▼
ALCATEL
SPACE

HERSCHEL / PLANCK

Herschel/Planck System Design Report

Product Code:000000

Rédigé par/*Written by*	Responsabilité-Service-Société *Responsibility-Office -Company*	Date	Signature
H/P Engineering Team			
Vérifié par/*Verified by*			
P. RIDEAU	System Engineering	31/07/01	
Vérifié par/*Verified by*			
C. MASSE	Product Assurance	31/07/01	
Approbation/*Approved*			
J.J. JUILLET	Project Manager	31/07/01	

Entité Emettrice : Alcatel Space - Cannes
(détentrice de l'original) :

ENREGISTREMENT DES EVOLUTIONS / *CHANGE RECORDS*

ISSUE	DATE	§ : DESCRIPTION DES EVOLUTIONS *§ : CHANGE RECORD*	REDACTEUR *AUTHOR*
01/00	31/07/01	First Issue	

TABLE OF CONTENTS

1. SCOPE

1.1. OBJECTIVES

The Herschel/Planck design report is issued to support the formal System Requirements Review (SRR) of the Herschel/Planck programme.

The objectives of this document are to:

- describe the system designs of the Herschel and Planck satellites

- demonstrate the compatibility of the design against the System Requirements Specifications.

In accordance to the share of work among the Core Team members, this document focuses on the system aspects. It is completed by Module Design Reports describing:

- the Herschel and Planck Service Module Design: SVM Design Report written by ALENIA

- the Herschel Extended Payload Module Design: HEPLM Design Report written by ASTRIUM

- the Planck Payload Module Design: PPLM Design Report written by ALCATEL.

These documents are part of the SRR data package submitted to ESA.

1.2. ORGANIZATION OF THE DOCUMENT

Section 2 gives the list of applicable and reference documents which have been used to build the design

Section 3 gives an overview of the main requirements driving the design.

Section 4 presents the mission design resulting from the discussions held since the beginning of Phase B with ARIANESPACE and ESOC.

Section 5 presents the experiment interfaces and accommodation constraints. As, at the time of preparation of the present document, the situation concerning the instrument interfaces is not frozen, this chapter will present the instrument interface baseline as well as the modifications presented by the instrument teams during meetings or in various versions of IID-B's. Preliminary assessment of this modifications will be presented which will be further detailed in Section 6.

Section 6 presents the overall system design of the Herschel and Planck satellites. It presents a summary of the various trade-offs conducted since the beginning of Phase B.

Section 7 presents the system budgets as well as the system analyses for Herschel and Planck.

2. DOCUMENTS

2.1.   ESA DOCUMENTS

2.1.1. Technical specifications

AD01.1   FIRST/PLANCK System Requirements Specification (SRS)
SCI-PT-RS-05991.

AD01.2   FIRST/PLANCK System Assembly Integration and Verification (AIV)
Requirements
SCI-PT-RS-07430.

AD01.3   FIRST/PLANCK Product Assurance Requirements
SCI-PT-RS-04683.

AD01.4   PLANCK Telescope Design Specification
SCI-PT-RS-07024.

2.1.2. ESA Undertakings

AD02.1   FIRST Telescope Specification
SCI-PT-RS-04671.

AD02.2   PLANCK Primary/Secondary Reflectors and Inner Baffle Specification
SCI-PT-RS-07422.

2.1.3. Satellite System Interface Specifications

AD03.1   FIRST/PLANCK Operations Interface Requirement Document (OIRD)
SCI-PT-RS-07360.

AD03.2   FIRST/PLANCK Space/Ground Interface Requirement Document (SGICD)
SCI-PT-RS-07418.

AD03.3   FIRST/PLANCK Packet Structure ICD
SCI-PT-ICD-07527.

2.1.4. Instrument interface specifications

AD04.1   FIRST/PLANCK IID Part A
SCI-PT-IIDA-04624.

AD04.2   IID Part B: Bolometer Instrument
SCI-PT-IIDB/SPIRE-02124.

AD04.3   IID Part B: Heterodyne Instrument
SCI-PT-IIDB/HIFI-02125.

AD04.4   IID Part B: Photoconductor Instrument
SCI-PT-IIDB/PACS-02126.

AD04.5   IID Part B: HFI
SCI-PT-IIDB/HFI-04141.

AD04.6   IID Part B: LFI
SCI-PT-IIDB/LFI-04142.

2.1.5. Mission support documents

AD05.1   FIRST/PLANCK Consolidated Report on Mission Analysis
FP-MA-RP-0010-TOS/GMA.

AD05.2   FIRST L2 Radiation Environment
ESA/ESTEC/wma/he/FIRST/3.

2.1.6. ARIANE STANDARDS

AD06.1   ARIANE 5 User's Manual Issue 03/Rev. 00 - March 2000.

AD06.2   CSG Safety regulations Volume 1 - General rules CSG-RS-10A-CN
Issue/Rev./Date 5/1/03.03.99 (Volume 1 taken precedence).

AD06.3   CSG safety regulations, CSG-RS-22A-CN Issue 5/0 (Volume 1)
and CSG-RS-22A (Volume 2) Edition 04, August 1991.

AD06.4   CSG Volume 2 Part 1. Ground Installations
GSG-RS-21A-CN Issue 05/Rev. 00 - Dec 1997.

AD06.5   ARIANE Specification SG-0-01 - Issue 03.

2.2.   PRIME DOCUMENTATION

2.2.1. System Specifications

AD07.1   General Design and Interface Requirements
                Document n° H-P-1-ASPI-SP-0027.

AD07.2   Environment and Test Requirements
                Document n° H-P-1-ASPI-SP-0030.

AD07.3   Cleanliness Requirement Specification
                Document n° H-P-1-ASPI-SP-0035.

AD07.4   EMC Specification
                Document n° H-P-1-ASPI-SP-0037.

AD07.5   EMC/ESD Control Plan
                Document n° H-P-1-ASPI-PL-0038.

AD07.6   Software Requirement Specification
                Document n° H-P-1-ASPI-SP-0046.

2.2.2. Product Assurance Requirements

AD08.1   Radiation Requirements
                Document n° H-P-1-ASPI-SP-0017.

AD08.2   Safety Requirements for Subcontractors
                Document n° H-P-1-ASPI-SP-0029.

2.3.   REFERENCE DOCUMENTS

RD01.1   System functional analysis
            Document n° H-P-1-ASPI-AN-0074.

RD01.2   HERSCHEL/PLANCK data rates
            Document n° H-P-1-ASPI-TN-0186.

RD01.3   PLANCK Straylight Evaluation of the Carrier Configuration
            Document PT-TN-05967.

RD01.4   PLANCK Payload Module Architect Technical Assistance- Impact of the
            SVM and Solar Array Temperature Fluctuations on the Temperature
            Stability of the PLM
            Document PT-07547, PL AS TN 033.

RD01.5   Application to Use ARIANE (DUA)
            Document H-P-1-ASPI-IF-0066.

3. KEY SYSTEM REQUIREMENTS AND DESIGN DRIVERS

3.1. GENERAL

Both Herschel and Planck payload presents stringent requirements which drives the system design. The main constraints which have to be taken into account are:

– cryogenic requirements for Focal Plane Units (FPU) of Herschel and Planck

– complex payload implementation: both instruments features a large number of equipment. Apart from the ones operating at cryogenic temperatures, some of these equipment have constraining requirements in terms of temperature range or stability

– attitude control: Herschel instruments requires accurate pointing as well as manoeuvrability. Planck mission imposes a slow spinning spacecraft. In both cases, attitude has to be controlled to avoid lighting of PLM's by Sun radiation in any cases.

– operation from L2 point of the Sun/Earth system. This allows to have optimum conditions for cryogenic spacecraft but constrains the launcher capacity, imposes long distances for telecommunications and drives system autonomy as visibility to ground is only possible 3 hours per day with one ground station.

These primary requirements drives the overall spacecraft layout and configuration as well as most of the subsystems performance. They are translated in system requirements as described in the following paragraphs.

The presence of a cryogenic payload leads to a separation of the spacecraft into 2 separate modules. The PLM (PayLoad Module) houses the cold FPU and provides the cryogenic environment:

– superfluid Helium cryostat for Herschel

– passive radiator at 60 K for Planck, plus accommodation of the active cooling chain provided by the experiments.

The SVM (SerVice Module) houses the warm equipment: payload warm units and platform equipments. Efficient thermal decoupling has to be provided between the two modules in terms of conducted and radiative heat load. This imposes further design requirements as the use of specific electrical harness (cryo harness) providing low thermal conductivity between PLM and SVM.

On both spacecraft, Sunshield/Sunshade shall be provided in order to protect the PLM from Sun illumination and to provide thermal insulation from Solar heat flux.

Injection of the spacecraft to L2 is performed using an ARIANE 5 launcher in its ES/V version. The spacecraft are set in a classical dual launch configuration. The overall launcher capacity to L2 is 5310 kg to which the mass of adaptors (SYLDA 5, 2624 adaptors, USF) have to be substracted. An overall mass ESA reserve of 200 kg has also to be kept. The launch configuration drives the available envelope for the spacecraft at launch. To meet the injection performance to L2 with ARIANE 5 ES/V, a parking orbit is planned, leading to a long launch sequence of 133 minutes. This has to be taken into account for the battery sizing.

Nominal lifetime requirements for Herschel and Planck are the following:

- 3.5 years for Herschel

- 21 months for Planck.

Full spacecraft performance, including margin shall be achieved at the end of this nominal lifetime. Extended lifetime is also envisaged:

- 6 years for Herschel

- 2.5 years for Planck.

This imposes to size the Fuel for attitude and orbit control for this duration. The items which degrade with time or usage shall be compatible with this extended duration. However, at the end of the extended duration, performance has to be met under nominal conditions, not taking into account margins.

Concerning Solar Array sizing, an additional margin of one year is required (SENV-095). Full performance of the Solar Array, including margins, shall be met for 4.5 years on Herschel and 2.75 years on Planck.

Autonomy requirements are similar for Herschel and Planck: the spacecraft have to operate during 48 hours without ground contact without interrupting the planned operations. Reconfiguration mechanisms and cross strapping have to be implemented to avoid the spacecraft to enter the survival mode on a single failure.

3.2.   SYSTEM REQUIREMENT SPECIFICATION

The top level applicable document specifying the spacecraft design is the (SRS) System Requirement Specification (AD01.1). Since the Phase B kick-off, the requirements in this document have been discussed between ALCATEL and ESA. This has resulted in the issue of an Issue 2 on the 13/07/01.

The design presented in this document follows the requirements from AD01.1 Issue 2.

The main open issue concerns the cleanliness requirements. The requirements in SRS Issue 2 have not been updated since the Issue 1, while different agreement have been reached during the Contamination Working Group meetings. The requirements presented in the Cleanliness Requirement Specification (AD07.3) are derived from the agreements of the Contamination Working Group. The sections of the design report related to contamination and cleanliness have been written in accordance with AD07.3.

Other open issues are:

– MISS-115 requires the Herschel spacecraft to be compatible with a transient (of TBD minutes) sun aspect angle of 90° + 95°/- 30° from the +X-axis. According to MISS-105, this requirement shall be met **after** separation from launcher. During discussion with ESA, ALCATEL suggested that in fact this requirement applies for the launch phase, **before** separation. No modification was introduced in Issue 2 and the need for such requirement is not understood.

– An inconsistency has been found between SMTT-120 and SMTT-135. The $Eb/N0$ of 2.7 dB specified in SMTT-120 corresponds to a Probability of Frame Loss (PFL) of 10^{-5}, not 10^{-6} as specified in SMTT-135. The value of 10^{5} for PFL is also the one required in the SGICD (AD03-2). The link budgets in the design report takes into account a PFL of 10^{-5} and $Eb/N0$ of 2.7 dB.

3.3.   MECHANICAL MARGINS REQUIREMENTS

As various requirements in terms of mechanical margins have been modified between Issue 1 and Issue 2 of the specification, the main margin requirements are recalled in this section.

a. Stiffness Requirements

As one of the major requirements for structural items dimensioning, SCMD-005 expresses that the structure resonance frequencies shall meet the launcher requirements as specified in ARIANE 5 Users Manual in AD07. Herschel and Planck shall achieve the following frequencies, when hard-mounted at their separation plane, with use of adapter 2624 of ARIANE 5:

– F_p lateral   > 9 Hz for S/C with mass ≤ 4500 Kg

– F_p longitudinal   > 31 Hz for S/C with mass ≤ 4500 Kg.

According to SCVE-040, the analytically predicted frequencies shall show positive margin on top of these requirements.

b. Strength Requirements

As a general rule, strength requirements for structural items are translated into margins of safety requirements. According to SCMD-020, margins of safety for Herschel and Planck shall be positive under the worst case combinations of mechanical and thermal loads. In addition SGEN-055 requires the dimensioning to cover a potential growth of 10 % of Herschel and Planck masses.

According to SINT-015, the structural design shall be compatible with an increase of the instrument units of 20 % above the nominal values from IID-B's. As the margins of the instruments between nominal mass and allocation are lower than 20 %, this will result in having a structural design compatible to the instrument mass allocations of the SRS or IID-A with some additional margin.

As a particular case, and according to SCVE-050, MoS shall be greater than 0.2 in case of a protoflight approach.

c. Safety Factors

According to SCMD-040 and SCMD-045, Safety Factors (SF) account for inaccuracies in predicted allowable and applied stresses, and shall be determinated according to the type of loads used for dimensioning:

	YIELD SF	ULTIMATE SF	BUCKLING SF
Conventional metallic materials	1.25	1.5	2
Unconventional materials	1.4	2	2
Inserts and joints	1.5	2	NA

d. Loads and Margins of Safety

As a recall, the **Limit loads** are defined to be the envelope of the mechanical and thermal load combinations (99 % probability of not being exceeded) during the entire life of the structure, including manufacturing, handling, transportation, ground testing without qualification, launch and on-orbit operations.

For launch, the **Limit loads** shall be derived from the various locations on the spacecraft from the quasi-static loads applied at the spacecraft Centre Of Mass (COM) and the loads resulting from the spacecraft vibration.

The **Design loads** are simplified load cases, which shall envelope the limit loads, and the qualification loads of the environmental testing.

Yield Loads, Ultimate Loads, Buckling Loads are Design loads multiplied by the respective yield, ultimate or buckling safety factors.

e. Preliminary design loads

According to SCMD-065, preliminary design loads shall be used for initial design. They are superseded for SRR by the values presented in EVTR (AD07.2)

f. Margins Of Safety (MOS)

According to SCMD-070, the Margin of Safety (MoS) shall be calculated as follows:

$$- \quad \text{MoS} = \frac{\text{Allowable load or stress}}{\text{Applied load or stress}} - 1.0$$

with Applied loads corresponding to Yield Loads, Ultimate Loads or Buckling Loads, derived from Design loads with application of the relevant Safety factors (see above under Point **c.**)

with Design loads and Qualification lads derived from Limit loads by application of the test factor of 1.25.

3.4. THERMAL MARGIN REQUIREMENTS

During discussion between ALCATEL and ESA on System Requirement Spec, the thermal margin philosophy for conventional temperature range was reviewed and it was agreed that:

– an acceptance test margin of 5° C shall be taken into account on both ends of the TCS Design Temperature Range. This defines the Acceptance Test Temperature Range

– a qualification test margin of 5° C shall be taken into account on both ends of the Acceptance Test Temperature Range. This defines the Qualification Test Temperature Range.

This definitions are reflected in the following figure and are in accordance with the GDIR (AD07.1) and EVTR (AD07.2).
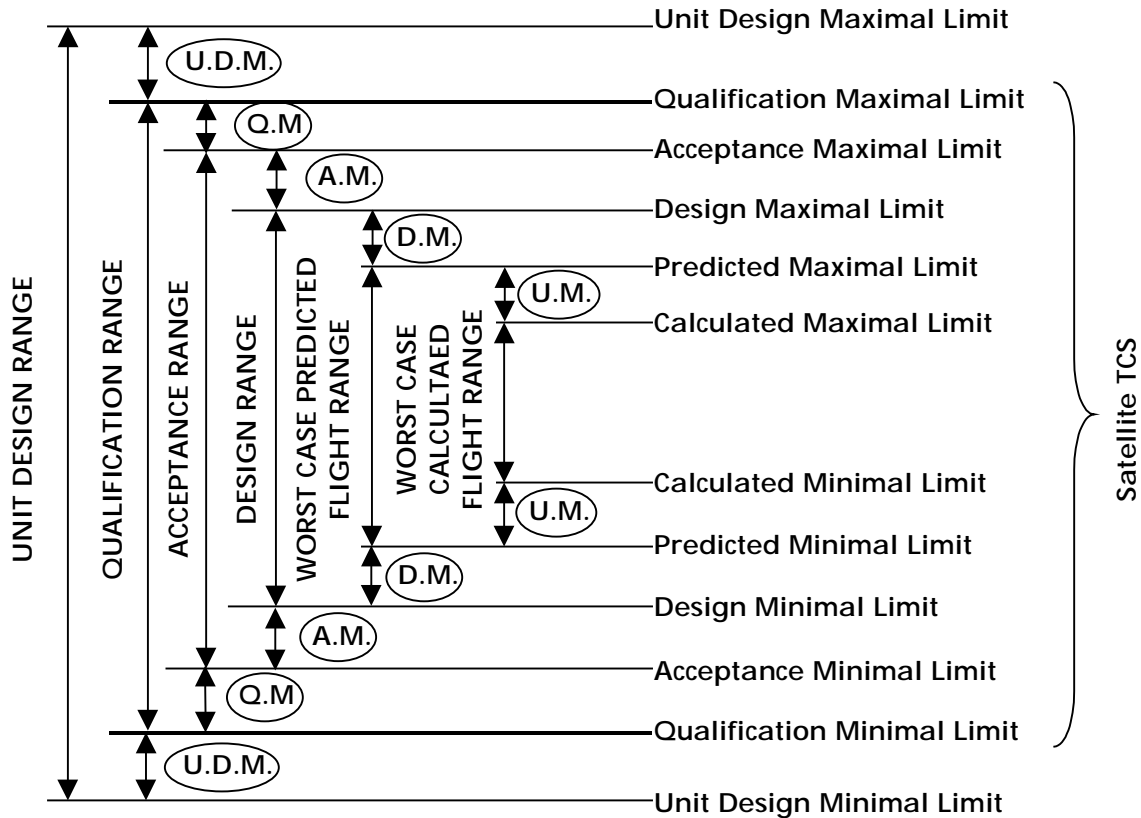
NOTES:

- UM = Modelling Uncertainty Margin

- DM = Thermal Control Design Margin/ABS (DM) > 0° C

- AM = Acceptance Margin/AM = 5° C

- QM = Qualification Margin/QM = 5° C

- UDM = Unit Design Margin/UDM > 0° C

with

- UM + DM = 7° C for internal equipment at conventional temperature range (for Phase B)

- UM + DM = 10° C for external (antennas, thrusters) (for Phase B).

4. HERSCHEL/PLANCK MISSION OVERVIEW

4.1.   OPERATIONAL ORBIT

Both HERSCHEL and PLANCK spacecraft are planned to operate from Lissajous orbits around the Lagrange point L2 of the Sun/Earth system. As shown in Figure 4.1-1, this point is aligned with the Earth and the Sun and located at $1.5 \ 10^6$ km from the Earth, away from the Sun.

Such orbits present the following advantages for the satellite operations:

- thanks to the Earth and Sun almost constant distances, the thermal environment is very stable. The thermal radiation from the Earth are reduced and induces a cold environment which is favourable for operating cryogenic satellites such as HERSCHEL and PLANCK

- the radiation environment is very low compared to an eccentric orbit such as ISO or XMM or even compared to geostationary orbits

- as the Sun and the Earth remain close together from the spacecraft, the shielding of the Sun thermal radiation will also prevent straylight effects from the Earth. The satellite communication with the Earth is facilitated as the satellite remains sun pointed.

During Phase A, many studies and trade-off have taken place to select the optimum orbits and transfer strategies for HERSCHEL which is dedicated to far infrared astronomy and PLANCK whose mission is to map the microwave background over the whole sky.

Both spacecraft are not sitting at L2 but orbiting around that point. The HERSCHEL and PLANCK orbits are described hereafter.
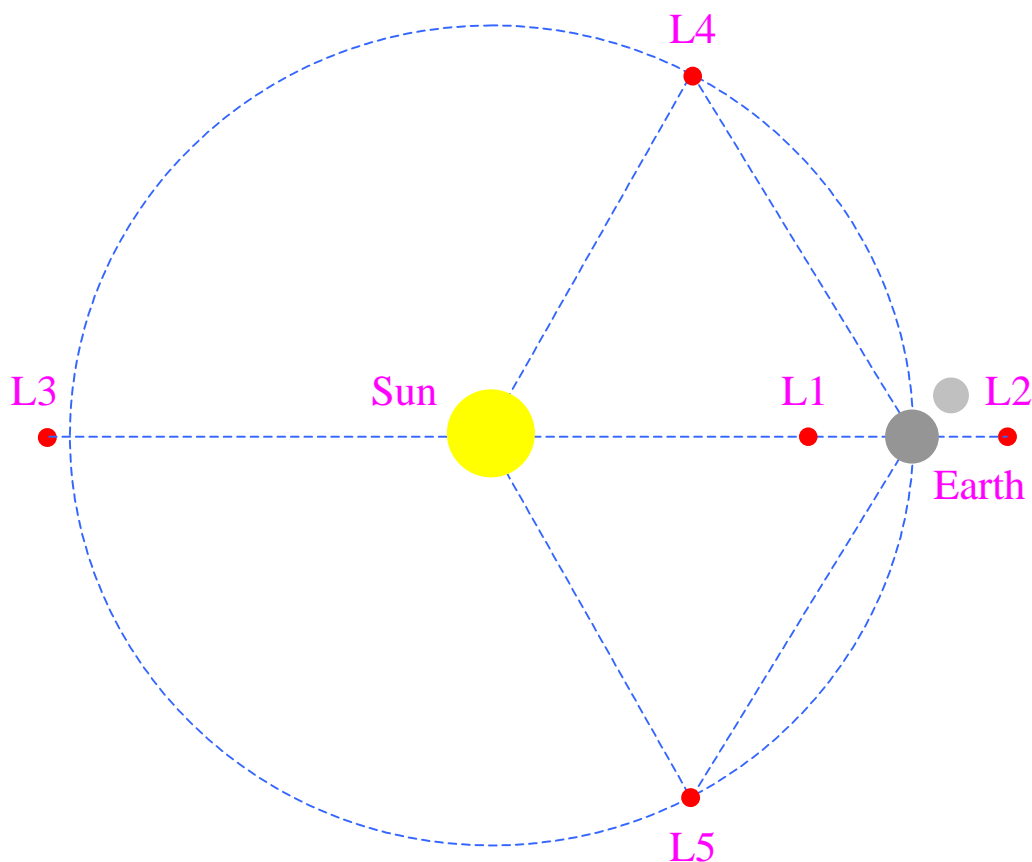
FIGURE 4.1-1   L2 LAGRANGE POINT HERSCHEL ORBIT

4.1.1. HERSCHEL orbit

A Large Lissajous orbit has been selected for HERSCHEL, its main characteristics are large amplitudes: up to 800 000 km amplitude in Y direction (as referenced in Figure 4.1-1), up to 500 000 km amplitude out of ecliptic plane (Z direction).

Figure 4.1-2 shows the orbit evolution of HERSCHEL from launch on the 15th Feb 2007 to 4.5 years of propagation in Earth centred XYZ rotating axis. The large amplitudes implies that the maximum Sun/Spacecraft/Earth angle can reach values above 30° and that the declination to Earth can be up to 40°, which is compatible with the satellite design.

This orbit can be reached without insertion manoeuvre.
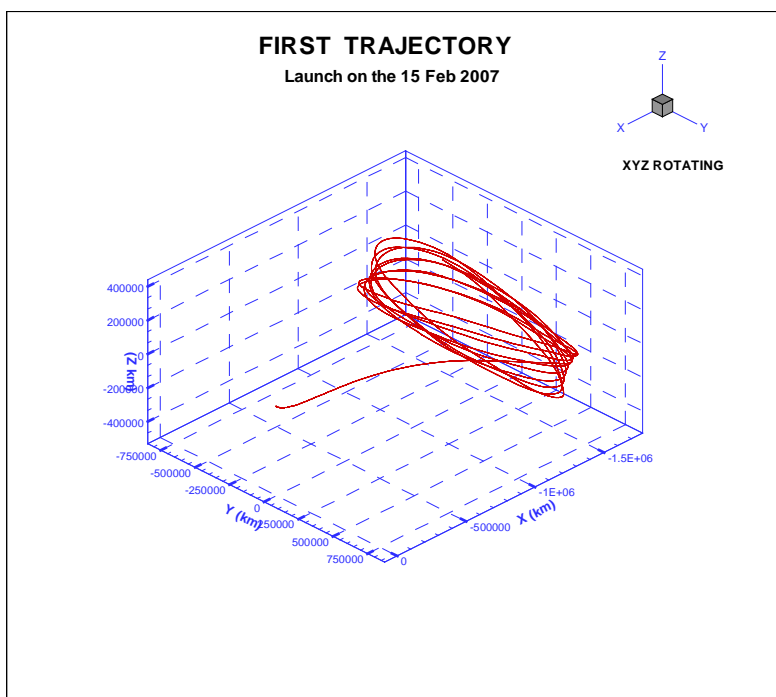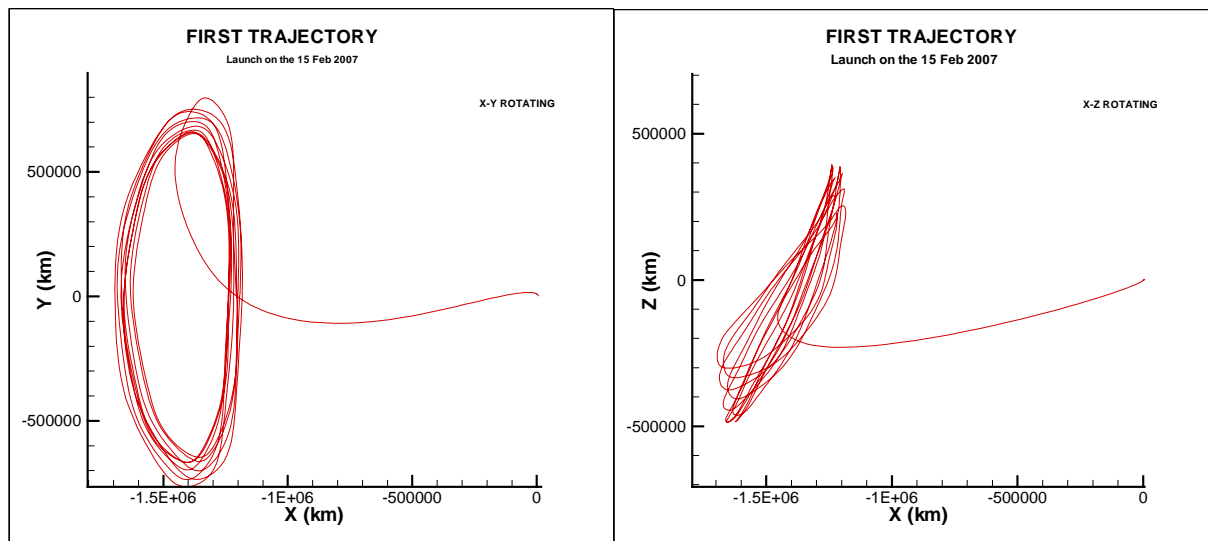
FIGURE 4.1-2 HERSCHEL LARGE LISSAJOUS ORBIT AROUND L2

4.1.2. PLANCK orbit

PLANCK is a Sun-pointed spacecraft with little manoeuvrability. In order to prevent the Earth and the Moon to enter the PLANCK field of view and generate unacceptable straylight, the chosen baseline is a Small Lissajous orbit with a Sun/Spacecraft/Earth angle limited to 10 degrees. This imposes an insertion manoeuvre at the arrival at L2 to reduce orbit amplitude. This manoeuvre has a magnitude of 250 m/s which is acceptable.

Figure 4.1-3 shows an example of a small Lissajous orbit from launch on the 15th Feb 2007 to 2 years of propagation in Earth centred XYZ rotating axis. The Y amplitude is 200 000 km and the Z amplitude is 250 000 km.
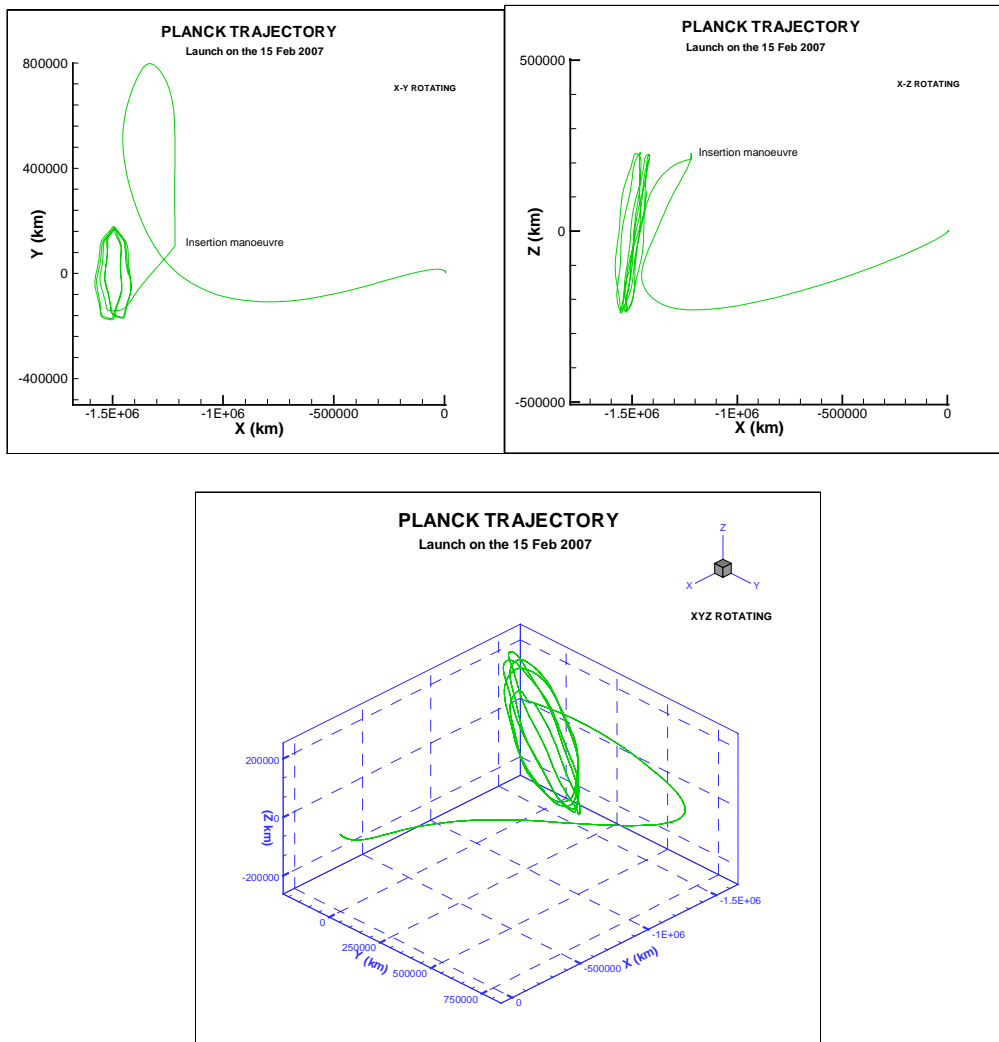
FIGURE 4.1-3 PLANCK SMALL LISSAJOUS ORBIT AROUND L2
The Sun/Spacecraft/Earth angle is limited to 10 deg.

4.2.   ATTITUDE CONSTRAINTS

4.2.1. HERSCHEL

HERSCHEL is a 3 axis stabilized, observatory type satellite. Its typical scientific mission consists in pointing successively at various targets in the sky according to a predefined schedule.

At any time in the mission, the whole sky is not accessible. This is due to the fact that the cold payload has to be protected from the Sun to remain operational. Any rotation around the Sun direction is allowed as it does not change the lighting conditions. Rotations around the perpendicular to the Sun direction are constrained in order to limit the size of the shield protecting the payload. The constraints are shown in Figure 4.2-1.

- 90 +/- 30 deg from X-axis around Pitch axis (Y axis).

- 5 deg around Roll axis (X axis = telescope line of sight).

The sunshield protecting the payload has thus to be designed such that no part of the cryostat or telescope are hit by the Sun light for any Sun direction within the allowed ones.

These constraints have top be met during the whole mission, from launcher separation (MISS 105). During launch, the launcher constraints leads to violation of the Sun aspect Angle requirements. This is described in Section 4.1.3.1.
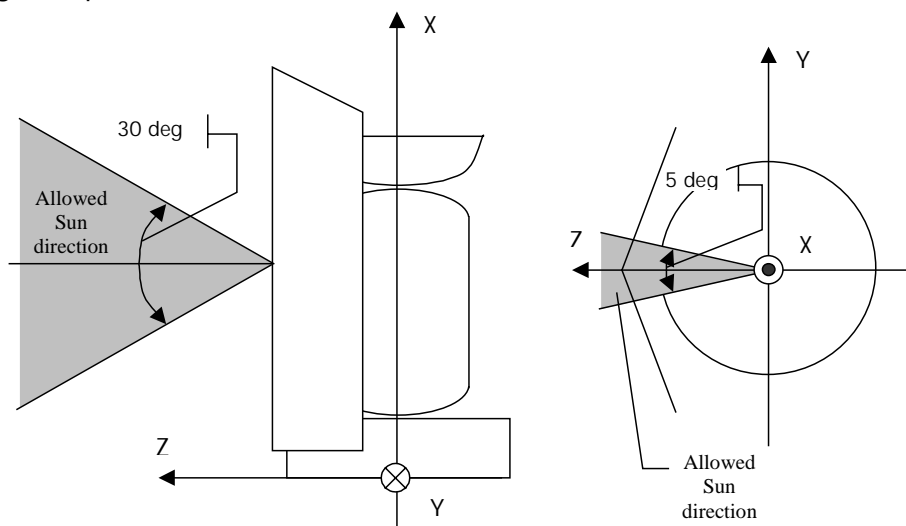
FIGURE 4.2-1 HERSCHEL ATTITUDE CONSTRAINTS
A ± 30 deg. rotation is allowed in Pitch (Y), while ± 5 deg. is allowed in Roll (X). The spacecraft is free to rotate around Z

4.2.2. PLANCK

The PLANCK attitude profile is very different from the one from HERSCHEL. PLANCK is a spinner which systematically scans the celestial sphere to produce a sky map. As shown in Figure 4.2-2, the PLANCK spin axis is normally opposite to the Sun, with the telescope line of sight at 85 deg. from the spin axis. During one rotation, the instruments scan a sector of the celestial sphere with an angular diameter of 85 deg.

In order to view the celestial poles, it is thus mandatory to be able to depoint the spin axis by from the Sun direction. A scanning law which depoints the spin axis at 10 deg. maximum from the Sun will be defined, in order to achieve scientific objectives. This means that the spacecraft has to be compatible with a maximum angle of 10 deg. between the spin axis and the Sun. This is shown in Figure 4.2-3.
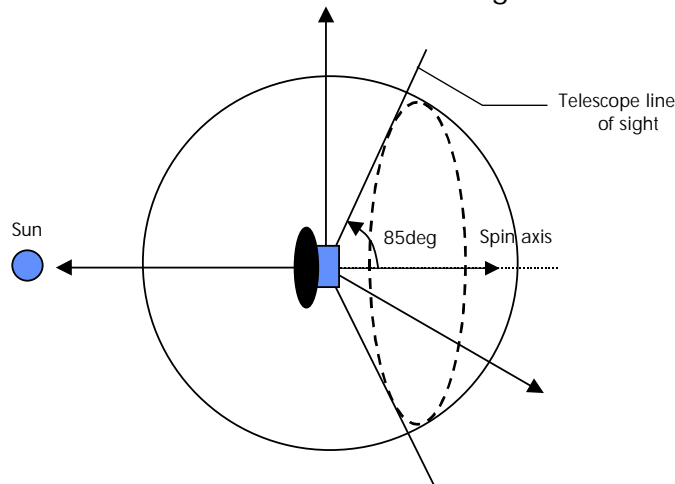
FIGURE 4.2-2   PLANCK OBSERVATION STRATEGY
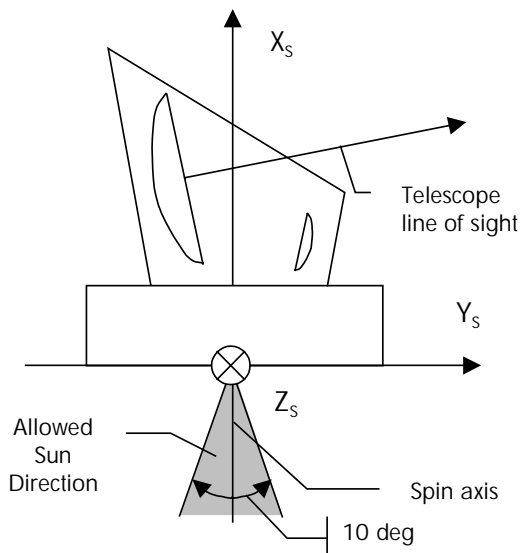
FIGURE 4.2-3 PLANCK ATTITUDE CONSTRAINTS
The Sun in constrained to remain within 10 deg from the spin axis

Due to the fact that PLANCK is in orbit around L2, it makes one rotation around the Sun per year. The spin axis has also to rotate at the same rate to remain Sun pointed. This is achieved by making regular precession manoeuvres which also includes out of plane motion to achieve the PLANCK scanning law. This scanning law is constrained by the fact that the angle between the spin negative axis (-X) and the direction from satellite to Earth has to remain below 10 deg.

4.3. MISSION PHASES

4.3.1. Launch phase

PLANCK and HERSCHEL missions have been combined for a launch in 2007. The nominal scenario consists in a dual launch with HERSCHEL and PLANCK targeting an injection of both spacecraft toward L2. An alternative strategy consists in the injection on a very elliptical parking orbit, this is described in Section 4.3.1.2. A trade-off is being driven on the choice of the injection orbit as described in Section 4.5.3.

4.3.1.1. Nominal scenario: direct injection to L2

The driving system constraints are the overall transfer cost and spacecraft mass, the Sun-spacecraft-Earth angle, the eclipse avoidance strategy and the sensivity with respect to launch date and hour.

The baseline ARIANE 5 Launcher is the ARIANE 5 EVOLUTION/SV with a delayed ignition of the EPS upper stage which can bring 5310 kg in transfer orbit. After burn-out of the lower composite, the upper stage and the satellites perform a ballistic phase around Earth of about 107 min. The upper stage is fired during 17 min at the end of the coast arc to inject successively HERSCHEL and PLANCK toward L2. Table 4.3-1 gives a time table for the launch sequence.

TIME	EVENT	
To	Lift-off	
T0 + 145.7 sec	Booster jettisoning	
T0 + 196.6 sec	Fairing jettisoning	HERSCHEL Sun constraint applies
T0 + 545.3 sec	Lower composite jettisoning	
T0 + 116 min	End of the coast arc, Upper stage ignition	Eclipses during coast arc
T0 + 133.2 min	Spacecraft separation	HERSCHEL is separated in 3 axis mode, PLANCK is separated in spin mode

TABLE 4.3-1 LAUNCH SEQUENCE

The orbit Apogee altitude targeted is around 1300 000 km.

For a dual launch, the sequence of events for the spacecraft separations is:

   – HERSCHEL separated in 3 axis mode with Z pointed to the Sun

   – ARIANE 5 upper stage re-orientation to have –X axis Sun pointed

   – SYLDA5 separation

   – PLANCK spin-up and ejection.

During Launch, TC are sent to HERSCHEL to open valves in the cryostat and power is provided to PLANCK coolers to their launch lock mode. From launcher separation, the attitude of the spacecraft will be controlled to meet the attitude constraints described in § 4.2.

Eclipse duration

The maximal eclipse duration during launch is expected to be about 43 minutes max during the coast phase.

Roll and Pitch control

One major constraint during the launch is the Solar Aspect Angle (SAA: angle between the Sun and the launcher axis) which must remain in the allowed area for both spacecraft as described in Chapter 4.2. As soon as the fairing is jettisoned, the point is to ensure that HERSCHEL does not receive any Sun light out of its acceptable range during the launch phase. The satellite Roll angle is limited to +/- 11° due to Sun shield configuration.

Two aspects must be considered:

   – the Sun must be close to HERSCHEL X, Z plane to meet the requirement around X. This imposes a Roll law for the launcher

   – the Sun must, as far as possible be at 90 +/- 30° from the X axis: once proper Roll has been achieved and during propulsive phases, the Sun angle from the X-axis is imposed by launcher attitude which is derived from mission analysis. It is however possible to have the Sun at 90 + 90 deg from X axis. Furthermore, Herschel is shaded by the EPS when the Sun in at 90 + 85 deg from X axis for any Roll.

Until EAP separation which occur before fairing separation, the roll angle is imposed by the launcher. After boosters jettisoning, the payload can impose its Roll Law, allowing correct orientation at fairing jettison. The launcher Roll constraint occurs 30 sec before EPC extinction: the EPC attitude must be oriented in order to ensure its atmospheric reentry. The judicious choice of the clocking of the satellites will ensure the compatibility of this launcher constraint with respect to HERSCHEL constraint.

For a given launch date and hour, the SAA can be solved by the Roll law optimization of the launcher. The period during which the SAA can be solved by the Roll law of the launcher is limited to about 15 days and to meet this constraint, it is necessary either to build a new Roll law (means a new software) or to clock the satellite differently.

Over a duration of 15 days, the variation of the Roll law is in the order of 10 deg.

Another contribution is the Roll attitude control of the EPC. It is controlled inside a deadband which has a nominal width of 25 deg with a target 13 deg. Added to the Roll law variation, this leads to a total rotation of the Sun of 23 deg around X, above the Sunshield/Sunshade shadowing capacity. The various ways investigated to solve this problem are the following:

– check possibility to improve launcher roll control: EPC Roll control on ARIANE 5 ES/V will be done with the same propellant as the main engine. Tighter Roll control can mean launcher performance degradation

– analyse possibility to improve H-PLM protection by the Sunshield/Sunshade

– investigate impacts on H-PLM to be illuminated by the Sun.

During the coast phase, the launcher EPS is nominally spinned at 2 deg/sec in one direction and the other. With ARIANE 5 Evolution, the attitude can be inertial and the accuracy of the attitude control drives the fuel consumption of the SCA (EPS attitude control system). The nominal attitude accuracy is +/- 20° in longitudinal accuracy pointing which is not compatible with HERSCHEL satellite. Higher accuracy could be reached in counter part of higher hydrazine consumption which is under analysis in ARIANESPACE.

Collision analysis

One other important point will be the trajectory analysis of HERSCHEL and PLANCK after the separation, in particular a collision risk analysis will demonstrate that there is no risk of collision between both spacecraft.

A slight and sufficient difference in the semi-major axis will be have to be introduced by the launcher spring separation system. First assessment indicates that, according to the semi-major axis differences, the ejection Delta-V and to the instability of the target point, there is no risk of collision between both spacecraft.

Injection Accuracy

The ARIANE 5 Launcher dispersions are determinant for the navigation study. The first manoeuvre has the objective to correct the launcher injection error and is planned 2 days after lift-off. One important parameter is the delayed ignition of the launcher injection onto the escape orbit which is traduced by a correction Delta-V allocation in the propellant budget.

A first Analysis shows that true anomaly is the driving parameter for inaccuracy due to the Schüler effect. Table 4.3-2 synthesises the results issued by ARIANESPACE which has taken 20 % margin on its results. The injection accuracy is the driving parameter as it dimensions the first orbit correction manoeuvre which takes place 2 days after the separation. The amplitude of this correction has been estimated to 43.3 m/s with an updated method generating a Monte-Carlo simulation with re-optimization of the transfer (save in Delta-V of 20 m/s compared to a classical navigation study). For the budget, a round-up value of 50 m/s will be considered for the first orbit correction.

Classical Orbit parameters	Orbit parameters	Estimated dispersions	Estimated dispersions with 20% margin
Semimajor axis a (km)	656493.132	47510	57010
Eccentricity e	0.99	0.000602	0.0007221
apogee (km)	1299995	95010	114020
perigee (km)	235	0.52	0.62
Inclination i (°)	6.107	0.01462	0.01755
Argument of perigee w(°)	110.129	0.249	0.2988
Right ascention of the ascending node W(°)	-120.914	0.2373	0.2847
Mean anomaly M	0.028	0.002521	0.003025

TABLE 4.3-2 INJECTION ACCURACY

4.3.1.2. Alternative scenario: injection on a parking orbit

Another strategy consists in the injection on a very elliptical orbit with an Apogee range of 500000 km to 700000 km called a parking orbit. The advantage for the launch phase are the following ones:

–   higher launcher performances as illustrated in Figure 4.3-1. Targeting an Apogee of 500000 km instead of 1300000 km could lead to an additional performance of about 150 kg which gives a total launch mass of 5460 kg

–   No major impact on the launch sequence and launch timeline have been identified with respect to previous section. The injection accuracy are considered as the same order of magnitude for the injection, the main difference lies on the fact that the spacecraft will not correct the launcher dispersions two days after but it will be combined with its Perigee manoeuvre. This is detailed in Section 4.3.3.2

–   no need to consider an additional Delta-V provision of 14m/s for the flight software compatibility.

Performances as function of the apogee altitude for AR5 ESV delayed ignition
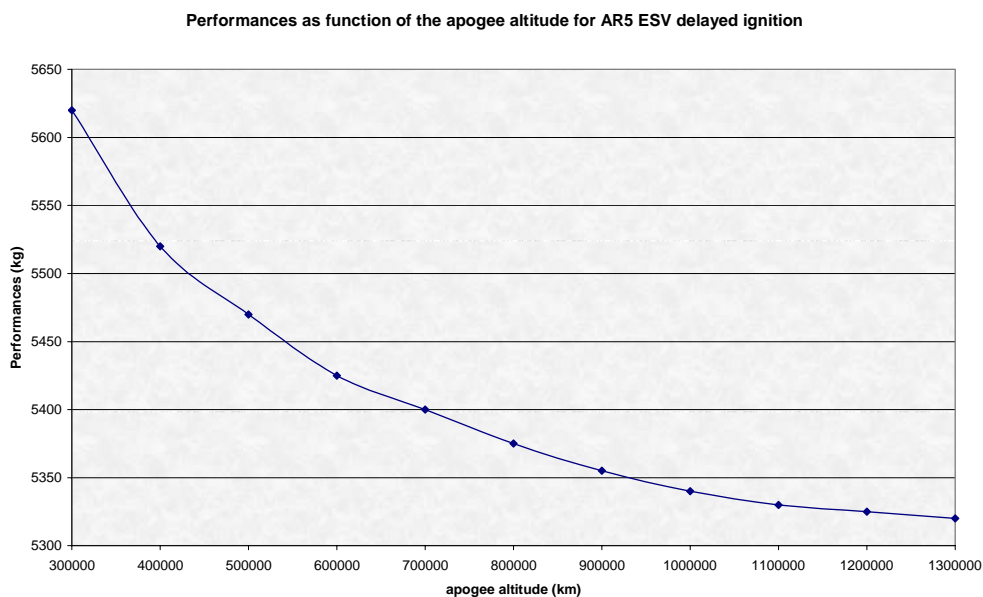
FIGURE 4.3-1 ARIANE 5 ESV PERFORMANCES VS APOGEE ALTITUDE WITH A DELAYED IGNITION

4.3.2. Transfer phase: direct injection toward L2

Transfer phase baseline is a direct injection toward L2 for both spacecraft. An alternative strategy is the parking orbit strategy described in Section 4.3.3. A trade-off between these two strategies is under assessment and is synthesised also in Section 4.5.

4.3.2.1. Transfer timeline

Table 4.3-2 shows the transfer phase timeline for HERSCHEL. The allocation for transfer to L2 Lissajous orbit is 6 months (SPER-005). In fact, when all commissioning and performance verification are completed. HERSCHEL can begin its scientific observation even if it is not yet arrived in its orbit around L2 point.

At the beginning of the transfer phase, HERSCHEL telescope is heated to prevent deposition of contaminant coming from the spacecraft outgassing. This heating lasts for 3 weeks (HERSCHEL telescope specification, TEPE-040), followed by cool down to telescope operational temperature (between 70 and 90 K). At the end of commissioning phase (T0 + 1 m) the telescope has not yet finished its cool-down: the temperature will be around 110 K.

PHASE	DURATION	ACTIVITIES
IOP	from T0 to T0 + 2d	– 3 axis stabilization acquisition – Ground contact acquisition – Switch ON telescope heaters – Orbit correction manoeuvres at day 1 and 2
Commissioning Phase	from T0 + 2d to T0 + 1 m	– P/F checkout – P/L switch-ON and checkout – End of telescope heating (T0 + 3 w) – Telescope cool-down – Cryo cover opening
Performance verification phase	from T0 + 1 m to T0 + 3 m	– End of telescope cool-down – Performance verification of AOCS and sensors calibration – P/L performance verification and calibration

TABLE 4.3-2   TRANSFER PHASE TIMELINE FOR HERSCHEL

The commissioning phase ends by cryo-cover opening. Timing optimization of the commissioning phase will be performed in Phase B to determine the best sequence of telescope heating and cryo-cover opening, in order to avoid any contamination of the instruments.

Table 4.3-3 shows the transfer phase timeline for PLANCK. It lasts from launcher separation up to the insertion manoeuvre onto the small Lissajous orbit.

PHASE	DURATION	ACTIVITIES
IOP	from T0 to T0 + 2d	– Spin mode acquisition – Ground contact acquisition – Orbit correction manoeuvres at day 1 and 2
Commissioning Phase	from T0 + 2d to T0 + 1 m	– P/F checkout – P/L swith-ON and checkout – Passive cool-down to 50 K ($\rightarrow$T0+1w) – Switch ON 20 K cooler and cool-down to 20 K ($\rightarrow$ T0 + 2w) – Switch ON 4 K cooler and cool-down to 4 K – Switch ON 0.1 K cooler and cool-down to 0.1 K ($\rightarrow$ T0 + 4w)
Performance verification phase	from T0 + 1 m to T0 + 6 m	– Performance verification of AOCS and sensors calibration – P/L performance determination and calibration – Injection manoeuvre to small Lissajous

TABLE 4.3-3 TRANSFER PHASE TIMELINE FOR PLANCK

4.3.2.2. Transfer orbit correction manoeuvres

The orbit correction manoeuvres have been computed with the assumptions described hereafter. Few manoeuvres have been scheduled as presented in Table 4.3-4.

Each manoeuvre has been determined using a guidance scheme which targets to remove the velocity component along the escape direction. A modified approach with a Monte-Carlo simulation with re-optimisation of the transfer Delta-V helps to reduce the required Delta-V. The main hypothesis of the computation are:

– launcher performances as given in previous section (including 20 % margin)

– orbit Determination accuracy (typical data)

– manoeuvre execution error less than 1 % in size and 1° in pointing at 1 sigma

– Solar radiation bias error of 10 %.

All the orbit manoeuvres are considered inertial for PLANCK and HERSCHEL.

DATE	DELTA-V	PURPOSE	SOLAR ASPECT ANGLE	MANOEUVRE DIRECTION
T lift-off + 2 hours	14 m/s	Launcher interface	[150° – 180°]	Tangent to the velocity direction
T lift-off + 2 days	50 m/s	Remove launcher dispersions	[0° – 30°] or [150° – 180°]	
T lift-off + 12 days	4 m/s	Remove first manoeuvre execution error	[0° – 180°]	Along the unstable direction which is close to the velocity
Injection – 20 days	3 m/s	Remove accumulated error during cruise and fine targeting	[0° – 180°]	Along the unstable direction in-plane or out of plane
Injection (only for **Planck**)	250 m/s	Lissajous orbit manoeuvre (specification for 6 months launch window)	[123° – 125°]	Match velocity conditions for Lissajous orbit
Injection + 2 days (only for **Planck**)	5 m/s	Remove injection manoeuvre execution error	[28.4° - 151.6°]	Along the unstable direction

TABLE 4.3-4 HERSCHEL AND PLANCK ORBIT CORRECTION MANOEUVRES

Additional orbit correction manoeuvre may be necessary during transfer. The first orbit correction manoeuvre is dependant on the launch date and hour but a representative value has been estimated with the given launch window.

4.3.2.3. Environmental conditions

Environmental conditions are driving constraints for the HERSCHEL/PLANCK mission and operations.

Figure 4.3-2 presents the distances to the Earth, which will drive the telecommunications and the radiation and thermal environment, and also to the Moon. The red curve represents HERSCHEL and the green one PLANCK.
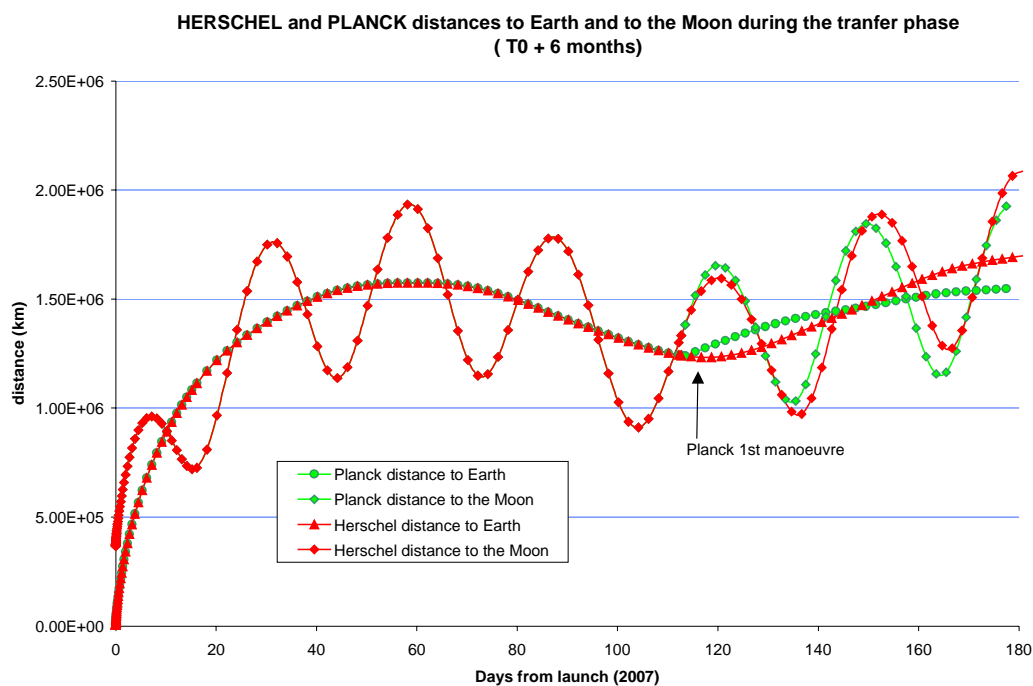
FIGURE 4.3-2 HERSCHEL AND PLANCK DISTANCES TO THE EARTH

The Sun-Satellite-Earth aspect angle is very constrained for both spacecraft due to the nature of the mission and the equipments embarked. This angle has to be checked during all the phases of the mission and particularly during the transfer when it is submitted to big variations.

Figure 4.3-3 shows the Sun-Satellite-Earth angle for HERSCHEL (red) and PLANCK (green) during the transfer phase.

Before PLANCK insertion manoeuvre, the SSCE angle reaches 31 degrees around day 80 after lift-off. The PLANCK insertion manoeuvre reduces the SSCE angle to a maximum value of 10°.

HERSCHELand PLANCK SUN-Satellite-Earth angle during the transfer phase
(T0 + 6 months)
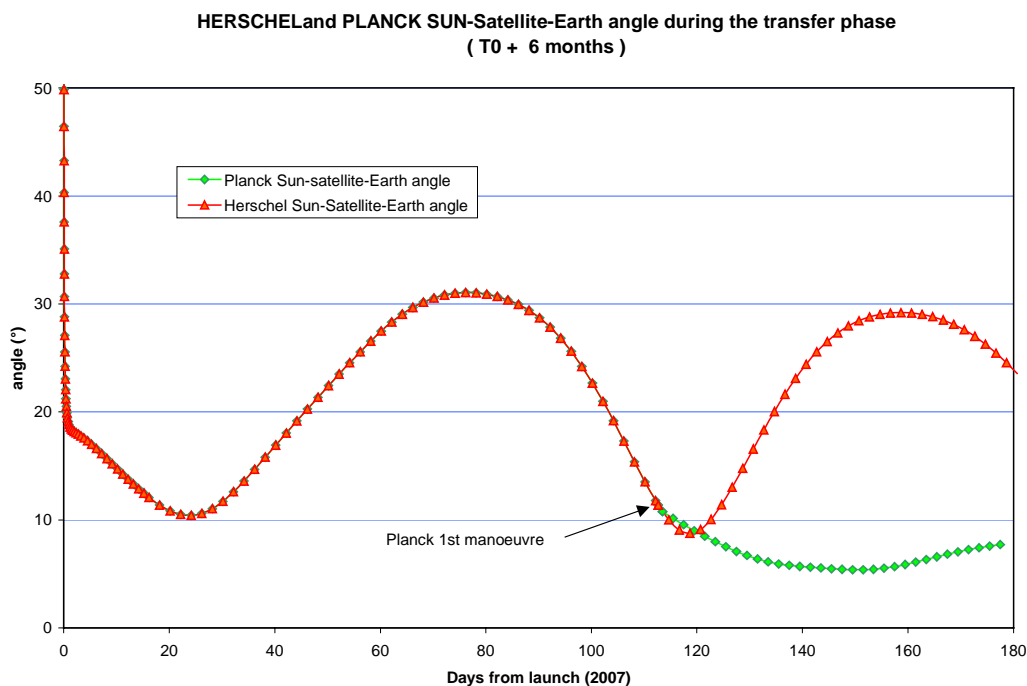
FIGURE 4.3-3 HERSCHEL AND PLANCK SUN-SATELLITE-EARTH ANGLE DURING TRANSFER

4.3.2.4. Ground station visibility

The ground station visibility during transfer is also a driving constraint for the mission. Both spacecraft will be controlled by the following ground stations: PERTH, KOUROU and VILLAFRANCA. These stations belong to the ESA network and their locations is illustrated in Figure 4.3-4.
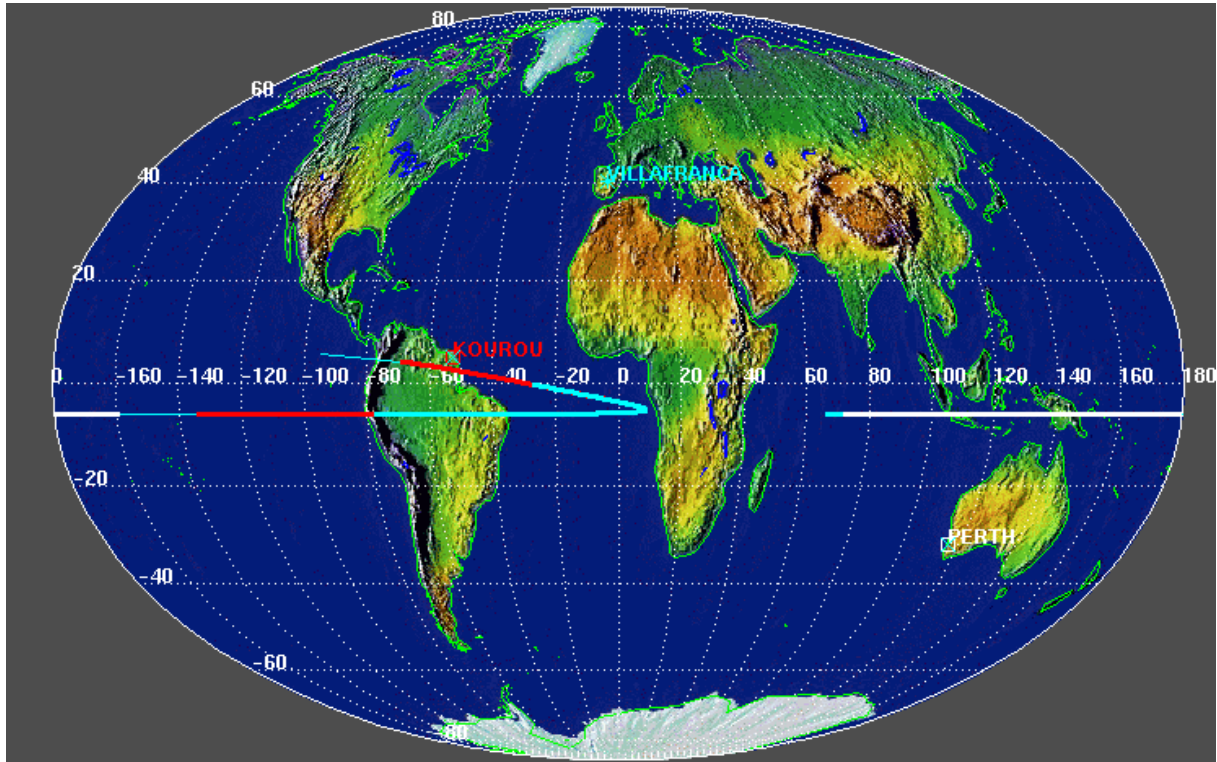
FIGURE 4.3-4 GROUND STATIONS COVERAGE DURING TRANSFER

The minimum elevation is taken to 5° for each station. The colour of the curves indicates the ground stations coverage periods on the orbit associated to the colour of the ground station names. It is possible to see that the coverage is ensured from lift-off to the first day of the mission except for about 1 h 40 minutes 13 hours after launcher separation.

During all the transfer phase, the coverage is ensured successively by one of the three ESA ground stations for a duration of about 10 to 12 hours, which will allow the monitoring of the satellite, the commanding of the attitude and orbit correction manoeuvres, as illustrated in Figure 4.3-5.

Ground stations coverage during transfer (T0 + 7 days)
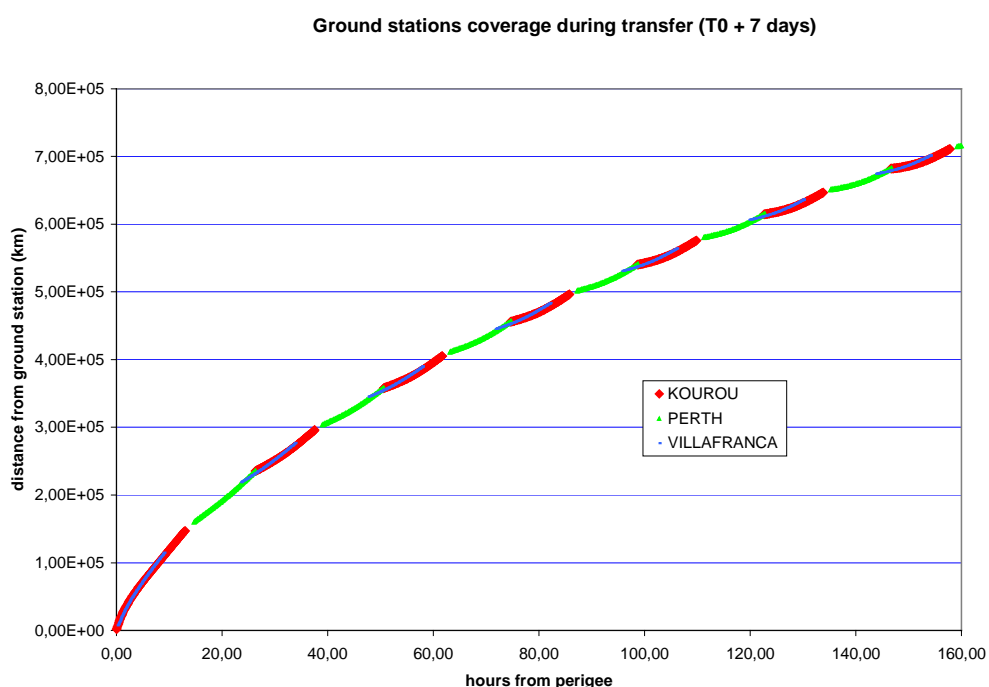
**FIGURE 4.3-5 ESA GROUND STATIONS VISIBILITY
Simulation duration: first day of the mission
(launch on the 15th Feb 2007 17h30)**

4.3.2.5. Launch window

The launch window has also been subject to many analyses. As both satellites are launched together, the launch window must be compatible with HERSCHEL and PLANCK but only PLANCK does really constraint the launch window; HERSCHEL does not introduce any launch window constraints.

The main constraints satisfied by the launch window are described:

– minimization of the injection DV on the Lissajous orbit: for PLANCK which needs a reduction manoeuvre to reach the small Lissajous orbit, the Delta-V is limited to 250 m/s assuming an injection on a Lissajous orbit with a maximum Sun-spacecraft-Earth angle less than 10° (higher case are not covered)

– the eclipse occurrence on the Lissajous orbit shall be avoided, as they are correlated with injection point on the Lissajous orbit and an eclipse avoidance manoeuvre which is included in the Delta-V budget of 250 m/s.

– no eclipses during transfer phase

– ARIANE 5 performances compatibility.

The launch window presented in Figure 4.3-6 has been computed for the all year 2007 (January to December). Two periods around Equinoxes are favourable due to the small angle between the transfer orbit inclination and the ecliptic plane:

– from February 2007 to May 2007

– from July 2007 to October 2007.

For the other periods, the injection cost for PLANCK may reach the value of roughly 370 m/s. The launch window is closed few days around Equinox due to eclipses occurrence.

The launch times of minimum Delta-V (200 m/s) are around begin of March and end of July centred at about 17 h 00 UT launch time.

The launch hour is between 15 h 30 and 18 h 30 in UT which corresponds to 12 h 30 to 15 h 30 in Kourou time. Associated system impact for the launching operations will be defined in the specific documentation.

The launch window has a daily duration of about 3 hours which is compatible with the ARIANESPACE constraint of 45 minutes. This constraint is satisfied for all the possible launch dates in 2007.

The launch window sensibility for the value of 250 m/s is bigger in terms of hours within a day rather than from a day to another one due to the relative rotation speed of the Earth.

The eclipses occurs during about 30 days for the worst launch hour cases.
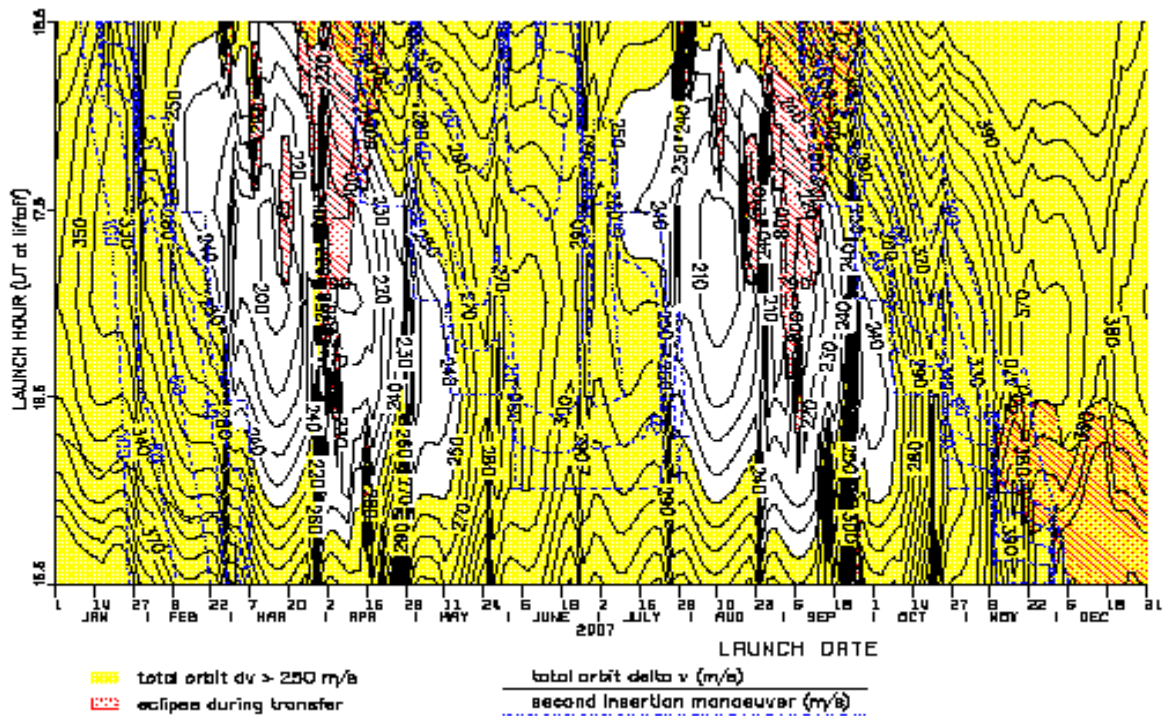
FIGURE 4.3-6 LAUNCH WINDOW FOR HERSCHEL/PLANCK
There is a 6 months launch window between February 2007 and October 2007

The date and time of the launch drive the following parameters of HERSCHEL and PLANCK mission:

- the Perigee velocity

- the maximum Sun-Satellite –Earth angle in orbit

- the exact time of the insertion manoeuvre for PLANCK

- the date and the amplitude of the eclipse avoidance manoeuvre

- and finally the size of the reached Lissajous amplitude orbits (in Y and Z).

Thus the overall mission will be strongly dependent on the selected launch date and time.

4.3.3. Alternative transfer phase: injection on a parking orbit

An alternative strategy which consists in the injection of both spacecraft on a parking orbit has been identified. All the impacts in terms of mission analysis and system are described in the following paragraphs. Possible parking orbit apogee altitudes remain in the range [500 000 km - 700 000 km] which induces additional 15 to 25 days of transfer duration (20 days average value).

4.3.3.1. Transfer timeline impact

Table 4.3-5 shows the transfer phase timeline for HERSCHEL.

The major impact of this parking orbit is an additional Perigee passage after one revolution on the high elliptical orbit which will impact the satellite cool-down timeline and the satellite lifetime as the CVV temperature will increase to 95 K (TBC) at Perigee.

Depending on the date of Perigee passage w.r.t. the end of telescope heating, the delay due to CVV heating at perigee will vary between 0 and 2 days for telescope cool-down, and 1 and 7 days for CVV cool-down.

The impact on CVV lifetime has still to be determined by simulations performed by ASTRIUM.

PHASE	DURATION	ACTIVITIES
IOP	from T0 to T0 + 2d	– 3 axis stabilization acquisition – Ground contact acquisition – Switch ON telescope heaters
Commissioning Phase	from T0 + 2d to T0 + 1 m	– P/F checkout – P/L switch-ON and checkout – Apogee manoeuvre around T0 + 10 days – Perigee manoeuvre around T0 + 20 days – End of telescope heating (around T0 + 23 days) – Telescope cool-down – Cryo cover opening
Performance verification phase	from T0 + 1 m to T0 + 3 m	– End of telescope cool-down – Performance verification of AOCS and sensors calibration – P/L performance verification and calibration

TABLE 4.3-5 TRANSFER PHASE TIMELINE FOR HERSCHEL WITH PARKING ORBIT

Table 4.3-6 shows the transfer phase timeline for PLANCK in the parking orbit case. It lasts from launcher separation up to the insertion manoeuvre onto the small Lissajous orbit.

To assess the different impacts of this scenario on the PLM cool-down timeline, the following hypotheses have been made:

    – no telescope heating since no major contamination is expected to occur at that time

    – coolers OFF before and at Perigee pass (since PLM will heat up at perigee pass, starting the coolers before is useless)

    – coolers ON only when third groove temperature is nominal.

The third hypothesis means that third groove nominal temperature achievement is the criteria to determine the delay induced by PLM heating at perigee pass on coolers switch-on time.

Following these hypotheses, the third groove will reach its nominal temperature one week after Perigee pass, which means that the total delay is around 3 weeks (the period of the parking orbit).

PHASE	DURATION	ACTIVITIES
IOP	from T0 to T0 + 2d	– Spin mode acquisition – Ground contact acquisition
Commissioning Phase	from T0 + 2d to T0 + 7w	– P/F checkout – P/L switch-ON and checkout – Apogee manoeuvre around T0 + 10 days – Perigee manoeuvre around T0 + 20 days – Passive cool-down to 50 K ($\rightarrow$ T0 + 1 m) – Switch ON 20 K cooler and cool-down to 20 K ($\rightarrow$ T0 + 5w) – Switch ON 4 K cooler and cool-down to 4 K – Switch ON 0.1 K cooler and cool-down to 0.1 K ($\rightarrow$ T0 + 7w)
Performance verification phase	from T0 + 7w to T0 + 6 m	– performance verification of AOCS and sensors calibration – P/L performance determination and calibration – Injection manoeuvre to small Lissajous

TABLE 4.3-6 TRANSFER PHASE TIMELINE FOR PLANCK

4.3.3.2. Transfer orbit correction manoeuvres impact

Parking orbit scenario implies that the spacecraft perform its injection toward L2 with its propulsive system and satisfying all the system constraints. Additional manoeuvres are to be performed with respect to the direct injection scenario as presented in next Table 4.3-7.

The main hypothesis of the computation are the same as in Section 4.3.2.3.

The main advantages of this parking orbit strategy are:

– the main orbit correction manoeuvre which removes the launcher dispersions is then combined with the Perigee (and possible Apogee) manoeuvres for the injection toward L2

– reduced sensitivity of the manoeuvres with respect to launcher dispersions which are, at the moment, not really accurately known and which correspond to the most important contribution in the Delta-V budget

– parametric study of possible Perigee manoeuvres realisation shows that a parking orbit strategy ensuring a fixed SAA for Planck close to 125 deg (Lissajous orbit injection value) or 180 deg (along spin axis) is close to the optimum in terms of Delta-V, which means that satellite system constraint satisfaction does not bring manoeuvres strategy desoptimization.

DATE	DELTA-V	PURPOSE	SOLAR ASPECT ANGLE	MANOEUVRE DIRECTION
T lift-off + 10 days	0 - 20 m/s	Apogee manoeuvre to counteract the orbit unstability	[60° – 80°]	
T lift-off + 20 days	20 - 70 m/s	Perigee manoeuvre to inject the satellite to L2 (includes gravity loss)	[125° or 180°] for PLANCK along SC X axis for HERSCHAL	**PLANCK:** Inertial thrust and manoeuvre location optimized with respect to SAA constraints (min thrust 11N) **HERSCHEL:** Constant turn rate (7°/min) assumed for the Perigee manoeuvre (thrust 40N)
Perigee Man + 2 days	5 m/s	Perigee manoeuvre execution correction	[0° – 180°]	
Injection – 20 days	3 m/s	Remove accumulated error during cruise and fine targeting	[0° – 180°]	Along the unstable direction in-plane or out of plane
Injection (only for **PLANCK**)	250 m/s	Lissajous orbit manoeuvre (specification for 6 months launch window)	[123° – 125°]	Match velocity conditions for Lissajous orbit
Injection + 2 days (only for **PLANCK**)	5 m/s	Remove injection manoeuvre execution error	[28.4° - 151.6°]	Along the unstable direction

TABLE 4.3-7 HERSCHEL AND PLANCK ORBIT CORRECTION MANOEUVRES

The drawbacks of this parking orbit strategy highlighted during the first study assessment are the following ones:

– optimum targeted Perigee in the range of 500000 km to 70000 km depends on the launch date and hour as illustrated in next Figure 4.3-7, which would induce a finite set of targeted orbit for ARIANE 5 (still to be worked out with the launcher)

– the SAA constraints must be applied during the additional manoeuvres of the satellites which constrains the range of possible manoeuvres orientation

– important gravity loss are to be foreseen for the spacecraft Perigee manoeuvre, which induces that the satellite propulsive system must have a minimum thrust level in purely axis direction, as illustrated in Figure 4.3-8. For HERSCHEL, a thrust of 40N available with an optimized thruster configurations compatible with the parking orbit strategy whereas, for PLANCK, the thrust associated to the satellite design is about 5N which is not compatible with the scenario. Satellite design would have to be reviewed to ensure at least 11N in purely axial thrust

– accuracy of the Perigee manoeuvre must be ensured to avoid a big increase of its execution correction (factor 7 for a manoeuvre correction 2 days after).

A trade-off between extra consumption due to Perigee (and Apogee) manoeuvres and additional launcher performances will be driven until the PDR for the final strategy evaluation.
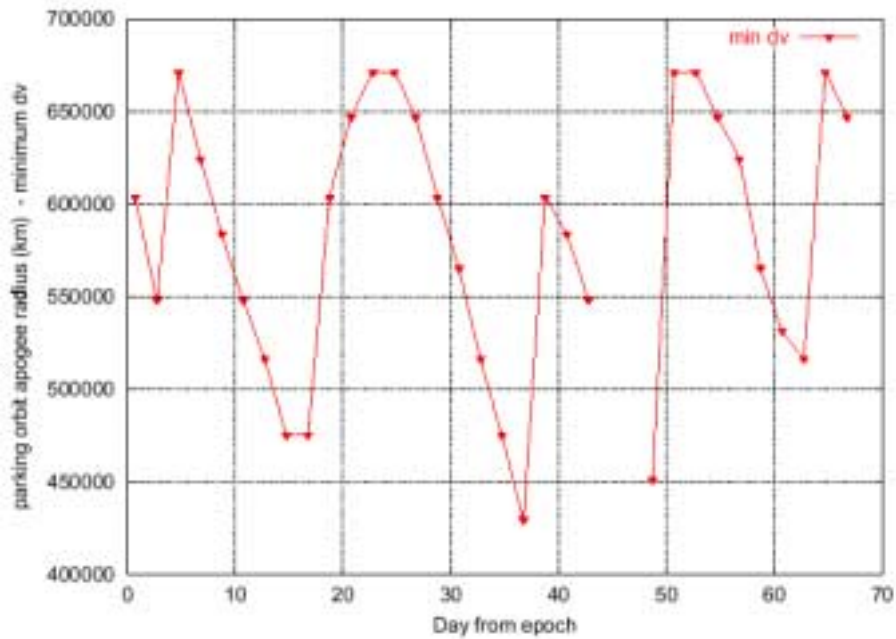
FIGURE 4.3-7 MINIMUM DELTA-V SOLUTION (125° - 20 N)
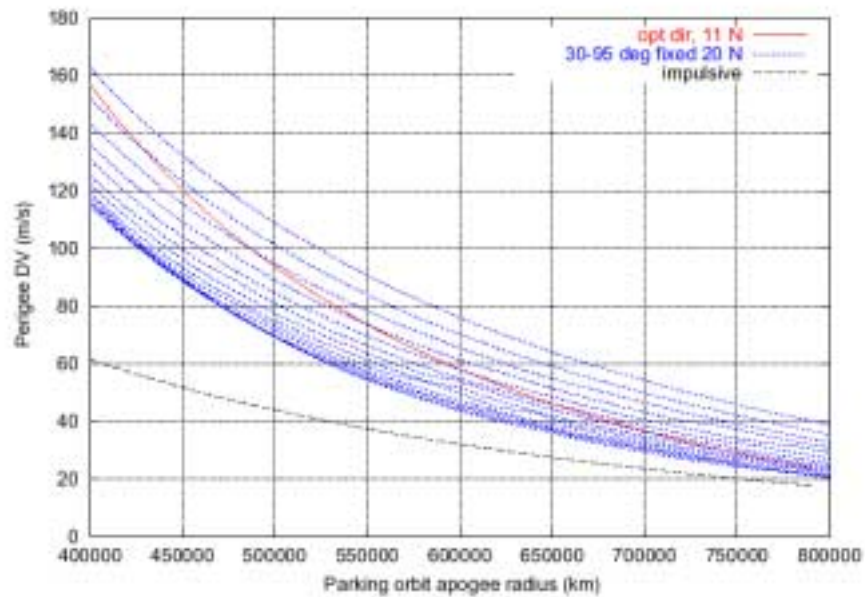
FIGURE 4.3-8 GRAVITY LOSS (CONSTANT MANOEUVRE DIRECTION)

4.3.3.3. Environment conditions impact

The environment conditions are the same as the ones with a direct injection given in Section 4.3.2.2 except that an additional Perigee passage around the Earth has to be considered.

Due to PLM exposition to Earth albedo and aerothermal fluxes, PLM temperature will increase around Perigee.

Moreover the spacecraft will have to pass trough the radiation belts two more times compared to the direct injection scenario.

The total transfer duration is increased by the duration of the parking orbit period which lasts between 15 and 25 days max.

4.3.3.4. Ground stations visibility impact

The Ground station visibility will be computed for the parking orbit scenario in order to ensure the contact during all the manoeuvres.

No major impact is expected from this mission parameter. This will be confirmed after refined analysis to be performed until the PDR.

4.3.3.5. Launch window impact

An updated launch window has been computed in accordance with the parking orbit scenario. The constraints which open or close the launch window are the same as presented in Section 4.3.2.5. Additional inputs are taken into account concerning the Perigee and Apogee manoeuvres Delta-V limit and no eclipse on parking orbit.

Figure 4.3-9 presents the preliminary parking orbit scenario launch window from 17 h to 19 h, from the 10/02/2007 to the 25/04/2007.
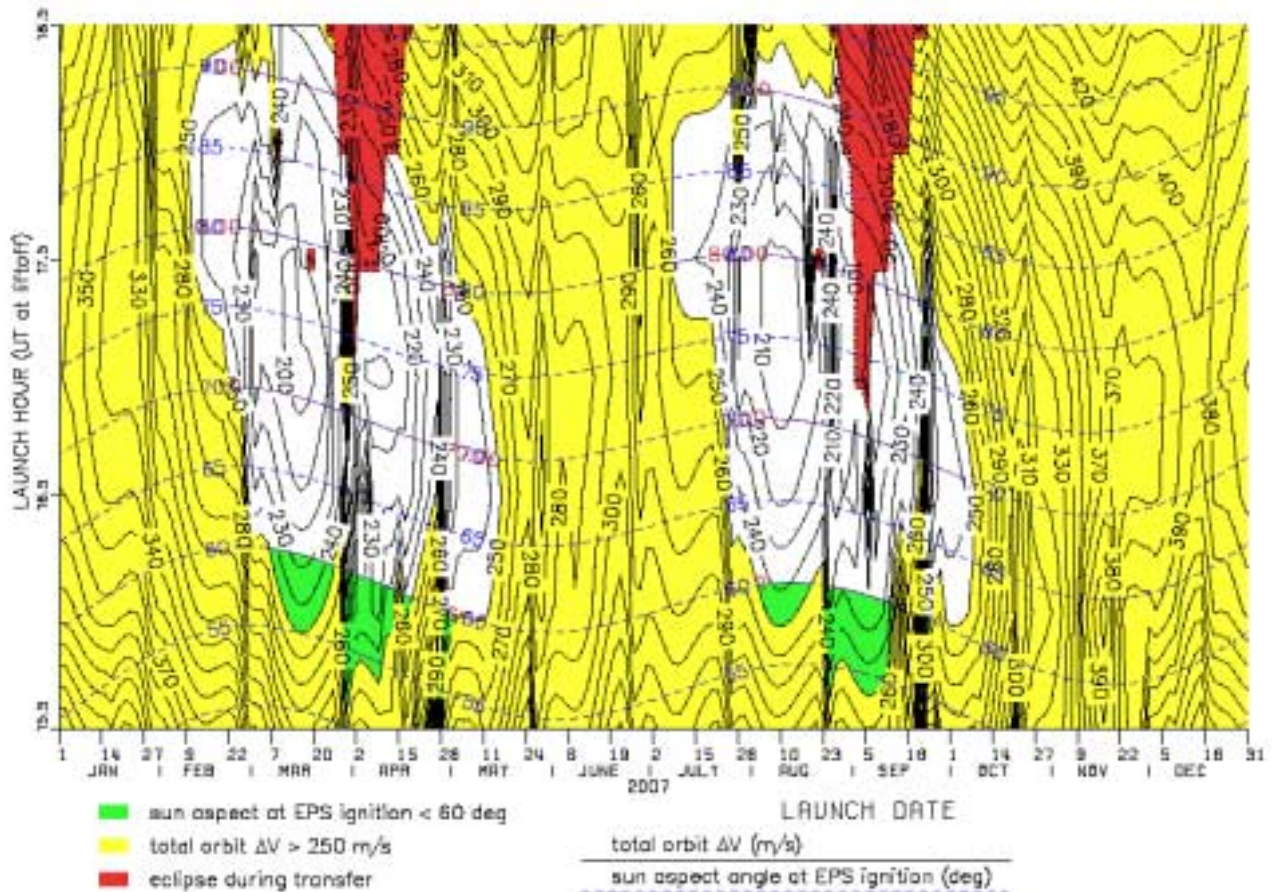
FIGURE 4.3-9 LAUNCH WINDOW IN CASE OF PARKING ORBIT SCENARIO

The launch window for parking orbit scenario is reduced with respect to the nominal one. Two months instead of 3 months are available in order to ensure the Delta-V limit of 20 m/s + 50 m/s , thus 70 m/s maximum for Perigee and Apogee manoeuvres plus the Lissajous orbit injection manoeuvre of 250 m/s. This Delta-V limit ensured by the launch window is 320 m/s.

It is possible to recover the nominal width of the launch window by increasing the global Delta-V budget of about 20 m/s thus giving a global Delta-V of 340 m/s.

Apsides line rotation is not included in the computation and this would lead to a small delay of the launch time of about 8 minutes for 2 degrees, no system impact foreseen.

4.4. SCIENTIFIC OBSERVATION PHASE

After the Performance Verification phase has been completed, the routine Operation Phase will begin. The mission last 3.5 years for HERSCHEL and 21months for PLANCK from launcher separation.

HERSCHEL and PLANCK observation phase will be shared between:

–   Observation Phase (PO): 21 hours scientific observation per day with storage of scientific data in the mass memory

–   TeleCommunication Phase (DTCP): 3 hours communication with Earth including uplink observation program, downlink of stored data and house keeping activities. On PLANCK, the scientific observation plan will continue undisturbed during telecommunication phase while, on HERSCHEL priority will be given to the attitude compatible with telecommunication constraints.

Additionally, orbit maintenance manoeuvres and attitude repointing manoeuvres will be performed regularly by both spacecraft as described in the following paragraphs.

The prime ground station for all the mission control is PERTH, the back-up is ensured by Kourou.

4.4.1. HERSCHEL and PLANCK orbit maintenance strategies

The objective of the orbit maintenance strategy is the correct the deviations observed on the satellites. Due to the instability of the Lagrangian point, it is necessary to correct these orbit deviations without to much time delay and with a good accuracy.

The Lissajous orbits are not stable orbits: if one solves the linear equation for arbitrary initial conditions, exponential terms with positive exponent appear in the solution for the X and Y components. The initial conditions have to be carefully chosen to get a non-escape orbit with periodic terms and decreasing exponential terms only in the solution.

It can also be proven that any Delta-V performed along a specific direction in the (X,Y) plane, called the non-escape direction, produces a transfer from a non-escape orbit to another non-escape orbit with a different amplitude. This non-escape direction lies in the (X,Y) plane at an angle 61.6 deg from the X axis (see Figure 4.4-1).

On the other hand, Delta-V performed along the escape direction, perpendicular to the non-escape direction, produce a transfer from a non-escape orbit to an escape orbit or vice versa.

The escape direction, with an angle of 28.4 to the X axis, is the one used for orbit maintenance: it allows to cancel any unstable terms appearing in the orbit due to external disturbances.
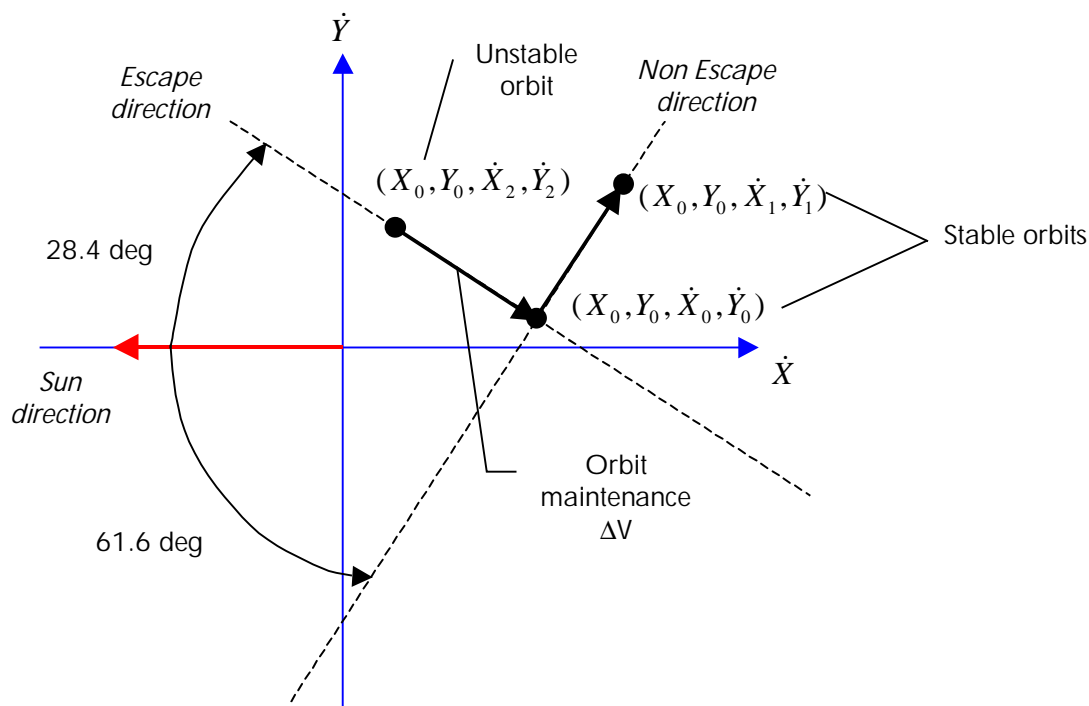
FIGURE 4.4-1 ESCAPE AND NON-ESCAPE DIRECTIONS

One major factor is the eclipse avoidance which is ensured by the orbit maintenance strategy. This is performed by eclipse avoidance manoeuvre which can be performed, for instance, along the non-escape direction.

Several methods have been applied to compute the orbit correction strategy for both spacecraft. The results give an orbit maintenance cycle including one manoeuvre per month. The amplitudes of the correction may vary but averaged values of 12 m/s for HERSCHEL and 6 m/s for PLANCK have been selected for all their mission duration.

4.4.2. Ground station coverage

The ground station visibility on the routine orbit is ensured by PERTH. On Lissajous orbits, the coverage is available around 7 hours to 13 hours per days during the Mission.

Figure 4.4-2 shows the coverage period from PERTH ground station for HERSCHEL and PLANCK. The minimum elevation is taken equal to 5° for this computation, if this value is changed to 10°, the visibility duration is reduced to about little more than 1 hour.

Coverage from PERTH during the routine phase
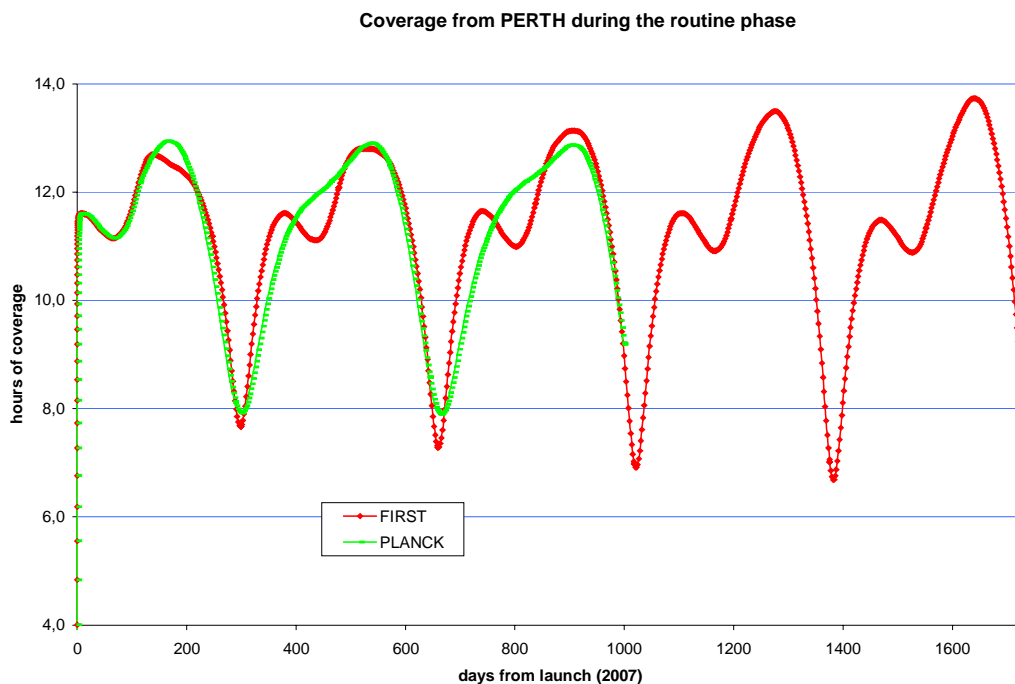
FIGURE 4.4-2 PERTH COVERAGE DURING THE MISSION

4.5. COMMUNICATION ASPECTS

Observation phase

On HERSCHEL, the MGA half cone aperture of 10° combined with the SAA constraints of 90 ± 30 deg from X-axis enable the spacecraft to communicate at high rate with Earth with a SSCE up to 40°.
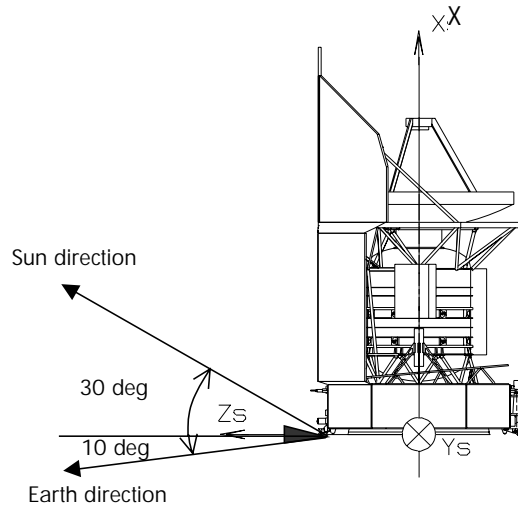
On PLANCK, the 10° half cone aperture MGA combined with a proper depointing up to 10° enables the spacecraft to communicate through the MGA with the Earth with a SSCE up to 20°.
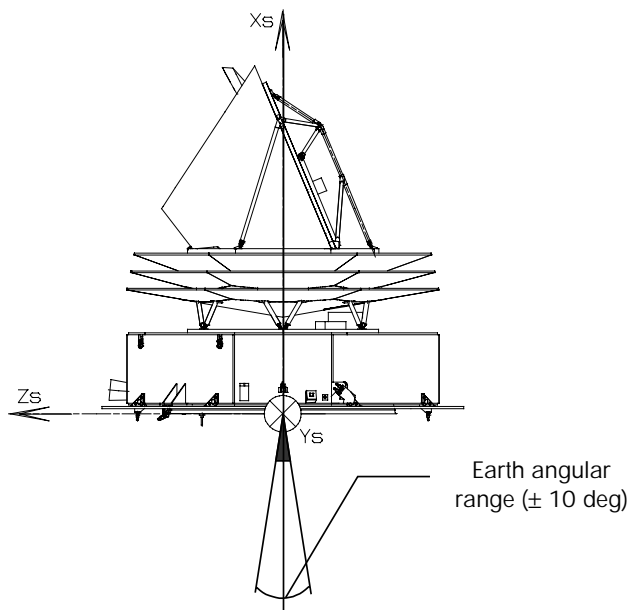
Transfer phase

When no high rate telemetry is needed (until the beginning of the Performance verification phase, from T0 to T0 + 1 m for HERSCHEL and PLANCK), omni-directional coverage is provided by the LGAs for both spacecraft.

Afterwards, SSCE has to be inferior or equal to 40 deg for HERSCHEL and 20 deg for PLANCK in order to use the MGA for high rate telemetry.

On PLANCK, SSCE exceeds 20 deg from day 45 up to day 105. This period starts 2 weeks after the beginning of the Performance Verification Phase which requires high data rate to test the instruments scientific performance. This means that this phase, which is planned to last 2 months, will have to begin a T0 + 1 month to T0 + 45 days and then from T0 + 105 d to will finish 1 month before the transfer phase maximum allocation of 6 months.

4.6.   MISSION DELTA-V BUDGET

This paragraph synthesises the Delta-V results for both spacecraft and both strategies which will allow to compute the satellite mass budget breakdown from beginning of life to end of life.

It includes the contributions from the transfer phase described in Section 4.3.2.2. and in Section 4.3.3.2. and also the orbit maintenance contribution explained in § 4.4.1.

4.6.1. Nominal scenario: direct injection

Table 4.6-1 and Table 4.6-2 present the Delta-V budgets for PLANCK and HERSCHEL for the direct injection scenario.

PLANCK MANOEUVRE	DELTA-V	DELTA-V TOTAL INCLUDING MARGINS	DIRECTION OF DELTA-V (SAA)
Perigee velocity correction Day 1: T_0 = lift off + 2 hr	14	14	150°/180°
Removal LV dispersions Day 2	50	50	150°/180° or 0°/30°
Manoeuvre 2 Day 12 from Perigee	4	4	0°/180°
Mid course corrections T_{inj} – 20 days	3	3	0°/180°
Orbit injection ECL avoidance 85 to 125 days	250	250	123°/125°
Correction for injection T_{inj} + 2 days	5	5	28.4° or 151.6°
Orbit maintenance for specified lifetime	5	6	28.4° or 151.6°
Total	331	332	-

TABLE 4.6-1 DELTA-V BUDGET FOR PLANCK FOR DIRECT INJECTION SCENARIO

HERSCHEL MANOEUVRE	DELTA-V	DELTA-V TOTAL INCLUDING MARGINS	DIRECTION OF DELTA-V (SAA)
Perigee velocity correction Day 1:T_0 = lift off + 2 hr	14	14	150°/180°
Removal LV dispersions Day 2	50	50	150°/180° or 0°/30°
Manoeuvre 2 Day 12 from Perigee	4	4	0°/180°
Mid course corrections T_{inj} – 20 days	3	3	0°/180°
Orbit injection ECL avoidance 85 to 125 days	0	0	-
Correction for injection T_{inj} + 2 days	0	0	-
Orbit maintenance for specified lifetime	12	12	28.4° or 151.6°
Total	83	83	-

TABLE 4.6-2 DELTA-V BUDGET FOR HERSCHEL WITH DIRECT INJECTION SCENARIO

4.6.2. Alternative strategy: parking orbit strategy

Table 4.6-3 and Table 4.6-4 present the Delta-V budgets for PLANCK and HERSCHEL for the parking orbit injection scenario.

PLANCK MANOEUVRE	DELTA-V TOTAL INCLUDING MARGINS	DIRECTION OF DELTA-V (SAA)
Apogee manoeuvre (Apogee 1) 1Bis) Perigee manoeuvre (Perigee 1)	~10 (0 to 20) ~60 (50 to 70)	60°/80° 125°/180°
Removal Perigee manoeuvre error Day 2	5	0°/180°
Manoeuvre 2 Day 12 from Perigee	4	0°/180°
Mid course corrections T_{inj} – 20 days	3	0°/180°
Orbit injection ECL avoidance 85 to 125 days	250	123°/125°
Correction for injection T_{inj} + 2 days	5	28.4° or 151.6°
Orbit maintenance for specified lifetime	6	28.4° or 151.6°
Total	343	-

TABLE 4.6-3 DELTA-V BUDGET FOR PLANCK WITH PARKING ORBIT SCENARIO

HERSCHEL MANOEUVRE	DELTA-V TOTAL INCLUDING MARGINS	DIRECTION OF DELTA-V (SAA)
Apogee manoeuvre (Apogee 1) 1Bis) Perigee manoeuvre (Perigee 1)	0 to 20 20 to 50	60°/80° along SC X axis
Removal Perigee manoeuvre error Day 2	5	0°/180°
Manoeuvre 2 Day 12 from Perigee	4	0°/180°
Mid course corrections T_{inj} – 20 days	3	0°/180°
Orbit injection ECL avoidance 85 to 125 days	0	-
Correction for injection T_{inj} + 2 days	0	-
Orbit maintenance for specified lifetime	12	28.4° or 151.6°
Total	94	-

TABLE 4.6-4 DELTA-V BUDGET FOR HERSCHEL WITH PARKING ORBIT SCENARIO

4.6.3. Trade-off summary

This section compares the two strategies foreseen: direct injection and parking orbit scenario from a system view in order to help in a close future for the choice between one of those two strategies.

In term of total Delta-V, the Delta-V budget is quite equivalent between the two strategies as illustrated in Table 4.6-5.

DELTA-V COMPARISON	DIRECT INJECTION	PARKING ORBIT
PLANCK	332 m/s	343 m/s
HERSCHEL	83 m/s	94 m/s

TABLE 4.6-5 DIRECT INJECTION AND PARKING ORBIT SCENARII DELTA-V BUDGET COMPARISON

Taking into account the efficiency of the manoeuvres (strongly related to the SAA of the manoeuvre), Table 4.6-6 gives the corresponding propellant mass for each scenario.

PROPELLANT MASS COMPARISON	DIRECT INJECTION	PARKING ORBIT
PLANCK	302.3 kg	302.4 kg
HERSCHEL	161.9 kg	175 kg

TABLE 4.6-6 DIRECT INJECTION AND PARKING ORBIT SCENARII PROPELLANT MASS BUDGET COMPARISON

For PLANCK, the propellant mass is the same in both scenario thanks to an increase of the efficiency of the manoeuvres, whereas on HERSCHEL there is no significant gain in the efficiency, and the propellant mass increases by 13 kg.

However, with an Apogee between 500000 km and 700000 km for the parking orbit, the ARIANE 5 ESV performance lies between 5400 kg and 5460 kg (see Figure 4.3-1), which gives 90 kg to 150 kg of additional performance compare to the direct injection scenario.

In terms of dry mass, this scenario yields an additional margin between 77 and 133 kg. This margin doesn't take into account the few kilograms of the additional thrusters required to reach a minimum thrust of 11 N on PLANCK.

A synthesis at system level is given in next Table 4.6-7 and will be developed in the subsystem following sections.

MISSION ASPECT	DIRECT INJECTION	PARKING ORBIT SCENARIO	SYSTEM IMPACTED
Dry mass increase		77 to 133 kg	
	-	+	
Compatibility with ARIANE 5 ECA	Not compatible	Compatible	
	-	+	
Criticality on LEOP operations	First orbit correction at lift – off + 2 days	Orbit manoeuvre at Perigee and Apogee passage	LEOP operations
	-	+	
Dependency on launcher error	Strong	Weak	Delta-V budgets
	-	+	
Dependency on launch date	More robust	Apogee radii function of the launch date	Launcher operations
	+	-	
PLANCK thrusters		11N thrust required at 125° SAA	Double the thrusters capacity at least in the flat direction on PLANCK
	+	-	

TABLE 4.6-7 MISSION AND SYSTEM IMPACT

MISSION ASPECT	DIRECT INJECTION	PARKING ORBIT SCENARIO	SYSTEM IMPACTED
Perigee pass number	1	2	CVV lifetime Radiation protection Spacecraft cool-down timeline
	+	-	
Transfer duration		Extended by 20 days	Compatible with 6 months transfer allocation
	0	0	
Herschel manoeuvres	Constant direction	Turning required	Small impact on HERSCHEL AOCS
	0	0	

TABLE 4.6-7 MISSION AND SYSTEM IMPACT (CONT'D)

5. PAYLOAD INTERFACE REQUIREMENTS

5.1. GENERAL

This chapter describes the status of the requirements for the interfaces between HERSCHEL and Planck, and the 5 instruments SPIRE, PACS, HIFI for HERSCHEL, and LFI + HFI for Planck.

The first (§ 5.1.) part will compare the main possible satellite allocations compatible with the current design at SRR with the instrument demands.

In the second part is described the status of the interfaces for HERSCHEL (§ 5.2.) and Planck (§ 5.3.).

5.1.1. Evolution of Instrument and satellite design

The satellite configuration proposed as response to the ITT was compatible with the instruments interfaces definition described in the IID-B 1.0.

During the period Sept 2000 - summer 2001, the instrument evolved significantly. A set of Instrument reviews took place between February and April 2001 with the goal of freezing the instrument definition (IIDR = Instruments Intermediate Design Review, corresponding to the instruments end of Phase B).

During the first part of Phase B, definition of instrument interfaces relied on the following set of information:

- IID-Bs 1.0 (Sept 2000, part of ITT package), describing the instruments

- IID-A 1.0 (Sept 2000) giving the allocations from the spacecraft as defined by ESA for the ITT

- outcome of the Instrument working sessions

- IIDR documentation

- multiple instruments proposed updates ro the IID-B to reflect the instrument evolution.

The instrument proposed modifications in the interface documents, especially w.r.t. power and mass, were often larger than their margins and could not be fully accepted. In these cases, the instruments have been requested to re-address the design.

The modifications of the instruments have been taken into account in the following way:

– ALENIA SVMs baseline detailed design and specifications are based on Instruments IID-B 1.0. Some aspects of proposed instrument modifications have been analysed

– ASTRIUM EPLM baseline design is based on IID-B 1.0, plus updates of FPU definition based on an intermediate definition frozen by ESA, and formalized on faxes SCI-PT-09267 and 09390. Harness definition is based on IID-B + Instrument internal Harness description documents (produced for IIDR) handed over to ASTRIUM during the HPLM Critical Item review meeting (HP-ASPI-MN-99) on 8/6/01.

– ALCATEL System baseline design is using the ITT (SRS & IID-A) instrument mass and power allocation and design, the instrument latest proposed modifications have been analysed to evaluate their feasibility

5.1.2. Margin Philosophy at instrument and system level

In order to avoid adding margins to margins at both instrument and spacecraft levels, the instruments margin philosophy is based on the following:

– in the IID-A (and SRS), instruments are given allocations of the satellite resources (mass, power, heat rejection, data rate,…). This allows the spacecraft to be designed on a stable basis with respect to the resources allocated to the instruments. The relevant information (resource) for the spacecraft is the sum of the allocations for all instruments. However, to simplify the design on both sides, the total instrument allocations have been shared between instruments, and also between warm and cold units

– in parallel, the instruments are being designed, and their nominal budgets are published in their respective IID-Bs. The difference between the nominal budget and the allocation can be considered as margin.

- In addition, the SRS specifies:

  - that the satellite structural design shall be compatible with the instrument nominal mass as agreed in the IID-B, at beginning of Phase B + a 20 % margin (SINT-015)

  - and that the thermal design shall be compliant with the instruments nominal IID-B dissipations + 20 % at cryogenics temperatures and + 10 % for the SVM (SINT-035).

A major difficulty arises from the fact that the instruments' IID-B are not frozen, and that the instrument requests are far from stable (they have in some cases fluctuated by more than 20 % over a period of a few months).

Since the proposed IID-B updates have not yet been approved by ESA they should not be formally used for the satellite design. Nevertheless a critical assessment of these instrument proposed modification and their impacts on the system design has to be performed to evaluate the acceptability of the corresponding changes.

In cases where the total resources requested by the instruments exceed the allocations, the on-going satellite design is confronted with uncertainty in instrument interface requirements and the instruments have been requested to re-address design issues.

Currently the SRR spacecraft system budgets are based on instruments allocations (IID-A or SRS).

5.1.3. Satellite resource allocation for instruments (proposed updates to IID-A) versus Instrument demand

In the following chapter, we propose the resources that we can allocate to the instruments (which should ultimately update the IID-A) and compare them to the current instrument demand as reflected in both the IID-B 1/0 from the ITT and latest updated requests from the instruments.

At the time of the ITT, the demand and allocation where compatible with the proposed design, including some margin in between. The situation is slightly different now, which is why we try to adjust the allocation as far as possible, or we have to negotiate with instruments to reduce their demand.

5.1.3.1. Mass Allocation

As the system mass margins are limited, the mass allocation for the instruments cannot be increased compared to what it was at the ITT.

The following table gives the distribution of the Payload allocated mass per instruments, and for each satellite, the distribution of this mass between the FPU, the SVM, and the cryostat (HERSCHEL only).

Instruments Mass Allocations

	ITT kg	SRR Total kg	FPU kg	Cryostat kg	SVM kg
Herschel	**415**	**415**	**179**	**35**	**201**
SPIRE	90	90			
PACS	133	133			
HIFI	192	192			
Planck	**445**	**445**	**62**		**383**
HFI	244	244			
LFI	89	89			
Sorption Cooler	112	112			

5.1.3.2. Power demand and power dissipation Allocations

For the power, we consider 2 types of allocations: The maximum average power demand (at input of the instrument), and the average power dissipation (at output of the instrument) which should be similar[1].

---

[1] These 2 values should be similar, except for RF components. The main difference for standard units will come from the difference in definition between maximum average power demand and the average dissipation.

The maximum average power demands (ref IID-A, § 5.9, GDIR § 6.7.5) assumes a moving averaging window of 5 mn, whereas the average power dissipation is smoothed by the thermal time constant of the unit + radiator (can be hours), therefore the difference between the 2 averages could be of a few % (Maximum average Power Demand ≥ Average Power dissipated).

The difference between demand and dissipation is even larger for the power peaks (IID-A § 5.9, GDIR § 6.7.6). In that case, the peak power dissipated can be very large due to heat storage, as illustrated by the sorption cooler on Planck.

The situation for the Power is slightly different for HERSCHEL and Planck, due to the design (non-deployable) and position of the Solar Arrays.

On Planck the Solar Array is located on the back of the spacecraft, and its size limited to 4.2 m by the diameter of the launcher fairing. Deployment is not advised for temperature stability. Therefore the Solar Array area has no growth potential. In addition, most of the Planck power is allocated to the payload (1 KW out of 1.375 kW), and most of it to the LFI/HFI/sorption cooler.

On HERSCHEL, the Solar Array is on the side of the spacecraft, and has some growth potential. In addition at the time of the ITT, there was a margin of 96 W between the IID-A allocation (454 W), and the SRS requirement (550 W, SINT020).

The following table gives the Power allocation for the instruments at the ITT, and the proposed update at the SRR.

We propose to increase the HERSCHEL Power allocation in the IID-A (including Instrument margins) from 454 W to 500 W.

For Planck, the situation is more delicate. There is no room for increasing the power allocation.

We proposed to the instrument teams, for the power demand allocation, to group LFI and the Sorption cooler together to manage commonly their margins (74 + 655 + 1 = 730 W allocated). However, the power dissipation of the sorption cooler is so large that it impacts the thermal design of the SVM, and therefore the allocation for dissipation depends of the design of the radiator, and of the SVM thermal control.

We proposed here a new envelope of 600 W for the sorption cooler + its Electronics (was 400 + 135 before). This must be consistent with the power demand, therefore 130 W remains for LFI.

This point has not been agreed at the present but is further pursued. The current definition of the sorption cooler margins (or contingencies) seems to be compatible with the proposed approach. It is distributed as follows: Compressor: 432 W Nominal + 88 W Margin = 512 W, Electronics: = 135 W.

Instruments Power Demand Allocations

	ITT			SRR	
	Max Average	Peak		Max Average	Peak
	W	W		W	W
Herschel	**454**			**500**	
SPIRE	86			100	
PACS	88			100	
HIFI	280			300	
Planck	**984**			**985**	
HFI	255			255	
LFI	74			730	
Sorption Cooler	655				

Instruments Power Dissipation Allocation

	ITT			SRR	
	Max Average	Peak		Max Average	Peak
	W	W		W	W
Herschel	**452**			**500**	
SPIRE	86			100	
PACS	86			100	
HIFI	280			300	
Planck	**984**			**985**	
HFI	255			255	
LFI	74			130	
Sorption Cooler	655			600	950

5.1.3.3. Instrument Mass and power budgets demands

The following tables show the evolution of the instrument estimated nominal mass and power resources since the ITT. Except for HIFI where the mass budget has decreased (mainly due to a better estimation of the LOU radiator) and was not updated in their comments to IID-B. For consistency with the other instrument (budgets based on Nominal masses) we used here nominal mass from HIFI IIDR documentation (SRON/U/HIFI/RP/2001).

In most of the cases then the need for resources has increased by about 10 % between the ITT and the SRR (except for HIFI for which the ITT mass budget had already negative margins due to the LOU radiator better estimated now).

The increase can always be justified by some selection of a design. The number of warm units has increased (the HIFI Wide Band Spectrometer has one more box (3→4), the PACS DECMEC is now split into DEC and MEC, LFI propose to split the DAE into DAE, and DAE control box, the SPIRE JFET box on the FPU has also split), which increases both the quantity of structure, and the dissipation.

Herschel current instrument proposed Mass & Power

	FPU	Cryostat shell		SVM		Total Mass			Total Power		
	Nominal Mass request	Nominal Mass request	Power Dissipation	Nominal Mass request	Power Demand/ Dissipation	Nominal Mass request SRR	Nominal mass ITT	mass allocation	Power demand / Dissipation SRR	Power demand ITT	Power allocation
	kg	kg	*	kg	W	kg	kg	kg	W	W	W
SPIRE	53.5	0.0	0	32	91	85.5	75.0	90	91.0	86.0	100
PACS	73.8	2.5	0.2	51.1	136.2	127.4	110.8	133	136.4	87.8	100
HIFI	46.0	39.9	7	90.6	280.6	176.5	201.1	192	287.6	280.0	300
total SRR	**173.3**	**42.4**	**7.2**	**173.7**	**507.8**	**389.4**	**386.9**	**415.0**	**515.1**	**453.9**	**500.0**
ITT (IID-B 1.0)	158	58.5	14.5	170.4	439.25		386.9			453.9	486
Change in instrument request since ITT						2.6 0.7%			61.3 13.5%		
Delta compared to allocation Instrument margin						25.6 6.6%			-15.1 -2.9%		

Planck current instrument proposed Mass & Power

	PPLM		SVM		total Mass			Total Power demand		
	Mass	Power Dissipation	Mass	Power demand / Dissipation	Mass Request SRR	Mass request ITT	Mass Allocation	Power demand/Dissipation SRR	Power demand ITT	Power allocation
	kg	W	kg	W	kg	kg	kg	W	W	W
HFI	25.9	0.000	196.8	264.0	222.7	213.0	244	264.0	254.0	255
LFI	37.7	0.581	68.1	112.8	105.8	74.0	89	113.4	73.6	130
Sorption cooler	3.04	0.000	111.46	655.0	114.5	100.2	112	655.0	655.0	600
total SRR	**66.6**	**0.581**	**376.4**	**1031.8**	**443.0**	**387.2**	**445.0**	**1032.4**	**982.6**	**985.0**
Total at ITT (IID-B 1/0)	50.2	0.55	337	982		387.2			982.6	984
Change in instrument request since ITT					55.8 14.4%			49.9 5.1%		
Delta compared to allocation Instrument margin					2.0 0.4%			-47.4 -4.6%		

The margin is negative for the power for both payloads, even with the allocation increase for HERSCHEL, which mean than effort is still required for instruments power control.

For the mass, the margin is considered not adequate and actions have be initiated to control/reduce the masses.

5.1.3.4. Allocation for temperatures and Power dissipation on FPU's

The instrument power dissipation and heat leaks on the cryogenic focal planes should be managed closely at system level to guarantee the compatibility between the various components, and a proper operation of the complex cryogenic systems.

The total allocation is defined by the heat lift available at a given temperature stage, and shall be split between the payload (support, radiation, …), and the instruments.

HERSCHEL

On HERSCHEL, the thermal interfaces between the instruments and the spacecraft are on 3 identified levels.

Level 0 (< 2 K) on the Helium tank, Level 1 (< 5 K) and Level 2 (< 15 K) on the Helium vent line.

The following table summarizes the cryogenic power allocation of the instruments on these 3 levels, at the ITT, unchanged for the SRR.

Herschel	ITT				SRR		
	Temperature		heat lift		Temperature		heat lift
Cooling system Heat Lift allocation	Min	Max			Goal	Max	
for Instruments only	K	K	mW		K	K	mW
Level 0		2	10			2	10
Level 1		5	25			5	25
Level 2		15	50		10	15	50

Note
allocation is for all instruments
For each instrument, we assume 1/3 of the time in ON mode, 2/3 in OFF mode
then equirepartition for each instrument modes (Phot:1/2, Spect:1/2, HIFI chanels:1/6)
Depending of the nature of the heat lift on a given level, the following duty cycle have to be used.

Comments

It is to be noted that this is global allocation, for all 3 instruments but only one instrument operates at a given time (except for parallel mode with PACS and SPIRE that is not expected to need more than 3 months of the mission).

This means that for each instrument, the allocation has to be aligned taking into account the instrument modes and performing a realistic averaging (in a first approach this can be done by giving a preliminary allocation of 1/3 of this budget, and a duty cycle of 1/3 for dissipative elements (including the sorption cooler), and of 1 for conduction/radiation).

For the sorption cooler of SPIRE and PACS, each recycling is equivalent to 48 h of usage, whatever the real duration of use. As a baseline it is agreed to use a duty cycle of 1/3 for each sorption cooler. (this will require optimisation of the mission profile, fixing minimum usage duration (48 h..66 h) for an instrument with sorption cooler, or defining a procedure to do a partial recycling of cooler).

The estimation of the available heat lift allocation is different for Level 0, where it translates directly into lifetime (10 mW allocated for a total heat load on the tank about 50 mW), and on the Vent line, where it depends of the mass flow rate ($Q=m_{dot}.Cp.(T_{i+1}-T_i)$). The total available heat lift (Instruments + Optical bench support, radiation + thermal straps support + harness) versus the mass flow rate, and temperatures of level 1 and 2 can be extracted from the following Figures 5.1.3.1: On level 1, 2 mg/s gives 24.5 mW available on level 1 at 4 K if the tank is at 1.7 K, 35 mW at 5 K. For a level 2, 2 mg/s at 10 K, 63 mW is available (2.5 mg/s, 4 K on level 1), 115 mW would be available at 15 K. These values include thermal loads form the cryostat and are <u>not</u> to be considered for the instrument budgets. This will be confirmed by the detailed simulation to be performed by ASTRIUM.
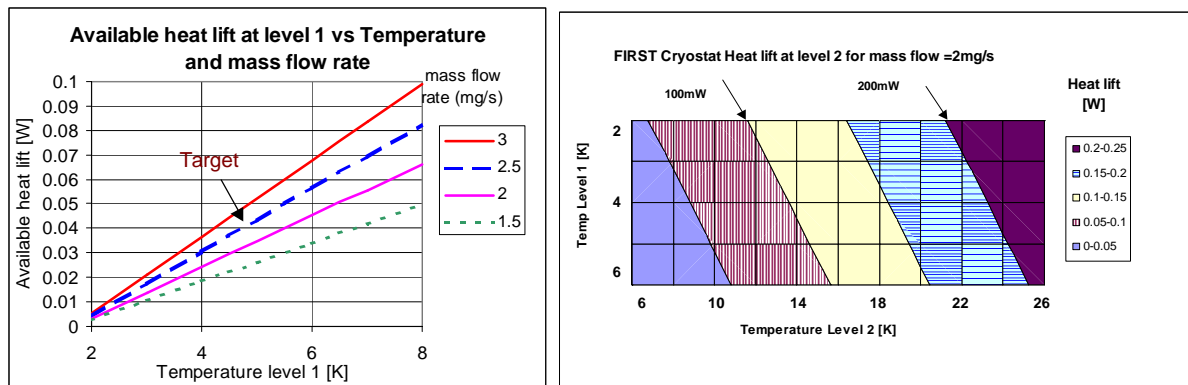
FIGURE 5.1.3.1 HEAT LIFT ON LEVELS 1 & 2 VS MASS FLOW RATE AND TEMPERATURES

The HERSHEL instruments FPU simplified thermal models have been delivered by the instruments to ESA, ALCATEL and ASTRIUM, and are under evaluation (refer to ASTRIUM SRR report Thermal section). The objective is to check the validity of the design, and the Impacts on the temperature distribution on the FPU, and on the cryostat lifetime and to come back to the instruments to refine the FPU design to be compatible with the Cryostat and lifetime.

Planck

The situation is different, as our responsibility in term of control of the heat leaks ends up at the 60 K stage (V-Groove 3). The principle of the insulation via the V-Grooves relies on the heat interception of all conductive paths on the intermediate V-Groove shield, therefore we have to propose allocation at each level (V-Groove 1, 2, and 3).

Planck FPU	ITT				SRR		
	Temperature		heat lift		Temperature		heat lift
Radiator & V-Groove	Goal	Max			Goal	Max	
Heat Lift allocation (Instruments + PPLM)	K	K	mW		K	K	mW
V-Groove 3 (Cold)	< 50	< 60			< 50	< 60	**2930**
V-Groove 2 (Medium)						100	**1320**
V-groove 1 (Warm)						160	**7150**

These heat lift capabilities of the passive cooling system can be distributed among the known contributions as follows:

Dissipations and Heat losses allocation	ITT				SRR			
Planck FPU	20K	V-Groove 3	V-Groove 2	V-Groove 1	20K (***)	V-Groove 3 (Cold)	V-Groove 2 (Medium)	V-Groove 1 (Warm)
Total						**2930**	**1320**	**7150**
HFI						**620**	**20**	**50**
JFET Dissipation		150				150		
Harness (Conduction (*)+Dissipation)		35	160			40	20	50
Cooler pipes 0.1K (Cond (*)+ Enthalpy)		160				170		
Cooler pipes 4K (Cond(*) + Enthalpy)		230				260		
LFI						**610**	**560**	**5370**
Dissipation	550							
Harness (Cond(*)+Dissip)						100	60	730
Wave-Guides (Cond(*) + Dissip + Rad)		350	300	450		510	500	4640
Sorption cooler						**1380**	**500**	**860**
Cooler Pipes (Cond(*) + Enthalpy)		1200	580	900		1380	500	860
Harness (Cond(*)+Dissip) (***)						0		
PPLM						**320**	**240**	**870**
Supports						220	70	530
Harness (Cond(*)+Dissip) (**)						100	170	340

*   Conduction / radiation allocation on level (i) represent the summ of the heat comming from level i+1 minus the one leaving to level i-1

**   Includes provision for Decontamination heaters on mirrors

***   sorption cooler harness included with pipe

These Heat losses allocations are **Maximum Values** acceptable by the Planck Payload.
This mean that the instrument estimated dissipations or losses **should include 20% of design margin** before reaching these values.
With these allocations, the calculated temperature at the sorption cooler interface iscurrently (SRR) **52K -0K+7K**

5.1.3.5. Request for dissipation on FPU in IID-B

The heat loads on the focal planes have dangerously increased since the ITT:

–   increase of the size of the sorption cooler in PACS and SPIRE

–   reinforcement of the structures adding heat leaks (SPIRE, PACS)

–   change of the number and nature of cryo-harness

–   doubling of the LFI wage-guide cross section, requirement for a wave guide support

–   …

This will impact the lifetime and FPU temperature on HERSCHEL, and endanger the cooler operation (by inadequate precooling) for Planck.

This topic is currently being analysed both by ASTRIUM for the HERSCHEL FPU, and by Alcatel for the Planck PLM. Refer to ASTRIUM proposal (Chapter 5.3.1 Influence of Design Parameters on Life Time and Telescope Temperature) for the HERSCHEL FPU's, and to ALCATEL PPLM report Chapter 7.4 for the Planck FPU.

It is important that both sides of the interface respect the proposed allocations for these dissipations: provide the heat lift for the payload, respect the heat losses for the instruments.

Description of this post should be improved in the IID-B, as the current information is not sufficient to make a diagnostic.

Dissipation, conduction should be separated, for instance by using the description of the simplified thermal model.

Estimation of total heat losses should be made for a given set of interface temperatures, for instance [1.7 K, 5 K, 15 K] for HERSCHEL levels [0, 1, 2], and for Planck V-Groove [3, 2, 1]: [50 K, 100 K, 150 K].

5.1.3.6. Data rates Allocation

The data-rate allocation has not been changed since the ITT, except that the Planck allocation has been set similar to the one of HERSCHEL to reflect the similar electrical architecture.

There has been some work performed to estimate the actual capability of the proposed data bus, by analysing the traffic on the bus (See discussion in § 6.5.4.). A technical note has been issued (annex to SRR design document, RD01.2, HERSCHEL/Planck data rates, Document n° H-P-1-ASPI-TN-0186), giving a maximum average data-rate capability of 140kbps, and a burst capability of 300 kbps, including Science data, housekeeping and overheads. The constraints comes currently from the down-link rate (1.5 Mbps).

This is a starting point for a discussion with ESA and the instruments, as the interpretation of the PS-ICD is not the same for all parties. Conclusion of this debate might allow increased data-rate allocation for both HERSCHEL and Planck.

Data rate IID-A Allocation		ITT	SRS	
Herschel	Science prime instrument	96	96	kb/s
	Housekeeping prime	2	2	kb/s
	Science non prime	2	2	kb/s
	Science + housekeeping	**100**	**100**	**kb/s Average 24h**
	Storage MMU	48	48	h
	Burst mode	300	300	kbps
Planck	**Science + Housekeeping**	**60**	**100**	**kb/s Average 24h**
	Storage MMU	48	48	h
	burst	240	300	kb/s

5.1.3.7. Data-Rate demand

The requirement for data rate was marginally compatible with the allocation at the ITT has now evolved.

The following tables summarizes the situation in the current proposed IID-Bs.

HERSCHEL

from IID-B	Herschel Instruments data rates in kb/s													
	SPIRE						**PACS**					**HIFI**		
modes	Prime		parallel	Serendipity	Burst	standby	Prime		parallel	burst	standby	prime	burst	standby
	Spectrometer	Photometer					spectrometer	Photometer	photometer					
Science uncompressed	97.4	93.6	10	87			3600	1600				98	300	
Science compressed	97.4	93.6	10	87	200	0	120	120	50	400		98	300	
Housekeeping	4.2	4.2	2.1	4.2	4.2	4.2	4	4	4	4	4	2	2	2
command verif							2	2	2	2	2			
Event handling							2	2	2	2	2			
duration of burst mode					short					30mn			short	
Total	**101.6**	**97.8**	**12.1**	**91.2**	**204.2**	**4.2**	**128**	**128**	**58**	**408**	**8**	**100**	**302**	**2**

IID-A Allocation		
Science prime instrument	96 kb/s	
Housekeeping prime	2 kb/s	
Science non prime	2 kb/s	
total	**100 kb/s**	**24h**
Storage MMU	48 h	
Burst mode	300 kbps	

System requirement specifications

	Herschel MODES				Data Rate (kb/s)				
MODE	SPIRE	PACS	HIFI		SPIRE	PACS	HIFI	total	
#1	Standby	Standby	Prime		4.2	8	100	112.2	
#2	Standby	Prime P	Standby		4.2	128	2	134.2	<-- Driver
#3	Prime	Standby	Standby		101.6	8	2	111.6	
#4	Parallel	Parallel	Standby		12.1	58	2	72.1	

additional modes from IID-B data

#2 S	Standby	Prime S	Standby		4.2	128	2	134.2	option with PACS Spectrometer
#3 S	Serendipity	Standby	Standby		91.2	8	2	101.2	Spire in Seredipity mode

IID-A Allocation								100	

The comparison between current allocation shows some discrepancy between demand and allocation, especially on HERSCHEL when PACS is prime. This should be solved at the end of the current on-going discussion about data-rates.

Planck

from IID-B	Planck instruments demand for Data rate (Kbps)							
	LFI			**HFI**			**Sorption**	
modes	Nominal	Burst	standby	Prime	burst	standby	ON	Burst
Science uncompressed				141				
Science compressed	51	100	0	48	100			
Housekeeping	3	3	3	2	2	2	0.5	10
duration of burst mode		short			short			
Total	**54**	**103**	**3**	**50**	**102**	**2**	**0.5**	**10**

IID-A Allocation	normal			burst	
Science prime instrument	100	kb/s	24h	300	kb/s
Storage MMU	48	h			

System requirement specifications

MODE	Planck MODE				Data Rate				
MODE	HFI	LFI	sorption		HFI	LFI	sorption	total	
#1	Prime	Prime	ON		54	50	0.5	**104.5**	nominal mode
#2	Prime	Standby	ON		54	2	0.5	**56**	degraded mode
#3	Standby	Prime	ON		3	50	0.5	**53**	degraded mode

| **IID A Allocation** | | | | | | | | **100** | |

5.1.3.8. EMC

Proposed updates to IID-A

The following updates to IID-A have been agreed with ESA:

−   CE, primary bus (IID-A § 5.14.3.1.1./2.): separate measurement of "true" DM and CM conducted emissions, and little relaxation of the CE CM requirement in order to be less stringent at converter switching frequencies:
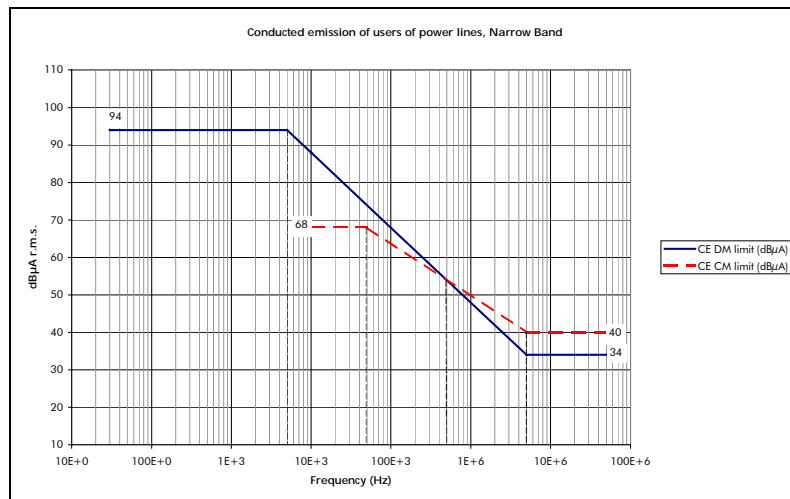
- CS common mode steady state, primary bus (IID-A § 5.14.3.4.): it has been agreed to go on using bulk current injection but to express the requirement in terms of voltage instead of current: 2 V_{pp} between return and chassis, to avoid reaching unrealistic voltage values at the lower frequencies (from 10 kHz).

- A CS common mode transient specification on the primary bus has been added in order to ensure that no equipment undergoes a change of status in case of short circuit failure of another equipment. The transient characteristics will be 28 V/5 μs with MIL-STD-461 CS06 shape.

- CS differential mode transient, primary bus: the step load transient shown on next figure has been introduced by ESA. The shape is the expected worst case envelope at regulation point. The rise time between 10 and 100 μs has been derived assuming C_{bus} = 1 mF (minimum) and ΔI = 20 A.
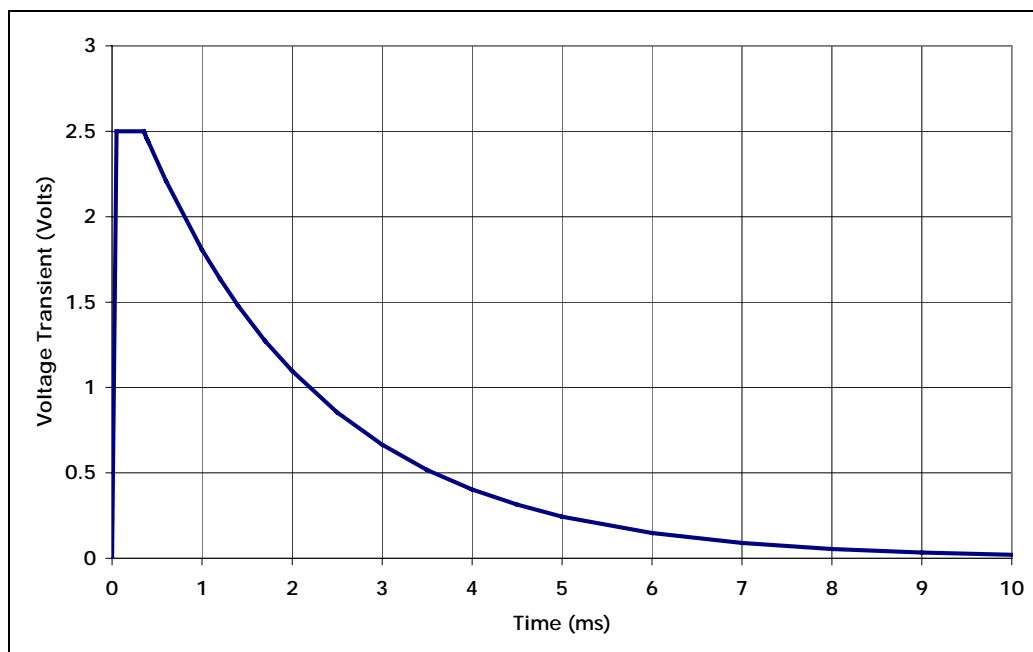
– Radiated Emission (IID-A § 5.14.3.9.): a less permissive RE requirement has been agreed, on the basis of classical RE test results on space programs; notches for ARIANE 5 destruction band (applicable to units on at launch) and spacecraft's TC band have been added:

Radiated Emission, E-Field
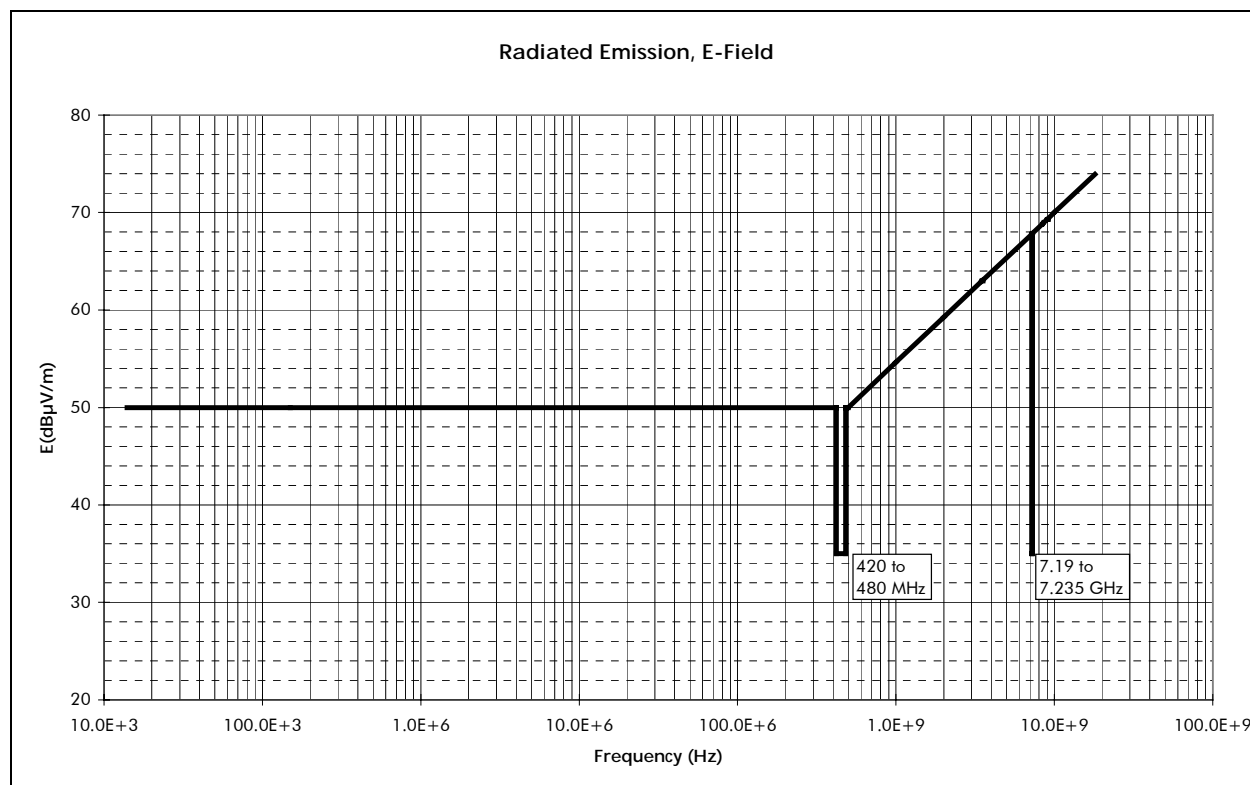
– A few paragraphs of IID-A 5.10.3 Chapter (grounding and isolation) have been modified or reworded in order to reflect ESA and ALCATEL common understanding of "DSPG" implementation, cf. § 6.3.7. "EMC approach".

– The LISN impedance has been specified (cf. IID-A Issue 02 or EMC spec Issue 02).

− The Common Mode Signal Isolation specification for receiver interface (IID-A § 5.14.1.2.) has been relaxed from 20 kΩ to 7 kΩ following Intersil confirmation that 26C32 RS-422 receiver common mode isolation ranges from 7 to 10 kΩ, based on both measurements and analysis:

HS-26C(T)32RH LINE INPUT STRUCTURE	For the + input: $$R_{CM}=((R3||R4)+R5)||R0$$ For the − input: $$R_{CM}=((R16||R15)+R12)||R17.$$ By calculation, the common-mode input impedance for any of the inputs is about 9.2 kΩ.
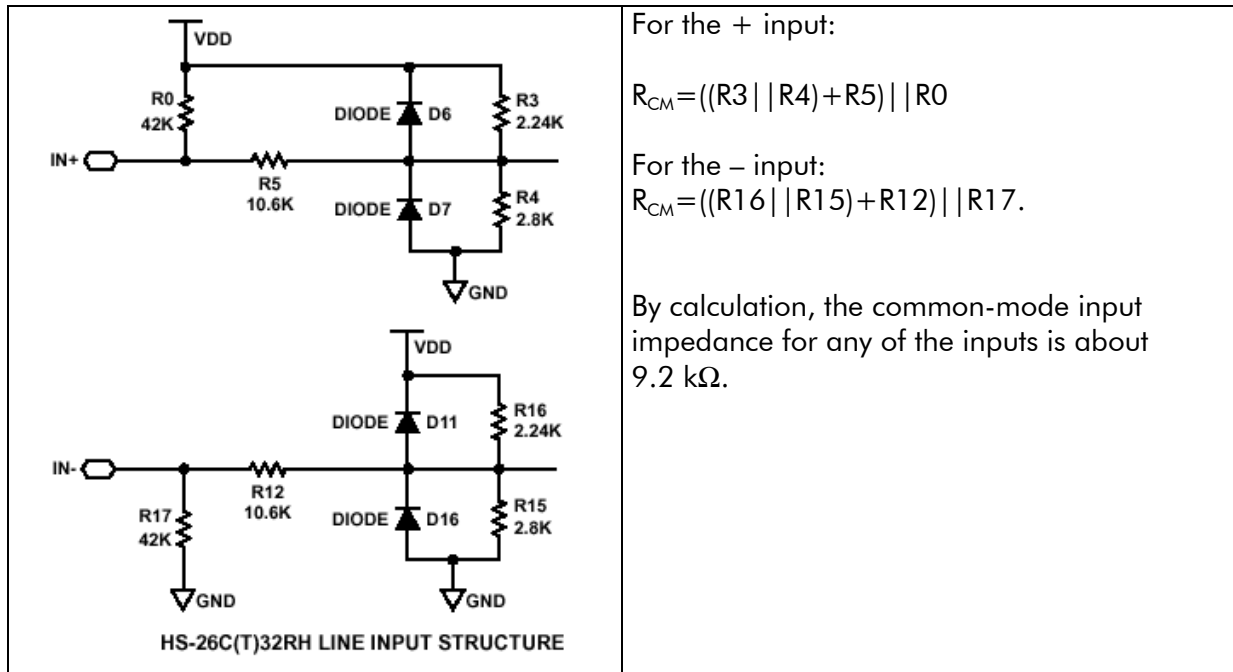
Instruments EMC critical issues

Low frequency low level signal common mode rejection:

For all the Instruments of both satellites, the main subject of concern is the common mode between SVM and PLM.

The common mode sources may be field to cable coupling (either E or H field) or structure currents flowing in metallic links between SVM, PLM and FPUs. These links (e.g. LFI wave guides and cryogenic piping for Planck; HIFI coaxial cables, cryogenic piping and harness over-shielding for HERSCHEL) will have a conductance limited by thermal constraints and an important total length (> 5 meters). cf. § 6.3.7. "EMC approach".

Most of detection lines and bias lines are single ended on one side only for common mode rejection at low frequency purpose, but this rejection will decrease with the frequency because of unavoidable parasitic capacitance's.

Various common mode rejection strategies may be chosen by the Instruments.

For HIFI, the common mode rejection of IF amplifiers bias lines is analysed in "Filtering of FCU – IF amplifiers interface" SRON-U/FCU/TN/2000-003, Draft 2.
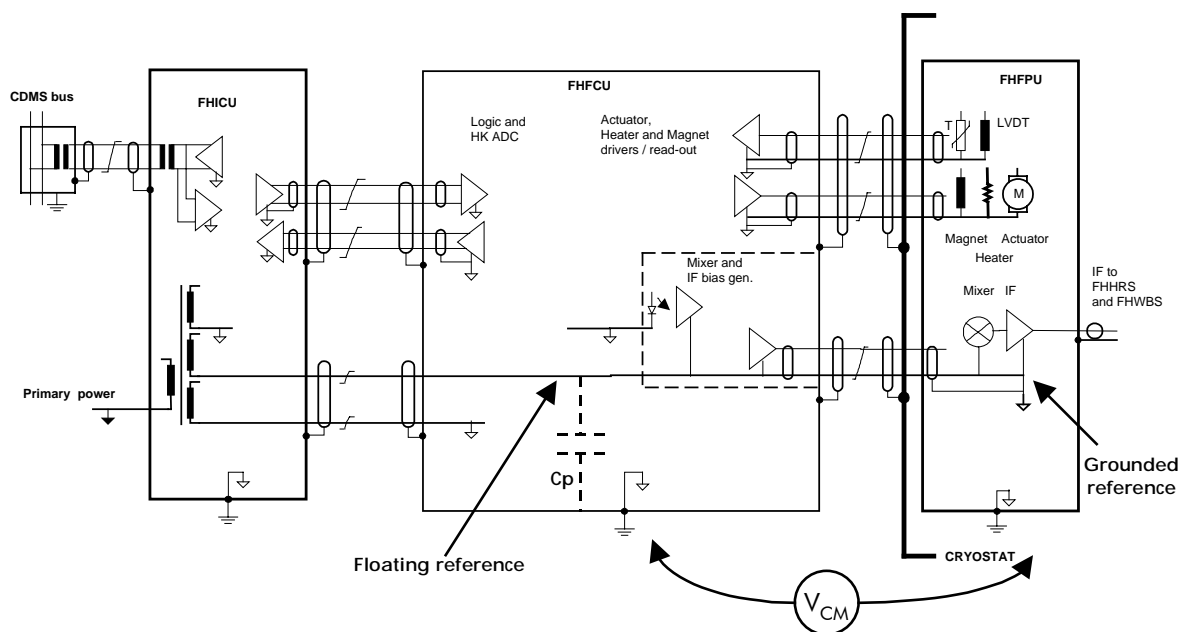
The problem is the following: the FCU delivers biases to the FPU IF amplifiers located in the cryostat at the end of 5 m cable length. The noise level on these links need to be low enough to ensure a sufficient stability of gain of the IF amplifiers.

In the FCU, the IF amplifier bias circuits are isolated from the structure in order to ensure common mode rejection at low frequency (cf. § 7.2.5. "HERSCHEL EMC analyses – Common mode rejection of SVM to PLM links"). However, a parasitic capacitance of several nF is expected between these circuits and the chassis. This capacitance, together with the resistance of the cryo return wires (estimated resistance per polarisation ≤ 50 Ω) creates a (first order) high pass filter with a w.c. cut-off frequency of 300 kHz that decreases common mode rejection according to F (the link inductance is still to be taken into account).

SRON conclusion is that some filtering in the FPU will be necessary, i.e. for each of the 70 IF transistors:

  – a drain filter consisting of a single 100 nF capacitor

  – a second order low pass gate filter with 5 kHz cut-off frequency consisting of 2 resistors and 2 capacitors.

It must be noted that among all the EMC susceptibility specifications of IID-A, the main contributor to the common mode noise budget is the requirement 5.14.3.6 "Conducted Susceptibility Common Mode Voltage – Steady State" that specifies $2\ V_{pp}$ between the equipment signal reference and ground plane in the frequency range 50 kHz to 50 MHz.

Detectors susceptibility to static magnetic fields

In the answers to the EMC questionnaire sent by ESA to the Instruments, at least too Instruments indicated a potential susceptibility to DC magnetic fields: HIFI (for the mixers) and PACS.

SST cryogenic pipes, for example, may be a source of DC magnetic field close to the Instrument sensitive areas.

Instruments requirements in terms of DC magnetic field susceptibility should be specified so that any potential compatibility problem with ferromagnetic materials can be identified.

Detectors susceptibility to dynamic magnetic fields

Because of the S^3R regulation, the Solar Array strings are a potential source of dynamic magnetic field.

Some detection chains may be susceptible to AC magnetic field. Because of the $1/R^3$ decreasing of low frequency magnetic field, no problem is expected on Planck. On HERSCHEL, the closest Instrument to the Solar Arrays is PACS.

A minimization of fields emitted by the S/A panels at the harmonics of the shunt regulators switching will have to be achieved by a proper string and string polarity layout.

Detectors susceptibility to RF

SPIRE detectors (bolometers) are thermal sensors, so sensitive to all types of energy including RF. RF sources on HERSCHEL are X-band telemetry and LOU. SPIRE concept is to RF filter every wire entering the Faraday shield formed by the 4K Instrument enclosure.

<u>HIFI compatibility with TTC X-Band emission</u>

HIFI asked for a RS E-field specification relaxation in the [3.5 – 9 GHz] band, from 2 V/m to 0.1 V/m for compatibility with IF signal sensitivity. They also asked for X-Band switch off during observations. So far ALCATEL disagrees with both of these requirements. An analysis supporting ALCATEL point of view is given in § 7.2.5. This topic will be discussed in the frame of EMC Working Group meetings.

<u>LFI compatibility with TTC X-Band emission</u>

Thanks to the position of the TTC antenna and to the high decoupling brought by the circular Solar Array, the 3 grooves and the baffle between the MGA and Planck telescope, no compatibility problem between X-Band TM harmonics and LFI lower frequency band is expected, cf. analysis § 7.3.5.

<u>Equipment susceptibility to ESD</u>

Like on ISO, it is assumed that no direct ESD can occur inside HERSCHEL cryostat and that it protects FPUs from external potential ESDs.

However it must be noted that the cryo-harness is a potential path for ESD coupling to sensitive I/F (cf. § 6.3.7. "EMC approach").

Also, SRON have announced that HIFI LOU cannot sustain ESD. This statement will have to be consolidated at a later stage and suitable protection means will have to be defined.

5.2.   HERSCHEL

The HERSCHEL satellite accommodates 3 instruments: **PACS**, **SPIRE** and **HIFI**, which are distributed into distinct zones:

–	the cryogenic Optical Bench:	Instrument FPUs
–	the outer region of the HERSCHEL cryostat:	HIFI Local Oscillator Unit (LOU) and PACS Bolometer Amplifier (BOLA)
–	the warm SVM:	Instrument warm electronic boxes.

In addition, the HIFI instrument includes RF wave-guides and semi-rigid co-axial cables, which provide connections between the warm electronics and (respectively) the LOU or HIFI FPU.

The optical bench accommodation of the 3 instrument FPUs, together with the SPIRE JFET box, is illustrated in Figure 5.2-1.
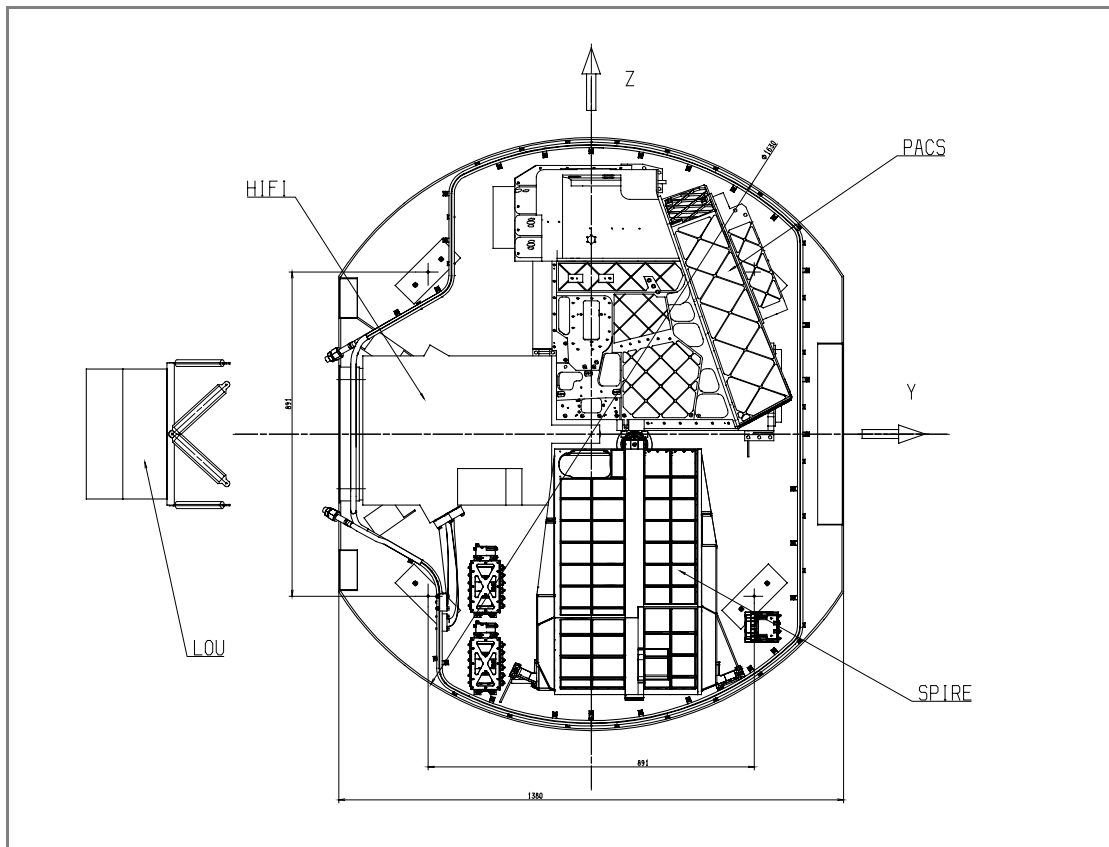
FIGURE 5.2-1 HERSCHEL FOCAL PLANE UNITS ON OPTICAL BENCH/DRAFT VIEW FROM ASTRIUM

5.2.1.   PACS

The following references are used to describe the documents from which design descriptions, requirements, specifications, etc. are drawn for PACS:

- **Ref 1.**   IID-A 1.0   (01-Sept-2001)

- **Ref 2.**   PACS IID-B 1.0   (01-Sept-2001)

- **Ref 3.**   PACS IID-B 1.1   (10-May-2001) – for impact assessment (see also § 6.2.2.).

Ref. 2 describes the PACS design, at the time of proposal submission, whereas Ref. 3 corresponds to the update design as proposed by the PACS instrument consortium on 10.05.01.

The following provides a description of the current status of the PACS instrument design. It also reflects the *changes* or *evolutions* described in Ref. 3. Whenever spacecraft/instrument interfaces are found by ALCATEL to be unacceptable, the acceptable design criteria/specifications are provided, and the corresponding discrepancies are highlighted.

To facilitate comparisons of the present document with the above references, the IID-B chapter references are identified in the following.

5.2.1.1. PACS Mechanical/thermal interfaces

Instrument Units (Ref. 2; § 5.1.)

The previous (Ref. 2) "Detector + Mechanism" (nominal & redundant) control units (FPDMC1 & FPDMC2) have now been split into 4 units, thereby separating Detector and Mechanism control functions: FPDEC1, FPDEC2, FPMEC1, FPMEC2. The (Ref. 3) PACS design thus includes two additional units.

This change is accepted and agreed by PACS to be implemented by stacking the two boxes on top of each other in two groups (2 x 2).

Location and Alignment (Ref. 3; § 5.3.1.2.)

The harness between the BOLA pre-amplifier unit and the PACS FPU is required to be **not more than 2 m** in length. This requirement is to be checked by ASED. However it should also be pointed out that the ultimate objective is to keep the impedance below a certain level, such that the harness characteristics of L, C and R needs are achieved.

Instrument Alignment (Ref. 3; § 5.3.2.)

An optical alignment requirement of ± 2 arcmin has been requested by PACS and is assessed by ASTRIUM.

Size and mass properties (Ref. 3; § 5.5.)

As discussed above, the *dimensions* and *number* of the warm electronic boxes can be accepted under certain conditions.

The Ref. 3 proposed nominal mass of the PACS units (125.82 kg) is uncomfortably close to the total mass allocation of 133 kg (only 5.4 % margin). This demonstrates mass criticality and the need for control of mass margins throughout design phase.

Although no per-instrument allocation has been defined in the IID-A 1.0, a total FPU allocation of 179 kg (i.e. for the 3 instruments) is stipulated. Further analysis has been requested by ESA to ASTRIUM in order to evaluate the acceptability of any excess in **total FPU mass**, beyond the 179 kg allocation)to secure for potential increases.

Mechanical fixation of FPU (Ref. 3; § 5.6.1.)

The fixation point location and interface is still in optimisation on PACS side and not yet frozen.

5.2.1.2.   PACS Electrical interfaces

Power outside cryostat – on CVV (Ref. 3; § 5.9.2.)

The predicted dissipation has now been decreased from 2.5 to 0.2 W. This new level will be considered in the design.

Power on the SVM (Ref. 3; § 5.9.3.)

Budget: The ITT power consumption was given as 85.3 W, for an allocation of 86 W. It has been proposed to increase the power allocation to 100 W for PACS. However,

their requested average power dissipation has now increased to 136 W – which is not accepted at present.

Interface circuit (Ref. 3; § 5.9.5.1.2.)

The circuit diagram provided does not contain enough detail. The equivalent impedance elements of each warm unit I/F circuit have been requested.

PACS electrical interfaces with the S/C
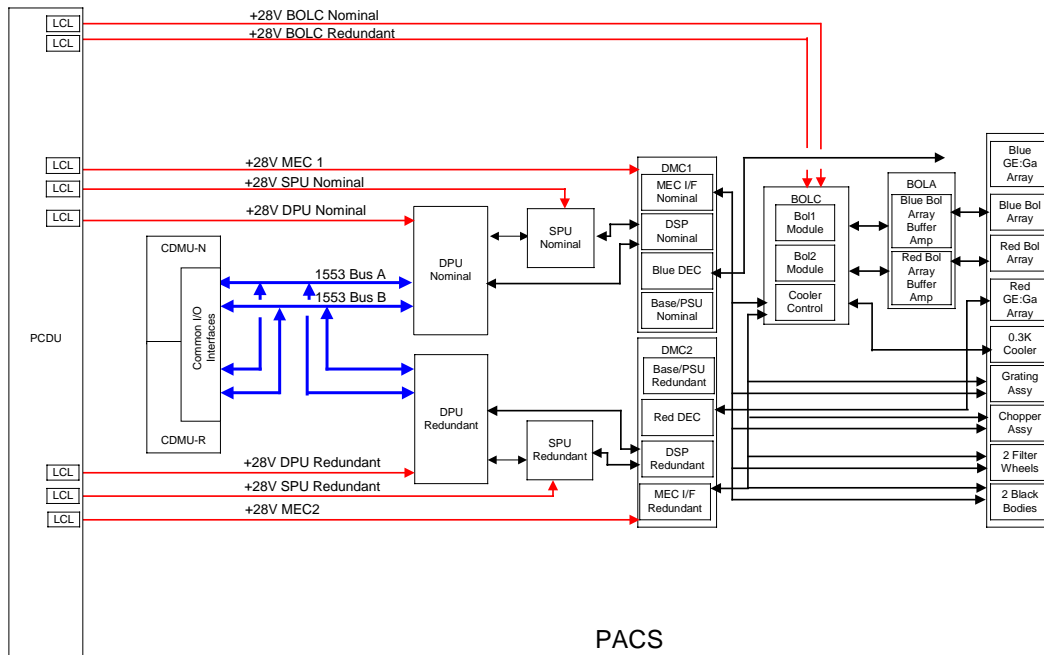
FIGURE 5.2-2 ELECTRICAL INTERFACES BETWEEN PACS AND THE SATELLITE

Power Interfaces

The following power lines (each one to be protected with an LCL) have been identified for PACS:

- – DPU Nominal

- – DPU Redundant

- – SPU Nominal

- – SPU Redundant

- – BOLC Nominal

- BOLC Redundant

- MEC1

- MEC2.

2 + 2 of these LCLs have to be fault tolerant, while the other 2 + 2 may use the "normal" LCL.

It is anticipated that each LCL will be of the standard 5A class. Precise current values are still TBD.

TM/TC & Synchronization Signals

The nominal and redundant MIL-1553 buses will be provided to PACS, connections to be made according to the 1553 standard using the "long stub" with an isolating and coupling transformers.

No other discrete TM/TC line are requested by PACS.

5.2.2. SPIRE

The following references are used to describe the relevant documents from which design descriptions, requirements, specifications, etc. are drawn for SPIRE:

- **Ref 1**.   IID-A 1.0   (01-Sept-2001)

- **Ref 4**.   SPIRE IID-B 1.0   (01-Sept-2001)

- **Ref 5**.   SPIRE IID-B 1.1   (06-June-2001) –   for   impact assessment

- **Ref 6**.   SPIRE IID-B 2/3(JD)   (29-June-2001) –   latest   update received from SPIRE.

5.2.2.1. SPIRE Mechanical/Thermal interfaces

Location and alignment (Ref. 5; § 5.1. & 5.5.)

Cryogenic units: The JFET amplifiers previously housed in a single unit (FSFTB, Ref. 4) are now split into 2 separate units: HSJFS and HSJFP. This evolution does not appear to have an impact on FPU accommodation or the SPIRE envelope on the OB.

<u>SVM Warm Units</u>: The number of warm electronic boxes has increased wrt Ref. 4: instead of 2 there are now 3 – the FSDRC has now been split into HSDCU + HSFCU. The new warm unit dimensions are not supplied in the IID-B Ref. 5 or Ref. 6. Principal moments for the warm units have not yet been provided.

Size and mass properties (Ref. 5; § 5.5.)

The Ref. 4 proposed nominal mass of the SPIRE units (78 kg) had a small margin with respect the total mass allocation (Ref. 1) of 90 kg. The Ref. 5 mass indicates a total SPIRE mass of 99.6 kg (including a margin allocation by SPIRE) and this clearly demonstrates the mass critically and the need of the implemented measures to control the mass.

Micro-vibrations (Ref. 6; § 5.6.1.1. – only TBD in Ref. 5)

A request for micro-vibration levels not in excess of 10 μg has been released by SPIRE. Results are discussed in Section 7.2.2. Preliminary results indicate that reaction wheel imbalances could lead to micro-vibrations (resonance peaks at OB level) typically in the range 1 to 10 mg (i.e. 2 to 3 orders of magnitude above the level requested by SPIRE). This situation appears critical and requires further analysis/justification by SPIRE.

Thermal interfaces/SVM (Ref. 5; § 5.7.3.)

A request on the stability on the warm units of 3 K/hr has been added (see also § 6.3.3.2.).

Temperature channels (Ref. 5; § 5.8.)

Accuracy and resolution requirements of the temperature sensors should be specified. The sensors shall be provided by the spacecraft, at fixation points on the SVM panels close to each respective box.

5.2.2.2.   SPIRE Electrical interfaces

Timing & synchronization (Ref. 5; § 5.14.3.)

The requested accuracy for a "start of scan" flag is 5 milliseconds, however the underlying observational requirement should be clarified. The accuracy with which this signal can be provided is probably closer to 100 ms (TBC).

Attitude and orbit control (Ref. 5; § 5.15.1.)

General: Some details of the S/C performance, wrt the requested pointing modes, are still TBC.

Raster mode: The requested step size is 1.7 to 30 arcsec. The S/C system requirement is for a step resolution not smaller than 2.0 arcsec.

SPIRE Electrical interface with the S/C
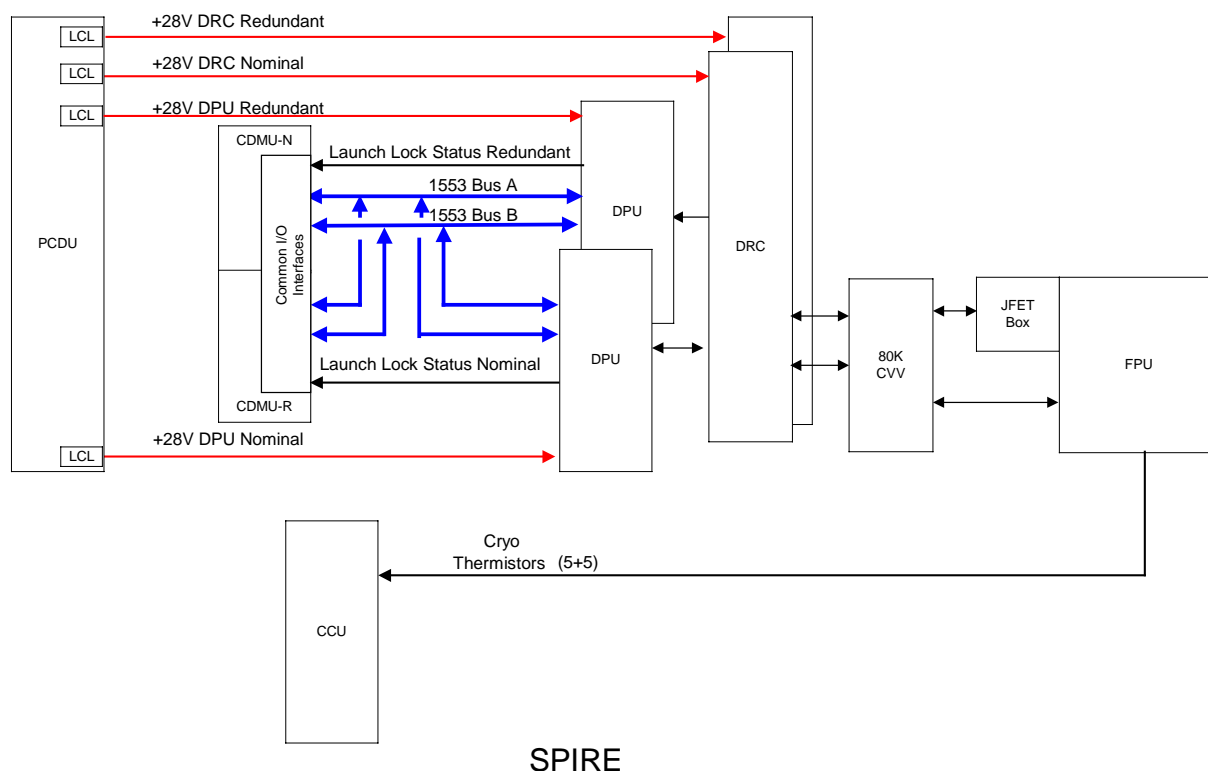
FIGURE 5.2-3 ELECTRICAL INTERFACES BETWEEN SPIRE AND THE SATELLITE, PROPOSED BY ALCATEL

Power Interfaces

The following power lines (each one to be protected with an LCL) have been identified for SPIRE:

– DRC Nominal

– DRC Redundant

– DPU Nominal

– DPU Redundant.

It is anticipated that each standard LCL will be of the 5A class. Precise current values are still TBD. It is not known if these LCLs need to be fault tolerant for the command OFF.

TM/TC & Synchronisation Signals

The nominal and redundant MIL-1553 busses will be provided to SPIRE, connections to be made according to the 1553 standard using the "long stub" with an isolating and coupling transformers.

No other discrete TM/TC line have been formally requested by SPIRE, however the status of the shutter launch lock may have to be acquired. If necessary this can be achieved by the use of relay status interfaces within the CDMU being connected to micro-switches on the shutter and connected to the CDMU via a SPIRE warm unit.

5.2.3. HIFI

The following references are used to describe the relevant documents from which design descriptions, requirements, specifications, etc. are drawn for HIFI:

– **Ref 1**. IID-A 1.0   (01-Sept-2001)

– **Ref 7**. HIFI IID-B 1.0   (01-Sept-2001)

– **Ref 8**. HIFI IIDR   (12-April-2001) – mass breakdown summary

– **Ref 9**. Comments to HIFI IID-B 1.0   (30-May-2001) – for impact assessment.

Ref. 7 describes the HIFI design at the time of proposal submission, whereas Ref. 8 corresponds to the updated design as proposed at the time of their IIDR (April 2001), and Ref. 9 are the most recent updates/comments to the IIDB 1.0.

5.2.3.1. HIFI Mechanical/Thermal interfaces

Instrument Units (Ref. 9; § 5.1.)

The number of HIFI units has evolved since the date of the ITT. The WBS (Wide Band Spectrometer) warm units previously named: "FHWBI", "FHWBO" and "FHWBE" have now been re-arranged into:

– FHWEH: HIFI WBS Electronics – Horizontal Polarization

– FHWEV: HIFI WBS Electronics – Vertical Polarization

– FHWOH: HIFI WBS Optics – Horizontal Polarization

– FHWOV: HIFI WBS Optics – Vertical Polarization.

In addition to the above modifications, the WBS baseplate has been removed, which - has relaxed accommodation constraints on the SVM panel. The WBS mass has nevertheless increased by around 5 kg since the design of Ref. 7.

Size and mass properties (Ref. 9; § 5.5.)

The **Ref. 7** proposed "nominal" mass of HIFI (201.1 kg) was already in excess of the total mass allocation (Ref. 1) of **192 kg**. The budgets provided by HIFI in **Ref. 8** include both "basic" and "with-contingency" mass estimations (totals of respectively 176.5 kg and 205.9 kg), whereas in **Ref. 9** the announced total "allocated" mass is given as 201.1 kg.

It should be noted that HIFI's <u>definition of "allocated" mass,</u> the given in Refs. 8 and 9, corresponds neither to their "basic" mass, nor to their "with contingency" mass, but rather to a notion of self-allocated mass the total of which has always been greater then the Ref. 1 allocation for HIFI.

Since the time of Ref. 9, the concept of the LOU radiator + support structure, mounted outside the CVV, has been refined, thus bringing its estimated mass down from 25 kg to 6 kg. Exact dimensions and design are still TBD. Taking into account the above change in radiator design, a more recent communication from HIFI (via ESA) indicates a revised mass estimate of 182 kg (TBC). The margin w.r.t. allocation is 5% thus demonstrating mass criticality and the need for control of mass margins throughout design phase.

The warm units FHHRH and FHHRV (Ref. 7 and Ref. 9) are noted to be very flat (height just 20 % of their length and width – see also § 6.2.2.2.) and thus wasteful in terms of SVM accommodation area. Stacking of these units could also be unacceptable because of thermal dissipation requirements. The design of these boxes should be justified, or reviewed.

Thermal Interface/outside CVV (Ref. 9; § 5.7.2.)

Requested min. and max. operating temperatures (respectively 90 K and 150 K) for FHLOU will depend on the LOU radiator design and support, and are to be confirmed by ASTRIUM.

Thermal Interface/SVM (Ref. 7; § 5.7.3.)

The requested temperature stabilities of the warm units are difficult to achieve and are assessed by ALENIA.

The requested max. operating temperature of FHWBO (now FHWOH & FHWOV) is 10° C. This appears acceptable in orbit, but not for ground tests.

5.2.3.2. HIFI Electrical interfaces

Interface circuit (Ref. 7; § 5.9.5.2.)

The circuit diagram provided does not contain enough detail. The equivalent impedance elements of each warm unit I/F circuit has been requested.

EMC Requirements (Ref. 7; § 5.14.)

The sensitivity of HIFI to EM interference is an important issue, and a request for waiver has been submitted to ESA. Acceptability of the requested maximum power levels (see frequency plan, Ref. 7; § 5.14.3.) is TBC (see also § 5.1.2.3. of the current document).

HIFI electrical interfaces with the S/C

<u>Power Interfaces</u>

The following power lines (each one to be protected with an LCL) have been identified for HIFI:

– FHLCU Nominal

- FHLCU Redundant

- FHLSU Nominal

- FHLSU Redundant

- FHICU Nominal

- FHICU Redundant

- FHHRH

- FHHRV

- FHWEH

- FHWEV.

Using the power consumption figures provided by the HIFI IIDB, each LCL will be of the 5A class. It is not known if these LCLs need to be fault tolerant for the command OFF.
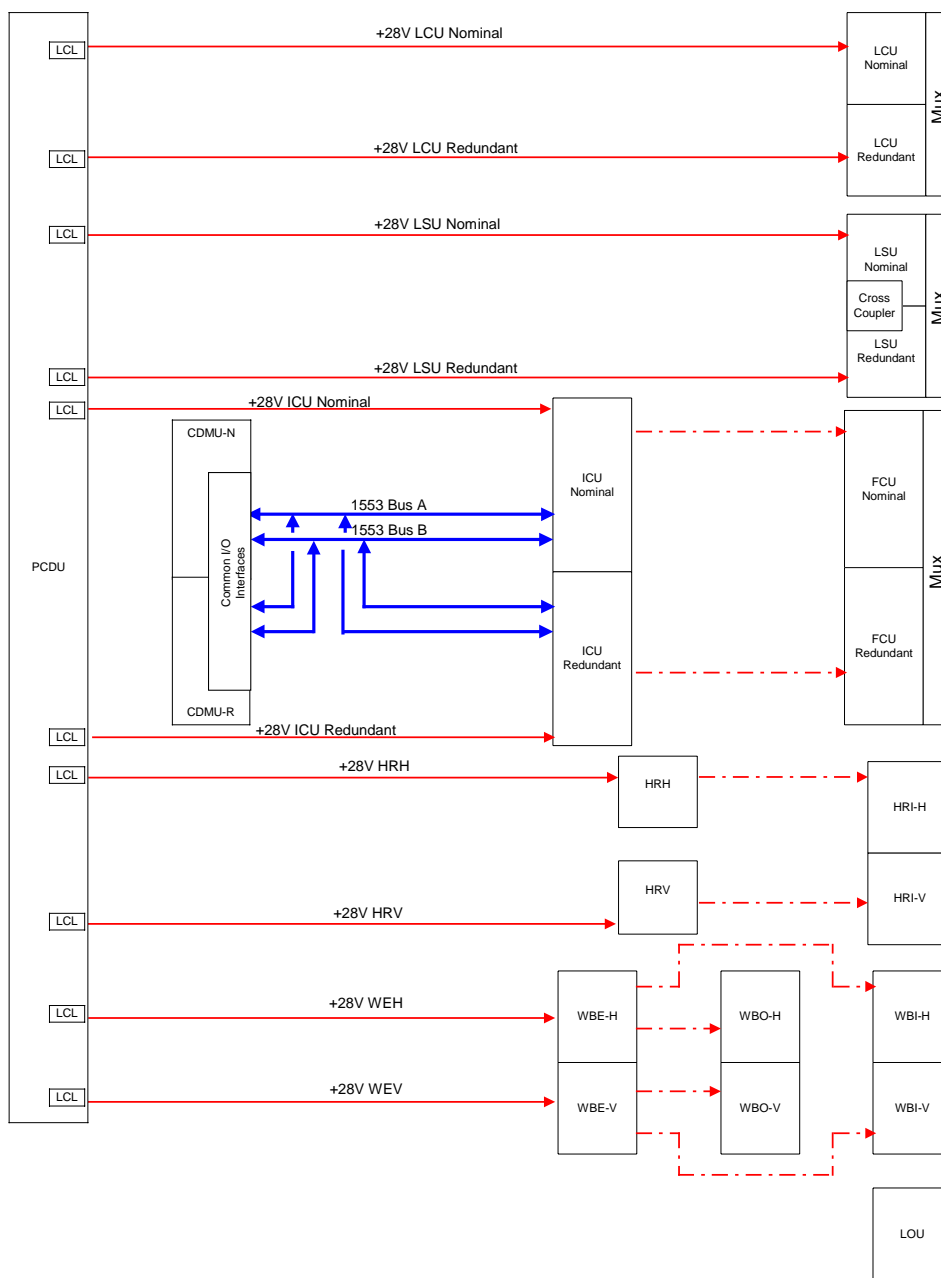
HIFI

FIGURE 5.2-4 ELECTRICAL INTERFACES BETWEEN HIFI AND THE HERSCHEL SATELLITE

TM/TC & Synchronization Signals

The nominal and redundant MIL-1553 busses will be provided to HIFI, connections to be made according to the 1553 standard using the "long stub" with an isolating and coupling transformers.

No other discrete TM/TC line are requested by HIFI.

5.3. PLANCK

The Planck Satellite accommodates 2 instruments: LFI developed by a Consortium led by N. Mandolesi (TESRE-Bologna-I) and HFI, developed by a Consortium led by J.L. Puget (IAS-Orsay-F).

Common to the 2 instrument is the sorption cooler, developed by JPL (one of the 6 US contributions to the HERSCHEL/Planck program). The Sorption cooler is a subsystem of LFI, and managed by LFI. The Sorption cooler electronics is developed under the responsibility and funding of HFI.

Both instruments have a cryogenic Focal Plane Unit (FPU) that receive and process the CMB signal, hosted by the Planck Payload Module (PPLM) and a set of warm units that amplify, digitise and process the electrical signal and that are accommodated in the Planck Service Module. The link between FPU and SVM is via Wave guides + Harness (LFI) and Harness (HFI).

Both instruments have also dedicated chains of coolers that provide the instrument with their ultimate temperatures (20 K for LFI, 0.1K for HFI), and that interface the satellite at in the SVM (compressors, control electronics), in the PPLM (heat exchangers and pipes).

The Satellite provides the services (Power, data handling, pointing, TM/TC, security,...) and the proper environment (Mechanical at launch, thermal) both for the warm units (270 - 300 K) and the PPLM (Telescope, Precooling at 50 K for the coolers, Straylight insulation).

The key issues to succeed the Planck mission is to master the cryogenic chain which is complex and with distributed responsibility, and to control the systematics (ie all perturbations (thermal, EMC, straylight, vibrations) which might affect the signal)
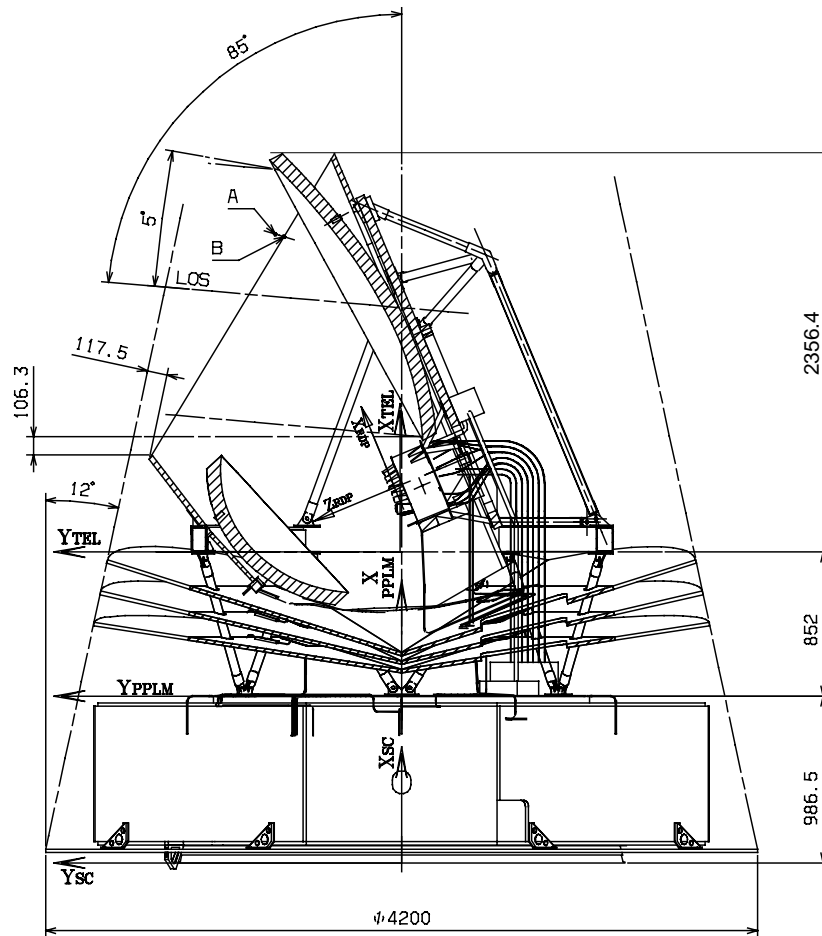
5.3.1. HFI

HFI (High frequency instrument) is based on very sensitive bolometers cooled at 0.1 K, and will map the CMB temperature fluctuations with 48 spider web bolometers split in 6 channels from 83 GHz to 1 THz.

5.3.1.1. HFI Mechanical & Thermal interfaces

FPU mechanical architecture

- 0.1 K stage
- 1.6 K stage
- 4 K stage
- 18 K plate

- single LFI mounting interface @ 18K
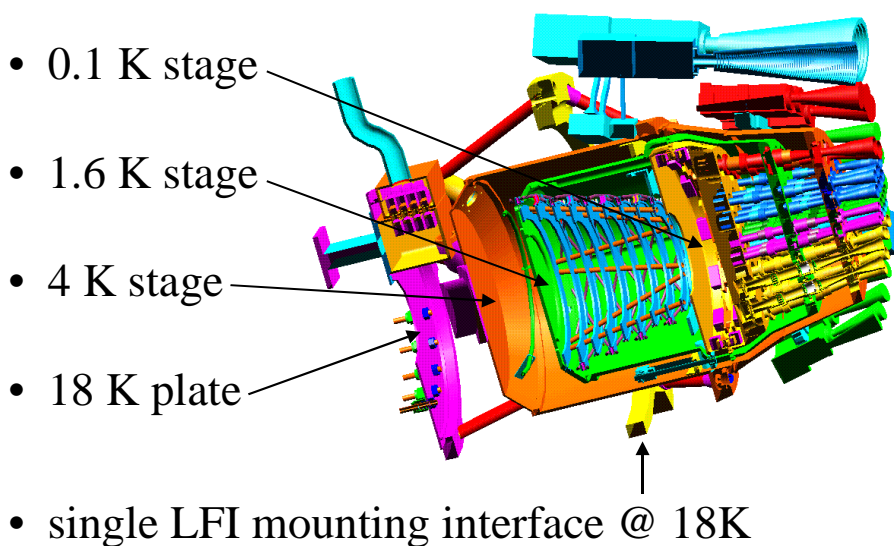
Location & Alignments

Some cable length still need to be clarified (JFET to PAU), and HFI is requiring the length of its cables to make a better estimate of the mass.

Size & mass properties

The following table compares the Mechanical interfaces of the HFI instrument at ITT and how it is proposed now.

The main changes is a new redundant DPU (but which shall be stacked with the nominal one), new size for boxes (Some large inflation, reduction of tanks and Fill & vent panel) a better description of the harness, the tanks, resulting in a mass increase of about 10 kg (5 %).

Interfaces of the FPU with LFI and envelopes volumes have been clarified during technical meetings.

The cabling seems very complex and heavy, especially between the PAU and REU, where the cable weight has doubled.

The DCCU and fill & vent panel size has been reduced to be compatible with the SVM shear webs, and these units seems to be far from being designed. In particular, the need of handling access and leak checking has still to be clarified (Open actions on this subject).

Location	unit	WBS	description	Size	Nominal Mass	Nominal Mass	Size	Mass	Mass
			HFI (Ref HFI proposal for IID-B : hfi-05-1-B.doc)				**ITT version (IID-B 1/0)**		
				LxWxH, m3	kg	kg	LxWxH, m3	kg	kg
PPLM	PHFPU	PHA	Instrument Focal Plane Units	0.44x Ø0.25	16.5	25.9	0.44x Ø0.25	15	19
PPLM	PHFET	PHCA	J-FET Box	0.22x0.16x0.12	2		0.22x0.16x0.16	2	
PPLM		PHAD	Cryoharness between FPU & JFETbox	0.50x0.00x0.00	2				
PPLM		PHCBB	Cryoharness PAU-JFET box	2.00x0.00x0.00	4.3				
PPLM	PHJCE	PHDD	4K Cooler Cold Unit		1.1			2	
SVM						196.84			194
SVM		PHB	**Instrument Main Electronics**						
SVM	PHDPU	PHBA-N	Data Processing Unit (DPU)	0.28x0.28x0.10	6.5		0.20x0.25x0.20	13	
SVM		PHBA-R	Data Processing Unit (DPU) redundant	0.28x0.28x0.10	6.5				
SVM		PHBB	Harness from DPU	L 1.0	4.59				
SVM		PHC	**Instrument Detection Units**						
SVM	PHPAU	PHCBA	Pre-Amplifier unit (PAU)	0.42x0.25x0.23	9		0.31x0.18x0.95	3	
SVM	PHREU	PHCBC	Readout Electronics Unit (REU)	0.41x0.41x0.32	32		0.34x0.37x0.28	25	
SVM		PHCBD	harness REU-PAU	L 2.5	10				
SVM		PHD	**Instrument 4K Cooler Units**						
SVM	PHJTC	PHDA	4K Cooler Compressor Unit	0.46x0.25x0.20	16		0.46x0.25x0.20	16	
SVM	PHJTA	PHDB	4K Cooler Ancillary Unit	0.35x0.35x0.10	5.1		0.35x0.35x0.10	8	
SVM	PHJTE	PHDC	4K Cooler Electronics Unit (4KCDE)	0.22x0.22x0.20	7		0.22x0.22x0.20	7	
SVM		PHDE	4K Cooler piping between compressor unit & Ancillary unit	1.00x0.00x0.00	0.1		TBD	2	
SVM		PHDF	Harness from 4K CDE	L 1.0	2.19				
SVM		PHE	**Instrument 0.1K Cooler Units**						
SVM	PH3HE	PHEAA	0.1K Dilution Cooler 3He Tank (1)	Ø 0.48	16		Ø 0.46	19	
SVM	PH4HE	PHEAB	0.1K Dilution Cooler 4He Tanks (3)	Ø 0.48	48		Ø 0.46	57	
SVM		PHEB	0.1K Cooler harness	L 3.0	1.22				
SVM	PHCDU	PHEC	0.1K Dilution Cooler Control Unit	0.66x0.60x0.26	25		1.00x0.40x0.26	25	
SVM		PHED	0.1K Dilution Cooler filling & venting panel	0.66x0.35x0.26	5		0.50x0.40x0.26	5	
SVM		PHEE	0.1K Cooler piping	L 2.0	2.64				
							Harness + pipes All	14	
			LFI Nominal Mass		222.7	222.7	0	213.0	213.0
			Allocation IID A / System Specification	9.5%		244.0	14.6%		244.0
			Total incl 20% margin	20.0%		267.3	0.2	0	255.6
			Delta Now/ITT		5%	9.7			

Mechanical Interfaces

Concerning the mechanical interfaces, there are still indication of micro-vibrations susceptibility (0.1 to 1 mg), which will have to be refined.

Thermal interfaces

The following table summarizes the HFI thermal requirements, which are very similar to the one of the ITT.

The main difference is the temperature stability requirement on the PAU (0.1 K/h) which will be difficult to guarantee (and verify). The main perturbation will be the sorption cooler (Preliminary calculation shows that this stability might be achieved, see § 7.2.3.).

Location	unit	WBS	description	Power demand / Dissipation		Power Density	Operating Min		Operating Max		Start up		Switch off		non Operating Min		non Operating Max		stability	Power demand ITT	
				W	W	W/m2	K	°C	K	°C	K	°C	K	°C	K	°C	K	°C	K/h	W	W
PPLM	PHFPU	PHA	Instrument Focal Plane Units	0	0.15	-	-	-	50	-	50	-	-	-	-	-	-	-	-		0.15
PPLM	PHFET	PHCA	J-FET Box	0.15		4	30	-	70	-	50	-	-	-	-	-	-	60	-	0.15	
PPLM	0	PHCBB	Cryoharness PAU-JFET box	0			-	-	-	-	-	-	-	-	-	-	-	-	-		
PPLM	PHJCE	PHDD	4K Cooler Cold Unit	0			-	-	-	-	-	-	-	-	-	-	-	-	-		
SVM																					
SVM		PHB	**Instrument Main Electronics**																		
SVM	PHDPU	PHBA-N	Data Processing Unit (DPU)	42	264	536	-	-10	-	40	-	-	-	-	-	-20	-	50	-	42	254
SVM			Data Processing Unit (DPU) redundant	0																	
SVM			Harness from DPU	0																	
SVM			**Instrument Detection Units**																		
SVM	PHPAU	PHCBA	Pre-Amplifier unit (PAU)	10		95	-	-20	-	30	-	-	-	-	-	-20	-	50	0.1	10	
SVM	PHREU	PHCBC	Readout Electronics Unit (REU)	90		528	-	-10	-	30	-	-	-	-	-	-20	-	50	-	90	
SVM		PHCBD	harness REU-PAU	0			-	-10	-	40	-	-	-	-	-	-20	-	50	-	60	
SVM		PHD	**Instrument 4K Cooler Units**				-	-	-	-	-	-	-	-	-	-	-	-	-	12	
SVM	PHJTC	PHDA	4K Cooler Compressor Unit	60		522	-	-10	-	40	-	-	-	-	-	-20	-	40	-	60	
SVM	PHJTA	PHDB	4K Cooler Ancillary Unit	12		98	-	-10	-	40	-	-	-	-	-	-20	-	50	-	12	
SVM	PHJTE	PHDC	4K Cooler Electronics Unit (4KCDE)	30		620	-	-10	-	40	-	-	-	-	-	-20	-	50	-	30	
SVM		PHDE	4K Cooler piping between compressor unit & Ancillary unit	0			-	-	-	-	-	-	-	-	-	-	-	-	-		
SVM		PHDF	Harness from 4K CDE	0			-	-	-	-	-	-	-	-	-	-	-	-	-		
SVM		PHE	**Instrument 0.1K Cooler Units**				-	-	-	-	-	-	-	-	-	-	-	-	-		
SVM	PH3HE	PHEAA	0.1K Dilution Cooler 3He Tank (1)	0			-	-10	-	40	-	-	-	-	-	-20	-	50	-		
SVM	PH4HE	PHEAB	0.1K Dilution Cooler 4He Tanks (3)	0			-	-10	-	40	-	-	-	-	-	-20	-	50	-		
SVM		PHEB	0.1K Cooler harness	0			-	-	-	-	-	-	-	-	-	-	-	-	-		
SVM	PHCDU	PHEC	0.1K Dilution Cooler Control Unit	10		25	-	-10	-	40	-	-	-	-	-	-20	-	50	-	10	
SVM		PHED	0.1K Dilution Cooler filling & venting panel	10		43	-	-10	-	40	-	-	-	-	-	-20	-	50	-		
SVM		PHEE	0.1K Cooler piping	0			-	-	-	-	-	-	-	-	-	-	-	-	-		
			LFI Nominal Power	264.2	264.2															254.2	254.15

Concerning the need of temperature sensors, there will be only one type provided and powered by the spacecraft (ie no distinction between SPT & SHT), located on the spacecraft, at the instrument interface point (not on the instrument). The information will be part of the spacecraft housekeeping.

Optical Interfaces

There is a good understanding in optical interfaces, and information has been exchanged to perform the PPLM optical and straylight design. An open point is how to define the orientation of the Instrument horns (wrt polarization)

5.3.1.2. HFI Electrical interfaces

Figure 5.3.1.2.1 shows the electrical interfaces between HFI and the satellite.
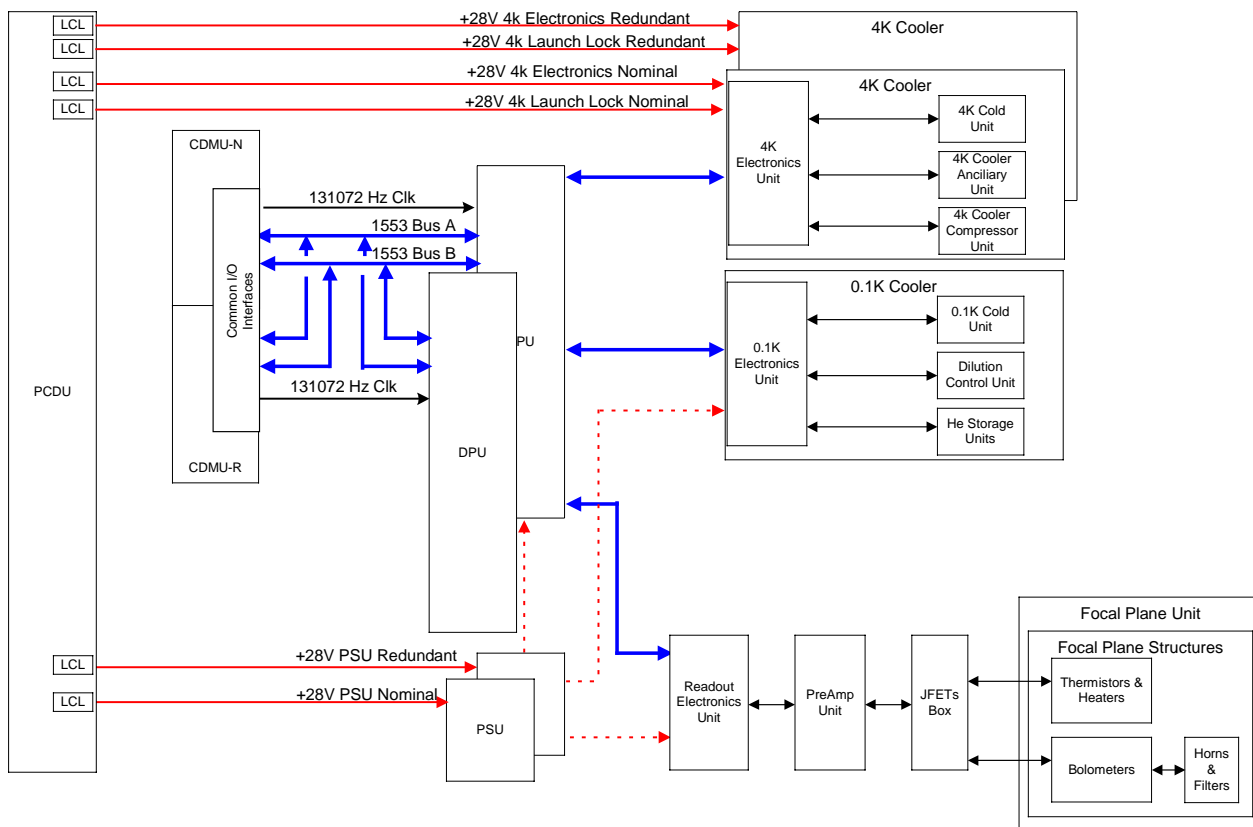
HFI

FIGURE 5.3.1.2-1

Power Interfaces

As stated on power allocation and demand, HFI has no margins wrt allocations. Some margin should be restored.

The following power lines (each one to be protected with an LCL) have been identified for HFI:

- PSU Nominal

- PSU Redundant

- 4k Electronics Nominal

- 4k Electronics Redundant

- 4k CEU Launch Lock Nominal

- 4k CEU Launch Lock Redundant.

It is anticipated that each LCL will be of the 5A class. Precise current values are still TBD. It is not known if these LCLs need to be fault tolerant for the command OFF.

TM/TC & Synchronization Signals

The nominal and redundant MIL-1553 busses will be provided to HFI, connections to be made according to the 1553 standard using the "long stub" with an isolating and coupling transformers.

1 Nominal + 1 Redundant (TBC by HFI) 131072 Hz clock signal will be distributed to the HFI using SBDL (Standard Balanced Digital Link) interfaces for HFI timing purposes.

Pointing

Based on the findings of the Boomerang and Maxima balloon missions, HFI (and LFI) have both issued technical note to require improvement in the pointing capability of Planck. This requirement for improvement represents one order of magnitude compared to the Planck pointing requirement form the SRS.

This is not likely that these wishes can be satisfied. We will design the ACMS to satisfy the requirement, and define under which conditions to reach the goals expressed in the SRS could be reached.

5.3.2. LFI

LFI (Low Frequency Instrument) is complementary to HFI. It will map the CMB with 27 coherent receivers split in 4 channels from 30 to 100 GHz.

The receivers are split into the cold Front End Modules (FEM), located in the Front End Unit (FEU) in the Focal Plane Unit (FPU) at 20K, and the Back End Modules (BEM) part of the Back End Unit (BEU) located on the upper platform of the SVM, and connected to the FEM by a set of 4 x 27=108 wave guides.
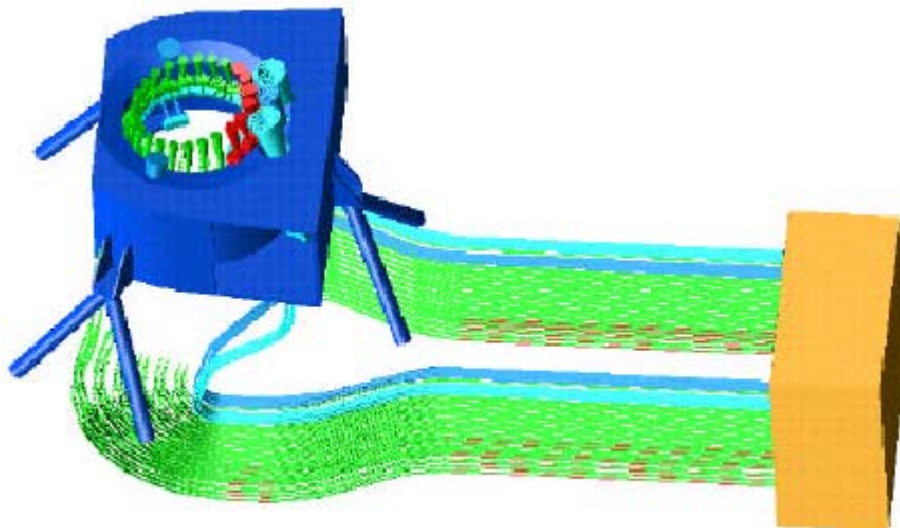
FIGURE 5.3-1 LFI FEU, WAGE-GUIDES AND BEU

One of the Key issue for the LFI detectors is to maintain them at 20K despite of a large dissipation (580 mW), and the large number of wave-guides connected the BEU to room temperature.

5.3.2.1. LFI Mechanical/Thermal interfaces

Location and Alignment requirements

The requirements on alignment and location are well understood, and should not be a major problem. The main concern is the integration of the Radiometer Array Assembly (RAA), composed of the FEU, BEU and wave-guide which has to interface all cooling stages.

Mass & Size properties

They are summarised in the following table.

Location	unit	WBS	description	Size	Mass	Mass	Size	Mass	Mass
	LFI		Ref: LFI proposal for IID-B LFI _ IIDB_updates_June27_01.doc				**ITT version (IID-B 1/0)**		
				LxWxH, m3	kg	**kg**	LxWxH, m3	kg	**kg**
PPLM	FEU	PLAA0	Front End Unit, without struts	0.40x0.43x0.60	26.15	**26.82**	0.40x0.43x0.60	22.4	**22.4**
on HFI	0	PLAF0	4K ref Load		0.67				
SVM-PPLM	WG	PLAxE	Wave-guide & Coax Cables Section - (4 bundles)	1.20x0.00x0.00	10.84	**10.84**	1.20x0.00x0.00	5	**5**
SVM	BEU	PLAB0	Back End Unit , without strut	0.40x0.40x0.20	33.52	**68.11**	0.40x0.40x0.20	30	**46.6**
			DAE Control Box	0.25x0.20x0.20	20.9				
			DAE Internal Harness		2.6				
SVM	REBA	PLBAA	REBA Nominal	0.30x0.30x0.50	4.045		0.30x0.30x0.50	6.8	
SVM		PLBAB	REBA redundant	0.30x0.30x0.50	4.045		0.30x0.30x0.50	6.8	
SVM		PLE00	Interconnecting Harness		3		0	3	
			Total		105.8	105.8		74.0	74.0
			Allocation IID A / System Specification	-15.9%		89.0	20.3%		89.0
			Total incl 20% margin	20.0%		126.9	20.0%		88.8
			Delta Now/ITT		43%	31.8			

The main change since ITT is the growth of the Back end Module and in particular the Data Acquisition Electronics (DAE). It gave birth to a new warm unit (DAE control box). LFI mass and power budgets are now exceeding allocations. A design reveiw process has been initiated with LFI in order to identify and implement a design compatible with resources.

Mechanical Interfaces

Supporting the copper part of the wave-guides is a new potential requirement arising from the instrument working sessions. Definition of the supporting system is an on-going activity. Provision for interfacing a new structure on the 60 K panel has been made.

Thermal interfaces

<u>Power dissipation</u>

Due to the DAE refined design, the Power budget of LFI has increased significantly (+ 54 %).

There are no changes in the temperature requirement, except a new temperature stability for the DAE which might be of the order of 0.2 K/h, et similar to the HFI PAU.

Concerning thermal interfaces, there is a change in the wave-guide cross section by a factor of 2 that is critical the heat budget on the 60 K shield.

There is also a new provision for interfacing the heat switch on the 50 K panel, and additional connection to the 20 K via the supporting of the copper part (20 K) of the wave-guides.

Location	LFI unit	WBS	description	Power demand / Dissipation		Power Density	Temperatures at interface																Power demand / Dissipation ITT	
							Operating				Start up		Switch off		non Operating				stabil ity			
							Min		Max								Min		Max					
				W	W	W/m2	K	°C	K	°C	K	°C	K	°C	K	°C	K	°C	K/h	W	W
PPLM	PLAA0	FEU	Front End Unit, without struts	0.581	0.581	3	40	-	65	-	-	80	-	-	-	-	-	50	-	0.55	0.55
on HFI	PLAF0		4K ref Load																		
SVM-PPLM	PLAxE	WG	Wave-guide & Coax Cables Section - (4 bundles)	0		-	20	26	-	28	-	-	-	-	-	-	-	-	-		
SVM	PLAB0	BEU	Back End Unit , without strut	45.72	112.82	286	-	-20	-	28	-	-	-	-	-	-	-	-	0.2	40.7	73
			DAE Control Box	31.5		630															
			DAE Internal Harness	0																	
SVM	PLBAA	REBA	REBA Nominal	35.6		396	-	-20	-	50	-	-	-	-	-	-30	-	70	-	32.3	
SVM	PLBAB		REBA redundant	0		-	-	-20	-	50	-	-	-	-	-	-30	-	70	-		
SVM	PLE00		Interconnecting Harness	0		-	-	-	-	-	-	-	-	-	-	-	-	-	-		
			Total	113.4	113.4															73.55	73.55
			Delta ITT / Now	39.9	54.2%																

5.3.2.2. LFI Electrical interfaces

Figure 5.3.2.2-1 shows the electrical interfaces between HFI and the satellite.
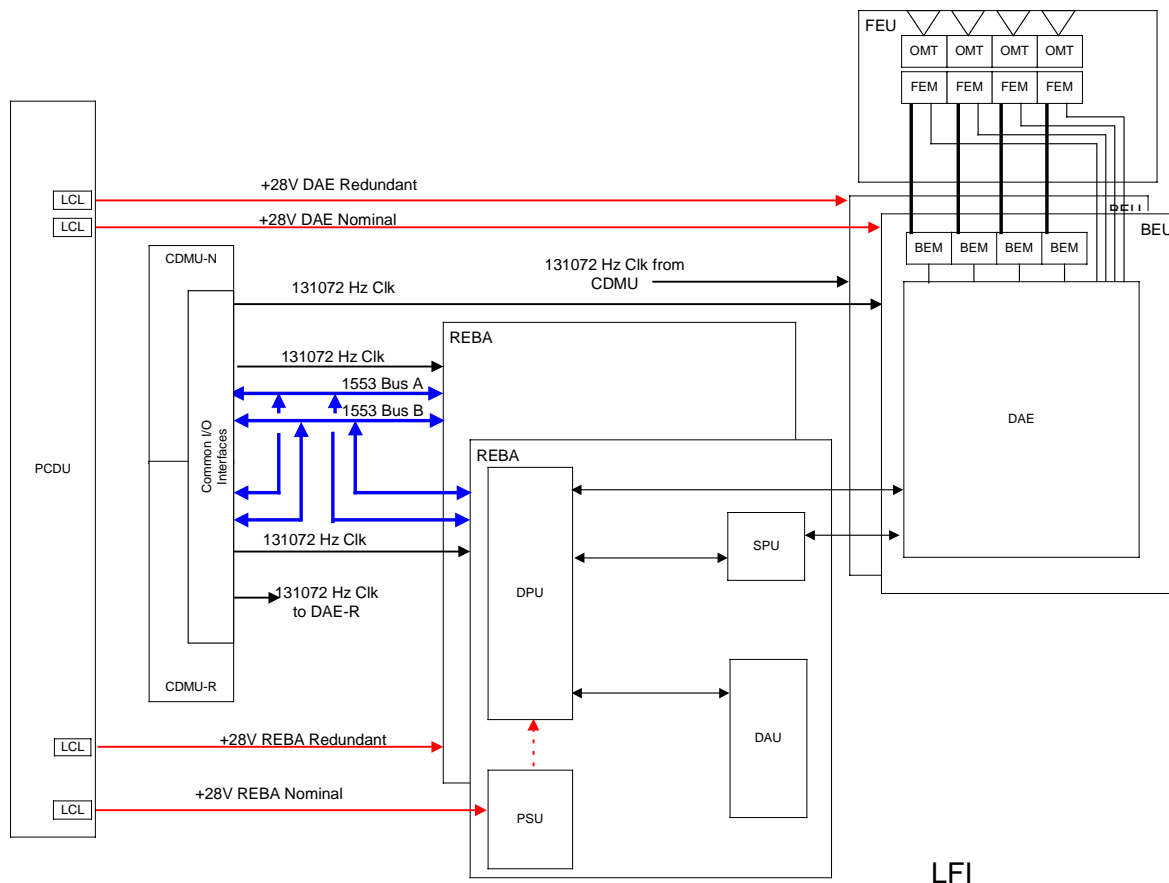
FIGURE 5.3.2.2-1

Power Interfaces

The following power lines (each one to be protected with an LCL) have been identified for LFI:

- REBA Nominal

- REBA Redundant

- DAE Nominal

- DAE Redundant.

It is anticipated that each standard LCL will be of the 5A class. Precise current values are still TBD.

All of these LCLs have to be fault tolerant ensuring that they may always be switched OFF.

TM/TC & Synchronization Signals

The nominal and redundant MIL-1553 busses will be provided to LFI, connections to be made according to the 1553 standard using the "long stub" with an isolating and coupling transformers.

The following 131072 Hz clock signals will be distributed to the LFI using SBDL (Standard Balanced Digital Link) interfaces for LFI timing purposes:

- one to the nominal REBA

- one to the redundant REBA

- one to the nominal DAE

- one to the redundant DAE.

Harness

LFI harness has changed, and impact of the new harness on the cryogenic performances has yet to be assessed.

5.3.3. Sorption cooler

The sorption cooler is a subsystem of LFI. It is also used as precooler for HFI, which in return provides the sorption cooler electronics. Because of its impact on the mission reliability, is is composed of 2 units, one in cold redundancy. It is designed to provide 1100 mW of cooling power at 20 K for LFI (including 135 mW at 18 K for HFI). It is based on a H2 closed cycle Joule Thomson cooler, with a sorption compressor based on thermal cycling of metal hydrides (LaNi4.78Sn0.22).

As it requires substantial resources from the satellite (112 kg for 2 coolers, 600 W, 3/8 SVM panels), and because it is common to both instruments, it is described in an independent document: The sorption cooler ICD, annex to LFI IID-B, and having the same structure than any IIDB document.

5.3.3.1. Sorption cooler Mechanical & Thermal interfaces

External configuration drawings

They will have to be updated after common agreement on the exact pipe routing.

Size and mass properties

The mass has increased by 14 % since the ITT, and the size of the electronics has grown by 20 %.

Location	**Sorption cooler** unit	**WBS**	Sorption cooler ICD - PL-LFI-PST-TN-011 v 1/1 description	Size LxWxH, m3	Mass kg	Mass kg	ITT version (IID-B 1/0) Size LxWxH, m3	Mass kg	Mass kg
PLFEU	SCCE	PSM1	Sorption Cooler Cold End Nominal		1.52	**1.52**	0	1.9	1.9
SVM-PPLM	SCP	PSM2	Sorption Cooler Pipes Nominal	9.50x Ø0.0064	4.43	**4.43**	9.50x Ø0.0064	2.8	2.8
SVM	SCC	PSM3	Sorption Cooler Compressor Nominal	1.00x0.75x0.25	39.8	**51.3**	1.00x0.75x0.10	34.4	45.4
SVM	SCE	PSM4	Sorption Cooler Electronics Nominal	0.30x0.30x0.15	8.5		0.25x0.20x0.14	8.5	0
SVM	harness	PSM5B	SCE to SCC harness Nominal	1.50	2		2.00	2	0
SVM-PPLM	harness	PSM5C	SCE to SCCE harness Nominal	5.00	1		1.00	0.5	0
PLFEU	SCCE	PSR1	Sorption Cooler Cold End Redundant		1.52	**1.52**	0	1.9	1.9
SVM-PPLM	SCP	PSR2	Sorption Cooler Pipes redundant	9.50x Ø0.0064	4.43	**4.43**	9.50x Ø0.0064	2.8	2.8
SVM	SCC	PSR3	Sorption Cooler Compressor redundant	1.00x0.75x0.25	39.8	**51.3**	1.00x0.75x0.10	34.4	45.4
SVM	SCE	PSR4	Sorption Cooler Electronics redundant	0.30x0.30x0.15	8.5		0.25x0.20x0.14	8.5	0
SVM	harness	PSM5B	SCE to SCC harness Redundant	1.50	2		2.00	2	0
SVM-PPLM	harness	PSM5C	SCE to SCCE harness Redundant	5.00	1		1.00	0.5	0
			Total Sorption Cooler		114.5	114.5	**0**	100.2	100.2
			Allocation IID A / System Specification	-2.2%		112.0	11.8%	0.0	112.0
			Total incl 20% margin	20.0%		137.4	20.0%	0.0	120.2
			Delta Now/ITT		14%	14.3			

Sorption cooler Thermal interfaces

The thermal interfaces are probably the most challenging.

There are several changes in the new proposed ICD version which are are highly critical w.r.t. technical realization.

1. Increase of the nominal average dissipation from 400 to 520 W→ SVM radiator not large enough →SCC Temperature above requirement.

2. Increase of the Peak dissipation from 950 to 1250 W → Large heat density on heat pipes → Dry heat pipe, associated to a reduction of the contact area to the radiator (- 30 %).

3. Wish to achieve a maximum temperature fluctuation of 0.5 K on the radiator (applicable to adsorbing beds) on a cycle which is not compatible with the response of the radiator to SCC interface to the peak power dissipation (3 K).

Our position on these modifications are the following:

1. At ITT, the nominal average dissipation of the Sorption Cooler Compressor was 400 W (with an allocated maximum average power demand of 520 W on the main bus)The SVM radiator design has been made with 470 W (400 W + 30 W (from delivered model) + 10 %) from the compressor. The impacts are described in the thermal section The thermal design of the radiator is compatible with a maximum value of 600 W, what includes an allocation of 130 W for the sorption cooler electronics. In view of the margins understood to be included in the sorption cooler compressor allocation, it is believed that a maximum average dissipation of 470 W allows viable design.

2. The second point is currently solved by changing the sorption cooler beds footprint (increasing contact area).

3. The impact of the power peak on the radiator fluctuation is being analysed (Ref § 7.3.3 of this document, plus § 7.4 of the Planck design report (HP-3-ASPI-RP-050).

5.3.3.2. Sorption Cooler Electrical interfaces

Figure 5.3.3.2-1 shows the electrical interfaces between Sorption Cooler and the satellite.
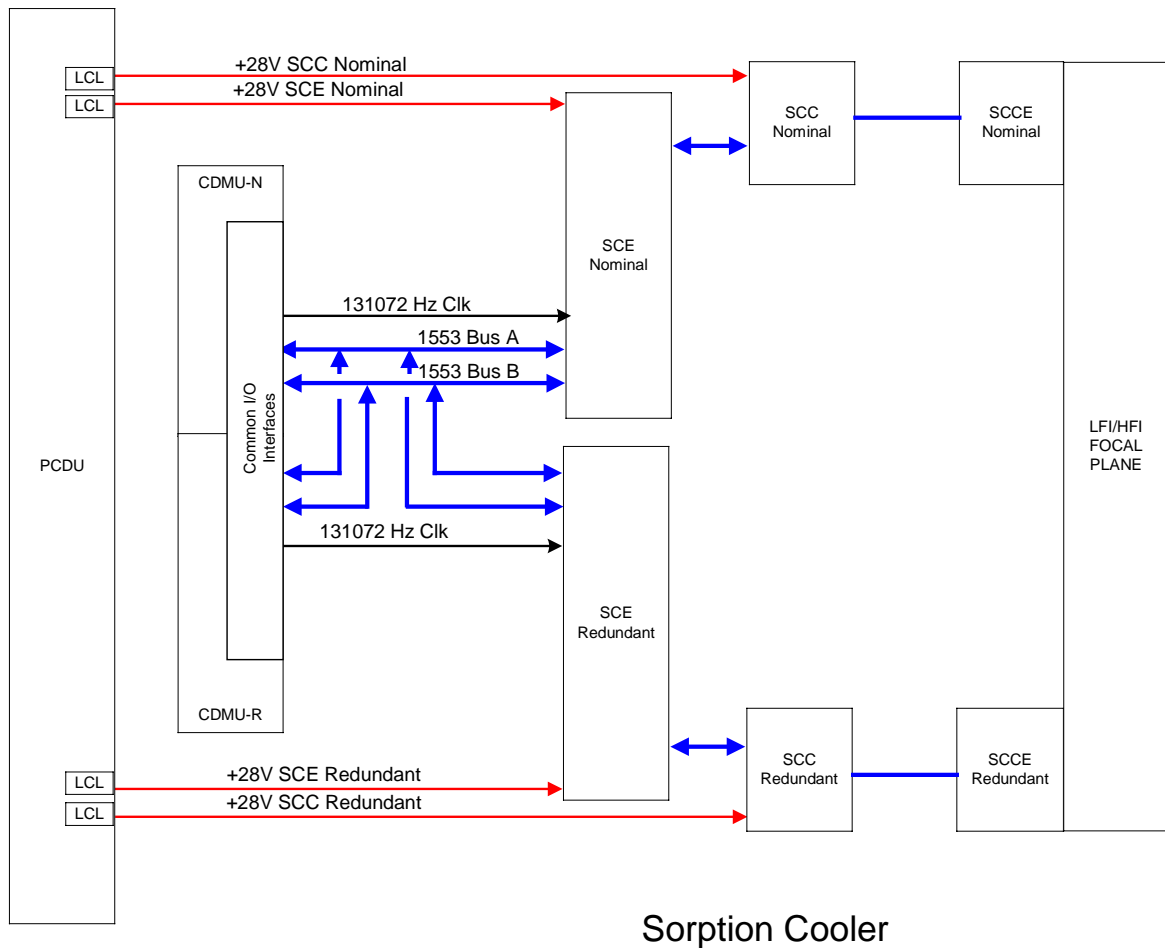

Sorption Cooler

FIGURE 5.2.3.2-1

Power Interfaces

The following power lines (each one to be protected with an LCL) have been identified for Sorption Cooler:

- Sorption Cooler Electronics Nominal

- Sorption Cooler Electronics Redundant

- Sorption Cooler Compressor Nominal

- Sorption Cooler Compressor Redundant.

It is anticipated that each LCL for the Sorption Cooler Electronics will be of the 5 A class, the Sorption Cooler Compressor LCLs are expected to be 20 A. The present power figures for the sorption cooler indicate that a 20 A LCL would not be sufficient but it would have to be increased to a 25 A LCL, in particular to be able to cope with the trip values. Precise current values are still TBD. It is not known if these LCLs need to be fault tolerant for the command OFF.

TM/TC & Synchronization Signals

The nominal and redundant MIL-1553 busses will be provided to the Sorption Cooler, connections to be made according to the 1553 standard using the "long stub" with an isolating and coupling transformers.

The following 131072 Hz clock signals will be distributed to the Sorption Cooler using SBDL (Standard Balanced Digital Link) interfaces for LFI timing purposes:

- one to the nominal SCE

- one to the redundant SCE.

Sorption cooler Harness

The sorption cooler cryo-harness is defined using cables gauge 26 (0.4 mm diameter), which is certainly not acceptable.

5.4.   OPEN POINTS

This paragraph is to summarise the open points concerning the technical interfaces with the instruments that will have to be resolved during the period between the SRR and the PDR.

Mass budget (HERSCHEL, Planck)

Instrument Nominal masses + margins and Satellite allocations will have to converge to an agreement before the PDR. This will be achieved by close control of the instrument design, and optimisation (redistribution) of margin.

Power budget (Planck)

Similarly, the power demand of the instrument + margins and the power allocation will have to be in agreement at the PDR. In that case, the evaluation of triple junction cells might generate extra margin.

Sorption cooler Compressor thermal interfaces (Planck)

The thermal interfaces of the Sorption cooler compressor is in a dangerous situation at the SRR, due to important changes of the interface data since the ITT. The problems are being solved, but Agreement on a revised allocation might be difficult.

Cryogenics heat budgets (HERSCHEL/Planck)

The cryogenic heat budget has evolved significantly since the ITT, and endanger the lifetime in HERSCHEL, and the cooler operations on Planck. Heat budget allocations and rules on how to use them have been proposed for the SRR, to have a closer control on these points. Status should be followed in the system budgets. On HERSCHEL Impact on the instrument usage during the mission is even possible.

Mechanical load on FPU (HERSCHEL)

The Random mechanical vibration levels proposed in the IID-A are considered as high by some instruments. The problem is being solved by allowing instrument subsystems to be notched during subsystem tests.

Micro-vibrations (HERSCHEL/Planck)

The microvibration levels are now proposed (in the latest proposed IID-B) by HERSCHEL SPIRE/PACS (10 μg) and indicated by Planck HFI (goal 0.1 to 1 mg). Preliminary analysis show that the response of the complete satellite to the excitation (Reaction wheel on HERSCHEL, 4 K cooler on Planck) is 3 orders of magnitude above the proposal for HERSCHEL, and near the upper limit of the goal for Planck. A first action is to re-assess the proposed microvibration requirement.

Temperature stability (HERSCHEL/Planck)

Both satellites have units very sensitive to temperature fluctuation. HIFI Wide Band Spectrometer (0.03 K/100 s) on HERSCHEL, HFI PAU (0.1 K/h), LFI DAE (0.2 K/h).

In addition, the Planck payload although highly damped by the thermal insulation, is very sensitive to temperature fluctuation (in the microK range). Both satellites have sources of fluctuations: response of the Satellite tilting wrt Sun for HERSCHEL, sorption cooler heat peaks for Planck.

Software controlled heaters (adjustable duty cycle) is the baseline on both satellites for the thermal control, but detailed analysis of the performances will be performed.

Cooling Time cooling/failure recovery time for Planck

The cooling time of the Planck payload, especially the coldest parts inside the instruments is estimated to be long (a few months), having impact on the mission lifetime, the feasibility and representativity of thermal testing, and on the mission continuity in case of cooler or satellite failure. Heat switches have been implemented between the instruments cooling stages to significantly shorten cooldown times of he cryogenic elements of the FPUs.. They have still to be developed, qualified and tested.

6. SYSTEM DESIGN

6.1. TRADE-OFFS SUMMARY

6.1.1. Battery cells capacity

The battery cell capacity and redundancy tradeoffs are fully explained in Doc. n° H-P-RP-AI-0002, the following paragraphs provide a summary of this document. Two tradeoffs have been performed, the first to select the type of battery cells, either low capacity of high capacity and the second tradeoff to select the number of batteries.

The Cell type tradeoff compares two types of cells, the low capacity cells from AEA Technology and the high capacity cells from SAFT and Diehl & Eagle Picher.

The low capacity cells are derived from commercially produced cells suitably screened. They are connected in series to achieve the required voltage, and these strings are then connected in parallel to achieve the required capacity. This configuration is analogous to the Solar Array, the battery must be sized to tolerate a single string failure and so a battery of low capacity cells is by definition single point failure free. Since the cells are screened and well matched there is no need for external electronics to balance the cell charge/discharge. A battery of low capacity cells would use 24 parallel strings, each string having 6 cells in series.

This configuration provides:

- – 544 Wh at 70 % DoD
- – mass of 6.74 kg
- – dimensions of 320 x 220 x 100 mm
- – loss 4.2 % energy in case of 1 string loss.

The high capacity cells as their name implies offer a higher cell capacity per cell (with a similar cell voltage), thereby fewer cells are required per battery, in this case one string of 6 cells yields 832 Wh at full capacity assuming the End of Charge Voltage is terminated at 4.1 V per cell in order to be compatible with a 28 V bus. However since each cell provides a significant portion of the overall power, dedicated battery management electronics have to be utilized to ensure that the cells are correctly balanced in terms of charge, and the loss of one cell can be tolerated by using a by-pass switch. In case of a cell failure the switch losses of the lost cel battery will have significantly less capacity, which can only be compensated by the use of two batteries.

This configuration using the SAFT cells provides:

- 582 Wh at 70 % DoD with no cell failure and cells charges upto 4.1 V max.

- mass of 10 kg (including electronics)

- dimensions of 270 x 150 x 240 mm (including electronics)

- loss 16.6 % energy in case of 1 cell loss.

The Eagle Picher cells offer a similar performance to the SAFT cells but the uncertainties of the battery control electronics required by these cells (the Supplier suggests that this electronics is incorporated in the PCDU) makes these cells unattractive.

The conclusions of the cell type trade-off is that the low capacity cells offer the best mass/effects after cell failure/and price and will be selected for the next level of trade-off – the number of batteries.

The second trade-off considers the number of batteries to be used on each satellite, one, two and three battery solutions have been compared.

As already indicated in the low capacity battery description, this type of battery is designed to tolerate a loss of one cell resulting in the loss of one string. Therefore one battery could satisfy the requirements in terms of capacity and reliability aspects.

The use of two batteries offers additional redundancy with mass and additional impacts on the BDR (and of the cost of the battery procurement).

Three batteries have been considered using recurrent design from Rossetta in order to reduce procurement costs. However this solution requires an additional BDR and harness which offsets the cost savings.

The trade-off is summarized in the following table:

	One Battery	*Two Batteries*	*Three Batteries*
Configuration	One module x 6 series x 24 parallel	Two modules x 6 series x 24 parallel	Two modules x 6 series x 11 parallel
BDR Configuration	2 x 350 W BDR	2 x 350 W BDR	3 x 200 W BDR
Theoretical Energy	777Wh	1554 Wh	1068 Wh
Mass	6.75 kg	13.5 kg	10 kg
Harness and BDR modules Mass	1 kg	1.5 kg	2 kg
Dimensions	320 x 220 x 100 mm (7l)	2 x 320 x 220 x 100 mm (14 l)	3 x 260 x 125 x 100 mm (10 l)
Energy at 70 % DoD with One Cell failed	521 Wh	1065 Wh	725 Wh
Energy at 70 % DoD with One Battery failed	NA	544 Wh	498 Wh
Overall Price	X	1.5x	1.5x

Conclusion of this trade-off is that the one battery solution satisfies the power needs and provides adequate failure tolerance for the HERSCHEL - PLANCK missions.

6.1.2. PND vs AND

The trade-off related to the method to be used for nutation control on PLANCK was already performed during the proposal phase. At that time, the Passive Nutation control was selected as it was considered feasible and was leading to a simple and robust design.

At ESA request, the trade-off was re-opened at the beginning of Phase B. The actions conducted were the following:

– reassess feasibility of the PND solution

– analyse in more depth the AND solution. The related issues are:

  • required sensors for on-board nutation estimation

  • adequacy of the 1N thrusters usef for momentum control to perform control.

The detailed trade-off can be found in ALENIA document "Active Versus Passive Nutation Damping Trade-Off", Doc. n° H-P-TN-Al-0004. The following paragraphs give a summary of the results.

Concerning the PND solution, it was confirmed that the required design parameters for the PLANCK mission were outside of the conventional and already flown dampers parameters. During the proposal, this was not considered as a show stopper. However, more in depth investigation has shown that the process of detailed simulation and development testing to validate the concept was long and expensive and final proof of the concept was not ensured. For these reasons, the PND activities were put on hold and the studies focused on the AND concept.

The following methods have been envisaged for nutation estimation:

1. Star Tracker

2. STar Mapper (STM).

3. Gyro.

The solution 1 was discarded due to the high rotation rate of PLANCK (6 deg/s)

Solution 2 was analysed in detail by ALENIA and proved to be adequate. Various case have been simulated which are summarized in the following table.

Simulation case	Nutation amplitude (arcmin)	Nutation estimation error (arcmin)	Nutation estimation error (%)	Nutation phase error (deg)	Remarks
Case 1 with noise	0.9	0.074	8.2	9	Cylindrical inertia tensor
Case 1 without noise	0.9	0.022	2.4	9	
Case 2	0.1	0.02	20	34.6	
Case 3	12	0.08	0.7	9	
Case 4	1	0.123	12.3	5.6	Realistic inertia tensor

For nutation values in the order of 1 arcmin, comparable to the RPE requirement of 1.5 arcmin, the performance of the nutation estimation based on STM are good. The accuracy is in the order of 0.1 arcmin and the error on phase estimation is below 10 deg. For very low nutation amplitude (0.1 arcmin), the STM noise degrades the estimator accuray but the error remains low at 0.02 arcmin.

Simulation performed with a gyro similar to the one used on HERSCHEL showed it adequacy for nutation estimation, even in the presence of drift. For low nutation amplitude (0.02 arcmin) estimation, a signal processing algorithm had to be implemented to obtain good results.

Simulation combining estimation of the nutation by the STM and the actuation by the 1N thrusters shows that the performance of the system is acceptable. The main limitation in nutation control performance comes from the thrusters and no improvement can come from the use of a gyro.

Considering the results of this feasibility analysis, the baseline is to use AND with attitude estimation based on STM. In order to accurately estimate the control performance, a sensitivity analysis will have to be performed on influencing parameters such as inertia characteristics (inertia measurement accuracy, cross products, inertia variation along mission).

6.1.3. Turbo-coding

One trade-off requested in the system requirements (SGICD/§ 2.1.6.) is to evaluate the use of turbo encoding instead of the standard concatenated encoding scheme, (convolutional & RS encoding) on the telemetry link.

The required telemetry link quality is to have a PFL (Probability of Frame Loss) better than 10^{-5}.

This link quality is achieved with an Eb/No of 2.7 dB when using the concatenated encoding scheme (Doc. n° ESA PSS 04 103) and only with an Eb/No of 0.3 dB with the Turbo code (rate ¼, CCSDS 101.0-B-4).

Obviously this difference in bit energy/noise density is directly translated to an additional mean to improve the link budgets margin (on telemetry recovery) or to reduce the transmitted power on-board (presently sized to 30 W with a TWTA).

The aim therefore of this trade-off is to evaluate the pros and cons of this turbo encoding implementation.

The essential criterias used in this trade-off are the development status of turbo code encoders, the complexity increase in the on-board architecture, the resulting occupied frequency bandwidth and the gain on the link budgets.

On top of the trade-off on the encoding scheme it must be reminded as well that two potential modulations are evaluated for the high data rate telemetry link, one is the OQPSK modulation with baseband filtering (Roll-off 0.5), so called SRRC-OQPSK, and the other is the GMSK modulation (BTb ¼). Both modulations are also addressed in this trade-off.

The table here after summarizes this comparison:

	CONCATENATED Code	TURBO Code
Resulting coded bit rate	3.441.300 bps	6.024.300 bps
Link quality/required Eb/No	PFL < 10^{-5} Eb/No > 2.7 dB	PFL < 10-5 Eb/No > 0.3 dB
Occupied bandwidth/ spectrum shape	(see plots here after)	(see plots hereafter)
Spectral occupancy for **99%** of the transmitted power (to be compared to the allocated bandwidth of 7 MHz)	SRRC-OQPSK ~ 2.8 MHz GMSK ~ 3 MHz	SRRC-OQPSK ~ 5 MHz GMSK ~ 5.2 MHz
On-board implementation/ complexity	Existing off-the-shelf ASIC, supported by the proposed CDMU	Not yet available at CDMU level for bit rate higher than 100kbps. Possibility in the TTC transponder with existing ASICs (FPGA) already qualified.
Impact on link budgets margins	All link budgets have positive margins. **(see section § 7.1.4. of Design report)**	The use of the turbo code brings 2.4 dB additional margin on the TM recovery section for all TM rates. However the Carrier and ranging tone recovery margins are not improved.

TM spectrum bandwidth

SRRC-QPSK Power Spectrum

SRRCQPSK(f)

Frequency [GHz]

GMSK Power Spectrum

GMSK_QPSK(f)

Frequency [GHz]
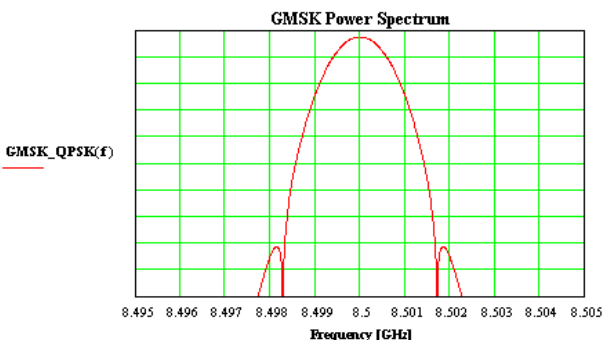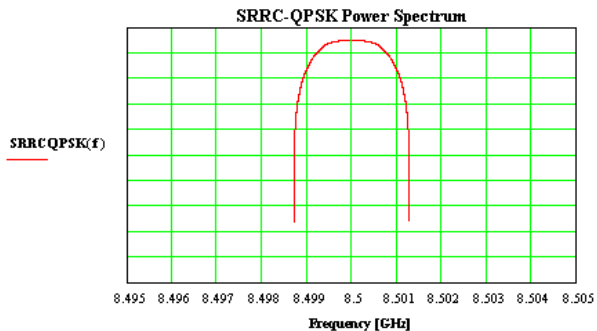
**PLOT 1: CONCATENATED
ENCODING/TM SPECTRUM**

SRRC-QPSK Power Spectrum

SRRCQPSK(f)

f1(f)
Frequency [GHz]

GMSK Power Spectrum

GMSK_QPSK(f)

f1(f)
Frequency [GHz]
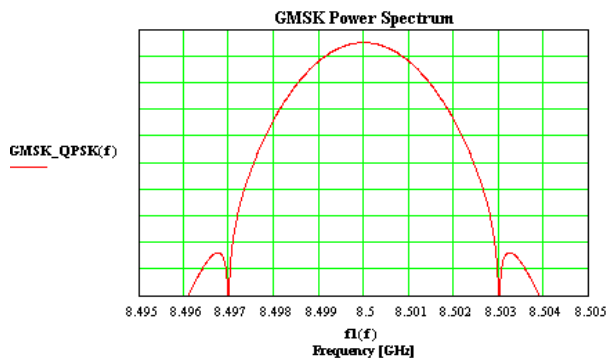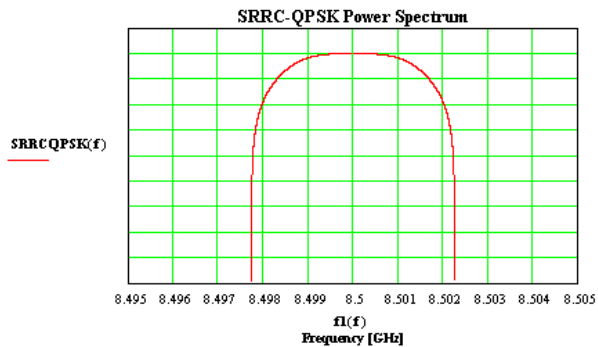
**PLOT 2: TURBO CODE
ENCODING/TM SPECTRUM**

Link budgets margins analysis

The following tables show in which way the carrier recovery margin is degraded if the turbo code is used together with a reduction of the transmitted power associated to the use of a SSPA instead of TWTA. Nota, only Kourou ground station is reported here because no problem identified when using New Norcia station.

For sake of completeness, both types of antennae (see § 6.1.5.) are still considered.

The present Tx chain uses a 30 W TWTA, and the highest RF output power available from an SSPA is 22 W (- 1.34 dB).

TYPE 1 Antennas

Herschel /Planck DOWNLINK budgets margins Comparison 30W TWTA R/S - 22W SSPA TURBO

Performances			G/S: Kourou					
			TM + RANG	TM + RANG	TM only	TM only	TM + RANG	TM + RANG
			LGA	LGA	Redundant LGAs	Redundant LGAs	MGA	MGA
			PCM(NRZ-L)/PSK/PM	PCM(NRZ-L)/PSK/PM	PCM(NRZ-L)/PSK/PM	PCM(NRZ-L)/PSK/PM	PCM(SP-L)/PM	PCM(SP-L)/PM
			30W	22W	30W	22W	30W	22W
TM Bit Rate	bps		**500**	**500 TURBO**	**500**	**500 TURBO**	**107K**	**107K TURBO**
Carr. Recov. Margin (dB)	Nom.	ESA Margin = 3dB	4.96	3.62	2.40	1.05	18.84	17.49
	Mean - 3 Sigma	ESA Margin = 0dB	2.62	1.27	0.11	-1.23	13.23	11.88
	WC-RSS	ESA Margin = 0dB	3.18	1.83	0.67	-0.68	14.22	12.87
TM Recov. Margin (dB)	Nom.	ESA Margin = 3dB	5.31	6.36	2.74	3.79	5.02	6.08
	Mean - 3 Sigma	ESA Margin = 0dB	3.50	4.55	0.90	1.95	3.37	4.43
	WC-RSS	ESA Margin = 0dB	4.03	5.08	1.44	2.49	3.84	4.90

TYPE 2 Antennas

Herschel /Planck DOWNLINK budgets margins. Comparison 30W TWTA R/S - 22W SSPA TURBO

Performances			G/S: Kourou					
			TM + RNG	TM + RANG	TM only	TM only	TM + RANG	TM + RANG
			LGA	LGA	Redundant LGAs	Redundant LGAs	MGA	MGA
			PCM(NRZ-L)/PSK/PM	PCM(NRZ-L)/PSK/PM	PCM(NRZ-L)/PSK/PM	PCM(NRZ-L)/PSK/PM	PCM(SP-L)/PM	PCM(SP-L)/PM
			30W	22W	30W	22W	30W	22W
TM Bit Rate	bps		**500**	**500 TURBO**	**500**	**500 TURBO**	**107K**	**107K TURBO**
Carr. Recov. Margin (dB)	Nom.	ESA Margin = 3dB	5.20	3.85	3.12	1.77	21.85	20.50
	Mean - 3 Sigma	ESA Margin = 0dB	2.08	0.74	0.10	-1.24	16.24	14.89
	WC-RSS	ESA Margin = 0dB	2.78	1.43	0.71	-0.64	17.23	15.88
TM Recov. Margin (dB)	Nom.	ESA Margin = 3dB	5.55	6.60	3.46	4.52	5.02	6.08
	Mean - 3 Sigma	ESA Margin = 0dB	2.71	3.77	0.73	1.78	3.37	4.43
	WC-RSS	ESA Margin = 0dB	3.44	4.49	1.36	2.41	3.84	4.90

From the here above data it is not seen as acceptable to move to the turbo code & SSPA architecture because the carrier recovery margins would become negative.

The only rationale to use the turbo code would then be to get more comfortable margins on the telemetry recovery but as presented also in the here above summaries, the concatenated coding & TWTA are already meeting the required link budgets margins.

It must be realized also that the use of an SSPA would decrease significantly the DC power efficiency (25 % for SSPA against 50 % for a TWTA) leading to a power increase from 65 W (TWTA) to 90 W (SSPA).

Conclusion

The use of turbo code brings additionnal margin on the TM links for all data rate which makes the system margins more comfortable, but doesn't bring any advantage for the Ranging link, nor at Carrier level.

It is excluded to reduce the transmitted power by for instance using an SSPA instead of a TWTA, because this would lead to negative margins on the Carrier recovery and Ranging recovery sections.

No particular concern exists about the space qualification of the intended ASIC (well known technology and proven device) but the hosting unit (CDMU or TTC transponder) will require a design upgrade for the turbo code implementation.

Also, the preferred modulation scheme is in any case the SRRC-OQPSK because it offers a higher spectral efficiency and belongs to the existing on-board modulators, whereas the GMSK is still not off-the-shelf.

The resulting occupied bandwidth is acceptable, i.e. 99 % of the transmitted power fits in the allocated band, but assuming the use of a baseband filtering if the OQPSK modulation is chosen, or without any filtering if the GMSK modulation is selected.

Compatibility with the ground segment has still to be confirmed and inputs from ESA are expected to close this assessment.

In the view of here above arguments, it is not recommended to use the turbo code, because the expected risks in terms of cost and delay with a new design development for CDMU or TTC transponder are not justified by the existing system telemetry margins obtained with the standard concatenated encoding.

6.1.4. Instrument Data Rate

In RD01.2 "Instrument data rates Technical Note" a preliminary study of the Packet Structure ICD has been performed together with how this maybe implemented on the HERSCHEL PLANCK satellites.

The purpose of RD01.2 was to identify if the data rates requested by the instruments are compatible with the MIL-1553 bus, ESA Packet Structure Protocol and with the mass memory and RF downlink constraints.

It became clear in the early part of the study that the use of data rate expressed in kbps (kilo bits per second) is misleading. Due to the packet structure, the requested data rate can only be achieved if the packets are completely full of useful data, i.e. if the user decides to send very small packets (inefficient), then while the datarate on the bus remains the same, the actual data rate of real useful data is very low since a smaller packets have a proportionately higher overhead. Also the use of high data rates for the burst mode (as requested by a couple of instruments) can be accomplished by the data bus but there are other constraints in the storage of his data and of downlinking it to ground.

The MIL-1553 bus is a serial, full multiplex bus running at 1 Mb/s. At 1553 level data is moved around as 20 bit words, of which 16 bits are useful data, the other 3 bits are for synchronisation and 1bit for parity check. The MIL-1553 protocol requests control words and data words. A control word will be a word which may specify the type of data for up to the next 32 MIL-1553 words. A MIL-1553 message may be up to 32 words long, that means 32 x 20 bits = 640 bits of which only 16/20 bits are useful = 512 bits. In addition to the control word overhead there are also delays on the bus which are identified as TBD in the Packet Structure ICD. However the Packet Structure ICD simplifies the life for the bus user and insulates the user from the MIL-1553 constraints by specifying a higher level protocol by introducing introduces the notion of Frames, Subframes and Message Slots.

A 1 second interval is defined as 1 FRAME. This FRAME is divided by 64 to produce a subframe, the resulting time duration of a subframe is 15.625 mS.
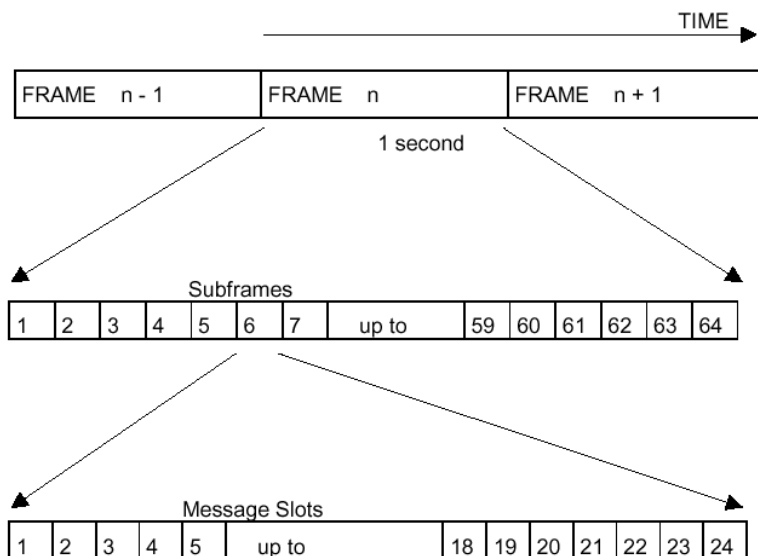
Definition: 1 FRAME = 64 SUBFRAMES ; 1 SUBFRAME = 24 MESSAGE SLOTS

Duration: 1 FRAME = 1 second: 1 SUBFRAME = 1/64 second; 1 SLOT = see table 4.1

Each subframe is divided (not equally) as 24 slots, some slots are for subsequent subframe control and low level TC/TM, however the majority of these slots (16) are reserved for Packet Transfers.

Each Packet Transfer Slot has a duration of 750uS, which is enough time for 1 complete MIL-1553 message (with the control word and bus delay times), i.e. 512 useful bits of data can be sent in one Packet Transfer Slot, so since there are 16 slots per subframe there can be a maximum of 8192 bits of Packet transfer data sent per Subframe. (8192 bits just happens to correspond to 1 kbyte or 1 ESA packet of the maximum size) !

We can conclude that each subframe can be used to transfer up to 1 kbyte to/from one user per subframe, so if we want to increase the user data rate we should increase the number of subframes allocated to that particular user.

At the risk of repetition, it must be stressed that a particular subframe is dedicated to a particular user for the packet transfer of data, if the user fills the subframe with data then the data rate will be optimized, if the user selects to transfer very small packets then the effective data rate will be low.

Only one packet will be sent per subframe, this simplifies the allocation of the subframes since in this way we can guarantee that there is no risk of trying to send several packets (each one could be of different length) with the result that the last packet is too long and would be truncated.

Considering the nominal needs of the instruments for HK TM and science data traffic on the databus and the probable needs of the platform systems, the outcomes of the initial study are:

- 1 subframe allocated for each user for HK data

- 4 subframes allocated for TC and time distribution

- 2 subframes allocated for AOCS TM

- 1 subframe allocated for AOCS TC

- 1 subframe allocated for PCDU TM

- 5 subframes allocated for TC acknowledge (but these subframes may be used for HK TM/TC since the TC acknowledge my be sent via event TM packets as described in the Packet Structure ICD)

– all TC to the PCDU sent using the low level commands within each subrame

– all Event and reporting to use the 1 asynchronous packet available within each subframe

– users polled every 6 subframes to see if they have an event packet to deliver (this implies that there will be a latency of up to 100 mS between reporting the event and the event packet being acquired)

– 18 subframes to be allocated for HERSCHEL Science data (for HIFI + PACS + SPIRE) in nominal mode, which is the equivalent of 147.5 kps if all the available packet capacity is utilized

– 18 subframes to be allocated for PLANCK Science data (for LFI + HFI).

The number of subframes may be increased for the science data to cope with the "burst" mode of the instruments, however the overall amount of data must be limited so that the mass memory and downlink constraints are not exceeded. A maximum average data rate of 140 kps has to be considered for the **total of all** instruments for both HK + science data for each satellite to be compatible with mass memory storage and downlink capabilities.

6.1.5. PLANCK redundant LGA

The PLANCK TTC subsystem includes three Low Gain Antennae (LGA), located on the side walls and the bottom of the SVM in order to provide an omnidirectionnal coverage without any interference with the telescope.

The antenna located on the bottom is the nominal LGA, oriented toward Earth, that ensure a perfect TM/TC link at L2 point whereas the two lateral ones are considered as redundant antennae to be used in case of emergency. By analysis at system level the precise positioning of these two redundant antennae with respect to the structure has been optimized in order to make maximum use of the reflections on the structure and reach an omnidirectionnal coverage.

The optimized configuration is the following:
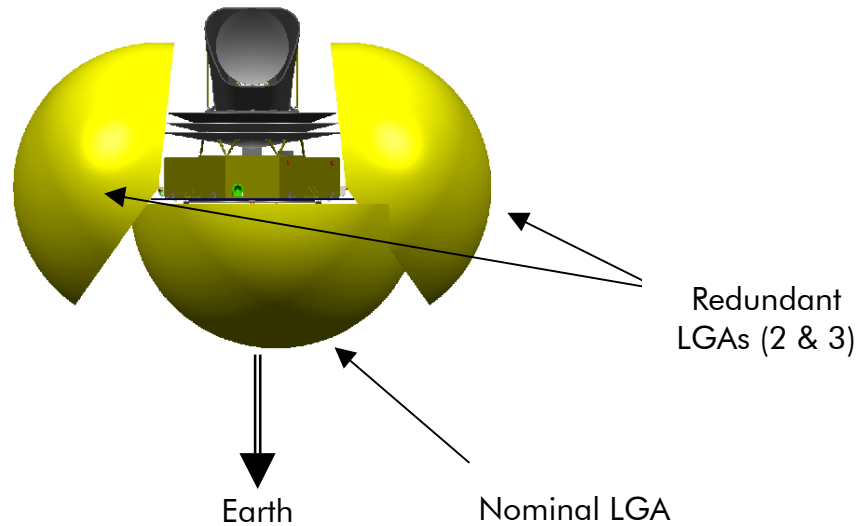
To refine this ideal coverage, two potential antennae have been then considered, a printed helices antenna (Type 1) and a horn type antenna (Type 2).

From the far field radiated pattern without any structure, the system modelling has been updated to compare both types of antenna.

The Type 1 pattern is derived from an existing S-Band antenna, scaled to the X-Band frequency:
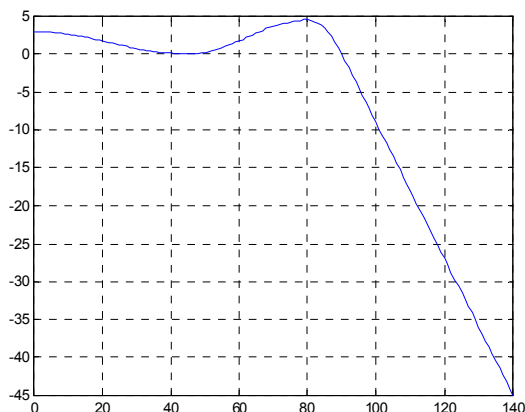
FIGURE 6.1.5-1 TYPE 1 ANTENNA/FAR FIELD GAIN PATTERN

The Type 2 antenna corresponds to an existing X-Band horn:
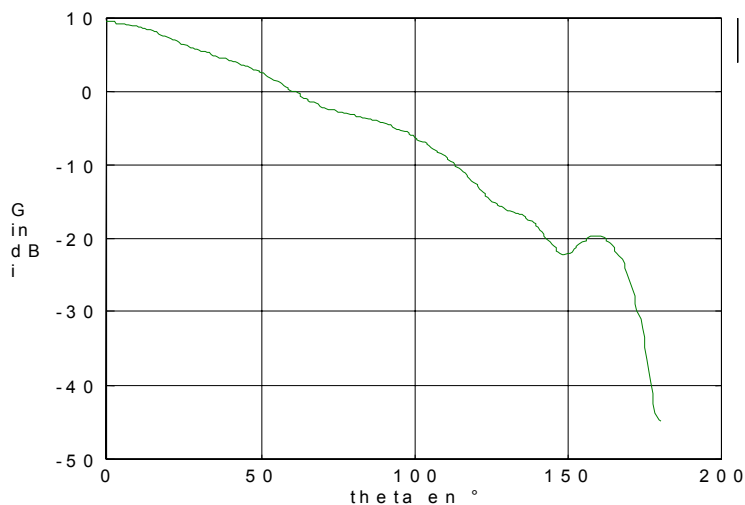
FIGURE 6.1.5-2 TYPE 1 ANTENNA/FAR FIELD GAIN PATTERN

The aim of the modelling at system level has been to assess the resulting coverage of the two redundant LGAs, with interferences to the structure.

The following 3Ds views show which antenna gets closer to the expected hemispheric coverage, for a given gain of - 3 dBi which corresponds to the nominal figure of the TTC link budgets:
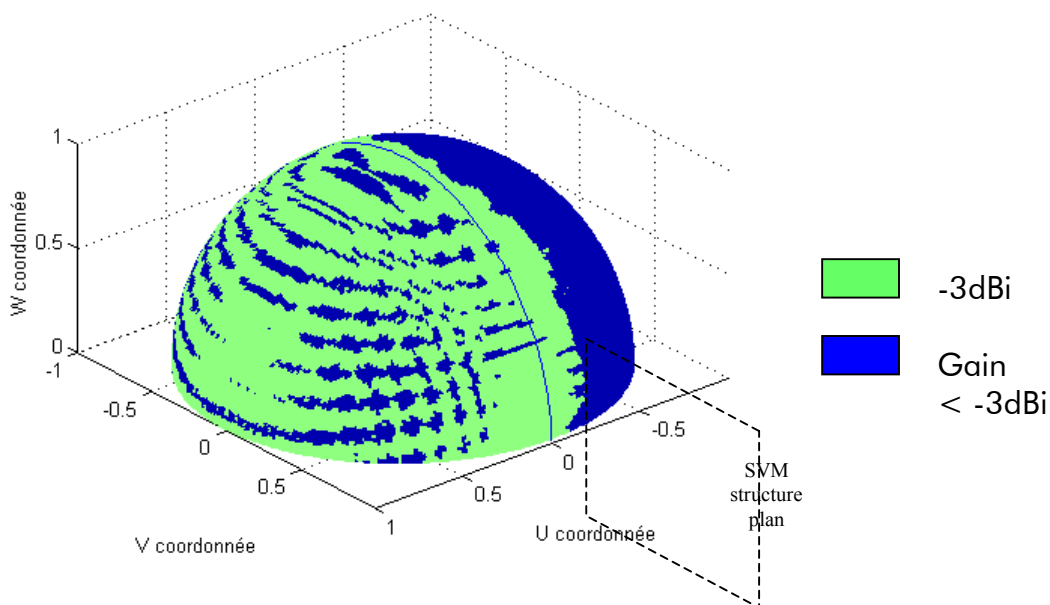
FIGURE 6.1.5-3 TYPE 1 ANTENNAE/GAIN PATTERN WITH STRUCTURE IMPACT
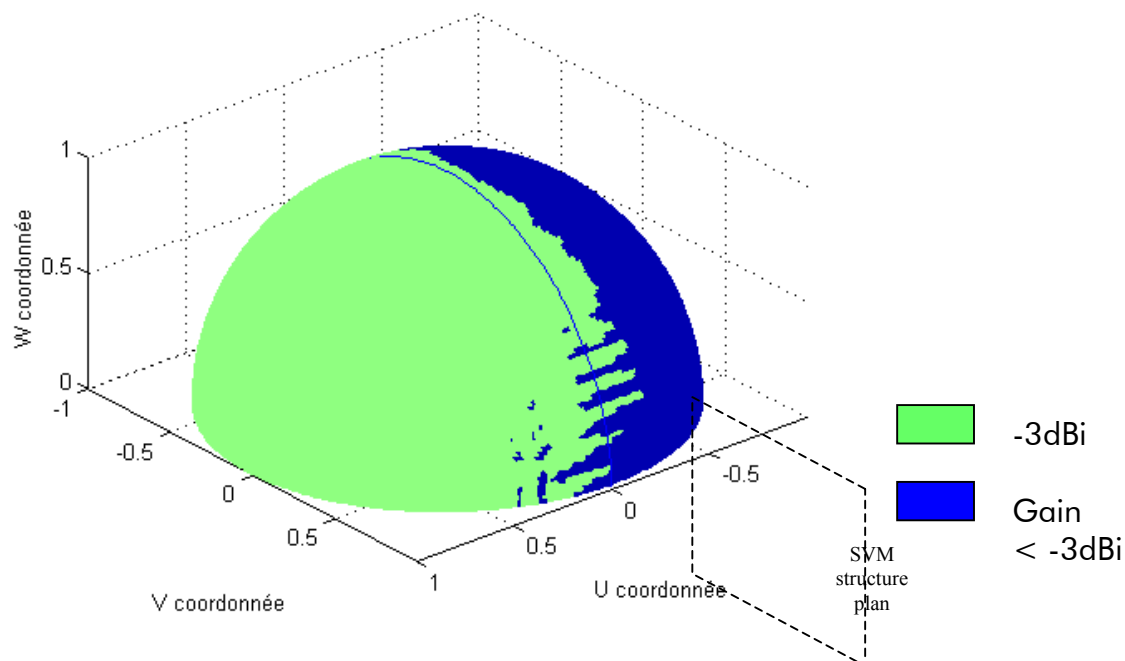
FIGURE 6.1.5-4 TYPE 2 ANTENNA/GAIN PATTERN WITH STRUCTURE IMPACT

From this reduced modelling, including only one half of the structure, it clearly appears that the upper elevation angles of the Type 2 antenna contribute to a more homogeneous hemispheric coverage with the structure impact.

To confirm this engineering feeling the modelling has been completed with the second redundant LGA in order to show that the dark area of the figure here above is compensated by the second redundant antenna.
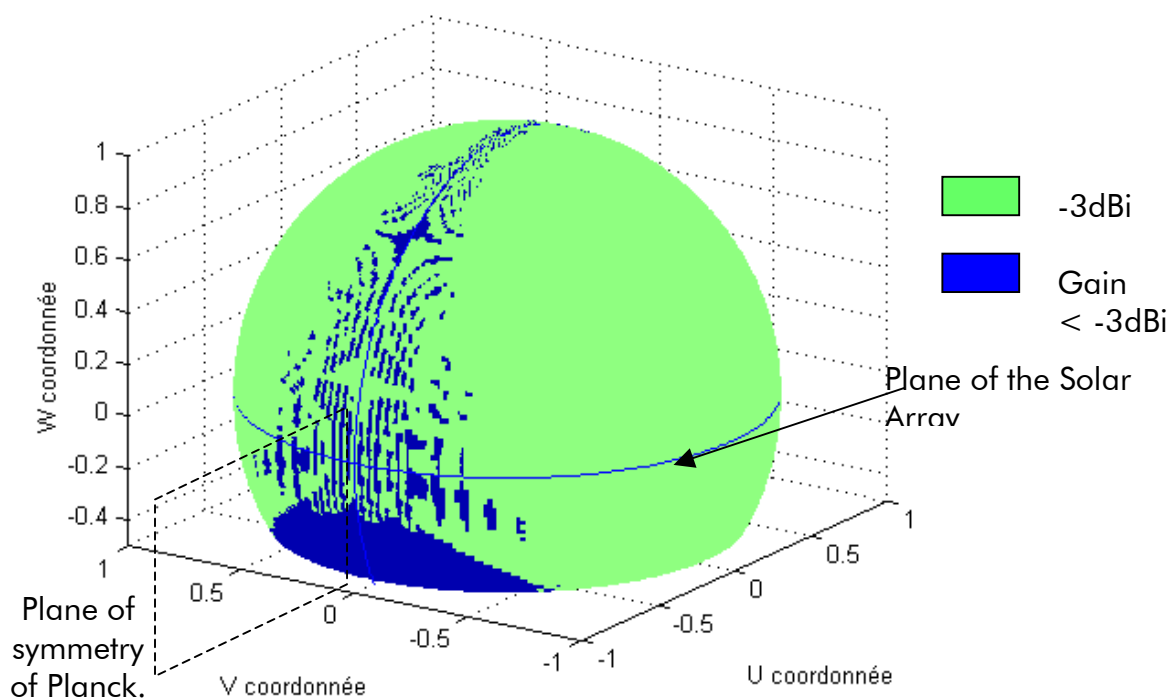
FIGURE 6.1.5-5 REDUNDANT LGAS COUPLED PATTERN/TYPE 2 ANTENNAE

Conclusion

The LGA positioning on PLANCK was originally optimized with ideal hemispheric antennae, however the Type 2 antenna taking into account the multiple reflections on the structure, is getting very close to the expected omnidirectionnal coverage. A precise modelling of the three LGAs (including the nominal one) leads to about 95 % with a - 3 dBi gain, and 97 % with a gain of - 5 dBi.

It is therefore recommended to select and antenna of the Type 2 design (horn) instead of the Type 1 (printed helices).

6.1.6. Sunshield/Sunshade

During the proposal phase, the Sunshield/Sunshade (SSH/SSD) activities for HERSCHEL have been performed in parallel by ALCATEL and ASTRIUM. This resulted in two different configurations, sharing however large commonalities (see following figure).

ALCATEL DESIGN   **ASTRIUM DESIGN**
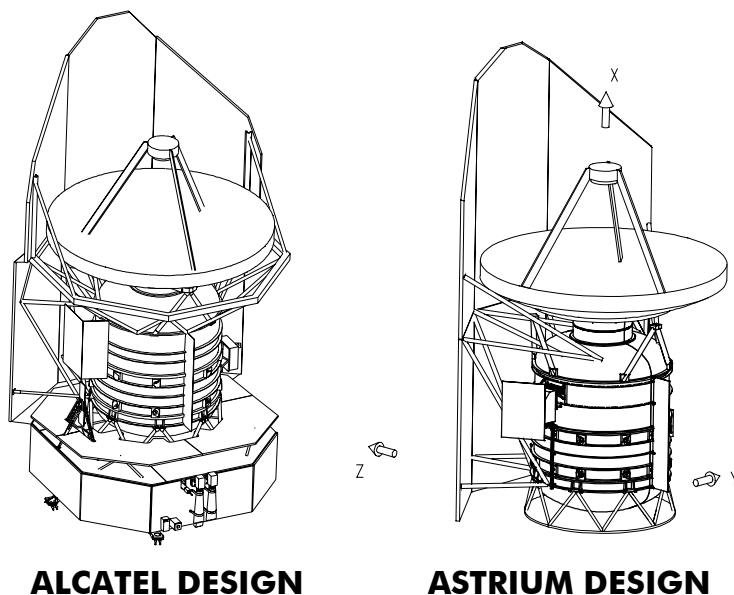
In the work share among the core team members, the SSH/SSD is part of the H-PLM, so definition of the new SSH/SSD baseline was performed by ASTRIUM. An analysis of the 2 configurations was performed and the most promising design features of each variant were introduced into the baseline.

The two designs from the proposal are built around the same elements:

– a Sunshield protecting the Cryostat. It also has the function of solar generator and thus is covered by solar cells

– a Sunshade protecting the Telescope. It is covered with OSR in order to minimise the Telescope temperature

– a supporting truss linking the SSH/SSD to the CVV.

Both Sunshield and Sunshade consists in 3 flat panels made of sandwich form with CFRP sheets. Their back side is covered with 20 layers of high efficiency MLI.

The main difference between the ALCATEL and ASTRIUM came from the supporting truss:

- in the ALCATEL solution the Sunshield and Sunshade were not coupled mechanically, thus leading to good thermal decoupling: this resulted in the implementation of a large circular frame to implement the Sunshade. The orientation of the SSH and SSD lateral panels were different to be optimal w.r.t. the fairing envelope

- in the ASTRIUM solution, the SSH and SSD forms and integrated assembly. The mechanical link between SSH and SSD has also to provide thermal decoupling. Additional attachment points on the CVV were used to connect the struts. The main drawback of this solution was that it did not meet the SSH/SSD frequency requirement of 40 Hz defined to avoid coupling with the satellite main modes.

The new baseline takes the same integrated SSH/SSD concept than the ASTRIUM solution. This allows to delete the SSD supporting frame which was inducing a heat load of 0.23 W to the CVV radiator. Work has then focussed on the optimization of the supporting truss to meet the 40 Hz frequency requirement. The main modifications w.r.t. the ASTRIUM proposal configuration was to add an additional stage of struts attaching the SSD to the CVV. In addition, the struts linking the SSH lower end to the CVV are now connected to the SVM to reduce the heat flow into the CVV. The final configuration is shown in the following figure. Details on the SSH/SSD are given in the H-EPLM Design Description.
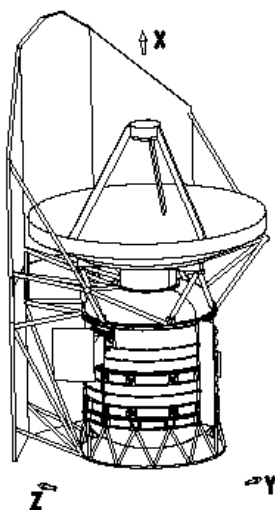
Further work is planned to be performed to optimize the struts sizing. Possible relaxation of the frequency requirements will also be investigated to analyse its impact on mass and lifetime.

6.1.7. DC/DC Synchronization

The need for the DC/DC synchronization has been discussed in depth with all the instruments, since it is the instruments needs which would require the implementation the synchronization, either only at instrument level or for the complete satellite. The outcomes of these discussions may be summarized in the following table:

Cons for the use of DC/DC synchronisation.	Pros for the use of DC/DC synchronization.
Extra complexity of DC/DC converter design.	A completely synchronized system will ensure that the noise spikes are within a fixed and defined frequency range.
Extra complexity & mass of providing & routing DC/DC sync lines.	If a synchronized system is implemented, then the synchronization can always be turned off should it be found to be unnecessary during testing.
Synchronization to system supplied clock is not always optimum for the instrument DC/DC.	
Even a "synchronized" system is not totally synchronized due to different delays and reaction times of the different DC/DC converters.	
The proposed design comprises many "Off-the shelf" units which do not offer the synchronization capability and would require modification if DC/DC sync were utilized.	
Instruments would have to be able to operate in free-running mode anyway.	
Increased number of configurations to test at unit, instrument and system level.	
Instruments have no need to synchronise with the system or other instruments, synchronisation within the instrument maybe desirable for HFI.	

The instruments did not demonstrate any real need for synchronization, either with the other instruments or with the SVM units, and after initial discussions PACS specifically wanted the sync to be removed.

HIFI did not indicate any preference for a non-sync or a synchronized system.

LFI identified a need for having a number of instrument DC/DC converters synchronized with each other, they will manage this within the LFI instrument and select and generate the most appropriate synchronization frequency.

HFI did not require DC/DC sync, they only need a stable 131072 Hz clock for timing aspects. This clock will be provided as derived from the system CDMS master clock and it has nothing to do with the synchronization of DC/DC converters.

Conclusion

The discussions with the instruments have concluded that no advantages of having a synchronized system have been identified, and the complexity of implementing the DC/DC synchronization and the extra testing does not justify the slight possibility that a synchronised system may improve instrument performance. It has been commonly agreed not to have system synchronized DC/DC converters for the HERSCHEL & PLANCK satellites.

6.2.   MECHANICAL AND THERMAL SYSTEM DESIGN

6.2.1.   Spacecraft overall configuration

6.2.1.1.   HERSCHEL Spacecraft

Recall of overall configuration

The overall configuration of HERSCHEL spacecraft is displayed in Figure 6.2.1-1.

The current HERSCHEL configuration is still close from HERSCHEL configuration at start of Phase B.

HERSCHEL S/C is of a modular concept, and is basically composed of two modules:

- the **H-PLM** (HERSCHEL PayLoad Module) which includes:

  - a cryostat in which the focal plane units are implemented, carrying external instruments as the LOU (part of HIFI) and the BOLA (part of PACS)

  - a 3.5 m Telescope supported on the top of the cryostat

  - a sunshield and sunshade shadowing the cryostat and telescope from Sun illumination. The sunshield also carries the Solar Array.

- The **SVM** (SerVice Module) is formed by an octagonal box built around a conical tube, which:

  - houses the equipment of the Avionics and Servicing S/S's, the payload "warm" boxes for HIFI, PACS and SPIRE Instruments; HERSCHEL SVM is designed to provide the various equipment and instruments housed in it with suitable mechanical and thermal environments during launch and in orbit phases

  - supports with the H-PLM Cryostat support truss; it supports also the SVM Shield on its top, used for radiative de-coupling with the cryostat

  - ensures the mechanical link with the Launcher adaptor, and therefore ensures the main load path during launch.

As a recall HERSCHEL and Planck SVM present a lot of communality at SVM level, as explained in details in the SVM Design Report.

FIGURE 6.2.1-1 HERSCHEL SPACECRAFT OVERALL CONFIGURATION

Main updates since ALCATEL proposal of December 2000

Main updates since proposal refer to the System configuration, H-PLM configuration, and to a lower extend to the SVM configuration.

–   Update of System configuration:

It is fed by all detailed changes part of Instruments, and SVM and H-PLM update as detailed below. This conducts to a S/C overall configuration very close to the original configuration.

However, it is to be mentioned that a certain number of configurations changes affect SVM and H-PLM configurations:

•   change of LOU wave-guides supporting from the SVM to the H-PLM, for design and interface simplification.

- Translation of H-PLM to SVM interface, from the top of the CVV supporting to the bottom of it:

  This change corresponds to the transfer of CVV supporting from SVM responsibility to H-PLM responsibility. It is associated also with a transfer of responsibility for the SVM shield. These changes require a complete review of mechanical and thermal interfaces between SVM and H-PLM, as developed under § 6.2.2.2.

– Instruments update: reflected under SVM and H-PLM configurations update.

– Update of H-PLM configuration: refer to the H-PLM Design Report. A summary of the modifications is given in Section 6.2.2.2.

– Update of SVM configuration:

  It is mainly related to the update of Instruments accommodation in a few area, according to the first discussions with Instruments. It includes also a consolidation of the SVM mechanical design in some area.

Additionally, it is to be mentioned that a certain number of evolutions for HERSCHEL configurations are currently in study. Refer to § 6.2.2.2. for more details.

6.2.1.2.   Planck Spacecraft

Recall of overall configuration

The overall configuration of Planck spacecraft is displayed in Figure 6.2.1-2.

As for HERSCHEL, Planck configuration does not present important changes relatively to Planck configuration at start of Phase B, as issued from ALCATEL proposal of December 2000.

Planck S/C remains also of a modular concept, and is basically composed of two modules:

– the **PLM** (PayLoad Module) which houses the "cold" part of the satellite and the focal plane unit. Its main constituents are:

  - the Cryo structure supporting the telescope

  - the Focal Plane Unit with associated electronics and cooling systems accommodated on the PPLM, and on the SVM structure via the Payload sub-platform and lateral panels

- the main baffle enclosing the telescope and the FPU, for stray-light protection.

– The **SVM** (SerVice Module) is formed by an octagonal box built around a conical tube, which:

- houses the equipment of the Avionics and Servicing S/S's, the payload "warm" boxes for HFI and LFI Instruments; Planck SVM is designed to provide the various equipment and instruments housed in it with suitable mechanical and thermal environments during launch and in orbit phases

- supports with the H-PLM Cryostat support truss; it supports also the SVM Shield on its top, used for radiative de-coupling with the cryostat.

- ensures the mechanical link with the Launcher adaptor, and therefore ensures the main load path during launch
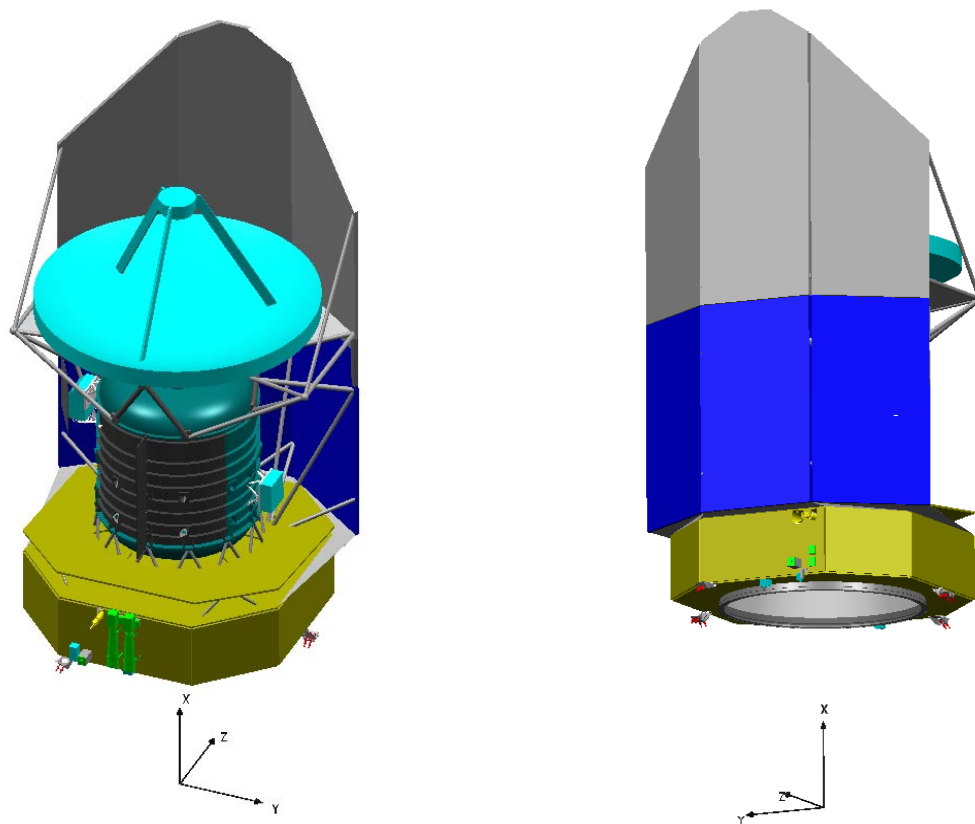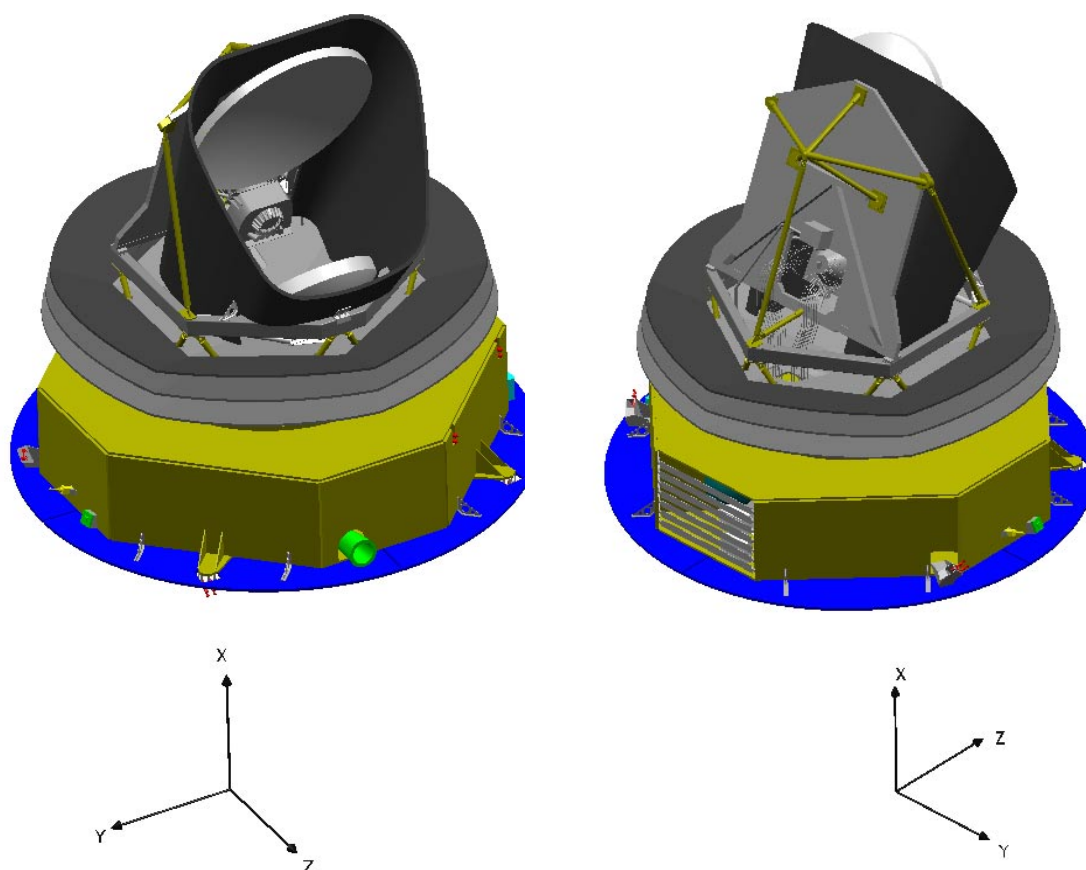
FIGURE 6.2.1-2 PLANCK SPACECRAFT OVERALL CONFIGURATION

Main updates since ALCATEL proposal of December 2000

Main updates since proposal refer to the System configuration, P-PLM configuration, and to a lower extend to the SVM configuration.

– Update of System configuration:

- update of S/C configuration:

It is feed by all detailed changes part of Instruments, and SVM and P-PLM modules update as detailed below. This conducts to a S/C overall configuration which is apparently rather similar to the original configuration. The most visible change stays in the P-PLM configuration, with an height increase affecting by the fact the overall S/C height.

– Instruments update: reflected under SVM and P-PLM configurations update.

– Update of P-PLM configuration: refer to the P-PLM Design Report. A summary of the modifications is given in Section 6.2.3.2.

– Update of SVM configuration:

It is mainly related to the update of Instruments accommodation in a few area, according to the first discussions with Instruments. It includes also a consolidation of the SVM mechanical design in some area.

Additionally, it is to be mentioned that a certain number of evolutions for HERSCHEL configurations are currently in study. Refer to § 6.2.3.2. for more details.

HERSCHEL configuration

6.2.2.1. Axis convention

HERSCHEL satellite reference frame (O, X_X, Y_X, Z_x) is a right-handed Cartesian system with:

- its origin O is located at the point of intersection of the longitudinal launcher and the satellite/launcher separation plane; the origin coincides with the centre of the satellite/launcher separation plane

- Xs-axis coincides with the nominal optical axis of HERSCHEL telescope. Positive XS-axis is oriented towards the target source.; the XS-axis coincides with the launcher longitudinal axis

- Zs is in the plane normal to XS-axis, such that nominally the Sun will lie in the (XS, ZS) plane (zero Roll angle with respect to Sun). Positive ZS-axis is oriented towards the Sun

- Ys completes the right handed orthogonal reference frame.
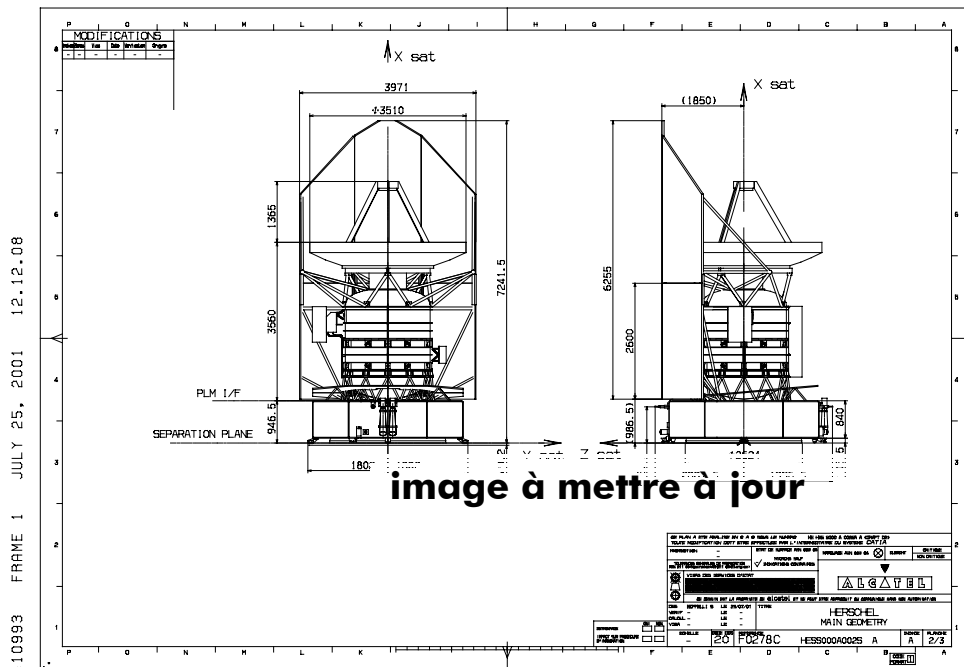
FIGURE 6.2.2.1 HERSCHEL SPACECRAFT AXES

HERSCHEL mechanical design

As explained above, HERSCHEL configuration presents for SRR a certain number of evolution and possible further evolutions in study. These configuration updates, constituting the current baseline or auguring a new baseline are presented hereafter with some details.

Update of System configuration

Update of S/C configuration

HERSCHEL overall configuration is rather similar to the proposal configuration. The most visible change stays in the SSH/SSD configuration with a modified SSH/SSD supporting and modified SSD shape. The S/C overall dimensions are almost unchanged.
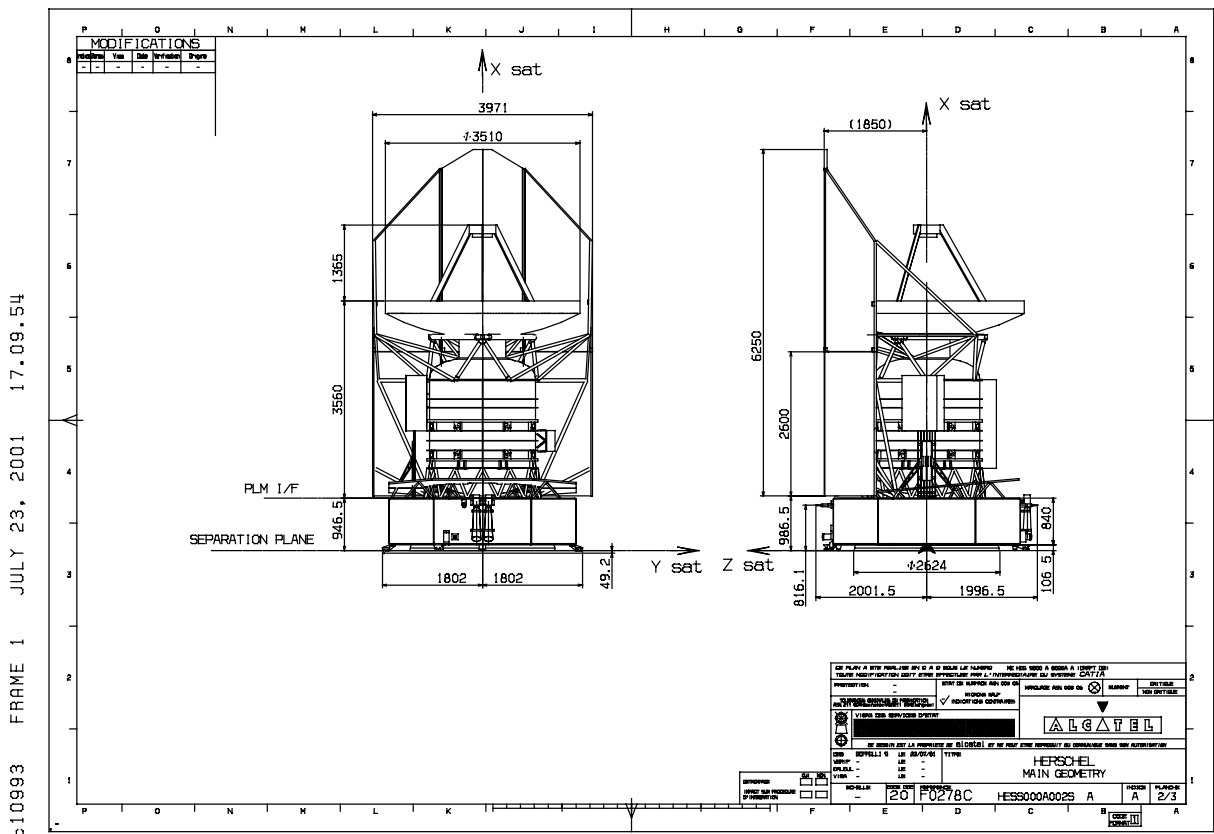
Status of H-PLM to SVM interface

The H-PLM to SVM interface was to be modified at beginning of Phase B to take into account the inclusion of the PLM supporting truss into the PLM, while the previous interface definition was including this truss in the SVM.

This change required a lot of effort to update module specifications impacted by this change, namely the SVM Interface specification and H-PLM Interface specification. From a mechanical point view, it conducted to review completely the definition of allocated volume, module interfaces and stiffness requirements and interface loads.

The current definition of these interfaces is as follows.

Allocated volumes for SVM and H-PLM

As shown in the following figures, allocated volume for HERSCHEL SVM and PLM are consistent and complementary, at their common boundary.

Both have to respect allocated volume beneath ARIANE 5 fairing, at the difference that:

  – HERSCHEL SVM has to deal with limits at the bottom of the separation plane with the Launcher

  – HERSCHEL PLM has to deal with limits at the top of the fairing.

Additionally, the definition of HERSCHEL PLM allocated volume with vertical flats takes consideration of TTC antennae field of view, accommodated on SVM panels.

ME.FST.RPA0.F.0017B.C

GENERAL VIEWS IN ALLOCATED VOLUME

SHEET 1/3

SUN SHADE

PLM

SUN SHIELD

SVM SHIELD

HERSCHEL PLM OVERALL GEOMETRIES
AND ALLOCATED VOLUME

14.16.08   JUNE 27, 2001   FRAME 1   c10993

ME.FST.RPA0.F.0018A.B

GENERAL VIEW IN ALLOCATED VOLUME

SHEET 1/3

SVM BOX

HERSCHEL SVM OVERALL GEOMETRY
AND ALLOCATED VOLUME

10.15.06   JULY 10, 2001   FRAME 1   c10993

DRAFT
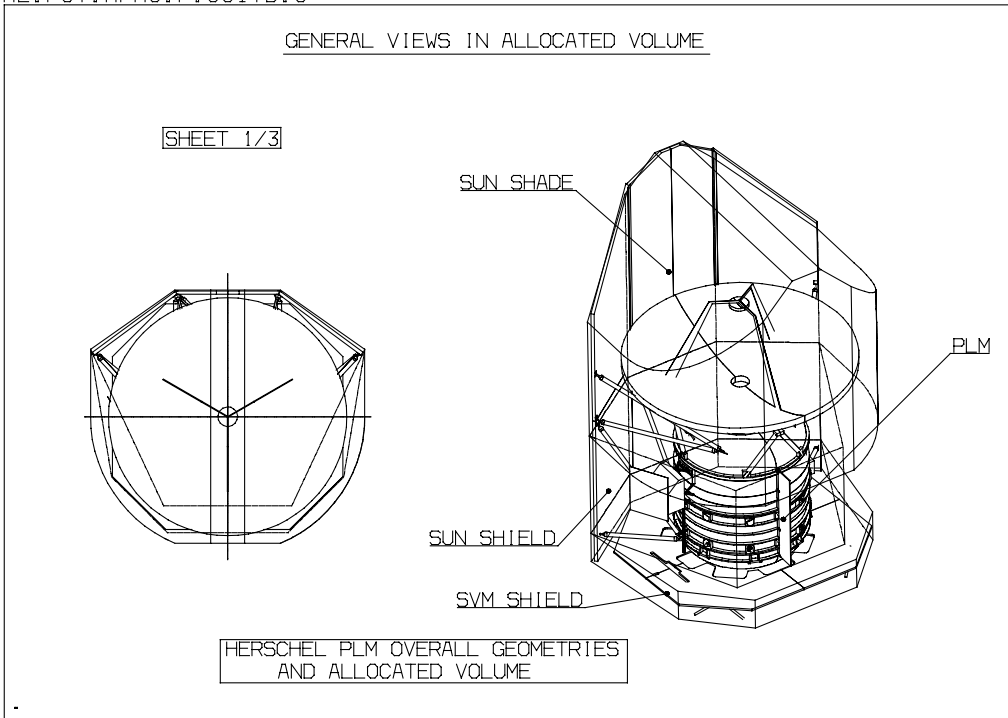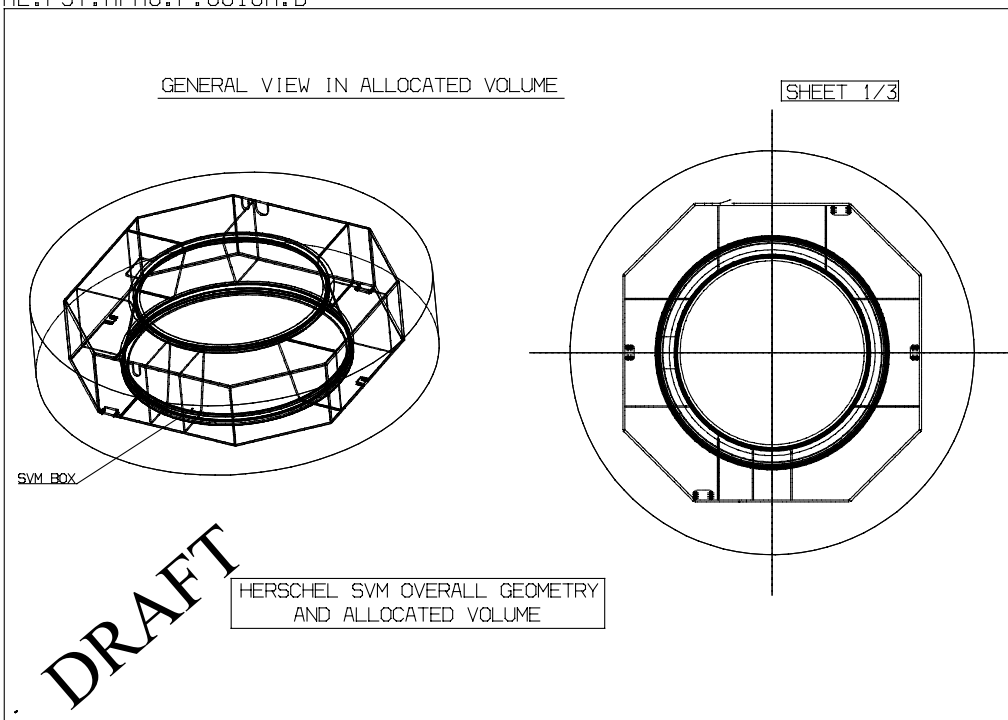
Module interfaces

At the present time, it is considered that Modules interfaces are preliminary defined, considering that the SSH/SSD supporting design may evolve, and that the CVV supporting struts with 24 struts as to be confirmed as baseline. The following figures shows this preliminary interface definition.

ME.FST.RPA0.F.0002A.C

HERSCHEL SVM: INTERFACE WITH CCV STRUTS

SHEET 2/3

ME.FST.RPA0.F.0002A.C

HERSCHEL SVM: INTERFACE WITH SSH STRUTS

SHEET 3/3
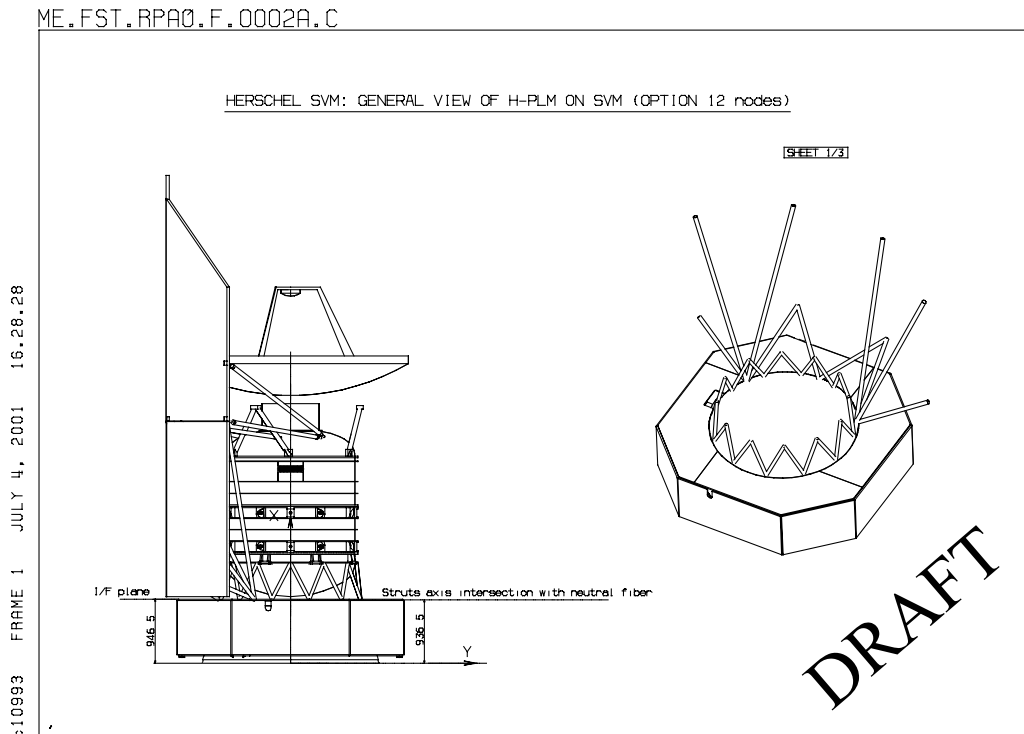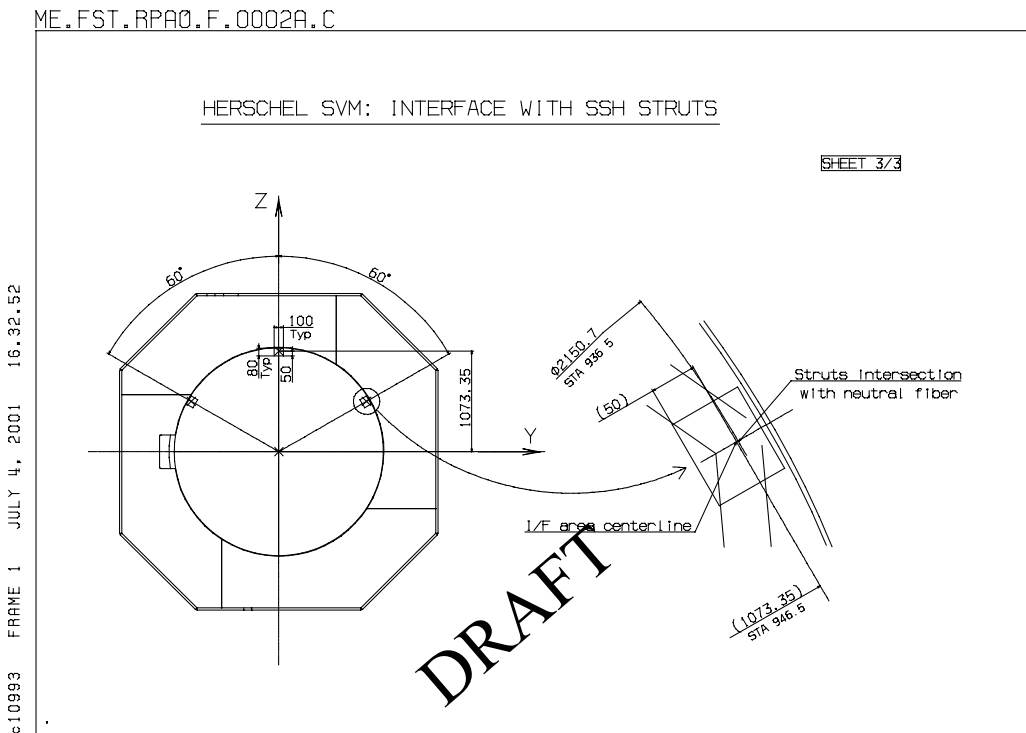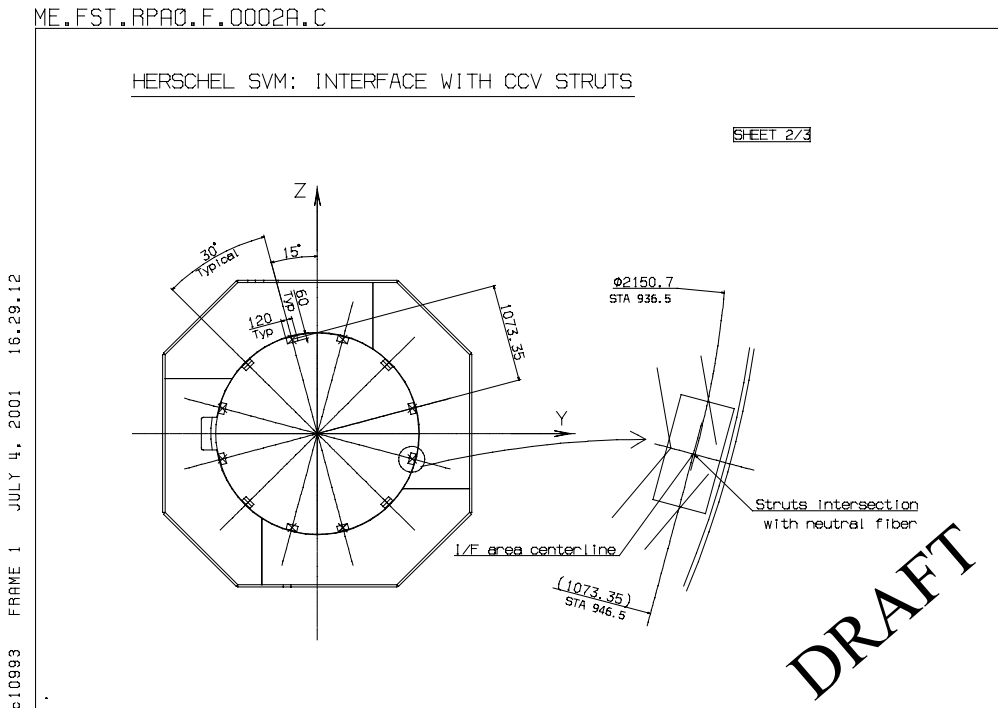
Stiffness requirements

In the same way, stiffness requirements have been defined considering CVV supporting struts combined with H-PLM. Stiffness requirements are declined in frequency requirements and rigidity requirements. Frequency requirements qualify the global stiffness behaviour of these modules, in consistency with stiffness requirements to be achieved at System level. On the other hands, rigidity requirements are defined at SVM level only, in complement to frequency requirements, to qualify local stiffness needs at specific interfaces.

As examples, frequency requirements for SVM and H-PLM are defined as follows:

SVM frequency requirement

SVM design shall ensure that eigen frequencies of Herschel main global modes fulfil the following requirements:

- longitudinal main mode > 58 Hz

- lateral main mode   > 23 Hz

considering a H-PLM of **2127 Kg** at an absolute location X = **2.71 m.**

H-PLM frequency requirement

The eigen frequencies of H-PLM main global modes shall fulfil the following requirements:

- longitudinal main mode > 35 Hz

- lateral frequency   > 13Hz

considering following local stiffness at each of SVM interface nodes:

- k circumference   >   5.7 E 7   N/m

- k radial   >   2.5 E 7   N/m

- k longitudinal (X)   >   5 E 7   N/m

- rotational dof are free.

Interface loads

At the present time, it is also onsidered that interfaces loads are preliminary defined, considering that the SSH/SSD supporting design may evolve, and that the CVV supporting struts with 24 struts as to be confirmed as baseline.

As an example, the basic interface loads at SVM to H-PLM interface (CVV struts roots) are to be simply calculated by application of QSL loads at CVV CoG, considering same H-PLM characteristics as for SVM frequency requirement:

LOAD CASES	X AXIS	Y AXIS	Z AXIS
1	10 g	/	0.5
2	/	3. g	/
3	/	/	3.25 g

TABLE 6.2.2.2-1 H-PLM TO SVM INTERFACE LOADS

Status of instruments interfaces and accommodation

As a general rule, all agreed changes in Instruments definition and interfaces, changes in Instruments accommodation in H-PLM or in SVM, will lead to update Instruments interfaces in a next IID-A Vversion.

However, it is to be recalled that a lot of Instruments changes since IID-B Issue 1/0 are not agreed, and are still in discussion with the Instruments.

6.2.2.2.2. Update of H-PLM configuration

The mechanical description of the H-PLM baseline can be found with details in the H-PLM Design Report. The main design updates can be summarized as follows:

- CVV supporting and SVM shield implemented in H-PLM

- update of SSH/SSD configuration: one baseline (achieving mechanical stiffness req.), and an option (more favourable for thermal performances, but with degraded mechanical performances).

- Update of CVV design, including mainly:

  - consideration of new SSH/SSD struts fixation on CVV structure

- refinement of OB concept, which is now in Aluminium

- refinement of He Tank and supporting concepts (suspensions and SFW), close anyway to proposal concept.

– Set-up of MLI blankets at the bottom edge of SSH/SSD (not yet shown in ASTRIUM configuration), for SAA protection during L2 injection by the Launcher.

6.2.2.2.3. Update of SVM layouts

Baseline description

As presented in the SVM Design report, the SVM configuration baselined for SRR is close to the baseline proposal of December 2000. It is to be mentioned that changes implemented in baseline concern mainly changes in equipment or Instruments accommodation. Changes in Equipment accommodation are mainly dictated by Thermal constraints, when changes in Instruments accommodation result from Instruments request recorded during the first meeting with the Instruments.

HERSCHEL SVM - LAYOUT - BASELINE FOR SRR
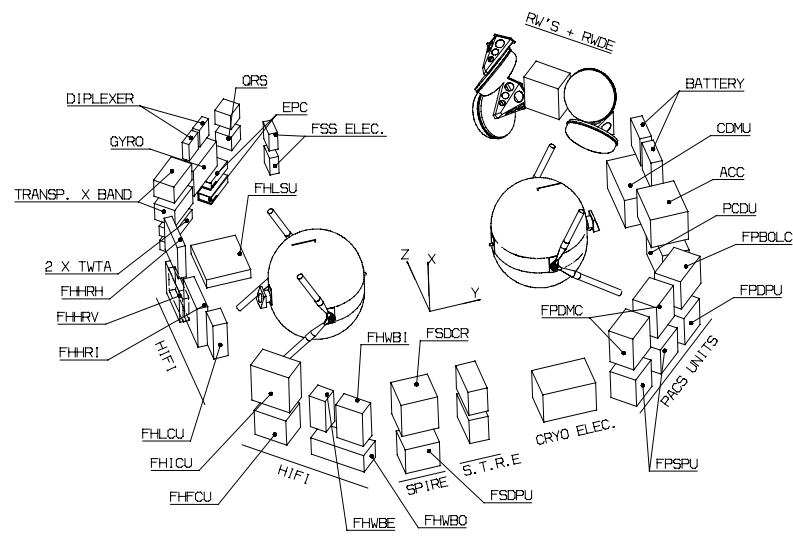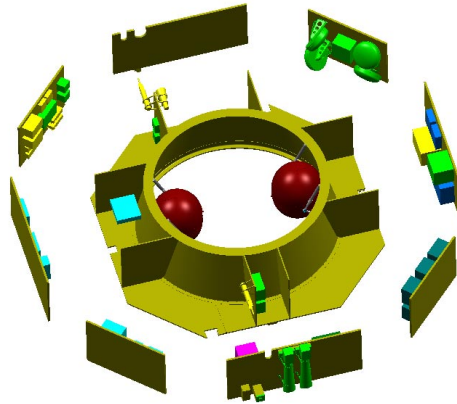
FIGURE 6.2.2.2-1 HERSCHEL SVM GENERAL LAYOUT

The changes described hereafter refer to changes in Equipment or Instruments accommodation wrt to proposal baseline of December 2000, but not to changes in equipment or Instruments definition, reference remaining IID-A and IID-B Issue 1/0. Further Instruments changes and impact on SVM configuration are discussed after the baseline description.

Change of PCDU/CDMU accommodation

PCDU/CDMU accommodation on panel +Y have been modified on HERSCHEL in order to improve equipment Thermal control. PCDU and CDMU have been inverted, to place the more dissipative equipment at the opposite side to the Sun. This measure is requested to control the CDMU temperature in the specified temperature range. This measure is implemented on PLANCK without any other impact.
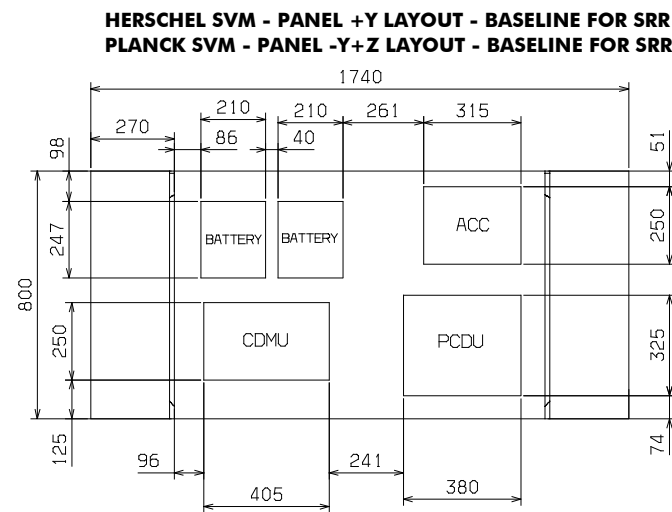
As a last minute change, the decision to keep only one battery is not yet reflected in the configuration. The same applies to the PND, which will have to be removed following conclusion of the PND/AND trade-off.

HIFI changes: Remove of HIFI baseplate on 2 HIFI panels: allows to relax accommodation constraints, and should result in a mass decrease at Instrument level.

HERSCHEL SVM - PANEL -Y-Z LAYOUT - BASELINE FOR SRR
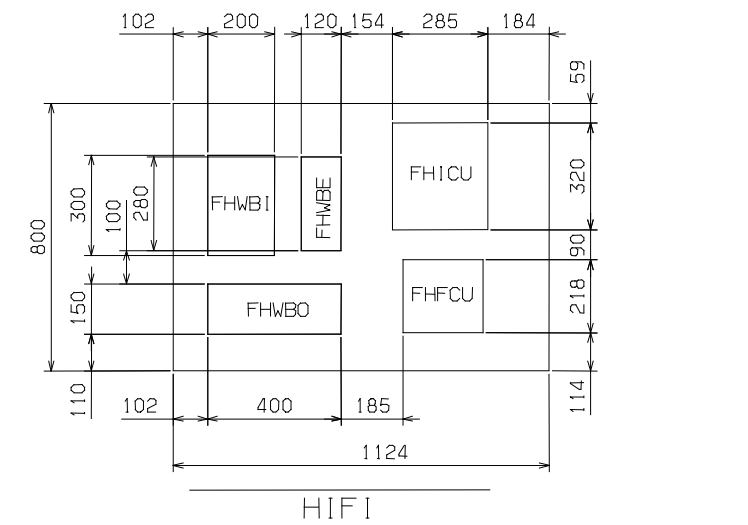
PACS change: Inversion of FPSPU with FPDPU on HIFI panel +Y-Z: to optimize warm harness length.

HERSCHEL SVM - PANEL +Y-Z LAYOUT - BASELINE FOR SRR
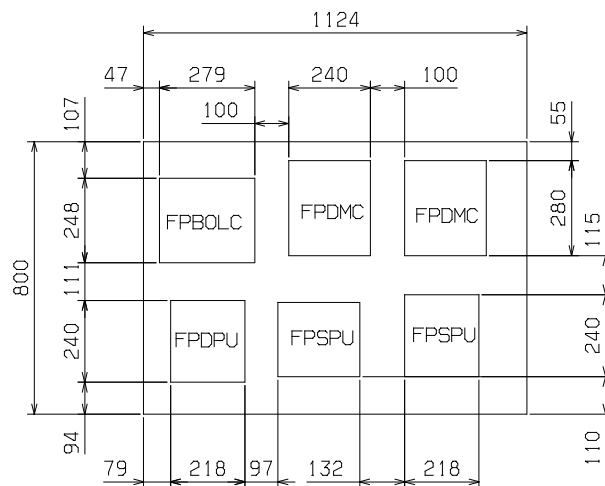
HIFI panel: Alternative accommodation for FHLSU:

–   FHLSU is currently accommodated below the Upper platform on +Y side.

HERSCHEL SVM - PANEL +X LAYOUT - BASELINE FOR SRR
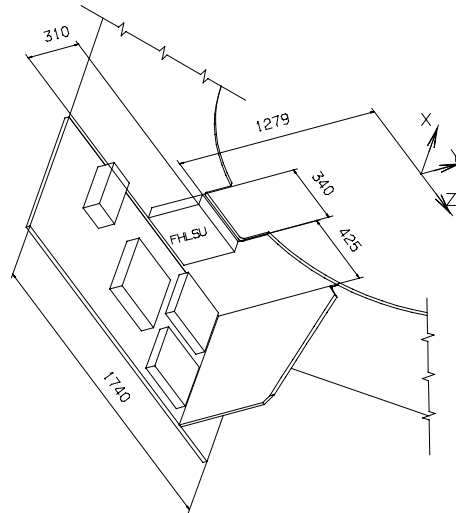
Idea is to move FHLSU on lateral panel +Y to improve its Thermal control. Instrument temperature can be better controlled in its specified temperature range. This accommodation on panel +Y is made feasible by HIFI baseplate deletion see above).

This alternative is to be further investigated regarding harness routing, wave guide impact (integration, length increase), and Instruments evolution as discussed hereafter.

HERSCHEL SVM - PANEL -Y LAYOUT - STUDY FOR SRR
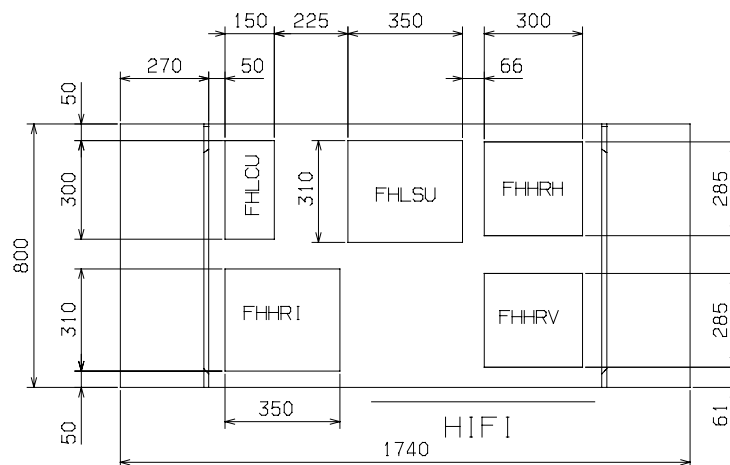
Study of baseline evolution

Preliminary assessment of coming Instruments changes has been started on the basis of Instruments evolution presented during Instruments meetings, and/or preliminary edition of IID-Bs Issue 2/0.

This preliminary assessment results in:

— check and update of SVM configuration Vs Instruments changes in dimension

— check of mass increase impact on mechanical analysis, and balancing when relevant

— recommendations for Instrument design optimization.

HIFI changes:

— growth of FHLCU/FHHRI/FHHRH & FHHRV on panel –Y which leads to a very high equipment density on this panel; problem even critical without FHLSU moved on the panel

HERSCHEL SVM - PANEL -Y LAYOUT - STUDY FOR SRR
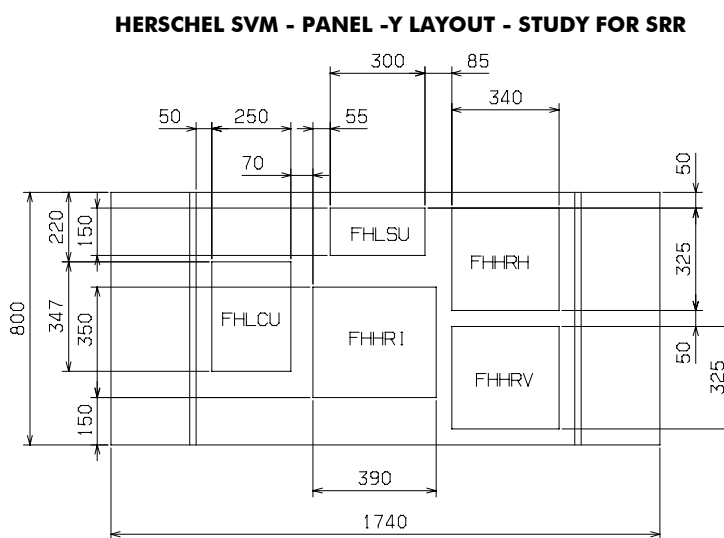
— problem is to define harness routing, to find appropriate harness channel between boxes

— problem is also to have not sufficient clearance between boxes to enable connectors mounting and dismounting.

Problem is made critical because of excessive growth and non convenient design of Instruments. As an example FHHRH & FHHRV are very flat boxes taking a too large place on the panel. HIFI is requested to review the design of these Instruments and to make them more compacts: the basis of FHHRH & FHHRV together shall not be greater than one actual box.

HIFI changes:

− 3 instruments FHWBO/I/E changed in 4 new instruments

− new accommodation to be consolidated by study of harness routing and connectors accessibility.

HERSCHEL SVM - PANEL -Y-Z LAYOUT - STUDY FOR SRR
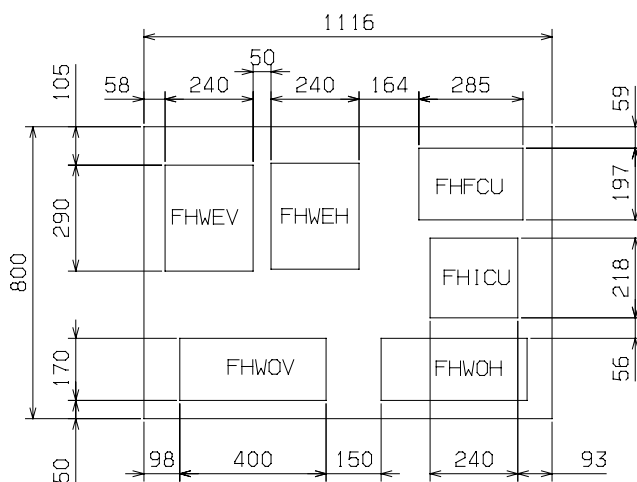
PACS changes:

–   growth of BOLC and other Instruments on +Y-Z panel requires a refinement of the Instruments accommodation

–   new accommodation seems to be acceptable, but is to be consolidated by study of harness routing and connectors accessibility.

HERSCHEL SVM - PANEL +Y-Z LAYOUT - STUDY FOR SRR
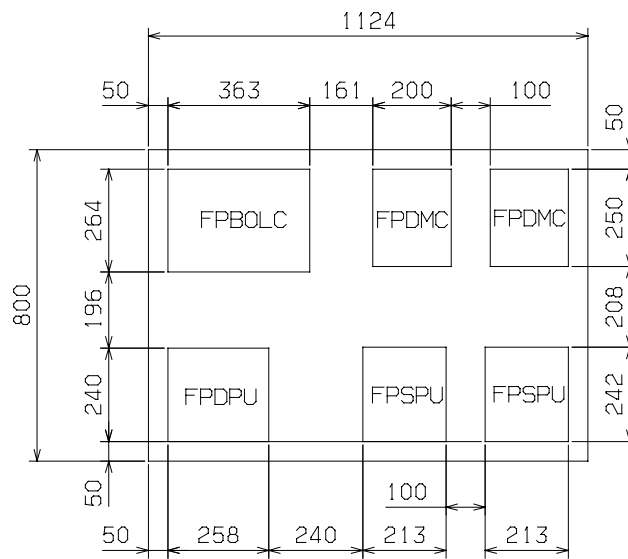
SPIRE change:

The following layout is TBC and preliminary:

Inside of SVM -Z panel
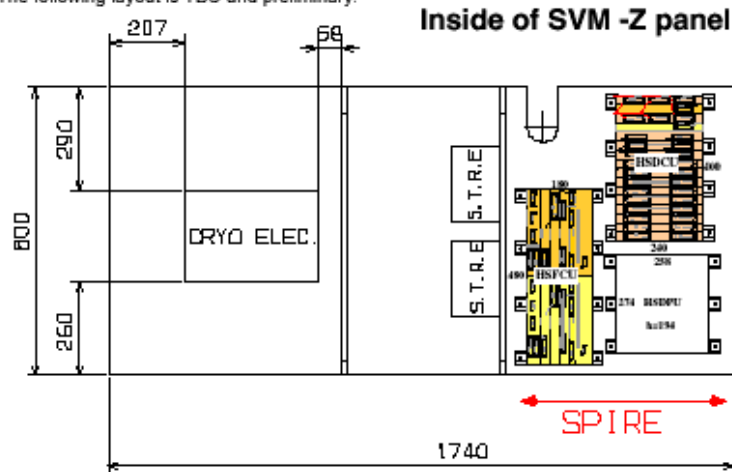
— a new box to be accommodated, according Instruments proposal:

— proposed accommodation leads to a very high Instrument density on the
   right side, when the left side is not very loaded.

ALCATEL proposal is to move one Instrument on the Cryo-elec side to balance
Instruments accommodation. Instruments to review and to comment ALCATEL
proposal in return (Instruments dimensions and accommodation).

HERSCHEL SVM - PANEL -Z LAYOUT - STUDY FOR SRR
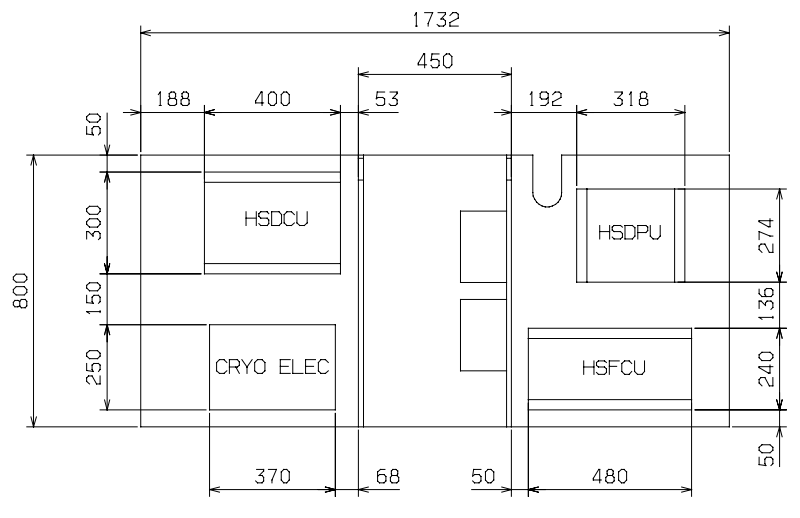
6.2.2.2.4. Sensors, antennae and RCTs accommodation

The sensors, antennae and RCTs configuration is similar to the sensors, antennae and RCTs configuration in ALCATEL proposal of December 2000. This is briefly recalled in the following sketches.

Star Trackers: 2 sensors pointing –X safe from sun illumination, accommodated on – Z side.
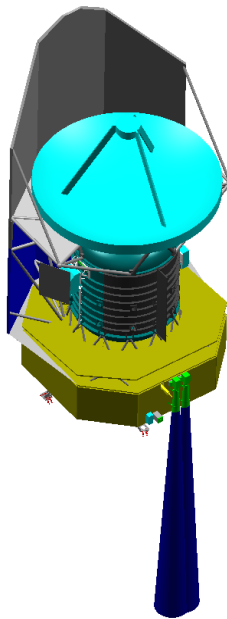
SAS and FSS sensors

Herschel is implementing a set of 2 SASs on ± Z side of the SVM. The 2 SASs provide a full sky coverage that allows to locate the Sun position whatever is the S/C attitude (nominal or survival mode). The FSS is accommodated on+ Z side, and is used only for fine attitude control in normal mode.
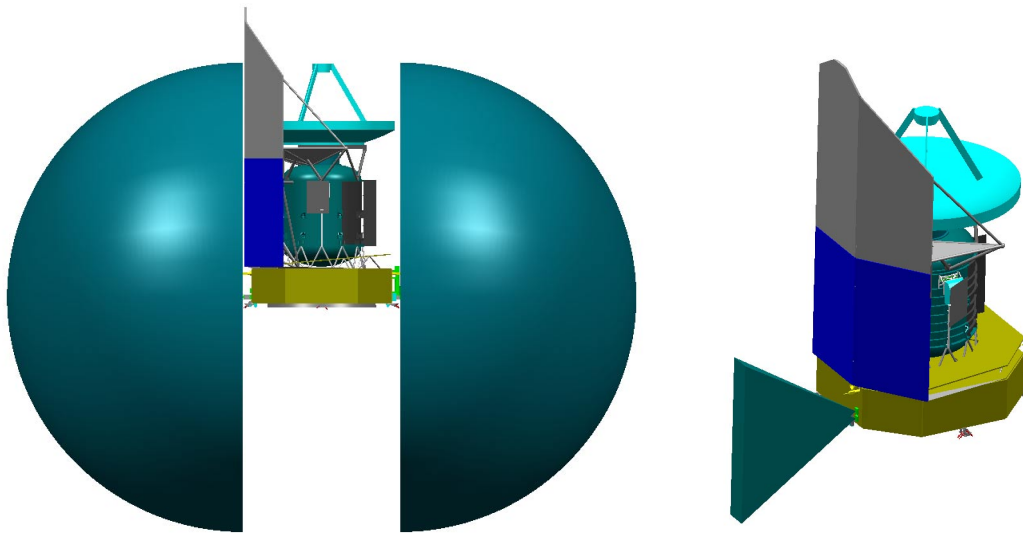
SREM and VMC accommodation

The SREM is located on – Z panel in a protected area (anti-Sun side), with a clear FoV. The VMC is located on +Z panel (illuminated side), and looking downwards, in order to make possible a recording of the FIRST-to-SYLDA 5 separation.
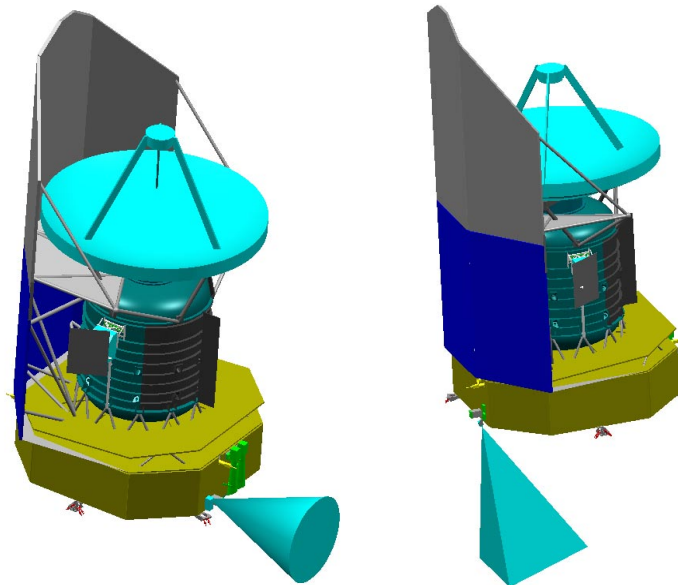
TTC antennae accommodation

The 2 LGAs antennae are accommodated on ± Z side of the SVM, and are required:

–   to cover the normal telecommunication mode (nominal S/C attitude) with + Z antenna pointing Earth

–   to cover the launcher separation subsequent phase and survival mode with the union of the 2 LG/As providing a full sky coverage.

The MGA antenna is nominally pointing Earth, and covers only the normal telecommunication mode.
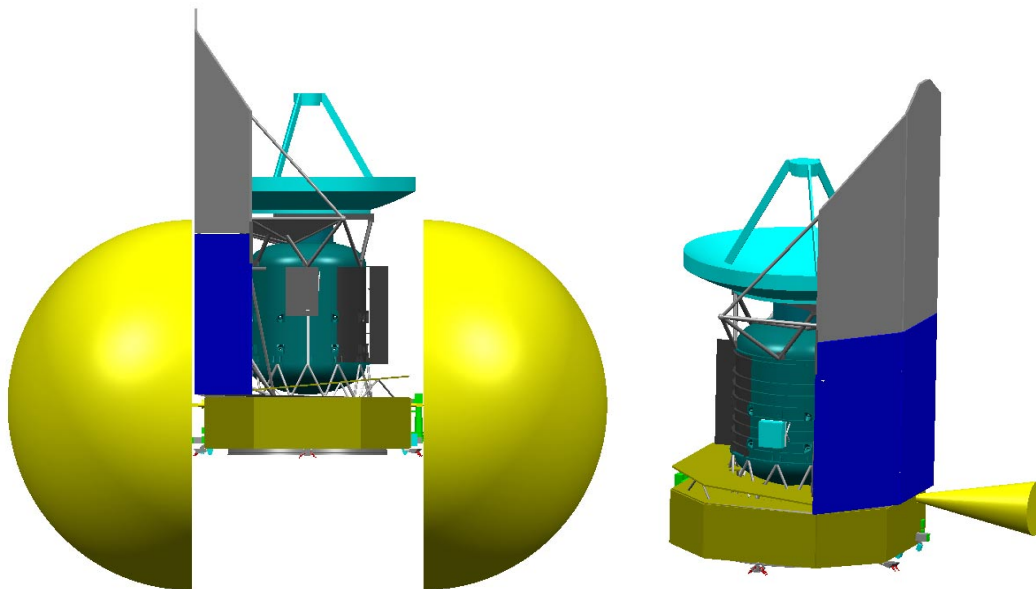
RCT accommodation

The RCTs system comprises 12 RCTs of 10N force, organised in 4 clusters located below the SVM box. The RCT are commanded by the ACMS system, for correction of launcher dispersion, attitude control or for reaction wheels unloading.
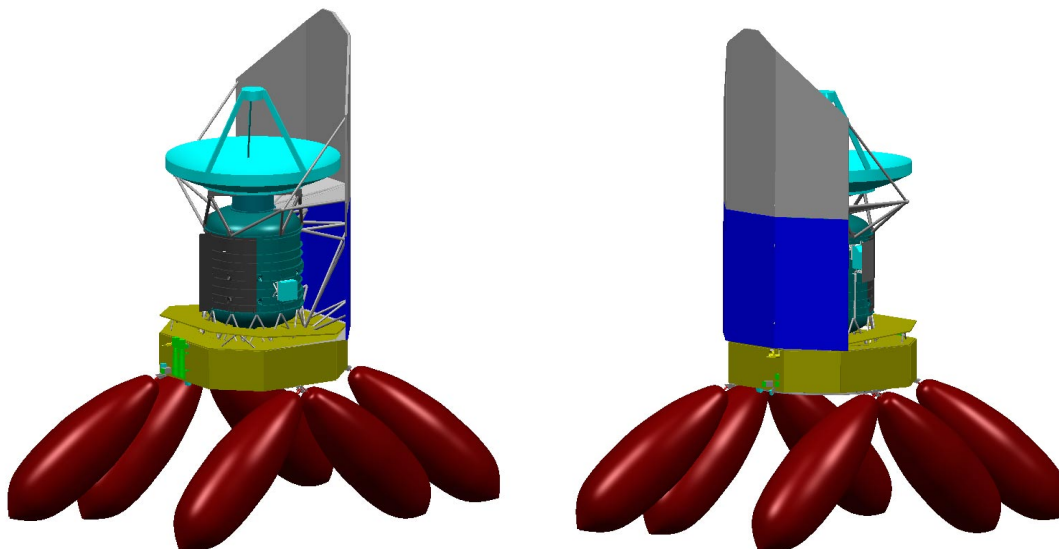
6.2.2.2.5. Satellite mechanical architecture

Following evolutions are currently in study at ASPI, ASTRIUM and ALS.

Study of SSH I/F and design

Position of the problem

As discussed with ESA and ASTRIUM at several occasions, it is thought that the SSH supporting could take benefit of a direct fixation to the SVM top. As a recall, the current baseline consists to support the SSH bottom by lower struts inclined and connected at the same level as the CVV struts (even if interface nodes are not the same). This is an evolution of the previous baseline with lower struts horizontal and connected on the CVV interface flange.

ME.HES.PHAA.A.0002A.A
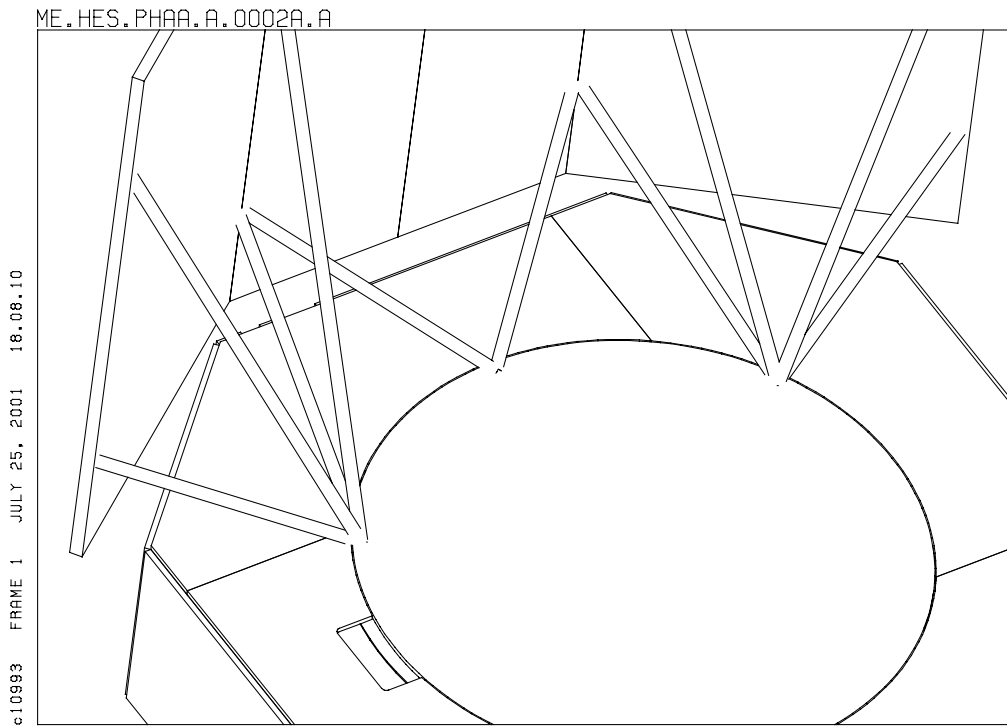
FIGURE 6.2.2.2-2 SSH SUPPORTING - BASELINE
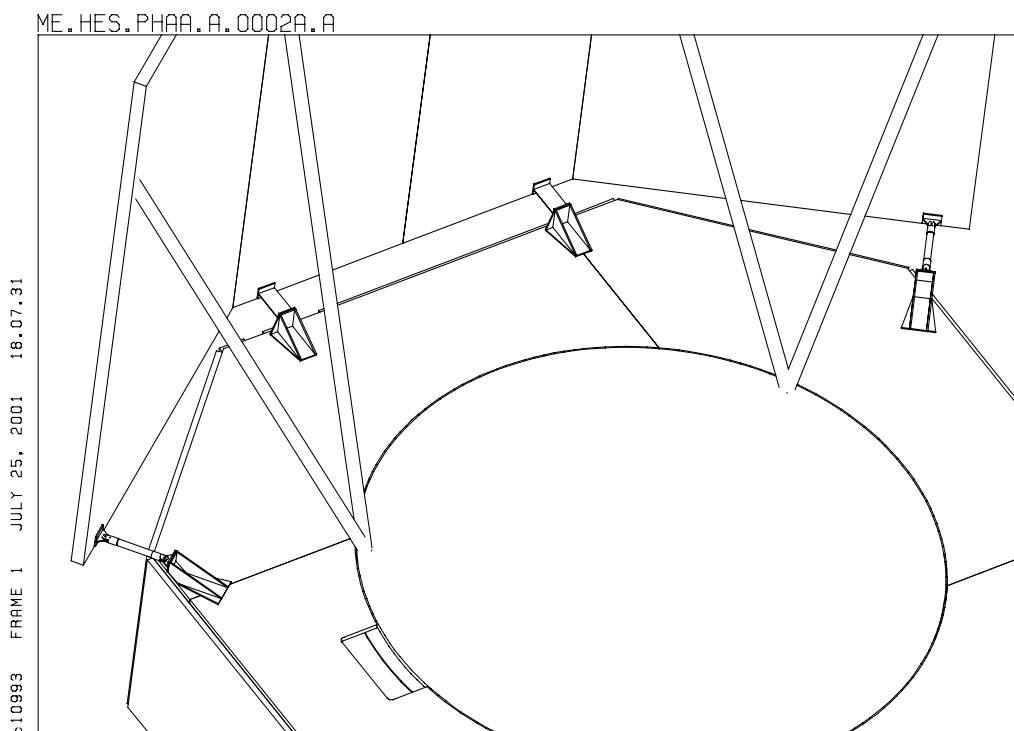
FIGURE 6.2.2.2-3 SSH SUPPORTING - PROPOSAL

Expected advantage

The basic improvement is to replace 4 struts by simple brackets, which should allow for stiffening and mass saving at the same time.

Additionally, it should allow:

- to reduce the density of interface nodes between SVM, CVV struts and SSH converging at the top of the PLM sub-platform, which should simplify interfaces and management

- to prevent additional cut in SVM shield, that could penalize its thermal performance.

Predictable drawbacks: No evident drawback.

Conclusion and recommendation

This proposal is to be discussed and evaluated with ASTRIUM and ALENIA, possibly implemented in design and specifications if judged positive by all parties.

Study of Telescope I/F and supporting

Position of the problem

As discussed with ESA at several occasions, the question about the need of an Interface triangle for the Telescope is to be re-opened. As a recall, the present estimated mass for the Interface triangle is about 30 Kg.

The question, more precisely in fact, is about the needs for a flight Interface triangle. The need is to clarified regarding different aspects as:

- structural role during Launch, and impact on dimensioning

- mechanical and thermal behaviour in-orbit, and impact on dimensioning

- role during on-ground integration activities

and subsequent impact on Telescope design.

Structural role during Launch

It is thought that a better arrangement of the Telescope supporting struts might allow limiting the structural role of the Interface triangle. The main interest of this adaptation is to make it lighter, or even to make it non-useful from a structural point of view.

The basic idea is to modify the geometry of the Telescope supporting struts as follows:

- the struts axis shall be convergent with the Telescope blades hinges, which prevents the need to have stiff Interface triangle bars in torsion (moment annulled at Telescope interface)

- the struts axis shall be in the same plane as the Telescope blades, which prevents the need to have stiff Interface triangle bars in tension/compression (out of plane loads annulled at Telescope interface).
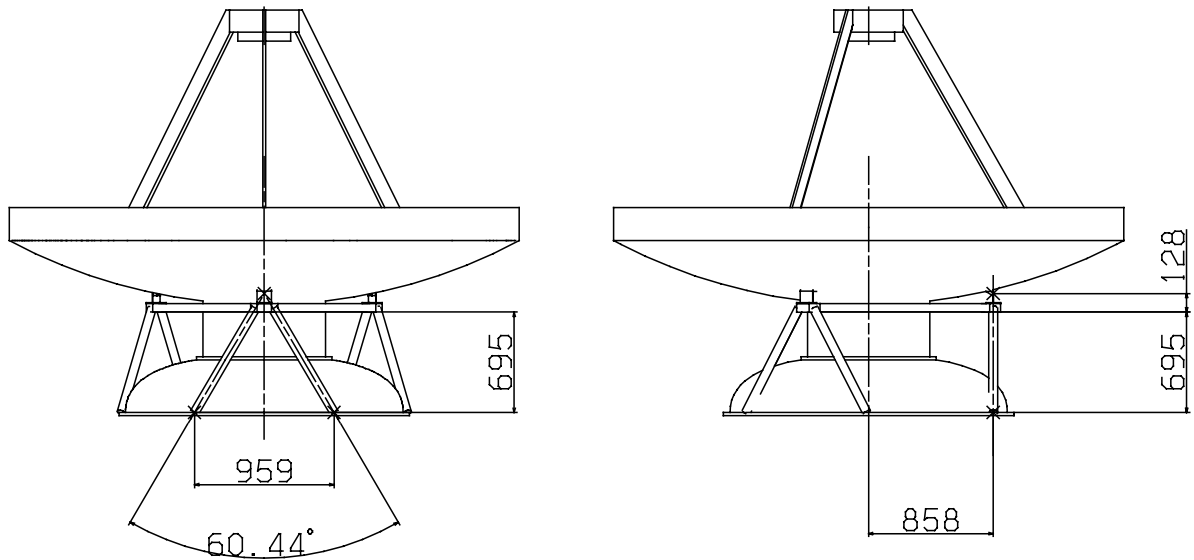
FIGURE 6.2.2.2-4 CURRENT GEOMETRY OF TELESCOPE SUPPORTING
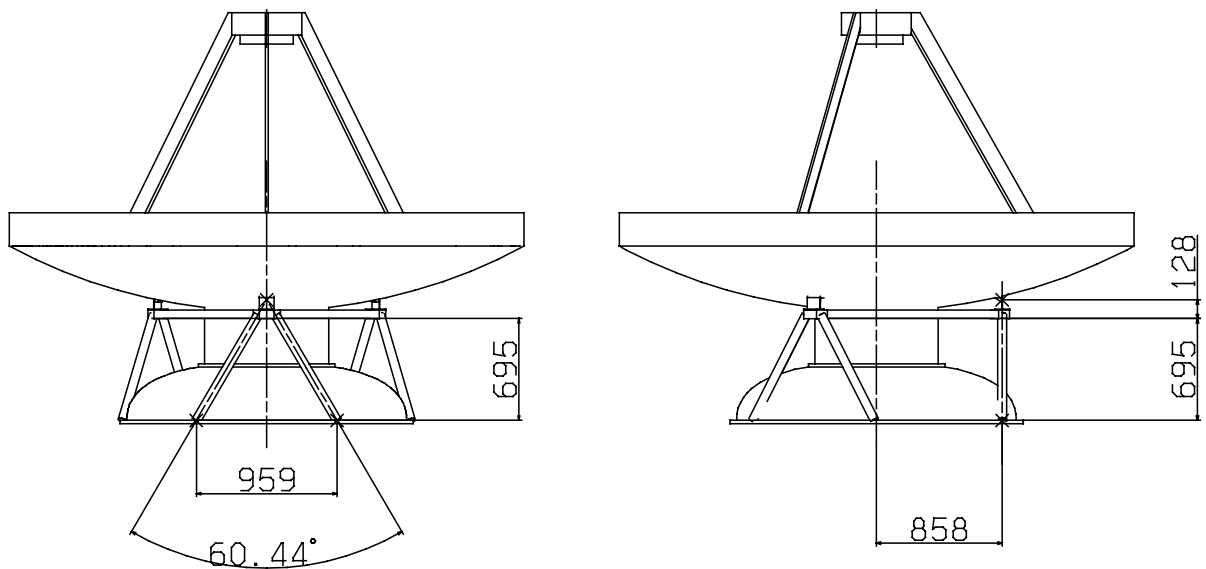
FIGURE 6.2.2.2-5 NEW GEOMETRY FOR TELESCOPE SUPPORTING

As a matter of fact, these recommendations impose to define new constraints or new requirements for the Telescope and Telescope supporting.

For the Telescope, it would lead to specify that Telescope blades and Telescope nodes to be in the bipode roots line. Concretely, it would impose to set the Telescope supporting and Telescope blades at a distance of 858 mm (current position of Telescope struts on CVV) from the Telescope centre line. This distance is to be compared to the distance of 1037 mm in the Telescope specification.

This obliges to modify the Secondary mirror supporting, and to change its bars inclination to make them converge to the new Telescope nodes location. This may impact the Secondary mirror performance, as this modification (bars will be less inclined) should favour its axial stiffness to the detriment of its lateral stiffness.

An other possibility could be to built the Telescope supporting and Telescope blades in tilted planes passing by the bipode roots line at the bottom, but passing by the Telescope nodes at the top (at a distance of 1037 mm for instance). This may allow to optimise the Primary Mirror and Secondary Mirror supporting (more or less) independently of the Telescope supporting, but with some design complications (Telescope blades and hinges will be tilted wrt Telescope normal plane).

An other action of the Interface triangle is to fight against bucking inside the system, as its stiffness reinforces the struts and the blades at their extremities. This point is to be carefully assessed in any case, if the Interface triangle is made lighter or if it is removed.

Mechanical and thermal behaviour in-orbit

The major drivers in this area are the temperature gradient residing between the various elements (Telescope, Interface triangle, Telescope supporting, CVV), and the different materials of these elements.

The presence of the Interface triangle allows to strain the thermo-elastic deformations from the CVV transmitted via the Telescope supporting. Without Interface triangle the deformation imposed on the telescope blades could be quite high, due to the high CTE of the Aluminium CVV and depending of the relative stiffness in bending between Telescope struts and blades. With and Interface triangle in CFRP, the difference of material between telescope (in SiC) and the triangle may introduce thermo-elastic deformations wich are however expected to be lower than without interface triangle.

Role during on-ground integration activities

The Interface triangle may play a role mainly:

– for Telescope handling during integration

– to secure Telescope and blades integration (mating on Telescope struts can be delicate without)

– to perform Telescope alignment.

The removal of the Interface triangle, or its replacement by a MGSE will have to be carefully assessed by the Telescope Contractor.

Preliminary conclusion and recommendations

From the above discussion, it is retained the following main idea:

– because of flight considerations, a removal or a lightening of the Interface triangle cannot be envisaged without a common optimization of the Telescope blades and Telescope struts, with impacts to be accepted at Telescope level

– the thermo-elastic effects are to be more accurately assessed to check impact on Telescope performance

– because of on-ground considerations, need of Interface triangle or MGSE for handling, integration and alignment on S/C is to be clarified by the Telescope Contractor.

Discussions with the different partners involved in this area (ESA, ASPI, ASTRIUM-D, Telescope Contractor) have to be initiated soon, in order to initiate a proper trade-offon the question of the Interface triangle, to clarify impacts on S/Ss design and interface specifications.

Move of PLM to SVM interface

Position of the problem

The idea is to connect PLM supports directly to the top of the SVM Central Tube, and not on the top of the PLM sub-platform. The basic motivation and expected advantages concern the possible mass saving that could be achieved at PLM sub-platform level, by avoiding implementation of structural inserts for PLM connection.

The following figure shows a principle view for implementation on HERSCHEL and PLANCK.
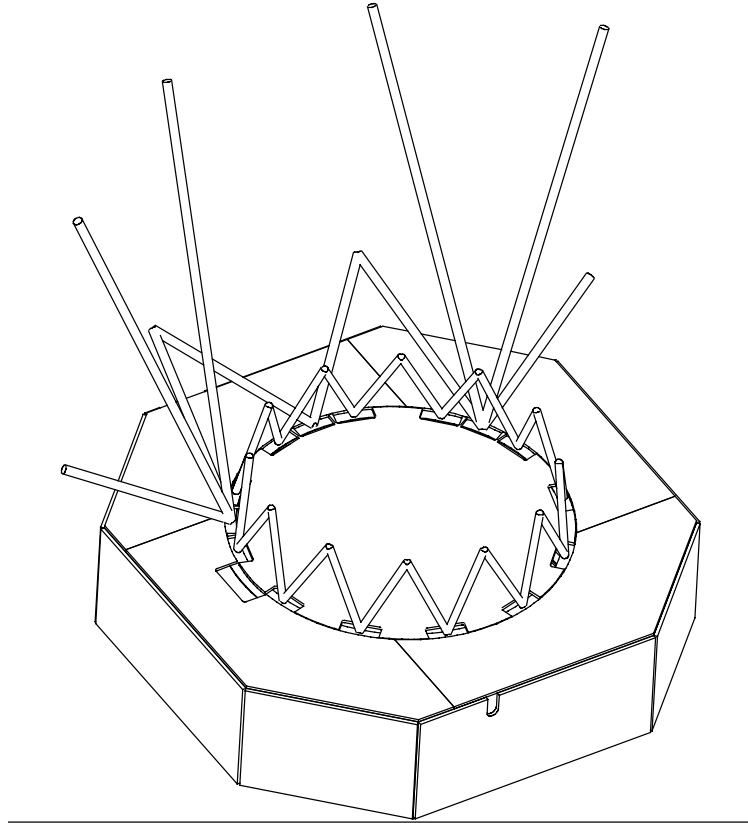
This change proposal is to be carefully assessed to some additional expected advantages or drawback, as discussed below.

Expected advantages

- Improved development flexibility as interface less dependant of PLM sub-platform change (platform thickness has been modified several time for PLANCK.

Predictable drawbacks

- Necessary implementation of structure brackets on the central cone, that could penalize the expected mass saving.

- Weakening of the PLM sub-platform structural role, as the platform stiffness cannot by fully transmitted to the central cone (reduced fixation area on Central Tube top).

This problem could be particularly critical for HERSCHEL, as it should be necessary to make a number of large cuts in the PLM sub-platform to avoid CVV struts plus SSH struts.

- Interface accessibility that could be more difficult through cuts in platform.

- Integration sequence that could be made more difficult.

As an example for PLANCK, the logic is to integrate together the PLM sub-platform and the PLM, to keep in place wave guides connection between the BEU (on top of the platform) and the FPU delivered and tested in these conditions.

Then, in order to maintain this logic, it should be envisaged to use MGSE to restore a mechanical link between these elements during P-PLM integration. This conducts to additional MGSE, and additional complexity in P-PLM integration on S/C.

Also, it is envisaged at PLM level to use the PLM sub-platform as mechanical basis for the P-PLM assembly.

- Reduced commonality if a common solution cannot be found to optimize HERSCHEL and PLANCK at the same time.

Preliminary conclusion and recommendations

This modification before to be implemented requests a common analysis and agreements between all partners involved in this area, i.e. ALCATEL (System and P-PLM), ASTRIUM (H-PLM) and ALS (SVM). A final decision on this change implementation will be taken after consultation and evaluation of impacts at each level.

6.2.2.3. HERSCHEL thermal design

6.2.2.3.1. Overall thermal design

The main objectives of the HERSCHEL Thermal Control System are unchanged since the Technical Proposal. Indeed, the thermal requirements haven't evolved. There are recalled hereafter.

–   fulfilment of the mission lifetime requirement of the Super-fluid Helium cryostat (3.5 years from launcher separation)

–   telescope temperature controlled in a 70 K – 90 K operating range

–   control of the SVM units and Solar Array in the required temperature range (~20° C for the SVM units and >100° C for the Solar Array in operation).

From a thermal point of view, HERSCHEL is divided into two entities under two different Prime responsibility: the SerVice Module (SVM) housing the instruments warm box and S/C resources, and the HERSCHEL PayLoad Module (H-PLM). Specific heat exchange constraints between the two modules are required in order to fulfil the overall specifications recalled above. Basically, the H-PLM is characterized by sub-modules classified in two separate temperature ranges, a conventional one (120 K – 420 K according to ESA ECSS standard) and a cryogenic one (< 120 K). The H-PLM sub-modules are recalled hereafter.

Conventional range

–   Sunshield/sunshade assembly (operating temperature between ~-10° C on sunshade and ~100° C on sunshield).

Cryogenic range

–   CVV and the instruments equipment attached on it (respectively BOLA for PACS and LOU for HIFI).

–   Telescope.

–   SVM shield.

In order to limit the heat exchanges between the SVM and cold parts of H-PLM, cautions have to be taken in order to minimize both conductive and radiative thermal coupling. For this purpose, Glass Fibre Reinforced Plastic struts are widely used, as well as MLI blankets. As far as possible, mechanical fixations between SVM and warm part of the H-PLM have been preferred to fixations onto cold part of H-PLM.

Lifetime requirement

From the cryostat lifetime requirements, are directly derived constraints on the CVV external temperature. The maximum value not to exceed during operational phase is driven by the heat loads onto the He II (Super-fluid) bath. These loads depends on one side on the mechanical and thermal design of the inner CVV, and on the other side on the loads carried by the SPIRE, HIFI and PACS instruments.

At the time of the technical proposal, the objective to reach on the external CVV temperature was the following: a 3.5 years lifetime without margin on the Helium quantity was achieved with a CVV external temperature of 80 K. Adding 10 % system margin (see AD01.1 SPLM-035 H) on the Helium quantity required a CVV external temperature at 73 K.

Thermal analyses performed for the ITT have shown that with the ALCATEL baseline at this time, the calculated external CVV temperature was 69.6 K nominal, and 76.4 K adding uncertainties and margin. The performances were then considered as marginal taking into account all uncertainties and margin.

Moreover, the instruments IID-Bs proposed updates feature an increase of the thermal loads onto the HeII bath. This leads to a reduction of the lifetime as calculated so far. An optimisation work is then required on both the internal CVV design and external environment.

A trade-off activity have been initiated by ALCATEL in order to reduce as much as possible the heat loads on the external CVV, while meeting the mechanical requirements.

The first proposition deals with the CVV supporting truss. The configuration used for the ITT was related to a "ISO type" truss, i.e. 16 struts of 50 mm outer diameter, 6 mm thickness and 675 mm GFRP length. With this hypothesis, and using conductance value correlated from ISO thermal balance tests, the conductive heat loads onto the CVV was calculated around 1 W. This is to be compared to a total of 4.3 W, therefore ~20 % of the loads, which is not negligible. A sensitivity analysis on the GFRP conductance has shown an impact of ~ 1 K with a 25 % reduction of the truss conductance. 1 K is an improvement to be taken into consideration, as it is equivalent to 25 days lifetime increase.

Preliminary results performed by ALCATEL have shown that it should be possible to improve the mechanical behaviour of the H-PLM while reducing the overall cross section/length of the struts, using 24 struts instead of 16. Recommendations have been made to ASTIUM in order to perform detailed mechanical and thermal analyses to support the trade-offs on the possible configurations.

The second major optimization activity is linked to the SSH/SSD configuration and supporting. The trade-offs undergoing are presented in ASTRIUM H-PLM Design description. Besides the improvement of the thermal performances, the aim is clearly to end up to the best solution taking into account mechanical requirements and mass budget reduction. Finally, the wave guides/harness from the instruments as well as cryo-harness for the payload servicing will be routed from SVM to PLM in a way that the thermal loads onto the CVV are reduced at a minimum level. If required, direct mechanical fixations onto the CVV shall be carefully addressed.

Details on CVV thermal design and lifetime budget can be found in the H-EPLM Design Report and Budget Document.

Telescope Decontamination

The telescope decontamination requirements have a large impact on the H-PLM thermal design. The decontamination temperature has been specified at 313 K. It shall be maintained during the first three weeks after launch. The impacts on the thermal design are the following:

- a thermal discoupling between the CVV and telescope is mandatory in order to minimize the impact on the CVV lifetime

- a thermal discoupling with cold space in order to reach 313 K with the allocated power supply (600 W maximum)

- the copper cable to feed the heaters on the telescope must be routed in a way to minimize the heat loads both onto the CVV and telescope.

For the technical proposal, a routing and thermal anchoring along the cryostat was considered.

Potential lifetime savings are possible if this cable is routed to the LOU, and then directly to the telescope. This design optimization shall be performed by the H-PLM Subcontractor.

IOP thermal constraints

Work have been initiated in order determine the thermal environment during the Initial Orbit Phase. The objective is to identify potential critical areas and to provide design solutions. This concerns mainly HERSCHEL spacecraft for which the heat loads onto the CVV radiator must be minimized as far as possible for Helium mass saving. The CVV radiator is actually permanently exposed to the external environment after fairing jettison (unlike ISO CVV). The impact which has been studied first is due to the Solar flux which may be encountered during the EPC phase.

Configuration studies have shown that it was possible to tolerate higher Pitch and Roll angles compared to what was possible at time of the ITT with additional MLI blankets. A Roll of up to 11 deg can be accepted by adding closure MLIs between the Sunshield/ Sunshade lower part and the SVM (see Section 6.2.2.2). However, the current status is that during launch phase, the Sun motion in Roll can exceed this 11 deg limit.

The maximum duration of potential H-PLM sun illumination during EPC phase is 380 s. Consequently no thermal impact are foreseen on bulky structure like the CVV, telescope, and SVM shield (time constant much larger than 380 s).

The impact on "light" components like LOU, BOLA and SVM shield is to be assessed because their time constants are in the same order of magnitude than the 380 s maximum duration illumination. However the temperature may not exceed 50° C.

The MLI blankets have a low time constant then react quickly to a changing thermal environment. All of them present an Aluminium coating on their external layer, with the following thermo-optical properties:

– infrared emissivity =0.05

– solar absorptance = 0.15.

The "equilibrium temperature" of the external layer may reach consequently 250° C. This may have impact on the MLI design, using for instance Kapton and Tissu Glass as interlayers instead of the classical Mylar and Dacron Net materials.

All the potential impacts listed above are considered as non critical points. The remaining uncertainty concerns "hot spots" phenomenon (rays concentration on a single point). This could be destructive for part of MLI blankets. Some design rules are followed by "classical" spacecraft in order to limit the occurrence probability. Sharp angles are for instance avoided as much as possible, and diffuse coatings are widely used. The MLI layout and shape will avoid as far as possible to create any "cavity".

However, to our present knowledge, it seems impossible get a low emissive and diffuse coating at the same time. Nevertheless, investigations will be carried out to confirm or not this first opinion.

6.2.2.3.2. H-PLM thermal design

The H-PLM thermal design has not evolved in a significant manner, except at the sunshade level. The overall configuration is described in details in the H-PLM design description. The main features are recalled hereafter, as well as the modifications since the ITT technical proposal.

The mechanical links between the warm and cold modules are achieved with low conductance supports. They are commonly obtained with composite materials. The selection of the material must be optimised with the temperature range: usually, Glass Fibre Reinforced Plastic (GFRP) is used between room temperature and 50 K. The supports between warm and cold parts of the spacecraft are the following:

– truss between the SVM and the CVV: this truss is at this time under study, for mechanical/thermal design optimization

– supporting struts between the sunshield/sunshade and CVV: as for the CVV truss, the SSH/SSD supporting is being optimized. The objective is to reduce at a minimum level the heat loads onto the CVV, while meeting the mechanical requirements. From a thermal point of view, the basis for this work is a reduction of the total cross section over length of the supporting struts between SSH/SSD and CVV, compared to what it was for the ITT baseline. Work performed so far both by ALCATEL and ASTRIUM have lead to a modification of the sunshade shape, associated to a modified supporting layout. The main change deals with the deletion of the sunshade supporting ring described in ALCATEL ITT technical proposal. It is an improvement considering the reduction of the radiative loads onto the CVV radiator, which unless calculated low (0.23 W), were submitted to significant uncertainties due to the reduced TMM used for computations. In other words, even if the calculated CVV temperature does not change, the uncertainties on the value are reduced. Work are still undergoing on the optimisation of the supporting layout.

Radiative insulation is obtained with high efficiency MultiLayers Insulation (MLI) blankets (20 layers), using aluminium coating on the external layers to limit the radiative exchange between warm and cold modules. The MLI blankets cover all sides of the warm components oriented towards the Cryostat and telescope, i.e. the rears side of sunshield and sunshade.

Additional MLI blankets are necessary for blocking solar radiation and/or Straylight:

– between SVM and sunshield, the shape/size of this MLI has changed since the ITT technical proposal in order to improve the H-PLM shadowing during the initial orbit phase

– between the primary reflector and CVV, to stop Straylight propagation from the SVM to the telescope, through multi-reflections between the sunshield rear side and the CVV. It has been shown during the FIRST System Optimization Study that this MLI blanket is also profitable for thermal reason, as it allows actually to reduce the thermal loads onto the telescope.

For these 3 MLI blankets, specific care shall be taken to avoid any gaps or any light traps at the edges.

The use of a CVV additional radiator as well as a SVM shield is maintained as a baseline.

The Sun-illuminated side of HERSCHEL is covered with AsGa cells on the sunshield, to provide the electrical resources, and Optical Solar Reflectors on the sunshade to get the telescope environment as cold as possible.

6.2.2.3.3. SVM thermal design

On SVM side, the TCS must fulfil more "classical" requirements compared to the TCS of the Payload. The SVM TCS is described in details in the SVM design report from ALENIA. We will deal in this chapter only with the main results obtained by ALENIA.

According to the inputs coming from the instruments IID-Bs Rev. 1.0 as well as S/C units characteristics defined by ALENIA, all the equipment's are maintained within their temperature limits. In hot case, the TMM results have been obtained adding 10 % system margin on all the dissipation and 7° C temperature margin. The conclusion will be however modulated for the FHLSU unit (HIFI instrument), which is actually mounted under the SVM upper platform.

Indeed, part of the MLI blanket has been removed around the unit footprint, in order to radiate part of the power towards cold space. This configuration has been assumed for the SRR data package because previous studies have shown that otherwise the FHLSU temperature was at the upper design limit (40° C).

The impact of this configuration is that part of the radiated power is absorbed by the SVM shield (~10 W), which temperature increases and therefore implies a CVV lifetime reduction. The impact have been evaluated by ASTRIUM around 20 days which is significant.

It is then proposed to study the feasibility to move the FHLSU unit onto − Y panel. Thermal aspects, as well as integration and impact on the wave guides design will be taken into consideration. The alternative and preferred solution is a relaxation of upper temperature limit. It is proposed to detail the TMM to get a good accuracy of what would be the maximum temperature obtained with a complete radiative insulation of the unit. The will give a basis for negotiation with HIFI PI.

The second point to be discussed is related to the stability constraints on HIFI instruments. Equipment's mounted on −Y panel as well as FLHSU are out of the requirements. It seems however that the hypotheses to perform the transient thermal computations are much more stringent than what actually happen in-orbit. ALENIA will refine the input data in order to get more realistic results. It is then more than likely that all the temperature stability requirements will be fulfilled, with perhaps the exception of FHLSU. Lets recall that this was the situation at time of the ITT technical proposal.

An optimization work related to the external coating of the S/C will be then performed by ALENIA in order to minimize the impact of a change in attitude on the FHLSU temperature stability (white paint on external MLI blanket, Sulfuric Anodization Oxydation on adapter ring…).

6.2.2.3.4. Impact of instruments units evolution

We deal in this chapter only with the thermal SVM interfaces as well as the thermal external CVV interfaces. Instruments foreseen evolutions on the Optical Bench is treated in the H-PLM design description. The modifications are related to the IID-Bs Rev. 2.0 proposed updates, and are compared to the IID-B Rev. 1.0 used as a baseline for the SVM design. For each instruments, we recall first the hottest case temperature obtained by ALENIA with instrument inputs at time of the IID-Bs.

NOTA: For each case, a 10 % system margin is applied on the dissipation and the temperature results include 7° C uncertainties and margin.

HIFI

ALENIA results at SRR.

HIFI	TMM results (°C)	Operating Design Range (°C)
FHICU	33,8	[-25 , 40]
FHFCU	23,6	[-10 , 40]
FHLCU	23,8	[-10 , 40]
FHLSU	32,7	[-10 , 40]
FHHRI	29,9	[-10 , 40]
FHHRH	35	[-10 , 40]
FHHRV	33,6	[-10 , 40]
FHWBI	16,9	[0 , 25]
FHWBO	10,2	[0 , 10]
FHWBE	11,4	[0 , 40]

All the equipments are maintained in their design temperature range, with all the necessary uncertainties and margin (FHWBO temperature is considerd as acceptable).

Main thermal interfaces evolution (from IID-B Rev. 1.0 to proposed Rev 2.0).

HIFI	T OPERATING RANGE (°C)		DISSIPATION (W)		LOCATION
	Rev. 1,0	proposed Rev. 2,0	Rev. 1,0	proposed Rev. 2,0	
FHICU	[-25 , 40]	[-25 , 40]	22	35	- Y , - Z
FHFCU	[-10 , 40]	[-10 , 40]	15	11,5	- Y , - Z
FHLCU	[-10 , 40]	[-10 , 40]	18	15,5	- Y
FHLSU	[-10 , 40]	[-10 , 40]	20	20	SVM upper platform
FHHRI	[-10 , 40]	[-10 , 40]	29	38,8	- Y
FHHRH	[-10 , 40]	[-10 , 40]	47	45,6	- Y
FHHRV	[-10 , 40]	[-10 , 40]	57	45,6	- Y
FHWBI	[0 , 25]	NA	7	NA	(- Y , - Z)
FHWBO	[0 , 10]	NA	25	NA	(- Y , - Z)
FHWBE	[0 , 40]	NA	18	NA	(- Y , - Z)
FHWEH	NA	TBD	NA	29,7	- Y , - Z
FHWEV	NA	TBD	NA	29,7	- Y , - Z
FHWOH	NA	[0 , 10]	NA	4,6	- Y , - Z
FHWOV	NA	[0 , 10]	NA	4,6	- Y , - Z
TOTAL HIFI			258	280,6	

For HIFI, the main evolutions in the thermal configuration and their consequences are:

  – a new accommodation of the WideBand Spectrometer (WBS) components: FHWBI, FHWBO and FHWBE become FHWEH, FHWEF, FHWOH and FHWOV with an overall dissipation increasing from 50 W to 68.6 W (~14 %)

  – increase of the overall dissipation: from 258 W to 280.6 W (+ ~ 9 %)

  – large increase of the WBS dissipation on (- Y , - Z) panel: from 87 W to 115.1 W (+ 32 %)

- deletion of the WBS base-plate

- increase dissipation on -Y panel: from 151 W to 165.5 W (∼ + 10 %).

Impacts

The large power increase of the WBS is considered as critical due to the rather low operating temperature required (10° C on FHWOH & FHWOV). Several points need to be investigated:

- increase of the radiator area, potentially associated to the addition of an optimised heat sink between the units and panel (optimization in term of thickness to achieve the best compromise between thermal and mass constraints)

- modification of the internal thermal control of the FHWOH and FHWOV units in order to implement a thermo-electric cooler, item widely used both in spatial application and to thermally control LASER diodes.

The evolution concerning the LOU box fixed onto the CVV is presented below:

	T OPERATING RANGE (°C)		DISSIPATION (W)		LOCATION
	Rev. 1,0	proposed Rev. 2,0	Rev. 1,0	proposed Rev. 2,0	
LOU	[80 K- 200 K]	[90 K - 150 K]	12	7	External CVV

The reduction of the dissipation is clearly a good improvement leading to a better design. The radiator size will be reduced, allowing a better accommodation with limited interference with the CVV radiator. Some of LOU box external sides could be used also to reject the dissipation, reducing all the more the radiator size. Potential mass saving should be obtained, as well as heat loads reduction onto the CVV due to mechanical requirements relaxation. This point shall be carefully addressed during Phase B.

NOTA: The heat loads from the LOU supporting truss was estimated at 40 mW for the ITT. However the design was considered not mature enough to get a high level of confidence in this result.

PACS

ALENIA results at SRR.

PACS	TMM results (°C)	Operating design range (°C)
FPDPU	29,2	[-15 , 45]
FPSPU	28,1	[-15 , 45]
FPDMC	32,2	[-15 , 45]
FPBOLC	26,2	[-15 , 45]

Main thermal interfaces evolution (from IID-B Rev. 1.0 to proposed Rev 2.0)

PACS	T OPERATING RANGE (°C)		DISSIPATION (W)		LOCATION
	Rev. 1,0	proposed Rev. 2,0	Rev. 1,0	proposed Rev. 2,0	
FPDPU	[-15 , 45]	[-15 , 45]	15	25	+ Y , - Z
FPSPU	[-15 , 45]	[-15 , 45]	13,65	28	+ Y , - Z
FPDMC	[-15 , 45]	NA	40	NA	+ Y , - Z
FPDEC1+FPMEC1	NA	[-15 , 45]	NA	18 + 12	+ Y , - Z
FPDEC2+FPMEC2	NA	[-15 , 45]	NA	18	+ Y , - Z
FPBOLC	[-15 , 45]	[-15 , 45]	16,6	35	+ Y , - Z
TOTAL PACS			85,25	136	

For PACS, the main evolutions in the thermal configuration are the following:

- new accommodation of the Detectors and Mechanism Electronics boxes (4 boxes), which becomes one DEC1/MEC1 (prime) box and one DEC2/MEC2 (redundant box)

- increase of the overall dissipation on + Y , - Z panel: from 85.25 W to 136 W (~+ 60 %).

Impact

- The huge increase in dissipation then the temperature increase need to be assessed by ALENIA. As for HIFI instruments, not all the allowable radiative surface is used. However, opening the radiative window could lead to use heat sinks, then impact the mass budget.

The evolution concerning the BOLA box fixed onto the CVV is presented below:

	T OPERATING RANGE (°C)		DISSIPATION (W)		LOCATION
	Rev. 1,0	proposed Rev. 2,0	Rev. 1,0	proposed Rev. 2,0	
BOLA	[120 K- 150 K]	[100 K - 150 K]	2,5	0,2 max	External CVV

The large reduction of the dissipation allows to envisage a different supporting concept of the box onto the CVV (e.g. deletion of the GFRP struts). The benefit is foreseen only on the mechanical behaviour as the heat load calculated for the ITT was small enough to have no impact on the CVV external temperature (20 mW to be compared to a total of 4.3 W).

SPIRE

ALENIA results at SRR.

SPIRE	TMM results (°C)	Operating design range (°C)
FSDRC	33	[-15 , 45]
FSDPU	25,8	[-15 , 45]

Main thermal interfaces evolution (from IID-B Rev. 1.0 to proposed Rev 2.0).

SPIRE	T OPERATING RANGE (°C) Rev. 1,0	proposed Rev. 2,0	DISSIPATION (W) Rev. 1,0	proposed Rev. 2,0	LOCATION	T stability Rev. 1,0	proposed Rev. 2,0
FSDRC	[-15 , 45]	NA	71		(- Z)	NA	NA
FSFCU	NA	[-15 , 45]		67 (FCU + DCU)	- Z	NA	< 3 K/hour
FSDCU	NA	[-15 , 45]			- Z	NA	< 3 K/hour
FSDPU	[-15 , 45]	[-15 , 45]	15	24	- Z	NA	< 3 K/hour
TOTAL			86	91			

SPIRE instrument present few evolution s, the most important one being the split of FSDRC box into FSFCU and FSDCU units. Concerning the new proposed dissipation, the increase ($\sim + 6$ %) is under the dissipation margin already applied (10 %). This increase is therefore estimated as acceptable from a thermal point of view.

Recommendations for Instruments

The next tables summarize the instruments units dimensions and proposed updated power dissipation. From these informations can be computed the so-called "power density" of a dissipating equipment, i.e. the dissipation divided by the external surface of the box. From this value can be derived the type of thermal control needed by the box:

- for a power density lower than typically 50 W/cm^2, it can be envisaged that the box can reject it's dissipation through radiation of it's external surface

- for a higher power density, the internal thermal design of the box must be mostly driven by heat conduction towards a base-plate in contact with a radiator.

This criteria is of course to be considered as a indication, and have to be modulated depending on the operating temperature range of the unit (e.g. FHWOH and FHWOV).

HIFI units power density.

	DISSIPATION (W)	Power Density (W/m²)	Baseplate Need
HIFI	proposed Rev. 2,0		
FHICU	35	124	YES
FHFCU	11,5	34,5	NO
FHLCU	15,5	38	NO
FHLSU	20	111	YES
FHHRI	38,8	92	YES
FHHRH	45,6	155	YES
FHHRV	45,6	155	YES
FHWEH	29,7	81	YES
FHWEV	29,7	81	YES
FHWOH	4,6	14,5	YES (10 °C max)
FHWOV	4,6	14,5	YES (10 °C max)

PACS units power density.

	DISSIPATION (W)	Power Density (W/m²)	Baseplate Need
PACS	proposed Rev. 2,0		
FPDPU	25	79	YES
FPSPU	28	143	YES
FPDEC1+FPMEC1	18 + 12	111	YES
FPDEC2+FPMEC2	18 (+12)	up to 111	YES
FPBOLC	35	67	YES

The SPIRE units power density has been calculated only for the DPU. Height of the FCU and DCU are not indicated in the proposed IIDB.

	DISSIPATION (W)	Power Density (W/m²)	Baseplate Need
SPIRE	proposed Rev. 2,0		
FSFCU	67 (FCU + DCU)	TBD	TBD
FSDCU		TBD	TBD
FSDPU	24	70	YES

6.2.3. PLANCK Configuration

6.2.3.1. Axis convention

The Planck satellite reference frame (O, X_X, Y_X, Z_x) is defined such that:

–   its origin O is located at the point of intersection of the longitudinal Launcher and the Satellite/Launcher separation plane; the origin coincides with the centre of the Satellite/Launcher separation plane

–   Xs coincides with the nominal spin axis of Planck. Positive X_S axis is oriented opposite to the Sun in nominal operation. The X_S axis coincides with the launcher longitudinal axis

–   Zs is such that the Planck telescope line of sight is in the (X_S, Z_S) plane. The telescope is pointing in the $+Z_S$ half-plane

–   Ys completes the right handed orthogonal reference frame.
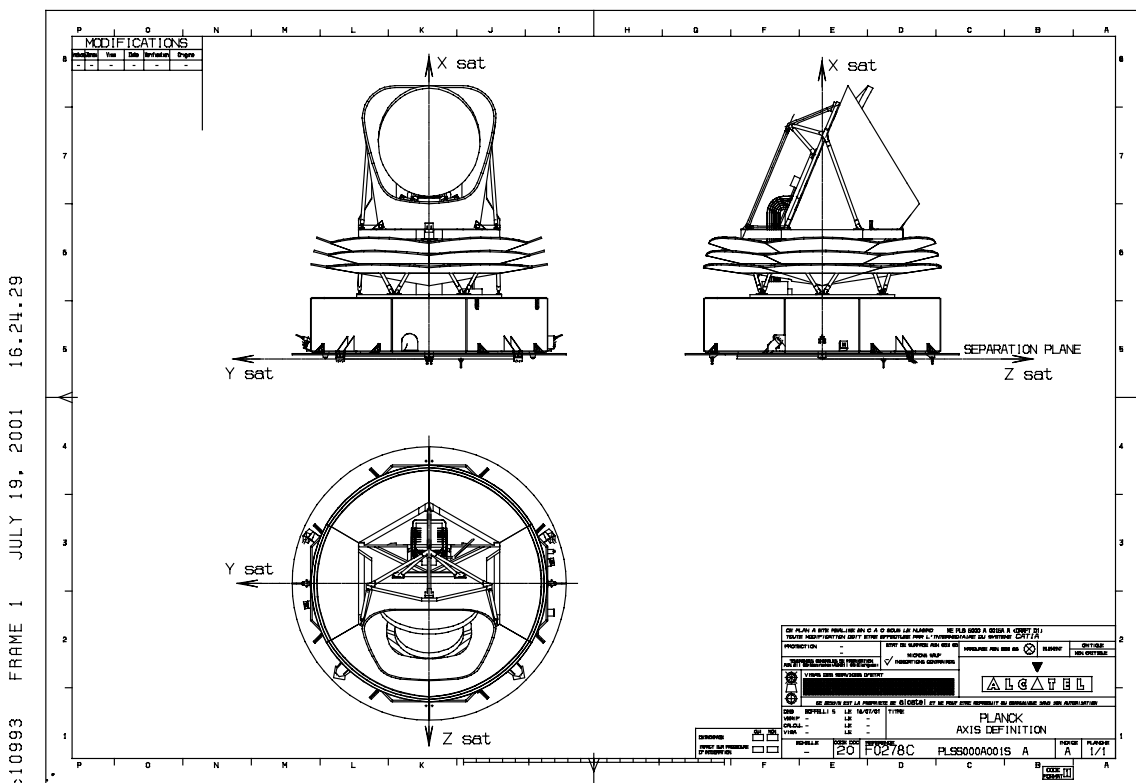
FIGURE 6.2.3.1 PLANCK SPACECRAFT AXIS

6.2.3.2. PLANCK mechanical design

As explained above, PLANCK configuration presents for SRR a certain number of evolution and possible further evolutions in study. These configuration updates, constituting the current baseline or auguring a new baseline are presented hereafter with some details.

6.2.3.2.1. Update of System configuration:

Update of S/C configuration

Planck overall configuration is similar to the proposal configuration. The most visible change stays in the P-PLM configuration changes with V-grooves of modified shapes, and with an overall P-PLM height increase. The S/C height and overall dimensions are updated accordingly.
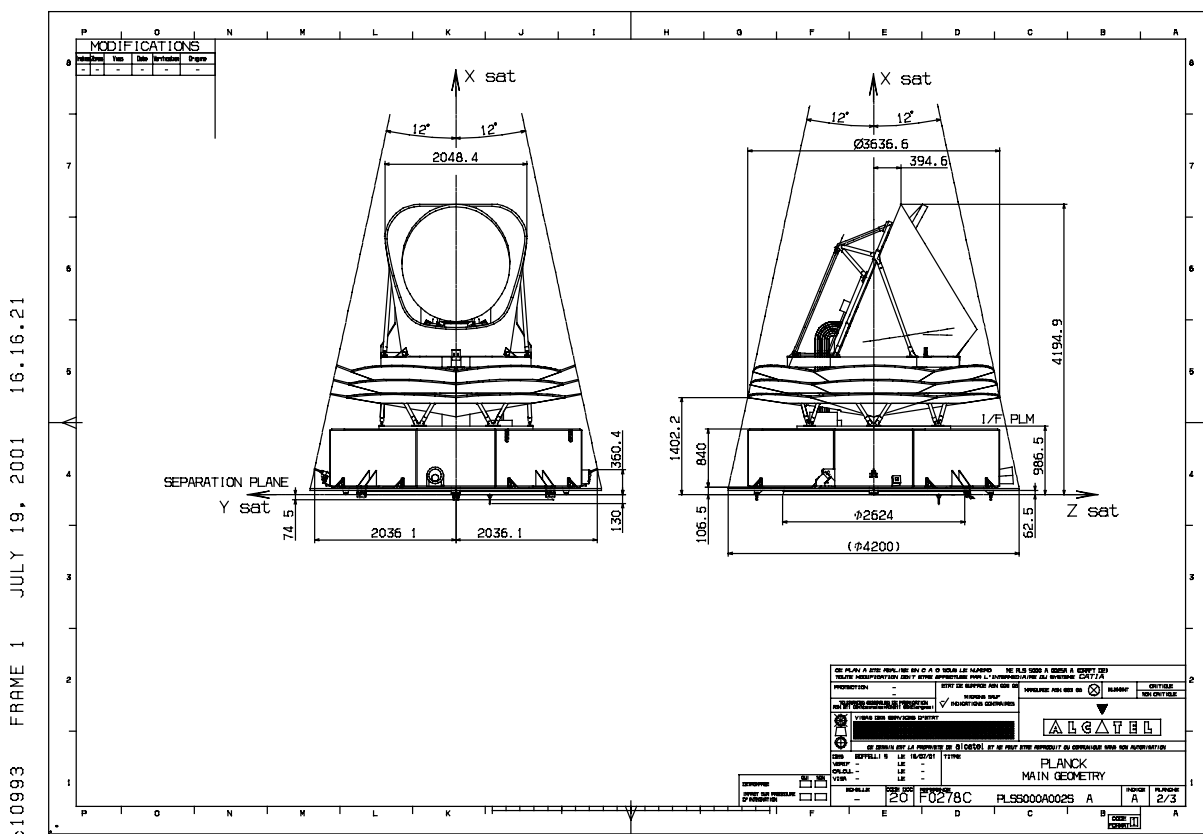
Status of P-PLM to SVM interface

The definition of this interface is under consolidation following same baseline as before:

– P-PLM supported by a set of 12 struts, connected on SVM top at 6 interface nodes

– P-PLM struts set at the level of the PLM sub-platform, at a station of 986.5, depending of the platform height.

Allocated volumes for SVM and P-PLM

As shown in the following figures, allocated volume for Planck SVM and PLM are consistent and complementary, at their common border.

Both have to respect allocated volume beneath ARIANE 5 constraints, at the difference that:

– PLANCK SVM has to deal with limits at the bottom of the separation plane with the Launcher, and limits with SYLDA 5 on the side

– PLANCK PLM has to deal with limits at the top of SYLDA 5.

ME.FST.RPA0.F.0022A.A

GENERAL VIEWS IN ALLOCATED VOLUME   SHEET 1/2

PLM

PLANCK PLM OVERALL GEOMETRIES
AND ALLOCATED VOLUME

DRAFT

c10993   FRAME 1   JULY 25, 2001   17.08.34

ME.FST.RPA0.F.0019A.B

GENERAL VIEWS IN ALLOCATED VOLUME

SHEET 1/3

SVM BOX

SOLAR ARAY

DRAFT

PLANCK SVM OVERALL GEOMETRY
AND ALLOCATED VOLUME

JULY 10, 2001   10.33.43

c10993   FRAME 1
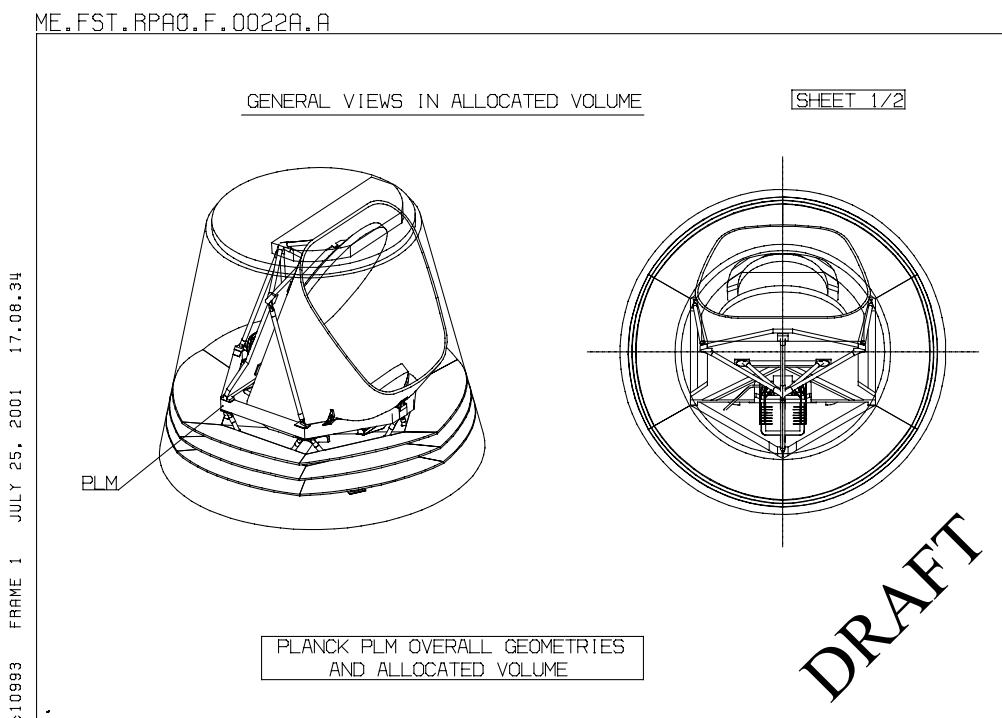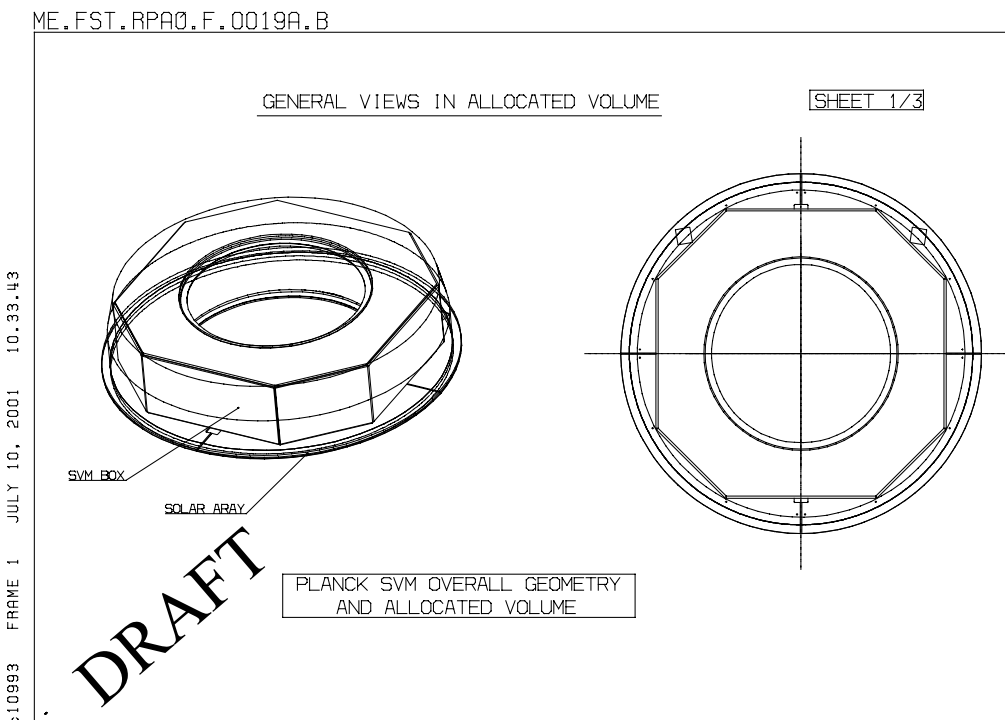
Module interfaces

Preliminary interface definition between SVM and PLM is shown in the following figure.

MODIFICATIONS

Z pplm

Z pplm

100
80

24 I/F HOLES DIAMETER TBD

789

30°

1044

Y pplm

60°

X pplm

60°

Φ2126

PLANCK PPLM
CRYOSTRUCTURE STRUT

ALCATEL

0278C   PLARRACE2020   A   A   01
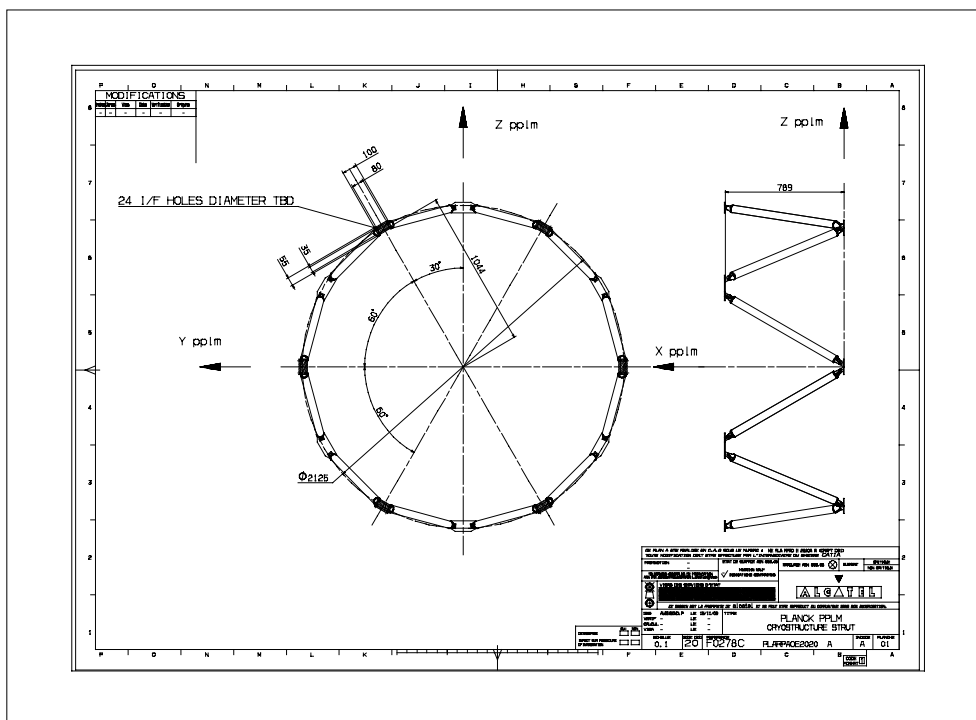
Stiffness requirements

Also, stiffness requirements have been refined as for HERSCHEL. Stiffness requirements are declined in frequency requirements and rigidity requirements. Frequency requirements qualify the global stiffness behaviour of these modules, in consistency with stiffness requirements to be achieved at System level. On the other hands, rigidity requirements are defined at SVM level only, in complement to frequency requirements, to qualify local stiffness needs at specific interfaces.

As examples, frequency requirements for SVM and P-PLM are defined as follows:

SVM frequency requirement

SVM design shall ensure that eigen frequencies of HERSCHEL main global modes fulfil the following mathematical expressions:

  – longitudinal main mode > 60 Hz

  – lateral main mode   > 35 Hz

considering a P-PLM of **310 Kg** at an absolute location X = **1.83 m.**

P-PLM frequency requirement

The eigen frequencies of P-PLM main global modes, on a rigid support, shall fulfil the following mathematical expressions:

  – longitudinal main mode > 85 Hz (effective mass > 25 % of total mass)

  – lateral frequency   > 32 Hz (effective mass > 50 % of total mass).

It is to be noted that the P-PLM stiffness can be specified in a simpler way than Herschel (no springs specifications at the limits) as the P-PLM modes can be de-coupled with the Satellite main modes.

Interface loads

At the present time, interfaces loads are preliminary defined.

As an example, the basic interface loads at SVM to P-PLM interface (Cryo structure struts roots) are to be simply calculated by application of QSL loads at PLM CoG, considering same P-PLM characteristics as for SVM frequency requirement:

LOAD CASES	X AXIS	Y AXIS	Z AXIS
1	13g		2g
2		5g	
3			7g

TABLE 6.2.3.2-1 P-PLM TO SVM INTERFACE LOADS

Status of Instruments interfaces and accommodation

As a general rule, all agreed changes in Instruments definition and interfaces, changes in Instruments accommodation in P-PLM or in SVM, will lead to update Instruments interfaces in a next IID-A version.

However, it is to be recalled that a lot of Instruments changes since IID-B Issue 1/0 are not agreed, and are still in discussion with the Instruments.

6.2.3.2.2. Update of P-PLM configuration

Evolution of P-PLM baseline configuration since ALCATEL proposal can be simply described as follows:

−   groove configuration have been changed from 10°/15°/20° to 5°/10°/15 configuration. This new design allows an easier integration and a better accessibility of these critical parts of the cryo-structure

−   increase of the cryo-structure height in order to keep an acceptable clearance between the SR and Groove 3 and between grooves

−   recentring of the telescope for mechanical behavior and balancing optimization

−   increase of the telescope frame diameter (from 2088 mm to 2400 mm) for maximum volume implementation

−   optimization of the grooves geometry wrt manufacturing and integration aspect: design made of 6 flat sectors of 60° each have been selected.

6.2.3.2.3. Update of SVM layouts

Baseline description

As presented in the SVM Design report, the SVM configuration base-lined for SRR is relatively close to the baseline proposal of December 2000. It is to be mentioned that changes implemented in baseline concern mainly changes in equipment or Instruments accommodation. Changes in Equipment accommodation are mainly dictated by Thermal constraints, when changes in Instruments accommodation result from Instruments request recorded during the first meeting with the Instruments.

PLANCK SVM - LAYOUT - BASELINE FOR SRR
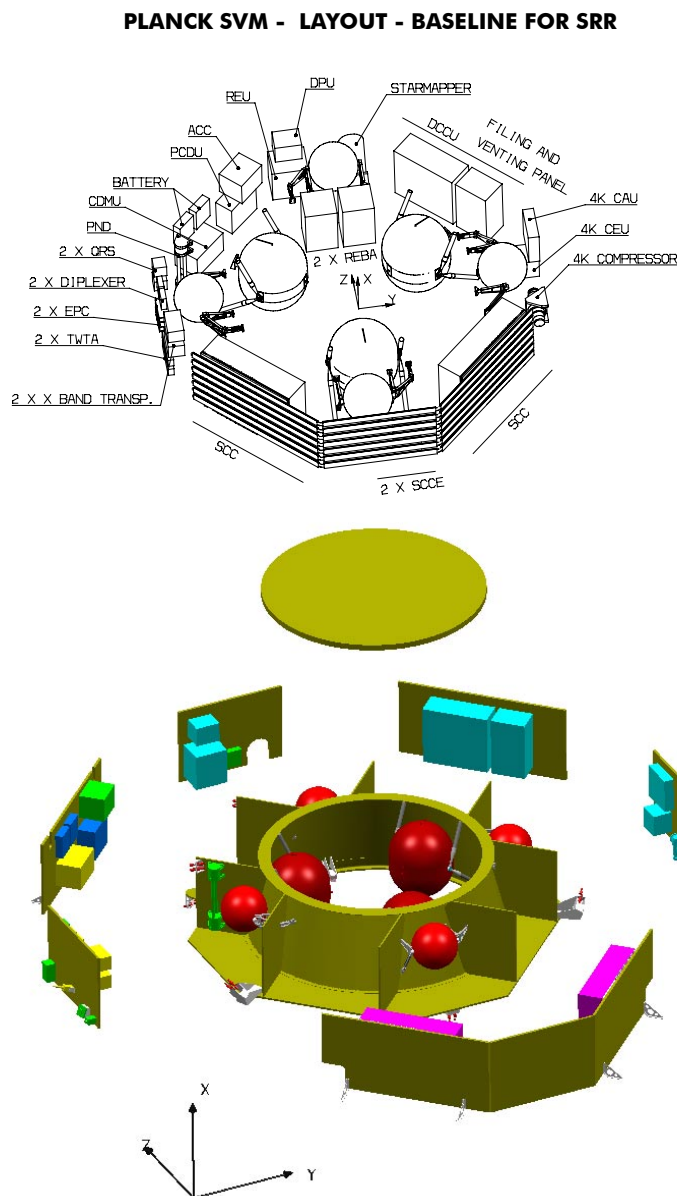
FIGURE 6.2.3.2-1 PLANCK SVM GENERAL LAYOUT

The changes described hereafter refer to changes in Equipment or Instruments accommodation wrt to proposal baseline of December 2000, but not to changes in equipment or Instruments definition, reference remaining IID-A and IID-B Issue 1/0. Further Instruments changes and impact on SVM configuration are discussed after the baseline description.

Change of PCDU/CDMU accommodation

− PCDU/CDMU accommodation on panel +Y have been modified on Herschel in order to improve equipment Thermal control. This measure is implemented on PLANCK without any other impact.
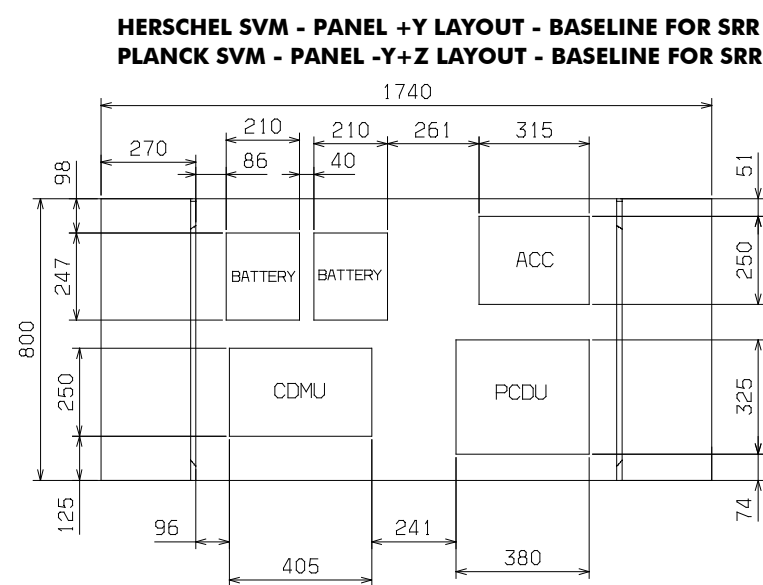
HERSCHEL SVM - PANEL +Y LAYOUT - BASELINE FOR SRR
PLANCK SVM - PANEL -Y+Z LAYOUT - BASELINE FOR SRR

As a last minute change, the decision to keep only one battery is not yet reflected in the configuration.

HFI change

− DCCU and FV panel change in dimensions on ALCATEL request.

− Instruments more compact, compatible with shear webs accommodation.

PLANCK SVM - PANEL +Y+Z LAYOUT - STUDY FOR SRR
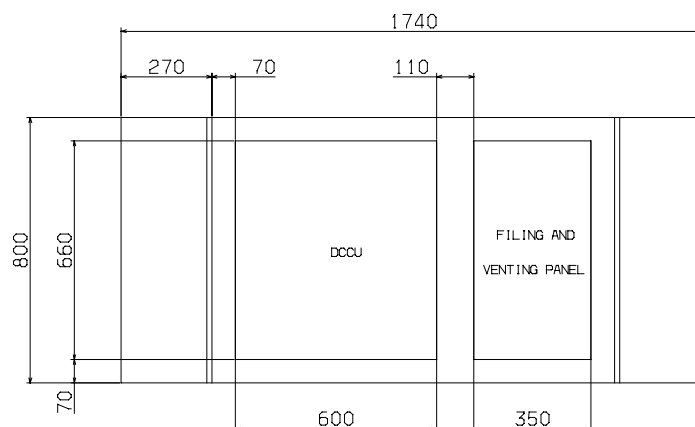
Study of baseline evolution

As for HERSCHEL, preliminary assessment of next coming Instruments changes has been started on the basis of Instruments evolution presented during Instruments meetings, and/or preliminary edition of IID-Bs Issue 2/0.

This preliminary assessment results in:

- check and update of SVM configuration Vs Instruments changes in dimension

- check of mass increase impact on mechanical analysis, and balancing when relevant

- recommendations for Instrument design optimization.

HFI changes

- Growth of REU and DPU in dimensions on panel +Z.

- Leads to interference with current He Tank accommodation.

A new accommodation for REU and DPU can be found with move of He Tank, and consideration of more realistic Instruments shape (clearance are not any way very large).

Layout to be consolidated with study of harness routing and connectors accessibility.
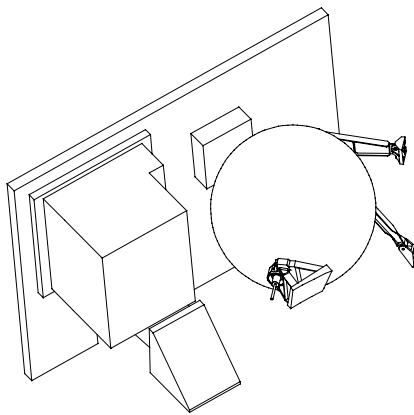
PLANCK SVM - PANEL +Z LAYOUT - STUDY FOR SRR
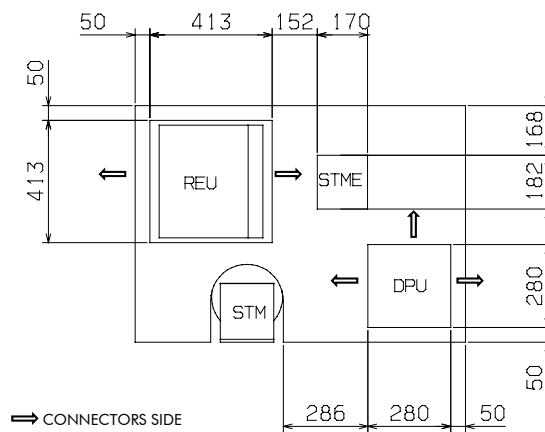
LFI changes: of REBA change in dimensions

    –   Instrument is smaller and lighter.

    –   Convenient to preserve actual accommodation, but remove kilo which participating to the spacecraft balancing.

LFI: BEU becomes 1 x BEU + 1 x DAE control unit

    –   BEU instruments have larger dimensions and mass than previously.

    –   Additional Instrument DAE control box to be accommodated.

    –   Best location for DAE control box is at the opposite side to BEU for balancing (then balancing is improved: gain is 2 Kg in balancing mass compared to additional mass of 21 Kg for DAE control box, and 3.5 Kg for BEU).

    –   Concern is about DAE control box temperature, which is not sure to be maintained in the specified temperature range (PLM sub-platform is not an ideal radiator).

    –   Refer to § 6.2.3.3. for thermal analysis of new DAE accommodation.

6.2.3.2.4. Sensors, antennae and RCTs accommodation

The sensors, antennae and RCTs configuration is similar to the sensors, antennae and RCTs configuration in ALCATEL proposal of December 2000. This is briefly recalled in the following sketches.

Star Mapper accommodation

The Star Mapper is accommodated on +Z side of the SVM, fixed to the lower platform. The Star Mapper line of sight is parallel to the line of sight of the Telescope, and oriented in XZ plane with an elevation of 5 deg. The Star Mapper accommodation constraints to operate one hole in +Z panel to ensure its field of view.
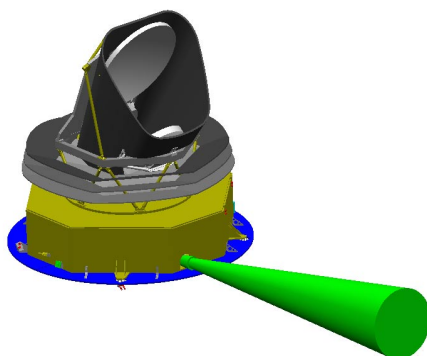
SAS sensors

Planck is implementing a set of 3 SASs. The first SAS is installed at the bottom of the Central Tube box and is pointing –X-axis for attitude control in nominal mode. The 2 other SASs are installed on ± Y side of the SVM, and provide in association with the first one a full sky coverage that allows to locate the Sun position whatever is the S/C attitude (nominal or survival mode).
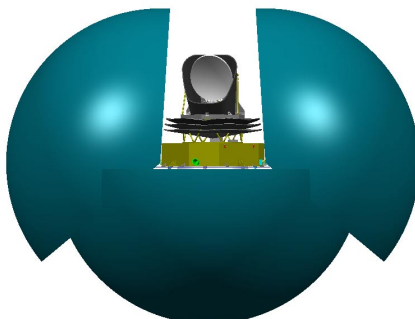
SREM and VMC accommodation

According to ESA request a SREM and a VMC will be installed on Planck SVM. The SREM is located on –Y panel in a protected area (shadowed area), with a clear FoV.

The VMC is located on -Y panel, and looking in lateral direction, in order to make possible a recording of the SYLDA 5 ejection.
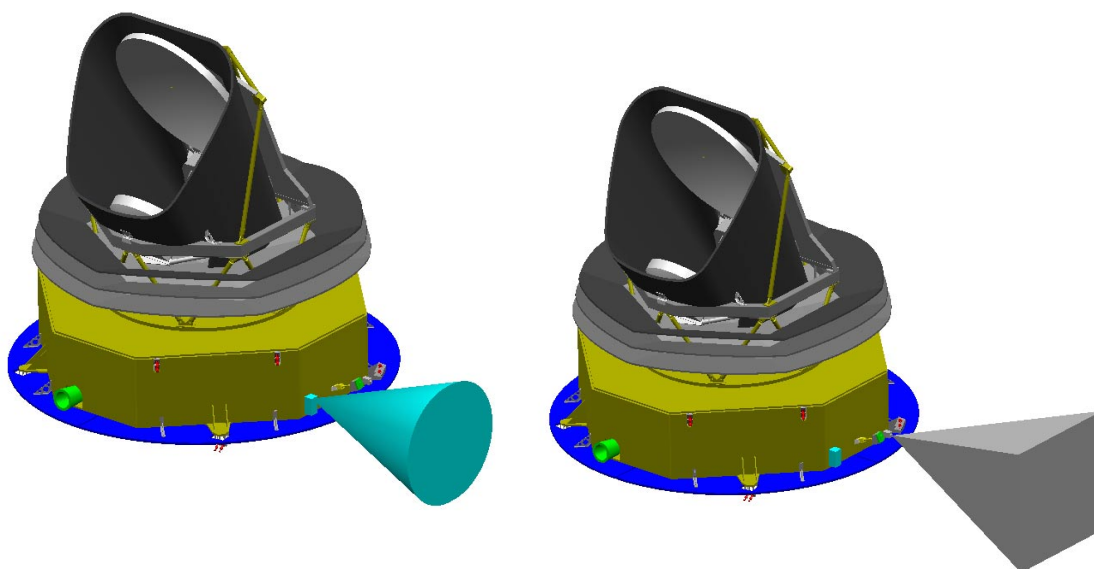
TTC antennae accommodation

The TTC antennae comprise 3 LGas antennae and one MGa antenna.

Three LGas are required to cover the launcher separation subsequent phase and survival mode providing a full sky coverage:

– first LGa antenna is accommodated at the bottom of the central cone

– 2 other antennae are accommodated on ± side of the SVM.

The MGa antenna is nominally pointing Earth, and covers only the normal telecommunication mode.
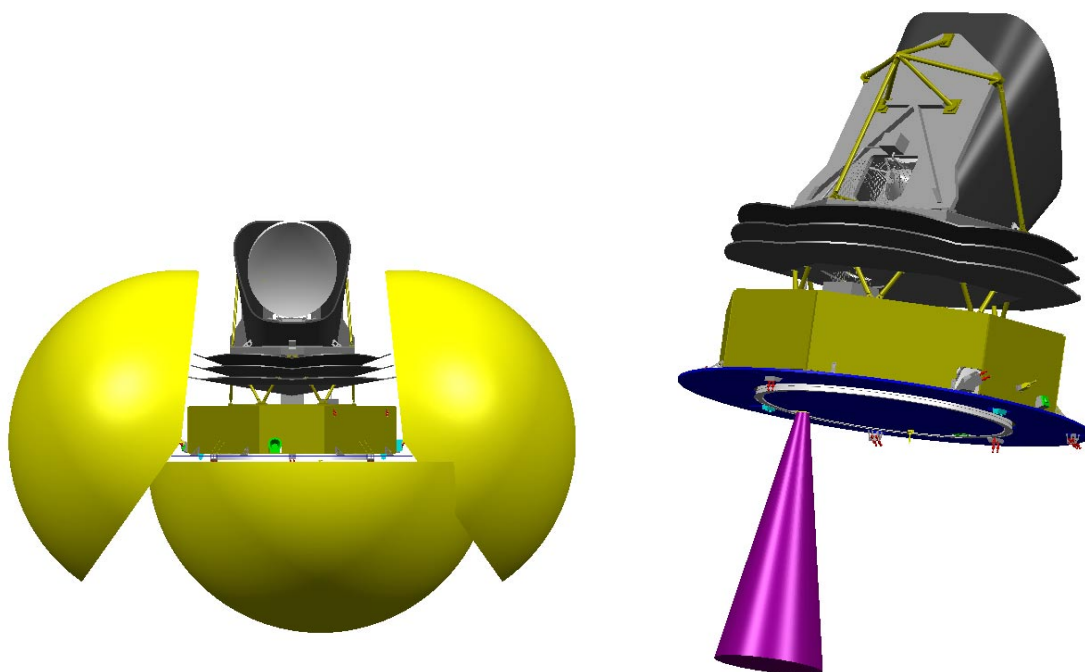
RCT accommodation

The RCTs system comprises:

–   12 RCTs of 10 N force, organized in 4 clusters located below and on the side of the SVM box

–   4 RCTs of 1 N force, organized in 2 clusters located on the side of the SVM box.

The RCTs are commanded by the ACMS system, for injection to L2 manoeuvres, correction of launcher dispersion, attitude control.
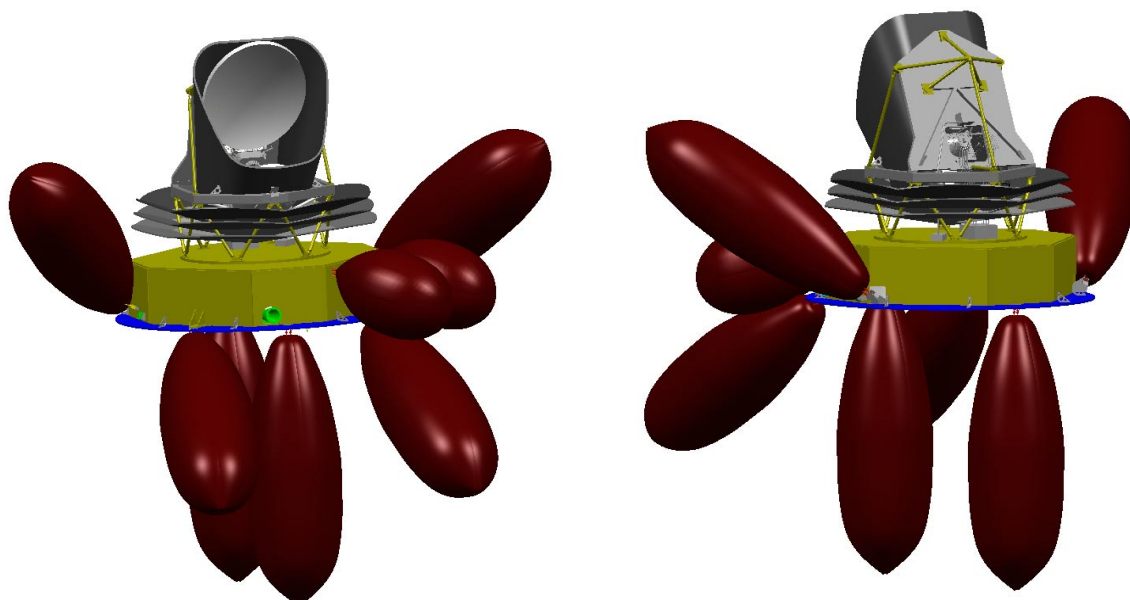
6.2.3.2.5. Mechanical architecture study

Following evolutions are currently in study at ASPI, ASTRIUM and ALS:

Move of PLM to SVM interface

This point is discussed in details under § 6.2.2.2. of this document. Main identified drawback for Planck is the conflict with the current P-PLM integration sequence that takes benefit of a P-PLM supported by the PLM sub-platform. A change of baseline would conduct too initiate a reflection work on P-PLM integration sequence and new MGSE that should be needed to replace the PLM sub-platform.

Change on PLM sub-platform

A change of the PLM sub-platform design should be necessary to reduce acoustic noise response on Instruments located on this platform.

The problem is that Instruments mass are spread on a large platform, which conducts to predict a high acoustic response (ratio mass/panel surface is low about 20 Kg/m^2). As an example, this leads to random loads of about 1 g^2/Hz for BEU.

An improvement is to reduce the platform surface (a large hole at the centre may be adequate), and to provide an additional support to the heavy Instruments (BEU) via supporting struts, or beams from below.
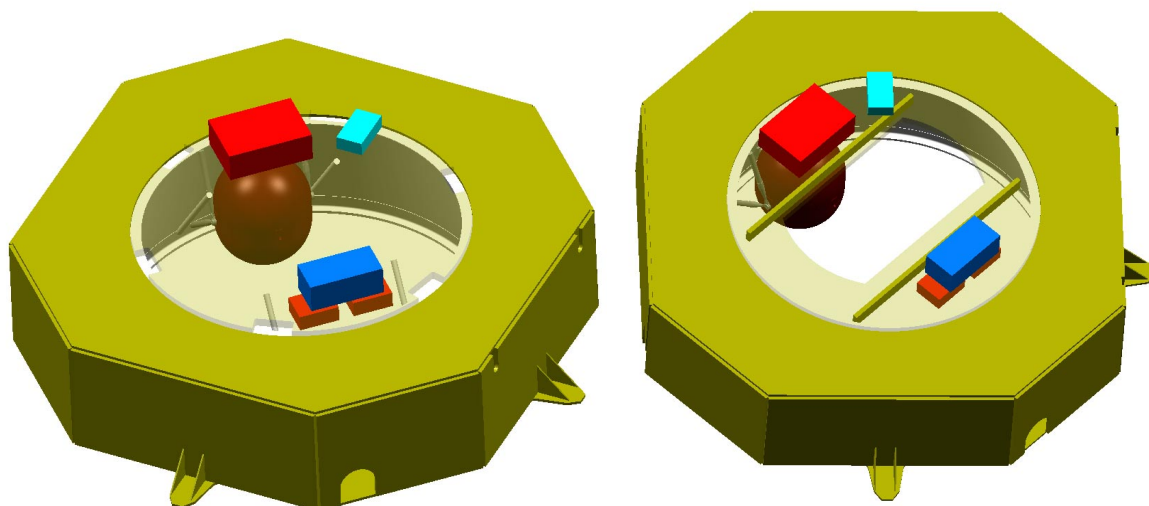
This could allow reducing random loads by a factor 5 approximately.

In that case, mass impact is to be accurately assessed as additional mass for struts can be compensated (TBC) by the sub-platform which is made lighter (large hole, plus re-sizing to account for supporting struts).

The next step would be to assess gain in random load reduction that could benefit to the Instruments on the PLM sub-platform, Vs possible mass impact on SVM.

6.2.3.3. PLANCK thermal design

6.2.3.3.1. Overall Thermal Design

The main features of the overall PLANCK spacecraft thermal design are unchanged since the technical proposal. It is recalled that the thermal concept is based on a high level of thermal insulation between the two sub-modules making up the spacecraft:

- the SerVice Module (SVM), which maintain all the equipment mounted on basically around 20° C and support the Solar Array (operating temperature >100° C)

- the PayLoad Module (PLM), which temperatures of its components are mostly set in the cryogenic range (<120 K).

The thermal insulation between SVM and PLM is required for several purposes:

– first of all, the PLM accommodates a cryogenic radiator in order on one hand to operate the instruments coolers, and on the other hand to provide a low temperature environment for the telescope and Focal Plane Unit. Due to the very low temperature needed on the PLM coldest stage (60 K at the Sorption Cooler pipes interface, including uncertainties and design margin), it is mandatory to reduce to their minimum the radiation and conduction heat flux between SVM and PLM

– another important Thermal Control System design driver is related to the requirements on the temperature fluctuation levels, out coming from the Strayligth constraints. Basically, temperature variations of the SVM must be kept under limits defined by Straylight analysis, in order not to induce unacceptable perturbations on the PLM, therefore on the instruments detectors. Those perturbations are all the more damped than there is a good thermal insulation between SVM and PLM.

Previous analyses have shown however that the practical level of thermal insulation obtained was good enough to achieve the required temperature specifications on P-PLM side. However, it has been evaluated as not high enough to meet all the Straylight requirements. Preliminary specifications have been deduced from the "PLANCK Strayligth Evaluation of the Carrier Configuration RD01.3" study, based on the temperature fluctuation levels calculated in the frame of the study "Impact of the SVM and Solar Array Temperature Fluctuations on the Stability of the PLM" RD01.4. These requirements will be updated according to the straylight analyses undergoing. They will be however in the same order to magnitude than what have been specified so far.

This leads to drive some interfaces requirements on the SVM prime, in term of design and performances:

– for radiative insulation purpose, the +X side of the SVM must be covered with a high efficiency MLI blanket, in order that the PLM have a view factor with a part of the SVM which temperature is as low as possible. For the same reason, the backside of the Solar Array shall be covered with a MLI blanket as well. In both cases, the external layer of the blankets is Aluminium coated in order to present a low emissivity, therefore reducing the radiative coupling with the cold PLM.

  – the SVM TCS must limit the temperature fluctuations at the PLM I/F truss attachment on SVM in the following range:

  $\leq \pm 325\ \mu K$ on a 325 s. time period

  $\leq \pm 0.25\ K$ on a 2 hours time period.

  – The SVM TCS must limit the average temperature fluctuations of each radiative panel in the following range:

  $\leq \pm 0.2\ K$ on a time period of 325 s

  $\leq \pm 0.5\ K$ on a time period of 2 hours.

From the above requirements, important additional features of the SVM TCS design have been deduced:

  – use of compensation heaters on equipments which dissipation changes when shifting from observation mode to telecommunication mode (Travelling Wave Tube Assembly and X-Band Transponders)

  – thermal discoupling of the three Sorption Coolers panels from the rest of the SVM to damp as much as the possible the induced temperature fluctuations towards the PLM

  – the temperature of the panels supporting the equipments shall be actively controlled in order to maintain a constant temperature level, even if the dissipations are not constant within a given operating mode, or if there is a spin axis re-orientation. For this purpose, it is proposed to use a well-proven active control design, i.e. a thermal regulation based on Pulsed Width Modulation. This concept is implemented on numerous satellites and payloads, which require stringent temperature stability.

Thermal design and analyses of the SVM is reported in the SVM design Report. PLANCK PLM design and analyses described in the P-PLM design report.

6.2.3.3.2. Impact of Instruments units evolution

As for HERSCHEL, we deal in this chapter only with the thermal interfaces at SVM level. Instruments thermal interfaces at P-PLM side are described in detail in the P-PLM design report.

The instruments data used by ALENIA for the SVM thermal design are based on the IID-Bs Rev. 1.0. The inputs from the instruments are consequently the same as for the ITT technical proposal. The important feature to keep in mind is that thermal analyses have been performed adding 10 % system margin on the dissipation of all units. The temperature results are moreover including 7° C margin for cover uncertainties and design margin.

For both LFI and HFI instruments, we recall first the hottest case temperature obtained by ALENIA. The modifications discussed after are related to the proposed IIDBs Rev. 2.0.

6.2.3.3.2.1. HFI instruments

ALENIA results at SRR.

	Units	TMM results (°C)	Operating design range (°C)
HFI			
PHDPU	DPU	22,5	[-10 , 40]
PHPAU	Pre-Amplifier Unit	32	[-20 , 30]
PHREU	Read Out Electronics	31,1	[0 , 30]
PHJTC	4K Cooler Compressor Unit	29,5	[-10 , 40]
PHJTA	4K Cooler Ancillary Unit	29,4	[-10 , 40]
PHJTE	4K Cooler Electronics Unit	27,6	[-10 , 40]
PH3HE	0,1K Dilution Cooler ^{3}He tank	23,7	[-10 , 40]
PH4HE	0,1K Dilution Cooler ^{4}He tank	25,2	[-10 , 40]
PHCDU	0,1K Dilution Cooler Control Unit	19,3	[-10 , 40]
	0,1K Filling & Venting panel		

Two units are slightly out of their specifications. The PAU, located on the PLM sub-platform, as well as the REU, located inside the central cone.

The recovery action for the REU would be a change of its location on to the panel, in order to increase the distance from the highly dissipative PCDU (123 W). The result is however estimated not critical as the temperature presented here includes significant margin. This conclusion is all the more valid that no dissipation growth of the HFI units have been identified in the IID-B proposed update.

With regard to the PAU, we will come back on this subject after presentation of the proposed LFI evolutions. Indeed, the total dissipation on the PLM sub-platform should increase a lot according to the proposed IID-B update. An overall solution should be consequently found.

the only evolutions (from IID-B Rev. 1.0 to proposed Rev 2.0) identified is related to the PAU temperature stability:

– PAU temperature stability during observation: ≤ 0.1°/hour.

It is not foreseen to thermally control the equipments located on the PLM sub-platform, as it would bring at even higher temperature the PAU and BEU, which would be clearly out of the specifications. The PAU will be submitted then to changing heat fluxes coming mainly from:

– the SCC panels

– a SAA change.

The PAU is highly conductively coupled with the P-PLM sub-platform. The time constant of this box is then equal to the time constant of the whole panel on which it is attached. Results obtained with the ITT Thermal and Mathematical Model shows that the impact of the SCC dissipation oscillations on the PLM sub-platform temperature fluctuations amplitude was around 5 µK. This gives a good estimation of the huge damping of the SCC panel temperature fluctuations. Computations will be however performed with the updated SVM TMM (used for SRR Design Report) to assess this point. Concerning the impact of a SAA change, ALENIA has computed with the updated TMM an impact of 0.2° C with a 10° angle spin re-orientation. This preliminary result is close to the requirements. It shall be checked after refinement of the PLM sub-platform nodal breakdown.

6.2.3.3.2.2. LFI instruments

ALENIA results at SRR.

NOTA: Evolutions linked to the Sorption Cooler Compressor are treated in the next chapter.

	Units	TMM results (°C)	Operating design range (°C)
LFI			
PLBEU	DAE	**32,3**	[-20 , 28]
PLREN	REBA Nominal	38,3	[-20 , 50]
PLREB	REBA Redundant	28,1	[-20 , 50]
PLSCE	SC Electronics	20,2	[-10 , 40]

The DAE box, located on the PLM sub-platform is out of the specifications, after inclusion of the 7° C temperature margin. This platform do not present a radiative surface towards the cold environment because it needs to be thermally discouled from the P-PLM.

The situation, which was not so critical at time of the ITT, would become much worse taking into account the proposed updates of the LFI instrument.

The first change concerns the BEU. A new dissipative box has appeared, the "DAE control box", which dissipate 31.5 W. Due to layout and integration constraints, the location of this box is stringently constrained on the PLM sub-platform. In the same time, the DAE dissipation has slightly decreased from 45.7 to 35.2 W.

The net dissipation increase on the sub-platform is however important (26 W), considering it's thermal control concept. This value is higher than the dissipation margin used for the SRR computations (10 % of 10 W + 45.7 W = 5.6 W).

It has to be noted that the results presented before are obtained with a PLM sub-platform nodal breakdown not detailed enough to have a good accuracy on the calculated temperature. It needs first to be refined by ALENIA. A clear status of the impact of such a dissipation evolution will then follow. The remarks and recommendations we can bring at this stage of the study are the following:

- the design temperature of the equipment on this sub-platform is reduced (~30° C) compared to "classical" units, which can operate up to 40° C – 50° C: investigations have to be made at instruments level in order to relax the requirements

- the specifications given in the LFI IID-B shows that the "the main requirement is not in the absolute temperature limits but in the temperature stability" (BEU): once again, it is recommended to clearly define the need in order not to put too high constraints on TCS design. One point to take into considerations is that the LFI wave guides are connected to the BEU. Care must be paid in order to check that a potential increase of the BEU temperature does not lead to an unacceptable level of heat losses on the PLM cold stages.

A potential recovery action to decrease the temperature of the PLM sub-platform units is to allow them to radiate towards cold space. This means to remove part or total of the MLI blankets on the box, and eventually add dedicated radiator panels if the external surfaces of the boxes are not large enough to efficiently reject the heat. Even if this configuration shall be studied, it is considered as the worst one, as it means a degradation of the thermal insulation between the SVM and PLM, then an impact on the PLM performances.

The situation on the PLM side does not allow at this stage of the study to relax the thermal interface requirements on the SVM design. An other potential impact concerns the additional mass due to the foreseen dedicated radiators for the BEU and DAE control box. Indeed, a design requirement criteria allows evaluating the need of a base-plate to control a box (see next chapter). It appears that the BEU and DAE control box are at the edge related to this criteria, and would probably require a base-plate due to the low maximum temperature design, at least for the BEU. This means that the heat has to be collected by the base-plate, and then driven to a radiator, involving a mass impact. Besides, the implementation of a radiator between the PLM sub-platform and the first "V-groove" shield would significantly alter the first shield view factor with space, then raise its temperature. Finally, it is strongly recommended to relax some requirements on the instruments side, in order not to induce a degradation of the overall system optimisation and performances.

Another requirement foreseen after working meeting with LFI instruments (but not reflected within the proposed IID-B updates) is the temperature stability of the BEU:

– BEU temperature stability during observation: ≤ 0.2 °/hour.

This level of stability is equivalent to the one required for the PAU, located also on the PLM sub-platform. The remarks made for this unit are therefore totally applicable.

6.2.3.3.3. Sorption Cooler Compressor Thermal Interface

The proposed thermal interface of the SCC shows an important increase of both the mean dissipation (400 W to 520 W, then + 30 %) and the peak dissipation (950 to 1250 W, again ~+ 30 %) at the I/F radiator. The mean disspation increase have a direct impact on the required radiator surface to maintain the SCC in its temperature range (260 K – 280 K), as well as on the heat pipes layout. In other words, a higher dissipation must be supported by a higher heat pipes number.

The data taken into account by ALENIA to design the SCC radiator are in coherence with the IID-B rev. 1.0. The mean power used was even larger than what was specified (430 W vs. 400 W in the IID-B 1/0), because the analyses have been performed using a table from a previous Sorption Cooler Agreement, showing the distribution of the power over the 6 elements of the SCC. Indeed, this distribution was necessary to design with confidence the radiator and this information on the dissipation was then not available in the IID-B. Taking 10 % system margin on this mean 430 W dissipation (as required in AD01.1/SINT-035: requirement to take 10 % margin over IID-B dissipation for warm payload units), the temperature of the SCC I/F absorbing beds fluctuate between 0° C and 1° C, without adding margin on the temperature. The important point is that all the available surface of the 3 dedicated SCC panels is used as a radiator (3.926 m^2), with a coating presenting an emissivity value of 0.78 (OSR).

NOTA: the crossing heat pipes number is 19 (as for ITT proposal), and have not been reduced to take into account the actual bed's footprint length provided recently by JPL. The impact of such a reduction is estimated as negligible. The SVM TMM shall be however updated to take into account this modification.

The impact of an increase of the mean dissipation to 520 W (+ 10 % system margin) has been assessed by ALENIA. The results obtained (calculated temperature without margin) are out of the right operating temperature range (see next figure).
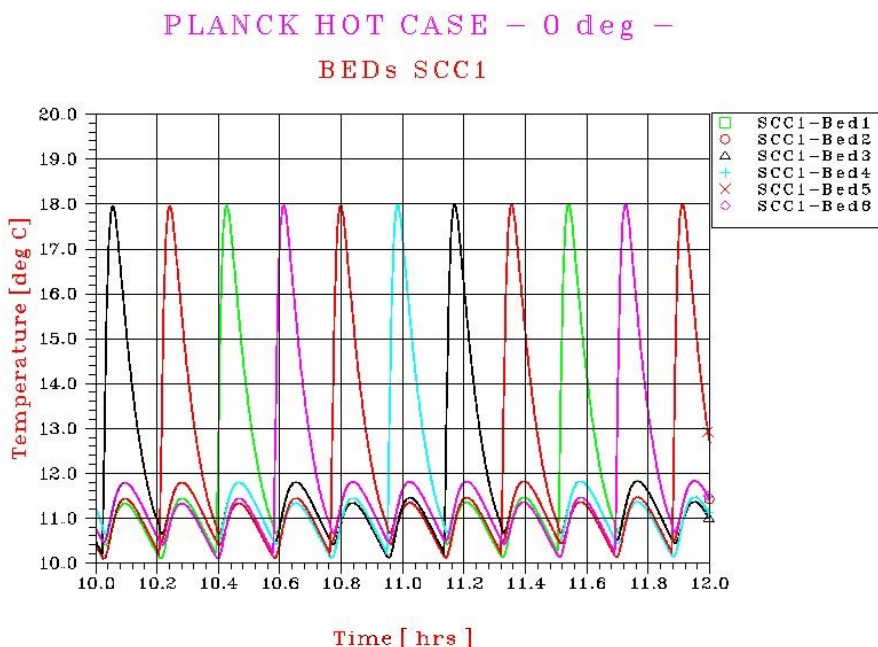
FIGURE 6.2.3.3-1 SCC BEDS CALCULATED TEMPERATURE PROFILE WITH 520 W + 10 % MARGIN

The calculated temperature range of the SCC I/F bed is [283 K – 285K], then higher than the specified range [260 K – 280 K]. As the whole panels surfaces are used as a radiative area, there is no way to enlarge the surface. The possibility to increase the emissivity of the coating shall be investigated (black paint instead of OSR).

The solution to use an open honeycomb (as for PLANCK cold radiator) will be also evaluated to increase by geometrical effect the emissivity of the coating applied inside the cell. However, it is not foreseen as the right solution, because in opposition with PLANCK PLM, the heat flux to be rejected towards space is huge, leading to a temperature gradient along the cell, so a reduced efficiency compared to the PLANCK PLM situation.

The right way to find out solutions to overcome the problem is to clearly identify the different dissipation margins ans contingency at the SCC level.

Besides the impact of the mean dissipation increase, the peak power dissipation increase brings additional problems dealing with the crossing heat pipes operation.

The outer shell interface has been greatly clarified since the beginning of the Phase B study. It appeared that the hypothesis taken for the proposal (and for the previous analyses performed during the P-PLM architect study) were far from the actual one. So far, we had assumed a contact surface under each compressor bed of 475 mm length and 41 mm width. Those two values had been derived from the SCC fixation layout. In response to clarification actions taken during the first working meeting with PLANCK instruments, the bed footprint have been provided by JPL (see next figure).
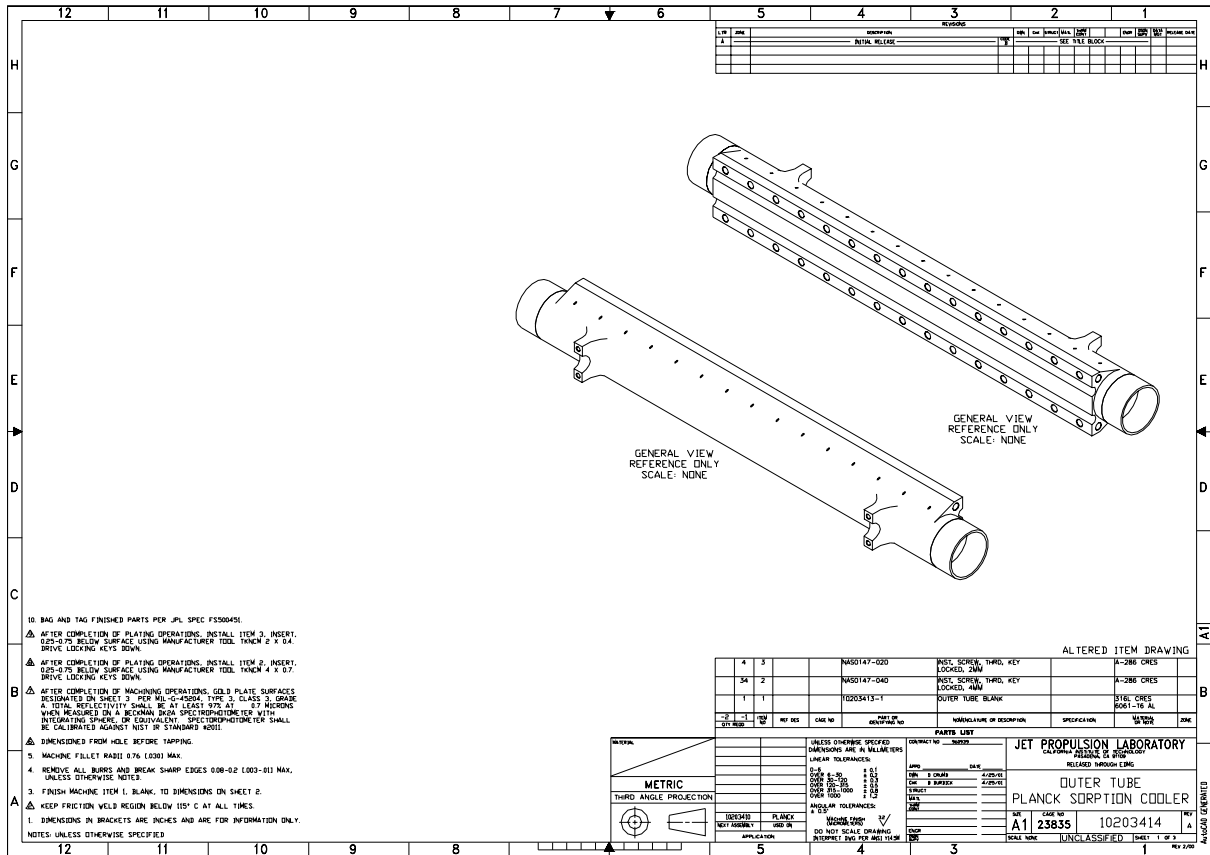
FIGURE 6.2.3.3-2 OUTER SHELL INTERFACE DRAWING (1)
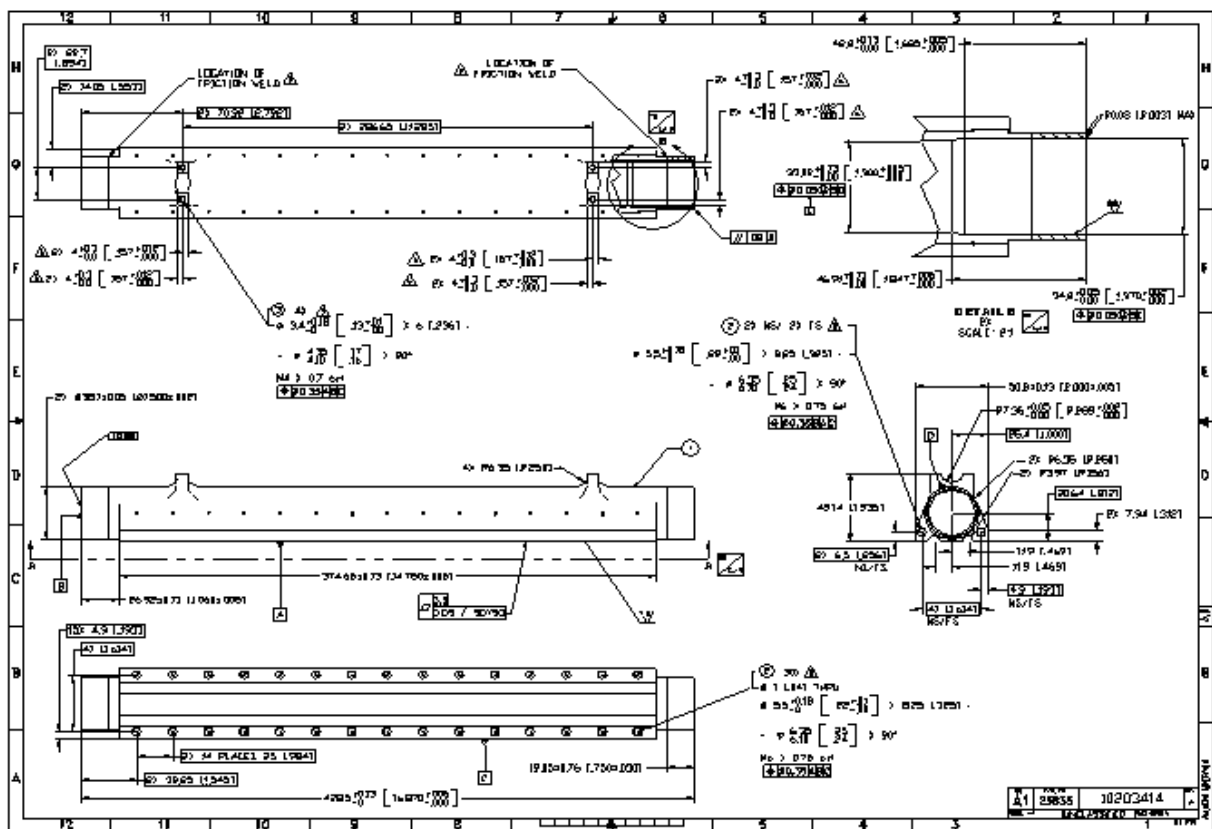
FIGURE 6.2.3.3-3 OUTER SHELL INTERFACE DRAWING (2)

The bed length is reduced with regards to what have been considered for the technical proposal, i.e. 374.8 mm. The consequence is the reduction of the crossing heat pipes number, from 19 to 15, taking into account the heat pipes wing width (25 mm). Let's note that the wing width is set by the fixation layout of the SCC, i.e. 25 mm between each screw along the bed length. All the results presented here are then related to an unchanged SCC fixation layout with regards to what is proposed by the instrument. Possible modifications of this fixation layout could be envisaged later if required, in order to optimize the whole system.

The width on which the bed is in contact with the radiator is 34.9 mm, to be compared to the 41 mm used so far. Taking into account the huge peak dissipation proposed increase, 950 W to 1250 W, so + 30 % (so 1020 W under an individual bed), the maximum power density on a heat pipe is 8.6 W/cm^2, taking into account 10 % system margin on the dissipation. This data has been considered as marginal, and well above the specification usually adopted by ALCATEL for the design of the heat pipes layout on Telecommunications spacecraft, which use widely heat pipes on their radiator panels.

Recovery action has been then required to JPL in order to slightly modify the bed footprint. This action has been accepted and the surface in contact with the heat pipes under each bed is now 374.8 mm * 50.8 mm. In this case, the maximum power density falls down 5.9 W/cm^2, still with 10 % system margin on the dissipation. The final power density to be specified to heat pipes Suppliers has been then put again in a commonly used range.

Work with JPL is undergoing in order to end up on a compromise on the heat dissipation budget. What is clear is that the design of the SCC radiator cannot withstand a mean dissipation higher than 470 W, and a peak dissipation higher than 1000 W. These values are **maximum** ones, including all JPL contingency and system margin. The corresponding relevant SCC interface temperature is 7° C, including 6.3° C margin. This margin is related to uncertainties (TMM, design not completely frozen in the details...). The studies undergoing are mainly a careful crosscheck of the SVM TMM delivered by ALENIA, which will be followed by an optimization of the present design. In particular, the impact of an increased emissivity of the SCC radiators will be addressed (use of black paint instead of Optical Solar Reflector). The aim of the studies is clearly to recover some margin on this critical area, which are considered as low at this stage of the study.

A different layout of the SC electronics will be also investigated. The "thermal ideal solution" is to remove these dissipative boxes (135 W) from the SCC panels, and to accommodate them on the adjacent panels. This would have a huge impact onto the overall SVM configuration, and will have to be studied carefully before taking any decision.

An alternative and very promizing solution to reduce the dissipation of the SCC is related to the reduction of the I/F temperature on the last stage heat exchanger (coldest "V-groove shield level). Indeed, the SCC dissipation is all the more important that the I/F temperature is low, for a given cooling power at 20 K. The present SCC dissipation is linked to an I/F temperature at 60 K. Studies are undergoing at P-PLM level to reduce maximum predicted temperature at this interface (now around 60 K). A significant improvement is foreseen due to the implementation of an optimised heat exchanger. The aim is especially to reduce the "hot spot" around the heat exchanger level. All the details concerning this study are described in the P-PLM design report.

Problems of the thermal interface between the SCC and the crossing heat pipes have been solved with minor change in the SCC design. The SCC presents now the correct interface in order to operate the heat pipes in the right way and with the best thermal performances.

The last point to be addressed is related to the new and very stringent temperature stability requirements on the I/F beds temperature identified in the Sorption Cooler ICD proposed update. This subject is treated in § 7.3.3.

6.2.3.3.4. Recommendations for instruments units thermal design

As depicted in HERSCHEL thermal design section, we have gathered in the next table the baseplate need for the different instruments units. The input taken into account are related to the IID-Bs proposed Rev. 2.0.

INSTRUMENT	Units	Length (mm)	Width (mm)	Height (mm)	Heat dissipation (W)	Power density	Baseplate
HFI							
	DPU (Nominal & Redundant stacked)	280	280	200	42	110	YES
PHPAU	Pre-Amplifier Unit	422	250	232	10	19	YES
PHREU	Read Out Electronics	340	370	280	90	139	YES
PHJTC	4K Cooler Compressor Unit	460	250	200	60	117	YES
PHJTA	4K Cooler Ancillary Unit	350	350	100	12 (20 non - op possible)	31	NO
PHJTE	4K Cooler Electronics Unit	220	220	200	30	44	NO
PH3HE	0,1K Dilution Cooler ^{3}He tank	diameter : 480			0		
PH4HE	0,1K Dilution Cooler ^{4}He tank	diameter : 480			0		
PHCDU	0,1K Dilution Cooler Control Unit	670	600	260	10	7	NO
	0,1K Filling & Venting panel	350	600	260	0		
LFI							
PLBEU	DAE	570	400	200	35,2	42	YES
	DAE control box	250	500	200	31,5	57	YES
PLREN	REBA Nominal	300	300	500	35	45	NO
PLREB	REBA Redundant	300	300	500	[35]		
SORPTION COOLER							
SCC	Sorption Cooler Compressor Nominal	1000	750	250	520 mean, 1250 max		
SCC	Sorption Cooler Compressor Redundant	1000	750	250	[520 mean, 1250 max]		
SCE	Sorption Cooler Electronics Nominal	250	200	140	135	597	YES
SCE	Sorption Cooler Electronics Redundant	250	200	140	[135]		

As shown in the previous table, the units internal design is not considered as critical, except for the SCE box (597 W/m^2). The dissipation is indeed very important compared to the dimensions. An additional feature to take into account for the thermal internal design is that the baseplate is not linked to the radiator on its whole surface, as it is mounted onto the SCC panels longitudinal heat pipes.

6.3. ELECTRICAL AND FUNCTIONAL SYSTEMS DESIGN

This section describes, from a system point of view, the way each of the main Herschel and Planck spacecraft functions are implemented, via hardware or software. The functions implementation is described through a breakdown into subsystems, and the EMC issue is also addressed, as a constraint on the baseline electrical design. Details on the different subsystems can be found in the SVM Design Report.

6.3.1. Design Overview

This chapter aims at giving an overview of the functional architecture of Herschel and Planck spacecraft's. Its main drivers are first recalled then the main features of the architecture are presented for each of the main functions : data handling, attitude control, power and TTC, as a response to the retained drivers.

6.3.1.1. Drivers

The main HERSCHEL and Planck electrical and software design features are derived from the System Requirement Specification following a top-down approach of the mission constraints.

The baseline solution is driven by the following criteria covering the overall system design, development and validation aspects:

 – compliance to technical and fault tolerance requirements, furthermore including sufficient flexibility to accommodate upgrade of the main requirements

 – commonalty between HERSCHEL and Planck designs; this is one of the programme challenge

 – optimization of the hardware impact towards minimization of mass and cost aspects

 – favour software based solution to improve design flexibility in the development and mainly validation phases

 – match the industrial development and validation constraints.

6.3.1.2.   Electrical architecture

The overall electrical architecture is designed to satisfy both the instruments and spacecraft mission needs. It is described in Fig 6.3.1-1 for Herschel, and Fig 6.3.1-2 for Planck and is basically identical for both spacecraft's.

As far as instruments services are concerned, it generally provides:

– power distribution to a number of instrument units of 28 V regulated and protected lines

– general 1553 data bus interface for data collection and payload commanding under packet formats. The communication protocol is addressed in AD 03.3 (Packet Structure ICD).

– indirect access to ground control centre via the spacecraft TTC subsystem when in ground station visibility

– storage in mass memory of science and housekeeping data for up to 48 hours, based on the specified instruments average rates.

– Signals to synchronise the payload operations with the spacecraft ones :

• accurate stamps of the Spacecraft Central Reference Time using dedicated 1553 Mode Commands

• On Target Flags to indicate to HERSCHEL instruments that the required pointing is achieved; OTF is distributed via 1553 Messages.

• accurate indication of the Reference Star Pulse to Planck instruments; RSP is distributed via 1553 Messages.

• 131072Hz clock, synchronized with the Spacecraft Central Reference Time.

– Conditioning of HERSCHEL and Planck Payload Modules specific temperature sensors.

While the functions mandatory for the proper spacecraft operation and mission achievement are:

– the power conditioning and distribution to the spacecraft units under a regulated and protected form.

− The satellite data handling tasks:

- reception via the X-Band receiver and storage of ground telecommands of the Mission Timelines under packet format specified in AD03.2 (SGICD) and AD03.3 (PS ICD)

- collection and storage on Mass Memory of science packets and satellite housekeeping for the 48 hours specified functional autonomy duration

- capability to store the Mission Timeline for a minimum of 48 hours of continuous operation

- downlink of this data under the format specified in the SGICD and packet ICD using the X-Band transmitter

- active thermal control of the satellite in nominal mode, and autonomous heating capabilities in survival case

- spacecraft accurate time maintenance and distribution to instruments and spacecraft users (ACMS)

- payload instruments interfacing and synchronization with the spacecraft operation via the 1553 bus commands and dedicated Sync lines.

− RF signal reception and demodulation for the uplink, modulation and transmission for the downlink, in line with AD03.2 requirements.

− Satellite attitude and orbit control, including ACMS sensors acquisition and processing, and actuators, including thrusters, commanding.

− Satellite Failure Detection Isolation and Recovery to satisfy fault protection and autonomy requirements.

These functions are implemented by both hardware and software components through the Avionics chain, which includes both Command & Data Management and Attitude & Orbit Control subsystem and the corresponding softwares, the Power Control Subsystem, the Telemetry/TeleCommand subsystem and the Harness subsystem.

FIGURE 6.3.1-1 HERSCHEL ELECTRICAL ARCHITECTURE

PLANCK ARCHITECTURE

FIRST/PLANCK COMMON PART

Cold redundant Modules

Hot redundant Modules

Redundancy by groups

FIGURE 6.3.1-2 PLANCK ELECTRICAL ARCHITECTURE
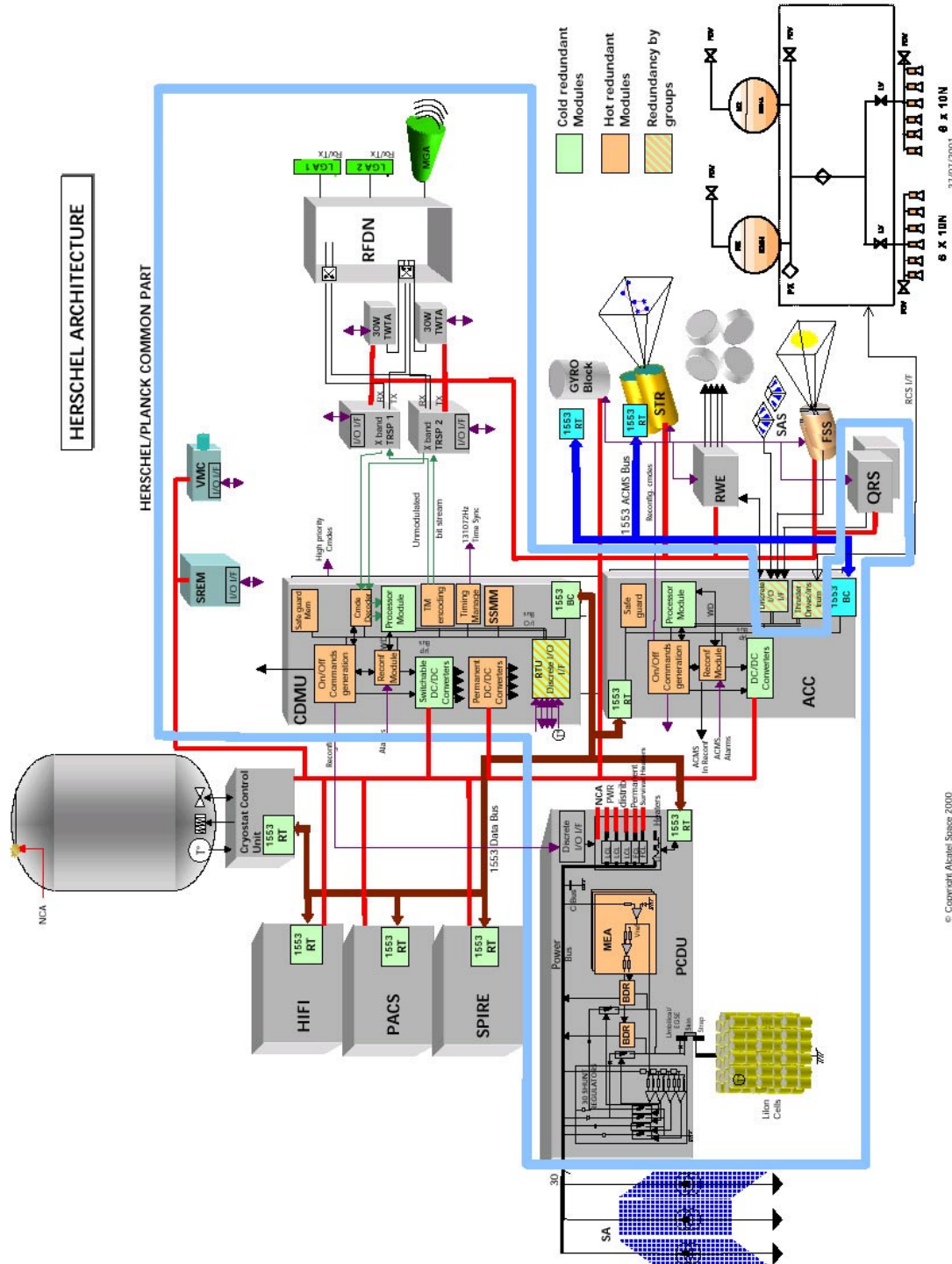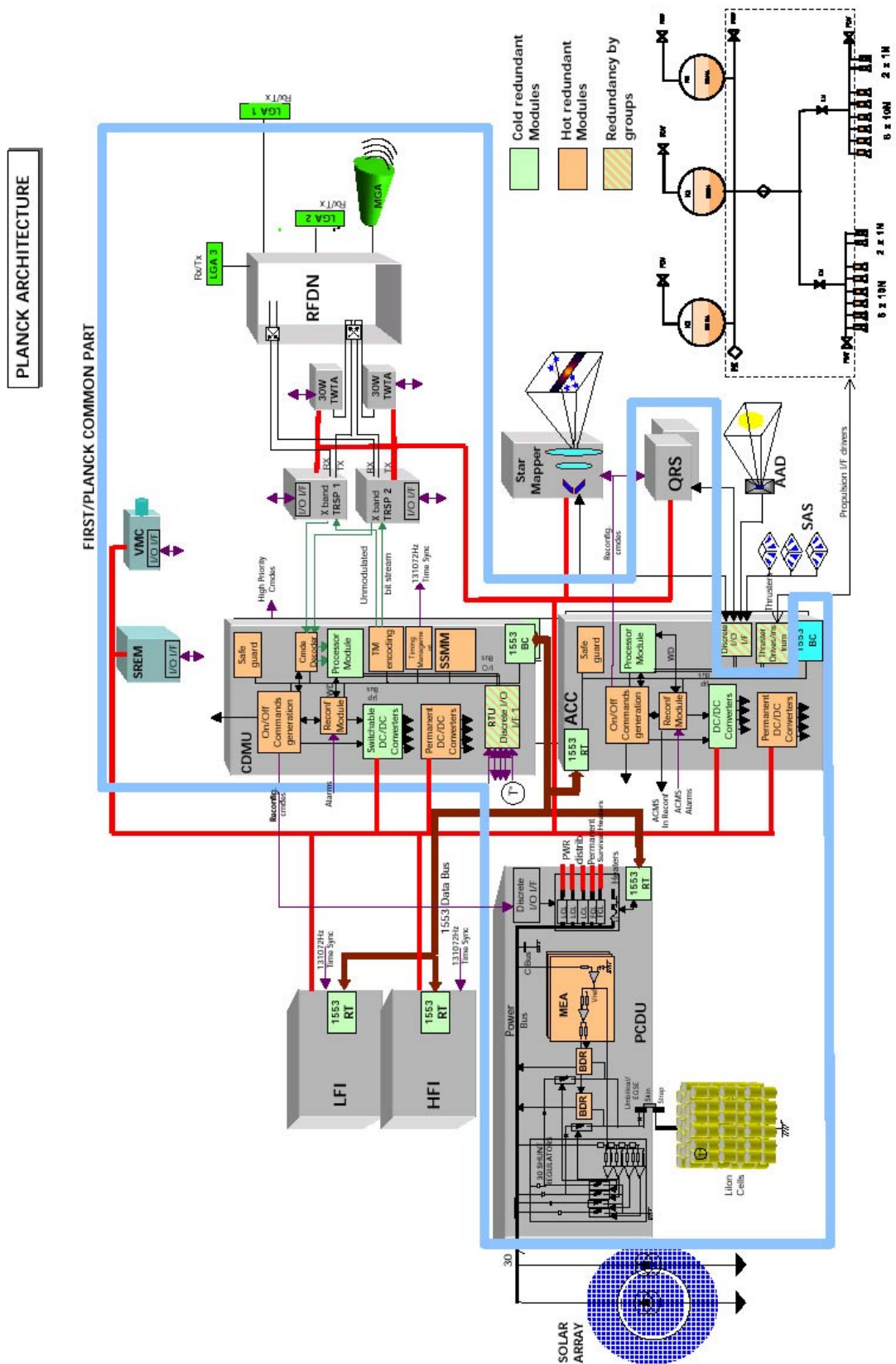
© Copyright Alcatel Space 2000

Avionics chain

It comprises both Command and Data Management and Attitude Control and Measurement susbsystems.

The Avionics architecture is essentially based on a decentralised approach, with Data Handling and Attitude Control tasks running on 2 distinct computers. On the contrary, the data handling function on the one hand, and the Attitude Control and Monitoring function on the other hand are themselves highly centralised around 2 main units.

The **C**ommand and **D**ata **M**anagement **U**nit (CDMU), the data handling cold redundant computer, is identical for both spacecraft. This is basically made feasible by taking, where applicable, the envelope case between the 2 spacecraft:

  − in the I/Os allocation (see SVM Design Report§ 9.7.7)

  − for the mass memory storage sizing (see § 6.3.2)

  − for the up and downlink data rates (see § 6.3.4).

It distributes a 1553 data handling bus to the Payload Module units, including each of the payload instruments (and the Cryo Control Unit for HERSCHEL), but also to the **P**ower **C**onditioning and **D**istribution **U**nit and the **A**ttitude **C**ontrol **C**omputer for commanding and telemetry collection. However, the data rate with PCDU and ACC is expected to be low in normal operation, leaving the maximum data bus bandwidth to the payload for science collection. A bus throughput preliminary analysis is performed in Section 6.1.4 and in RD01.2 for the two spacecraft's.

The CDMU hot redundant TC decoders receive telecommands from one of the 2 hot redundant X-Band receiver under a packetized format. Commands are either executed (High Priority Commands), or forwarded to the processor module of the CDMU, which either executes the commands, or forward them, still under packet format to the end user, instrument or ACC.

The telemetry is sent to one of the cold redundant X-Band transmitting chain during the communication sessions via up to 8 virtual channels getting data directly from the mass memory, or from the processor memory. The telemetry rates can be set from programmed values, to cope with the different spacecraft modes, and the capabilities of the 2 ground stations allocated to HERSCHEL and Planck missions: Perth and Kourou as back-up.

The CDMU interfaces with the PCDU for telemetry collection, but also:

- to turn on and off or enable units according to the Mission Timeline, ground commands, or reconfiguration orders

- to implement the spacecraft thermal control by suitably commanding the heaters.

The CDMU houses the Data Handling on board software and provides to it all the features, storage & processing capabilities and mechanisms necessary to the performance of the spacecraft control and management tasks and to the implementation of the services stated in OIRD (AD03.1).

High level failures recovery is ensured by a cold redundant Reconfiguration Module (CDMU_RM) which distributes the appropriate High Level Commands internally and to the PCDU according to the spacecraft data handling context saved in failure proof safeguard memory (CDMU_SGM). Lower level failure identification and recovery is managed by the Data Handling software. The overall fault protection strategy is described in Section 6.4.3.

The Spacecraft Central Reference Time is maintained via a hot redundant timing module driven by an adequate Oscillator to guarantee the stability requirements.

Also, in addition to the above standard CDMU function, the HERSCHEL and Planck CDMUs include all the other CDMS functions:

- the RTU function, performing the point to point interfaces

- the 25 Gbits Solid State Mass Memory module, with its dedicated controller, to store science data and housekeeping outside communication sessions (sizing is justified in Section 6.3.3).

The **A**ttitude **C**ontrol **C**omputer (**ACC**), cold redundant, centralises the whole Attitude Control and Measurement tasks, in line with the spacecraft modes, based on sensors data and on the spacecraft actuation capabilities. Attitude orders and spacecraft modes changes commands are received from the CDMU via the 1553 data handling bus.

In an ultimate purpose of implementation of the commonality, ACCs are identical for both HERSCHEL and Planck. However, HERSCHEL (resp. Planck) ACC runs HERSCHEL (resp. Planck) ACMS software, and is configured to interface the HERSCHEL (resp. Planck) sensors and actuators, including the Reaction Control System. ACC distributes an ACMS 1553 data bus to interface complex units : Star Trackers and gyros.

The respective HERSCHEL and Planck ACMS configurations are detailed from an overall satellite point of view in Sections § 6.3.3 and from a subsystem point of view in SVM Design Report § 9.5.

The ACC houses the ACMS software and provides to it all the features, storage & processing capabilities and mechanisms necessary to the performance of the spacecraft attitude control and monitoring tasks and to the implementation of a limited set of data handling services.

The ACC, is able to autonomously manage the configuration of its connecting units via on/off interfaces implemented at equipment (sensor/actuator) level, provided that its units have been "enabled" by the CDMU through PCDU.

The ACC implements similarly to the CDMU, high level ACMS reconfiguration capabilities, ACC_RM and ACC_SGM, as required by the fault protection system approach described in Section 6.4.3. The lower level failures isolation and recovery is performed by the ACMS software.

Power Control Subsystem

As far as power generation and distribution are concerned, the HERSCHEL and Planck missions are mainly characterised by the following features:

- both missions have a pretty similar power need; about 10 % of difference between both is currently expected

- both mission feature identical orbit conditions: the illumination conditions are very close, with a Sun spacecraft angle of up to 10° For Planck, and 30° for HERSCHEL

- for both missions, a 133min non illuminated phase happens at Launch, while a up to 75 minutes eclipse can happen during the transfer orbits to L2

- the number of power and heater lines for both spacecraft is very similar.

These points justify a **unique** implementation of the subsystem between HERSCHEL and Planck. It is built around a single **P**ower **C**onditioning and **D**istribution **U**nit (**PCDU**) including the 2 main power functions: power conditioning and regulation, and power distribution. The subsystem level design is addressed in Section 9.3.

The conditioning consists in the management of the 2 power sources in order to be capable to deliver the power demanded under 28 V regulated power lines, as specified. The voltage regulation is based on the S3R concept: the Solar Array is subdivided into 30 non redundant elementary electrical sections, such that the loss of one of them impacts the spacecraft power budget by not more than 3 %.

Depending on the power demand, each section is either closed, connected on the power bus, or switching in order to maintain in any case the voltage at a bus capacitor bank within its 28 V range.

As far as the secondary power source is concerned, the design is based on one single rechargeable battery for each satellite. The charge of this battery is performed via dedicated Solar Array shunt sections ("S4R" concept), while the discharge is via two parallel Battery Discharge Regulators.

The power conditioning, including the battery charge control, is autonomously performed by the PCDU.

The second main function of the PCDU consists in the distribution of the regulated power to the user. It is performed via redundant, individual Latching Current Limiter (LCL), or Fold Back Command Limiter (FCL) lines, for the units, while the heaters lines are distributed though switchable lines, protected by groups.

Commanding of the distribution lines, heaters and telemetry collection, is managed by the spacecraft CDMU via the 1553 data handling bus.

Finally, a, limited, number of heaters controlled by thermostats, connected to the Main Power Bus via FCL ensure the spacecraft survival heating function while not introducing additional bus failure modes. Their operating range is set such that they do not nominally interfere with the thermal control function.

Telemetry & TeleCommand Subsystem

It addresses the RF communication up and downlink between the spacecraft and the 2 ground stations baselined for HERSCHEL and Planck missions, Perth and Kourou.
As far as TTC is concerned, the HERSCHEL and Planck missions are essentially characterised by the following features:

- both use X-Band for up and downlinks. Frequencies allocations however are specific for each spacecraft

- the Earth to spacecraft distances during operation are very comparable for both spacecraft: 1.8 Mkm for Herschel (large Lissajous, 1.6 Mkm for Planck (small Lissajous).

- the spacecraft to Earth aspects angles from telecommunication point of view are similar for both spacecraft: 10° maximum for Planck and 0° for HERSCHEL

– the uplink and downlink data rates requirements, mainly driven by the science data, are identical between the 2 spacecraft's.

This, again, calls for an obvious hardware commonality between HERSCHEL and Planck TTC subsystems.

It thus comprises:

– two X-Band transponders, operated in hot redundancy for the receiving part and cold redundancy for the Tx one. They are identical for HERSCHEL and Planck with the obvious exception of the carrier frequencies setting; especially, the down and uplink data rates Telecommand and Telemetry streams are made common between HERSCHEL and Planck, for sake of highest commonality, HERSCHEL case being the envelope of both with:

  • 500 bps, 5 kbps, 107 kbps and 1.5 Mbps for the downlink rates depending on the ground station and the receiving on-board antenna

  • 125 bps and 4 kbps for the uplink rates depending on the ground station and the receiving on-board antenna.

In addition, the data is transmitted by the CDMU to the transponders under a non modulated NRZ-L or SP-L, depending upon the actual data rate. It is received by the CDMU from the transponders under 2 digital chains format.

– 2 cold redundant 30W TWTA amplifying stages, to guarantee the above downlink rates

– one single frequency X-Band Medium Gain Antenna, to perform the high data rate downlink during the planned telecommunication sessions. The use of the MGA in receiving mode offers a back up to the nominal commanding via the LGA's

– identical Dual band Rx/Tx Low Gain Antennae, to perform the low rate downlink, mainly at start of the missions and in emergency cases, and to receive the telecommand uplink streams. The antennae are accommodated, for each satellite, in order to guarantee a quasi omnidirectional coverage in both TM and TC, thus making the spacecraft robust to the "attitude loss" failure mode. Specificities due to the different geometries, different attitude controls, and different Payload Module constraints, lead to define 2 LGAs for HERSCHEL, and 3 LGAs for Planck.

The TTC architecture also comprises the suitable set of diplexers, hybrids and switches integrated in the so-called RFDN, such as to reduce to a minimum the number of commands to send in case of change in the TTC configuration.

6.3.1.2.1.   Summary

The Table 6.3.1-1 recapitulates the different payload and spacecraft functions to be provided, and indicates which unit(s) permits to fulfil them.

INSTRUMENT FUNCTION	FULFILLED BY
Power distribution	**PCDU**: LCLs
Data I/F	**CDMU**: 1553 Bus and direct lines (TBC)
Ground I/F	**CDMU** + **TTC**
Data storage	**CDMU**: acquisition via 1553 data handling bus and storage in mass memory
Synchronisation	**CDMU**: 1553 DH bus messages + hardware lines (TBC) **ACC**: Attitude sync lines (TBC)
T° monitoring	**CDMU** **Cryostat Control Unit** for HERSCHEL

SPACECRAFT FUNCTION	FULFILLED BY
Power generation & conditioning	**Solar Array** + **1 battery** + **PCDU**: S4R concept
Power distribution	**PCDU**: LCLs, FCLs for permanent lines **ACC**: distribution of secondary lines to sensors & actuators **ACMS units**: additional ON/OFF switching at unit level for units on main bus
Data acquisition	**CDMU**: 1553 data handling Bus and direct interface lines **ACC**: 1553 ACMS Bus and direct interface lines
commanding	**CDMU:** 1553 data handling Bus and direct lines **ACC**: 1553 ACMS Bus and direct interface lines
Ground I/F	**CDMU** + **TTC**
Data storage	**CDMU**: acquisition via 1553 and direct lines and storage in mass memory
Time maintenance	**CDMU:** Central Reference Time driven by hot redundant oscillators
Synchronisation	**CDMU**: 1553 messages + 131072Hz hardware lines
Thermal control	**PCDU**: heaters supplying ; survival heaters supplying **CDMU**: Temperature acquisition, Proportional Integral control laws implementation
Attitude Control and Monitoring	**ACC** + **Sensors/actuators**
FDIR	**CDMU**: via CDMU_RM and CDMU_SGM (see § xxxx.) **ACC**: via ACC_RM and ACC_SGM (see § xxxx.) for ACMS fault protection

TABLE 6.3.1-1 IMPLEMENTATION OF INSTRUMENTS AND SPACECRAFT FUNCTIONS

6.3.2.   Avionics electrical design

The chapter 6.3.1 has given an overview of the avionics design : it includes 2 main functions, the data handling function, and the attitude control function.
The overall design, as discussed in the previous chapter, is basically identical for both satellites, and is based on a decentralised architecture which allows to clearly associate 2 subsystems to the 2 functions : the **C**ommand and **D**ata **M**anagement **S**ubsystem (**CDMS**), and the **A**ttitude **C**ontrol and **M**onitoring **S**ubsystem (**ACMS**), linked together via a 1553 Bus.

6.3.2.1.   CDMS

6.3.2.1.1.   Functions

The Command and Data Management Subsystem performs the following general tasks :

– Telemetry acquisition and formatting

– To perform the Spacecraft monitoring and manage the emission of transfer frames as defined in the Packet TM Standard from the assembling into a frame to the encoding.

– Telecommand acquisition, decoding validation and distribution

– To manage the reception of TC segment as defined in the Packet TC Standard from their acquisition to the routing towards the corresponding user.

– Data storage

– To manage the saving of data to insure their integrity until dump to ground.

– Time distribution and time tagging

– To generate the required synchronisation signals, on board datation and its distribution especially to manage time tagging.

– Autonomy supervision and management.

– To monitor that the others functions are running without failure. In that case, it manages the corresponding reconfiguration to bypass this failure.

In order to perform these functions, the CDMS interfaces with the payload instruments, the ACMS, the Power Control System and the Telemetry and TeleCommand subsytem.

6.3.2.1.2.   CDMS Design

As already described in section 6.3.1, and illustrated in Figure 6.3.1-1 and 6.3.1-2, the CDMS design is essentially centralised, and <u>unique for both spacecraft's</u> : it is reduced to a single unit, the CDMU, which performs all the identified functions.

The CDMS hardware configuration is summarized in table 6.3.2-1.

6.3.2.1.3.   CDMU Design

The CDMU design implemented to satisfy the identified CDMS tasks mainly comprises :

− A Telecommand Decoder and routing module which has to fulfil the telecommand acquisition, decoding validation and distribution function requirements.

− A Telemetry encoder and multiplexer module which has to fulfil the telemetry acquisition and formatting function requirements.

− A processor module run the CDMS On board software, and has especially in charge to acquire messages, commands and provide responses via the Platform Interface bus, to perform overall commanding, housekeeping collection and monitoring. It also support the software in the high level management of the Mass memory

− A mass memory area which has to fulfil the data storage function requirements.

− A Reconfiguration Module which has to fulfil the autonomy supervision and management function requirements.

− A command generator which has to generate command associated to a request from the TC decoder, the processor module or the reconfiguration module requirements.

− An On Board Time module which has to fulfil the Time distribution and synchronisation signals generation sub-function requirements.

– An I/O module to perform the elementary commands distribution and parameters acquisition

As a consequence of the CDMS design approach, system level requirements, and especially reliability requirements, are directly applicable to the unit level. The CDMU detailed internal design is therefore driven by major high level FDIR constraints, which apply to the different modules listed above :

– The CDMU does not include any single point failure.

– Electrical and thermal insulation between nominal and redundant circuits is provided to eliminate failure propagation.

– The redundancies is testable without dismounting the unit.

– The Reconfiguration Module is robust to SEU (register's state shall be guaranteed) and SEL free.

– The RM is failure independent from the functions which are observed by itself. In practice, a failure occurring in units observed by RM does affect the functioning of RM itself.

– The RM is only reconfigurable by ground. Any interaction from Processor Module to Reconfiguration Module is forbidden.

– A single failure on PM does not cause the loss or corruption of both Safe Guard Memories.

– A reconfiguration sequence has precedence on any other task. It is not possible to interrupt a reconfiguration sequence.

– Single failure inside the CDMU does not lead to the generation of spurious commands.

– The CDMU implements a means of inhibiting internal and external commands which are functionally independent from the command generator.

– It is possible to passivate a failed Telemetry Module so that it does not affect the output of the correctly functioning TM module.

- It is possible to passivate a failed On Board Time module so that it does not affect the output of the correctly functioning OBT module.

- A single failure inside the CDMU does lead to the loss of both nominal and redundant TC modules.

The Figure 6.3.2-1 is a functional description of the CDMU, showing the various modules organisation, and how this organisation satisfies the system constraints listed above.
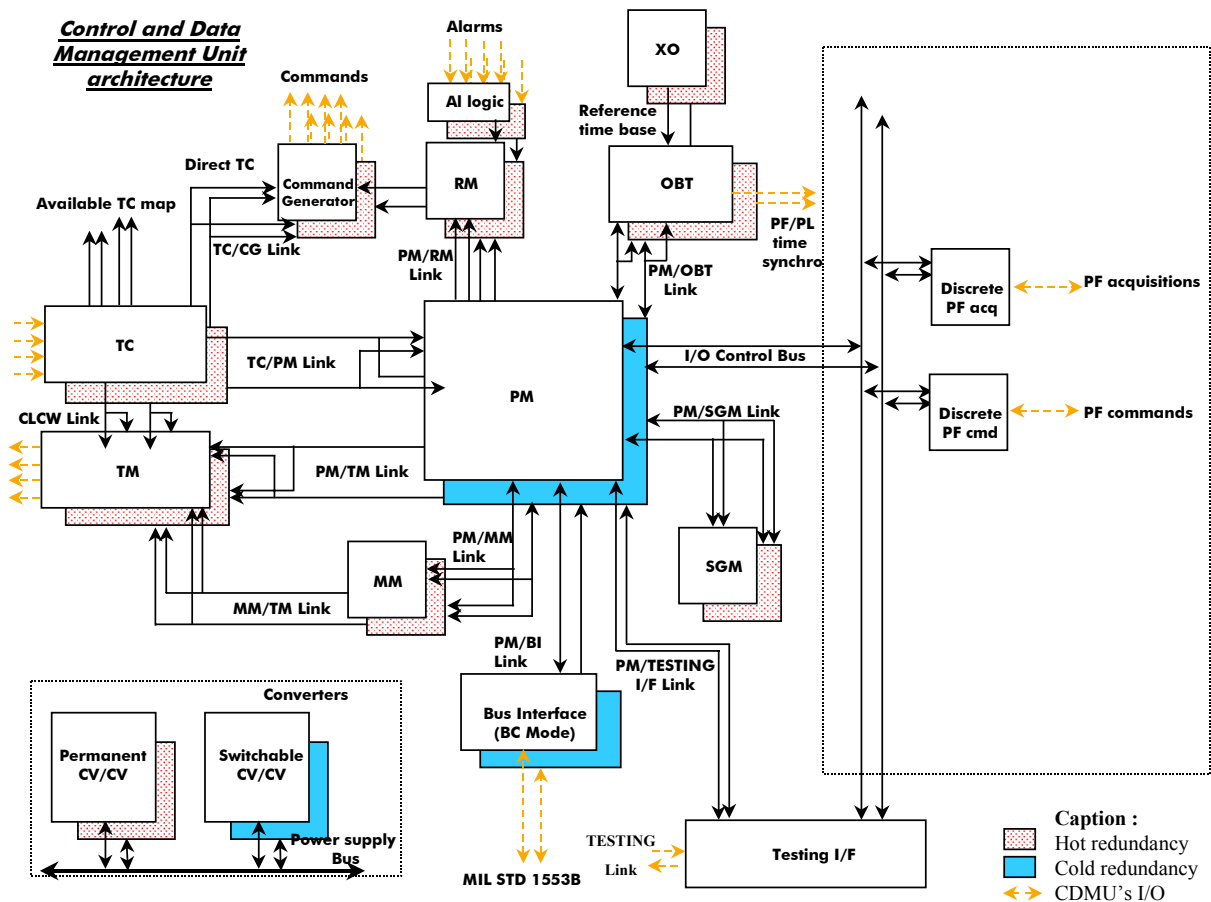
FIGURE 6.3.2-1   CDMU FUNCTIONAL ARCHITECTURE

The following sub-sections hereafter detail, for each module of the CDMU, the main system requirements applicable to their design.

6.3.2.1.4.   TC Management

The CDMU provides 2 TC Decoders that are running in hot redundancy, each one being active.

The TC bit rates are identical for Herschel and Planck:

- – low TC bit rate :   125 bps.

- – High TC bit rate : 4 kbps.

6.3.2.1.5.   TM Management

TM Encoding

The telemetry data stream is in nominal Reed Solomon and Convolutional encoded (concatenated code) which permits to achieve a minimum E_b/N_0 of 2.7 dB for a frame loss probability of 10^{-5}. Also, the TM bit stream is forwarded to the TTC transmitter under NRZ-L or SP-L format, depending on the selected bit rate. No modulation is performed at CDMU level to leave the entire link performance responsibility within one single subsystem (TTC).

The down stream telemetry frames are assembled from up to 8 virtual channels allocated to the mass memory or to the processor module.

The frame structure complies with the Packet Telemetry Standard.

TM bit rates

As far as the downlink telemetry is concerned, the same data rates are now specified for Herschel and Planck.. Three rates are to be considered:

- – 500 bps, 5 kbps on LGAs

- – 107 kbps on MGA with Kourou

- – 1.5 Mbps on MGA with Perth.

It shall be pointed out that these data rate figures could possibly be slightly tuned (still in line with mission requirements), in the course of the Phase B, to adapt to simpler hardware design solutions.

6.3.2.1.5.1. Processor Module

The main functional blocks of the Processor Module function are:

- ERC32SC Processor

- Boot PROM

- EEPROM

- RAM

- Oscillator

- Serial I/O Bus (to SCIO)

- Mil-STD-1553B Interface

- Internal Control Bus Interfaces (for TM/TC)

- Test Interfaces.

Processor

The Processor Module implements processing capabilities in line with the operating system and application software performance requirements, including real time constraints.

Memories

The exact amount of memory needed for the Processor Board will be consolidated during Phase B. For the baseline design the following memory types and sizes (excluding check bits) are foreseen:

- 64 Kbytes PROM for the boot memory

- 1 Mbytes EEPROM for the program memory, power switched for a better SEU tolerance

- 4 Mbytes RAM, EDAC protected.

MIL-STD-1553B

A MIL-STD-1553B Bus Controller interfacing with payload instruments, PCDU, Attitude Control Computer and Cryo Control Unit (on Herschel only), is implemented on each PM.

Test Interface

A test interface is provided on the Processor Board allowing communication with the S/W. The bit rate for this interface is 19200 bps.

6.3.2.1.6. Mass Memory

The CDMU provides an-board storage medium with a size sufficient to record the spacecraft science and housekeeping data generated during 48 hours.

The major contributor to mass memory sizing is the payload, which generates data rates of at least 100 kbps. Therefore, taking into account a 5kbps rate for the transmission of the spacecraft housekeeping, the Mass Memory size shall be, as a minimum :

$(100+5)$ x 3600s x 48h = 18Gbits.

25 Gbit EOL solid state mass memory modules are actually implemented : this offers a 40% capacity margin, or would permit to extend the payload allocation to 140kbps assuming the most optimized use of the Mass memory content. A dedicated mass memory controller is in charge, inside the CDMU, to manage the mass memory internal and external interfaces, the CDMU data handling software running the filing system.

6.3.2.1.7. Reconfiguration Module

The CDMU provides one hot redundant reconfiguration module basically consisting in a state machine capable to process a limited number of hardware alarms, and as a result to issue sequences of pre-programmed ON/OFF commands to the PCDU, and for internal purpose, and 2 x 1 Mbytes Safe Guard Memory for the storage of the spacecraft context, to be used in case of reconfiguration after a failure. The overall FDIR approach, including the hardware alarms definition, is described in §6.4.3.

The Reconfiguration Module also receives the Launcher separation strap status and initiates the post separation activities.

6.3.2.1.8. On board time Module

The On Board Time (OBT) module implements a reference time function according to the TAI reference, which is possible to synchronise to a master time source. The On Board Time module may also be used as a master reference time source, i.e. sending synchronisation pulses to slave reference time functions. The module also contains functions for sampling current On Board Time and generating pulses at a specific time.
The CDMS maintains the time reference and distributes this time to all on board users. The main specific features of the reference oscillator are :

  – 1 ppm over 30 days including all parameters influencing the stability.

  – The On-Board Time function is a protected resource.

The CDMU provides synchronization signals and timing signals as required by the science instruments or spacecraft units : as required by IIDs (AD-05.1 to 05.6) 131072 Hz synchronization signals have to be generated and distributed

6.3.2.1.9. I/O Modules

The CDMU provides the data handling software with the hardware facilities necessary to perform the platform monitoring, processing and control, and especially:

  – **housekeeping and thermal monitoring,** of service module units and also Payload Module & Instruments for Planck

  – **units configuration control** via a set of ON/OFF commands

  – **thermal control,** from temperatures acquired both from the directly from the CDMU

  – **battery surveillance** (battery control is autonomously performed inside PCDU)

  – **Visual Monitoring Camera** interface. The camera data is acquired via fast (up to 3 Mbps) RS422 serial link, packetized, then stored in the mass memory (**TBC**)

  – **SREM** interface. The Standard Radiation Environment Monitoring unit is acquired via standard ML16/DS16 serial lines, as service module housekeeping data.

EQUIPMENT	NB	REQUIRED PERFORMANCE	ALCATEL BASELINE
Data Handling			
CDMU	1	- Processing capability > **5 Mips** - Mass memory storage **>** **= 25 Gbits** - 1553 Data Handling Bus Controller - VMC interface - RTU, function - Internal Reconfiguration Module and Safeguard Memory - Spacecraft time accuracy < 10^{-8} - TM rate selectable from 500 bps up to 1.5Mbits/s - 8 virtual channels - TC rate between 125 bps and 4 kbps	- Unit based on ERC 32 monochip processor (~8Mips) – 4 Mbytes RAM, 1 Mbytes E²PROM - 2 x 1 Mbyte SGM - Reconf Mod: 80 HLC – SSMM = 25 Gbits EOL - Spacecraft time driven by internal OCXO - RTU standard I/O: 80 DR, 80 ANA, 192 TH,80 Bi-level, 88 HP, 14 ML16, 14 DS16 - 1553 Bus Controller - TM rate selectable by NCO - Mass < 15 kg - Electrical consumption < 44 W

TABLE 6.3.2-1 CDMS HARDWARE

6.3.2.2.   ACMS

It implements the full set of functions and units dedicated to attitude and orbit control of the satellites, including sensors, actuators, processing capability, and attitude and orbit control fault protection system.

HARDWARE DESIGN

The **ACMS** architecture, is shown in Figure 6.3.2-3 and 6.3.2-4 for the 2 satellites. It is integrated and built around a single, internally redundant, Attitude Control Computer (**ACC**), identical for both satellites and interfacing with "intelligent" sensors via a 1553B ACMS data bus, the other sensors and actuators, including RCS thrusters, being interfaced via dedicated elementary digital or analogue I/F lines.

The **ACC** functional architecture is shown in Fig 6.3.2-2. The core processor is essentially identical to the CDMU one and most of the CDMU design drivers mentioned in section 6.3.2.1.3 are applicable to the ACC; it thus implements:

– a processor board built around an ERC32 monochip μp

– a 4 Mbytes RAM and 1 Mbytes EEPROM processor board

– one hot redundant Reconfiguration Module consisting in a state machine capable to issue sequences of pre-programmed ON/OFF commands to the ACMS sensor and actuators connected on the main power bus, and internally, and 2 x 1 Mbytes safe guard memory for the storage of the ACMS context, to be used in case of reconfiguration after a failure.

In addition, the ACC provides the ACMS software with the hardware facilities necessary to perform the attitude control function, monitoring, units management and especially:

– ACMS sensors and actuators interfaces

– ACMS units configuration control via a set of ON/OFF commands.
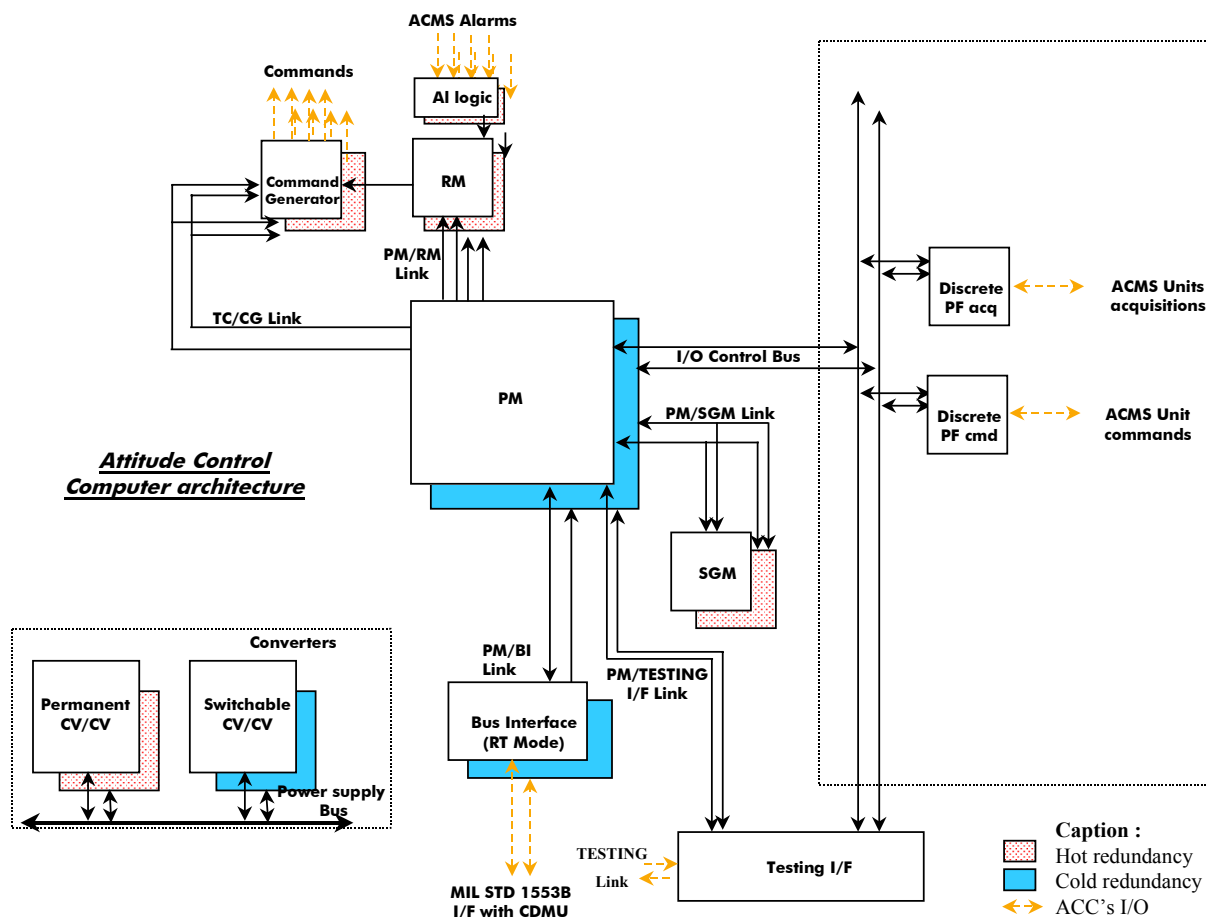
FIGURE 6.3.2-2 ACC FUNCTIONAL ARCHITECTURE

The Herschel **sensors**, discussed and justified in SVM Design Report Section 9.5, consist in:

- two small field of view STar TRackers (**STR**), used in cold redundancy, and located on the service module. Both are aligned with the $X_{S/C}$ axis, looking toward -$X_{S/C}$ (opposite to the telescope line of sight). The STRs are connected to the ACMS 1553 Bus; they are not autonomous due to their reduced field of view, and thus do not contain any star catalogue

  The two STR, similarly to ISO configuration, are complemented by two fine Sun sensor

- 2 **FSS** (Fine Sun Sensor) to ensure the required pointing performance via the Roll axis control. The FSS are located on the XY plane to point the +$Z_{S/C}$ axis, thus providing a highly accurate measurement of the spacecraft to Sun angle along X and Y, acquired via dedicated digital lines. It is planned to have the 2 FSS connected to the 1553 ACMS Bus. A dedicated FSS output provides the attitude anomaly detection signal to the ACC reconfiguration module

- a 4 skewed **Gyroscope Block** complete the STR data in Normal Mode, during science observation, in order to improve the pointing stability and to propagate the attitude during the slews. The gyro blocks are connected to the ACMS 1553 Bus

- two Quartz Rate Sensors (**QRS**), behaving as coarse gyros, are used for the Sun acquisition mode, then for the loose monitoring of the low spin in ACMS safe mode. They are acquired by the ACC via dedicated digital lines

- two Sun Acquisition Sensors (**SAS**) monitor the spacecraft absolute orientation w.r.t. Sun. One SAS (internally redundant) is oriented along +$Z_{S/C}$. The second is oriented along -$Z_{S/C}$ such that in total, basically the whole sky is covered. They provide an indication of the Sun orientation w.r.t. spacecraft via dedicated analogue lines.

Herschel **actuators** are discussed and justified in SVM Design Report section 9.5. Theyconsist in 4 Reaction wheels and 12 x 10N thrusters, commanded via dedicated lines

- the Reaction Wheels (**RW**) are implemented to provide the necessary torque and accuracy capability for the slew maneuvers during nominal operation. They are also employed to control FIRST slow spin during Safe Mode. They are mounted in an homogenous skewed configuration, and the nominal maneuver performance is achieved with the use of 3 wheels only.

The RWS system, even in case of 1 RW failure, is compatible of the 20 Nms daily momentum accumulation. Reaction wheels are commanded via analogue interfaces providing for each wheel, the torque and the direction to apply.

−   The **THR**usters configuration is driven by the needs to provide:

- a 3-axis torque in order to ensure the attitude control and to unload the RW

- the capacity to perform all orbits control maneuver with a good geometric efficiency (> 94 % in worst case).

  The thrusters configuration is organized in two branches of 6 thrusters:

- 2 thrusters are used to produce the desired acceleration in ΔV mode (one for ΔV with SAA < 90°, the other for ΔV with SAA > 90°)

- 4 thrusters to produce the control torque both in ΔV mode and in wheel unloading phases. All thrusters are inclined by ~45° towards the −X satellite axis, thus avoiding contamination risks for SVM equipment.

Herschel ACMS hardware configuration is summarized in table 6.3.2-1
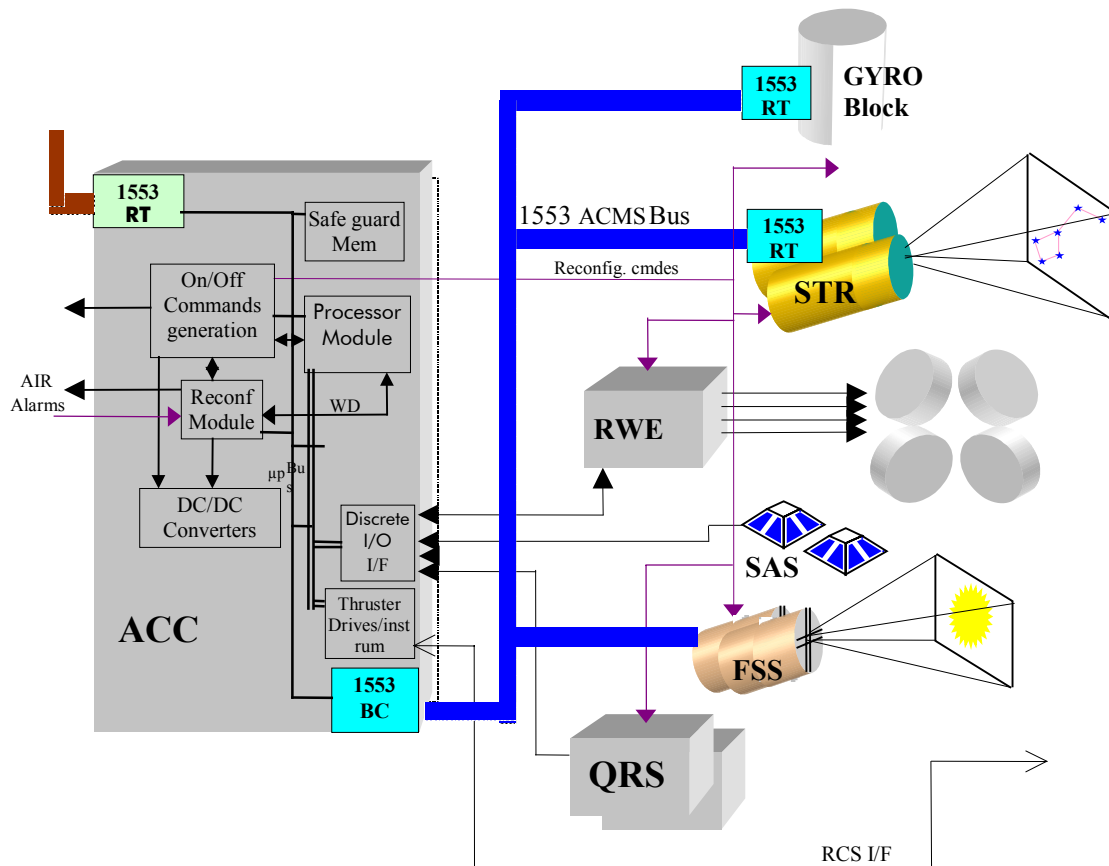
FIGURE 6.3.2-3 HERSCHEL ATTITUDE CONTROL AND MONITORING SUBSYSTEM

EQUIPMENT	NB	REQUIRED PERFORMANCE	ALCATEL BASELINE
HERSCHEL ACMS			

ACC		- Processing capability > **5 Mips**
		- 1553 ACMS Bus Controller
		- 1553 Data Handling Bus Remote Terminal
		- ACMS units I/F function
		– ON/OFF cmdes capability
		- Internal Reconfiguration Module and Safeguard Memory
			Processor Module = ERC32, 8 Mips 4 Moctets RAM, 1 Moctets EEPROM, Bus 1553,
			- 2 x 1Mbytes SGM
			- I/O: 40 HLC, 40 DR
			- Reconf Mod: 80 HLC
			- I/O ACMS:
			    4 Reaction wheels I/F
			    4 SAS I/F
			    12 thrusters I/F
			    2x3 axis QRS I/F
			- Mass < 12 kg
			- Power consumption < 22 W

Star Trackers	2	FOV = 4x4° Bias < **1arcsec** Bias spatial variation < 1 arcsec Noise < 1.3 arcsec (2 Hz)	
Gyrometers (4 axis)	1	Drift < **0.05°/h over 1 Hr** ARW $2.10^{-13}(rad/s)^2$/Hz readout nose < 0.1 arcsec	
Fine Sun Sensors	2	Bias **100arcsec** bias stability < 60arcsec Noise < 5 arcsec FOV (+/-10° x +/-35° AAD function	
Sun acquisition sensors	2	Accuracy **0.1°**	
Quartz Rate Sensor	2	**Accuracy < 0.01°/s**	
Reaction Wheels	4	**0.2 Nm** up to 25 Nms	
Thrusters	12	Double valves **10N**	

TABLE 6.3.2-1 HERSCHEL ACMS HARDWARE

The Planck **sensors**, discussed and justified in SVM Design Report Section 9.5, consist in :

– one internally redundant STar Mappers (**STM**), essentially provides the spin and nutation information via phase and height signals to be used by ACMS, and by the payload instruments to synchronize their operations. They are located on the service module and are aligned with the $Z_{S/C}$ axis. The STMs interface with the ACC via dedicated analogue lines

– two Quartz Rate Sensors (**QRS**), behaving as coarse gyros, are used for the sun acquisition mode, and for the loose monitoring of the spin in ACMS normal mode. The two QRS blocks are mounted in order to form a 6 axes. Each measurement is achieved on a different axis, thus enabling to perform checksums to detect up to QRS failure they are acquired by the ACC via dedicated digital lines

– three Sun Acquisition Sensors (**SAS**) passively monitor the spacecraft absolute orientation w.r.t. Sun. One SAS (internally redundant) is oriented along $-X_{S/C}$. The second and third SAS are located in the YZ plane, and oriented in opposite directions such that in total, basically the whole sky is covered. They provide an indication of the Sun orientation w.r.t. spacecraft via dedicated analogue lines

– one redundant Attitude Anomaly Detector (**AAD**) provides the ACC with a highly reliable, passive, attitude loss indication to the ACC for initiation of the attitude recovery process. It is accommodated to point along $-X_{S/C}$ spin axis. Sun presence flags are acquired by the ACC via specific status acquisition lines

Planck **actuators** and consist in 12 x 10N thrusters + 4 x 1N thrusters, commanded via dedicated ACC lines.

The **THR**usters configuration is driven by the needs to provide:

– the capacity to perform orbit correction maneuvers

– the capacity to perform angular momentum correction (orientation and value).

And by the architecture constraints:

the protection of the payload instrument.
These constraints combined with the necessary redundancy for failure tolerance, lead to the THR implementation in 2 branches (one nominal, one redundant), containing each:

– 3 pairs of 10N thusters for ΔV corrections:

- 1 pair directed towards the +X hemisphere ("up thrusters")

- 1 pair directed downwards ("down thrusters")

- 1 intermediate pair ("flat thrusters")

- 1 pair of 1N thrusters for angular momentum correction.

This configuration enables to provides at minimum one level redundancy and enables the complete separation of the thrusters used in operation and those used in safe mode.

Planck ACMS hardware configuration is summarized in table 6.3.2-2
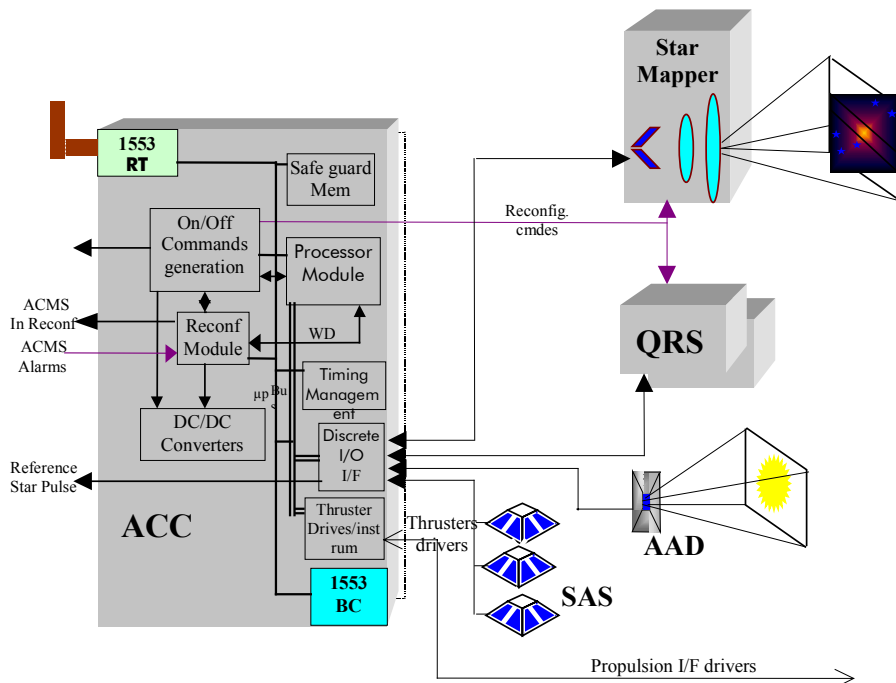
**FIGURE 6.3.2-4 PLANCK ATTITUDE CONTROL AND MEASUREMENT
SUBSYSTEM ARCHITECTURE**

EQUIPMENT	NB	REQUIRED PERFORMANCE	ALCATEL BASELINE
PLANCK ACMS			

ACC		- Processing capability > **5 Mips**
		- 1553 ACMS Bus Controller
		- 1553 Data Handling Bus Remote Terminal
		- ACMS units I/F function
		- On/off cmdes capability
		- Internal Reconfiguration Module and Safeguard Memory
			Processor Module = ERC32, 8Mips 4 Moctets RAM, 1 Moctets EEPROM, Bus 1553
			- 2 x 1Mbytes SGM
			- I/O: 40 HLC, 40 DR
			- Reconf Mod : 80 HLC
			- I/O ACMS :
			    2 Star Mappers I/F
			    6 SAS I/F
			    2 AAD I/F
			    12 10N thrusters I/F
			    4 1N thrusters I/F
			    2x3 axis QRS I/F
			- Mass < 12 kg
			- Power consumption < 22 W

Star Mappers	1	Bias < **0.17 arcmi** Noise < **0.17 arcmin**	
Attitude Anomaly Detectors	1		
Sun acquisition sensors	3	Accuracy **0.1°** FOV = 180°° x 180°	
Quartz Rate Sensor	2	**0.01°/s**	
Thrusters	16	12 Double valves **10N** Calibration dispertion on impulse < +/-5 4 Double valves **10N** Calibration dispertion on impulse < +/-5 %	

TABLE 6.3.2-2 PLANCK ACMS HARDWARE

SATELLITES ACMS MODES

The **Herschel ACMS** Modes are designed to ensure both the best state of the art attitude determination (< 2.3''), pointing (< 2.2'') and stability (< 0.25'') performances and the mission robustness and especially to always ensure the instrument Sun guard.

The Modes transition logics is shown in Figure 6.3.2-5, while usage of equipment for each mode is shown in Figure 6.3.2-3.

The scientific observation is performed in a single **Normal Operation Mode** relying on the inertial attitude determination based on the accurate 2-axes STR combined with the FSS. For higher stability and scanning modes, gyrometers are used to propagate the attitude and reduce the sensors noise impact on the control. The actuation is performed by a set of 4 Reaction Wheels. The RW unloading is performed in the **Wheel Unloading Phase**, by a sequence of opened loop THR pulses.

To provide the best robustness, independent sensors QRS and SAS measurement are used for the FDIR, to avoid any anomalous attitude.

In case of Major failure, a robust **Sun Acquisition Mode** is entered. The attitude determination is based on the SAS and the QRS rate measurement, and the 3-axis control is performed by the Thrusters. When the Z-axis is safely pointed toward the Sun, the Safe Hold Mode is entered and the 3-axis attitude control is performed on RW. A slow rotation rate (0.5 Round/hour) is commanded by transferring 5 Nms from the RW to the +Z-axis, thus ensuring a reduced momentum accumulation due to solar torque integration. Consequently a several days control autonomy can be ensured without required the use of THR.

A **Star Acquisition Mode** ensures the inertial attitude acquisition. A slow rotation rate about the Sun axis is commanded to acquire the guide star and enable under ground command the transition to the Normal Operation Mode.

The **Orbit Correction** are performed on 3-axis THR control and the inertial attitude propagation on the gyrometers (**Orbit Correction Mode**).
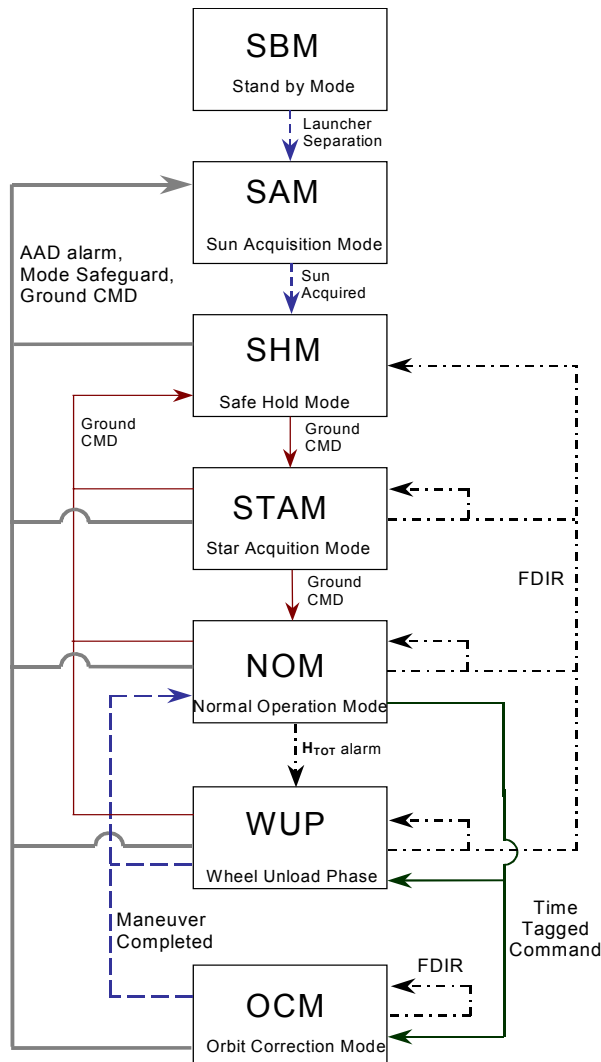
FIGURE 6.3.2-5 HERSCHEL MODES TRANSITION LOGIC

	SAM	SHM	STAM	NOM	WUP	OCM
SAS	C-F	C-F	F	F	F	F
QRS	C-F	C-F	F	F	F	F
GYR	---	---	C-F	C-F	C-F	C-F
FSS	---	---	C-F	C-F	C-F	---
STR	---	---	C-F	C-F	C-F	---
RWS	---	C-F	C-F	C-F	C-F	---
THR	C-F	---	---	---	C-F	C-F
C: unit used in control						
F: unit used for FDIR function						
--- unit not used						

TABLE 6.3.2-3 HERSCHEL MODES VS UNIT USE

The **Planck ACMS** is based on a simple and robust architecture, with a minimum of ACMS modes and only two actively controlled mode. All modes are spin stabilized ; the nutation is <u>actively</u> damped via thrusters use to ensure a low nutation compatible of the science observation.

The Planck ACMS modes are briefly described hereafter, while the modes transition logics is illustrated in Figure 6.3.2-6. The sensors use versus modes is shown in Table 6.3.2-4.

The Science is performed in the passive **Normal Operation Mode**. The Star Mapper data are collected to provide the telemetry necessary for the payload data exploitation but also to determine the satellite inertial attitude. For High Robustness, the FDIR is performed by additional coarse rate sensors (QRS) and Sun Acquisition Sensors.

An **Angular Momentum Correction Mode** (HCM) is implemented to enable the angular momentum orientation and control. The Momentum correction is based on the attitude determination performed by STM processing and achieved by a 3 THR pulses tuned to perform the slew and avoid the nutation.

The **Orbit Control Mode** enables to perform the necessary orbit correction. As the 10 N THR perturbation are rather high, the stabilization is no longer based on the gyroscopic stiffness but on closed loop 3-axis control based on the QRS integration and a SAS and STM for drift calibration and inertial reference. 2 THR are used for ΔV and two pairs are off-modulated for the 3-axes attitude control

For initial acquisition and in case of attitude anomaly, the robust **Sun Acquisition Mode** is used. A 3-axis THR based control based on QRS rate measurement and SAS, for Sun reference, ensures a rapid Sun acquisition, whatever the entry conditions, thus ensuring the payload safety. Based on equipment independent from NOM, this mode is very robust.

The **Stand-By Mode** is then entered after the Sun Acquisition. The spacecraft is fully passive; the Sun aspect angle and speed rate are monitored by the SAS and the QRS.
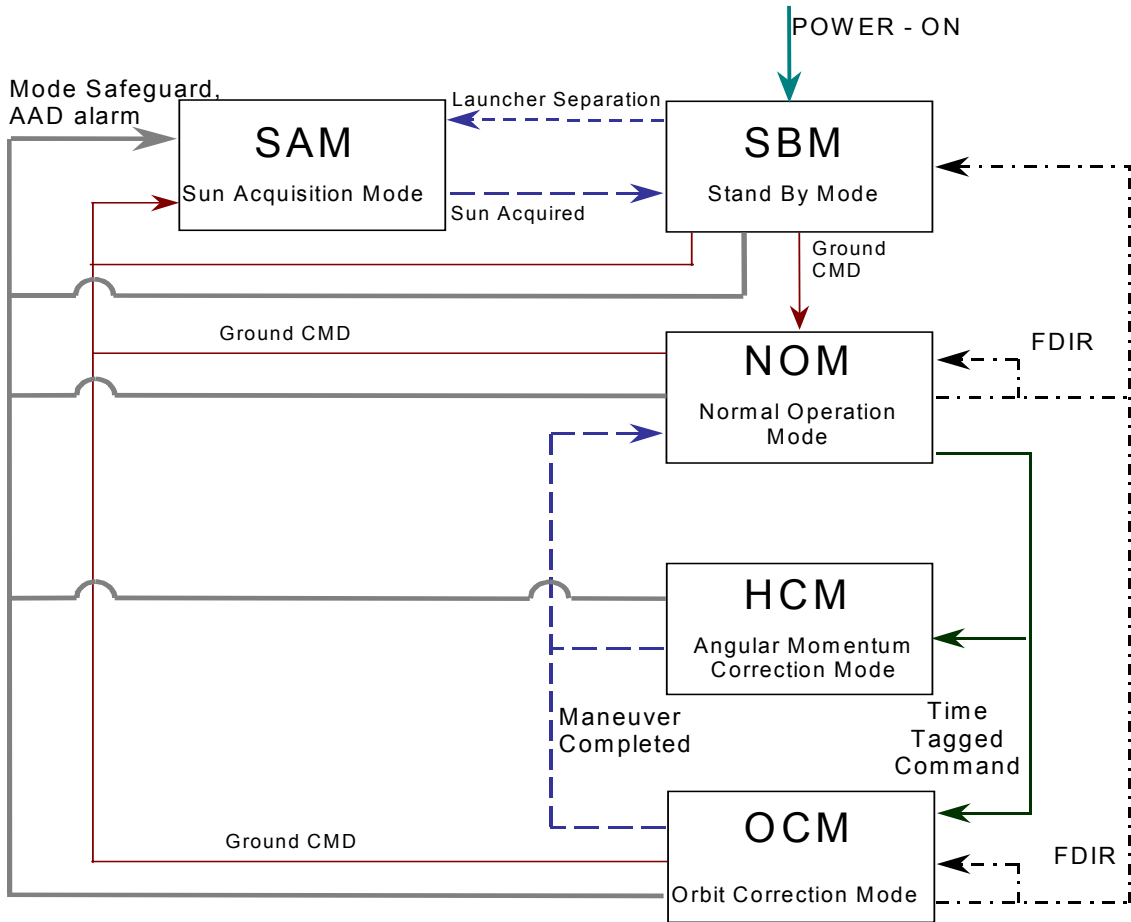
FIGURE 6.3.2-6 PLANCK MODES TRANSITION LOGIC

	SBM	SAM	NOM	HCM	OCM
SAS	F	C-F	F	---	C-F
QRS	F	C-F	F	---	C-F
STM	---	---	M-F	---	C-F
THR1N	---	---	F(1)	C	---
THR10N	---	C-F	---	---	C-F
C: unit used in control					
M unit used for measurement					
F: unit used for FDIR function					
--- unit not used					

TABLE 6.3.2-4 PLANCK MODES VS UNIT USE

6.3.3.   Avionics software architecture

The functions devoted to the Herschel/Planck avionics software are generally :

Data handling functions

- overall mission and spacecraft management

- interface to the ground for operation

- TM/TC packet flow management

- time synchronization

- payload instrument interface.

Attitude Control and Measurement functions

- ACMS modes management

- attitude control algorithms processing

- ACMS S/S management, including fault protection.

These functions are implemented from a software point of view through the design of a number of dedicated services and tasks :

Data handling services

- Telemetry acquisition and formatting services, supported by the AD03.1 services 3 (periodic reporting) and 5 (event reporting), and in compliance with the ESA Packet Telemetry Standard,

- Telecommand acquisition, decoding, validation and distribution services, supported by the AD03.1 services 2 (device commanding) and 20 (information distribution), and in compliance with the ESA TC Packet standard

- Data storage, supported by the AD03.1 services 15 (on board storage) and 22 (context saving)

   − Time distribution and time tagging, supported by the AD03.1 service 9

   − Autonomy supervision, fault protection and mission management, supported
     by the AD03.1 services 11 (on board scheduling), 12 on board monitoring),
     18 (on board control procedures) and 19 (Event/actions).

Attitude Control and Measurement

   − Sensors data processing and actuators commanding.

   − Modes management service.

   − Spacecraft attitude fault protection and management.

The chapters 6.3.1 and 6.3.2 have presented the baseline avionics architecture. From
this architecture, it is possible to break the Flight software down into avionics software
components capable to perform the overall tasks and services described above. This
breakdown is illustrated in Figure 6.3.3-1, while Figure 6.3.3-2 shows the overall flight
software organization including the interfaces between software products and with the
hardware addressed in §6.3.1 and §6.3.2.
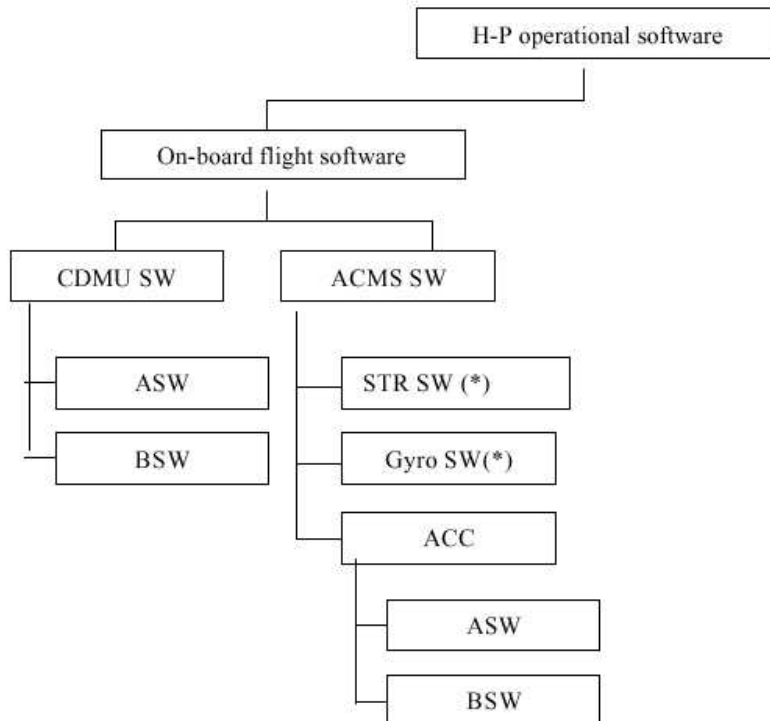
(*) Herschel only

FIGURE 6.3.3-1 AVIONICS FLIGHT SOFTWARE BREAKDOWN
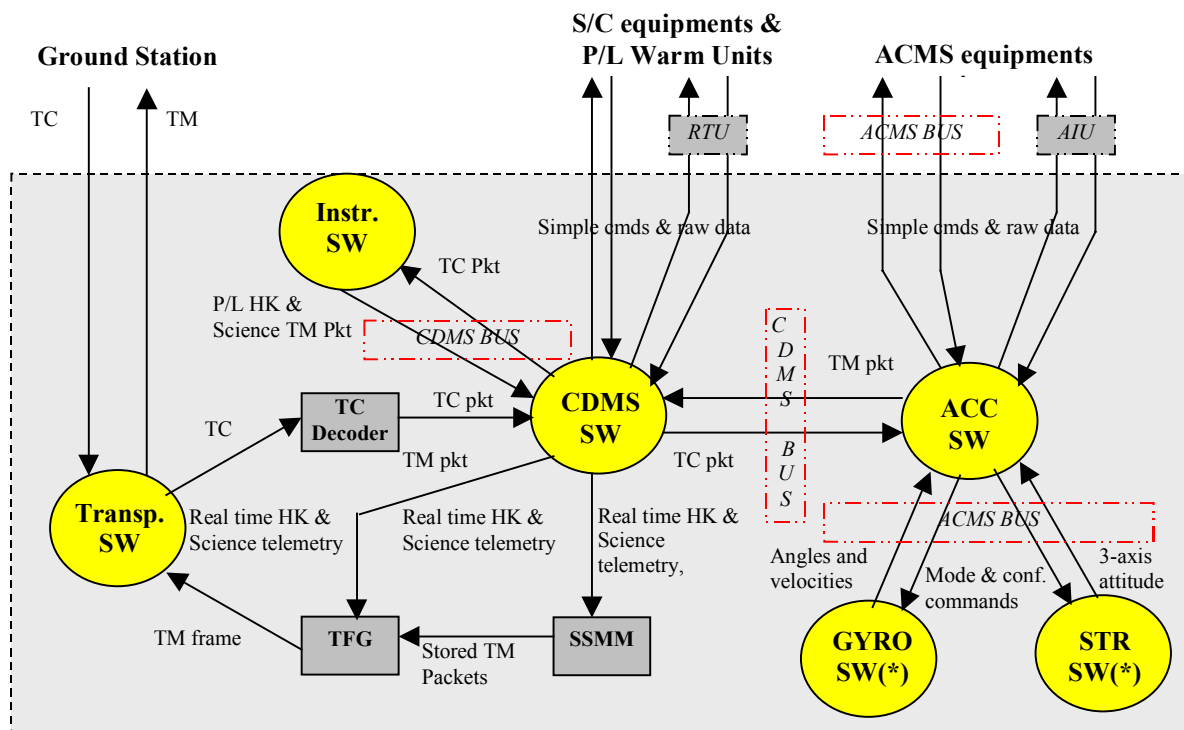
(*) FIRST only

FIGURE 6.3.3-2 SATELLITE SOFTWARE ARCHITECTURE AND INTERFACES

The main avionics software components are the CDMS SW and the ACC SW; these flight software's are conceived taking into account the following drivers :

- The CDMU and ACC use the same type of microprocessor unit

- The HW subcontractor shall be in charge of low-level drivers definition and implementation, due to his intrinsic knowledge and experience in this area

- The SW architecture shall be based on various different SW layers

- The degree of commonality between the CDMU SW and ACC SW shall be maximized.

As a consequence, a convenient avionics software layers breakdown is presented in Figure 6.3.3-3, applicable to both software types:
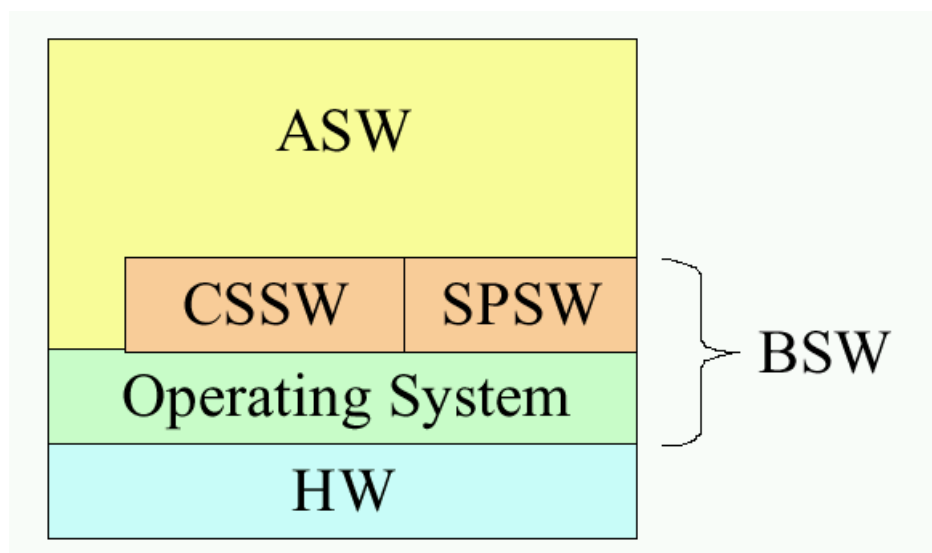
FIGURE 6.3.3-3 AVIONICS SOFTWARE LAYERS

The **HW** layer is related to the physical services which must be supported : 1553 Bus, I/O's

The **Operating System** layer directly interfaces the HW layer, and comprises the real time kernel with task scheduling, inter tasks communication facilities, events management, …, the I/O devices drivers, the bootstrap

The **C**ommon **S**ervice **S**oft**W**are represents the core package common to Herschel and Planck CDMU and ACC. It eg. includes the Patch/Dump, self tests services.

The **SP**ecialized SoftWare includes the services specific to CDMU and ACC but which cannot be considered as part of the Application SW; these are eg. the Mass Memory high level management service, the Mission Timeline management service for the CDMS SW, or the sensor actuators services for the ACC SW.

Finally, the **A**pplication **S**oft**W**are is the highest level component.
The ASW makes use of the lower level services, and includes the high level satellite functions : thermal control, satellites modes management, FDIR, data management, instruments management for the CDMS SW, and ACMS modes management, Control Law, ACMS FDIR for the ACC SW.

The CDMS ASW is unique for both satellite, the respective satellite database identifying Herschel or Planck. On the contrary, Herschel and Planck ACMS specificity lead to the design of 2 distinct products.

These software layers and the corresponding allocation of the software modules are illustrated in Figure 6.3.3-4

CDMS ASW

- Mission Time Line Management
- FDIR at System Level
- FDIR at CDMS Level
- CDMS HK collection
- Thermal Control
- Battery Monitoring

ACC ASW

- First/Plank Specific Control Algorithms
- Mode Management
- FDIR at ACMS Level
- Standard Control Algorithms Execution
- Sensors acquisition
- Actuators commanding
- ACMS HK & ARD collection

BASIC SW

CDMS SPSW
- TM/TC Management
- OBCP Management
- MTL Support
- On Board Monitoring
- SSMM Management

ACC SPSW
- Services common to Herschel and Planck ACMS software but not provided by CSSW, e.g.
  - ACMS SW Subcontractor's libraries and utilities)
  - Reduced set of OIRD services

HW layer, OS & CSSW

- General Services for higher SW level (Event logging, OBT acquisition, Data Packetization, Memory Patch & Dump, etc.)
- Real Time OS/Scheduler (Process Scheduler, IP Communication, etc.)
- PM Bootstrap & Initialization Firmware
- Processor Management & Health Status Check
- MIL-STD-1553B drivers (BC & RT) & I/O Drivers

FIGURE 6.3.3-4 HERSCHEL/PLANCK SOFTWARE LAYERS ALLOCATIONS

6.3.4.   Telecommunication design

This section describes the overall TTC subsystem for both HERSCHEL and PLANCK satellites. First, a discussion of open points from the SRS (AD01.1) is given. Then, the TTC architecture is presented with emphasis on the commonality reached between both satellites in order to reduce the development cost and number of tests.

6.3.4.1.   Open points from SRS requirements

The following points from the SRS requires clarification/discussion with ESA

SMTT-020 The TT&C Subsystem shall be compatible with the following ESA Standards:
- Ranging Standard, ESA PSS-04-104
- Radio Frequency and Modulation Standard, ESA PSS-04-105
☛Compliant with the MPTS ranging standard. Tone frequency anyway still to be defined by ESA.

SMTT-035 The TT&C Subsystem shall support the following modes for the downlink:
- Carrier only
- Telemetry
- Ranging
- Simultaneous Telemetry and Ranging
- Doppler
☛ Carrier only mode will be achieved by inhibiting the TM data transmission from CDMU to the TTC transmitter (see SMTT-045 here after).
No problem to handle the other modes for off-the-shelf transponders. However the 'Doppler mode' needs to be precisely defined by ESA. Missing in the ESA PSS-04-105.

SMTT-050 The TT&C subsystem shall provide a range and/or range rate measurement capability. For ranging, it shall be capable to demodulate ranging tones from the uplink carrier and modulate the downlink carrier with them.
☛ capability for ranging measurement is ensured with the built-in ranging channel in the transponder. Note however that only one tone (MPTS standard) is expected here.

SMTT-120 The link budget margins shall be computed under the following assumptions:
- Telemetry:
Telemetry bit error rate associated with 99.999% of transfer frame delivery corresponding to Eb/No = 2.7 dB theoretical for ESA standard concatenated FEC coding. For optional TURBO coding at rate ¼ the equivalent Eb/No is 0.3 dB.
- Telecommand :
a) Under all conditions specified by the mission Telecommand Bit Error Rate of 10^{-5} corresponding to Eb/No = 9.6 dB (theoretical),

b) Under "no signal" conditions, the mean rate of spurious command generation must be less than one per two years.

☞ Regarding the telemetry link quality, as per ESA PSS 04 103, the corresponding PFL to the specified Eb/No of 2.7dB is 10^{-5} (and not 10^{-6} as per SMTT-135). All TTC link budgets have been established on this basis.

6.3.4.2. TTC subsystem architecture

The following sketches show the proposed architecture for both missions, keeping in mind a maximum commonality between HERSCHEL and PLANCK SVMs.

HERSCHEL TTC architecture
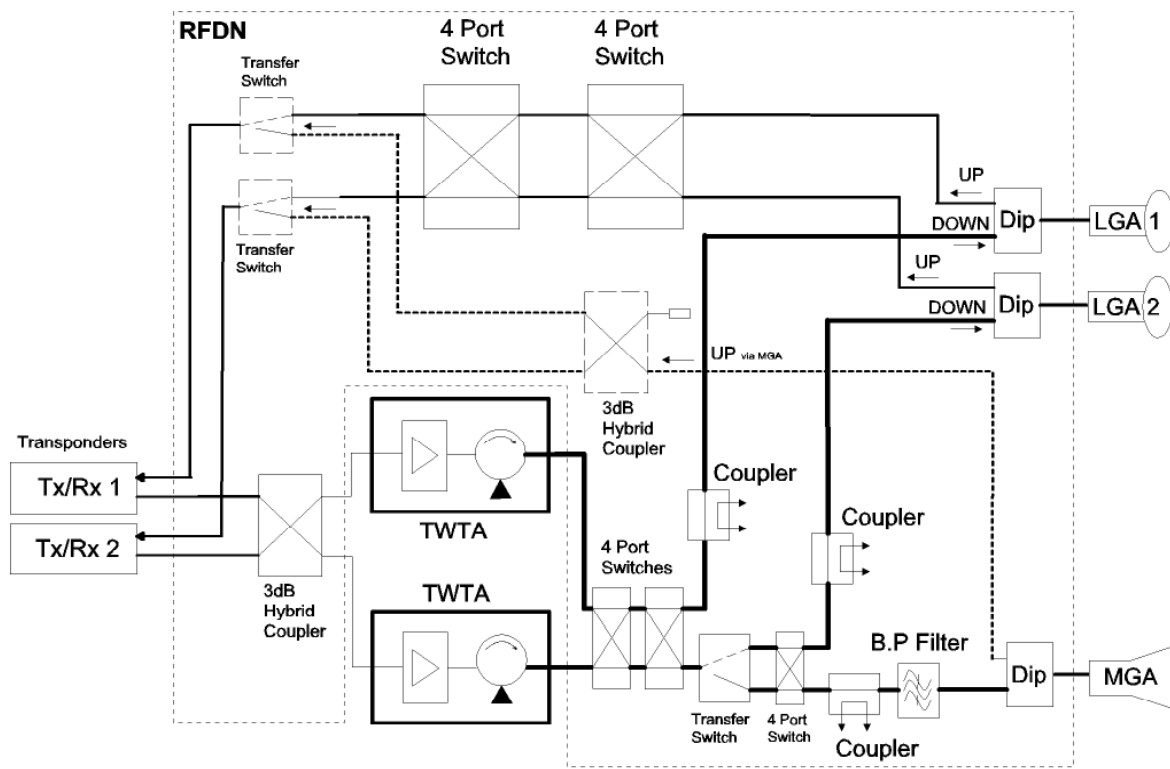
HERSCHEL RFDN configuration

File: Herschel_RFDN.ds4 - 02-07-2001

FIGURE 6.3.4-1a   HERSCHEL TTC SUBSYSTEM ARCHITECTURE

Receive section

The uplink RF signal can be received by the two LGA (Low GAin) or by the MGA (Medium GAin), depending on the spacecraft attitude and mission phase.

The 4 port switches allow any kind of combination LGA 1/LGA 2 with receiver 1/receiver 2.

NOTA: Two 4P switches are envisaged to avoid any SPF at this level.

The medium gain antenna can also be used for telecommand, by using the Transfer switch located right after the 4P switches.

Then as per system requirement the two receivers are always ON, working in hot redundancy, which allows to select the highest RF signal between the different antennae just by monitoring the receiver adequate telemetry (typically called AGC TM).

Transmit section

In downlink the output from one of the two transponders feed a 3 dB Hybrid Coupler that supply contemporarily the two TWTA. This solution seems more reliable with respect to 4 Port Switch solution because it is only passive connection without any moving mechanical parts.

Note also that only one Transmitter and one TWTA will be active at the time, in line with the system requirement to have a cold redundancy for the transmit section.

The RF losses due to the 3 dB Hybrid Coupler insertion are negligible because the RF signal will be amplified by the TWTA, which will deliver about 30 RF power.

Each TWTA output supplies two 4 port switches (SPF free), that permit a connection either to the nominal LGA 1 or to the redundant LGA 2/or MGA.

A Band-Pass filter is also foreseen in the MGA path to avoid interferences to other satellites, when transmitting high data rate (wider spectrum).

Note that this filter could be integrated in the TTC transmitter as baseband or RF filtering, while putting this filter after the TWTA leaves the freedom to work in a more saturated area with a better power efficiency (to the detriment of the linearity obviously).

Diplexers and test-points

With each antenna a diplexer uplink_frequency/downlink_frequency is foreseen to keep the flexibility of using each antenna in uplink or in downlink.

On each downlink physical path a test-point is available in order to control the transmitted RF power. However the positioning of these test-points is not definitive and could be integrated in the Antennae itself, which would allow during test campaigns to measure the antennae uplink and downlink gain patterns, as well as the transmitted RF power at antenna port level. This option will be investigated on the time of the antennae procurement.

Commonality Herschel ⇔ Planck

The proposed architecture for PLANCK is directly derived from the HERSCHEL one with a further 3 dB Hybrid Coupler on the redundant LGA path, to handle the third LGA.

PLANCK TTC architecture
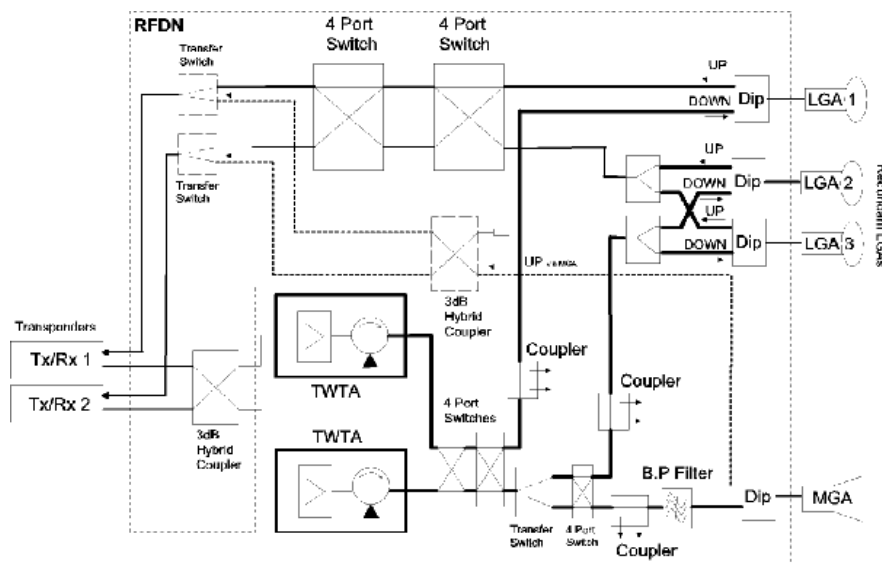
FIGURE 6.3.4-1b   PLANCK TTC SUBSYSTEM ARCHITECTURE

Receive section

Same architecture as for HERSCHEL with in addition the possibility of receiving the uplink RF signal from the nominal LGA on one Receiver and the signal from both redundant LGAs on the other Receiver.

Transmit section

Fully identical to the HERSCHEL one.

Technology

The downlink distribution network, characterized by high RF power, between the output of two TWTAs and the different antennae, will use a wave guide technology while the uplink path and low power downlink distribution network between the Transmitters output and the TWTAs will use coaxial technology.

6.3.4.3. Functional description

As per system requirement (SGICD) each satellite will carry three different data rates on the telemetry link and two on the uplink.

To maintain the required performances in terms of link quality (BER or PFL), a limited cross-strapping between data rates and antennae has been defined:

Uplink data rate ⇔ antennae correspondence

BIT RATE	GROUND STATION	S/C ACTIVE ANTENNA
125 bps	Kourou	Nominal or redundant LGA(s) or MGA
4 kbps	New Norcia	Nominal or redundant LGA(s) or MGA

Downlink data rate ⇔ antennae correspondence

BIT RATE	GROUND STATION	S/C ACTIVE ANTENNA
Low data rate		
500 bps	Kourou	Nominal or redundant LGA(s)
5 kbps	New Norcia	Nominal or redundant LGA(s)
Medium data rate		
107 kbps	Kourou	MGA
High data rate		
1.5 Mbps	New Norcia	MGA

All above combinations are fully supported by the HERSCHEL and PLANCK architectures depicted in previous section § 6.3.4.2.

Another system requirement (SGICD) regards the type of modulation to be supported by the TTC transponder, depending on the telemetry data rate.

The required modulation schemes are:

Telemetry data rate ⇔ modulation scheme

BIT RATE	MODULATION SCHEME	SUBCARRIER FREQUENCY
Low	PCM(NRZ-L)/PSK/PM	45884.000 Hz (sine) or 80324.000 Hz (sine)
Medium	PCM(SP-L)/PM	N/A
High	SRRC-OQPSK or GMSK	N/A

Note that so far the choice of the modulation scheme for telemetry high data rate is not yet done, but the SRRC-OQPSK is known to be available with existing transponders.

The GMSK modulation remains an alternative, which presents the advantage of not requiring any baseband filtering. Choice will be made during TTC transponder procurement phase. Refer to section § 6.1.3. (turbo code trade-off) for more details about the spectral efficiency of each modulation.

All these modulation schemes can be supported by the transmitter by the use of two separate phase modulators and one unique serial data interface as shown on the following sketch:
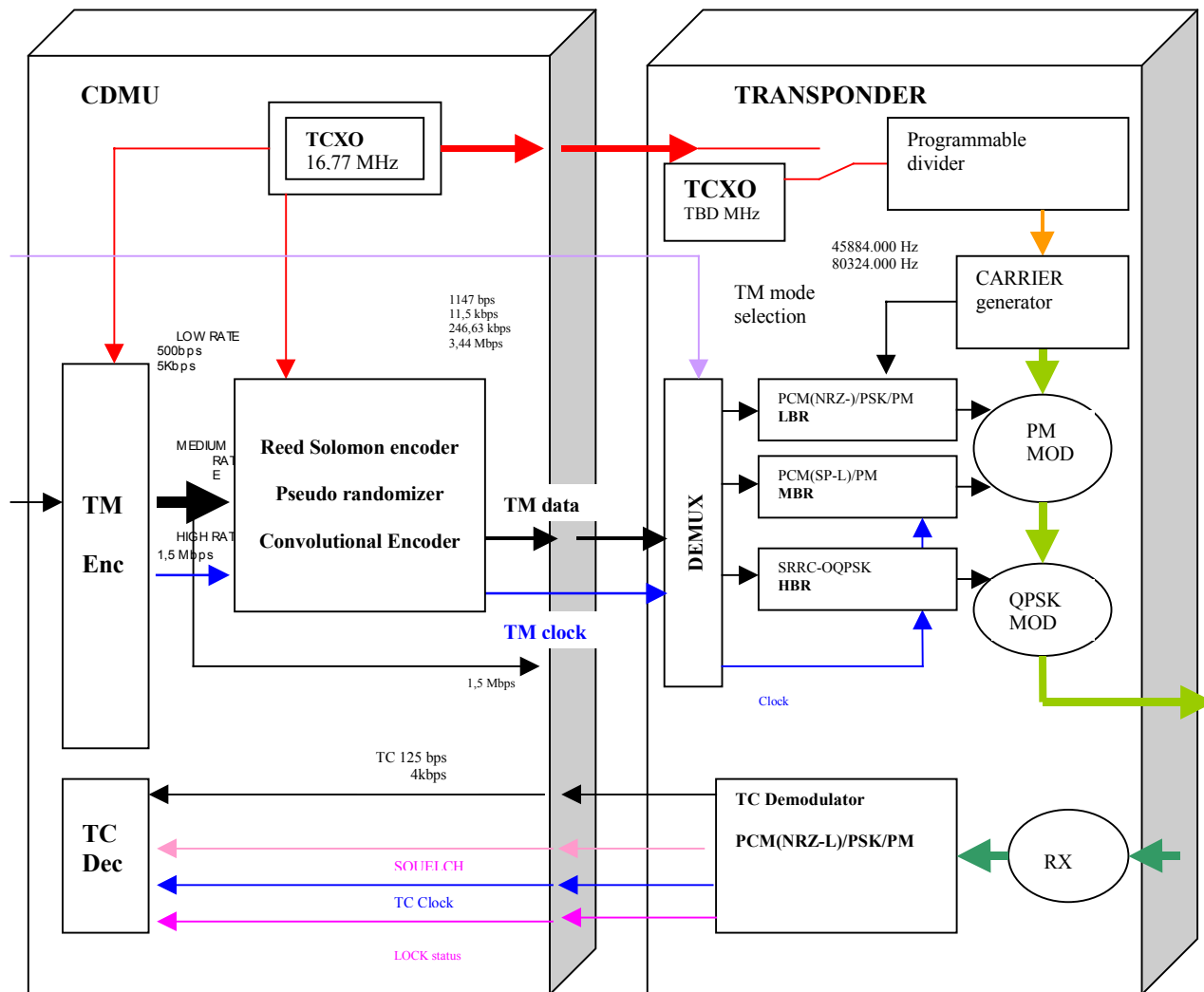
FIGURE 6.4.3-2   CDMU ⇔ TRANSMITTER FUNCTIONAL LINKS

NOTA: From the here above sketch a pseudo randomizer function is envisaged as per system requirement (SGICD) but its need has still to be confirmed. Kept as an option.

Obviously the uplink modulation being of the standard modulation scheme PCM (NRZ_L)/PSK/PM with 16KHz sine subcarrier is fully supported by the existing transponders.

6.3.4.4. Antennae configuration

For each satellite, based on the payload module constraints (interferences with the telescope), also on the satellite dimensions and final attitude, a different set of antennae and configuration has been proposed.

– HERSCHEL configuration

Up and Downlink with 2 LGAs (LGA 1 nominal - LGA 2 redundant) and Up and Downlink with one MGA.
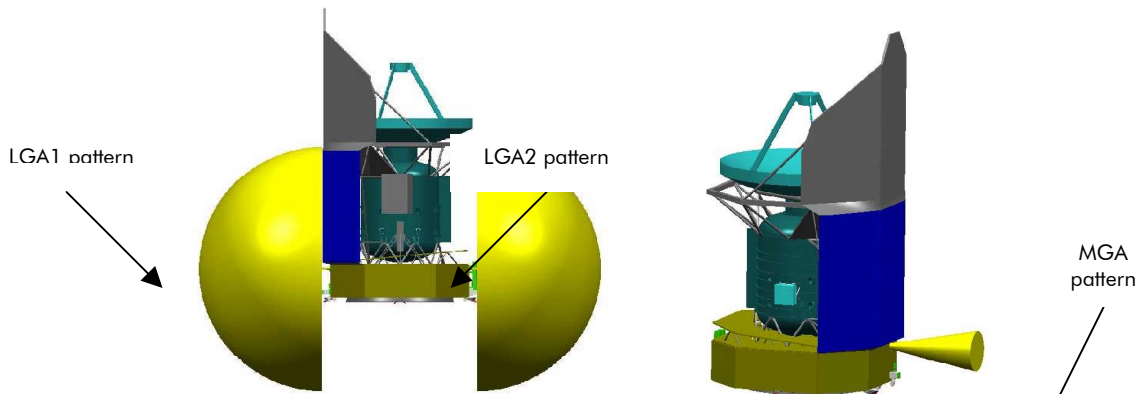
FIGURE 6.4.3.3   HERSCHEL ANTENNAE CONFIGURATION

– PLANCK configuration

Up - Downlink with 3 LGAs (LGA 1 nominal - LGA 2 & 3 redundant and used simultaneously) and
Up and Downlink with one MGA
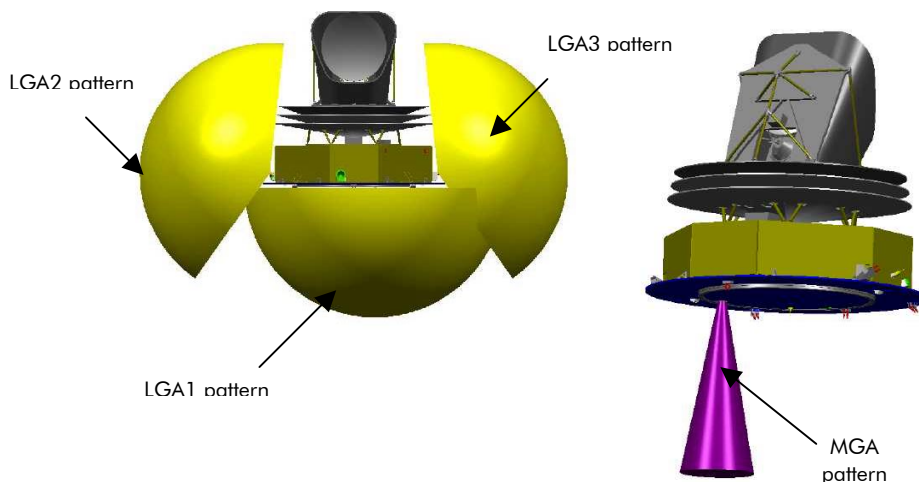
FIGURE 6.4.3.4   PLANCK ANTENNAE CONFIGURATION

The use of the LGA antennas assures an almost complete coverage independently on the spacecraft attitude and operational phases of the mission.

See also section § 6.1.5 PLANCK LGAs trade-off for more details about the LGA 1/2/3 combined coverage.

6.3.4.5. Main performances

TTC frequencies

- HERSCHEL uplink = 7207.8483 MHz

- HERSCHEL Downlink = 8468.5 MHz

- PLANCK uplink = 7196.3580 MHz

- PLANCK downlink = 8455.0 MHz.

Occupied bandwidth

3 MHz for the TC spectrum and 7 MHz for the TM spectrum.

Transmitted RF power

The radio frequency output power from the transponder is raised through a TWTA up to 30 W. The output power from TWTA and the gain assured by the MGA are sufficient to transmit the high data rate required for the long range distance (1.8 MKm) in accordance with the ESA requirements.

Antennae Gain

For the LGAs a nominal gain of − 3 dBi has been assumed, whereas for the MGA + 17 dBi has been assumed.

Both figures are confirmed to be realistic from usual antennae Suppliers.

Modulation indices

So far on the uplink, 1.0 Radpk for the Telecommand and 0.4 Radpk for the Ranging are assumed in the link budgets.

On the downlink, 1.2 Radpk for the Telemetry and 0.6 Radpk for the Ranging.

6.3.5. Power Design

The **P**ower **C**onditioning **S**ystem (**PCS**) aims at providing the Planck and Herschel satellites units and payload instruments with the power and energy compatible with all the phases of their respective missions, over their specified lifetimes. This power demand ranges from about 150W to 1350W for Herschel, and 230 W to 1600 W for Planck, including margins, depending upon the mode of operation and the life phase.

The power system shown in Figure 6.3.4-1 is identical for Herschel and Planck, and mainly organized around the Power Conditioning and Distribution Unit (**PCDU**). This equipment autonomously receives and conditions the power delivered by 30 identical electrical sections of one $\sim$10 m^2 Solar Array, organized in 2 areas at the bottom of the spacecraft, perpendicular to the spin axis for Planck, and one $\sim$11m^2 organized in 3 identical panels on the top of the cryostat for Herschel. The selected power system topology is a regulated bus, with the array power regulation based on a S^{3}R concept.

The Solar Arrays provides power to the satellites users typically from the launch time until physical separation from the rocket. Note that a 75mn long eclipse in transfer phase is also to be taken into account, but is not a driver for the solar array sizing.

The panels are fixed for both satellites and essentially face the Sun during all the operating phases in flight.

The selected solar cells technology is **dual junction Gallium Arsenide**, which currently provides the efficiency consistent:

-   with the limited available surface, mainly for Planck

-   with the high temperature reached at cell level while in operation.

When illuminated, the Solar Array power is directly used to maintain one single batteries in a pre-defined, autonomously controlled by the PCDU, state of charge. This concept is called S^{4}R. The conditioning is performed via the commanding of specific digital shunt sections of the Solar Array. The number of connected sections is set to allow a recharge of the battery in a reasonable time. This solution is consistent with a battery below bus principle, which is the best mass/cost compromise for the considered power range ($\sim$1500 W).

During the whole launch phase duration (sizing case), in case of peak power bursts (reaction wheels consumption during maneuvers) or in case of attitude loss type failure, **1 x 36 Ah** battery, able to deliver up to 521 Wh in worst case, provides the requested energy via two Battery Discharge Regulators (BDR). 4 x S^{4}R sections are allocated for the recharge; this allows to guarantee a minimum recharge ratio of C/5.

The distributed voltage is 28 V, regulated by the mean of a single failure proof 3 domains main error amplifier and a suitable capacity bank.

The selected battery type is based on **LiIon** cells for their very favorable energy/mass efficiency, and the proposed design features a serial/parallel arrangement of low capacity cells. Battery strings failure cases are limited to open circuit, thus leading to a slow degradation of the available energy. The initial battery sizing takes into account a one battery string loss failure case; this is considered as the most credible failure mode.

2 hot redundant BDR modules are implemented to discharge the battery, each of them being able to draw the maximum discharge current.

The power distribution is performed via nominal + redundant individual lines which are protected and switched inside the PCDU (centralized distribution principle) by the mean of Fold back Current Limiter's (FCLs) or Latching Current Limiters (LCLs) upon commanding from the data handling computer.

LCL's are specified to have the following characteristics:

  – Commandable ON/OFF

  – Fault tolerant so that LCL can always be switched OFF; this feature is intended to be used only for a limited number of LCLs, for those users who cannot function with both redundant units operating, or those which failure in ON is not acceptable from a system point of view (eg. too high power consumption).

The heaters lines are individually switched, and protected by an electronic fuse per group of heaters.

The Power System hardware configuration is summarized in Table 6.3.5-1, and the LCL's allocation for Herschel and Planck is shown in tables 6.3.5-2 and 6.3.5-3.

Detailed justification and subsystem trade-off related to the battery selection, are provided in SVM Design Report §9.3. The Power and energy budgets are presented in § 7.1.2.
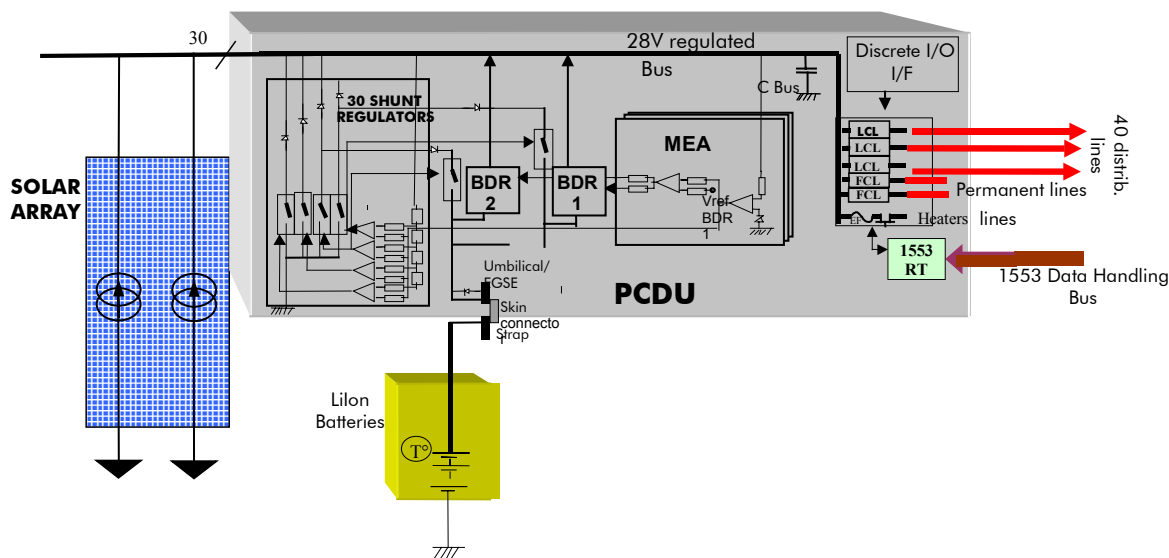
FIGURE 6.3.5-1 POWER CONTROL SUBSYSTEM

EQUIPMENT	NB	REQUIRED PERFORMANCE	ALCATEL BASELINE
Power Control Subsystem			
PCDU	1	- Distributed power > **1600 W** - Regulated **28Vbus** - Users line number (N+R) > **40** - Heaters lines number (N+R)> **40** - temperature acquisition> **120**	- S3R principle for regulation - battery charge by Solar Array sections-> S4R topology; discharge via BDR - 64 power lines available - Switching/protection by LCLs & FCLs - 40 Heaters lines distribution via electronic fuses/electronic switches - capability for 192 Temp acquisition - 1553 Bus I/F - Mass < 22kg
Solar Array	1	Fix array - **1500 W** under worst illumination conditions for Planck - **1200 W** under worst illumination conditions for Herschel	- 10m² GaAs Dual Junction cells array - Planck : Mass < 45kg - Herschel : Mass < 37kg - 1700 W in the specified conditions for Planck - 1600 W in the specified conditions for Herschel
Battery	1	E > **526 Wh** at 70 % DoD with **Vbatt < 28 V**	- 1 batteries of 6s24p LiIon 1.5 Ah Cells - - Vbatt < 27.2V - BOL capacity = 1 x 521 Wh Worst case - Mass < 7 kg.

TABLE 6.3.5-1 POWER S/S HARDWARE

LINE #	ALLOCATION	TYPE	CLAS
1	CDMU Hot Nom	FCL	I
2	CDMU Hot Red	FCL	I
3	XPND1 Rx Nom	FCL	I
4	XPND1 Rx Red	FCL	I
5	XPND2 Rx Nom	FCL	I
6	XPND2 Rx Red	FCL	I
7	ACC Hot Nom	FCL	I
8	ACC Hot Red	FCL	I
9	Survival Heater Line Nom	FCL	I
10	Survival Heater Line Red	FCL	I
11	CDMU Cold Nom	LCL	I
12	CDMU Cold Red	LCL	I
13	XPND1 Tx Nom	LCL	I
14	XPND1 Tx Red	LCL	I
15	XPND2 Tx Nom	LCL	I
16	XPND2 Tx Red	LCL	I
17	QRS Nom	LCL	I
18	QRS Red	LCL	I
19	STR Nom	LCL	I
20	STR Red	LCL	I
21	CCU Nom	LCL	I
22	CCU Red	LCL	I
23	PACS MEC1	LCL	I
24	PACS MEC2	LCL	I
25	SREM	LCL	I
26	VMC	LCL	I
27	ACC Cold Nom	LCL	I
28	ACC Cold Red	LCL	I
29	TWTA 1 Nom	LCL	I
30	TWTA 1 Red	LCL	I
31	TWTA 2 Nom	LCL	I
32	TWTA 2 Red	LCL	I
33	GYRO Nom	LCL	I
34	GYRO Red	LCL	I
35	PACS DPU-Nom	LCL	II
36	PACS DPU-Red	LCL	II
37	PACS SPU-Nom	LCL	II
38	PACS SPU-Red	LCL	II
39	PACS BOLC Nom	LCL	II
40	PACS BOLC Red	LCL	II
41	SPIRE DPU Nom	LCL	II
42	SPIRE DPU Red	LCL	II
43	HIFI ICU-Nom	LCL	II
44	HIFI ICU-Red	LCL	II
45	HIFI LCU-Nom	LCL	II
46	HIFI LCU-Red	LCL	II
47	HIFI LSU-Nom	LCL	II
48	HIFI LSU-Red	LCL	II
49	HIFI WEH	LCL	II
50	HIFI WEV	LCL	II
51	HIFI HRH	HC-LCL	III
52	HIFI HRV	HC-LCL	III
53	SPIRE FCU Nom	HC-LCL	III
54	SPIRE FCU Red	HC-LCL	III
55	RWS1 Nom	HC-LCL	III
56	RWS1 Red	HC-LCL	III
57	RWS2 Nom	HC-LCL	III
58	RWS2 Red	HC-LCL	III
59	RWS3 Nom	HC-LCL	III
60	RWS3 Red	HC-LCL	III
61	RWS4 Nom	HC-LCL	III
62	RWS4 Red	HC-LCL	III
63	SPARE	20A-LCL	20A
64	SPARE	20A-LCL	20A

TABLE 6.3.5-1 HERSCHEL POWER LINES ALLOCATION

LINE #	ALLOCATION	TYPE	CLAS
1	CDMU Hot Nom	FCL	I
2	CDMU Hot Red	FCL	I
3	XPND1 Rx Nom	FCL	I
4	XPND1 Rx Red	FCL	I
5	XPND2 Rx Nom	FCL	I
6	XPND2 Rx Red	FCL	I
7	ACC Hot Nom	FCL	I
8	ACC Hot Red	FCL	I
9	Survival Heater Line Nom	FCL	I
10	Survival Heater Line Red	FCL	I
11	CDMU Cold Nom	LCL	I
12	CDMU Cold Red	LCL	I
13	XPND1 Tx Nom	LCL	I
14	XPND1 Tx Red	LCL	I
15	XPND2 Tx Nom	LCL	I
16	XPND2 Tx Red	LCL	I
17	QRS Nom	LCL	I
18	QRS Red	LCL	I
19	SPARE	LCL	I
20	SPARE	LCL	I
21	SPARE	LCL	I
22	SPARE	LCL	I
23	SPARE	LCL	I
24	SPARE	LCL	I
25	SREM	LCL	I
26	VMC	LCL	I
27	ACC Cold Nom	LCL	II
28	ACC Cold Red	LCL	II
29	TWTA 1 Nom	LCL	II
30	TWTA 1 Red	LCL	II
31	TWTA 2 Nom	LCL	II
32	TWTA 2 Red	LCL	II
33	LFI REBA Nom	LCL	II
34	LFI REBA Red	LCL	II
35	LFI DAE Nom	LCL	II
36	LFI DAE Red	LCL	II
37	HFI PSU Nom	LCL	II
38	HFI PSU Red	LCL	II
39	HFI 4K CEU Nom	LCL	II
40	HFI 4K CEU Red	LCL	II
41	SPARE	LCL	II
42	SPARE	LCL	II
43	SPARE	LCL	II
44	SPARE	LCL	II
45	SPARE	LCL	II
46	SPARE	LCL	II
47	SPARE	LCL	II
48	SPARE	LCL	II
49	SPARE	LCL	II
50	SPARE	LCL	II
51	SCE Nom	HC-LCL	III
52	SCE Red	HC-LCL	III
53	HFI 4K CEU Lock Nom	HC-LCL	III
54	HFI 4K CEU Lock Red.	HC-LCL	III
55	SPARE	HC-LCL	III
56	SPARE	HC-LCL	III
57	SPARE	HC-LCL	III
58	SPARE	HC-LCL	III
59	SPARE	HC-LCL	III
60	SPARE	HC-LCL	III
61	SPARE	HC-LCL	III
62	SPARE	HC-LCL	III
63	SCE SCC Nom	20A-LCL	20A
64	SCE SCC Red	20A-LCL	20A

TABLE 6.3.5-2 PLANCK POWER LINES ALLOCATION

6.3.6.   Harness Design

The Harness for the HERSCHEL PLANK satellites may be considered as the following main elements:

- PLM Harness maybe subdivided as:

  - cryo harness - harness which interconnects cold units and/or connect warm units to cold units. This harness is the responsibility of the PLM, but the routing, heat leakages and EMC aspects are also being considered by ALCATEL. In addition for HERSCHEL there will be an additional harness connecting the cryo temperature sensors and valve commands/ monitoring to the CCU, this is the responsibility of the HPLM. For PLANCK a cryo harness will connect the PPLM and instruments cold temperature sensors to the SVM, this will be the responsibility of ALCATEL to define the harness and routing while it will be supplied as part of the PPLM

  - telescope harness. The harness which provides power to the telescope heaters and connects the telescope sensors to the CDMU within SVM. As for the cryo harness it is the responsibility of the PLM, but the routing, heat leakages and EMC aspects are also being considered by ALCATEL.

- Instrument Warm Harness - provides the interconnections between the instrument units and is the responsibility of the instrument. ALCATEL will provide routing information and design rules for this harness are given in the ALCATEL GDIR documentation.

- SVM Harness - all harness which provides the interconnections between SVM units, including power TM/TC and clock signals. This harness includes the Solar Array to the PCDU. This harness including the routing and definition is the responsibility of the SVM.

- SVM to instruments Harness, this harness including the routing and definition is the responsibility of the SVM and may be subdivided as:

  - power harness - all power lines from the PCDU to the instruments

  - MIL-1553 Bus harness including coupling transformers and terminators

  - TM/TC harness, includes any discrete TM required by the instruments (e.g. thermistor, status), any discrete TC required by the instruments (none identified to date), and any timing clock required by the instruments (e.g. 131072 Hz).

Figure 6.3.6-1 shows the main elements of the HERSCHEL-PLANCK harnesses.
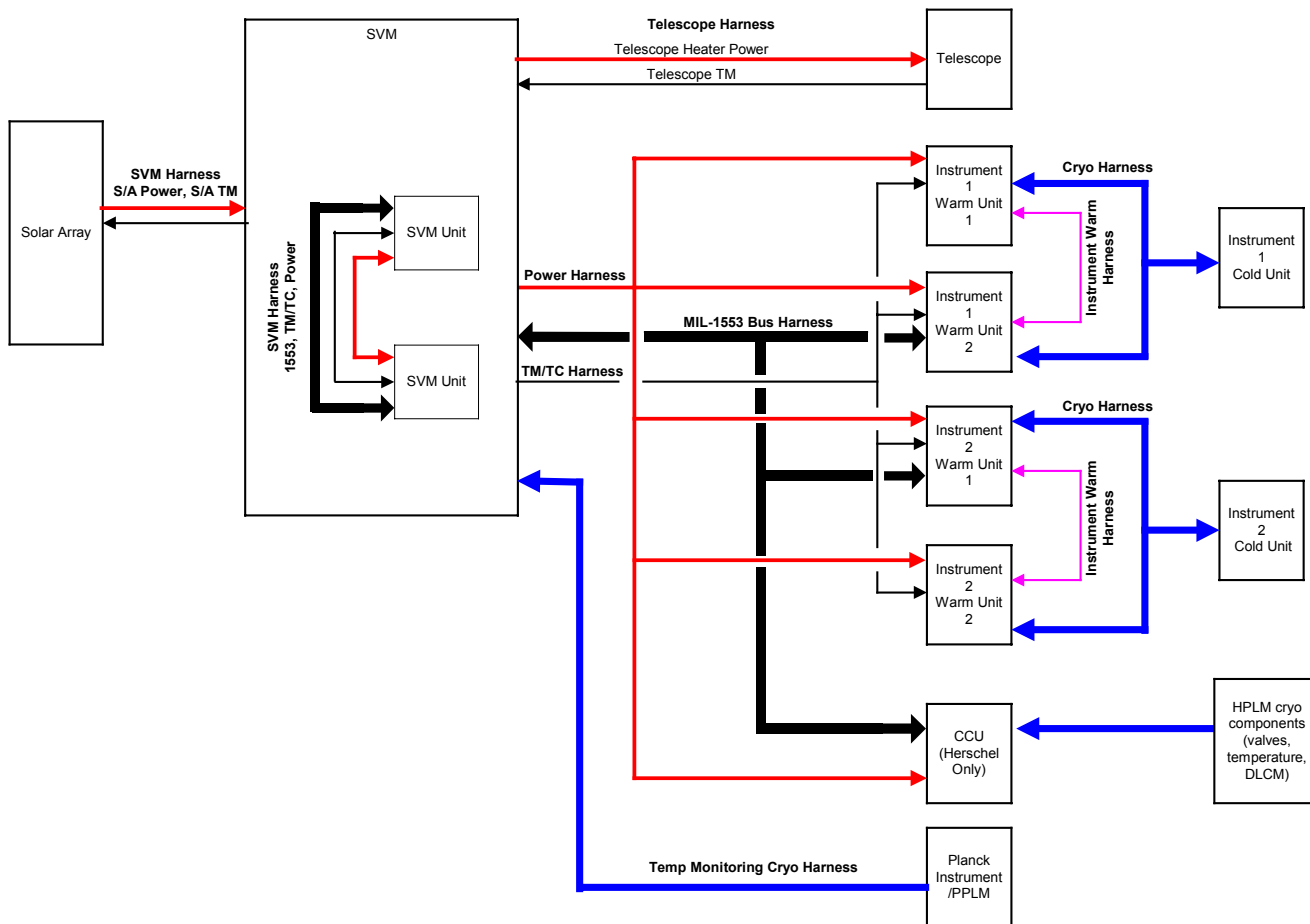
FIGURE 6.3.6-1 HERSCHEL/PLANCK HARNESS

6.3.7.   EMC approach

System Grounding/Shielding concept

General concept

The general system grounding and shielding concept is described in the GDIR § 6.2. The main issues are recalled hereafter:

- the distribution of the power lines follows a classic star concept ; the primary power return is grounded at one single point in the PCDU; this concept, together with the users primary EMI filters and with the active protections set in the PCDU provides and optimal decoupling between the various power lines, limiting as far as possible the noise propagation from one user to another through the power lines

- DC/DC converters must include galvanic isolation between the 28 V input and the secondary voltages supplying the electronics

- all equipment chassis are connected to the spacecraft structure through the lowest achievable impedance path (not only resistance), the goal being to build an equipotential voltage reference; as far as possible, the units metallic cases shall be in contact with the panels structure (where Aluminium face-sheets are used), so that the grounding strap(s) are not the only path for the common mode currents.

Secondary zero volts grounding

On lots of previous programs, a bad understanding of the DSPG (Distributed Single Point Grounding) concept implications on secondary 0 V grounding rules led to very bad grounding implementations from an EMC point of view, i.e. zero volt layers connected to one single point of a chassis with long wires, that is of course completely inefficient at high frequencies.

The result of this was more common mode emission, more radiated emission and threatens for signal integrity.

In order to clarify the DSPG concept and to avoid misunderstandings liable to encourage exotic EMC approaches, the following clarifications have been agreed with ESA, reflected in both IID-A and GDIR:

- GDEL-240: Each user secondary power return shall be connected to a single ground (ground point/ground plane). This ground point/ground plane shall be connected to chassis.

In the case of an equipment supplying another one, it has been agreed to connect the secondary power return in the supplied units instead of in the supplying unit:

– GDEL-270: When a single converter via multiple windings supplies one or more equipment, the secondary power return shall be grounded to a single location within the supplied unit(s); one secondary power output shall not be distributed to more than one unit.

Shielding concept

In order to control the radiated emission from harness transmitting digital signals, shielded twisted lines will be used. For that kinds of "high frequency" signals, the shielding if efficient only if grounded at both ends.

This should in particular be applied to all RS-422 lines and to the 1553.

For the 1553 this should be applied to the main bus and to the stubs (cf. Figure 6.3.7-1).

The shielding of digital lines does not always follow the here above rules in Instruments grounding diagrams ; this will be clarified in the near future.
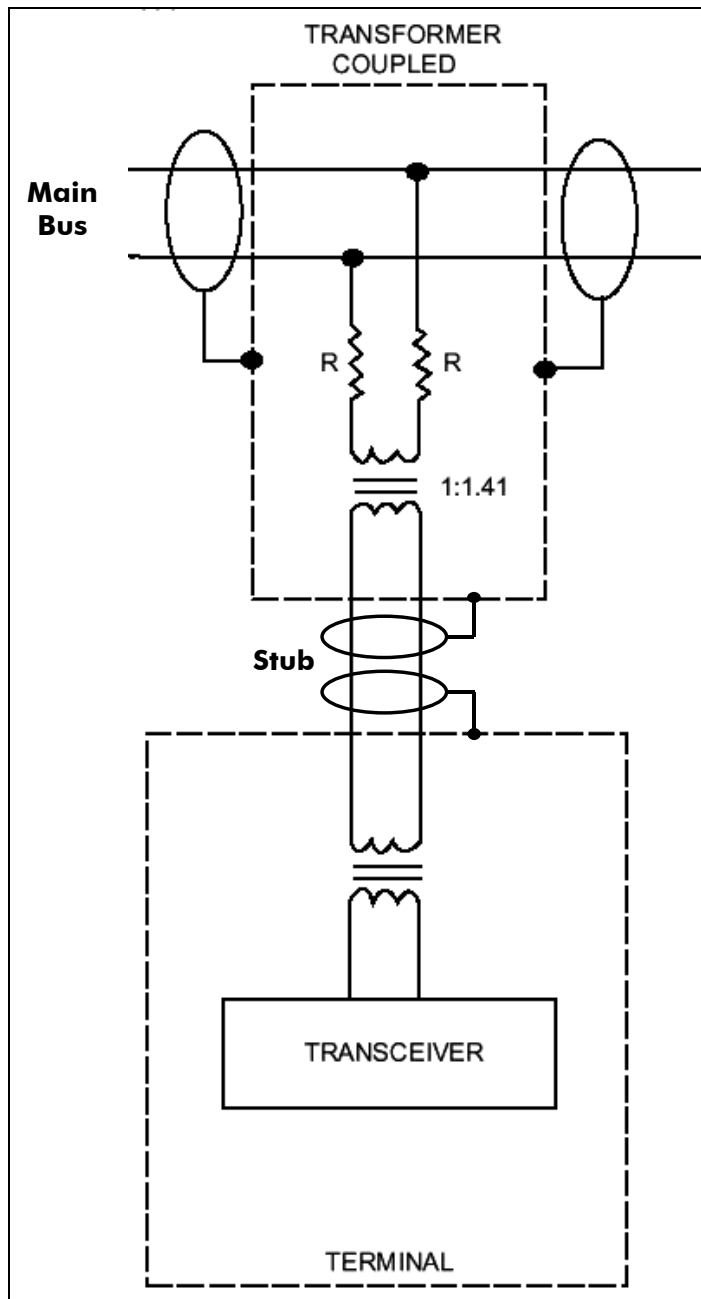
FIGURE 6.3.7-1 1553 BUS SHIELDING CONNECTION

The cryo-harness between the cryostat structure (HERSCHEL) or the FPU (PLANCK) and the SVM will be overshielded in order to protect the sensitive analogue signals and interfaces against high frequency common mode, field to cable coupling, and ESD. The shields connections to structure should be done over 360° at each end (cf. next "cryo-harness" paragraph).

SVM to PLM Grounding implementation

On both satellites, warm SVM and cold PLM are linked by isolating glass fibre struts for thermal decoupling purpose. This implies that the metallic links between SVM structure, PLM structure and optical bench are limited. Anyway on both satellites, some elements ensure structure electrical continuity.

HERSCHEL

Like on ISO, the optical bench is electrically linked to the Aluminium CVV through the cryogenic piping.

The CVV is then linked to SVM structure via the cryo-harness overshielding. On ISO the overshieldings were made of SST.

14 wave guides link HIFI LSU located in the SVM to HIFI LOU located outside the cryostat. Up to now, the baseline was to fix the LOU to the cryostat structure through isolating struts, but this is very liable to be changed for thermally and electrically conductive struts, so creating another conductive path between SVM structure and CVV.

Another metallic link between the optical bench and SVM structure is HIFI IF semi-rigid coaxial cables, with shields made of SST.

PLANCK

The electrical connection between FPU and SVM structures is ensured by:

- coolers piping

- LFI wave guides between FEM and BEM

- HFI bolometers signal cables overshielding.

It must be noted that as LFI BEM and DAE units are set on the SVM upper platform made of Carbon panels, an Aluminium grounding network should be foreseen.

On both satellites, as it was done on ISO, an analysis of structure impedance between cold detectors and Instrument warm electronics should be done, taking into account materials and geometry. The results is expected to be a RLC network valid up to 10 MHz.

Cryo-harness

One of the EMC concerns of ISO program was the consequence of an ESD current flowing between the SVM and the PLM (order of magnitude: 50 A, rise time = 10 ns, duration = 50 ns).

A part of such a discharge current could flow on the cryo-harness overshieldings and, according to the cryo-harness transfer impedance, create a transient voltage between the inner conductors and the overshielding, liable to create a failure of the interfaces.

Transfer impedance theory and typical values
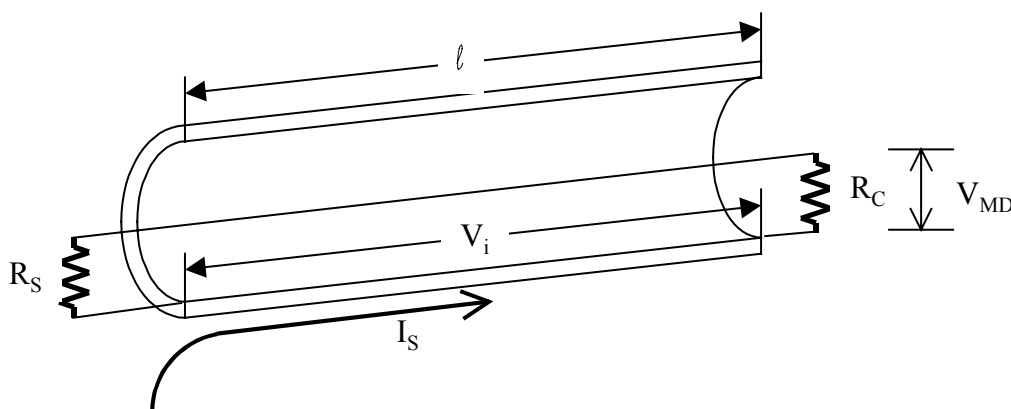
1 < λ/2.

In a shielded cable, the current induced on the shield by an external perturbation creates inside a longitudinal induced voltage V_i that distributes itself between the charging loads.

The transfer impedance is defined as $Z_t = \dfrac{V_i}{I_S \times 1} = \dfrac{2V_{MD}}{I_S \times 1}$ if $R_C = R_S$.

Z_t is expressed in Ω/m and characterises the shielding imperfection.

The better the shielding is, the lower Z_t is.

---

[1] From Mardiguian « Manuel pratique de compatibilité électromagnétique »

At low frequency (up to 10 or 100 kHz) Z_t is constant and equal to the shielding resistance.

For cables having a tubular shield (e.g. coaxial semi-rigid cables) Z_t is only driven by the diffusion of the electromagnetic fields through the tube (i.e. skin effect), and expresses as follows:

- at low frequency (T/δ <1):

$$\left|Z_t\right| = \frac{1}{2\pi a\sigma T} = R_0 \text{ with:}$$

  - a: shield diameter

  - σ: shield conductivity

  - T: shield thickness

  - δ: skin depth : $\delta = \dfrac{1}{\sqrt{\pi\mu\sigma f}}$

  - R_0: DC resistance of the shield per unit length.

- At high frequency (T/δ >1).

$$\left|Z_t\right| = 2\sqrt{2} \cdot e^{-T/\delta} \cdot R_{hf} \text{ with } R_{hf} = \frac{1}{2\pi a\sigma\delta}.$$

Braided-wire shields have a different behaviour at high frequency, especially because of the coupling by diffraction through the holes.

For most simple-braided shields, the transfer impedance can be expressed as:

$$Z_t = R_0 + jL_t\omega.$$

(R_0 being the diffusion component, and L_t the transfer inductance expressing the magnetic field penetration through the holes).

Some more complex coupling phenomena exist for braided shields that depend on the geometry: number of carriers (bands of wires) that make up the shield, number of carrier crossings per unit length, weave angle.

In the end, the following typical Z_t curves can be met:
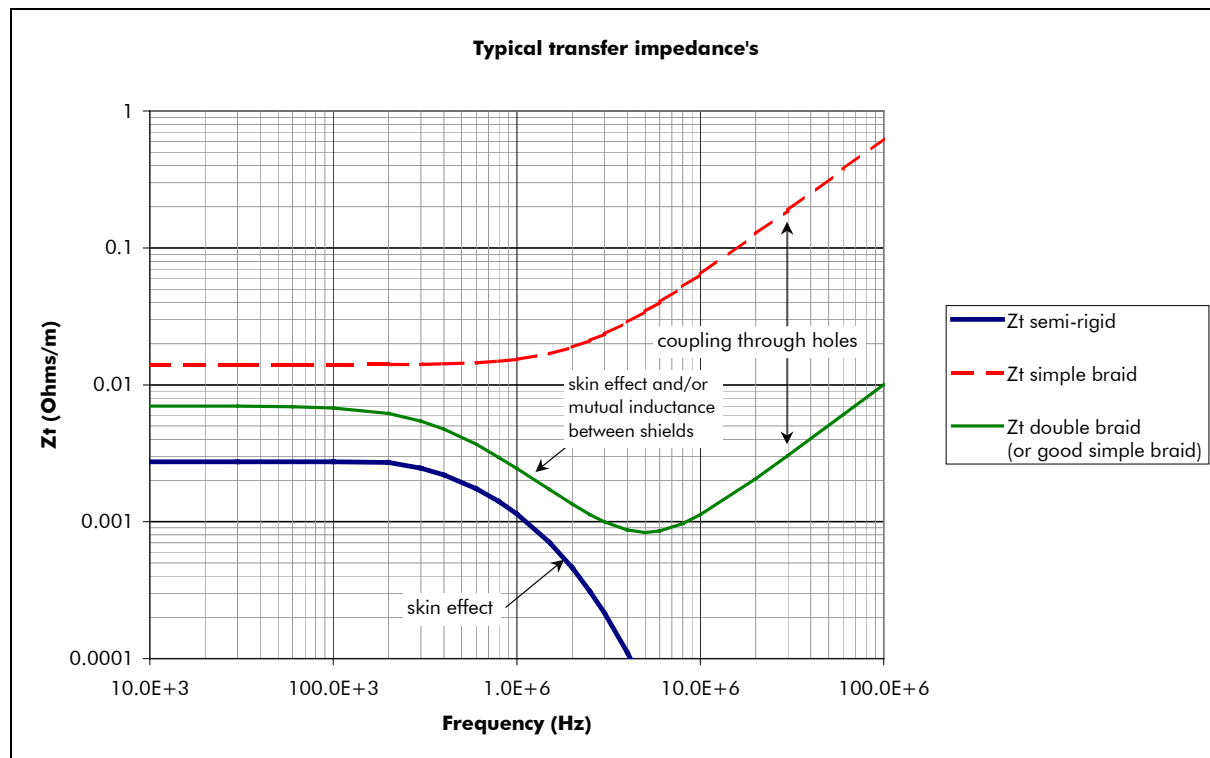
The characteristics of the cryo-harness braided overshieldings can have a major impact (± 20 dB) on transfer impedance's so will have to be carefully taken into account in the frame of future ESD analyses.

Choice of overshield material

Because of the thermal (decoupling of SVM from PLM) and electrical (having low resistance path) constraints, among the different overshield material candidates, the one presenting the maximal ratio $\alpha = \dfrac{\sigma(\text{electrical} \cdot \text{conductivity})}{\lambda(\text{thermal} \cdot \text{conductivity})}$ should be preferred a priori.

A rough comparison performed in the frame of ISO program was done at 0° C:

METAL	CU	AG	ALU	STAIN	GOLD	NI	LEAD	IRON	SST
α	145.10^3	145.10^3	174.10^3	128.10^3	133.10^3	197.10^3	133.10^3	162.10^3	87.10^3

This table evidences that there is no significant advantage for a specific metal (from a DC resistance point of view), so it should be chosen according to magnetic, mechanical or technological considerations.

This is in line with Wiedemann-Franz empirical law according to which for a solid metal around 0° C, $\lambda/\sigma = L.T$ with $L = 2.45.10^{-8}$.

Bundle configuration

On ISO, the trade-off was the following concerning the harness between SVM and PLM, routed on glass fibre struts:

– concentration of the whole allowed metal section between SVM and PLM in the bundle overshields

– lighter bundle overshields routed on thin aluminium tape set on the struts.

At low frequency, both solutions are equivalent, but we are confident that the best strategy for higher frequencies is to concentrate all the available metal section in the overshields in order to reach the best possible transfer impedances (thanks to good optical coverage), especially between 1 and 10 MHz for ESD protection purpose.

The overshield connections at both ends should be done over 360° with good contact and optical coverage so as not to deteriorate the overall transfer impedance, i.e. shielding efficiency.

An analysis will have to be done, taking into account the typical ESD current shape, the estimated transfer impedance, the terminal impedances and the components resistance to voltage transients to assess the system survival to a typical ESD.

It must be noted that the choice of proper cryo-harness overshielding strategy is important not only for ESD protection but also for protection of sensitive signals against field to cable coupling and against high frequency structure currents.

CS/CE margin on primary power lines

A very rough analysis was carried out in order to show that an intrinsic CS/CE margin exists between the specifications.

The CE DM specification of a unit consuming 1A was increased of 10Log60, considering a satellite consuming 60 A (worst case) and a statistical combination of unit CE (10Log(I) in stead of 20Log(I) variation law).

Then this value vas multiplied by the LISN impedance in order to get a rough idea of the voltage ripple at power bus star point.

Of course this approach is not fully valid, especially at high frequency, but it is a worst case as it doesn't take into account the decoupling between different power outputs of the PCDU.

Anyway, it allows to demonstrate a minimum CS/CE margin in differential mode between 26 and 32 dB, meaning that the CE and CS specifications are consistent (cf. following figure).
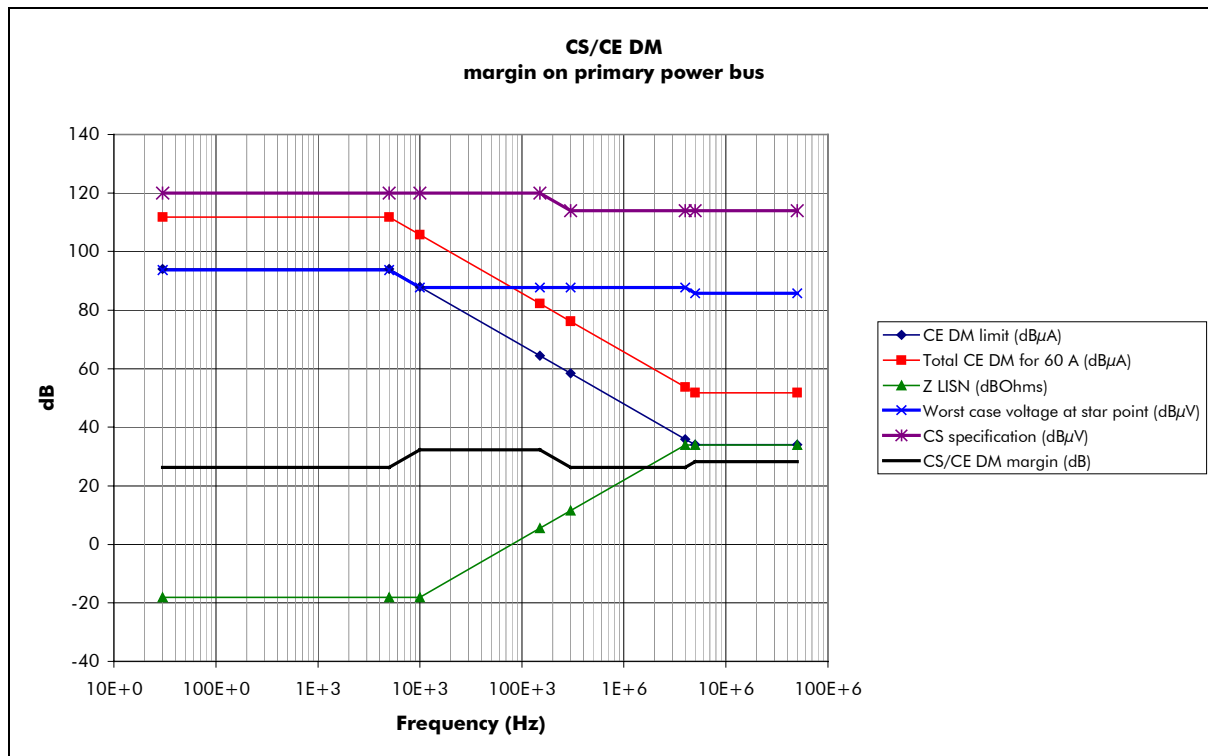
However, Planck 4K Cooler Drive Electronics may be OOS at low frequency.

Considering 60 W/80 Hz, we have assumed a CE of 127 dBμA up to 100 Hz, then decreasing of 20 dB/decade.

The previous results are then modified as follows:

CS/CE DM
margin on primary power bus

Legend:
- CE DM limit (dBµA)
- Total CE DM for 60 A (dBµA)
- Z LISN (dBOhms)
- Worst case voltage at star point (dBµV)
- CS specification (dBµV)
- CS/CE DM margin (dB)
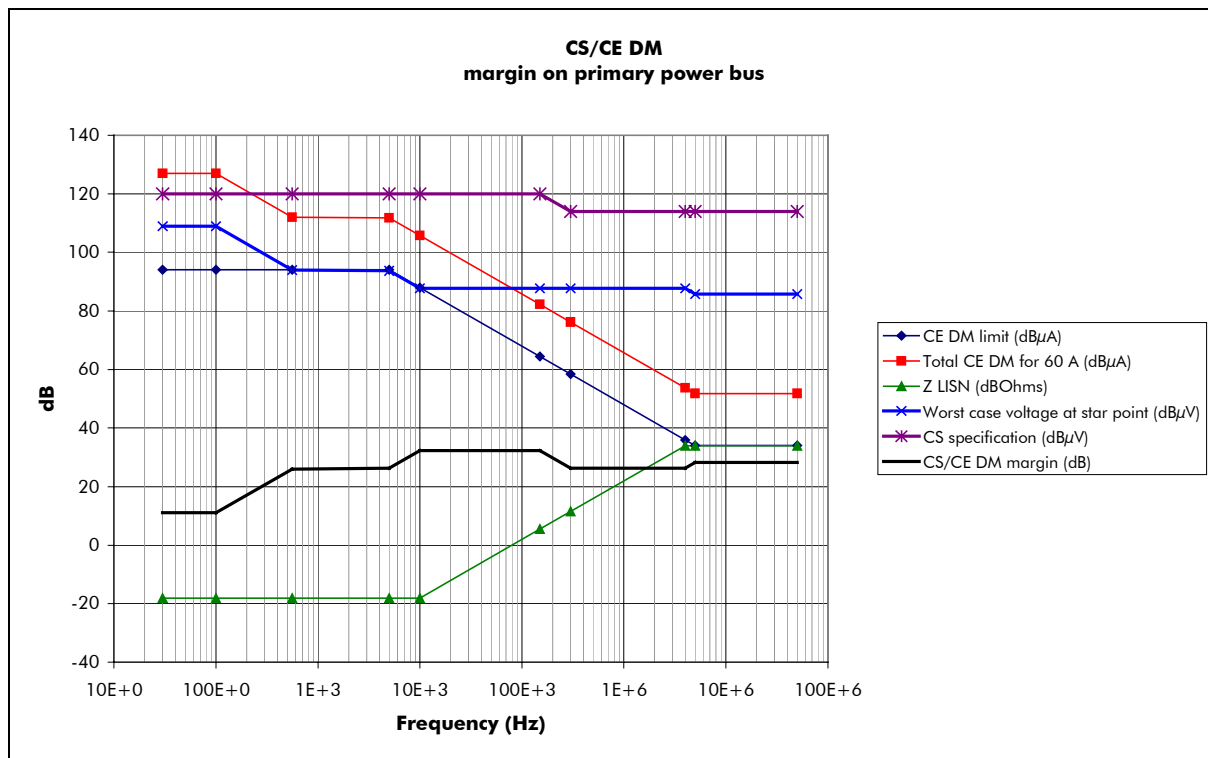
And we still have 11 dB margin at low frequency.

6.4. MISSION OPERATIONS AND AUTONOMY

6.4.1. Operations concept

The Herschel and Planck mission presents an intermediate status for operation between missions such as ISO or XMM/integral which are in constant ground contact, and deep space missions like ROSETTA for which long period of autonomy are foreseen. The basic operation concept in which the 2 spacecraft in orbit around L2 are operated from one single ground station (nominally Perth) leads to a ground contact of 3 hours per day for each spacecraft (DTCP: Daily Telecommunication Period). When ground contact is not available (OP: Observation Period), the spacecraft are fully autonomous, performing science observation according to a pre-defined schedule uploaded during a preceding ground contact period. The spacecraft have been designed to cope with this autonomy requirement, allowing operation without ground contact for 48 hours, the goal being to maximise the scientific return and to put the spacecraft in safe condition in case of major anomaly only.

Another major driver is to maximise commonality in the way the two spacecraft are operated. Even if they may exhibit differences (Herschel is a 3-axis stabilised spacecraft while Planck is a slow spinner), they share a number of commonalties:

- Similar orbits around L2

- Use of the same ground stations

- Same sharing of daily operations between OP and DTCP

- Common design for electrical subsystem of Herschel and Planck

- Identical data rates to ground.

Commonality in operation concepts will lead to reduction of the operational costs by allowing the use of the same procedure for the two spacecraft.

The Herschel and Planck spacecraft will be operated from the MOC (Mission Operation Centre) at ESOC, which interfaces with the Herschel Science Centre (HSC) and Herschel Instrument Control Centres (ICCs) and for Planck with the Data Processing Centres (DCP). Commanding of both spacecraft will be conducted by MOC based on inputs received from these centres. Housekeeping telemetry received from both platform and instruments will be processed by the MOC. Science telemetry as well as relevant housekeeping will be transferred to the scientific centres.

During scientific operation, both spacecraft will be operated from the Perth 35 m ground station. However other ground stations are envisaged during the various phases of mission. The planned usage of ground stations during the various phases of mission is shown in Table here after:

MISSION PHASE	GROUND STATION	
Initial orbit phase	ESA Network (Kourou, Perth, Villafranca)	
Commissioning phase	Perth/Kourou (routine)	Villafranca (emergency)
Performance verification phase	Perth/Kourou	Villafranca (emergency)
Routine operations phase	Perth 35 m (Prime station)	Villafranca, Kourou (emergency)

Communication to ground relies on X-Band for both TM and TC. TC is nominally via the Low Gain Antenna (LGA). TC via MGA at high bit rate is possible.

For telemetry, various modes are envisaged as shown in the following table. For commonality reasons, the same data rates have been selected for Herschel and Planck.

	Antenna	Ground Station	FIRST	Planck	TM/TC mode
TM Hi-rate	MGA	Perth	1.5 Mbps	1.5 Mbps	Real time HK + mem. dump. Real time HK + real time science + mem. dump.
TM medium-rate	MGA	Perth/ Kourou	107 kbps	107 kbps	Real time science + real time HK
TM low-rate	LGA	Perth	5 kbps	5 kbps	Real time HK (S/C + P/L).
		Kourou	500 bps	500 bps	Real time HK with Kourou 15 m.

Nominal TC rate is 4 kbps via LGA when communicating via Perth, and 125 bps when Kourou is used. In addition, commanding via MGA at 4 kbps is also possible. The various TC modes are summarised in the following table; they are identical for Herschel and Planck.

	S/C ANTENNA	GROUND STATION	DATA RATE	REMARKS
TC low rate	LGA	Kourou	125 bps	
TC nominal	LGA or MGA	Perth	4 kbps	

The figure hereafter summarises the ground segment for Herschel and Planck satellites.
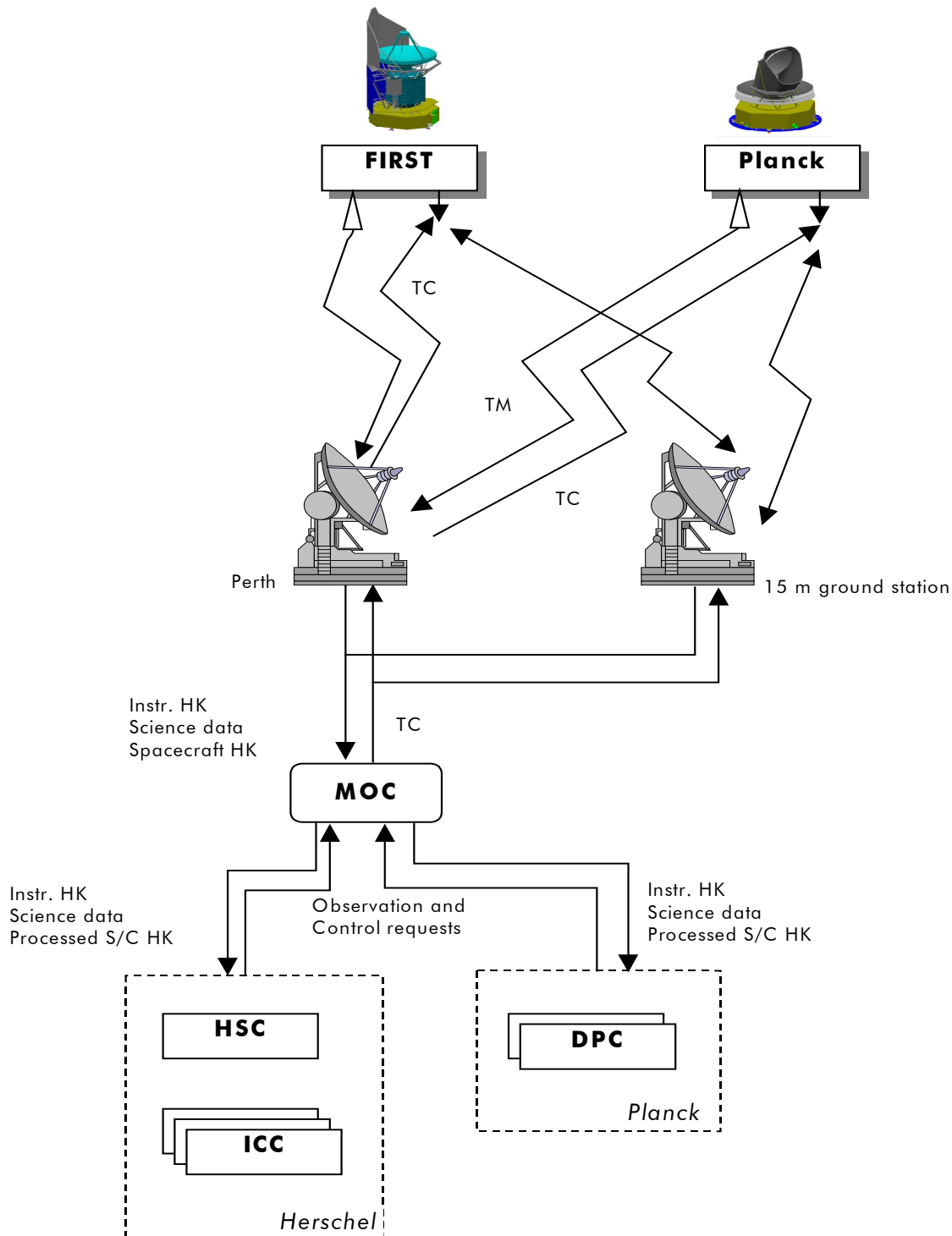
The basic concept of operations for the satellites is that all activities will be performed according to the on-board Mission TimeLine (MTL). This is the operational mode of the spacecraft during nominal scientific operations, even if the spacecraft is in ground visibility. Autonomy functions allowing spacecraft reconfiguration in order to maintain scientific activities are active on-board and do not require inputs from ground. Actions from ground are limited to receiving telemetry (real time and stored in the mass memory) and sending commands to update the Mission Timeline. The telecommands stored in the MTL can perform direct commanding or initiate OBCP, activate functions or pass parameters to the tasks.

Real time commanding of the spacecraft is also possible. However, when the spacecraft is under ground control, autonomy functions are still active on-board and ground commands are not required to maintain spacecraft safety. This is in accordance with the requirement that ground reaction within less than 3 minutes shall not be required (OIRD, CTRL-1). When, direct commanding is used, there is always the risk that the actual spacecraft status is different to the one known on-ground on which the command has been based. For instance, a reconfiguration can have occurred which is not taken into account on-board. Failure protection on-board includes protection mechanisms to avoid that such inconsistency leads to hazardous situations.

On-Board Control Procedures (OBCP)

A principle mode of operation of the Spacecraft will be by execution of pre-defined on-board control procedures (OBCPs) initiated from the mission timeline. OBCPs are flight procedures, which are resident on-board of the FIRST or Planck satellite. They are written by using a Spacecraft Control Language (SCL).

After activation they are interpreted and executed in the on-board system, e.g. the CDMS, the ACC, and potentially other intelligent on-board users, like instrument control units. They serve for controlling processes, which may be active for an extended period of time and which may involve the (conditional) execution of a (longer) sequence of commands. These on-board Telecommands may affect one or several application processes or functions. More than one on-board unit may be involved.

In order to retain predictable and robust behaviour of the spacecraft and its systems the number of OBCPs shall be kept to a minimum, and the internal structure of each OBCP must be kept simple.

OBCPs can be activated by:

-   Timeline

    – Ground command

    – On-board event, automatically.

6.4.1.   Spacecraft system modes

6.4.1.1.   Pre-launch/Launch Mode

This mode corresponds to a waiting phase of the on-board SW up to spacecraft separation from ARIANE. It ends by separation detection by majority voting in the CDMU Reconfiguration Module (RM). During this mode, the following equipment is ON:

    – CDMU nominal

    – ACC nominal (in standby mode)

    – PCDU

    – CCU (Cryogenic Control Unit)

    – Receiver (nominal + redundant).

The batteries provide power. After fairing separation, it is expected that the orientation of the launcher will be such that the Herschel Sun Aspect Angle requirements will be fulfilled. This means that the Herschel Solar Array will be exposed to Sun and that battery charging can occur. This is however not the case on Planck as its Solar Array will not be exposed to Sun.

The instruments are all in OFF mode, except HFI, which is in launch mode to provide power to the 4 K cooler for launch lock.

When the separation is detected by the CDMU, the House Keeping Mode 1 is engaged.

6.4.1.2.   Housekeeping modes

The housekeeping modes are the normal system modes when no scientific operations are performed.

Two modes have been defined:

−   HK1 which is the initialisation mode at separation

−   HK2 which corresponds to the routine mode when the spacecraft is in ground contact or in the absence of ground contact and in the absence of scientific activity.

HK1

The aim of this mode is to reach a stable sun-pointed attitude safe for payload, power and communication. HK1 is initiated on launcher separation detection. This initiates the separation sequence programme running in the CDMU which commands all activities required to perform Sun acquisition and acquire data link with Earth.

The following equipment are switched ON:

−   Transmitter and associated TWTA

−   AOCS sensors: QRS, SAS and FSS on Herschel

−   Thruster drivers and cat bed heaters

−   Reaction wheels on Herschel

−   RCS latch valve.

As, during launch, the CDMS and ACC are switched on, all functions of data handling and attitude control are available at launcher separation. 20 seconds after separation, the spacecraft is able to transmit telemetry and the AOCS is fully operational.

Both spacecraft are separated from the launcher in Sun pointed attitude. The ACC is then commanded to Sun acquisition mode which is performed on both Herschel and Planck using thrusters. This allows to compensate the launcher separation uncertainty and to re-point the spacecraft solar arrays towards Sun. Once successful Sun pointing is achieved, power generation is gracefully switched to Solar Array. Sun pointing will be observed by the Sun Acquisition Sensors of the AOCS; alternatively it can be detected by monitoring of the Solar Array delivered power. On Herschel, once rate damping by thruster is achieved, the AOCS transitions to safe hold mode in which attitude control is performed with the wheels. On Planck the initial spin direction will be defined by the launcher and will then not be changed during the mission.

If Sun acquisition is not achieved before a pre-defined time-out, a complete re-configuration of the AOCS will be performed and new Sun Acquisition sequence will be commanded.

During HK1, communication with Earth is performed using omni-directional coverage provided by the LGA. This is imposed by the fact that, at launcher injection and for few tens of minutes, the angle between Earth and Sun seen from the spacecraft is above 90 deg. In that case, if the spacecraft is Sun pointed, communication is ensured by the antennas covering the - Z hemisphere on Herschel and the + X hemisphere on Planck. Transmission of telemetry to ground is performed using the LGA on which TC is received.

In this mode, the payload instruments are OFF.

The autonomy mode is Ground Managed.

Transition to HK2 is performed by ground command.

HK2 is the basic housekeeping mode when no science is performed. It is used at the beginning of mission, during commissioning and performance validation phases. It allows transition from survival to fine pointing mode under ground control and will be used to resume scientific operation after a transition to survival mode.

In this mode, all AOCS modes are tested.

It has 2 sub-modes:

– When the spacecraft is in ground visibility: HK2/V

– When the spacecraft is not in ground visibility: HK2/NV.

Transition between the two sub-modes is nominally by ground command but can be by timeline.

This mode can be entered from:

– HK1 by ground command

– Survival Mode by ground command

– Science Mode by ground command or TimeLine.

This mode can be exited to:

- Science Mode by ground command or TimeLine

- Survival Mode in case of conditions given in § survival mode.

HK2/V

All AOCS modes, can be used. In particular, it is possible to perform the orbit control manoeuvres required at the beginning of mission.

Calibration will be conducted in AOCS observation modes:

- Fine Pointing Mode (FPM) or Line Scanning Mode (LSM) for Herschel

- Nominal Mode (NOM) for Planck.

On Herschel, the calibrations are:

- Fine Sun Sensor to Star-Tracker calibration

- Gyro calibrations.

Multiple calibrations will be performed with various Sun Aspect Angles and attitudes to reduce the calibration error.

Switching ON of the payload is performed and transition of the payload modes from OFF mode to standby mode can be commanded. Only housekeeping data from the payload will be collected and transmitted to ground. The spacecraft receives TC from ground and downloads housekeeping telemetry. The LGA (+ Z on Herschel, - X on Planck) is used for communication with the ground. The autonomy mode will be "Ground Managed" (GM).

HK2/NV

For Herschel the spacecraft will remain in fine pointing mode, 3-axis stabilised with the Z-axis Sun pointed. Planck will remain in normal mode with the spin axis Sun pointed. Spin axis re-orientation manoeuvres can be commanded in order to maintain the SC Sun pointed. Housekeeping data from the instruments (if switched ON) and platform are stored in the mass memory. The autonomy mode is "Autonomous Fail Safe" (AFS).

6.4.1.3.   Science Mode

This is the spacecraft mode of operation during scientific mission. It has 2 sub-modes:

– Autonomy (SCI/AUT) which corresponds to nominal science observation without ground contact.

– Telecommunications (SCI/TC) which correspond phases in ground contact during science activities.

Transition between the two sub-modes is nominally by ground command but can be by timeline. Ground command is always possible in autonomy as the receivers remain ON during the phase.

Line of sight calibrations will be conducted in this mode during performance verification phase. It will consist in measuring the relative angles between instruments line of sight with respect to the attitude reference sensors, or to calibrate attitude sensors between them (Star-Tracker calibration). On Planck, line of sight calibration will be performed by observing sources both in the instrument detectors and by the Star-Mapper. Typical sources, which can be used for such calibration, are external planets such as Jupiter or Saturn. In order to facilitate this calibration, the Star-Mapper is co-aligned with the telescope, allowing the object to be seen at the same time by the instrument and the Star Mapper.

This mode will also be used during commissioning and performance verification phase to validate proper functioning of the satellite and payload.

SCI/AUT

During **autonomy mode**, the operations on both Herschel and Planck follow the commands defined in the on-board mission timeline.

On Herschel, the observations will consist in a succession of slew and fixed pointing. Pre-programmed modes of observation in the on-board software will allow to perform complex observation sequences without requiring complex telecommand sequences from ground. These modes are:

– Raster pointing with or without OFF position

– Position switching

– Nodding.

In addition, a scanning mode is also specified for Herschel. It is used for the following scientific pointing modes:

- Line scanning with or without OFF position

- Tracking of solar system objects.

These observations are performed using the AOCS Fine Pointing Modes (FPM) or Line Scanning Mode (LSM). Wheel unloading can be performed autonomously based on a command included in the timeline. Similarly, orbit control manoeuvres can be programmed in the timeline and performed without ground link.

The Herschel scientific observation is basically performed by one instrument, which is in Prime mode while the other instruments are in standby. There are two other possible operational modes for the payload:

- PACS in Prime mode, SPIRE in parallel mode performing photometer observations with a degraded sensitivity and spatial resolution

- During slew, SPIRE can perform useful observations with its photometer in the so-called "serendipity" mode.

The following table summarises the payload modes.

MODE	HIFI	PACS	SPIRE	COMMENTS
1	Prime	Standby	Standby	
2	Standby	Prime	Standby	
3	Standby	Standby	Prime	
4	Standby	Prime	Parallel	TM bandwidth, to be shared between PACS and SPIRE.
5	Standby	Standby	Serendipity	During slew. All TM bandwidth available for SPIRE.

On Planck, the basic operational mode is based on parallel operation of HFI and LFI. Alternative modes exist with one of the experiment in Prime mode and the other in standby mode, as shown in the following table.

MODE	HFI	LFI
1	Prime	Prime
2	Prime	Standby
3	Standby	Prime

The instruments are constantly scanning the celestial sphere and the spin axis direction is adapted regularly to follow the Planck scanning law at up to 10 deg from the Sun, as defined in the on-board mission timeline. This is performed using the AOCS Nominal Mode (NOM) between slews and the HCM (angular momentum control) to adjust spin axis direction.

During autonomy mode, the housekeeping data from the platform and instruments as well as scientific data are stored in the mass memory for subsequent downloading during a telecommunication period. The mass memory is sized to store 48 hours of data with margins.

The FDIR has to ensure autonomous reconfiguration of the spacecraft to maintain continuation of the scientific observation. A small outage can be tolerated but the spacecraft shall go in survival mode only if major failure occurs on-board and after all reconfiguration path have been exhausted. The autonomy mode is then "autonomous fail operational".

SCI/TC

During **telecommunication mode**, the spacecraft is Earth pointed to download the scientific data stored in the mass memory during the whole duration of the visibility period. Communication nominally uses the MGA for high rate telemetry while commanding is performed via the LGA.

On Planck, the scientific observation shall continue nominally in parallel to telecommunication. This is ensured by a ± 10 deg field of view MGA, compatible with the maximum Sun/SpaceCraft/Earth (SSCE) angle during mission.

Ranging is done in TM/TC medium rate.

On Herschel, the scientific observations will be limited to attitude compatible with Earth pointing and compliance with the SAA constraints. As a MGA field of view of ± 10 deg has been considered for Herschel, some flexibility exists in Herschel pointing, allowing performing raster pointing or line scanning (with a limitation in the line length). Scientific data collected during telecommunication mode are either transmitted real time of stored in the mass memory for transmission at the end of the telecommunication period or during a subsequent one.

The payload modes of operations are similar for the 2 spacecraft to the ones in autonomy mode. However, on Herschel, some specific payload housekeeping tasks such as coolers recycling will be preferably conducted in telecommunication mode.

Even if the spacecraft is in ground visibility, an "Autonomous Fail autonomous" (AFO) FDIR will be maintained. This is particularly applicable to Planck for which the scientific mission goes on nominally during telecommunication phase: on-board reconfiguration will allow quicker reaction than using ground control and will minimise possible outage in the science mission.

6.4.1.4.   Survival

In survival mode, the spacecraft is put in safe condition and the requirement is that it shall survive for at least 7 days without ground contact. The safe attitude corresponds to a Sun pointed attitude allowing power generation and stable temperature conditions. The timeline is discontinued and the spacecraft is waiting for ground commands.

On Herschel, the spacecraft is first transitioned to SAM, allowing fast re-acquisition of Sun pointed attitude (Z-axis Sun pointed) using thrusters. To avoid staying 7 days under thruster commands, control is then autonomously transitioned to SHM (Safe and Hold Mode), where control is performed by the reaction wheels which maintain the spacecraft Z-axis Sun pointed.

On Planck, due to the spinning motion, the spacecraft is intrinsically stable in the absence of external torques. On transition to survival mode, the AOCS is commanded into SAM, allowing Sun reacquisition on thrusters. Once Sun pointed, the AOCS can be very passive due to the low disturbing torques. The spacecraft will remain inertially pointed, which means, that the Sun will move by around 1 deg per day w.r.t. the spin axis. After 7 days, the Sun will have moved 7 deg which is still acceptable. Surveillance of the Sun position is performed by the Attitude Anomaly Detector, which will detect any attitude constraints violation and will initiate a SAM in this case.

Communication to ground during survival is performed using the LGAs for TM and TC. Omni-directional coverage is provided by the LGAs which allows to receive TC and send TM in any spacecraft attitude.

This mode has two sub-mode:

–   SM1 in which the spacecraft is put in ACMS safe mode and the equipment are in standby.

–   SM2 in which the spacecraft is put in ACMS safe mode and the equipment are OFF.

Transition to survival mode can be initiated in various ways:

- From a ground command: this will happen when, the spacecraft being under ground control, the ground detects an on-board failure.

- From a command in timeline : transition to survival mode at predefined time is used to put the spacecraft in safe conditions in case of loss of ground contact. This will occur when all commands in the mission timeline have been executed and no update has been received from ground. As this transition to survival mode is pre-programmed, it can be preceded by a Sun pointing command in normal mode, thus avoiding a transition to SAM. The absence of timeline update can be due to no commands from the ground station but can also result from a failure in the TTC equipment. In order to differentiate the two cases a search phase will be initiated: switching between antenna and receivers will be modified to check if any signal is received from Earth in the new configuration.

- After major on-board failure or attitude loss, the satellite being autonomous (either Autonomous Fail Safe(AFS) or Autonomous Fail Operational (AFO)).

The sub-mode in which the spacecraft transitioned depends on the failure kind.

SM1

The spacecraft switch to ACMS safe mode (SAM or SHM for Herschel, and SAM for Planck). The instruments will be transitioned to a waiting mode. A safe mode flag will be sent to the experiment to initiate proper reconfiguration.

This mode is entered in case of:

- Loss of proper Sun Pointing (SP)

- Violation of Thruster On Time (TOT)

- Timeout on TC reception from CDMU for ACC

- Satellite over/under heating.

SM2

In case of transition to SM2, the spacecraft switch to ACMS safe mode (SAM or SHM for Herschel, and SAM for Planck) and the instruments will be switched OFF. A safe mode flag will be sent to the experiment to initiate proper reconfiguration. On Planck, the active cooling system has to be switched OFF. As this can result in the loss of 1 month of mission, spacecraft will switch to SM2 only in case of:

    − Bus Under Voltage (BUV)

    − Battery Depth of Discharge (DOD)

    − Timeout on TC reception from ground.

6.4.1.5.   Modes links and transitions

The following table summarises the Herschel operational modes.

SC MODE	SUB-MODE	TM/TC MODE	TM/TC ANTENNAS	TM DATA RATE	FDIR	AOCS MODE	PAYLOAD MODES	POWER MODE
Science (SCI)	Autonomy (AUT)	N/A	N/A	N/A	AFO	FPM, LSM, WUP	- 1 instrument Prime; others in standby. - PACS Prime, SPIRE parallel. - SPIRE in serendipity	SA
	Telecommunication (TC)	Real time HK + mem. dump	TC = LGA + Z TM = MGA	TM Hi-rate	AFO	FPM, LSM, WUP, OCM	- 1 instrument Prime; others in standby. - PACS Prime, SPIRE parallel.	SA
		Real time HK + real time sci. + mem. dump		TM Hi-rate				SA
		Real time HK + real time sci.		TM Medium-rate				SA
HK1		Real time HK	TM/TC by LGA +Z/-Z	TM Low-rate	GM	SAM/SHM	Instruments OFF.	Battery or SA
HK2	V	Real time HK	TM/TC by LGA + Z	TM Low-rate	GM	SAM/SHM,STAM,FPM, LSM, WUP, OCM	Instruments OFF or in standby.	SA
	NV	N/A	N/A	N/A	AFS	FPM, SAM, SHM, WUP	Instruments OFF or in standby.	SA
Survival	SM1	Real time HK	TM/TC by LGA +Z/-Z	TM Low-rate	N/A	SAM, SHM	Instruments in standby	SA or Battery
	SM2	Real time HK	TM/TC by LGA +Z/-Z	TM Low-rate	N/A	SAM	Instruments OFF.	SA or Battery
Launch	LUM	N/A	N/A	N/A	N/A	SBM	Instruments OFF.	Battery

FPM: Fine Pointing Mode – LSM: Line Scanning Mode - WUP: Wheel Unloading Phase – OCM: Orbit Correction Mode –
SAM: Sun Acquisition Mode - SHM: Safe Hold Mode – STAM: Star Acquisition Mode – SBM Stand By Mode

The following table summarises the Planck operational modes.

SC MODE	SUB-MODE	TM/TC MODE	TM/TC ANTENNAS	TM DATA RATE	FDIR	AOCS MODE	PAYLOAD MODES	POWER MODE
Science (SCI)	Autonomy (AUT)	N/A	N/A	N/A	AFO	NOM, HCM	- 2 instruments Prime. - 1 Prime, 1 in standby.	SA
	Telecom-munication (TC)	Real time HK + mem. dump	TC = LGA + Z TM = MGA	TM Hi-rate	AFO	NOM, HCM, OCM	- 2 instruments Prime. - 1 Prime, 1 in standby.	SA
		Real time HK + real time sci. + mem. dump		TM Hi-rate				SA
		Real time HK + real time sci.		TM Medium-rate				SA
HK1		Real time HK	TM/TC by LGA +X	TM Low-rate	GM	SAM	Instruments OFF.	Battery or SA
HK2	V	Real time HK	TC = LGA – X TM = LGA – X	TM Low-rate	GM	SAM,NOM, HCM, OCM	Instruments OFF or in standby.	SA
	NV	N/A	N/A	N/A	AFS	NOM, HCM	Instruments OFF or in standby.	SA
Survival	SM1	Real time HK	TM/TC by LGA + Z/- Z	TM Low-rate	N/A	SAM	Instruments in standby	SA or Battery
	SM2	Real time HK	TM/TC by LGA + Z/- Z	TM Low-rate	N/A	SAM	Instruments OFF.	SA or Battery
Launch	LUM	N/A	N/A	N/A	N/A	SBM	Instruments OFF.	Battery

NOM: Normal Operation Mode – HCM: Angular momentum Correction Mode - OCM: Orbit Correction Mode –
SAM: Sun Acquisition Mode - SBM: Stand By Mode

Modes transition logic

The main modes have been defined for Herschel and Planck, allowing having the same transition logic for the two spacecraft.
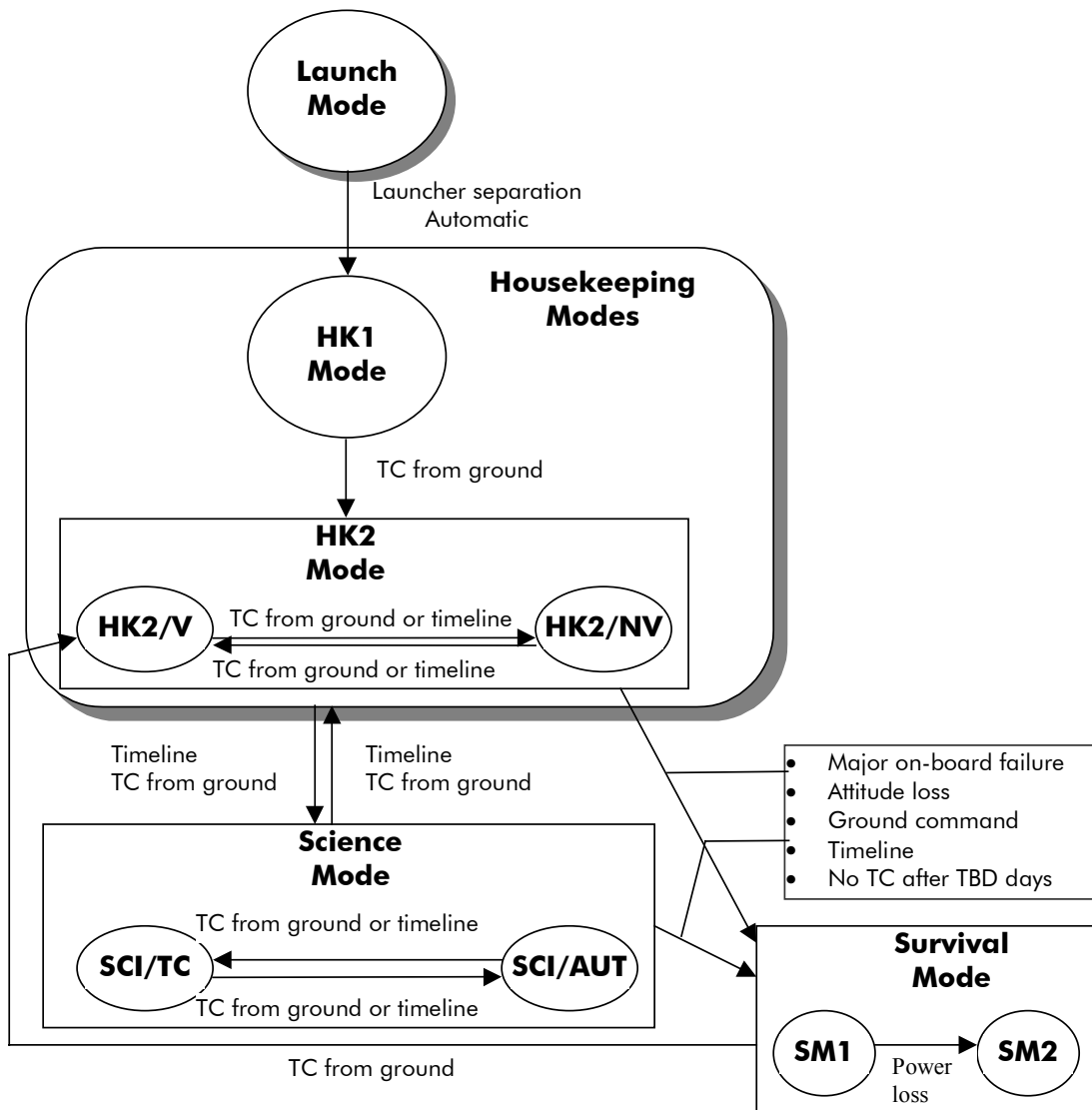
6.4.2.   FDIR concept

6.4.2.1.   FDIR modes

Ground Managed (GM)

The spacecraft are under ground control, and their operation is driven by the ground control data system. This happens at different stages of the missions: post launch activities, commissioning, and science calibration. It shall be pointed out nevertheless that the daily communication phases in L2 are not obligatorily, although under ground contact, GM from the autonomy point of view. The current flight programme, regularly uploaded, is executed. On anomaly or unforeseen event occurrence, the FDIR mechanism shall stop the nominal Mission TimeLine (MTL) and put the spacecraft in a safe configuration. Normal operation shall be resumed only upon ground authorisation.

Autonomous Fail Safe (AFS)

This autonomy mode answers to physical or operational constraints preventing any ground contact. It is typically applicable to the early phases of the FIRST & Planck missions, when the scientific observations are not yet entered and the main concern is to preserve the spacecraft safety while minimising the risks.

The flight programme, uploaded during ground contact, is autonomously executed. The FDIR principle shall follow the GM case: on anomalous event occurrence, the on board timeline shall be halted, the spacecraft shall be put in a safe mode, and the mission sequence shall only be resumed by the ground.

Autonomous Fail Operational (AFO)

This autonomy mode directly answers to the system requirements to maintain the continuity of the mission timeline and performance as long as healthy alternative functional path exits. It essentially applies for both spacecraft, to the scientific observation phases, possibly including the ground communication periods.

6.4.2.2.   FDIR general requirements

The main drivers for the FDIR strategy elaboration are the Herschel/Planck overall autonomy and safety requirements:

- The mission shall be nominally maintained without ground contact for any 48 hours period during the operational life, assuming no major failure condition. Mission shall be maintained as far as possible on the main cases of the single failures

– The spacecraft shall survive without ground contact for any 1 week period during the operational life when switched to survival mode

– Satellite life shall be preserved: fuel consumption shall be optimised, Herschel cryostat Helium shall be preserved, and reconfiguration and equipment loss shall be minimised.

This imposes the need to have any failure likely to induce a loss of the mission, or a damage to the spacecraft safety, autonomously detected, isolated then recovered. The requirements are identical for both Herschel and Planck, and, considering that the baseline Avionics architecture is also identical for both spacecraft, the FDIR philosophy is unique while the alarms definition and processing, and the details of the reconfiguration actions obviously differ from one spacecraft to the other one.

The strategy to apply in order to detect, isolate and recover failures is basically dependent upon the spacecraft life phase, or more precisely upon the current spacecraft mode. Each mode is associated to an autonomy mode: ground managed, autonomous fail safe or autonomous fail operational.

6.4.2.3.   General FDIR implementation

The requirements declined above following the spacecraft modes strongly suggest a **hierarchical** failure detection identification and recovery architecture. It permits to satisfy the top level requirement to have a visible impact on the mission operation, only in case of a major, high level failure, the equipment level failures being possibly processed and recovered autonomously at lower levels.

Generally, FDIR is focused on the vital spacecraft functions listed below:

– Attitude Control & Measurement (ACMS), managed by the ACC computer and the ACMS software. It includes the propulsion management

– Command/control, data handling and TTC, controlled by the CDMU and CDMS software

– Electrical power generation and distribution performed by the PCDU and monitored by the CDMU

– Thermal regulation, under CDMS SW control

– Payload management by the CDMS SW.

These vital functions, therefore, are performed or supervised by either of the 2 platform computers: the CDMU or the ACC. **The failures processing essentially depends on the current spacecraft mode and mission phase**, and the reconfiguration actions, in AFO mainly, are graduated w.r.t. failure criticality. Each computer, CDMU and ACC, applies a similar strategy to recover from a single failure:

- Software monitoring for the surveillance of low level failures, associated to a reconfiguration managed by software

- Hardware monitoring for the surveillance of high level failures, then a hardware based reconfiguration.

Major failures which can endanger the spacecraft vital functions, indeed, shall be detected by **dedicated hardware alarms** and handled independently from software tasks by the mean of high priority commands issuing.

The software monitoring is implemented within each computer for the functions units and interfaces under its respective control. Therefore the FDIR function, essentially system, as a consequence of the baseline decentralised architecture, is broken down into CDMS FDIR and ACMS FDIR, with simple interfaces between them. Each FDIR subset is implemented in hardware according to the same approach, as follows:

- Two separate hardware reconfiguration modules with direct hard-wired links from/to critical units, for alarm inputs and high priority commands outputs. The data handling reconfiguration module is called CDMU_RM, while the ACMS reconfiguration module is called ACC_RM

- Two-associated non-volatile safeguard memories, respectively the CDMU_SGM for the data handling safeguard memory, and the ACC_SGM for the ACMS safeguard memory.

The CDMS SW and the ACC SW shall detect low level alarms, while the CDM_RM and the ACC_RM shall detect high level alarms in input and order any reconfiguration by means of High Priority Commands called HPC_CDM when issued by the CDMU_RM, and HPC_ACC when issued by the ACC_RM.

The CDM_SGM and ACC_SGM shall memorise all the system and units configuration necessary to ensure autonomous failure recovery, and to save the failure context. Note that the design of CDMU is such that the spacecraft time keeps running in case of computer reconfiguration, and therefore does not require to be saved.

CDMS FDIR and ACMS FDIR communicate via either SW messages (e.g. events packets) for low level alarms, and HW signal for high level/system alarm.

An important feature is that at any failure detection, isolation and recovery procedure can be individually disabled and enabled by ground commands.

As it has already been underlined, the overall fault protection system relies on hardware for the processing of high level alarms and the sequencing of the associated reconfiguration actions. However, then, the hand is given back to the software for the post reconfiguration operations, the management of the spacecraft modes. This clearly differs from the approach retained e.g. on XMM/Integral spacecraft, where the ACMS safe mode is ensured by fully hardware mechanisms. It is strongly believed nevertheless, that the proposed solution offers the same level of reliability with in addition the benefit of:

– A simpler implementation (no Failure Detection and Control Electronics)

– Higher flexibility

– Simpler ground operational constraints.

6.4.2.4. Failures level

The failures detected by the FDIR function have been grouped into 5 main levels to allow for progressive detection and optimised reconfiguration. The failure level assignment is performed according to:

– The criticality of the failure

– The functions involved in failure detection (hardware or software functions)

– The recovery sequence.

The different levels are detailed hereafter:

– Level 0 failures

This level corresponds to a unit internal single failure, detected by the unit itself, and which can be automatically recovered thanks to the internal redundancy implementation, without any impact on the other part of the system.

Multiple (number selective by ground) occurrences of Level 0 failure shall lead to higher level recovery actions.

– Level 1 failures

A Level 1 failure is a failure, as seen by the ACMS computer (ACC) or the data handling one (CDMU), in a unit connected to either computer via the data bus (1553 bus), or dedicated acquisition lines and which cannot be automatically recovered by the unit itself. The surveillance of the unit is performed by the appropriate ACMS SW or CDMS SW via simple health check, and the same software, keeping in mind that the strategy for the complete processing of the failure is basically mode dependent, orders recovery actions.

Two sub-levels are considered:

- The Level 1a relates to failures which can be attributed to the unit level : ACMS sensors, ACMS actuators, PCDU, TTC transponders, … Any failure of these equipment implies only malfunction of the related ACC or CDMU software application. These failures are single application related. The failure detection is based on unit specific health data and operational parameters.

- Note that any ACMS unit reconfiguration action shall be reported to the CDMU, with the past and current unit contexts, and the safeguard memories shall be updated in accordance with the updated spacecraft configuration.

- The Level 1b relates to failures at communication modules level, and as such can be considered as multi-application related.

  Every bus coupler is checked by the mean of:

Specific internal health status depending on coupler design

1553 protocol errors including I/O time-out.

– Level 2 failures

A Level 2 failure is relative to an anomaly of a satellite vital function. The objective is to detect failures which have not/cannot be flagged at Level 1 by simple unit/communication health check, and, if possible, to process them before they may turn into a more severe (i.e. more mission impacting) system alarm. For each vital function, depending on the current mode, observed performances are compared to non-ambiguous thresholds and, depending on the current spacecraft mode, a recovery strategy is engaged, possibly leading to the reconfiguration of the whole functional chain.

The Level 2 failure detection and recovery are performed, depending on the function implicated in, by either of the two CDMS or ACMS on-board software.

– Level 3 failures

A Level 3 failure is considered as an internal processor module (CDMU or ACC) failure, much more severe than the Level 0, such that the processor module cannot neutralise it autonomously.

Corresponding errors are detected either by hardware or by software while the recovery is performed by H/W, via the CDM_RM or the ACC_RM.

The first occurrence of these alarms corresponds to the Level 3a, and the second occurrence to the Level 3b.

– Level 4 failures

A Level 4 failure is considered as a failure which is not detected/recovered by lower level procedures (Levels 0 to 3). The failure induces global system malfunction, which is detected by dedicated system alarms, hardwired to the relevant reconfiguration module: CDM_RM or ACC_RM.

Retained alarms are:

- Loss of proper Sun Pointing (SP)

- Violation of Thruster On Time (TOT)

- Depth Of Discharge (DOD)

- Bus Under Voltage (BUV)

- CDMS In Reconfiguration (CIR)

- ACMS In Reconfiguration (AIR).

Where SP, CIR and TOT alarms are handled by the ACC_RM and BOC, BUV and AIR alarms are handled by the CDM_RM.

It shall be pointed out that the failures leading to the listed alarms may be processed by lower level reconfigurations; this is the reason why a dedicated Δt time interval is allocated to each of them, significant of the duration given to the lower levels to successfully recover the alarm. Shall the alarms remain set after Δt, Level 4 reconfiguration will occur. For each alarm, in each mode, Δt is programmed to fit with the system constraints.

Level 4 recovery action is performed by the proper reconfiguration module (CDM_RM or ACC_RM).

6.4.2.5.   Feared failures

The tables below are preliminary lists of the failure cases to be detected and recovered by FDIR (via reconfiguration or change to safe mode).

ACMS function potential failure.

Herschel			
LEVEL 1 FAILURES	**LEVEL 2 FAILURES**	**LEVEL 3 FAILURES**	**LEVEL 4 FAILURES**
-STR unit failure. -FSS unit failure. -SAS unit failure. -GYRO unit failure. -QRS unit failure. -RW unit failure. -Thruster unit failure. -ACMS I/F board failure. -ACMS 1553 bus interfaces failure. -ACC_RM, ACC_SGM failure. -Multiple bus protocol errors. -Harness failure.	-Failure to achieve/maintain the requested attitude: ● mode initialisation failure, ● attitude acquisition failure, ● Sun searching failure, ● Sun, Star, Earth pointing failure, ● Rate control failure, ● Delta-V control failure. -Equipment data processing error. -Equipment command processing error. -Attitude control functions error : ● Attitude filter, ● Attitude error determination, ● Rate error determination …. -Thruster on time SW.	-ACC failure.	-Sun out of spec. angle. -Thruster over activation or thruster failure. -Timeout on TC reception from CDMU (Time Sync TC).
Planck			
LEVEL 1 FAILURES	**LEVEL 2 FAILURES**	**LEVEL 3 FAILURES**	**LEVEL 4 FAILURES**
-STM unit failure. -SAS unit failure. -QRS unit failure. -Thruster unit failure. -ACMS I/F board failure. -ACMS 1553 bus interfaces failure. -ACC_RM,ACC_SGM failure. -Multiple bus protocol errors. -Harness failure.	-Failure to achieve/ maintain the requested attitude : ● mode initialisation failure, ● attitude acquisition failure, ● Sun, Star, Earth pointing failure, ● Delta-V control failure. -Equipment data processing error. -Equipment command processing error. -Attitude control functions error : ● Attitude filter, ● Attitude error determination, -Thruster on time SW.	-ACC failure.	-Sun out of spec. angle. -Thruster over activation or thruster failure. -Timeout on TC reception from CDMU (Time Sync TC).

Propulsion function potential failure

Herschel			
LEVEL 1 FAILURES	**LEVEL 2 FAILURES**	**LEVEL 3 FAILURES**	**LEVEL 4 FAILURES**
-Thruster failure. -PROP I/F board failure. -Thruster misalignment. -LV blocked open. -LV blocked close. -Harness failure.	-Thruster command failure. -Thermal control failure.	-ACC failure.	-Fuel over consumption (= thruster over activation or thruster failure).
Planck			
LEVEL 1 FAILURES	**LEVEL 2 FAILURES**	**LEVEL 3 FAILURES**	**LEVEL 4 FAILURES**
-Idem Herschel.	-Idem Herschel.	-Idem Herschel.	-Idem Herschel.

Thermal regulation function potential failure

Herschel			
LEVEL 1 FAILURES	**LEVEL 2 FAILURES**	**LEVEL 3 FAILURES**	**LEVEL 4 FAILURES**
-Heater unit failure. -Thermistor unit failure. -RTU I/F board failure -PCDU failure. -Harness failure.	-Unexpected local thermal behaviour.	-CDMU failure.	-Satellite over/under heating.
Planck			
LEVEL 1 FAILURES	**LEVEL 2 FAILURES**	**LEVEL 3 FAILURES**	**LEVEL 4 FAILURES**
-Idem Herschel.	-Idem Herschel.	-Idem Herschel.	-Idem Herschel.

Electrical power conditioning and distribution function potential failure

Herschel			
LEVEL 1 FAILURES	**LEVEL 2 FAILURES**	**LEVEL 3 FAILURES**	**LEVEL 4 FAILURES**
-PCDU failure. -Battery unit failure. -Harness failure. -Solar array failure. -Solar array driver failure.	-Power management failure (power depth of discharge is incompatible with the mission).	-CDMU failure. -Battery overcharge.	-Bus undervoltage. -Battery DOD
Planck			
LEVEL 1 FAILURES	**LEVEL 2 FAILURES**	**LEVEL 3 FAILURES**	**LEVEL 4 FAILURES**
-Idem Herschel.	-Idem Herschel.	-Idem Herschel.	-Idem Herschel.

Payload management function potential failure

Herschel			
LEVEL 1 FAILURES	**LEVEL 2 FAILURES**	**LEVEL 3 FAILURES**	**LEVEL 4 FAILURES**
-Instrument failure. -Cryostat control unit failure. -Harness failure.	-N.A.	-CDMU failure.	-N.A.
Planck			
LEVEL 1 FAILURES	**LEVEL 2 FAILURES**	**LEVEL 3 FAILURES**	**LEVEL 4 FAILURES**
-Instrument failure. -Sorption cooler failure. -Harness failure.	-N.A.	-CDMU failure.	-N.A.

Command/control function potential failure

Herschel			
LEVEL 1 FAILURES	**LEVEL 2 FAILURES**	**LEVEL 3 FAILURES**	**LEVEL 4 FAILURES**
-RTU I/F board failure. -Data handling 1553 bus interfaces failure. -CDMU_RM,CDMU_SGM failure. -Multiple bus protocol errors. -Erroneous TC. -DC/DC failure. -Erroneous TM position. -Bus I/F error. -Receiver failure. -Harness failure.	-No TC reception during planned communication phases (TBC).	-CDMU failure.	-Timeout on-ground TC reception.
Planck			
LEVEL 1 FAILURES	**LEVEL 2 FAILURES**	**LEVEL 3 FAILURES**	**LEVEL 4 FAILURES**
-Idem Herschel.	-Idem Herschel.	-Idem Herschel.	-Idem Herschel.

6.4.2.6.   FDIR strategy

The FDIR strategy is defined for both spacecraft and each spacecraft: each phase, from an autonomy & FDIR point of view is declared as ground managed, autonomous fail safe or autonomous fail operational. For each mode, depending on the operational life phase, the top level requirements (GM, AFS, and AFO) are refined at lower levels.

Each FDIR subset, CDMS FDIR and ACMS FDIR, is nominally declared in the same mode (even a need to choose different operating modes for ACMS and CDMS FDIR could be evidenced at a later stage).

The proposed principles and protocol for the system level FDIR implementation, i.e. the synchronisation of the 2 FDIR subfunctions, are based on some general rules detailed in the table here after. The applicability for each autonomy mode is given.

SYSTEM FDIR RULES	GM	AFS	AFO
Any ACMS FDIR action leads, at a minimum, to suspend the MTL in CDMS SW; any ACMS FDIR action is sent as an event to CDMS SW.	X	X	X
Any successful ACMS mission recovery is reported as an Event to CDMS SW, and allows to resumes the MTL.	Level 1 only	Level 1 only	X
Any ACMS switch to SM1 mode when triggered by FDIR is reported to CDMS via the AIR high level alarm.	X	X	X
Any ACMS switch to SM1 when triggered by FDIR causes a CDMS FDIR action to initiate SM1.		X	
Any CDMS FDIR action leads, at a minimum, to suspend the MTL in CDMS SW.	X	X	X
Any successful CDMS mission recovery resumes the MTL.	Level 1 only	Level 1 only	X
Any CDMS switch to SM2 triggered by FDIR is reported to ACMS via the CIR high level alarm.	X	X	X
Any CDMS switch to SM2 triggered by FDIR causes on ACMS FDIR action to initiate SM2.	X	X	X
Any timeout on the reception of CDMU TC by ACC unchains an ACMS FDIR action to initiate SM1	X	X	X

SYSTEM FDIR GENERAL RULES

Failure level 1 to 2 in ACC is recovered by ACC itself and is reported to CDMU; the ACC must have the possibility to switch from an equipment to the other without CDMS (PCDU is commanded by CDMS): for that reason, all equipment are ON from PCDU point of view and the ACC can put ON or OFF the equipment in the equipment itself.

Failure level 1 to 2 in ACC is recovered by CDMU.

When the CMDS (ACC) is in reconfiguration, a delay of Δt seconds (TBD) as to be waited before the beginning of ACC (CDMS) reconfiguration in order to avoid a loop phenomenon i.e. ACC and CDMS reconfiguration in loop.

FAILURE LEVEL	DETECTION PROCEDURE	FAILURE RECOVERY		
		GM MODE	AFS MODE	AFO MODE
1a Equipment failure	OBSW acquisition of unit Health Check status.	- Stop boost (when applicable). - Suspend MTL. - Switch over to the redundant unit using SGM configuration. - After time-out, switch to safe mode (SM1 or SM2).	- Stop boost (when applicable). - Suspend MTL. - Switch over to the redundant unit using SGM configuration. - After time-out, switch to safe mode (SM1 or SM2).	- Stop boost (when applicable). - Suspend MTL. - Switch over to the redundant equipment. - Resume MTL to the next step.
1b Communication I/F failure	Monitoring of Communication protocol and bus couplers.	- Stop boost (when applicable). - Suspend MTL. - Switch over to the redundant bus coupler or direct interface using SGM configuration. - After time-out, switch to safe mode (SM1 or SM2).	- Stop boost (when applicable). - Suspend MTL. - Switch over to the redundant bus coupler or direct interface using SGM configuration. - After time-out, switch to safe mode (SM1 or SM2).	- Stop boost (when applicable). - Suspend MTL. - Switch over to the redundant bus coupler or direct interface k. - Resume MTL to the next step.
2 Main function failure	OBSW performance check.	- Stop boost (when applicable). - Suspend MTL. - Disconnect non essential loads. - Switch to safe mode (SM1 or SM2).	- Stop boost (when applicable). - Suspend MTL. - Disconnect non essential loads. - Switch to safe mode (SM1 or SM2).	- Stop boost (when applicable). - Suspend MTL. - Switch over to the redundant set of equipment units (from SGM conf.) related to the function. - Resume MTL to the next step.

TABLE 6.4.3-1 FDIR STRATEGY OVERVIEW

FAILURE LEVEL	DETECTION PROCEDURE	FAILURE RECOVERY		
		GM MODE	AFS MODE	AFO MODE
3a CDMU or ACC first failure occurrence.	Nominal processor module HW alarm or SW watch dog.	- Stop boost (when applicable). - Suspend MTL. - Disconnect non essential loads. - Switch over to the redundant processor module from SGM. - Switch to safe mode (SM1 or SM2).	- Stop boost (when applicable). - Disconnect non essential loads. - Suspend MTL. - Switch over to the redundant processor module from SGM. - Switch to safe mode (SM1 or SM2).	- Stop boost (when applicable). - Suspend MTL. - Switch over to the redundant processor module. - Load SGM (CDMU reps. ACC) context. - Attempt to re engage current operating mode. - Resume MTL to the next step.
3b CDMU or ACC second failure occurrence.	Nominal processor module HW alarm or SW watch dog.	N/A	N/A	- Stop boost (when applicable). - Disconnect non essential loads. - Suspend MTL. - Redundant PM cold restart from PROM. - Switch to SM2.

TABLE 6.4.3-2 FDIR STRATEGY OVERVIEW

| FAILURE LEVEL | DETECTION PROCEDURE | FAILURE RECOVERY | | |
		GM MODE	AFS MODE	AFO MODE
4	global satellite malfunction.	System alarm.	- Stop boost (when applicable). - Disconnect non essential loads. - Suspend MTL. - Switch over to the redundant processor module from PROM. - Switch to SM2	- Stop boost (when applicable). - Disconnect non essential loads. - Suspend MTL. - Switch over to the redundant processor module from PROM. - Switch to SM2	- Stop boost (when applicable). - Disconnect non essential loads. - Suspend MTL. - Switch over to the redundant processor module from PROM. - Switch to SM2.

TABLE 6.4.3-3 FDIR STRATEGY OVERVIEW
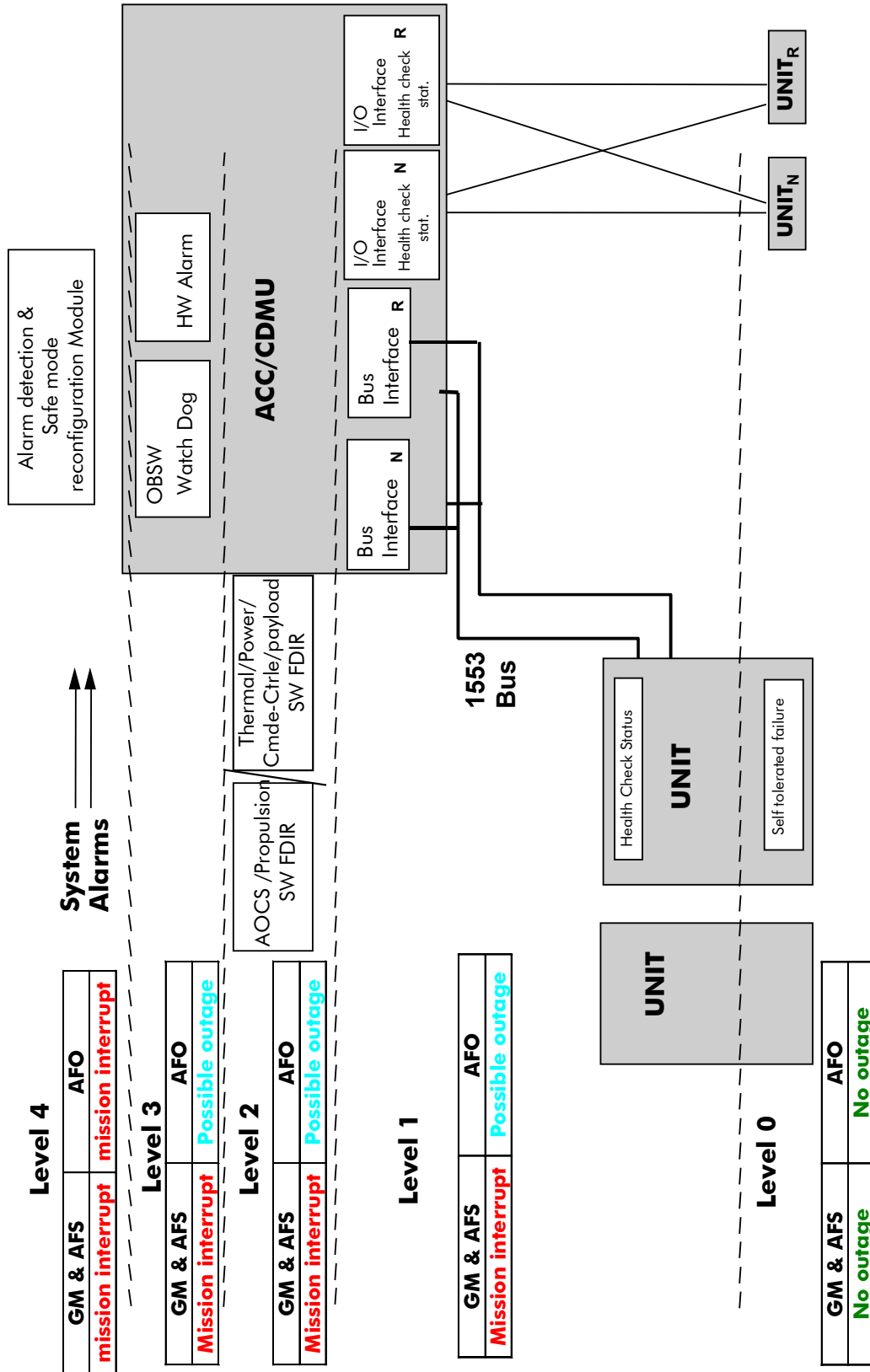
FIGURE 6.4.3-1 FDIR ARCHITECTURE & MISSION IMPACT

6.5.   EXTERNAL INTERFACES

6.5.1.   Ground segment interfaces

6.5.1.1.   General

The interfaces with the ground segment are specified via in two documents:

- Space to Ground ICD (AD03.2) which defines the telecommunication interface between spacecraft and ground

- Operational Interface Requirement Document (AD03.1) which defines the functional requirements for spacecraft operations.

During scientific observation, Herschel and Planck share the same Prime ground station: Perth 35 m. The main features of the interface with the ground are:

- daily ground contact of 3 hours for each spacecraft. During this ground contact the spacecraft shall as a minimum dump 24 hours of stored telemetry, and receive upload of the mission timeline. In fact, the memory is sized to store 48 hours of scientific data : to be able to download 2 days data, some margin shall be available in the daily time communication period in order to be able to recover from the loss of one telecommunication pass

- during Initial Orbit Phase and transfer, alternative ground stations are planned to be used. These are 15 m ground stations with characteristics similar to the Kourou one. In case of emergency, such ground stations are planned to be used in order to increase the daily coverage. Daily contact is however limited to 6 hours in case of emergency.

Herschel and Planck ground interface is illustrated in Figure 6.5.1-1.
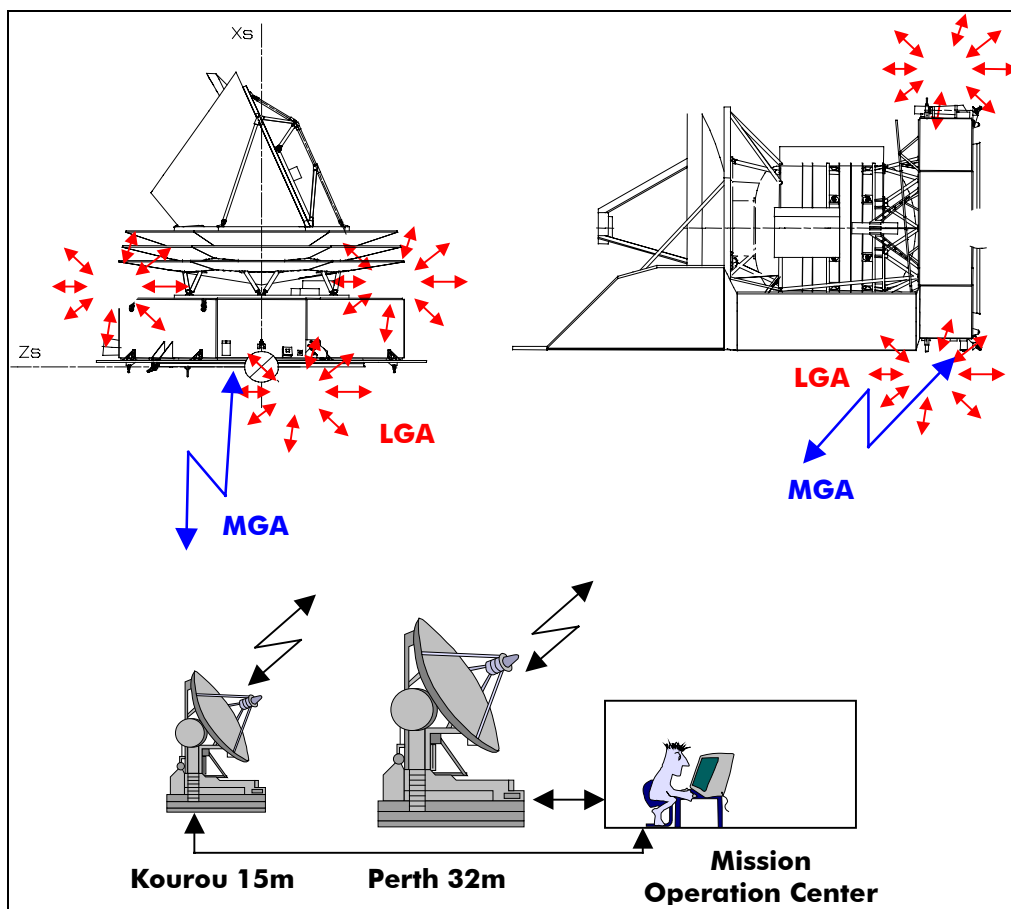
FIGURE 6.5.1-1 SPACECRAFT GROUND INTERFACE

6.5.1.2.   Downlink

The downlink communication between the spacecraft and Earth is performed in X-Band.

It is based on-board on:

- 2 LGAs for Herschel and 3 LGAs for Planck for near Earth operations and in case of emergency thanks to their quasi omnidirectional transmit capability

- 1 MGA for both spacecraft in nominal operational mode.

- It makes use of the following ground station:

- the Kourou 15 m station during post Launch activities and in emergency cases

- the Perth 32 m station during normal operation.

As far as the downlink telemetry is concerned, one single set of data rates is used common to both satellites :

low rate : 500 bps on LGAs

medium rate : 107 kbps on MGA with Kourou

high rate : 1.5 Mbps on MGA with Perth.

The downlink modulation scheme is :

- NRZ-L/BPSK/PM for low rates

- SP-L/PM for medium rate and

- NRZ-L/SRRC - OQPSK/PM or NRZ-L/GMSK/PM for high rates.

The telemetry data stream is Reed Solomon and Convolutional encoded (concatenated code) which permits to achieve a minimum E_b/N_0 of 2.8 dB for a frame loss probability of 10^{-5}. The frame structure complies with the Packet Telemetry Standard.

6.5.1.3.   Uplink

The up link communication between Earth and the spacecraft is performed in X-Band, and makes use of the Kourou and/or Perth ground stations.

It is based on-board on:

- 2 LGAs for Herschel and 3 LGAs for Planck. One single LGA is used in nominal for each spacecraft, the other one(s) implementing the required quasi omni directional coverage in TC.

- The MGA as a back up to the LGA's

- One single set of uplink data rate is specified. Two nominal rates are then considered:

- 125 bps on from Kourou, on LGA

4k bps on LGA and MGA with Perth.

The TTC design is compliant with the ranging signal used by the ESA Ground station and the TC frame structure is compliant with the ESA packet TC standard.

The uplink modulation scheme is a NRZ-L/PSK/PM onto a sine subcarrier, and no special encoding is applied.

6.5.1.4.   Link configurations

Regarding the switching function, the proposed RFDN design allows connecting the receivers and transmitters to the nominal LGA, or the redundant one in case of attitude loss, or/and to the MGA for high bit rate transmissions.

For the MGA, this is also valid for the uplink.

6.5.1.5.   Operations

6.5.1.5.1.   Operational interface

The main interface with operations is represented by the packet telemetry/ telecommand protocol, enriched by the specification of eighteen Services which mainly define the types of packets, and the way to elaborate and process them.

6.5.1.5.1.1. General spacecraft control

The following general features are implemented within the on-board telemetry/ telecommand system of Herschel and Planck.

Telecommand

–   All telecommands are received from ground as TC packets, and similarly, commands generated on-board and addressed to intelligent users (namely payload instruments and ACMS Computer) are forwarded as TC packets. Each addressee of the telecommands is identified by a unique APID, while each TC packet type is itself identified by a unique SID. The total number of SID depends on the operational interfaces with the reception, but is kept as low as possible.

–   All telecommand received on Board are stored in Mass Memory for possible checking purpose.

– Execution of Critical Commands (no hazardous commands is identified yet on Herschel/Planck) is implemented via 2 "arm" and "fire" commands. This shall basically be the case, for Herschel, of the commanding of the NCA to open the cryo cover after Launch. for the Execution of vital functions, which may cause mission degradation if not executed, is implemented via 2 differently routed, down to the source, main and redundant telecommands. For instance, LCLs switching is performed via the commanding of the nominal (resp. redundant) CDMU, then the transmission via the nominal (resp. redundant) bus interface to the nominal (resp. redundant) PCDU branch to switch the nominal and/or redundant limiter. These features rely on the electrical architecture design.

– A telecommand packet contains only one telecommand function.

– All on-board devices, i.e. units can be commanded individually from ground, except TC decoder modules, RF receivers and survival heaters which are permanently supplied via FCLs.

– An adequate buffering of transmitted commands is foreseen on-board to allow a verification, validation and unimpeded execution of the received TC in parallel to the reception of TCs with the maximum specified rate (4 kbps). Commands not compliant with the packet standard are rejected at decoder level then at software level.

– Besides general SW memory load commands, special commands are foreseen to change dedicated parameters and on-board data.

Telemetry

– Symmetrically, telemetry is collected from the intelligent units as TM packets, identified by the same APID than the one used for telecommanding.

– Data acquired as discrete signals or non packetised formats, from a given unit are packetised by the CDMS SW and stamped with the APID corresponding to that given unit. Nominally status information is provided from direct measurements instead of from secondary effects.

– TM packets are organised in:

  • housekeeping packets

  • science packets

  • TC report packets

- Event report packets

- Memory dump packets

- context packets (TBC).

Instrument science packets acquisition is performed according to a Data Bus Profile which allocates an agreed bus bandwidth and further a storage capability to each instrument depending upon its mode of operation and corresponding data rate.

– A predefined bandwidth is reserved for the event packets collection, ie the packets generated asynchronously to signal an event. All data which is collected on board is stored in Solid State Mass Memory.

– The housekeeping telemetry is generated such that the S/C status, performance, and the current on-board activities are recorded and stored, then transmitted to ground.

This means that TM is prepared such that:

- the S/C status can be determined directly without need to request further information by TC

- the status of the command executed on-board is provided

- all parameters used as inputs to OBCP's, Functions, and all changeable parameters are available in TM

- units level raw housekeeping data is accessible to ground

- critical TM data is provided under redundant paths, independently routed.

Autonomy and fault protection

The Autonomous phase is specified as 48 hours without ground contact and without mission interruption, and 7 days in a safe mode, without ground intervention.

– Sufficient memory is allocated to the Mission Timeline and control procedures buffers to cope with the 48 hours mission autonomy. Also, the size of the Mass Memory is adjusted to cope, with margins and in End of Life, with the storage requirements induced by the autonomy duration specification.

– As a design principle, the management of anomalies, as detailed in Section 6.4.3 (FDIR), is hierarchical, such that the anomalies are sought at the lowest possible level and does not lead to higher level recovery until low level reconfigurations have been tried. This ensures the best satisfaction of the 48 mission autonomy requirement.

– The survival Mode is entered:

- manually upon ground telecommand

- autonomously (default) when all possible lower level recoveries to an anomaly have been exhausted, in line with Satellites Modes description in §6.4.2 and FDIR strategy in § 6.4.3.

When in survival Mode, the spacecraft:

- maintains essential on-board functions, including fault protection mechanisms

- reports via event packets the anomaly conditions and the recovery actions

- generate a minimum set of TM packets to allow immediate identification of the survival mode, and makes available, stored in Mass Memory and in Safeguard Memory, the spacecraft detailed history before and after the anomaly occurrence.

– The fault protection system is detaily addressed in Section 6.4.3; it is designed such that:

- the fault protection processes can be individually enabled/disabled

- all the parameters used in the fault protection processes can be read and updated

- the spacecraft configuration is continuously saved in protected memory, nominally the Safeguard Memory (either the CDMS SGM or the ACMS SGM) to permit a safe automatic transition.

Packet services

As mentioned previously, eighteen services define the main tools made available for the satellites operation, based on the TM/TC packet protocol. These can be broken down into 3 categories: commanding, monitoring, management.

Services related to the **commanding** of the satellites:

– **Service 2** device commanding, defines the capability to directly command the hardware devices via the TC decoder and using specific APID. Service 2 is fully applied to CDMS. However, as far as Attitude Control Computer is concerned, the TC decoder being obviously not present, it is anticipated this service to be handled at the level of the 1553 protocol, via the use of Command Words.

– **Service 19** is a complement to service 5 addressed later. It implements the capability to react to an "exception event" by issuing a telecommand depending on, the event identifier. The service is table driven via the maintenance of an "action list".

– **Service 20** information distribution, establishes the principles of the distribution to all intelligent users connected on the spacecraft data bus (namely instruments and Attitude Control Computer), of a broadcast telecommand containing information of interest to the users.

– Services related to the **monitoring** of the satellites:

– **Service 1** Telecommand Verification, defines dedicated TM packets indicating within TBD seconds from the TC reception, the status of reception, execution and completion of the TC. The application source of the TC, (ground, mission timeline, OBCP,...) is clearly identified. It shall be pointed out that clustered acceptance and verification packets are foreseen to reduce the total number of TM packets related to TC verification. A realistic alternative is to implement this service using the service 5, event packets.

– **Service 3** deals with the expression of the spacecraft observability. It is implemented via 2 ways, and an appropriate downlink bandwidth is reserved accordingly:

  • synthetic pre defined TM to characterize the status of the spacecraft and indicate whether anomalous conditions have occurred. This TM is permanently generated and stored for transmission

  • special diagnostic TM packets to make possible accurate failure analysis or analysis of an event. This trouble shooting TM is defined upon need and downlinked upon request.

This implementation principle is applicable to CDMS SW and to ACMS SW. It may also be extended to payload instruments.

– **Service 5** supported by the Service 19, defines one of the principles of operation of the spacecraft. It is based on the events reporting, which consists in pre defined TM packets triggered upon the occurrence of on board events classified into:

- normal events, which refer to all important on-board activities, autonomous actions

- exception events, which refer to anomalies to be handled by the board. This category is the one involved in the service 19

- Alarms events, which refer to anomalies to be managed by the ground.

Each type of event packet is uniquely identified via its own APID, which permits its immediate detection on-ground thus making possible a reaction in less than 30 mn, as specified.

The downlink bandwidth allocated to events reporting is reduced by summarising the events, and mainly reporting anomalies in nominal on their first occurrence only. As mentioned before, it may be proposed to use this service to report the Telecommand Verification packets.

– **Service 16** a TM packet is defined to report the status and performance of the on board traffic, at packet level. Some statistics on the packet bus management are made available to ground. The on-board implementation of the packet management is table driven, which permits by simple telecommands to disable the routing of TC packets.

– **Service 17** in addition to the possible self checks, the capability for the ground to ask a synthetic "are you alive ?" question to all intelligent users (TBC for payload, but desirable) is defined. "Yes I'm alive" TM packet type is expected in response.

– **Service 21** the science data, as mentioned before, is table (IPT) driven; this table can be changed such that packet collection from a given instrument is enabled/disabled.

Services related to the **management** of the spacecraft:

Service 6 it relates specifically to the memory management

As a major principle, any SW, e.g. any memory area, except PROMs, can be loaded/patched from ground using a dedicated TC. Three types of memory areas are distinguished: code, fixed data variables and parameters.

Any memory load TC packet is self consistent and does not depend on previous packets. This TC is:

- capable to load contiguous memory area

- protected by CRC such that it can be checked on-board for consistency, and rejected before execution.

Symmetrically, any memory area (including non volatile and mass memories) can be dumped. Contrarily to the Memory Load TC, there is one single Dump TC for a given Dump, even though the area to dump is distributed over a number of TM source packets.

In addition, a check of a defined memory area can be commanded, consisting in the computation and report to ground of the checksum of this area.

Service 8 is related to the control of spacecraft Functions, possibly mixing hardware and software. Functions provide essential spacecraft functionality (e.g. Thermal Control is a Function). It is a major operation feature giving the possibility to act at Function level via dedicated TC packets. Functions can be started/stopped and received parameters.

Service 9 deals with the Time management: The spacecraft time reference is maintained within the CDMU and can be distributed to intelligent users, ACC and instruments) to have a common datation basis (e.g. to make ACMS sensors acquisition synchronised with payload datation). The synchronisation protocol is detailed in the Herschel/Planck Packet Structure ICD.

Specific TM permits to verify the proper units synchronisation.

Service 11 addresses the scheduling of the planned operations of the spacecraft. These are based on the Mission TimeLine, which is a facility to control and execute at pre defined times commands which have been loaded in advance from ground during visibility periods. Any telecommand, but those explicitly excluded, can be used in the MTL. The MTL runs only at CDMU level and the service is always active at start-up. It can however be suspended/resumed by TC.

Without stopping the MTL, it is possible to prevent the execution of a specified subset of commands using their APID, and to insert, append and delete commands to/from it. The deletion is performed using different filters:

- all commands

- from a specified time onwards

- between specified times

- individual commands

- commands within a dedicated APID.

For commands with the same execution time, the order of the uplink is applied.

The MTL granularity is 1 s (TBC) and as mentioned, the MTL buffer is sized to comply with 48 hours autonomous operations.

Service 12 addresses a major operation concept, the On-Board Monitoring Function. It is implemented solely in CDMU, on which it is active by default, and basically consists in monitoring defined parameters against limits and in initiating an event in case of out of limit detection.

All S/C housekeeping and non science telemetry packets can be used for monitoring. The parameters to be monitored are handled via a monitoring list including the following specifications per parameters:

- parameter identification by a unique mnemonic

- upper and lower limits

- enable/disable flag defining the status of the monitoring

- the monitoring time interval

- the number of allowed out of limits before triggering an event

- the identifier of the event triggered by the monitoring.

It is possible to modify only a subset of the monitoring list parameters, and the monitoring information.

Telemetry report packets containing the value which is out of limit, the limit itself and possibly the event triggered are generated.

On telecommand request, the monitoring list can be reported to ground.

Service 14 provides the facility, using dedicated TCs, to enable/disable the generation and/or transmission to ground and/or another user of selected TM packets. The selection is at the level of the APID and can include the following types:

- all packets

- specified types/subtypes

- specified HK packets

- specified diagnostic packets

- specified report packets.

Furthermore, each Application Process can provides a status information defining which packets are selected for transmission to ground and/or another Service, and the generation frequency.

Service 15 is related to the management of the storage unit. This capability is centralised at CDMU level only. All TM packets are stored on-board, regardless of the status of transmission to ground.

The storage is organised in virtual stores containing given packets identified by their APID and type. Storage is cyclic within a store: the oldest data is overwritten when the store is full.

The storage capability, i.e. the size of the SSMM is defined to cope with the storage of all packets generated on board over 48 hours + margin.

A selected privileged retrieval of stored packets is possible.

Dedicated HK TM provides status of the storage:

- the number of stored packets

- the size in words of the occupied storage

- the allocation for the different available subsets of telemetry which can be dumped independently.

The ground is allowed to enable/disable the storage of selected packets.

Finally, only the ground is authorised to clear the content of the Mass Memory (per APID, per packet store, type, ...).

Service 18 defines the management of the On-Board Control Procedures. OBCPs are Flight Control Procedures which execute on board. They are controlled via specific TC packets which:

- load OBCPs

- start OBCPs

- stop OBCPs

- suspend OBCPs

- resume OBCPs.

OBCPs are nominally initiated from the MTL and are able to access TM, issue telecommands and event packets, execute simple mathematical expressions and logical functions Several OBCPs can run concurrently without interference. They are developed in a simple language, the Spacecraft Control Language, which is interpreted on-board.

It is possible to communicate with an OBCP, ie. pass parameters or modify OBCPs variables).

Nominally, CDMS SW and ACMS SW could be users for spacecraft OBCP's (TBC for instruments). However, to simplify the management of the overall operations of the satellites, it is currently considered to restrict the use of OBCPs to the CDMS only.

Service 22 defines the implementation for all intelligent users of a service to store and retrieve the contexts, on request of these users.

6.5.1.5.2.   Applicability to ACMS

As it has been demonstrated throughout the previous chapter, the proposed operation concepts fully comply, at CDMS level, with the operational interface requirements.
The applicability of these requirements to the other users on-board, and especially to the ACMS Control Computer can however be disputed. As a matter of fact, referring to the architecture description in § 5.2.2., ACC does not interface with ground, but with the CDMU via a 1553 bus I/F. Also, the ACC may not be connected to intelligent users, i.e. users featuring a TM/TC packet interface. It is nevertheless believed to be of the highest interest to have available within the ACC, a limited set of Services in order to standardize some of the operation concepts.

As a consequence, the basic services related to commanding are extended to ACC and ACC SW, but applied to the CDMU-ACC link:

– device commanding to implement the ACMS units direct commanding

– event/action, as support to the event/reporting service, to initiate a telecommand as answer to an exception event.

Some services related to monitoring are also applied to ACC SW:

– telecommand verification, to report to CDMU, for storage or transmission, the status of TC reception and execution

– periodic reporting, as an extension of the service to ACMS to define synthetic TM and trouble shooting TM to report the health of ACMS

– event reporting, to trigger pre defined TM in case of an ACMS related event occurrence. Events are classified into normal, exceptions and alarms, as per CDMU.

Finally, a few management services are extended to ACC and ACC SW:

– the memory management service, to take profit of the commonality of processor modules and memory arrangement between CDMU and ACC, and support the ACC memory load, memory check, and memory Dump

Functions management service give to the ground the capability to control the execution of the Functions related to ACC SW.

It shall be pointed out that the Timing Management, On-Board Monitoring Function, Mission TimeLine services are centralised within the CDMU only, to simplify the ground management.
In the same attitude, On-Board Control Procedure service is not made available at ACMS level to concentrate the high level management features at CDMS level.

6.5.1.5.3.   On-Board Control Procedures

Thanks to their simple interface to operations (via simple spacecraft development language), and their flexibility, the OBCPs are a principle mode of operation of the satellites.

However, OBCPs as implemented via an On Board Interpretation of uplinked procedures have been recognised to have major drawbacks:

their execution time on-board, when compared to processes in native language (nominally in ADA), is very long. Even though Herschel/Planck CDMU is based on a powerful ERC32 processor, the general statement remain true in proportion

if considered as a principle of operation a significant part of the Application Software would be developed using OBCPs and the MTL would consist in calls to OBCP's. This means that from the early phase of the SW development, some OBCP's will be part of the software, some other ones being developed in the course of the satellites testing phase. This approach, indubitably questions the validity of the software acceptance, pronounced at a given time, since it integrates the fact that later OBCPs development does not significantly impact the software behaviour and does not impose a full revalidation. Although strict rules can be applied to OBCPs development to at least partly overcome this problem, it remains an issue of concern.

In addition, Herschel and Planck missions are characterised by regular, routine operations, contrarily to interplanetary missions which must keep a large flexibility to mission adaptation. There are consequently high probabilities that the major part of the control procedures and flight applications can be specified in time to be introduced in native software, and then fully validated via the whole software PA process.

It is therefore proposed to implement OBCP's via a simpler, and believed more robust, scheme :

- On ground, Development of an OBCP using a very basic Spacecraft Control Language with very strict rules,

- Conversion of this OBCP into high level language (C or ADA), as an independent piece of code

- Compilation in standalone and link of the generated code

- Validation of the new code in standalone, and of the OBCP, on ground

- uplink of the "OBCP" to the spacecraft

Storage of the "OBCP" as a new task : as such it can then be started, stopped, suspended, resumed, terminated upon ground command, timeline order or as a response to an event (if planned).

6.5.2.   Launcher interfaces

Both Satellites will be launched on the same ARIANE 5 in dual launch configuration. PLANCK Satellite will be in lower position and HERSCHEL satellite in upper position on top of the SYLDA 5 as illustrated by Figure 6.5.2-1.

Both HERSCHEL and PLANCK Satellites have a reference diameter of 2624 mm at the interface Satellite/launch vehicle interface plane and will use Standard 2624 adapters and separation systems.

Details concerning Launcher interfaces are provided by document RD01.5, Application to Use ARIANE (DUA).
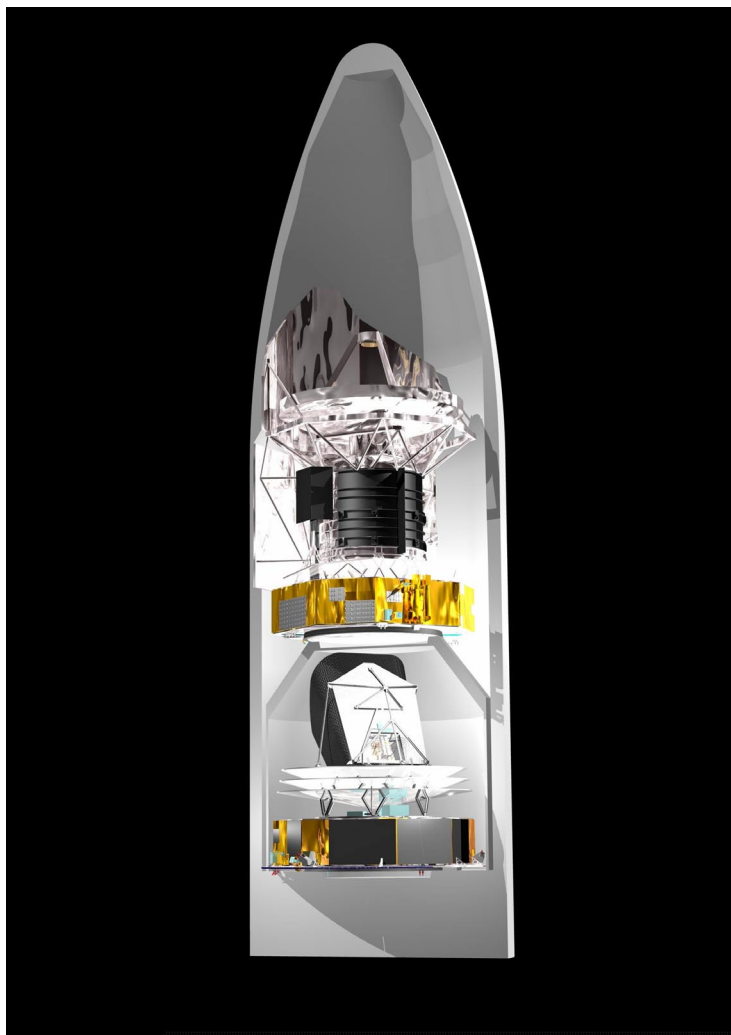
FIGURE 6.5.2-1 HERSCHEL & PLANCK LAUNCH CONFIGURATION

6.5.3.   GSE interfaces

The GSE interfaces are considered in the Satellites, Modules, Subsystem and unit design. For both HERSCHEL and PLANCK, three mains and common interfaces are considered.

Specific interfaces for HERSCHEL cryogenic operations and for PLANCK instruments integration are considered in the relevant PLM design.

Mechanical interfaces at Satellite level

The mechanical interfaces between the Satellites and the MGSE are defined by drawings to be issued. This applies mainly to:

- launcher interface

- hoisting and handling points.

Electrical interfaces at Satellite level

The electrical interfaces between the Satellites and the EGSE are defined by document to be issued. This applies mainly to:

- umbilical connectors (refer to DUA)

- flight connectors

- test and monitoring connectors

- safety plugs.

Filling, draining and pressurisation interfaces

The interfaces between the propulsion system (part of the SVM) and the TGSE is based on fill & drain valves located at the outer edges of the Satellite and accessible through the external MLI.

Specific GSE interfaces

For HERSCHEL, specific interfaces for cryogenic operations using the CVSE are defined by H-PLM Contractor.

For PLANCK, specific interfaces for installation of the instruments in the PLM are defined by drawings to be issued.

6.6. CLEANLINESS

At all stages of their on-ground and in-orbit live, elements of the spacecraft and instruments are submitted to particular and molecular contamination. Moreover, this contamination has a direct impact on optical/RF performances, particularly in terms of transmission loss and stray light enhancement via diffusion, and emissivity enhancement via self-emission.

Thus, dedicated working groups were led by ESA, including scientific and industrial representatives, in order to build acceptable particulate and molecular specifications and budgets. Main drivers were EOL performances and cost.

For each HERSCHEL and Planck programmes, the following performances drove End of Live cleanliness levels.

6.6.1.   Particulate contamination

HERSCHEL/Planck common features

– At HERSCHEL and Planck wavelengths, a level of 5000 ppm on telescopes has no significant impact on the image quality (PSF degradation or antenna gain losses).

On HERSCHEL

– The driving parameter on HERSCHEL is transmission losses for telescope, instruments, and HIFI LOU windows.

– From a transmission point of view, 5000 ppm end of live on the telescope and 1550 ppm end of live for the instruments (inside the cryostat) are enough to be compliant with EOL transmission goals. 5000 ppm is also required for HIFI LOU window, although the actual level on this element should be much lower thank to a relevant protection.

– 5000 ppm end of live on the telescope is enough to fulfill the straylight requirements of HERSCHEL. The corresponding BRDF will be taken into account in straylight analysis.

- From a thermal point of view, the main driver is the increase of emissivity of thermal shields. A level of 10000 ppm (emissivity increase of 0.01 for external reflective surface) is acceptable. The impact is estimated to be less than 1.5 K on the primary reflector and less than 0.5 K on the Cryostat Vacuum Vessel temperature. With such a contamination level, the thermal impact of specularity losses are negligible.

On Planck

- The driving parameter for Planck is the straylight induced by reflector scattering.

- From a straylight point of view, 5000 ppm on telescope and instruments is the upper acceptable limit for the higher frequency channels of Planck.

However, we have noticed that the radiated background due to particulate contamination of reflectors is the most limiting factor for HFI performances. It is why the reduction of particulate contamination should be a permanent goal during Planck development programme.

From a thermal point of view, the main driver is the increase of emissivity of thermal shields (V. grooves and external layers of MLI) A level of 10000 ppm (emissivity increase of 0.01 for external reflective surfaces) is acceptable. The impact is estimated to be less than 0.6 K (TBC) on the telescope and FPU environment temperature. With such a contamination level, the thermal impact of specularity loss is negligible.

6.6.2.   Molecular contamination

HERSCHEL/Planck common features

At HERSCHEL and Planck wavelength, optical/RF performances are not very sensitive to molecular contamination. A level of 4.10^{-6} g/cm^2 end of live is acceptable for both telescopes.

The main impact of molecular contamination will be an increase of the surface emissivity, inducing:

- from an optical point of view, transmission losses and an increase of the radiated background

- from a thermal point of view, an increase of thermal coupling (loss of thermal shield efficiency).

On HERSCHEL

From a thermal point of view, water ice coming from spacecraft outgassing could be trapped by cold thermal shields and mainly by primary mirror MLI. Not to affect the telescope temperature by more than 1 K, the total amount of contaminant on the cold thermal shields shall not exceed $6.10^{-6} g/cm^2$ (TBC).

On Planck

The most critical effect of the in-flight molecular contamination is the increase of PLM temperature due to V.groove contamination (water and ammonia ice). Not to affect the telescope and FPU environment by more than 2 K, the V. grooves shall not be contaminated by more than $3.10^{-5} g/cm^2$ (TBC).

Taking the previous considerations into account, acceptable contamination levels at S/C delivery and at End Of Live, are the following:

TELESCOPES CONTAMINATION LEVELS		UNITS	HERSCHEL & PLANCK
At S/C delivery	Particulate	ppm	1500
	Molecular	g/cm^2	10^{-6}
End of life	Particulate	ppm	5000
	Molecular	g/cm^2	$4\ 10^{-6}$

PLANCK INSTRUMENTS CONTAMINATION LEVELS		UNITS	PLANCK INSTRUMENTS
At instrument delivery	Particulate	ppm	300
	Molecular	g/cm^2	10^{-6}
End of life	Particulate	ppm	5000
	Molecular	g/cm^2	$5\ 10^{-6}$

HERSCHEL INSTRUMENTS CONTAMINATION LEVELS		UNITS	HERSCHEL INSTRUMENTS
At instrument delivery	Particulate	ppm	300
	Molecular	g/cm^2	$4\ 10^{-6}$
End of life	Particulate	ppm	1550
	Molecular	g/cm^2	$6\ 10^{-6}$

Budgets are presented and justified in § 7.1.7.

6.7.   ALIGNMENT

6.7.1.   Planck Alignment

6.7.1.1.   Alignment justification

The three elements that make up the optical payload are the primary reflector, the secondary reflector and the Focal Plane Unit (FPU). The reflectors must be well manufactured and correctly aligned with respect to each other, to the FPU, and to satellite spin axis to get:

– the angular resolution on the sky

– the ellipticity of the far field radiation pattern

– the line of sight with respect to the telescope axes (i.e the Absolute Pointing Error). The Line of Sight knowledge and stability are necessary for each detector to observe precisely the same location in the sky, seen many times during the sky survey

– the spill-over for each horn of the focal plane unit in order to minimize the straylight coming from sources external to the spacecraft in the far-field of the telescope.

6.7.1.2.   Requirements

6.7.1.2.1. Pointing Error- Line of Sight

The Absolute Pointing Error APE is the only pointing error directly applicable to the alignment plan: Requirements and goals are presented in the following table:

Angular ERROR	Requirement for LOS (arcmin)	Requirement around LOS (arcmin)	Goals for LOS (arcmin)	Goals around LOS (arcmin)
APE	37	37		25

LOS requirement comes from the classical scientific need of knowing in which direction each horn is looking.

Around LOS requirement is more specific: it is derived from the need for two horns aligned in the focal plane to look at the same direction during sky survey.

6.7.1.2.2.   Image quality - Wave front Error

Telescope performances are specified in terms of RF performance (gain), Image Quality performance (WFE) and ellipticity (see AD01.4). These performances are applicable to the telescope assembly.

The Image Quality requirement has been used to assess the required alignment performance and stability of the reflectors and the FPU since it is easier to manage with optical software.

WFE requirements defined in Planck telescope design specification (see AD01.4) for different frequency (to which are associated specific position of the focal surface) are applicable to alignment plan.

WFE degradation must not exceed 42 µm, 28 µm WFE degradation being the design goal.

Gain and ellipticity are covered by WFE specification, and thus do not drive alignment needs.

6.7.1.3.   Alignment philosophy

Alignment until telescope assembly level:

Until the PLM level, main alignment and stability needs of optical elements are driven by imaging quality concerns, and thus WFE. Thus, the following alignment sequence will be performed up to telescope assembly level.

The telescope is aligned to meet both the image quality and LOS requirements for the theoretical location of the FPA at cryogenic temperature.

For this alignment, the two reflectors are equipped with corner cubes and optical balls and an optical quality measurement device (Wave Front Sensor) is used. Moreover, a test FPU with optical references will be used to control the alignment at cryogenic temperature.

A coarse alignment based on theodolite measurement method using optical reference on the structure, the 2 reflectors and the FPU allows the adjustment of the primary mirror and a first adjustment of the secondary. This first alignment should be sufficient to meet the LOS requirement.

A fine adjustment of the secondary mirror is then performed by a wave front analysis method.

The thermo-elastic behaviour of the telescope structure must be taken into account when adjusting the telescope at ambient to implement the necessary focus offset which will give the correct focus location at cryogenic temperature.

The telescope optical and alignment performances are verified under mechanical and cryogenic environments, particularly the FPU stability at cryogenic temperature because this measurement cannot be performed during cryogenic test at PLM level (baffle around the telescope limiting the sighting possibilities).

Alignment from telescope assembly to PLM level

At PPLM and satellite level, alignment has no impact on WFE Error, and is thus driven by Absolute Pointing Error requirements.

There are two ways to fulfill LOS requirements:

- if LOS must be exactly aligned on it's theoretical direction (85 w.r.t. spin axis), then an adjustment of the satellite spin axis will be used. It uses an inertia measurement device, and the inertia axes are adjusted by adding balance masses. Another way can also be to align telescope assembly wrt cryo structure via shimming

- if the LOS need is not its absolute position wrt to satellite spin axis, but its deviation wrt to known (measured) position, then a spin axis adjustment will not be necessary for LOS.

Around LOS, a spin axis adjustment will certainly have to be done, in order to bring it perpendicular to horns line of scan. This alignment might also be performed via shimming between telescope assembly and cryo structure.

The current baseline is that, at satellite level, the spin axis is adjusted to match as best as possible its theoretical orientation (85°) w.r.t. actual LOS of Planck telescope. This concerns LOS and around LOS alignment. Thus:

- LOS positioning budgets until telescope assembly level are needed to assess the amplitude of spin axis adjustment

- data on spin axis adjustment accuracy, LOS stability budgets , and LOS knowledge budgets give final APE contribution, for both LOS and around LOS.

6.7.2.   Herschel alignment

Alignment of the HERSCHEL PLM is described in § 5.12. of the H-EPLM Design
Description. It describes alignment concept for:

– Focal Plane Units

– HIFI Local Oscilator (LOU)

– Herschel Telescope.

6.8. SAFETY

The HERSCHEL/PLANCK system will be developed with the overall objective to be free of conditions, both in design and operations, which could produce uncontrolled hazards for ground personnel and facilities. Several disciplines within ALCATEL organization including Product Assurance department are used to achieve this objective as described in detail in the Product Assurance plan.

For Subcontractor, safety requirements has been edited taking into account CSG safety regulation requirements and ARIANE 5 user's manual (see document Ref. 2.???).

The HERSCHEL/PLANCK design includes the following main safety impacted subsystems:

- hydrazine propulsion subsystem

- cryogenic subsystem

- electrical subsystem including avionics and Li-Ion batteries

- mechanical aspects: handling device, cryo-cover opening

- thermal aspects: use of heaters and heat pipes.

Safety discussion

Fracture Control Activities

The ESA PA PLAN requires that the structural design of satellite/items be based on the "safe life" principle.

The CSG safety regulations don't require Fracture Control and Fracture Mechanics Analysis for structures.

According to the CSG safety regulations, pressure vessels may require Fracture Mechanics Analysis depending on their Ultimate Safety Factor (USF) (not required if USF greater than 2).

Usually no Fracture Control Activities are performed for structures flying on non-manned launchers.

6.8.1.   Subsystem safety aspects

The precedence of telecommunication and scientific satellites and experiences gives to ALCATEL a solid safety experience with design and operations for all satellite dangerous aspects.

6.8.1.1.   Hydrazine propulsion subsystem

The three major hazards for hydrazine subsystem consist in:

- – toxic material: hydrazine

- – adiabatic detonation

- – pressure system.

Feared events are:

- – inadvertent hydrazine firing or leakage

- – explosion of hydrazine inside propulsion subsystem

- – explosion of pressure system.

Special control will take place for the adiabatic detonation problem inside propellant lines. The effects of this phenomenon is a catastrophic hazard category.

6.8.1.2.   Cryogenic subsystem

The explosion of the cryogenic vacuum vessel or accidental blast of Helium is a catastrophic hazard category. This may be due to:

- – incorrect structural strength for internal or external pressure

- – incorrect working of safety device

- – pressure generation inside cryogenic vacuum vessel.

The experience obtained with ISO gives us confidence for the processing of these points.

6.8.1.3.   Electrical Power subsystem

The main hazard points for Electrical Power System (EPS) are:

  –   Li-Ion batteries safety aspects: electrolyte leakage or firing, external short circuit, ...

  –   short circuit in EPS: selection of wire gauges and use of current limiters with regard to electrical power for each parts, this inside satellite and outside to EGSE and PO

  –   non protected lines short circuit: necessity of double insulation for wire between batteries and PCDU.

6.8.1.4.   Avionics

  –   Inhibits implementation against inadvertent thruster firing.

  –   Inhibits implementation against inadvertent cryogenic cover opening.

6.8.1.5.   Mechanical aspects:

Satellite handling, when tanks (Helium and Hydrazine) are filled, is a catastrophic hazardous aspect. Attention will be taken in place for handling as well for satellite as for MGSE handling device.

6.8.1.6.   Thermal aspects

The use of heaters and heat pipes is considered dangerous. Heaters aspects are taken into account with avionics and software studies. For heat pipes, ALCATEL had a long safety experience with design and operations.

6.8.2.   Instruments safety aspects

Experiment Safety Analysis

The safety analysis for each instrument will be performed by the instrument itself under ESA responsibility. ALCATEL will review these documents to analyse the ALCATEL personal hazard aspects. At minimum, the instruments have to comply with the CSG Safety Regulation Requirements.

System Safety Analysis

Concerning inclusion of Instrument Safety Analysis in the System Safety Analysis, ALCATEL intention is to introduce the Instrument Hazard Reports with others.

Instruments Subcontractors will have to support ESA in answering HERSCHEL/PLANCK related "CSG safety submissions sheets for Phases 1 & 2".

6.9.   RELIABILITY AND FAULT TOLERANCE

6.9.1.   General

This section describes the means which will be implemented in order to ensure the reliability of the satellites during their missions. These means will be applied to the extent necessary to satisfy the requirements of the project.

They are grouped in the following categories:

– Quality

- EEE parts procured with Hi-Rel quality levels (SCC-B for active parts, SCC-C for passive parts or Mil equivalent).

- Use of qualified processes for assembly of parts, boards... (e.g.: soldering, crimping performed according to specifications); use of qualified materials; respect of cleanliness conditions.

– Margins:

- Application of derating specification for EEE parts in order to assure stress margins (electrical, thermal).

- Application of specified margins for strength of structural elements.

- Application of specified margins on performance of mechanisms (e.g.: motorization margin of mechanisms).

- Existence of margins on performance of critical electronic circuits (Worst Case Analyses).

– Fault tolerant architecture

- Fault tolerance by implementation of redundancies, protections, and allowance of degraded performances (no Single Point Failure of EEE parts will be allowed for the vital functions).

- Implementation of cross couplings between redundant items.

  If single operator commands resulting in mission termination are identified, measures to reduce the risk will be implemented (arming, means for command verification before execution for errors having fast effect, telemetry for errors resulting in slow effect…).

– Tests

- Capability to test redundancies and protections as close as possible to launch (in particular when the satellite is integrated) gives the possibility to assure a reliability close to 1 at launch time.

– Reliability design rules, interface requirements in case of failure

- Reliability oriented design rules introduced in design and performance specifications as well as interface requirements in case of failure contribute to the construction of the satellites reliability from the early phases of the project. In particular, it contributes to avoid failure propagation to redundancies/protections and to other equipment.

6.9.2. Reliability features of the architecture

6.9.2.1. Structure (SVM or PLM)

Reliability of structural elements is assured by application of specified safety margins and by verifying their application through the environmental qualification and acceptance tests.

6.9.2.2. Thermal Control

a. Passive thermal control (SVM or PLM)

Items like MLI, paints, coatings, surface treatments, OSR are subject to known slow deterministic degradations for which design margins are provided. Besides, local defects have minor consequences.

b. Active thermal control (SVM)

The thermal regulation uses the following items:

heaters

thermal sensors

PCDU to control the electrical power applied to the heaters

CDMU which acquires the temperature for regulation via the thermal sensors, and performs the processing of the thermal regulation and its FDIR.

The PCDU includes two cold redundant sets of 40 lines each controlling the heaters. One set is divided into 8 branches of 5 lines, each branch being provided with one re armable electronic fuse (overcurrent protection of the power bus) and one safety switch (protection against permanent heating). Both sets are under control of the nominal and redundant bus couplers.

3 failure independent sets of 40 thermal sensors are implemented, 3 per heater set, in order to perform majority voting. Retained solution for their conditioning and acquisition is:

the 3 sets of 40 thermal sensors are conditioned in the CDMU shared I/O I/F in order that the DH CDMU can make majority voting. The conditioning circuits are in this case supplied by hot redundant supplies and arranged so that no single failure results in loss of more than one of the three groups of sensors. CDMU normal acquisition circuit requires in this case a 120 inputs capability. The health of the common link acquiring the temperature information (acquisition circuit) is verified by measurement of reference resistors put in the conditioning circuits in place of sensors (in case a voted temperature or the link between sensors and CDMU is declared as abnormal, the DH CDMU controls a switchover to the redundant set of 40 heaters).
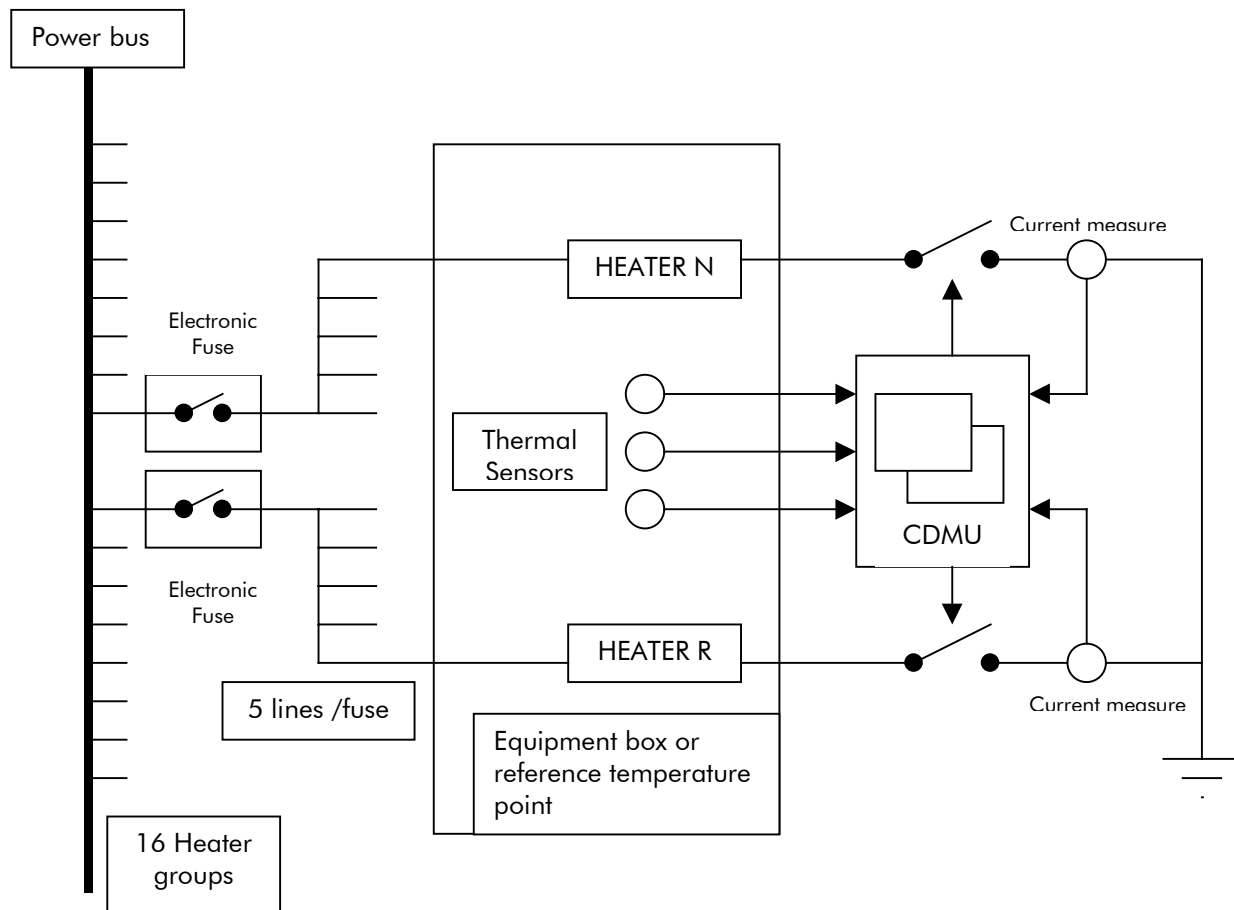
FIGURE 6.9.2-1 HEATER LINES

In addition, survival heaters (non redundant) controlling temperature by means of thermostats will be connected to the power bus through a Fold back Current Limiter (FCL). This permits to maintain an acceptable temperature at the level of the critical items (battery, tanks, ...) without any unit turned on (apart from the PCDU itself). Thermostat switching temperatures limits will be chosen lower than temperatures assured by nominal thermal regulation, so that no thermostat switching should occur on normal operation.
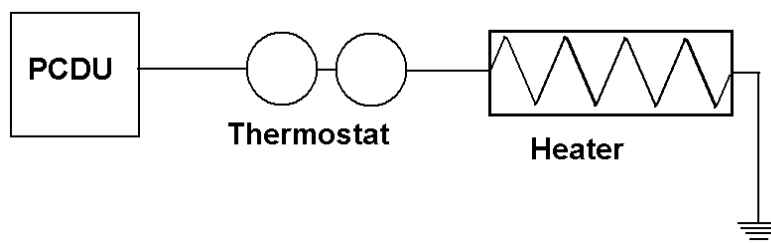
FIGURE 6.9.2-2 SURVIVAL HEATER LINE

6.9.2.3.   Solar Array

The Solar Array includes for both spacecraft an electrical network mounted on structural panels.

The reliability of the electrical network is obtained by the following means:

- a tolerated power loss corresponding to one section out of 30 to cover the power section failures within PCDU, (deterministic solar cells degradations being covered by other margins). The Solar Array, for both spacecraft, is therefore oversized by 3.3 %

- redundant wires and connectors will transmit the power from the electrical network to the PCDU (Redundant wires and connectors are requested as SA may be dismounted after environmental tests).

6.9.2.4.   Power S/S

The Power S/S is composed of one PCDU and one SPF free battery.

The Power S/S:

- provides a regulated 28 V on a main bus from the unregulated power delivered by the Solar Array or the battery

- assures the battery charge

- distributes the main bus power to the users

- controls the thermal control heaters.

- supply power to the non contaminating cover actuator for HERSCHEL.

The most general necessary fault tolerance characteristic for the main bus is that no single failure causes a permanent overvoltage or undervoltage (including due to users failures).

The Power S/S functional description is presented in Figure 6.9.2-3 it exhibits the following reliability features:

– Battery

  One battery is provided and is SPF free. It is composed of 144 cells (6 series of 24 parallels), this allows similarly to the Solar Array case, to loose one battery string with still enough power margin. Apart form the Launch phase, and possibly one single 75 mn long eclipse during transfer orbit, no eclipse is foreseen during nominal mission, so that battery is only necessary in case a failure results in an attitude loss and SA power decreases or in case of power demand during a short time (e.g. power peaks due to reaction wheels).

– PCDU

  Power bus 28 V regulation from Solar Array (SA) sections is performed by 30 shunt sections (one per SA section) controlled by one Main Error Amplifier (MEA).

  The sections are non redundant, therefore one shunt section is allowed to fail in open or short circuit. Short circuit is covered by a Solar Array power margin of 3.3 %, open circuit is covered by presence of a permanent load on the power bus. This load is guaranteed by the permanently supplied users and is consistent with the max current delivered by one section. The MEA (2/3 MEA hot redundant channels + reliable voter) is designed so that a single failure cannot cause an over or undervoltage on the power bus. MEA is hot redundant. It assures an autonomous fault tolerant power bus regulation (no possible control by TC).

  Battery charging is autonomously performed from 4 SA sections by specific charge circuits under MEA control. The current of the two sets of 4 SA sections, when not necessary for the power bus, is re-routed to charge the battery when necessary. Nominal charge control algorithm (voltage tapering) is implemented for the battery, via H/W in the PCDU. On top of that the CDMU monitors the battery voltage and temperature.

Main bus filter is composed of numerous in parallel capacitors, so that the open circuit of anyone has a negligible effect on the filtering performance. To prevent short circuit on the bus, either sets of two in series capacitors are used or self healing types.

Two parallel Battery Discharge Regulators (BDR) in series with the battery assure the 28 V on the power bus when the SA cannot deliver the necessary power. Risk to produce overvoltage on the power bus is covered by an overvoltage protection in the BDR. Besides, BDR modules are protected so that no single failure can short the battery or the power bus, nor directly connect the battery to the power bus. Also, each BDR is sized to handle the maximum discharge current, such that the design is tolerant to the loss of one BDR.

Auxiliary Supply (AS) for low power circuits is designed so that no single failure can result in over/undervoltage of supplied circuits, or in main bus short circuit (as well as no single failure in the low power circuit can short the auxiliary supply output). Circuits being permanently connected to both AS (hot redundant MEA, voters...) include protection so that a failure cannot result in overload of both AS. Circuits supplied by AS but cold redundant (TM/TC I/F, 1553 bus coupler) are for their normal part connected to AS normal side and their redundant part connected to AS redundant side.

Each bus coupler (A or B) has access to A and B 1553 buses.

– LCL Distribution Module

Main Bus power lines to users are provided with 64 LCL (Latching Current Limiters)/FCL (Foldback Current Limiter) which prevent excessive load on the main bus in case of users abnormal current consumption.

LCL are used for ON/OFF control of users.

Those users which turn off is critical:

from a power budget point of view or

for operational constraints reasons.

LCLs are provided with 2 level of independent switch-off.

FCL are used for permanently supplied users (RF Rx, CDMU TC decoder mass memory bank, Reconf Modules, …).

- Heater Distribution Module (HDM)

    HDM contains the redundant heating lines control and isolation items as described in section on active thermal control. Commands for isolating safety switches and thermal regulation switches are free of common cause failures resulting in permanent heating.

- Survival heater distribution
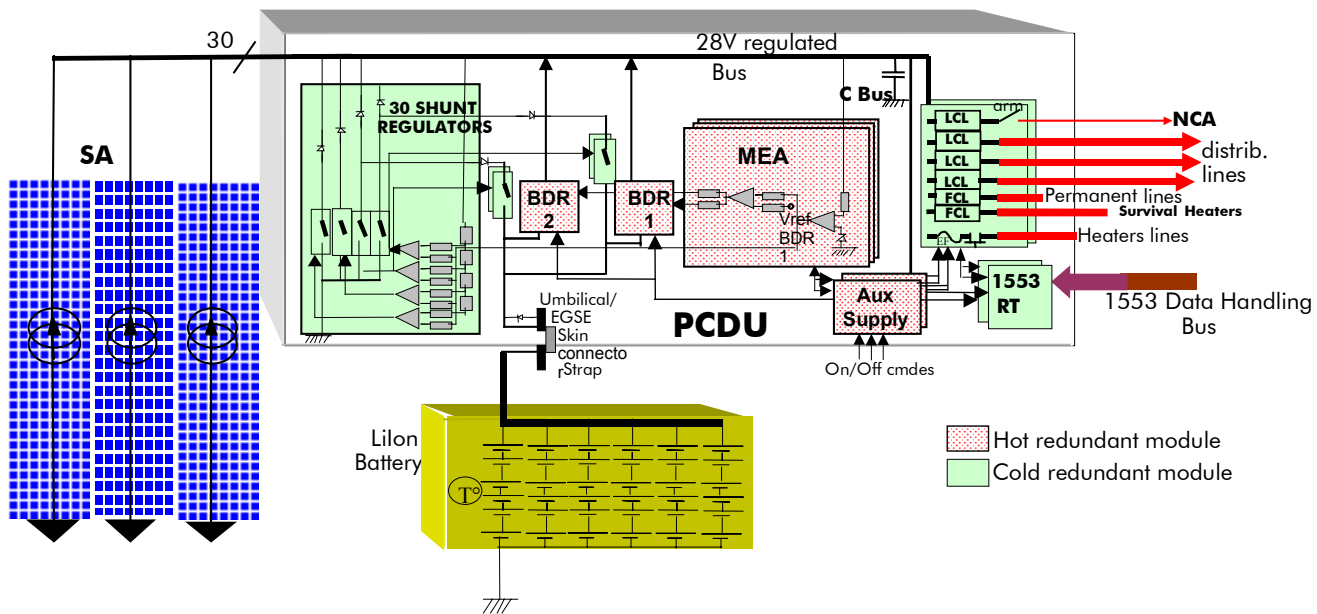
FIGURE 6.9.2-3 POWER SYSTEM FUNCTIONAL DESCRIPTION

6.9.2.5.   Data Handling (CDMS)

The CDMS is essentially composed of one internally redundant CDMU, identical for HERSCHEL and PLANCK. It is functionally described in Figure 6.9.2-4, and comprizes the following modules:

- 2 hot redundant RF Receiver interface modules

- 2 hot redundant TM/TC modules cross strapped with RF receiver I/F modules, each module including a Reconfiguration Module (RM) and a high accuracy timing module in hot redundancy

- 2 cold redundant Processor Modules (PM) cross strapped with TM/TC modules and Mass Memory Controllers, each PM having a 1553 I/F to A and B data handling buses

- 1 set of failure tolerant Mass Memory Banks

- 2 cold redundant Mass Memory Controllers both having access to Mass Memory Banks

- I/O I/F circuits providing cross strapped links between redundant PM and users redundant channels

- 2 hot redundant converters to supply the hot redundant circuits

- 2 cold redundant converters to supply the cold redundant circuits

- thermal regulation processing module.

It is to be noted that links between processors and users are done via I/O I/F circuits or 1553 bus. Any nominal or redundant chain of an user of the 1553 bus is provided with a bus coupler having access to normal and redundant 1553 physical buses.

Cross couplings are designed to be SPF free.
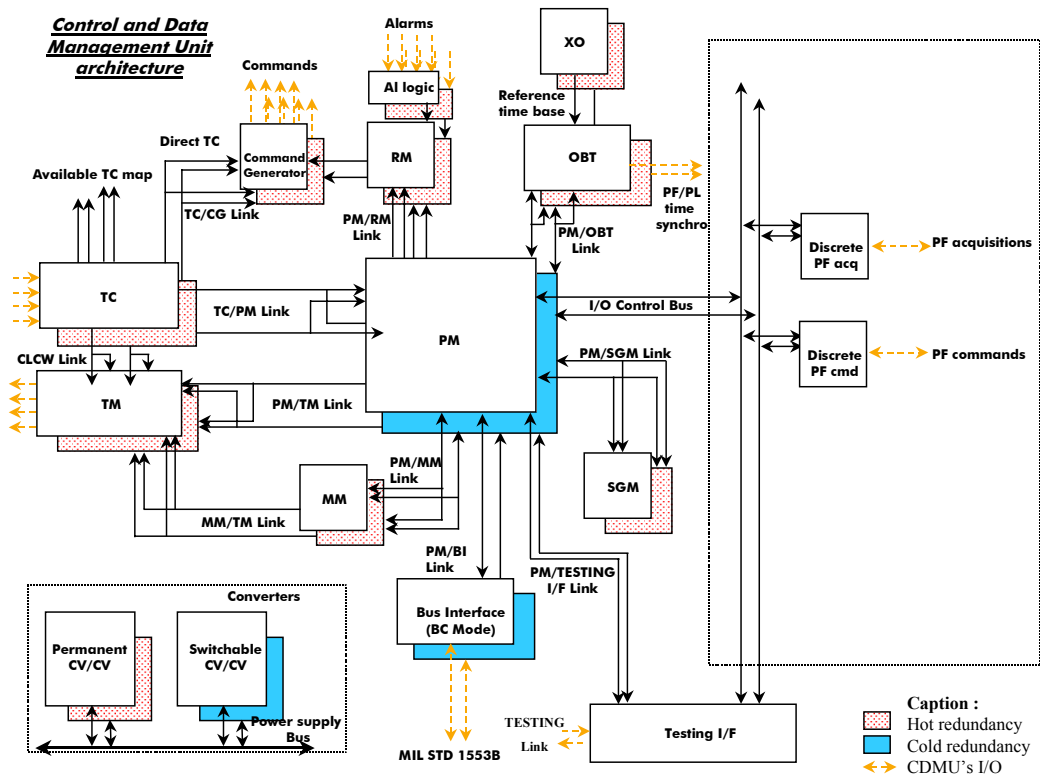
FIGURE 6.9.2-4   CDMU FUNCTIONAL BLOCK DIAGRAM

Concerning items of the spacecraft controlled through double in series switches or valves (protection against untimely operation) like heaters, thrusters, cryo valves, RF switches, the control switch and the safety switch will be controlled by failure independent command channels (so that no single failure can untimely activate or leave active both switches or both valves).

6.9.2.6. ACMS

The ACMS is composed of:

- 1 Attitude Control Computer (ACC) (same ACC is used for HERSCHEL and PLANCK) internally redundant. It is functionally described in Figure 6.9.2-5, and includes the following modules:

  - 2 cold redundant Processor Modules (PM). Each with RAM and PROM/EEPROM and 1553 I/F to A and B ACMS buses as bus controller and 1553 I/F to A and B data handling buses as remote terminal

  - 2 hot redundant Reconfiguration Modules (RM) having access to both PM

  - I/O I/F circuits assuring exchange of data between any processor and any user (in the particular case of the link with the 4 wheels, 4 failure independent physical links are provided)

  - 2 hot redundant converters to supply the hot redundant circuits

  - 2 cold redundant converters to supply the cold redundant circuits.

- Sensors for HERSCHEL

  - 2 Sun Acquisition Sensors (SAS): 2 SAS are necessary, each one is internally 2 for 1 hot redundant

  - 2 Quartz Rate Sensors (QRS) used in 2 for 1 hot redundancy

  - 1 GYRo blocks (GYR) of 4 skewed axes used in hot redundancy

  - 2 Star TRackers (STR) used in 2 for 1 cold redundancy

  - 2 Fine Sun Sensors (FSS) used in 2 for 1 cold redundancy.

- Actuators for HERSCHEL

  - 4 Reaction Wheel Systems (RWS) in 4 for 3 cold redundancy

  - 2 cold redundant branches of 6 10N thrusters each.

- Sensors for Planck

  - 1 Attitude Anomaly Detector (AAD): Sun presence alarm sensor

  - 3 Sun Acquisition Sensors (SAS): 3 SAS are necessary, each one being 2 for 1 internally redundant

  - 2 Quartz Rate Sensor (QRS) in 2 for 1 cold redundancy

  - 1 STar Mapper (STM) internally 2 for 1 cold redundant.

- Actuators for PLANCK

  - 2 cold redundant branches of 6 10N thrusters plus 2 1N thrusters each.

The functional connections of Planck (resp. Herschel) sensors and actuators to the ACC are shown in Figure 6.9.2-5 (Planck) and Figure 6.9.2-6 (HERSCHEL).
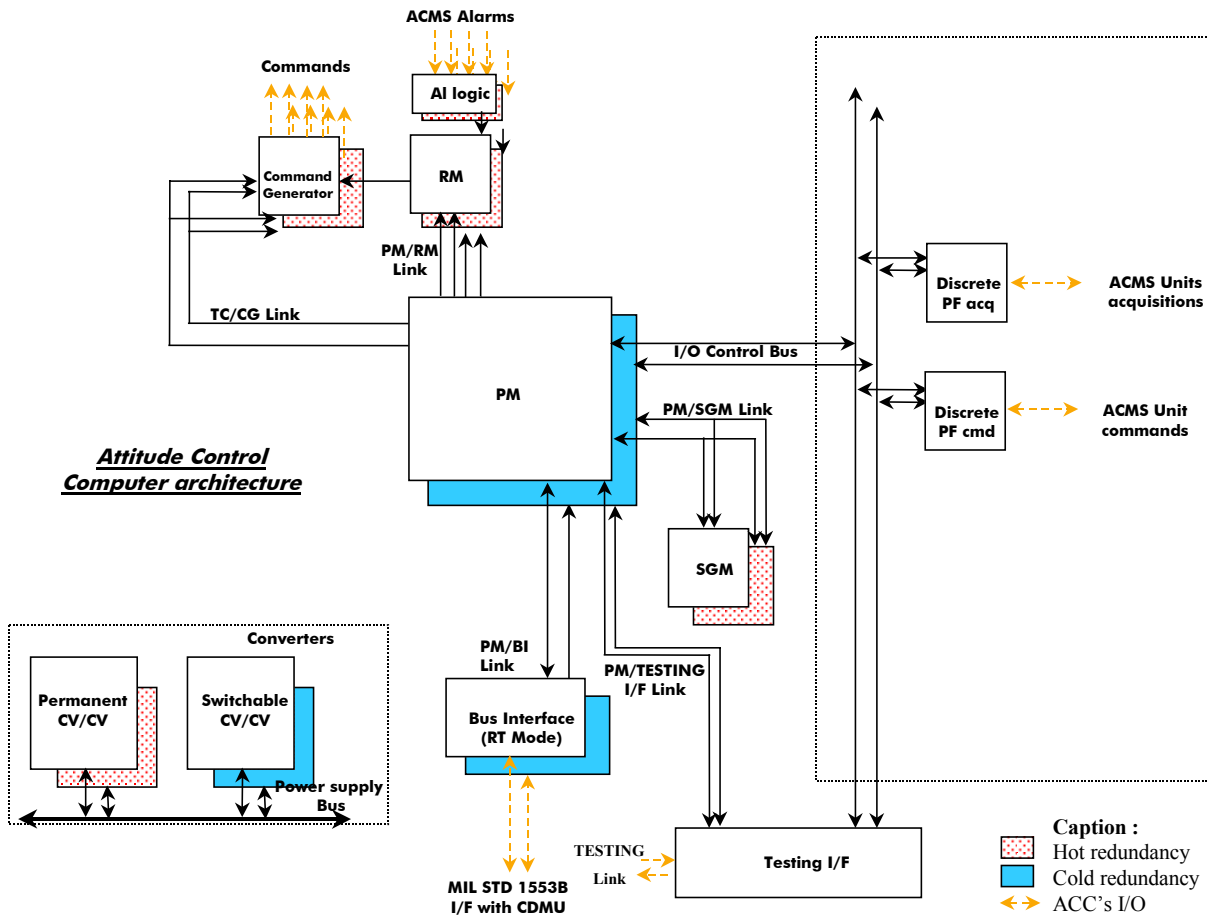
FIGURE 6.9.2-5   ACC FUNCTIONNAL BLOCK DIAGRAM

Any nominal or redundant chain of an user of the 1553 bus is provided with a bus coupler having access to normal and redundant 1553 physical buses.

Cross couplings internal to ACMS are designed to be SPF free.
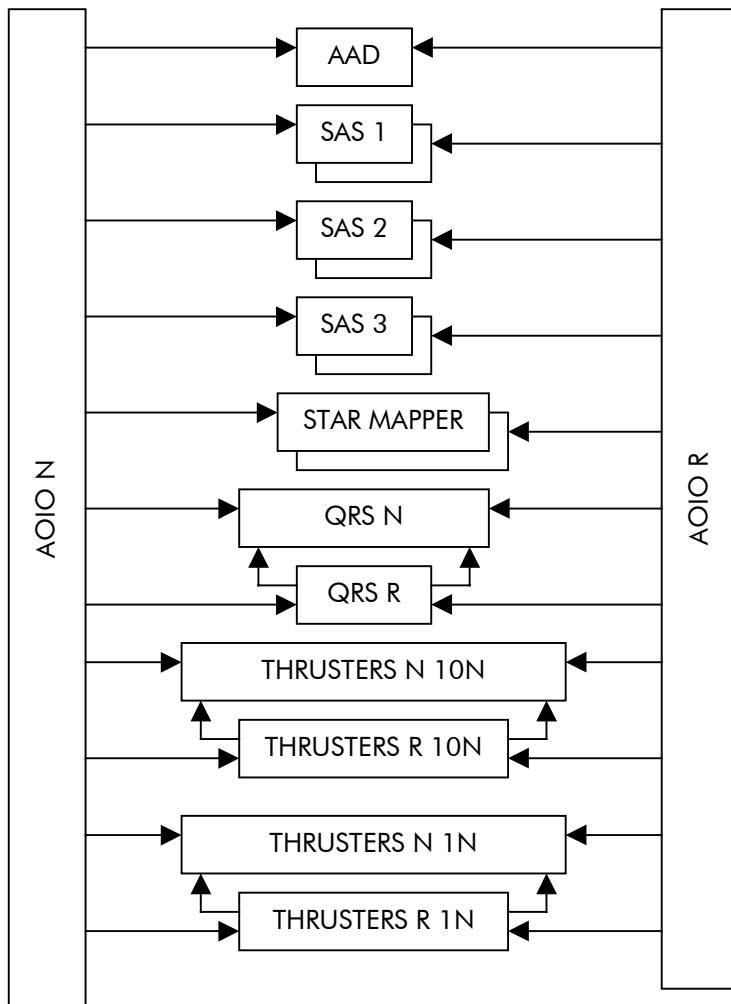
FIGURE 6.9.2-6 PLANCK SENSORS AND ACTUATORS INTERFACES
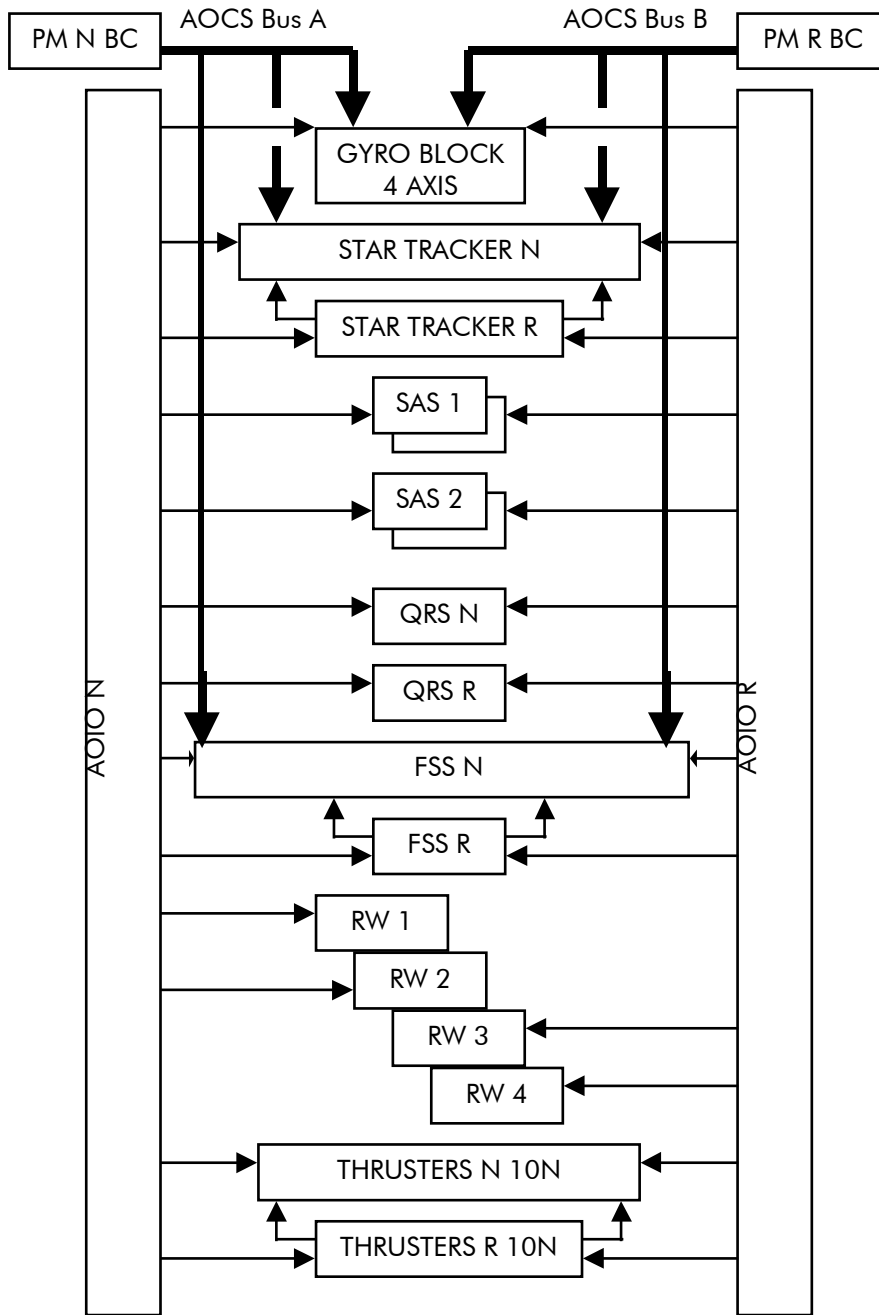
FIGURE 6.9.2-7   HERSCHEL SENSORS AND ACTUATORS INTERFACES

6.9.2.7. CDMS/ACMS FDIR management

FDIR principles for HERSCHEL and PLANCK are detailed in § 6.4.3. The main features of FDIR management are recalled below:

– FDIR management performed by CDMS and ACMS is based first on a reliable manager which is the processing part of the CDMU and ACC

– this reliable manager is obtained through the use of a specific Reconfiguration Module (RM) which in case of processor alarm or high level alarm, controls at least a switchover to the redundant processor. The RM independence from the other functions is such that no single failure mode (in particular common cause) can result in simultaneous processor failure and no detection/action by the reconfiguration module. Although a single failure can trigger an unnecessary reconfiguration, this reconfiguration will remain correct. 2 hot redundant RM are provided; the active one is selected by default, before launch, and can be changed by ground command

– this reliable processing made by CDMU or ACC assures a FDIR reliable action on the functions/equipment under their control (1553 I/F, Power, Thermal Control... for CDMU; 1553 I/F, Attitude Control sensors and actuators for ACC).

– Another point is that, in order to minimize frequency and cumulated duration of mission outages, several levels of fault processing are considered:

• Level 0, which corresponds to equipment failures internally recovered (no effect or action to/from another equipment)

- Level 1, in which a processor (of CDMU or ACC) reconfigures a user on basis of its alarms or incorrect response on 1553 bus

- Level 2, in which a processor reconfigures a user or a functional chain on basis of detected abnormal performance (cross check/consistency check, continuity check, threshold) at function level.

- Level 3a, in which a RM reconfigures a processor in case it issues alarms or if ACC 1553 bus is declared failed

- Level 3b, in which a RM performs a restart of the processor from PROM

- Level 4, in which a RM reconfigures a processor and some related equipment in case it receives high level (system) alarms.

– A Safeguard Memory (SGM) in the RM contains:

- the list of equipment on which to reconfigure

- the reconfiguration sequence

- the context necessary for the restart - after reconfiguration - of interrupted tasks: spacecraft status, current mission timeline, ….

– Activation of autonomous FDIR according to mode of control: Ground Managed (GM), Autonomous Fail Operational (AFO), Autonomous Fail Safe (AFS). In GM and AFS, failures triggering FDIR levels 1 to 4 put the spacecraft in Safe Mode, in AFO, failures triggering FDIR levels 1 to 3a result in mission continuation, and levels 3b and 4 put the spacecraft in Safe Mode.

6.9.2.8.   Propulsion

Redundant/isolating components are provided so that no single failure of hardware is identified which could result in critical/catastrophic situation except those leading to external leakage of propellant or burst (tanks, lines), and mixing of propellant/ pressurant in tanks.

Downstream tanks and filter, the thrusters are arranged in two redundant branches, each one being isolated by a latch valve. Besides, in order to satisfy the 3 inhibits safety requirement, each thruster valve has two in series independent seats.
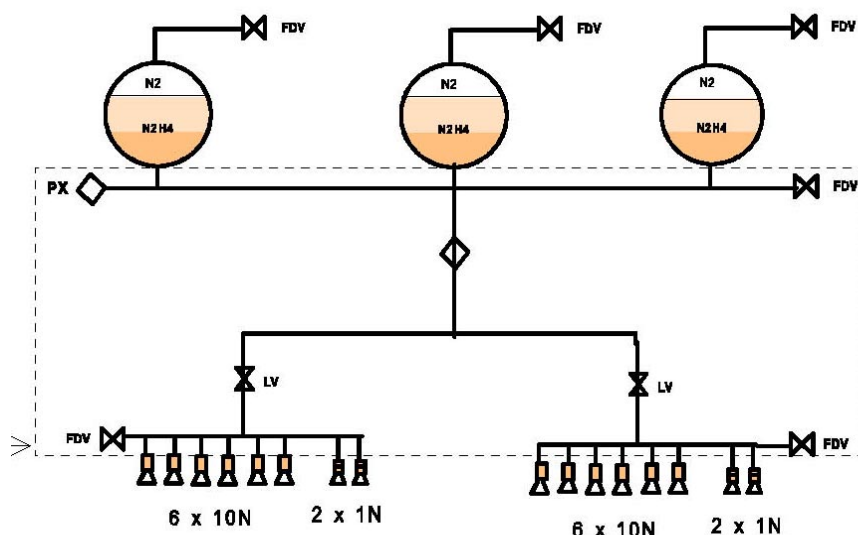
FIGURE 6.9.2-8 PLANCK PROPULSION EXAMPLE

6.9.2.9.   Telecommunication Subsystem

The subsystem can be represented as follows:

- two X-Band transponders in hot redundancy for the receiving part and cold redundancy for the transmitting one

- two cold redundant 30 W TWTA cross strapped (via a non redundant hybrid) with the transponders transmitters

- one non redundant MGA

- two non redundant LGA for HERSCHEL and three for PLANCK (assuring quasi omnidirectional coverage)

- items connecting the antennas to transponders receivers and TWTA. These items are wave guides, RF switches, hybrid, diplexers, MGA filter, test couplers. They are non redundant and SPF, except the RF switches which are all redunded. The failure mode "stuck in intermediate position" will be

covered by an operational procedure, sending double commands to ensure positive switching as on ISO/INTEGRAL.

LGA can be a back-up for MGA in case a low transmission rate is acceptable, and MGA is a back up to LGAs for TC uploading.

An automatism (part of the spacecraft level FDIR) periodically changes the crossing configuration between LGA in case both Rx do not detect any RF signal after a certain delay (timeout on TC reception from ground).

6.9.2.10.   Harness

The harness elements have the same level of redundancy than the units they connect. Besides, a verification of the application of technological design rules (e.g.: use of backshell to protect from EMC, use of mechanical keying to avoid permutation of connectors...) contributing to reduce the risks of failure propagation/common cause failures will be performed from Phase B. Separate connectors will be used to segregate the links between redundant items.

6.9.2.11.   HERSCHEL PLM

Reliability of optical elements is assured by application of specified safety margins, by qualification and acceptance tests, use of materials whose optical degradation in space environment is predictable and covered by margins.

Cryostat Control Unit (CCU) and valves arrangement are designed to assure the failure tolerance of the cryo valves control at Helium subsystem level. Cryo valves which are normally actuated after launch are redundant with regard to their critical failure modes. The cryo valves control in the CCU is such that redundant valves are controlled by separate redundant circuits, and that each valve is protected from premature control by an arming. For other functions (DLCM, temperature measurements...), no SPF is identified.

Helium tank SPF correspond to mechanical failures.

The Helium tank cover has no redundancy except that release of one NCA out of two is enough to assure the opening mechanism release and so the cryo cover opening. For Helium tank and its cover, the SPF list in provided in the table below.

6.9.2.12.   Planck PLM

Reliability of optical elements is assured by application of specified safety margins, qualification and acceptance tests, use of materials whose optical degradation in

space environment is predictable and covered by margins, qualification and acceptance tests.

6.9.3.   List of Single Point Failures

From preceding paragraphs, the following list of hardware SPF can be established. These SPF are proposed to be accepted due to the very low risk resulting from the risk reduction arguments. It can be noted that most SPF concern mechanical items, and that the failure modes of the electronic parts being SPF have an extremely low probability of occurrence.

SUB ASSEMBLY	IDENTIFIED SINGLE POINT FAILURE	RISK REDUCTION
Structure (SVM + PLM)	Rupture/distortion of structural item	Safety margins Qualification/acceptance tests
Optics (PLM)	Rupture/distortion of structural item	Safety margins Qualification/acceptance tests
	Degradation of optical characteristics (radiation)	Tests, learned lessons (space proven materials)
Thermal Control (SVM)	MLI, paints, coatings, surface treatments, OSR	Tests, learned lessons (space proven materials)
	Short circuit between redundant heaters on same support	Tests showing isolation between tracks, electrical margin, robustness of Kapton layer, Thermal Control performance tests
Propulsion (SVM)	Rupture/external leakage of item containing pressurant or propellant (tanks, F/D valves, pipes, filter, latch valves, pressure transducer, welds, screws)	Safety margins Qualification/acceptance tests Inspection Qualified weld process + X-ray inspection Screwing procedure Leak tests Proof/burst pressure tests
	Mixing of propellant/pressurant in a tank (tanks diaphragm)	Qualified and space proven diaphragm with N2H4, leak tested diaphragm Thrust possible tolerance to N2/N2H4 mixing
Power S/S (SVM)	Short circuit of film resistors Short circuit of self healing capacitors	Non credible failure mode Non credible failure mode if self healing energy is available
	Burst of battery	Pressure release lid or fissurable envelope prevent burst
	Leakage of battery	Battery overcharge/short circuit protections prevent overpressure/leakage

SUB ASSEMBLY	IDENTIFIED SINGLE POINT FAILURE	RISK REDUCTION
TTC Subsystem (SVM)	**HERSCHEL** Wave guides Coax cables and connectors 1 MGA 2 LGA 3 ports for the 2 LGA2/MGA RF SW 3 test couplers 1 filter 2 diplexers 2 ports for the 2 TWTA RF SW 2 ports for the 2 RF SW between LGA 1-2 and Rx	Simplicity of the items Functional tests after acceptance environmental tests Components with low failure rates Qualified technologies
	PLANCK Wave guides Coax cables and connectors 1 MGA 3 LGA 3 ports for the 2 LGA2-3/MGA RF SW 3 test couplers 1 filter 3 diplexers 2 ports for the 2 TWTA RF SW 2 ports for the 2 RF SW between LGA 1-2-3 and Rx	
	HERSCHEL/PLANCK LGA/MGA, RF SW blockage in intermediate position (6 SW)	RF switches having high margin with regard to number of switching Qualified item Item acceptance tests demonstrating correct switching at extremes of the temperature range Operational procedure

SUB ASSEMBLY	IDENTIFIED SINGLE POINT FAILURE	RISK REDUCTION
Helium S/S (HERSCHEL PLM)	External leakage of items containing Helium (tank, valves, pipes, seals …) Internal leakage of Helium valves or safety valves or rupture disk.	Safety margins Qualification environmental tests demonstrating no leakage Tightness monitoring capability on launch site via temperature information For valves: design preventing particle generation + filter upstream the valves + acceptance test report at valve level demonstrating correct tightness
	Unwanted opening or closure of valves due to launch environmental conditions (shock, acceleration, vibrations).	Safety margin Environmental tests passed without change of valve position
	Partial blockage of phase separator	Use of clean Helium Procedure to prevent presence of air PLM functional tests satisfactory
Cover S/S (HERSCHEL PLM)	Premature release of opening mechanism	Safety margin 2 independent levels of commanding
	No release of opening mechanism when necessary, cover stuck closed	Functional safety margin Use of anti cold welding material Cover opening tests
	Cryo cover damaging other items when released	Safety margin Cover opening test Low probability for a free part to enter the cryostat
	Insufficient tightness of cover/tank interface	Tests before launch demonstrating correct tightness

7. SYSTEM BUDGETS AND PERFORMANCE

7.1. SYSTEM BUDGETS

7.1.1. Mass properties budgets

Three mass properties budgets are established:

- Section 7.1.1.1: HERSCHEL mass, centring and inertia budgets.

- Section 7.1.1.2: PLANCK mass, centring and inertia budgets.

- Section 7.1.1.3: launch mass budgets, established from both spacecraft mass budgets and compared to ARIANE 5 capability for direct on to L2 (5310 kg).

7.1.1.1. HERSCHEL mass properties

7.1.1.1.1. HERSCHEL mass budget

HERSCHEL spacecraft mass budget is shown hereafter in Table 7.1.1-1. It has been built in accordance with the margin requirements of the System Requirements Specification:

- 20 % margin for completely new developments

- 15 % margin for new developments derived from existing hardware

- 10 % margin for existing units requiring minor/medium modification

- 5 % for existing unit.

With this margin philosophy, the mass budget is the following:

- maximum mass: **2911.8 kg**

- nominal mass: **2578.1 kg.**

The instruments mass is the allocation made in the IID-A (AD4.01).

The SVM and PLM element masses are the prime allocations. They have been used to derive the SVM and PLM allocated masses reflected in the modules specifications:

– 1625 kg for H-EPLM mass, excluding telescope and instruments but including Helium, SSH/SSD, SVM shield and support truss

– 415 kg for HERSCHEL SVM

The wet mass is calculated from the HERSCHEL Delta-v and fuel budget which is detailed in Section 7.1.3.1.

HERSCHEL SATELLITE			
	NOMINAL MASSES	MARGIN	MAXIMUM MASSES
PAYLOAD MODULE (DRY)	**1583.6 kg**	**235.3 kg**	**1818.9 kg**
Dry Cryostat (allocated)	**1185.2**	**153.2**	**1338.4**
Dry Cryostat excluding Instruments	*983.6*	*130.8*	*1114.4*
Instruments inside Cryostat	*158.0*	*21.0*	*179.0*
Cryo elec.	*8.6*	*1.4*	*10.0*
Instruments outside Cryostat	*35.0*	*0.0*	*35.0*
Telescope (allocated)	**224.0**	**56.0**	**280.0**
Sunshield with support (allocated)	**56.1**	**8.4**	**64.5**
Sunshade with support (allocated)	**79.6**	**11.9**	**91.5**
SVM shield with support (allocated)	**13.5**	**2.0**	**15.5**
Truss and fixation (allocated)	**25.2**	**3.8**	**29.0**
SERVICE MODULE (DRY)	**541.7 kg**	**74.2 kg**	**615.9 kg**
Payload in SVM (allocated)	**175.7**	**27.8**	**203.5**
HERSCHEL instruments inside SVM	*173.3*	*27.7*	*201.0*
SREM/VMC	*2.4*	*0.1*	*2.5*
SVM S/S and items (allocated)	**366.0**	**46.4**	**412.4**
Power	*32.5*	*4.5*	*37.0*
ACMS	*71.4*	*4.8*	*76.2*
DHS	*12.0*	*2.4*	*14.4*
RF	*14.5*	*2.0*	*16.5*
SVM Structure	*151.3*	*22.7*	*174.0*
Thermal Control	*16.2*	*2.6*	*18.8*
Harness	*25.0*	*5.0*	*30.0*
RCS	*38.1*	*2.4*	*40.5*
Assembling	*5.0*	*0.0*	*5.0*
DRY SATELLITE MASS	**2125.3 kg**	**309.5 kg**	**2434.8 kg**
FLUIDS	**452.8 kg**	**24.2 kg**	**477.0 kg**
Cryostat Helium (allocated)	**307.5**	**3.1**	**310.6**
Propellant plus pressurant (allocated)	**145.3**	**21.1**	**166.4**
WET SATELLITE MASS	**2578.1 kg**	**333.7 kg**	**2911.8 kg**

TABLE 7.1.1-1 HERSCHEL MASS BUDGET

7.1.1.1.2. HERSCHEL centring and inertia

The centring and inertia values are presented hereafter in Table 7.1.1-2.

HERSCHEL spacecraft centring and inertia have been computed with nominal values on the same basis as HERSCHEL mass budget.

The centring and inertia data are determined for launch (BOL) and in orbit extreme case (EOL). The knowledge of these data is requested for the following purpose.

Centering:

– verification of HERSCHEL centring at Launch (ARIANE 5 requirement)

– knowledge of HERSCHEL centring, and variation of HERSCHEL centring, for alignment of thrusters

– knowledge for on-ground activities (handling, MGSE dimensioning, ...).

Inertia:

– verification of HERSCHEL stability and commandability during attitude control or attitude maneuvers

– knowledge for on-ground activities (handling, MGSE dimensioning, ...).

The unbalance due to Sunshield/Sunshade CoG off-set is 150 m x kg. The mechanical architecture of HERSCHEL SVM has taken into consideration this parameter, and has been adapted to restore HERSCHEL balance at the maximum. This target is fully achieved as HERSCHEL does not request any balancing masses.

As a conclusion, it is evidenced that the present designs and mass properties of HERSCHEL:

– comply with Arianespace requirements: CoG at a maximum distance of 30 mm from the satellite axis at launch

– optimize the satellite inertia for commandability

– avoid balancing masses.

	CENTRE OF MASS [MM]					
DRY S/C	x		y		z	
	2155.0		-23.0		-12.4	
	R = 26.1 mm					
	INERTIA [KG.M²]					
	Ixx	Iyy	Izz	Ixy	Iyz	Ixz
	2960	4979	5063	-187	50	401

	CENTRE OF MASS [MM]					
WET S/C	x		y		z	
	2006.6		-18.6		-10.0	
	R = 21.1 mm					
	INERTIA [KG.M²]					
	Ixx	Iyy	Izz	Ixy	Iyz	Ixz
	3236	5570	5835	-194	50	396

TABLE 7.1.1-2 HERSCHEL CENTRING & INERTIA

7.1.1.2.   PLANCK mass properties

7.1.1.2.1. PLANCK mass budget

PLANCK spacecraft mass budget is shown hereafter in Table 7.1.1-3. It has been built in accordance with margin requirements of the System Requirements Specification:

- – 20 % margin for completely new developments

- – 15 % margin for new developments derived from existing hardware

- – 10 % margin for existing units requiring minor/medium modification

- – 5 % for existing unit.

With this margin philosophy, we have the following results:

- – maximum mass: **1472.0 kg**

- – nominal mass: **1283.8 kg.**

The instruments mass is the allocation made in the IID-A (AD4.01).

The SVM and PLM element masses are the prime allocations. They have been used to derive the SVM and PLM allocated masses in the module specifications:

- – 191 kg for dry PLM excluding reflectors (21 kg for primary, 11 kg for secondary) and instruments in PLM (113.4)

- – 485 kg for SVM

The wet mass is calculated from the PLANCK Delta-v and fuel budget which is detailed in Section 7.1.3.2.

PLANCK SATELLITE			
	NOMINAL MASSES	MARGIN	MAXIMUM MASSES
PAYLOAD MODULE (DRY)	**287.8 kg**	**49.0 kg**	**336.8 kg**
SERVICE MODULE (DRY)	**718.6 kg**	**98.5 kg**	**817.1 kg**
Payload in SVM	285.8	41.1	326.9
Instruments inside SVM	*283.4*	*41.0*	*324.4*
SREM/VMC	*2.4*	*0.1*	*2.5*
SVM S/S and items	425.3	57.4	482.7
Power	*32.5*	*4.5*	*37.0*
ACMS	*19.7*	*2.7*	*22.4*
DHS	*12.0*	*2.4*	*14.4*
RF	*14.8*	*2.0*	*16.8*
Structure	*171.5*	*25.8*	*197.3*
Thermal Control	*51.6*	*6.0*	*57.6*
Harness	*25.0*	*5.0*	*30.0*
RCS	*54.2*	*3.2*	*57.4*
Solar arrays	*39.0*	*5.8*	*44.8*
Assembling	*5.0*	*0.0*	*5.0*
Balancing masses	7.5	0.0	7.5
DRY SATELLITE MASS	**1006.4 kg**	**147.5 kg**	**1153.9 kg**
FLUIDS	**277.4 kg**	**40.7 kg**	**318.1 kg**
He PPLM	6.8	1.0	7.8
Propellant plus pressurant	270.6	39.7	310.3
WET SATELLITE MASS	**1283.8 kg**	**188.1 kg**	**1472 kg**

TABLE 7.1.1-3 PLANCK MASS BUDGET

7.1.1.2.2. PLANCK centring and inertia

The centring and inertia values are presented hereafter in Table 7.1.1-4. From these data the wobble and Lambda values are also derived.

PLANCK spacecraft centering and inertia have been computed with to nominal values on the same basis as PLANCK mass budget.

The centring and inertia data are to be determined for launch (BOL) and in orbit extreme case (EOL). The knowledge of these data is requested for the following purpose.

Centering:

– verification of PLANCK centring at Launch (ARIANE 5 requirement)

– knowledge of PLANCK centring, and variation of PLANCK centring, for alignment of thrusters

– knowledge for on-ground activities (handling, MGSE dimensioning, ...).

Inertia:

– verification of PLANCK wobble angle at launch: wobble to be lower than 1 deg (ARIANE 5 requirement)

– knowledge of PLANCK wobble angle in orbit, as contributor to the PPLM pointing budget

– knowledge of PLANCK Lambda factor for verification of PLANCK commandability during attitude control

– knowledge for on-ground activities (handling, MGSE dimensioning, ...).

The mechanical architecture of PLANCK SVM has taken into consideration the PPLM CoG offset, and has been adapted to restore PLANCK balance at the maximum. This target is fully achieved as PLANCK requests only 7.5 kg of balancing masses.

As a conclusion, it is evidenced that the present design and mass properties of PLANCK:

– comply with ARIANESPACE requirements: CoG at a maximum distance of 30 mm from the satellite axis and wobble to be lower than 1 deg at Launch

– optimize the wobble angle for attitude stability

– present inertia ratio compliant with command strategy

– minimize the balancing masses.

	CENTRE OF MASS [MM]					
	x		y		z	
	930.7		-21.7		-23.0	
DRY S/C			R = 31.7 mm			
	INERTIA [KG.M²]					
	Ixx	Iyy	Izz	Ixy	Iyz	Ixz
	1844	1636	1533	0	-54	0
	l = 1.16			wobble = 0.0°		

	CENTRE OF MASS [MM]					
	x		y		z	
	844.6		-17.5		-18.5	
WET S/C			R = 25.5 mm			
	INERTIA [KG.M²]					
	Ixx	Iyy	Izz	Ixy	Iyz	Ixz
	2098	1802	1699	-1.9	-54.3	-2
	l = 1.2			wobble = 0.55°		

TABLE 7.1.1-4 PLANCK CENTRING & INERTIA

7.1.1.3. Launch mass budgets

A mass budget at launch is set-up for HERSCHEL/PLANCK in order to verify that the total mass at launch does not exceed the capability of the launcher for HERSCHEL and PLANCK on the nominal injection orbit (direct injection to L2).

The total mass at launch is obtained by adding the masses of the 2 spacecraft (HERSCHEL and PLANCK) and the masses of the associated adapters which are to be carried with the S/C during the launcher injection maneuver.

A system margin of 200 kg has been counted on top of the S/C and adapters to achieve the maximum predicted mass at launch. The system margin of 200 kg is consistent with the ESA reserve to be considered in the calculation of the S/C maximum masses, as specified in the System Requirements Specification (SCMD-085).

For HERSCHEL and PLANCK in dual launch configuration, the following adapters are taken into account according to ARIANE User's Manual:

- 2 adapters 2624 of 98 kg each, for HERSCHEL and PLANCK respectively:

  - PLANCK adapter mounted on the top of the EPS cone

  - HERSCHEL adapter mounted on the top of SYLDA5.

- One adapter SYLDA5 of 425 kg, for HERSCHEL accommodation.

- One USF plate of 50 kg, mounted on the top of the EPS cone, to stiffen the EPS cone for launch.

The launch mass budget is shown in Table 7.1.1-5. The total mass of 5254.8 kg is compliant with the launch capacity of ARIANE 5 E/S of 5310 kg with a **55 kg additional margin**, which can be allocated to cover variations from module levels.

	MAXIMUM MASS
PAYLOADS	
HERSCHEL	2911.8 kg
PLANCK	1472.0 kg
TOTAL Payload	**4383.8 kg**

ADAPTERS	
PLANCK Adapter 2624	98.0 kg
HERSCHEL Adapter 2624	98.0 kg
Sylda 5	425.0 kg
USF plate on EPS cone	50.0 kg
TOTAL Adapters	**671.0 kg**

System margin	**200.0 kg**

TOTAL MASS AT LAUNCH	**5254.8 kg**
REQUIREMENT	< 5310 kg

TABLE 7.1.1-5 LAUNCH MASS BUDGET

7.1.2. Power and energy budgets

Mission Phases

The power budgets are given for each of the following phases, covering the whole mission around L2.

- The **Launch** phase corresponds to the status from umbilical disconnection until sepration from the Launch vehicule

- The so called **Pre-op** phase corresponds to the beginning of the transfer phase, when the payload is not switched ON and when decontamination of the Payload Module is performed

- The **Obs** phase corresponds to the nominal observation mode when no communication occurs

- The **Trans** phase corresponds to the 3-hour daily communication period

- The **Safe** phase corresponds to the spacecraft consumption in Safe mode

- The **Safe on battery** phase addresses the attitude loss failure mode.

For both spacecraft, the power budgets also include 100 W "ESA margin", as specified in SMPC-220. This margin however has not been taken into account for the Launch case regarding the low consumption and the low expected variation during this phase: it has been replaced by a large, 30 %, additional "system margin".

Margin Policy

For each of the budget items the margin policy in Table 7.1.2-1 has been applied, depending upon the development status of the given unit:

ITEM	MARGIN	UNITS
Units specified by ESA. and off the shelves hardware	0 %	Payload instruments. SREM. VMC
Existing items which budget is extrapolated	5 %	X-Band transponders. QRS. FSS
Items derived from existing hardware or off the shelves hardware which consumption depends on operating mode	10 to 15 %	TWTAs. PCDU. Gyros. Star Tracker
New design items. consumption resulting from analysis	20 to 25 %	CDMU. ACC. thermal control/ compensation heating. Cryostat Control Unit

TABLE 7.1.2-1 POWER MARGINS POLICY

Battery commonality

In order to benefit from a possible commonality between HERSCHEL and PLANCK, the battery sets design are identical on both spacecraft. The sizing case for the battery design over the two spacecraft, is the 133.2 min long launch phase for PLANCK.

The selected battery can deliver up to 521 Wh with 70 % DoD, assuming one cell loss (23 strings available within 24).

Assumptions on power consumption

The instruments power is the allocation made in the IID-A (AD4.01).

The power consumption of SVM and PLM elements are the prime allocations.

7.1.2.1. HERSCHEL power and energy budget

The Table 7.1.2-2 hereafter details the HERSCHEL spacecraft power consumption for the principal operating modes, from a power point of view, from Launch to operation around L2.

For each phase, the budget is in accordance with the baseline described in Section 6, i.e. mainly, from a power point of view:

- 30 W RF TWTAs in cold redundancy, and operated only during the programmed daily communication periods

- 600 W have been taken into account for HERSCHEL Telescope decontamination in pre-obs phase

- units nominally operated in cold redundancy

- thermal control heating budget in line with baseline implementation, per phase

- the total payload power consumption figures are those specified in the System Requirement Document; they are composed of the power consumption for each instrument as extracted from the IID-B 1/0 and a margin computed such that the total figure in nominal operation is the one allocated in the SRS (550 W).

These figures however, represent the maximum average power consumption over a given phase. The HERSCHEL operation comprises few power consumption short term changes within a given phase: especially the Reaction Wheels power consumption will strongly depend upon a given mission plan. The sizing of the power sources. and especially the Solar Array has therefore been optimized by an energetic simulation which results are presented in Figure 7.1.2-1.

Solar Array

The sizing case is the Obs phase, EOL, with the max 30° off pointing of the spacecraft from the Sun.

More precisely, two sizing cases have been identified:

- the minimum array string length voltage is defined by the first Winter Solstice period with HERSCHEL Solar Array axis oriented toward the Sun (hot case)

- the minimum required array power is defined by the lowest illumination conditions: lowest solar flux (Summer Solstice) combined with the highest Solar Array SAA (30°).

The Electrical Power System architecture baseline consists in having the Solar Array power conditioned via 30 non redundant sequentially shunted sections. A reliability margin is therefore included in the Solar Array sizing, to take into account a complete SA section failure inside the PCDU.

Finally, SMSA-015 requires to consider an additional 10 % margin on the dimension of the Solar Array. The implemented Solar Array thus permits to deliver up to 1450 W in the worst illimination condition, providing an additional margin of 28 % compared to the margined power requirement.

Battery

With the presented budget, 404 Wh are required for HERSCHEL early phases after launch, while the battery can deliver up to 521 Wh with 70 % DoD and one cell loss (giving 29 % margin).

A full operational phase energetic simulation has been performed with one single battery, and one Solar Array section lost, over one "worst case" day, consisting in a set of worst cases (from a power point of view) small slews, plus one large slew; the slews are also performed in Trans mode. This leads to power bursts on the reaction wheels power lines, with a number of peaks of up 200 W above. Each of the individual units power consumption is introduced with values depending on the satellite operation, and the baseline power regulation (S4R) and LiIon battery management is fully simulated. Figure 7.1.2-1 demonstrates the perfect adequacy of the proposed design, and sources sizing with the need, including with suitable margins.

COMPONENTS	LAUNCH	PRE OP	TRANS	OBS	SAFE	SAFE on battery
Max HIFI	0.0	0.0	281.0	281.0	0.0	0.0
Max PACS	0.0	0.0	85.3	85.3	0.0	0.0
Max SPIRE	0.0	0.0	86.0	86.0	0.0	0.0
Margin	0.0	0.0	98.0	98.0	0.0	0.0
MAX Instruments	0	0	550	550	0	0
Cryostat Control Unit	15.0	15.0	15.0	15.0	15.0	0.0
CCU	15	15	15	15	15	0
S/B TC receiver	25.2	25.2	25.2	25.2	25.2	25.2
S/B TM transmitter	0.0	6.3	6.3	0.0	6.3	6.3
TWTA	0.0	63.0	63.0	0.0	63.0	63.0
TTC SUBSYSTEM	25	95	95	25	95	95
SREM	0.0	2.0	2.0	2.0	2.0	2.0
Virtual Monitoring Camera	3.0	3.0	3.0	3.0	3.0	3.0
CDMU	30.0	48.0	48.0	48.0	48.0	48.0
CDMS SUBSYSTEM	33	53	53	53	53	53
ACC	15.0	26.4	26.4	26.4	26.4	26.4
RWDE	0.0	20.0	30.0	30.0	10.5	10.5
STRE	0.0	33.0	33.0	33.0	0.0	0.0
FSS	0.0	1.6	1.6	1.6	0.0	0.0
QRS	0.0	0.0	0.0	0.0	8.9	8.9
Gyros	0.0	16.5	16.5	16.5	0.0	0.0
ACMS SUBSYSTEM	15	97	107	107	46	46
Cat Bed Heaters	0.0	0.0	50.2	50.2	0.0	0.0
Press. Trans.	2.6	2.6	2.6	2.6	2.6	2.6

TABLE 7.1.2-2 HERSCHEL POWER BUDGET

RCS SUBSYSTEM	**3**	**3**	**53**	**53**	**3**	**3**
Tanks heaters	3.0	3.0	3.0	3.0	3.0	3.0
Pipes & valves heaters	12.0	28.0	28.0	28.0	28.0	28.0
Star trackers heaters	0.0	5.0	0.0	0.0	0.0	0.0
Batteries heaters	0.0	12.0	12.0	12.0	12.0	12.0
HERSCHEL Telescope heaters	0.0	600.0	0.0	0.0	0.0	0.0
payload heaters	0.0	0.0	28.0	47.0	47.0	0.0
Compensation heaters	0.0	165.0	0.0	32.0	0.0	0.0
THERMAL SUBSYSTEM	**15**	**813**	**71**	**122**	**90**	**43**
PCDU	21.5	73.2	63.3	62.5	29.5	30.8
Harness	3.4	34.0	29.8	29.2	9.5	8.1
Battery charge	0.0	56.5	0.0	0.0	0.0	0.0
POWER CONTROL SUBSYSTEM	**25**	**164**	**93**	**92**	**39**	**39**

TOTAL PLATFORM	**131**	**1239**	**487**	**467**	**340**	**278**

S/C REQUIREMENT (W)	**131**	**1239**	**1037**	**1017**	**340**	**278**
MARGIN (ESA reserve)	**0**	**100**	**100**	**100**	**0**	**0**
INCLUDING margin/ESA reserve	**170**	**1339**	**1137**	**1117**	**408**	**333**
actual SOLAR ARRAY POWER (W)	**0**	**1500**	**1350**	**1350**	**1350**	**0**
POWER MARGIN	**NA**	**12%**	**19%**	**21%**	**231%**	**NA**

TABLE 7.1.2-2 HERSCHEL POWER BUDGET (CONT'D)
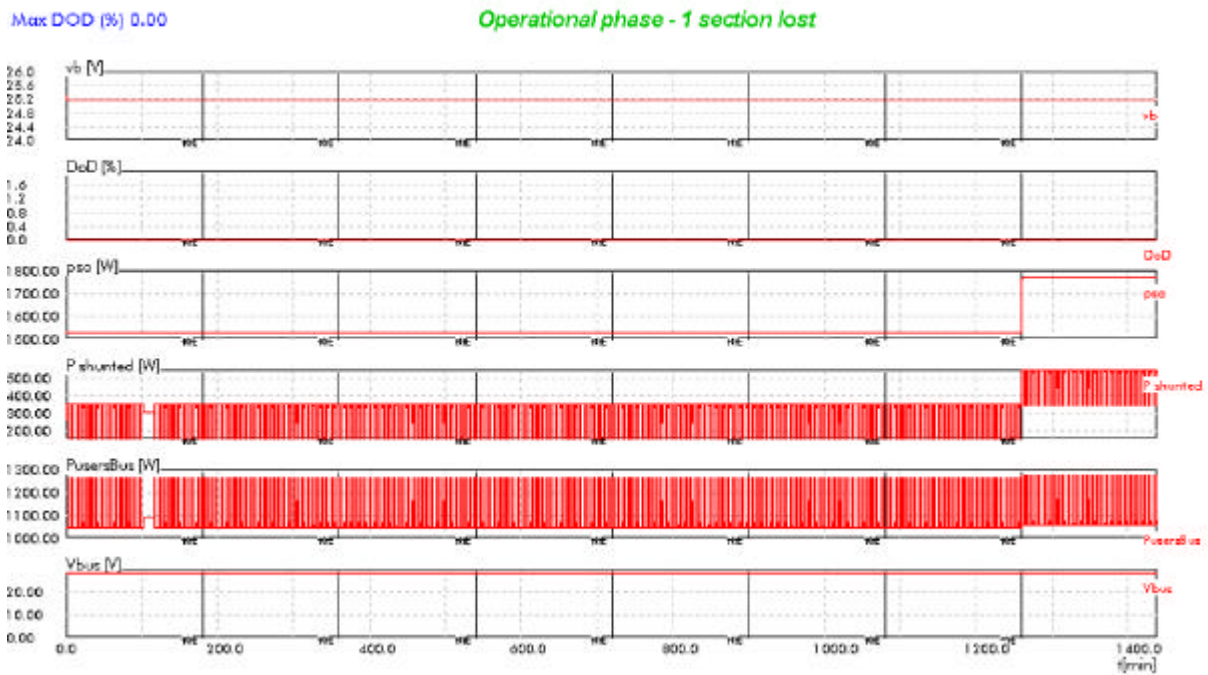
FIGURE 7.1.2-1 HERSCHEL WORST CASE POWER SIMULATION

7.1.2.2. PLANCK power and energy budget

The Table 7.1.2-3 hereafter details the PLANCK spacecraft power consumption for the principal operating modes, from a power point of view, from Launch to operation around L2.

For each phase, the budget is in accordance with the baseline described in Section 6, i.e. mainly, from a power point of view:

- 30 W RF TWTAs in cold redundancy, and operated only during the programmed daily communication periods

- an allocation of 300 W has been taken into account for possible Telescope decontamination in pre-obs phase. Even if this is not in the present baseline, this shows that the system resources are available.

- units nominally operated in cold redundancy

- thermal control heating budget in line with baseline implementation, per phase

- the total payload power consumption figures are those specified in the System Requirement Document; they are composed of the power consumption for each instrument, as extracted from the IID part B's and a margin computed such that the total figure in nominal operation is the specified one.

These figures however, represent the maximum average power consumption over a given phase. Considering the PLANCK operation comprises very few consumption short term changes within a given phase, they can directly be used for the sizing of the power sources.

Solar Array

The sizing case is the Trans phase, EOL, with the maximum 10° off pointing from the Sun.

More precisely, two sizing cases have been identified:

- the minimum array string length voltage is defined by the first Winter Solstice period, with PLANCK spin axis oriented toward the Sun (hot case)

- the minimum required array power is defined by the lowest illumination conditions: lowest solar flux (Summer Solstice) combined with the highest Solar Array SAA (10 degrees).

The Electrical Power System architecture baseline consists in having the Solar Array power conditioned via 30 non-redundant sequentially shunted sections. A reliability margin is therefore included in the Solar Array sizing, to take into account a complete SA section failure inside the PCDU.

Finally, SMSA-015 requires to consider an additional 10 % margin on the dimension of the Solar Array. The implemented Solar Array thus permits to deliver up to 1664 W in the worst illumination condition, providing an additional margin of 12 % compared to the margined power requirement.

Battery

From the budget presented, the Launch energy requirement amounts to 500 Wh.

The selected battery can deliver up to 521 Wh with a 70 % DoD and one cell loss, giving 4 % margin.

A full launch phase energetic simulation has been performed with one single battery over more than 10 hours, starting with Launch conditions, then the post launcher separation conditions, until the completion of the battery recharging process. Each of the individual units power consumption is introduced with values depending on the satellite mode, and the baseline power regulation (S4R) and LiIon battery management is fully simulated. Figure 7.1.2-2 demonstrates the perfect adequacy of the proposed design and sources sizing with the need.

Similarly, a whole one day PLANCK operation has been simulated, introducing the loss of one Solar Array section. The results summarized in Figure 7.1.2-3 again show the compliance of the design, and of the Solar Array sizing, with the mission power requirements.

COMPONENTS	LAUNCH	PRE OP	TRANS	OBS	SAFE	SAFE on battery
Max LFI (excl. sorption cooler)	0.0	32.3	73.6	73.6	0.0	0.0
Max sorption cooler	0.0	0.0	655.0	655.0	655.0	0.0
Max HFI	30.0	42.0	254.2	254.2	102.0	0.0
Margin	0.0	0.0	17.0	17.0	0.0	0.0
MAX PAYLOAD	30	74	1000	1000	757	0
S/B TC receiver	25.2	25.2	25.2	25.2	25.2	25.2
S/B TM transmitter	0.0	6.3	6.3	0.0	6.3	6.3
TWTA	0.0	63.0	63.0	0.0	63.0	63.0
TTC SUBSYSTEM	25	95	95	25	95	95
SREM	0.0	2.0	2.0	2.0	2.0	2.0
Virtual Monitoring Camera	3.0	3.0	3.0	3.0	3.0	3.0
CDMU	30.0	48.0	48.0	48.0	48.0	48.0
CDM+A59S SUBSYSTEM	33	53	53	53	53	53
ACC	15.0	26.4	26.4	26.4	26.4	26.4
Star Mapper	0.0	0.7	0.7	0.7	0.0	0.0
QRS	0.0	8.9	8.9	8.9	8.9	8.9
SAS	0.0	0.0	0.0	0.0	0.0	0.0
ACMS SUBSYSTEM	15	36	36	36	35	35
Cat Bed Heaters	0.0	0.0	50.2	50.2	0.0	0.0
Press. Trans.	2.6	2.6	2.6	2.6	2.6	2.6
RCS SUBSYSTEM	3	3	53	53	3	3
Thrusters heaters	32.0	0.0	0.0	0.0	0.0	0.0
Tanks heaters	2.0	2.0	0.0	0.0	2.0	2.0
Pipes & valves heaters	12.0	12.0	4.0	4.0	12.0	12.0
Payload compensation Heaters	0.0	152.0	1.0	1.0	0.0	0.0
Batteries heaters	0.0	12.0	12.0	12.0	12.0	0.0
Telescope Baffle heaters	0.0	300.0	0.0	0.0	0.0	0.0
Sorption cooler Compensation Heaters	0.0	595.0	0.0	0.0	0.0	0.0
SVM Compensation Heaters	0.0	0.0	0.0	76.0	0.0	0.0

TABLE 7.1.2-3 PLANCK POWER BUDGET

THERMAL SUBSYSTEM	**46**	**1073**	**17**	**93**	**26**	**14**
P C U	18.6	67.8	57.7	57.9	44.0	19.3
PDU	7.3	25.0	23.8	23.9	19.5	8.0
PCDU	25.8	92.8	81.5	81.8	63.6	27.2
Harness	5.3	42.8	40.0	40.2	31.0	6.8
Battery charge	0.0	79.7	0.0	0.0	0.0	0.0
POWER CONTROL SUBSYSTEM	**31**	**215**	**122**	**122**	**95**	**34**
TOTAL SVM	153	1474	375	382	306	233

S/C REQUIREMENT (W)	183	1549	1374	1382	1063	233
MARGIN (ESA reserve)	0	100	100	100	0	0
INCLUDING margin/ESA reserve	238	1649	1474	1482	1275	303
actual SOLAR ARRAY POWER (W)	0	1806	1664	1664	1664	0
POWER MARGIN		10%	13%	12%	30%	

TABLE 7.1.2-3 PLANCK POWER BUDGET (CONT'D)
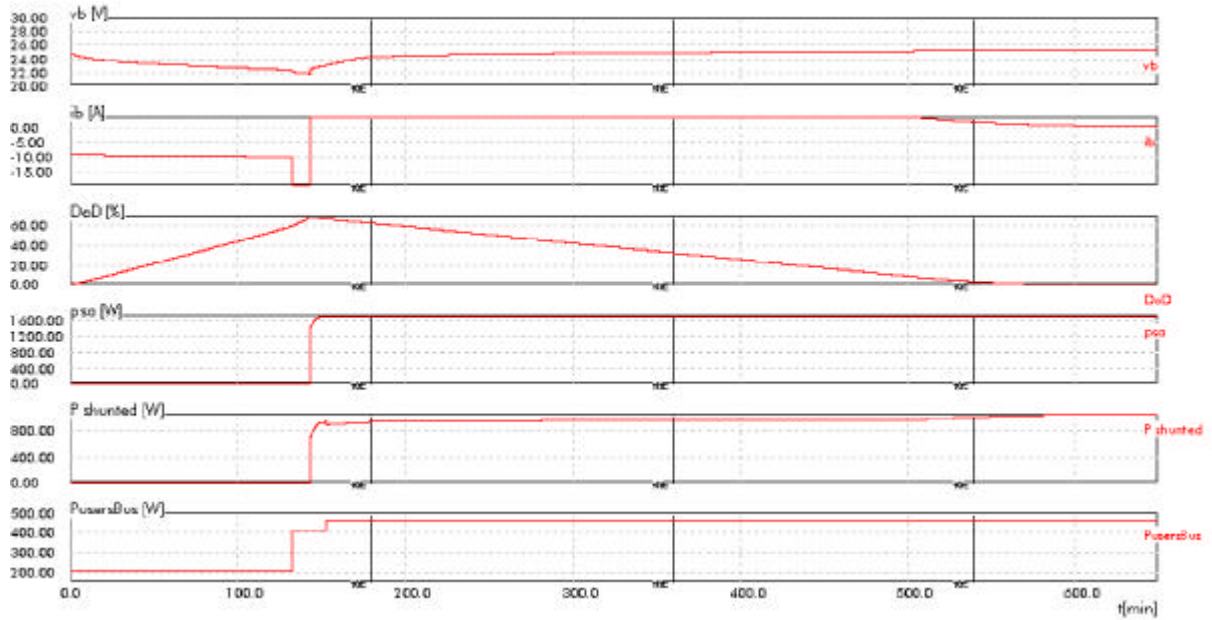
FIGURE 7.1.2-2 PLANCK LAUNCH POWER SIMULATION
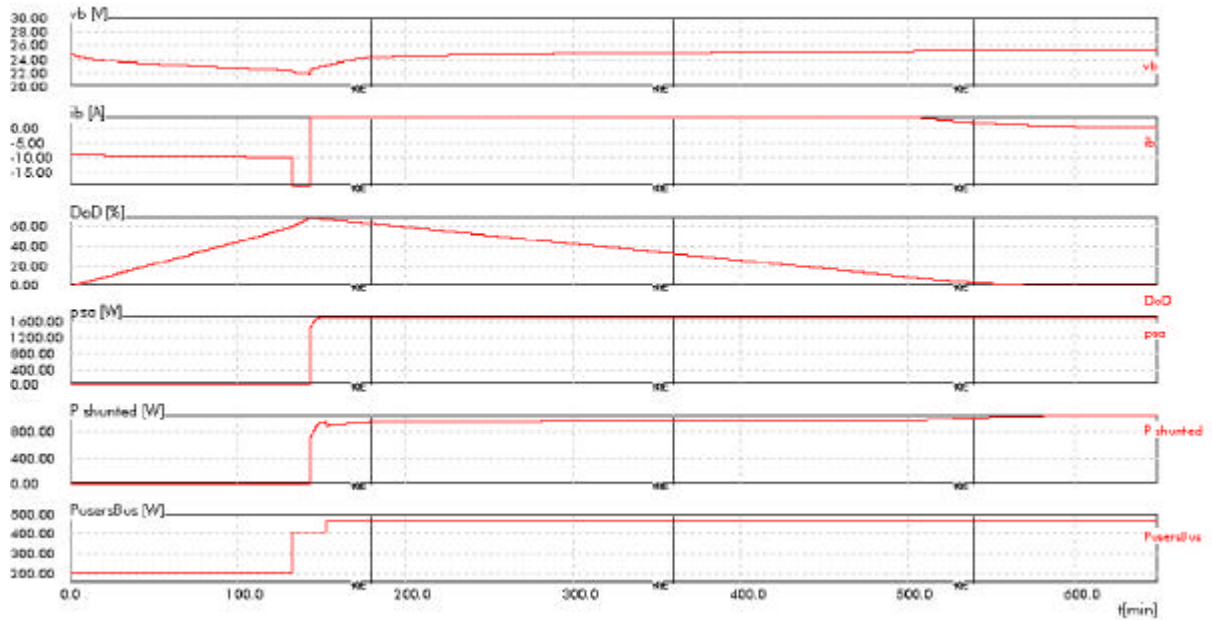
FIGURE 7.1.2-3 PLANCK WORST CASE OPERATION SIMULATION

7.1.3. Delta-V and fuel budget

In order to establish HERSCHEL and PLANCK Delta-v and fuel budget, the following assumptions are taken into account:

- mission analysis in accordance with Section 4.

- Delta-v margins as specified in the System Requirements Specification:

    - 10 % on orbit insertion propellant. This margins has been taken for all maneuvers, including launcher dispersion correction and trim corrections

    - 50 % on orbit maintenance and angular momentum management/ attitude control.

- Worst case sun aspect angles.

- Satellite dry masses in accordance with mass budgets of Section 7.1.1. For HERSCHEL, this mass includes the Helium inside the cryostat at the beginning of life.

- Thruster configuration in accordance with Section 6.

- The thruster specific impulse has been derived from 10N thrusters qualification data. Its sensitivity to the tank pressure has been taken into account in the calculation.

7.1.3.1. HERSCHEL Delta-V and fuel budget

The HERSCHEL delta-V and fuel budget in shown in Table 7.1.3-1.

The allocation for attitude control is sized to allow wheel unloading of 20 Nms per day during 6 years, plus an allocation for safe mode.

Taking into account the RCS subsystem configuration, a residual mass of 1.9 kg and a pressurant mass of 2.6 kg has been derived.

The fuel total mass of 163.8 kg fits into the baseline fuel tanks with a margin of 20 %, as specified in SMRC-025.

MANEUVER	Delta-V	SAA	Efficiency	Margin	Isp	Fuel [kg]	S/C Mass [kg]
Perigee velocity	14 m/s	150-180	90%	10%	220.79	22.9	2911.4
Removal of launcher dispersion	50 m/s	any	90%	10%	220.79	80.3	2888.5
Maneuver 2	4 m/s	any	90%	10%	214.49	6.5	2808.2
Midcourse correction	3 m/s	any	90%	10%	215.96	4.8	2801.7
Orbit inj/ecl avoidance	0 m/s	28.4 deg	97%	50%	214.55	0 kg	2796.9
Orbit maintenance (4½ years)	12 m/s	28.4 deg	97%	50%	210.00	25.0	2796.9
Attitude Control	10 m/s	180 deg	98%	50%	192.40	22.4	2771.8
SUB TOTAL	93 m/s					161.9 kg	2749.5
Residual Fuel						1.9 kg	
TOTAL						163.8 kg	

TABLE 7.1.3-1 HERSCHEL DELTA-V AND FUEL BUDGET

7.1.3.2. PLANCK Delta-V and fuel budget

The PLANCK Delta-v and fuel budget is shown in Table 7.1.3-2.

For PLANCK, due to the fact that the spacecraft attitude is almost fixed, the thrusters cannot always be aligned with the Delta-V direction. Even if the thruster configuration has been chosen to maximise efficiency, some maneuvers have to be decomposed. This leads to a loss of efficiency which has been included in the fuel budget.

The allocation for attitude control is sized to allow spin re-orientation maneuvers during 2.5 years, plus an allocation for safe mode.

Taking into account the RCS subsystem configuration, a residual mass of 2 kg and a pressurant mass of 5.3 kg has been derived.

The Fuel total mass of 305 kg fits into the baseline Fuel tanks, with a margin above the 20 % specified in SMRC-025.

MANEUVER	Delta-V	SAA	Efficiency	Margin	Isp [sec]	Fuel [kg]	S/C Mass [kg]
Perigee variation	14 m/s	150-180	83%	10%	221.59	12.5	1472
Removal of launcher dispersion	50 m/s	any	48%	10%	221.59	74.7	1459.5
Maneuver 2	4 m/s	any	48%	10%	217.94	5.9	1384.8
Midcourse	3 m/s	any	48%	10%	217.90	4.4	1378.9
Orbit insertion	250 m/s	125 deg	91%	10%	216.62	180.9	1374.5
Injection correction	5 m/s	28.4 deg	54%	10%	215.85	5.7	1193.6
Orbit maintenance	6 m/s	28.4 deg	54%	50%	215.63	9.3	1187.8
Attitude Control	9 m/s		98%	50%	171.79	9.6	1178.6
SUB TOTAL	341 m/s					303.0	1169.0 kg
Residual Fuel						2.0	
TOTAL						305.0 kg	

TABLE 7.1.3-2 PLANCK DELTA-V AND FUEL BUDGET

7.1.4. Link budgets

This section summarizes the system margins in the same format as the one used during the proposal. The complete set of link budgets is provided by ALENIA in Section 7 of the SVM Budget Report.

NOTE: The type 2 antenna gain data have been used here to refine the system link budgets, considering the outcomes of section § 6.1.5.

The uplink budget is given in Table 7.1.4-1.

The downlink budget is given in Table 7.1.4-2.

Common up- and downlink budgets are raised for HERSCHEL and PLANCK. The worst case is always taken into account, and is referred in the "Antennas" column of Tables 7.1.4-1 and 7.1.4-2.

As identified in the first issue of link budgets, the uplink peformances are marginal with Kourou ground station when using the Low Gain Antennae (LGA). Yet, the telemetry subcarrier recovery margins remain largely acceptable.

No criticality is identified on the uplink budgets.

Comfortable margins achieved on all downlinks except when using the redundant LGA (emergency mode) with Kourou ground station however this scenario remains a very worst case and the require link budgets margins are still justified.

Here as well no criticality identified on the downlink budgets.

UPLINK BUDGETS				KOUROU G/S				NEW NORCIA (PERTH) G/S			
			Mode	TC + RNG	TC only	TC + RNG	TC + RNG	TC + RNG	TC only	TC + RNG	TC + RNG
			Antennas								
			H/P nominal LGA	x				x			
			PLANCK redundant LGAs		x				x		
			H/P MGA			x	x			x	x
			BIT RATE (kbps)	0.125	0.125	0.125	4	4	4	4	4
			S/C ALTITUDE (* 10^6 km)	1.80	1.60	1.80	1.80	1.80	1.80	1.80	1.80
PARAMETER	MARGING	ESA Margin dB		calculated margins (dB)				calculated margins (dB)			
Signal Recovery	Nominal	3		4.50	4.42	21.40	21.40	20.55	19.45	37.45	37.45
	mean -3*sigma	0		0.48	0.50	19.00	19.00	16.73	15.73	35.19	35.19
	margin - wc RSS	0		2.29	2.22	20.01	20.01	18.34	17.25	36.06	36.06
Carrier Recovery	Nominal	3		4.20	4.66	19.87	19.87	20.35	19.16	35.83	36.01
	mean -3*sigma	0		0.02	0.68	17.34	17.34	16.37	15.37	33.46	33.65
	margin - wc RSS	0		1.79	2.25	18.16	18.16	17.94	16.74	34.12	34.30
Telecommand Recovery	Nominal	3		7.60	5.33	22.64	7.59	8.69	5.90	24.68	23.74
	mean -3*sigma	0		3.52	1.46	20.37	5.32	4.82	2.22	22.57	21.61
	margin - wc RSS	0		5.31	3.04	21.17	6.11	6.40	3.61	23.21	22.26

TABLE 7.1.4-1 UPLINK BUDGET MARGINS

DOWNLINK BUDGETS			Mode / Antennas	**KOUROU G/S**					**NEW NORCIA G/S**				
	DOWNLINKS		Mode	TM only	TM+RNG+TC echo	TM only	TM only	TM+RNG+TC echo	TM only	TM+RNG+TC echo	TM only	TM+RNG+TC echo	TM only
			H/P nominal LGA	x	x				x	x			
			PLANCK redundant LGAs			x					x	x	
			H/P MGA				x	x					x
			BIT RATE (kbps)	0.5	0.5	0.5	107	107	5	5	5	5	1500
			S/C ALTITUDE (* 10^6 km)	1.80	1.80	1.60	1.80	1.80	1.80	1.80	1.80	1.80	1.80
PARAMETER	MARGING	ESA Margin dB		*calculated margins (dB)*					*calculated margins (dB)*				
Carrier Recovery	Nominal	3		5.20	5.20	3.12	18.77	18.84	19.91	20.07	17.47	17.51	33.63
	mean -3*sigma	0		2.08	2.08	0.10	13.21	13.23	17.43	17.52	15.16	15.19	28.07
	margin - wc RSS	0		2.78	2.78	0.71	14.19	14.22	18.01	18.12	15.72	15.74	29.05
Telemetry Recovery	Nominal	3		5.54	5.55	3.46	4.95	5.02	7.25	7.41	4.81	4.84	5.33
	mean -3*sigma	0		2.71	2.71	0.73	3.30	3.37	5.45	5.62	2.98	3.03	3.72
	margin - wc RSS	0		3.43	3.44	1.36	3.77	3.84	6.00	6.17	3.52	3.56	4.15

TABLE 7.1.4-2 DOWNLINK BUDGET MARGINS

7.1.5. Pointing budgets

7.1.5.1. Definition of errors

The following terminology is used:

- **Absolute Pointing Error (APE):** is the angular separation between the desired direction and the instantaneous actual direction.

- **Pointing Drift Error (PDE):** is the angular separation between the short time average pointing direction during some time interval and a similar average pointing direction at a later time.

- **Relative Pointing Error (RPE):** is the angular separation between the instantaneous pointing direction and the short time average pointing direction during some time interval. This is also known as the pointing stability.

- **Attitude Measurement Error (AME):** is the instantaneous angular separation between the actual and the measured pointing direction. This performance requirement is referred to as 'a posteriori knowledge'.

- **Absolute Rate Error (ARE):** is the difference between the actual and the controlled angular rate about the satellite spin axis.

In addition, for the **HERSCHEL Mission**, the following "unconventional" term is definedwhich is specifically applicable to modes where a number of pointings are commanded relatively close to each other (e.g. for raster pointing).

- **Spatial Relative Pointing Error (SRPE):** is the angular separation between the average orientation of the satellite fixed axis and a pointing reference axis which is defined relative to an initial reference direction.

In addition, for the **PLANCK mission**, the following term is defined which is specifically applicable to efficiently cover portions of the sky which have been 'missed', by returning to a previous pointing with an accuracy compatible with the nominal scan width.

- **Pointing Reproducibility Error (PRE):** is the angular separation between the average actual pointing direction at one time and the achieved average pointing direction of that same commanded direction at a later time. The PRE is given over 20 days.

Unless otherwise specified, the pointing error specifications are expressed as half-cone angles of the optical axis and half-sector angle around the optical axis. They are specified at a temporal probability level of 68 %, which implies that error will be less than the requirement for 68 % of the time.

7.1.5.2. Herschel pointing budget

This sections is split into:

- – a synthesis of all pointing budgets, requirements and goals

- – a list of error sources

- – summation rules for budgets compilation

- – description and justification of sources

- – budgets compilation

7.1.5.2.1. Pointing Budget Synthesis

The following tables summarises Herschel pointing budgets:
All values are at 68% confidence level as required.

	Half cone (arcsec)			Roll (arcmin)		
	Reqt.	Perfo.	Goal	Reqt.	Perfo.	Goal
APE (inertial mode)	3.7	1.49	1.5	3.0	0.65	3.0
APE (scanning mode)	3.7 + 0.05 × ω	1.49 + 0.023 × ω	1.5 + 0.03 × ω	N/A		
PDE after 24 hours	1.2	0.29	N/A	3.0	0.34	N/A
RPE over 1 min (inertial mode)	0.3	0.25	0.3	1.5	0.16	1.5
RPE over 1 min (scanning mode)	1.2	1.1	0.8	1.5	TBD	1.5
AME (inertial mode)	3.1	1.57	1.2	3.0	0.66	3.0
AME (scanning mode)	3.1 + 0.03 × ω	1.57 + 0.021 × ω	1.2 + 0.02 × ω	3.0	TBD	3.0

Note: w is given in arcsec/sec.

Herschel pointing performance is compliant with the requirements.

The AME and RPE around LOS in scanning mode remain to be evaluated. However, it is expected that the compliance to the requirement (and the goals which are identical to the requirements) will be achieved, by similarity to all pointing requirements around LOS that are met with large margins.

The AME goals in inertial mode (1.2") and in scanning mode (1.2"+0.02×ω) should be achievable by reducing the impact of the star tracker bias (by calibration) and by using bright stars in the STR field of view.

The 0.8'' RPE goal is met when the scanning angular rate is below 40 arcsec/sec, i.e. two thirds of the maximum rate.

Other goals are achieved: APE in inertial and scanning mode (half-cone and Roll), RPE in inertial mode (half-cone and roll).

7.1.5.2.2. Pointing Budgets error sources and related time scales

The various error sources are summarised hereafter. There are 3 error classes:

- B = static (Bias)

- D = periodic or variable over time scales larger than the duration over which the RPE is specified (1 minute)

- N = high frequency.

All errors in the following table are given for a single axis, and at 68% confidence level (equivalent to 1σ for a gaussian noise):

ARCSEC		B	D	N	Comments
PLM support drift around Y	D_{PLM_Y}		0.22		Thermal analysis
PLM support drift around Z	D_{PLM_Z}		ε		Thermal analysis
SVM drift around Y	D_{SVM_Y}		0.17		Thermal analysis
SVM drift around Z	D_{SVM_Z}		ε		Thermal analysis
FSS bias	$B1_{FSS}$	33			Equip. Req.
FSS drift	$D1_{FSS}$		20		Equip. Req.
FSS noise	$N1_{FSS}$			1.66	Equip. Req.
STR bias full FOV	$B1_{STR}$	1			Equip. Req.
STR resolution	D_{STR}		0.06		Equip. Req.

ARCSEC		B	D	N	Comments
STR delay induced trail error	D_{STR_SCAN}			0.12	Equip. Req.
STR noise	N_{STR}			1.3	Equip. Req.
CTRL limit cycle inertial	N_{CTL1}			0.16	Simulation
CTRL limit cycle scan (scan axis)	N_{CTL2}			1.1	Simulation
Star catalogue error	B_{CAT}	0.1			-
Sun propagation error	B_{SUN}	7.2			-
Relative meas. Error inertial	N_{mes1}			0.24	Simulation
Relative meas. Error scan	N_{mes2}			1.15	Simulation
RW microvibration	N_{RW}			0.005	Preliminary analysis
PACS Centroid Bias	B_{PACS}	0.17			

7.1.5.2.3. Summation rules

In accordance with ESA Pointing Error Handbook (section 2-5, methods for budget compilations), the following rules are applied:

– budget are summed quadratically within a frequency class, except when they are dependent one from another. In this case, a linear sum is performed.

– for each axis, the pointing budget is obtained by the linear sum of the pointing contributions of all frequency classes.

– at a first step, the half cone budget at 68% confidence level is obtained by the quadratic sum of the 1σ budget of the two axes. During the design phase, a more fitting formula will be calculated.

7.1.5.2.4. Main contributor description and justification

– The thermo-elastic errors presented in the above table are derived from thermal analysis, considering worst attitude to Sun. This results in a gradient variation of +/- 4.5 K on the SVM and +/-1.5 K on the PLM around the Y-axis. Around Z-axis the gradient are very small and can be neglected. 1 ? values are determined considering an homogeneous repartition of the pointing attitude w.r.t. Sun.

Currently the thermal evolution of the structure can be modelled as a function of the attitude with a > 50 % accuracy, thus improving the budgets and providing margins.

– The **Star Tracker performances** are based on the equipment requirement, which performances are compatible of existing or on-going development equipment.

– **Control limit cycle:** the value is based on simulations. For Line scanning the error is evaluated for a worst case 60 arcsec/s rotation rate and is applicable along the rotation axis. Transverse error are the same as inertial pointing.

– **Star catalogue errors** are expected to be close to 0 based on Hipparcos catalogue. A value of 0.1 arcsec has been taken into account in the ACMS pointing budget.

– The **relative measurement error** is the short term measurement error. It is given by the performance of the gyro-stellar filter.

– **Attitude dynamic measurement and control error** contribution have been evaluated by simulations.

– **RW Microvibrations** induces minor error on the line of sight, below 0.005″ at low frequency (< 20 Hz), where the spacecraft can be considered as a rigid body. At higher frequencies, structural resonances can occur which can results in error amplification. Amplifications up to a pessimistic factor 20 are compatible to the pointing budgets. Such amplifications are of short duration, as the RW rotation rate is evolving, and have consequently minor consequences on a 1σ budget.

– **PACS centroiding bias:** PACS photometer in the short wavelength has a pixel field of view of 3.3 arcsec. Using a centroiding algorithm, the maximum deviation is estimated by analysis to 15% of a pixel. Considering this error is a 3σ value, this leads to a PACS bias of:

BPACS = 3.3 × 0.15 / 3 = 0.17 arcsec

7.1.5.2.5. Calibration

In order to achieve the best performances the long term error between the instrument reference and the scientific mode attitude sensors have to be calibrated. The calibration phase aims mainly at the suppression of the bias errors, though some thermal error calibration will also be performed to improve the pointing budget.

The following calibrations will be performed:

- **STR/FSS calibration:** The calibration will be performed by pointing the satellite in an attitude such that 2 well known reference stars are in the STR boresight. The 2 stars enable the determination of the rotation around the STR line of sight, which can be compared with the FSS measurements. In order to improve the measurement this calibration will be performed with different reference stars, thus enabling the averaging of noise, FOV non uniformity and star catalogue errors. As the errors are random, the uncertainty on the bias calibration can be driven down to 0.

$$A_{CAL1} = (\sqrt{D_{1,FSS}{}^2 + D_{STR}{}^2} + \sqrt{N_{CTL2}{}^2 + N_{1,FSS}{}^2 + N_{STR}{}^2}) / \sqrt{n_{Calibration}} = 2.0 \text{ arcsec}$$

- **STR/Instrument calibration:** The calibration will be performed such as to point both the instrument and the STR boresight toward stars with well known directions. The PACS photometer array in the short wavelength is the detector with the smallest pixel. It is thus the best suited to perform STR/instrument calibration. As the STR is pointing in the direction opposite to the telescope, pointing a reference star in the centre of the STR Field of view will be difficult, thus resulting in an STR FOV non uniformity driven calibration uncertainty. The Yaw driven uncertainty will previously have been driven to a residual random contribution by the STR/FSS calibration. As the uncertainties are random errors, the calibration will consequently be performed several times in order to reduce the uncertainty.

  The calibration will be performed in Sun pointed attitude to avoid the thermal error and will be completed by pointings with an offset w.r.t. the Sun to calibrate the thermal evolution. Taking into account the calibration duration and the limited amount of suitable reference stars, the number of measurements performed for calibration will be conservatively considered to be below $n_{Calibration} = 100$.

  The calibration error only depends of the following sources:

  - control limit cycle

  - relative measurement error

- PACS centroiding error.

The calibration error writes:

$$A_{CAL2} = (B_{PACS} + D_{STR} + N_{CTL1}) / \sqrt{n_{Calibration}}$$

Thus, $A_{CAL2} = 0.04$ arcsec

- **Gyro calibration (necessary for line scanning):** the gyrometers are used in closed loop in scientific modes. Their bias is continuously calibrated by a Kalman filter based estimator performing the hybridation of STR and FSS measurement with the gyrometers. Thus the STR and FSS outputs are used for the gyrometers bias calibration when available (essentially in inertial and raster pointing mode, unavailability are possible during line scanning). An estimation of the gyros drift is thus continuously available in scientific mode.

- **Star Tracker inter-calibration:** in order to avoid a large interruption of the mission in case of star tracker switching, the two sensors are inter-calibrated from time to time. The calibration residual order of magnitude will be much inferior to the star tracker noise. Since switching to the redundant star tracker is not a nominal operation, this case is not taken into account in the pointing budgets.

7.1.5.2.6.   Budget compilations

Budgets are separated between:

Half-cone = instrument line of sight pointing

Roll = pointing around line of sight

7.1.5.2.6.1. Absolute pointing error in inertial mode

Half-cone

Requirement	Performance	Goal
3.7 "	1.49 "	1.5 "

$$APE = \sqrt{A_{CAL2}{}^2 + B1_{STR}{}^2 + B_{CAT}{}^2} + \sqrt{D_{STR}{}^2 + (D_{PLM} + D_{SVM}{}^2)} + \sqrt{N_{CTL1}{}^2 + N_{RW}{}^2}$$

This leads to:

APE_Y = 1.09"

APE_Z = 1.02"

Roll

Requirement	Performance	Goal
3.0 '	0.65 '	3.0 '

$$APE = \sqrt{A_{CAL1}{}^2 + B1_{FSS}{}^2 + B_{SUN}{}^2} + \sqrt{D1_{FSS}{}^2 + (D_{PLM} + D_{SVM}{}^2)} + \sqrt{N_{CTL1}{}^2 + N_{RW}{}^2}$$

7.1.5.2.6.2. Absolute pointing error in scanning mode

Half-cone

Requirement	Performance	Goal
3.7" + 0.05 ω	1.49 "+ 0.023 ω	1.5" + 0.03 ω

The absolute pointing error in line scanning phases is degraded by two contributions along the rotation axis:

the relative pointing error raises to 1.1 arcsec on the scan axis

the trailing error due to the error on the datation of star tracker data (2 ms). This error is maximum (0.12 arcsec) at maximum scan rate (1 arcmin/sec).

Along the other axis, the APE is the same as in inertial pointing.

The resulting APE is 2.83 arcsec, for a scanning rate of 60 arcsec/sec. Though a comprehensive study for intermediate rates has not been performed yet, one can as a first step assume linearity between:

$\omega = 0$ APE = 1.49"

$\omega = 60$"/s   APE = 2.83"

The linear law is then:

APE = 1.49" + 0.023 ω < 1.5"+ 0.03 ω

7.1.5.2.6.3. Pointing drift error after 24 hours

The pointing budgets are identical in inertial and scanning modes.

Half-cone

Requirement	Performance	Goal
1.2 "	0.29 "	N/A

The pointing drift error over 24 hours is mainly induced by the thermo-elastic distortion. By definition of the PDE, no short time control error is taken into account.

The PDE reduces thus to:

$$PDE = \sqrt{D_{STR}^2 + (D_{PLM} + D_{SVM})^2}$$

PDE_Y = 0.06 arcsec

PDE_Z = 0.28 arcsec

Roll

Requirement	Performance	Goal
3.0 '	0.34 '	N/A

$$PDE = \sqrt{D1_{FSS}^2 + (D_{PLM} + D_{SVM})^2}$$

7.1.5.2.6.4. Relative pointing error in inertial mode over 1 minute

Half-cone

Requirement	Performance	Goal
0.3 "	0.25 "	0.3 "

Simulations have been performed in worst case conditions, i.e. in nodding mode: sequence of 5 arcmin slews in 34 sec. followed by 166 sec. observation cycles, during which the RPE is measured.

The simulations take into account the following features:

- sensors and actuators performance

- time delays between sensors acquisitions and actuators commanding

- dynamic perturbation

- under estimation of system parameters in control law.

The High frequency RW microvibration is added to the simulation results.

Roll

Requirement	Performance	Goal
1.5 '	0.16 '	1.5 '

As for the half-cone error, simulation results have been taken into account.

7.1.5.2.6.5. Relative pointing error in scanning mode over 1 minute

Half-cone

Requirement	Performance	Goal
1.2 "	1.1 "	0.8 "

Simulations have been performed in worst case conditions, i.e. for a scan rate of 1 arcmin/sec along 20 deg long lines. The resulting RPE is 1.1 arcsec on the scan axis.

The High frequency RW microvibration is added to the simulation results.

Combining with the RPE on the other axis (0.21 arcsec), yields a half cone RPE of 1.1 arcsec.

The resulting RPE of 1.1 arcsec is obtained for a scanning rate of 60 arcsec/sec. Though a comprehensive study for intermediate rates has not been performed yet, one can as a first step assume linearity between:

$\omega = 0$ RPE = 0.25"

$\omega = 60"/s$ RPE = 1.1"

The linear law is then:

RPE $= 0.25" + 0.014\ \omega$

The goal is achieved when $0.25" + 0.014\ \omega < 0.8"$, i.e. for $\omega < 40$ arcsec/sec.

Roll

Requirement	Performance	Goal
1.5 '	TBD	1.5 '

To be evaluated.

7.1.5.2.6.6. Absolute measurement error in inertial mode

Half-cone

Requirement	Performance	Goal
3.1 "	1.57 "	1.2 "

The absolute measurement error is given by:

$$AME = APE + N_{mes1} - N_{CTL1}$$

Roll

Requirement	Performance	Goal
3.0 '	0.66 '	3.0 '

The absolute measurement error is given by:

$$AME = APE + N_{mes1} - N_{CTL1}$$

7.1.5.2.6.7. Absolute measurement error in scanning mode

Half-cone

Requirement	Performance	Goal
3.1 " + 0.03 ω	1.57 " + 0.021 ω	1.2 " + 0.02 ω

The absolute measurement error in line scanning mode is

$AME = APE + N_{mes2} - N_{CTL2}$

The resulting AME is 2.85 arcsec, for a scanning rate of 60 arcsec/sec. Though a comprehensive study for intermediate rates has not been performed yet, one can as a first step assume linearity between:

$\omega = 0$ AME = 1.57"

$\omega = 60"/s$ AME = 2.85"

The linear law is then:

AME = 1.57" + 0.021 ω > goal = 1.2"+ 0.02 ω

Roll

Requirement	Performance	Goal
3.0 '	0.66 '	3.0 '

The absolute measurement error in line scanning mode is

AME = APE + N_{mes2} - N_{CTL2}.

7.1.5.3. Planck pointing budget

This sections is split into:

- a synthesis of all pointing budgets, requirements and goals

- a list of error sources

- summation rules for budgets compilation

- description and justification of sources

- budgets compilation

7.1.5.3.1. Pointing Budget synthesis

The following tables summarises Planck pointing budgets:

All values are at 68% confidence level as required.

	Half cone (arcmin)			Yaw (arcmin)		
	Reqt.	Perfo.	Goal	Reqt.	Perfo.	Goal
APE	37	16.8	N/A	37	13.4	25
PDE after 24 hours	6.2	2.0	N/A	6.2	1.6	N/A
RPE over 55 min	1.5	1.1	N/A	10	1.0	N/A
AME	1.0	1.0	0.5	6	3.0	3
PRE over 20 days	2.5	TBD	N/A	37	TBD	25

The pointing performances are compliant with the specifications.

The Pointing Reproducibility Error is to be evaluated.

The goal of 0.5 arcmin for AME may be met by improved calibration and on-ground processing of STM data. Further ACMS analyses will consolidate this statement.

The other goals are achieved: APE and AME in yaw.

7.1.5.3.2. Pointing Budgets error sources and related time scales

The various frequencies to be considered in the pointing error budget are:

B	Biases	0 Hz
C	Calibration frequency	$1/T_{cal}$ (T_{cal} = time between 2 calibrations)
D	Observation Period/PDE horizon	1/24 hours
R	Slew frequency/RPE horizon	1/1 hour
N	Nutation frequency	0.04 Hz = 1/260 sec

The various error sources are listed in the following table:

	ARCMIN	B	C	D	R	N
S1	STM/X noise					0.17
S2	STM/Y noise					0.17
S3	STM calib/X		0.17			
S4	STM calib/Y		0.17			
D1	Detector calib/X		0.35			
D2	Detector calib/Y		0.35			
D3	Detector calib/Z		3.00			
T1	Telescope alignment/XY	11.70				
T2	Telescope alignment/Z	7.80				
F1	Focal Plane alignment/XY	0.25				
F2	Focal Plane alignment/Z	0.25				
D4	Detector alignment/XY	1.35				
D5	Detector alignment/Z	1.35				
W1	Wobble/Y	4.00	0.00	1.60		
W2	Wobble/Z	6.00	0.43	0.80		
N	Nutation					1.0
SP	Solar Pressure			2.40	0.10	
ΔH	ΔH error				0.17	

7.1.5.3.3.   Summation rules

In accordance with ESA Pointing Error Handbook (section 2-5, methods for budget compilations), the following rules are applied:

– budget are summed quadratically within a frequency class, except when they are dependent one another. In this case, a linear sum is performed.

– for each axis, the pointing budget is obtained by the linear sum of the pointing contributions of all frequency classes.

– at a first step, the half cone budget at 68% confidence level is obtained by the quadratic sum of the 1σ budget of the two axes. During the design phase, a more fitting formula will be calculated.

7.1.5.3.4. Main contributor description and justification

Mechanical Alignment

The mechanical alignment are driving the pointing performances and cannot be compensated by calibration as the satellite is spinning.

The telescope alignment of 11.7 arcmin in XY plane and 7.8 arcmin along Z is consistent with the alignment budget of section 7.1.9.

<u>Star Mapper</u>

The star mapper performance is 1 arcmin, 1 σ over one satellite revolution in worst case conditions (3 stars detected). However, its precision is expected to be higher in most cases. A posteriori filtering of the star mapper data over 1 hour reduces its contribution to the AME to 10 arcsec on each axis (scan axis and elevation axis).

Solar pressure torque

The transverse solar pressure torque is maximum when the SAA is maximum (10 deg.). Its direction is constant in inertial space, and therefore causes an angular momentum drift, estimated to:

α = 0.5 arcmin / hr.

The deviation of the LOS from the average circle it describes over 60 min is:

$e(t) = \cos \boldsymbol{w} t \sin\left(\frac{t-30'}{60'}\boldsymbol{a}\right)$ where ω (=0.1 rad/sec) is the rotation rate

which 1σ deviation (in the sense of a temporal probability) is 0.1 arcmin.

The contribution to the RPE is thus 0.1 arcmin.

Nutation

There is only one nutation source: the inaccuracy of the THR pulses during NAMs.

An allocation of 1 arcmin is made, which is in consistent with the analyses in the PND/AND trade-off technical note. The option used is the "Star Mapper only", without gyrometer and PND.

Fuel sloshes

Sloshes of fuel excited by NAM have been shown to not significantly affect the pointing stability.

LOS Pointing requirement definition

The target trajectory of the LOS on the celestial sphere is a circle with a radius of 85 deg. The actual trajectory is derived from the theoretical by introducing 3 types of errors, illustrated on the following figure:
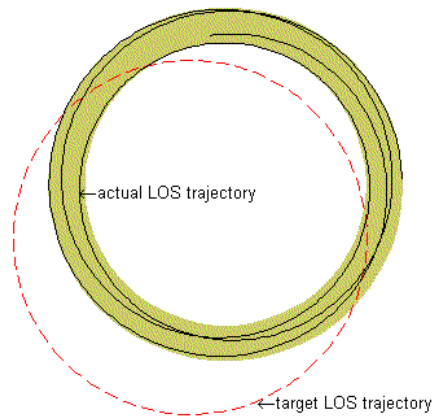
The 3 types of errors are:

– the **position error $\delta\alpha$ of the circles centre**, i.e. the orientation error of the satellite angular momentum w.r.t. inertial space.

– The **error $\delta\beta$ in the radius of the circle**, with 2 contributors:

  • the wobble projection in the XZ plane

  • the instrument LOS alignment error in the XZ plane.

– The **jitter of the LOS around the average circle**, due to the nutation and to the drift of the circle centre. The envelope of the LOS motion forms a strip with a width θ_{jitter}.

The Pointing budget items are defined as follow:

– the **Absolute Pointing Error** is the maximum distance from any point in the jitter strip to the target circle, i.e.:

$$APE = \delta\alpha + \delta\beta + \theta_{jitter}/2.$$

– The **Pointing Drift Error** is the angular drift over 24 hours of the average circle centre.

- The **Relative Pointing Error** is the half the width of the jitter strip $\theta_{jitter}/2$ + the drift of the circle's centre over 55 minutes.

- The **Absolute Measurement Error** is the instantaneous angular separation between the estimated LOS and the actual LOS direction in inertial space.

- The **Pointing Reproducibility Error** is than angular separation between the 2 average circles obtained in 2 pointing attempts performed at 2 different times with the same pointing target w.r.t. inertial space.

Around LOS pointing requirement definition

Due to the wobble, to the nutation the rotation axis in satellite frame is not exactly along X, as displayed on the following diagram:
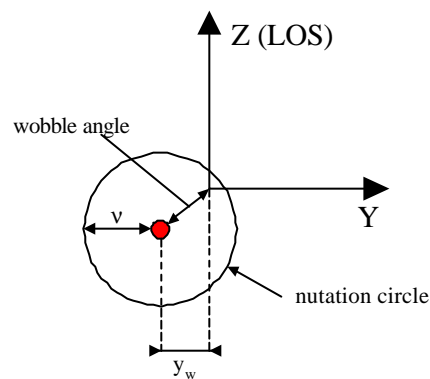
Nominally, the scan direction, in the focal plane should be along the Y satellite axis. Du to the wobble and to the nutation the actual scan direction is tilted by the angle θ:

$$\theta_{sat} = (y_w + \nu)/\sin(85°) \approx (y_w + \nu).$$

The total pointing error around the LOS is the sum of θ_{sat} and of the alignment error of θ_{inst}, the focal plane around the LOS.

The definition of the various errors is then derived as follows:

- The Absolute Pointing Error is:

$$APE = \theta_{sat} + \theta_{inst}.$$

- The Pointing Drift Error is the sum of the drifts over 24 hours of y_w and θ_{sat}.

- The Relative Pointing Error is the nutation angle ν.

- The Absolute Measurement Error is the estimation error of $\theta_{sat} + \theta_{inst}$.

- The Pointing Reproducibility Error is the sum of the drifts over 20 days of y_w and θ_{sat}.

7.1.5.3.5. Budget compilations

Budgets are separated between:

- **Half-cone** = instrument line of sight pointing

- **Yaw** = pointing around line of sight

7.1.5.3.5.1. Absolute Pointing Error

Half-cone

Requirement	Performance	Goal
37 '	16.8 '	N/A

The contributions to the Absolute Pointing Error budget are:

- the alignment between the telescope LOS and the star mapper LOS.

- The angular momentum pointing accuracy which contains two terms:

- the measurement error

- the nutation avoidance manoeuvre accuracy.

- The pointing drift error.

- The relative pointing error.

Combining the error sources yields:

$$APE_{LOS} = PDE_{LOS} + RPE_{LOS} + \sqrt{W2_B^2 + T1_B^2} + \sqrt{S3_C^2 + S4_C^2 + D1_C^2 + D2_C^2}$$

Yaw

Requirement	Performance	Goal
37 '	13.4 '	25 '

The absolute pointing error around LOS writes:

$$APE_{YAW} = RPE_{YAW} + PDE_{YAW} + \sqrt{W1_B{}^2 + T2_B{}^2} + D3_C$$

7.1.5.3.5.2. Pointing Drift Error after 24 hours

Half-cone

Requirement	Performance	Goal
6.2 '	2.0 '	N/A

The 1 σ PDE requirement for LOS is 6.2 arcmin over 24 hours.

The solar pressure contribution is 12 arcmin/day (maximum value, for SAA = 10 deg.). However, it is deterministic and can be taken into account in the NAM schedule.

It is computed as follows:

$$PDE_{LOS} = \sqrt{T1_D{}^2 + F1_D{}^2 + D4_D{}^2 + W2_D{}^2 + 48\,\Delta H^2}$$

Yaw

Requirement	Performance	Goal
6.2'	1.6 '	N/A

The 1 σ requirement for the PDE around LOS is 6.2 arcmin over 24 hours.

It is computed as follows:

$$PDE_{YAW} = T2_D + F2_D + D5_D + W1_D.$$

7.1.5.3.5.3. Relative Pointing error over 55 minutes

Half-cone

Requirement	Performance	Goal
1.5 '	1.1 '	N/A

The relative pointing error requirement is as follows:

- amplitude (68 % of time) < 1.5 arcmin

- time horizon = 55 minutes.

The time horizon is shorter than the expected interval between two angular momentum corrections. Therefore, only two significant contributions enter the RPE budget:

- the angular rate of the spin direction induced by solar pressure

- the satellite residual nutation at the end of the last nutation avoidance manoeuvre.

The RPE budget is summarised in the following table:

Solar pressure contribution	0.1 arcmin
Nutation contribution	1.0 arcmin
RPE_{LOS} (1 σ)	1.1 arcmin

Yaw

Requirement	Performance	Goal
10 '	1.0 '	N/A

The relative pointing error around LOS reduces to the nutation contribution:

$$RPE_{YAW} = 1.0 \text{ arcmin}$$

7.1.5.3.5.4. Absolute Measurement Error

Half-cone

Requirement	Performance	Goal
1.0 '	1.0 '	0.5 '

The restitution of the instrument LOS pointing history relies on the star mapper data.

The AME budget writes:

$$AME_X = S1_N + \sqrt{S3_C{}^2 + D1_C{}^2 + T1_C{}^2 + F1_C{}^2 + D4_C{}^2}$$

$$AME_Y = S2_N + \sqrt{S4_C{}^2 + D2_C{}^2 + T1_C{}^2 + F1_C{}^2 + D4_C{}^2 + W2_C{}^2}$$

$$AME_{LOS} = \sqrt{AME_X{}^2 + AME_Y{}^2}$$

The performance is mainly driven by the STM noise, the detector calibration, and the wobble calibration. The goal of 0.5 arcmin for AME may be met by improved calibration and on-ground processing of STM data. Further ACMS analyses will consolidate this statement.

Yaw

Requirement	Performance	Goal
6.0 '	3.0 '	3.0 '

The absolute measurement error around LOS writes:

$$AME_{YAW} = \sqrt{D3_C{}^2 + T2_C{}^2 + F2_C{}^2 + D5_C{}^2 + W1_C{}^2}$$

The performance is driven by the calibration of detector.

7.1.5.3.5.5. Pointing Reproducibility Error over 20 days

Half-cone

Requirement	Performance	Goal
2.5 '	TBD	N/A

Yaw

Requirement	Performance	Goal
37 '	TBD	25 '

7.1.6. Data handling and software budgets

7.1.6.1. CDMU Mass memory

The basic requirement for mass memory sizing is MOOM-220 which specifies that all mission data generated during 48 hours shall be stored on-board.

The major contributor to mass memory sizing is the payload, which generates data rates of at least 100 kbps (SINT-040 and SINT-045 of SRS).

Taking into account an allocated 5 kbps average rate for satellite housekeeping, the required storage is 18.1 Gbit. A mass memory of **25 Gbit** end of life is planned on HERSCHEL and PLANCK thus providing a margin of 38 %. This margin allows to go to an allocation of 140 kbps (maximum average), as described in section 6.1.4.

During the Daily TeleCommunication Period (DTCP), the volume of downlinked data can reach 16 Gbit (1.5 Mbps × 3 hours), i.e. more than the mass memory can store in one day (17.3 Gbit/2 < 9 Gbit). The DTCP is therefore not a sizing case for the mass memory capacity.

7.1.6.2. CDMU Bus traffic

The main contributors are the instruments:

– specified to 100 kbps in nominal conditions

– the prime allocation allows 140 kbps as a maximum average.

The SVM contributors are:

– PCDU

– ACC.

Their allocated contribution is evaluated to 5 sub-frames every second, to be taken from the 64 available in total.

The total sub-frame allocation (see Section 6.1.4) is **30 frames out of 64**, giving **113 % margin**.

7.1.6.3. CDMU TM/TC budgets

HERSCHEL and PLANCK budgets, including margins, are presented in Tables 7.1.6-1 and 7.1.6-2.

Subsystem	Unit	High Priority Cmds	High Level Cmds	Ext. High Level Cmds	Low Level Cmds	ML16	An Mn	Therm	Therm PT	Relay Status	Bi-level	SBDL Status Lines	DS16	RM Alert Inputs	131 kHz LOBT Sync
Power	PCDU	16					2			8	2			4	
	Battery						4								
TT&C	XPND1	2	2			2	12			4	2		6	2	
	XPND2	2	2			2	12			4	2		6	2	
	RFDN	16	8	8			6			16					
	TWTA1	4	4				2			2					
	TWTA2	4	4				2			2					
TCS								120							
ACMS	ACC	8	8		8		6				16			4	2
RCS	LVs									2					
CDMS	CDMU	8					8				24			2	
PLM	VMC					1							1		
	SREM					1							1		
	CCU		8												
HIFI	LOU														
PACS							12								
SPIRE	HSFCU									6					
								3							
Total		**60**	**36**	**8**	**8**	**6**	**54**	**135**	**0**	**44**	**46**	**0**	**14**	**14**	**2**
Allocated		**80**	**80**	**16**	**16**	**14**	**80**	**192**	**64**	**80**	**64**	**8**	**14**	**16**	**16**
Margin		**20**	**44**	**8**	**8**	**8**	**26**	**57**	**64**	**36**	**18**	**8**	**0**	**2**	**14**

TABLE 7.1.6-1 HERSCHEL CDMU TM/TC BUDGET

Subsystem	Unit	High Priority Cmds	High Level Cmds	Ext. High Level Cmds	Low Level Cmds	ML16	An Mn	Therm	Therm PT	Relay Status	Bi-level	SBDL Status Lines	DS16	RM Alert Inputs	131 kHz LOBT Sync
Power	PCDU	16					2			8	2			4	
	Battery						4								
TT&C	XPND1	2	2			2	12			4	2		6	2	
	XPND2	2	2			2	12			4	2		6	2	
	RFDN	16	8	8			6			16					
	TWTA1	4	4				2			2					
	TWTA2	4	4				2			2					
TCS								120							
ACMS	ACC	8	8		8		6				16			4	2
RCS	LVs									2					
CDMS	CDMU	8					8				24			2	
PLM	VMC					1							1		
	SREM					1							1		
HFI	DPU								28						2
LFI	REBA														2
	DAE							1	2						2
SCS	SCE														
Total		44	28	8	8	6	52	121	30	30	44	0	14	10	8
Allocated		80	80	16	16	14	80	192	64	80	64	8	14	16	16
Margin		36	52	8	8	8	28	71	34	50	20	8	0	6	8

TABLE 7.1.6-1 PLANCK CDMU TM/TC BUDGET

7.1.6.4. CDMU Processing load

The ERC32 is expected to have sufficient processing capability (**8 Mips**) for HERSCHEL and for PLANCK CDMS tasks.

The processing load margins will be quantified in the design phase.

7.1.6.5. CDMU Memory

The ERC32 is expected to have sufficient memory capability (**6 Mbyte RAM, 1 Mbyte EEPROM**) for HERSCHEL and for PLANCK CDMS tasks.

The memory margins will be quantified in the design phase.

7.1.6.6. ACC bus traffic

7.1.6.6.1. HERSCHEL ACC

HERSCHEL has four subscribers:

– **one** on the nominal Star Tracker

– **one** on the redundant Star Tracker

– **two** on the gyrometer (one unit with two couplers).

The bus traffic is sized by telemetry (Star Tracker and gyrometer measurements), and is dimensioned as a first step by:

– maximum rate 8 Hz

– star tracker: 40 16-bit words per cycle

– gyrometer: 40 16-bit words per cycle.

Even if all subscribers are used, i.e. one Star Tracker and gyro measurements used in the ACMS loop, while the other Star Tracker is monitored, the maximum telemetry rate is 15360 bps, **representing about 3 % of the bus capacity**.

7.1.6.6.2. PLANCK ACC

PLANCK has no 1553B data bus subscribers.

7.1.6.7. ACC TM/TC budgets

The following I/O interfaces are allocated to the ACC:

- for both spacecraft:

    - 40 HLC/40 DR

    - Reconfiguration module: 80 HLC.

- HERSCHEL ACMS equipment (not selected yet) on discrete lines:

    - 4 reaction wheels I/F

    - 4 Sun acquisition sensors I/F

    - 2 fine Sun sensors I/F

    - 12 10-newton thrusters I/F

    - 2 quartz resonating sensors I/F.

- PLANCK ACMS equipment (not selected yet) on discrete lines:

    - 2 star mappers I/F

    - 6 Sun acquisition sensors

    - 2 attitude anomaly detectors

    - 12 10-newton thrusters

    - 4 1-newton thrusters

    - 2 quartz resonating sensors.

7.1.6.8. ACC Processing load

The ERC32 is expected to have sufficient processing capability (**8 Mips**) for HERSCHEL and for PLANCK ACMS tasks.

The processing load margins will be quantified in the design phase.

7.1.6.9. ACC Memory

The ERC32 is expected to have sufficient memory capability (**6 Mbyte RAM, 1 Mbyte EEPROM**) for HERSCHEL and for PLANCK CDMS tasks.

The memory margins will be quantified in the design phase.

7.1.7. Cleanliness budgets

The following budgets have been built from budgets which were approved by the Cleanliness Working Group. They represent a compromise cost/performance at each state of life of the different parts. They are included in the Cleanliness Requirement Specification (AD07.3). They concern, for each of both particular and molecular aspects:

- Herschel instruments

- Herschel telescope

- Planck instruments

- Planck telescope.

Due to its particular design, LOU windows of HIFI instrument on Herschel does not have the same budgets of contamination, although specifications are the same. Realistic specific budgets are ongoing, and will be built during Phase B.

The following general hypothesis were made while building Herschel and Planck cleanliness budgets:

- 1 vacuum test (without any vacuum break) is equivalent to: 25ppm
  $2.10^{-8} g/cm^2$

- 1 day in Class 100 000 is equivalent to: 225ppm
  $3.10^{-9} g/cm^2$

- 1 day in Class 10 000 is equivalent to: 60ppm
  $3.10^{-9} g/cm^2$

- contamination during transport: 15ppm
  $< .10^{-8} g/cm^2.$

Dust particle have a statistical distribution: The particle size distribution is considered in accordance with the standard: MIL-STD-1246-B.

One of the main contributors for particulate contamination is the launch phase: time under fairing and vibro-acoustical redistribution during launch:

- under fairing is assimilated to Class 100000 (could be reduced to 10000 at the time of Herschel/Planck launch)

- considering values given by ESA and derived from acoustic tests of ARIANE 5 fairing, front exposed surfaces as the Herschel Primary mirror are supposed to receive 1600 ppm. Another - American- source leads to a cleanliness level equivalent to 1000 ppm.

On ground molecular contamination comes from environment, facilities, people, GSE, etc …

In order to reach required contamination allocation, bake out of some elements will have to be considered (in particular paints, harness, Carbon structure elements and MLI's). Bake-out of Herschel cryostat is planned to be performed.

Main in-flight molecular contamination sources are:

- water-ice deposition on cold optical and thermal surfaces from material out-gassing

- water ice and ammonia ice (NH3) deposition on cold optical and thermal surfaces from back-scattering of propulsion exhaust gas.

E-PLM and spacecraft integration shall not contribute to the molecular contamination for more than 10^{-6} g/cm^2.

Spacecraft subsystems and units shall be delivered with a molecular cleanliness better than 10^{-6} g/cm^2

7.1.7.1. Budget for particulate contamination for Herschel instruments (inside cryostat)

Following budget describes particulate contamination levels of Herschel instruments from the beginning to the end of life, taking into account the following hypothesis.

These instruments (except LOU windows) are inside a closed cryostat from cryostat closure to its in flight opening, and no particulate contamination is supposed to happen during this period.

The non-sensitive external surfaces of the spacecraft will have a contamination level lower than 10000 ppm (TBC) before encapsulation. With such a level, in-orbit particle redistribution is estimated to be negligible inside the cryostat.

Micrometeorite impact is estimated to be less than 100 ppm over the whole life in orbit (3.5 year).

PHASE		CONTRIBUTION	TOTAL	SPECIFICATION (TOTAL)
Instruments at delivery		300 ppm	300 ppm	300 ppm
PLM integration till cryostat closure	15 days in Class 10000	900 ppm	1200 ppm	1200 ppm
Spacecraft AIT till encapsulation	Instruments inside cry-cover	0 ppm	1200 ppm	1200 ppm
Spacecraft launch campaign	7 days under Class 100000 fairing	0 ppm	1200 ppm	
Launch		0 ppm	1200 ppm	
Micrometeorite and redistribution		350 ppm	1550 ppm	1550 ppm

OBSTRUCTION FACTOR IN PPM

7.1.7.2. Budget for particulate contamination for Herschel telescope

Following budget describes particulate contamination level of Herschel telescope from the beginning to the end of life, taking into account the following hypothesis.

The exposure time of the telescope during E-PLM and spacecraft integration is estimated to be 15 days in Class 10000. These days stand for AIT, alignment tests, vibration tests, acoustic tests, preparation to thermal tests … Out of this tests, the telescope is protected by a hard cover, which is removed before fairing installation (7 days before launch). During mechanical tests, it can be envisaged to protect the telescope by a protective foil.

The non-sensitive external surfaces of the spacecraft will have a contamination level lower than 10000 ppm (TBC) before encapsulation. With such a level, in-orbit particle redistribution is estimated to be less than 250 ppm (TBC) on the telescope.

Micrometeorite impact is estimated to be less than 100 ppm over the whole life in orbit (3.5 year).

PHASE		CONTRIBUTION	TOTAL	SPECIFICATION (TOTAL)
Telescope at delivery		300 ppm	300 ppm	300 ppm
Spacecraft AIT till encapsulation	15 days in Class 10000 without covers	900 ppm	1200 ppm	1500 ppm
Spacecraft launch campaign	7 days under Class 100000 fairing	1500 ppm	2700 ppm	
Launch		1600 ppm	4300 ppm	
Micrometeorite and redistribution		350 ppm	4650 ppm	5000 ppm

OBSTRUCTION FACTOR IN PPM

7.1.7.3. Budgets for particulate contamination for Planck instruments and telescope

Following budget describes particulate contamination levels of Planck instruments and telescope from the beginning to the end of life, taking into account the following hypothesis.

The exposure time of the reflectors during telescope, PLM and spacecraft integration is estimated to be 20 days in Class 10000. These days stand for AIT, alignment tests, vibration tests, acoustic tests, preparation to thermal tests … Out of this tests, the telescope is protected by a hard cover. During mechanical tests, it is envisaged to protect the reflectors with a protective foil. This cover is removed before installation of Planck under the SYLDA 5 on the launch pad. With the current Operation Plan, this operation is performed 8 days before roll-out. Taking into account a 1 day launch delay, a total duration of 10 days without protection has to be taken into account. As it is expected that at the time of Herschel/Planck launch, the cleanliness under fairing will be Class 10 000, the current allocation of 1500 ppm for launch campaign in the budget in compatible with this 10 days without protection.

The non-sensitive external surfaces of the spacecraft will have a contamination level lower than 10000 ppm (TBC) before encapsulation. With such a level, in-orbit particle redistribution is estimated to be less than 100 ppm (TBC) for 1.5 years in orbit life time.

Micrometeorite impact is estimated to be less than 50 ppm over the whole life in orbit (1.5 year).

PHASE		CONTRIBUTION	TOTAL	SPECIFICATION (TOTAL)
Instruments and reflectors at delivery		300 ppm	300 ppm	300 ppm
Telescope AIT	10 days in Class 10000	600 ppm	900 ppm	900 ppm
Spacecraft AIT till encapsulation	10 days in Class 10000 without covers	600 ppm	1500 ppm	1500 ppm
Spacecraft launch campaign	10 days under Class 10000 fairing	1500 ppm	3000 ppm	
Launch		1000 ppm	4000 ppm	
Micrometeorite and redistribution		200 ppm	4200 ppm	5000 ppm

OBSTRUCTION FACTOR IN PPM

7.1.7.4. Budgets for molecular contamination for Herschel instruments

Following budget describes molecular contamination levels of Herschel instruments from the beginning to the end of life, taking into account following hypothesis:

– cold units of instruments shall be submitted to a bake-out at 80° C prior delivery to PLM

– the cryostat will be submitted to a bake-out at 80° C before cool-down

– from cryostat closure until in flight cryostat opening, instruments are protected, and molecular cleanliness is preserved. Cryostat opening is planned to occur after around 1 month when spacecraft outgassing rate has become very low.

PHASE		CONTRIBUTION	TOTAL	SPECIFICATION (TOTAL)
Instruments at delivery		$4\ 10^{-6}$ g/cm^2	$4\ 10^{-6}$ g/cm^2	$4\ 10^{-6}$ g/cm^2
PLM integration till cryostat closure	Vacuum bake-out	$1\ 10^{-6}$ g/cm^2	$5\ 10^{-6}$ g/cm^2	
Spacecraft AIT till encapsulation	Instruments inside cry-cover	0^-g/cm^2	$5\ 10^{-6}$ g/cm^2	
Launch	Instruments inside cry-cover	0 g/cm^2	$5\ 10^{-6}$ g/cm^2	
In orbit redistribution and thruster plumes contamination		10^{-6} g/cm^2	$5\ 10^{-6}$ g/cm^2	**$6\ 10^{-6}$ g/cm^2**

7.1.7.5.   Budget for molecular contamination for Planck instruments

Following budget describes molecular contamination levels of Planck instruments from the beginning to the end of life.

PHASE		CONTRIBUTION	TOTAL	SPECIFICATION (TOTAL)
Instruments at delivery		10^{-6} g/cm^2	10^{-6} g/cm^2	10^{-6} g/cm^2
Spacecraft AIT till encapsulation		10^{-6}g/cm^2	$2\ 10^{-6}$ g/cm^2	$2\ 10^{-6}$ g/cm^2
Launch		10^{-6} g/cm^2	$3\ 10^{-6}$ g/cm^2	
In orbit redistribution and thruster plumes contamination		$2\ 10^{-6}$ g/cm^2	$5\ 10^{-6}$ g/cm^2	**$5\ 10^{-6}$ g/cm^2**

7.1.7.6.   Budget for molecular contamination for Herschel Telescope

Following budget describes molecular contamination levels of Herschel telescope from the beginning to the end of life.

One important source of telescope contamination in orbit is the spacecraft outgassing. To avoid this contamination, it is planned to heat up the telescope to 313 K during 3 weeks at the beginning of mission: this allows to get negligible contribution of outgassing to the telescope contamination. The remaining source is the contamination from thrusters. A preliminary assessment done during the proposal has shown that the expected contamination from thrusters is below $1\ 10^{-6}$ g/cm^2. This will be confirmed by an analysis to be conducted for PDR taking into account the actual definition of the thruster configuration and spacecraft.

PHASE		CONTRIBUTION	TOTAL	SPECIFICATION (TOTAL)
Telescope at delivery		$2\ 10^{-7}$ g/cm^2	$2\ 10^{-7}$ g/cm^2	$2\ 10^{-7}$ g/cm^2
before encapsulation		10^{-6} g/cm^2	10^{-6} g/cm^2	10^{-6} g/cm^2
Launch		10^{-6} g/cm^2	$2\ 10^{-6}$ g/cm^2	
In orbit redistribution and thruster plumes contamination		$2\ 10^{-6}$ g/cm^2	$4\ 10^{-6}$ g/cm^2	**$4\ 10^{-6}$ g/cm^2**

7.1.7.7.   Budget for molecular contamination for Planck Telescope

The following budget describes molecular contamination levels of Planck telescope from the beginning to the end of life.

The main source of in-orbit contamination comes from spacecraft outgassing at the beginning of mission. A worst case analysis performed during the proposal phase has shown that the telescope contamination due to spacecraft outgassing was reaching $2\ 10^{-6}$ g/cm^2 in the absence of telescope heating.

It was also demonstrated that telescope heating was leading to high contamination of the Focal Plane Unit (above $4\ 10^{-5}$ g/cm^2). In the case of telescope heating, it would also be necessary to perform FPU heating to avoid contamination, thus imposing heating lines on the FPU and resulting heat leak during scientific operations.

It is thus preferred to avoid heating of the telescope during in-orbit phase. The compliance with the cleanliness requirements will be confirmed by a detailed analysis to be conducted for PDR.

However, heaters should be implemented on the reflectors for on-ground testing: at the end of the cryogenic tests, it can be interesting to heat up the reflectors to avoid their contamination by the vacuum chamber cold screens during return to ambient conditions.

Contamination by thrusters has been estimated to be one order of magnitude lower than the contamination by spacecraft outgassing. This will be confirmed by an analysis to be conducted for PDR taking into account the actual definition of the thruster configuration and spacecraft.

PHASE		CONTRIBUTION	TOTAL	SPECIFICATION (TOTAL)
Reflectors at delivery		$2 \ 10^{-7}$ g/cm^2	$2 \ 10^{-7}$ g/cm^2	$2 \ 10^{-7}$ g/cm^2
Telescope integration		$3 \ 10^{-7}$ g/cm^2	$5 \ 10^{-7}$ g/cm^2	$5 \ 10^{-7}$ g/cm^2
Before encapsulation		$5 \ 10^{-7}$ g/cm^2	10^{-6} g/cm^2	10^{-6} g/cm^2
Launch		10^{-6} g/cm^2	$2 \ 10^{-6}$ g/cm^2	
In orbit redistribution and thruster plumes contamination		$2 \ 10^{-6}$ g/cm^2	$4 \ 10^{-6}$ g/cm^2	**$4 \ 10^{-6}$ g/cm^2**

7.1.8. Alignment budgets

7.1.8.1.   Planck Alignment budgets

7.1.8.1.1.   WFE budgets

Three stages until telescope assembly level have been identified, and for each one, an allocation has been given, in order to fulfill WFE requirements with a margin:

Telescope assembly WFE degradation
at 857 GHz
Requirement : 42 µm rms
Goal : 28 µm rms

Telescope WFE degradation at a defined field position
including apodization
Requirement : 31 µm rms
Goal : 24 µm rms

FPU WFE degradation at 217 GHz
including apodization
Requirement : 16.5 µm rms
Goal : 8.5 µm rms

Telescope - FPU integration

Requirement : 16.5 µm rms
Goal : 8.5 µm rms

Margin

wrt the requirement : 16.5 µm rms
wrt the goal : 8.5 µm rms

For each stages, WFE requirement induces relative positioning accuracy, knowledge and stability, which are described in alignment plan (doc HP-3-ASPI-PL-0078), and in the dedicated paragraph in the PPLM design report.

7.1.8.1.2. LOS budgets

The three alignment contributors to APE are the following:

– wobble angle adjustment accuracy, the accuracy of this adjustment is of 2 arcmin (TBC).

– On-ground LOS orientation knowledge, taking into account:

- the accuracy of LOS measurement during LFI end-to-end tests: 1 arcmin

- the knowledge of the measurement device orientation wrt satellite axes: 2 arcmin, we obtain a 3 arcmin for on ground LOS knowledge accuracy

– In orbit stability of PLM optical elements, the analysis described in Planck Alignment Plan takes into account:

- realistic behavior of mechanical telescope structure

- current stability requirement for FPU

- current requirements for cryostructure stability and leads to a total of 7.8 arcmin for LOS and 3.8 arcmin for around LOS.

Thus, we can derive the following LOS and around LOS budgets. This budgets are further justified in PPLM design report:

LOS
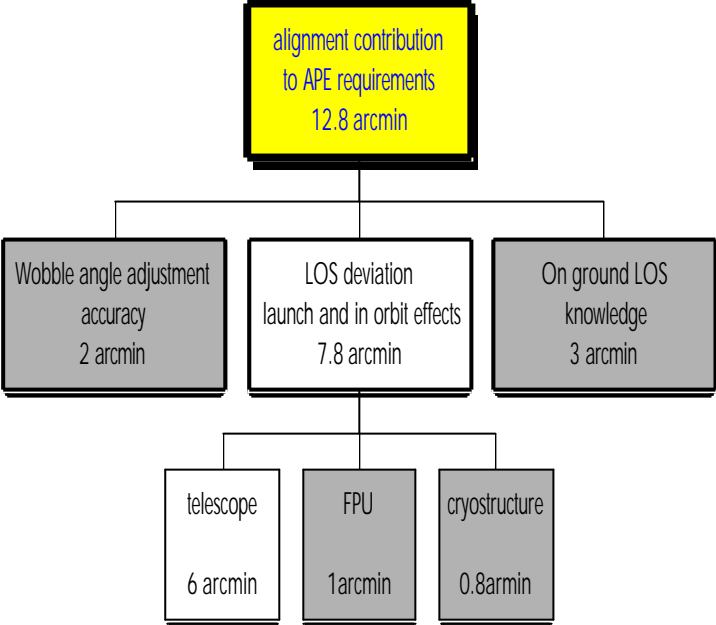
around LOS
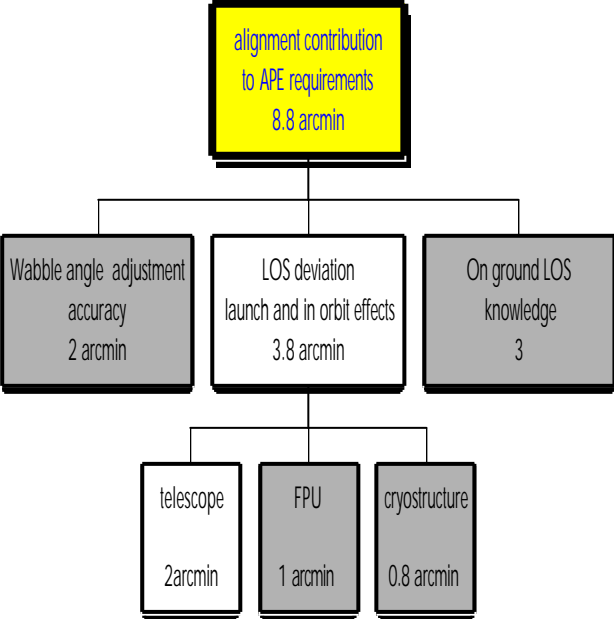
On another hand, the on ground LOS and around LOS offset contribute to the wobble angle adjustment range.

Taking into account the positioning accuracy of reflectors, FPU, cryostructure and SVM, the analysis (further described in PPLM design report) leads to the following LOS and around LOS budgets:

On ground LOS offset

```
                    ┌─────────────────┐
                    │   On ground     │
                    │      LOS        │
                    │     offset      │
                    │   5.5 arcmin    │
                    └────────┬────────┘
              ┌──────────────┴──────────────┐
    ┌─────────┴──────────┐      ┌────────────┴─────────┐
    │     on ground      │      │  PLM/SVM orientation │
    │ LOS orientation/PLM│      │                      │
    │     3.9arcmin      │      │      1.6 arcmin      │
    └─────────┬──────────┘      └──────────────────────┘
      ┌───────┴────────┐
┌─────┴──────────┐ ┌───┴──────────────────┐
│telescope assembly│ │ telescope assembly / │
│                  │ │    cryostructure     │
│   3.1 arcmin     │ │        0.8           │
└─────────┬────────┘ └──────────────────────┘
  ┌───────┼────────────────┐
┌─┴─────┐┌─┴─────────┐┌─────┴──────────┐
│telescope││   FPU    ││FPU manufacturing│
│        ││integration││                │
│2 arcmin││0.1 arcmin ││    1 arcmin     │
└────────┘└──────────┘└────────────────┘
```
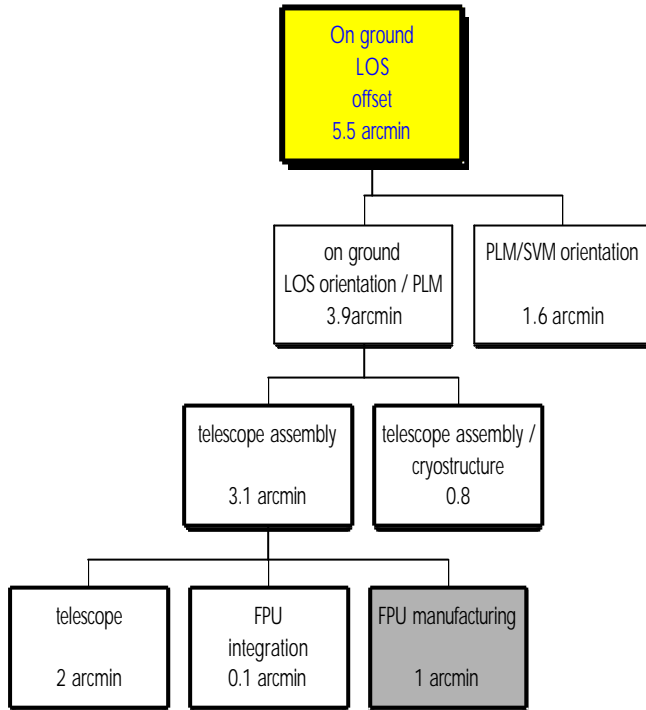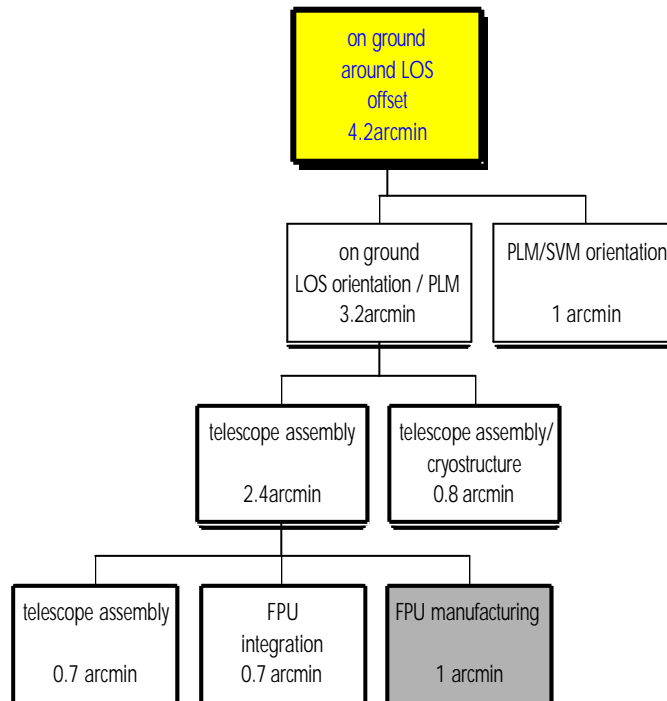
on ground around LOS offset

```
                         ┌─────────────────┐
                         │   on ground     │
                         │  around LOS     │
                         │    offset       │
                         │   4.2arcmin     │
                         └────────┬────────┘
                   ┌──────────────┴──────────────┐
         ┌─────────┴──────────┐      ┌────────────┴─────────┐
         │     on ground      │      │  PLM/SVM orientation │
         │ LOS orientation/PLM│      │                      │
         │     3.2arcmin      │      │       1 arcmin       │
         └─────────┬──────────┘      └──────────────────────┘
           ┌───────┴────────┐
     ┌─────┴──────────┐ ┌───┴──────────────────┐
     │telescope assembly│ │ telescope assembly/  │
     │                  │ │   cryostructure      │
     │    2.4arcmin     │ │     0.8 arcmin       │
     └─────────┬────────┘ └──────────────────────┘
       ┌───────┼────────────────┐
┌──────┴───────┐┌─┴─────────┐┌───┴──────────────┐
│telescope assembly││   FPU    ││FPU manufacturing│
│              ││integration││                │
│  0.7 arcmin  ││0.7 arcmin ││    1 arcmin     │
└──────────────┘└──────────┘└────────────────┘
```

7.1.8.2. Herschel Alignment budgets

Refer to H-EPLM Design Description (HP-2-ASED-RP-0003).

7.2. HERSCHEL SYSTEM ANALYSES

7.2.1. Mechanical analyses

7.2.1.1. Introduction

Several mathematical models (FEM) and mechanical analyses have been prepared and carried out in order:

- to assess the ability of the structural concept of HERSCHEL satellite (Launcher requirements)

- to define and update subsystem (H-PLM and SVM) structural requirements

- to update and complete the environment specification for Herschel equipment.

HERSCHEL mathematical model has been prepared from SVM FE model delivery coming from ALENIA and H-PLM FE model delivery coming from ASTRIUM D.

7.2.1.2. Analysis of Herschel satellite dynamic behaviour

7.2.1.2.1. Subsystem mechanical performances

7.2.1.2.1.1. HERSCHEL Service Module
General

The SerVice Module (SVM) finite element model has been received from ALENIA.

This mathematical model has sufficient detail for the stiffness simulation in the dynamic analyses.

SVM FE model description

- SVM cone:

    Honeycomb: height H/C=15 mm
    Three plies composite face sheet: T300 resin Epoxy CFC 0°/60°/-60°
    thickness for each sheet: t= 0.375 mm.

- SVM upper/lower closure platform:

    Honeycomb: total height H=20 mm
    Three plies composite face sheet: thickness for each sheet 0°/60°/-60°:
    t= 0.375 mm.

- SVM lateral panels:

    Honeycomb: height H/C=35 mm
    Aluminium face sheet: thickness for each sheet: t= 0.3 mm.

- SVM shear webs:

    Honeycomb: height H/C=15 mm
    Six plies composite face sheet: thickness for each sheet 0/60°/-60°/-60°/
    60°/0: t= 0.75 mm.

Local reinforcements have been implemented on the cone in the zones around the GFRP struts fixations. These reinforcements consist in increasing the stiffness of the local plate support of the cone. The total number of the plies of the composite face sheet has been increased, the honeycomb properties remaining unchanged.

H-PLM subplatform

The mechanical characteristics of the H-PLM sub-platform are:

- twelve plies composite face sheet thickness t = 1.5 mm

- honeycomb: height H/C =15 mm.

SVM FE model characteristics

The FEM model has been set up to the maximal mass. The maim characteristics of the model are:

Number of Nodes   : 8551
Number of Element   : 8804

SVM FEM has   : 51306 d.o.f
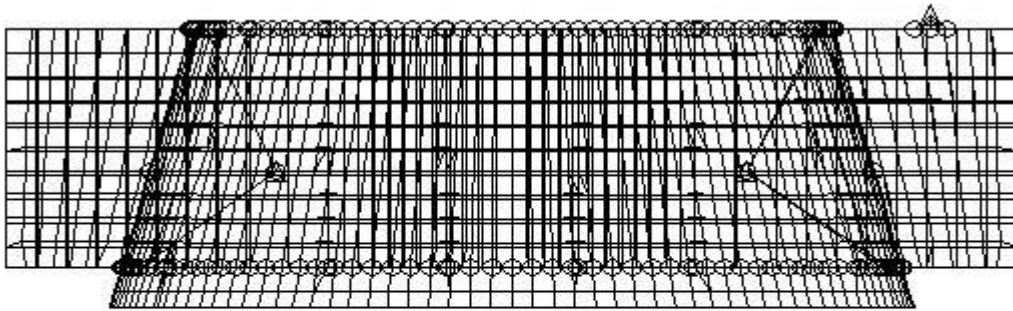SVM FEM mass is   : 716 Kg

X
Y Z

TABLE 7.2.1.2-1 HERSCHEL SERVICE MODULE MATHEMATICAL MODEL

SVM Dynamic performances

Herschel SVM dynamic global (global box modes, global lateral and longitudinal ones) and local stiffness (panels ..) are obtained from a modal analysis. These results are summarized in the following table.

Mode Frequency (Hz)	Effective Masses (Kg)			Mode description
	Mx	My	Mz	
25.9	20			H-PLM sub platform X mode
39		36.4	38.8	Out of Plane mode Y+Z- Lateral panel
41.3		32.8	44.4	Out of Plane mode Y-Z- Lateral panel
46.7			161	HERSCHEL SVM lateral Z mode
48.4		40.1	39.5	Out of Plane mode Y+Z+ Lateral panel
50.9			89.6	Fuel tank lateral mode
51.96		109		HERSCHEL SVM lateral Y mode
59.5		32.8	13.5	Out of Plane mode Y-Z+ Lateral panel
61.8		114.2		Lateral SVM Y mode + fuel tank
80.7	187			HERSCHEL SVM longitudinal X mode

TABLE 7.2.1.2-2 HERSCHEL SVM MAIN MODES

Comments

HERSCHEL SVM main modes are close to 47 Hz in lateral and 80 Hz in longitudinal direction. SVM is very stiff in the longitudinal direction.

HERSCHEL out of plane mode of lateral panel are located around 40 Hz which is still very close to the lateral SVM main modes frequencies.

7.2.1.2.1.2. HERSCHEL Payload Module
General

The HERSCHEL PLM finite element model implemented in the satellite system FE model has been received from ASTRIUM.

PLM FE model description

HERSCHEL Payload module is defined from the four following substructures:

– Telescope

In this H-PLM configuration, HERSCHEL Telescope is modelled with a concentrated. Global telescope Inertia are taken into account in telescope mass element.

– Sunshield/Sunshade structure

Sunshield/Sunshade structure is a stiff Sunshield/Sunshade configuration but doesn't correspond exactly to the stiff SSD/SSH baseline design. In fact, SSD/SSH structure connected to a rigid interface (simply supported boundary conditions) presents lateral SSD and SSH modes between 30 Hz and 40 Hz. In SSD/SSH baseline, all these lateral modes should be higher than 40 Hz. The SSD/SSH main modes are listed in the next table.

FREQUENCY [HZ]	MASS X [KG]	MASS Y [KG]	MASS Z [KG]	MODE SHAPE DESCRIPTION
32.6			1.57	HERSCHEL lateral SSD Z mode
36.1		2.6		HERSCHEL lateral SSD Y mode
38.5			12.8	HERSCHEL lateral SSH Z mode
41.4		4.96		Second lateral SSH Y mode
43.9			48.4	Third lateral SSD Z mode

TABLE 7.2.1.2-3 SSD/SSH MAIN MODES

NOTE: The stiff SSD configuration is a simply supported SSD configuration which gives all lateral SSD modes above 40 Hz.

– HERSCHEL Cryostat and GFRP struts support

CRYOSTAT strut support considered in these technical analyses is a 24 struts configuration which corresponds to the SRR baseline strut configuration. This CRYOSTAT strut support has been analysed from the HERSCHEL FE model of ALCATEL proposal. Sensitivity analyses have been performed :

- Considering 4 strut configurations (12, 16 ,24, 32 struts)

- Considering two upper interface diameter (2.1 and 2.3m)

Sensitivity analyses on strut section area have been performed in order to optimize the satellite mechanical behaviour increasing the thermal performances (higher life duration). In all these analyses, strut outer diameter has remained constant.

In the 24 struts configuration, the optimized strut section area has been identified with a tube thickness around 2mm instead of 4mm initially. This strut section reduction allows to save mass and reduce conductive thermal load from SVM to CRYOSTAT.

In the H-PLM FE model, thickness of the strut has been considered equal to 2 mm.

The Physical FEM model has been set up to the maximal mass. The main characteristics of the H-PLM FE model are:

Number of Nodes   : 12310
Number of Element   : 12698

HERSCHEL PLM FEM has   73860 dof
HERSCHEL PLM FEM mass is   2136 Kg

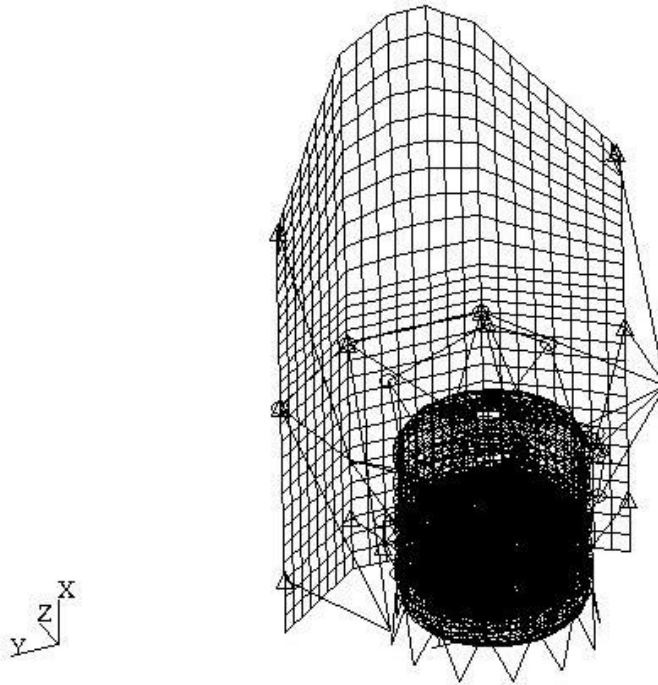The physical mathematical model is shown hereafter on the next figure.

TABLE 7.2.1.2-4 HERSCHEL PLM MATHEMATICAL MODEL

HERSCHEL PLM Dynamic performances

With telescope and Sunshield Sunshade structure, the frequencies of the HERSCHEL Payload module main modes computed with simply boundary conditions at the struts interface points with SVM are listed in next table.

Mode Frequency (Hz)	Effective Masses (Kg)			Effective Inertia (m²Kg)			Mode description
	Mx	My	Mz	Ix	Iy	Iz	
22			1756				HERSCHEL lateral H-PLM Z mode
22.96		1796					HERSCHEL lateral H-PLM Y mode
29.3				238			X rotation of O. Bench
31.2			24				HERSCHEL SSD lateral Z mode
32.55			16		830		Second Lateral H-PLM Z mode
33				114		357	Second SSD Lateral Y mode
33.8		2.6				1116	Second Lateral H-PLM Y mode
38			2.7				HERSCHEL lateral SSH Z mode
44.3	1173						HERSCHEL longitudinal H-PLM X mode

TABLE 7.2.1.2-5 HERSCHEL PLM MODAL ANALYSIS RESULTS

Comments

Main H-PLM lateral modes coming from the suspended masses are above 20 Hz and the longitudinal one is around 44.3 Hz.

Lateral main modes of the sunshield are between 30 and 40 Hz and lateral SSD modes are identified at 31-33 Hz and around 44 Hz-45 Hz.

This modal analysis shows that SSD/SSH modes and H-PLM satellite main modes are in the same frequency bandwidth which allows possible modal coupling between them at system level.

7.2.1.2.1.3. HERSCHEL Satellite FE model

The mathematical model of the whole HERSCHEL satellite is assembled using the models of the various subsystems previously described: service module, and HERSCHEL payload module. The SVM shield is not represented is the global satellite FE model.

Main characteristic of the model

The SVM and H-PLM models are connected to each other with Rigid bodies (RBE2) element. The main characteristics of the HERSCHEL satellite FE model are:

- Number of physical nodes: 20869

- Number of elements: 21532

- Total number of degrees of freedom: 125214.

Global Mass budget

The following table presents the mass budget of HERSCHEL satellite.

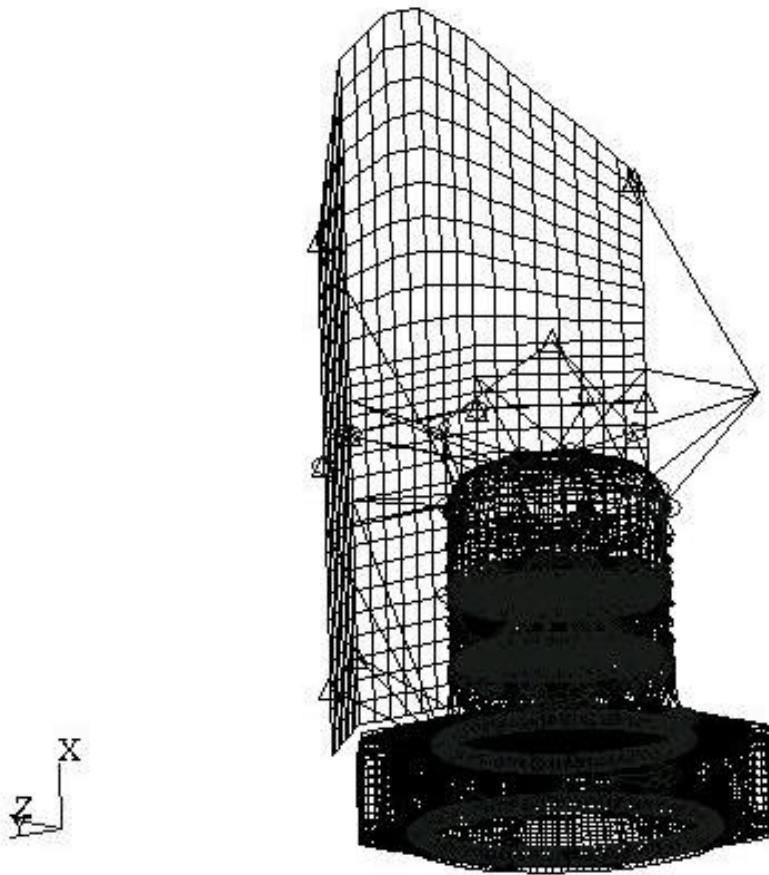| Subsystem	Mass in the model [Kg]
H-PLM	2136
SVM	716
Total mass	**2852**

TABLE 7.2.1.2-6 3D VIEW OF HERSCHEL FE MODEL

7.2.1.2.2.   Overall system mechanical analyses

7.2.1.2.2.1. General

The dynamic system analysis is carried out in two different steps:

–   an overall dynamic modal analysis is performed with NASTRAN software in order to identify

–   the primary and secondary main modes of HERSCHEL satellite and their effective mass and to check if there is no coupling between subsystems.

A dynamic response analysis is performed to predict the accelerations responses of:

- equipment during AR V launch. From the computed accelerations, quasi static loads are evaluated and design loads are defined for subsystems sizing and the equipment qualifications levels.

7.2.1.2.2.2. HERSCHEL Satellite overall dynamic analyses

HERSCHEL dynamic analysis (modal and sine response of the satellite) is performed up to 100 Hz which corresponds to the frequency bandwidth of the sine vibration tests.

Modal analysis

HERSCHEL satellite main modes with effective mass higher than 5 % of the total mass are presented in next table.

Mode Frequency (Hz)	Effective Masses [Kg]			Mode shape description
	Mx	My	Mz	
14.25			1765	HERSCHEL lateral global Z mode
14.9		1787		HERSCHEL lateral global Y mode
27.8			39.4	X rotation of O-Bench
28.4		89	164	second lateral global Z mode
28.7		147	75	second lateral global Y mode
30.7	13.1		1	SSD Lateral Z mode
36.2	1787			HERSCHEL lateral global X mode
39		35.1	36.5	SVM Y+Z- lateral panel
40.5	88.8		1	SSD lateral global Z mode
41.3		38.3	46.4	SVM Y-Z- lateral panel

TABLE 7.2.1.2-7 HERSCHEL SATELLITE MODAL ANALYSIS RESULTS

Comments

HERSCHEL satellite main modes

The HERSCHEL satellite main modes are located at the following frequencies:

- HERSCHEL longitudinal mode = 36.2 Hz   (Margin > 15 %)

- HERSCHEL lateral mode = 14.25 Hz   (Margin > 20 %).

HERSCHEL longitudinal mode is driven by the HERSCHEL longitudinal mode of CRYOSTAT (located above 44 Hz). The CRYOSTAT suspended mass (Helium tanks, optical bench) have a significant contribution in this mode. The frequency of the longitudinal mode fulfils the Launcher frequency requirement (> 31 Hz) in longitudinal direction.

HERSCHEL lateral main modes are determined by the stiffness of the primary structure (SVM cone, CRYOSTAT struts support). The frequencies of these lateral modes are more than 20 % higher than the minimal required frequency and are compliant with the lateral launcher frequency requirement (> 9 Hz).

The second lateral main modes of HERSCHEL satellite are located around 28.5 Hz and are driven by the HERSCHEL lateral mode of CRYOSTAT (located around 30 Hz).

HERSCHEL satellite secondary modes

HERSCHEL **Sunshade** modes are found at 30 Hz and 40.5 Hz and are mainly lateral Z mode. Lateral SSD mode located around 40.5 Hz is significantly coupled with the first longitudinal main mode of the satellite (36.2 Hz). This modal coupling is identified by the significant effective mass in the longitudinal axis X (89 Kg) at the frequency of the SSD lateral Z mode (40.5 Hz). This modal coupling is due to the proximity of the two modes (the longitudinal main modes one being around 36 Hz instead of 34-35 Hz in the previous study and SSD structure being not stiff enough).

Moreover, it has to be noticed that the SSD dynamic behaviour has probably be significantly moved because of low SVM interface stiffness introduced at the interface points of lower strut support of SSD/SSH structure with SVM. Indeed, initially located on a stiff CRYOSTAT ring interface, the interface points have been moved on SVM upper interface point without local structural reinforcement.

First HERSCHEL **Sunshield** modes are mainly local bending modes of panels (out of plane mode) and are identified around 38 Hz.

The HERSCHEL **service module** modes are found above 50 Hz which ensure the modal de-coupling with HERSCHEL satellite main modes (lateral and longitudinal ones).

Dynamic Sine Response analyses

– Methodology

The dynamic response analysis is performed using the following ARIANE 5 input flight levels.

- Longitudinal axis: ± 1 g from 5 Hz to 100 Hz

- Lateral axis: ± 0.8 g from 5 Hz to 25 Hz
  ± 0.6 g from 25 Hz to 100 Hz.

These levels are applied at the base of the spacecraft. No notching is considered at this step of the analysis. The reduced damping factor considered in this analysis is 2 % for each mode which is usually consistent with most of the experimental tests.

– Notching on the main modes

The following table presents the qualification maximal loads at the launcher interface due to the dynamic response (with qualification factor of 1.25), the maximum quasi static loads at the interface and the foreseen notching values.

The analyses and notching level evaluation have been performed from the main ARIANE 5 quasi static loads (6 g longitudinal and 2 g lateral).

The main ARIANE 5 quasi static load cases are summarized in the following table.

Flight Event	Longitudinal [g]	Lateral [g]
Max dyn pressure	-3.2	± 2
SRB end of flight	-6	± 1
Max tension case	2.5	± 0.9

The estimated notching levels are presented hereafter.

Item	ARIANE V QSL (g)	Quasi static Launcher interface loads	Dynamic Launcher interface loads	Frequency (Hz)	Flight Notching level	Qualif Notching level
Fx (N)	6	1.711 E+5	4.6000 E+5	36	0.37g	0.46g
Fy (N)	2	5.704 E+4	3.4000 E+5	14.8	0.134g	0.168g
Fz (N)	2	5.704 E+4	3.4000 E+5	14	0.134g	0.168g
My (N.m)	2	1.188 E+5	1.0815 E+6	14	0.088g	0.11g
Mz (N.m)	2	1.188 E+5	1.0780 E+6	14.8	0.088g	0.11g

For the primary main modes, the predicted qualification notching levels are:

- longitudinal direction   0.46 g

- lateral Y/Z direction   0.11 g.

These values are consistent with usual values found on other satellites with a similar weight.

NOTE: ARIANE 5 coupled dynamic analyses of similar satellite show lower longitudinal quasi static loads around 5 g instead of 6 g. Without agreement with Launcher authorities concerning the use of lower longitudinal quasi static loads, the mechanical analyses and quasi static loads evaluations have been performed with a Launcher longitudinal quasi static load factor equals to 6 g.

7.2.1.3. Inputs to support subsystem spec

Dynamic loads and mechanical environments of structures and instruments have to be evaluated and specified through EVTR and GDIR specifications. The following chapters give a descriptions of these loads, environment and the mechanical requirements applicable to subsystems.

For information, the frequency of the events (resonance) where quasi static loads have been computed and the load direction of the satellite are also presented.

Quasi static loads

The main flight limit loads extract from the dynamic response analysis are presented in next tables. Notching on primary main modes are taken into account in these loads.

－ **HERSCHEL TELESCOPE**

Flight limit loads

FLIGHT LIMIT LOADS			
Axial (g)	Lateral (g)	Frequency (Hz)	Load Direction
7	2	36	X
/	8	28.8	Y/Z

TABLE 7.2.1.3-1 FLIGHT LIMIT LOADS FOR HERSCHEL TELESCOPE

Comments

These telescope flight limit loads are lower than flight limit loads (around 16 g in axial direction and 10 g in lateral) proposed for sizing the telescope. The axial loads estimated at 36 Hz have been computed with a rigid FE Telescope model (Rigid mass). This modelling doesn't take into account the flexibility of the Telescope and reduces the quasi static loads. For this reason, Telescope flight limit loads which are similar to Primary Reflector remain at 16 g in longitudinal and 10 g in lateral.

For information, at 40.5 Hz, for the longitudinal satellite excitation, a modal coupling coming from SSD structure increase Telescope lateral Flight limit loads. This load case must not be taken into account for defining Telescope load specification because a de-coupling task will be done after SRR to reduce these loads below the flight levels computed at 28.8 Hz as it was previously.

－ **HERSCHEL INSTRUMENTS**

The main flight limit loads of the HERSCHEL PLM instruments are presented hereafter.

Flight limit loads

FLIGHT LIMIT LOADS				
Equipment	Axial (g)	Lateral (g)	Frequency (Hz)	Load Direction
PACS/HIFI/ SPIRE	14.3 2	1.5 6	36 28.8	X Y/Z
BOLA	6.5	3.2	75	Y
LOU	17	8.5	75	Y
Optical Bench	13	1	36	X

TABLE 7.2.1.3-2 QUASI STATIC LOADS OF PLM INSTRUMENTS

Comments

For optical Bench instruments and optical bench structure, quasi static loads extracted at the frequency of longitudinal main mode are similar to preliminary flight limit loads defined in ALCATEL proposal. However, a modal coupling occurring at 40.5 Hz increases a little the lateral loads (9 g instead of 8.4 g) and the longitudinal component up to 9.6 g.

These accelerations will be reduced during B Phase by decoupling SSD modes from longitudinal main mode. This modal decoupling task could be done:

- by optimizing the frequency location of HERSCHEL longitudinal main mode which should be reduced down to 34 Hz (softening the Central Tube for instance which is higher than the stiffness required at the moment..)

- by increasing the dynamic stiffness (all SSD natural frequencies > 45 Hz) of the SSD structure as it is specified in the SSD frequency requirement (at the moment, the SSD frequency requirement is not fulfilled by the delivered SSD structure).

These quasi static loads can not be considered as maximal loads because modal coupling can increase significantly the acceleration levels on the optical bench instruments if the frequencies of interest (longitudinal main mode at 36 Hz and SSD lateral Z mode 40.5 Hz) are closer even with low frequency shift. Sensitivity analyses should be performed to estimated the evolution of the loads and the frequency limits of coupled modes.

For CVV instruments, the acceleration levels are similar or have been little modified but these quasi static loads remain low and acceptable.

	FLIGHT LIMIT LOADS			
Equipment	^ (g)	// (g)	Frequency (Hz)	Load Direction
SVM lateral Panels	25	20	55.2	X
SVM Panel +Y /-Y	40 (*)	20 (*)	52	Y
Fuel tank	11.5	8	75	Z

TABLE 7.2.1.3-3 QUASI STATIC LOADS FOR SVM LATERAL PANELS

Comments

For SVM lateral panels, the flight limit loads have increased a little. The increase is probably due to a light modal coupling between SVM global box modes and out of plane lateral panel modes in Y direction. The analysis of quasi static loads modifications (modal analyses of global and local modes) will be done during B phase to reduce these flight limit loads down to loads used for testing and qualification. Moreover, the high frequencies of the SVM and lateral panel modes where the limit loads are computed will allow to expect a significant reduction of these loads with auxiliary notchings coming from preliminary LCDA results.

(*) these loads are not specified because these levels should be reduced by secondary notching.

− **HERSCHEL TANKS**

For Tanks, design loads have been computed. A design factor of 1.2 have been taken into account to determine the design loads. The flight limit loads are listed hereafter.

	FLIGHT LIMIT LOADS			
Equipment	Axial (g)	Lateral (g)	Frequency (Hz)	Load Direction
He II	13.2	0.8	36	X
	1.6	8	28.5	Y/Z
He I	19.2	0.8	36	X
	/	5.6	28.5	Z

TABLE 7.2.1.3-4 HERSCHEL TANKS FLIGHT LIMIT LOADS

Comments

Flight limit loads of PLM tanks have not been significantly modified compared to the flight limit loads of the ALCATEL proposal.

These loads have slightly increased and are probably influenced by the modal coupling between longitudinal main mode of the satellite and a lateral SSD mode.

The possible influence of modal coupling on the quasi static loads could come from a lower effective mass (5 %) on the satellite longitudinal main mode which probably could increase the notching levels and consequently the loads. The decoupling task previously defined should improved this dynamic situation by reducing these loads.

Unit sine environments

The sine environment are defined for qualification test from the quasi static loads in order to be consistent with quasi static loads and to be sure that the loads levels will be applied during these tests.

The sine vibration levels are defined between 5 Hz and 100 Hz. The acceleration levels applied in this range are the acceptance levels defined in consitency with quasi static loads. Notching will be allowed not to exceed quasi static loads.

Equipment	Load direction	Frequency Hz	Acc level (g)
FPU	Longit(X)	5 – 40 Hz	6
		40 – 100 Hz	3
	Lat(Y/Z)	5 – 100 Hz	14
LOU	Long.	5 – 80 Hz	17
		80 – 100 Hz	5
	Lat	5 – 100 Hz	9
BOLA	Long	5 – 100 Hz	7
	Lat		3.2
SVM	⊥	5 – 100Hz	25
	//		20

SINE ACCEPTANCE LEVELS

H-PLM sine environment

These loads are similar to H-PLM global dynamic loads (flight limit loads) presented in Chapter 6.3.1.4. At the interface, the flight dynamic environment of the H-PLM with SVM local stiffness is the launcher interface sine environment defined in the MUA 5:

– longitudinal axis X : 1 g from 5 Hz to 100 Hz

– lateral axes Y/Z : 0.8 g from 5 Hz to 25 Hz
: 0.6 g from 25 Hz to 100 Hz.

H-PLM Flight limit loads

The envelope of H-PLM Quasi static load cases computed for few CRYOSTAT strut support configurations are presented in the next table.

Load Case	X Axis	Y Axis	Z axis
1	10 g	/	± 1.25 g
2	/	3 g	/
3	/	/	3.25 g

TABLE 7.2.1.3-5 H-PLM QUASI STATIC LOADS

These loads have to be applied to the whole H-PLM structure (the resultant force is applied to H-PLM centre of gravity). Global Quasi static loads generate equivalent sizing forces in the struts at the interface points with SVM.

7.2.1.3.1. HERSCHEL Random vibration analyses

Methodology

The methodology for computing random acceleration levels on H-PLM equipment are based on two technical approaches which give estimated levels from the weight of the equipment (HERSCHEL approach with ESA formulae) and from experimental results (second approach with XMM experimental random curve) provided by ESA. The final random results are defined from equipment location analyses on the panels.

The random vibration level evaluation of equipment located inside CRYOSTAT doesn't take into account the acoustic attenuation of HERSCHEL CVV structure. Moreover, the influence of structural damping at low temperatures is not considered in the random vibration evaluation.

For PDR, detailed Acoustic Analyses will be done with acoustic FE model taking into account CVV acoustic attenuation for improving and increasing the accuracy of random vibration specification levels.

HPLM random vibration specification

The following levels presented in the next table are the random vibration levels specified for H-PLM equipment. These levels define a random spectrum with an horizontal maximal level:

- 20-100 Hz : +3 dB/Oct

- 100 Hz-300 Hz : PSD max [g²/Hz]

- 300 Hz-2000 Hz : -5 dB/Oct.

Maximal PSD values (PSD max) of qualification random spectrum are defined in the following tables.

H-PLM Equipment	In plane PSD [g²/Hz]	Out of Plane PSD [g²/Hz]
HIFI	0.05	0.1
PACS	0.05	0.1
SPIRE	0.05	0.1
LOU	0.1	0.2
BOLA	0.2	0.4
Telescope	0.15	0.3
He I	0.05	0.1
He II	0.1	0.2

TABLE 7.2.1.3-6 H-PLM RANDOM VIBRATION SPECIFICATION

HERSCHEL SVM equipment random vibration specification

The random qualification levels for HERSCHEL equipment located inside SVM are presented in the next table. These levels are the specified random vibration levels for SVM equipment.

Item	Mass [Kg]	Mounted Panel	Panel mass/surf [Kg/m²]	Out of Plane Level [g²/Hz]	In plane Level [g²/Hz]
FPDMC	8.25	[-Z;+Y]	52	0.2	0.1
FPBOLC	9			0.2	0.1
FPDPU	7			0.2	0.1
FPSPU	7.1			0.2	0.1
Battery	6.8	[+Y]	55	0.2	0.1
PCDU	18.2			0.2	0.1
AOCS IF/Unit	8.69			0.2	0.1
CDMU	13.33			0.2	0.1
Gyroscopes	5.24	[+Z;-Y]	20.5	1.2	0.6
QRS	1.43			1.2	0.6
X/B transponders	3.46			1.2	0.6
TWTA	0.75			1.2	0.6
EPC	1.4			1.2	0.6
Diplexer	0.3			1.2	0.6
FHFCU	10	[-Y;-Z]	45.6	0.2	0.1
FHWBI	8			0.2	0.1
FHWBO	10			0.2	0.1
FHWBE	6			0.3	0.15
FHICU	7			0.2	0.1
RWDE	6.5	[+Z;+Y]	38	0.4	0.2
RWDS	7			0.3	0.15
FHLCU	11	[-Y]	30	0.3	0.15

Item	Mass [Kg]	Mounted Panel	Panel mass/surf [Kg/m²]	Out of Plane Level [g²/Hz]	In plane Level [g²/Hz]
FHHRI	8.7	[option 1]		0.4	0.2
FHHRH	4.7			0.3	0.15
FHHRV	4.7			0.3	0.15
FHLCU	11	[-Y]	42	0.2	0.1
FHHRI	8.7	[option 2]		0.2	0.1
FHHRH	4.7			0.2	0.1
FHHRV	4.7			0.2	0.1
FHLSU	12			0.3	0.15
FSDPU	10	[-Z]	53	0.2	0.1
FSDCR	18			0.2	0.1
Cryo elec	8.6	[-Z]	16.3	1	0.5
FHLSU	12	Platf [+X]	15	1	0.5
FSS Elec	2.2	Web [+Z]	10	1.5	0.75
STR Elec	3.5	Web [–Z]	11	1.5	0.75

TABLE 7.2.1.3-7 SVM RANDOM VIBRATION LEVELS

7.2.1.3.2. HERSCHEL Shock analyses

General

A shock analysis is performed in order to evaluate the shock environment of the HERSCHEL equipment inside H-PLM and SVM. HERSCHEL spacecraft position is the upper position with SYLDA 5 interface.

Shock excitation assumptions

At the spacecraft interface, the shock response spectrum of shock excitation is supposed to be close to the shock response spectrum presented in the following table. This shock response spectrum is not the excitation shock response spectrum used in the ALCATEL proposal but this shock excitation is considered to be more representative (but still conservative) than the previous one.

Frequency [Hz]	Shock Acceleration [g]
100	20
600	1000
10000	3600

TABLE 7.2.1.3-8 LAUNCHER INTERFACE SHOCK EXCITATION

HERSCHEL-PLM Shock evaluation

Only launcher interface shock excitation is analysed in this section.

Shock attenuation inside sandwich panels due to the distance from the excitation source has been clearly identified from experimental tests. Considering this shock attenuation, shock levels at the interface with H-PLM strut support located at 970 mm from the launcher interface plane are estimated reduced by about 15 dB at high frequencies.

The estimated HERSCHEL-PLM Shock interface levels are presented in the following table. For the following shock specification, out of plane and in plane shock levels are supposed to be identical.

Frequency [Hz]	Shock Acceleration [g]
500	200
1300	600
10000	600

TABLE 7.2.1.3-10 H-PLM INTERFACE SHOCK RESPONSE SPECTRUM
(SRS H-PLM)

In H-PLM structures (not made with sandwich elements), shock level is not supposed to be significantly reduced except at interface points. The shock attenuation at each of interface point is supposed to be around 5 dB (conservative approach). For H-PLM equipment and instrument, severity shock level SRS 1 to be considered for shock specification is defined hereafter.

Frequency [Hz]	Shock Acceleration [g]
100	20
1300	200
10000	200

TABLE 7.2.1.3-11 SHOCK RESPONSE SPECTRUM SRS 1

HERSCHEL PLM Shock specification

Without any consideration of cryo cover release and taking into account the results defined previously, shock levels specified for HERSCHEL PLM equipment (PACS, SPIRE, HIFI..) are summarized in the next table.

H-PLM Equipment	Interface shock Spec
PACS	SRS 1
SPIRE	SRS 1
HIFI	SRS 1
LOU	SRS 1
BOLA	SRS 1
Helium Tank I	SRS 1
Helium tank II	SRS 1
Telescope	SRS 1

TABLE 7.2.1.3-12 HERSCHEL PLM EQUIPMENT SHOCK SPECIFICATION

For HERSHEL Payload, interface shock levels are defined in Table 7.2.1.3-11.

P-PLM Structure	Shock specification
HERSCHEL –PLM	SRS H-PLM

TABLE 7.2.1.3-13 HERSCHEL PLM INTERFACE SHOCK SPECIFICATION

HERSCHEL SVM Shock specification

Waiting for results of ARIANESPACE new shock damping test and new Launcher interface shock data, for HERSCHEL SVM shock levels, the proposal main results presented hereafter are considered unchanged. Out of plane and In plane shock levels are supposed to be identical.

Frequency (Hz)	Acceleration (g)
100	7
600	1300
3900	3400
10000	3400

Shock response spectrum Sa 1 (qualification levels)

For equipment connected to the upper plate-form, the qualification shock levels are:

Frequency (Hz)	Acceleration (g)
100	7
600	1600
10000	2000

Shock response spectrum Sa 2 (qualification levels)

HERSCHEL SVM Equipment		shock level
RCS components		Sa1 (TBC)
Lateral Panels		
-TWTA	-FPSPU	
-EPC	-FPDPU	
-GYRO	-FPDMC	
-QRS	-FPBOCC	
-DIPLEXER	-CRYO Elec	
-TRANSP	-FSPDU	
-FSDCR	-RWD Elec	Sa1
-FHFCU	-PLDU	
-FHWRO	-CDMU	
-FHWBE	-AOCS I/F unit	
-FHWBI	-BAT	
-FHICU	-FHLCU	
-FHHRH	-FHHRI	
-FHHRV		
Upper plate form		Sa2
-FHLSU		

SVM equipment Shock Level STATUS

7.2.1.4. Inputs to HERSCHEL SVM structural requirements specification

The mechanical design of HERSCHEL SVM has to be defined from mechanical environment and stiffness requirement to fulfil the Launcher frequency specification. These mechanical environment have been defined with the latest HERSCHEL SVM mass configuration and mechanical design.

HERSCHEL SVM Dynamic requirement specification

In order to avoid modal coupling between substructure, SVM dynamic requirements have been defined and concerns the frequency location of:

–   Global SVM modes with rigid Payload

In relation with the global stiffness of Central Tube, the global SVM modes with rigid Payload have to be defined to reach and fulfil the Launcher frequency requirements with HERSCHEL Payload.

- Frequency of the HERSCHEL longitudinal main mode > 58 Hz

- Frequency of the HERSCHEL lateral main mode   > 23 Hz.

–   SVM global Box modes

SVM global Box modes have to be de-coupled to HERSCHEL main modes (HERSCHEL longitudinal and secondary lateral). These technical considerations and the mechanical design lead to the following frequency requirements:

- Frequency of the HERSCHEL SVM longitudinal global box mode > 51 Hz

- Frequency of the HERSCHEL SVM lateral global box mode   > 48 Hz.

–   Tank support modes

To avoid modal coupling between SVM modes located around 50 Hz and fuel tank main modes, the frequency requirements:

- Frequency of HERSCHEL fuel tank longitudinal X main mode > 145 Hz

- Frequency of HERSCHEL fuel tank lateral main mode   > 80 Hz.

–   SVM Lateral panels

The lateral panel frequency requirements have been defined from the lateral behaviour of HERSCHEL satellite for decoupling out of plane modes of panels to second lateral Satellite main modes (around 30Hz). The main lateral panel frequency requirement is:

- frequency of out of plane lateral panel > 50 Hz.

HERSCHEL SVM Stiffness requirement specification

– Global lateral stiffness (Central Tube)

A global lateral and longitudinal stiffness is specified to ensure a satisfactory global dynamic behaviour of HERSCHEL satellite with respect to the Launcher frequency specifications. The lateral and longitudinal stiffness requirements specified for Central Tube are:

- $8.2E7 \text{ N/m} < K_{lateral}(Y) < 8.2E7 \text{ N/m} + 20\%$

- $8.2E7 \text{ N/m} < K_{lateral}(Z) < 8.2E7 \text{ N/m} + 20\%$

- $3.5.E8 \text{ N/m} < K_{longitudinal}(X) < 3.5E8 \text{ N/m} + 20\%$.

– Local interface stiffness (interface SVM/H-PLM)

Local stiffness at SVM interface points with GFRP strut support have to be specified in order to avoid the decrease of the SVM global stiffness due to low local stiffness. The local translation stiffness at interface points with SVM have been estimated. These local stiffness have to be specified for a good global satellite dynamic behaviour.

- $k_{circumference}$ > $5.7 \text{ E } 7 \text{ N/m}$

- k_{radial} > $2.5 \text{ E } 7 \text{ N/m}$

- $k_{longitudinal}(X)$ > $5.0 \text{ E } 7 \text{ N/m}$.

– Local interface stiffness (interface SVM/fuel tank)

To avoid a significant frequency decrease coming from local SVM stiffness, local interface points between fuel tank and SVM have been estimated and derived as a local stiffness requirement.

HERSCHEL SVM Interface specification

The global dynamic behaviour of HERSCHEL satellite generates forces (during sine test) at SVM/GFRP struts interface points. These dynamic local loads depend on the frequency location of subsystem modes (mainly SSH/SHH and CRYOSTAT). These loads are specified for local and global SVM interface sizing.

Local flight limit Loads

Local loads coming from dynamic behaviour of Sunshield/Sunshade structure have been also defined and specified in terms of local axial struts forces inside interface struts with SVM.

7.2.1.5. Inputs to H-PLM structural requirements specification

The objectives of the H-PLM structural requirements are to ensure a satisfactory global satellite dynamic behaviour with respect to the Launcher frequency requirements and to define the main global H-PLM dynamic loads for Payload Module sizing.

H-PLM frequency requirements

– Global H-PLM Lateral and longitudinal stiffness

CRYOSTAT strut support in H-PLM. Taking into account the local interface stiffness with SVM:

- $k_{circumference}$ > 5.7 E 7 N/m

- k_{radial} > 2.5 E 7 N/m

- $k_{longitudinal}(X)$ > 5 E 7 N/m.

H-PLM frequency requirements are:

- Frequency of the H-PLM longitudinal (X) mode > 35 Hz

- Frequency of the H-PLM lateral (Y/Z) mode > 13 Hz.

– Sunshield/Sunshade dynamic stiffness

The non symmetrical structure of Sunshade generates coupling motions mainly between lateral Z modes of SSD and lateral and longitudinal modes of HERSCHEL Satellite. In order to decrease these modal coupling, the frequencies of Sunshade lateral main modes must be higher than the SC lateral modes (located around 14 Hz and 28 Hz) and also the SC longitudinal one (around 34-35 Hz).

To reach the objective of de-coupling, the resulting frequency requirement of the Sunshade on H-PLM structure with local SVM interface stiffness is 45 Hz:

- frequency of the first Sunshade lateral mode > 45 Hz
  (All Sunshade modes must be higher than 45 Hz).

7.2.2. Microvibration analyses

This section present Microvibration analysis concerning optical instruments of HERSCHEL spacecraft.

7.2.2.1. Introduction

Microvibrations generate disturbances which can affect the instruments in two ways:

- accelerations on the optical bench which can generate perturbations on the optical instruments and in particular on bolometers

- accelerations on the cryostat exterior which can disturb the instruments via propagation of microphonic noise through the harness.

The aim of this analysis is to evaluate the level of those microvibrations:

- at the center of gravity of each optical instrument

- and at one point on the exterior of the CVV.

The main sources of perturbation identified on the HERSCHEL spacecraft are the reaction wheels used to adjust the orientation of HERSCHEL.

This study deals with the effects of one single wheel, which turns, in the range from 0 to 3600 rpm (0-60 Hz).

The configuration taken into account corresponds to the launch configuration, in which Helium tanks are full. Further studies should be carried out to know the response of the satellite when the tanks are empty.

The desired level of vibration given by SPIRE is to keep the acceleration level of the focal plane instrument below 10 µg.

7.2.2.2. Modelling and analysis

7.2.2.2.1. Numerical modelling

This micro vibration analysis is based on:

– a finite element model to predict the transfer function between the disturbance point and the instrument localization

– a model of the disturbance source.

The finite element model is the one used at the end of the proposal period, which was completed, with the physical model of the cryostat. Nodes which represent the optical equipment are the nodes: 48044, 48054, 48064 located at the center of gravity. of each instrument. The chosen node to study the CVV is the 50710, which has a central position on the shell of the CVV.

The node 12166 represents the reaction wheel.

7.2.2.2.2. NASTRAN analysis

The NASTRAN analysis is a free-free modal analysis (normalized on the generalized mass) of HERSCHEL spacecraft. Modes between 0 and 100 Hz have been taken into account for this study because they can influence the response from 0 to 60 Hz.

The output file contains the disturbing source displacements and the disturbed equipment displacements on each mode. These results are stored in a PUNCH file and are used for microvibration calculation.

7.2.2.2.3. Microvibration analysis

µVision is software developed by CNES and is specific to microvibrations. The results were checked with NASTRAN, which is well known in mechanical analysis.

The needed inputs to micro vibration calculations are:

– PUNCH file from NASTRAN analysis

– perturbing source definition: type (reaction wheel, magnetic wheel…), frequency, number of harmonics, excitation level, excitation type and direction of this excitation. Disturbance values have been derived from those typical of a 25 Nms wheel

– modal damping assumptions. They are estimated thanks to tests experience, and have been reduced in order to match with the worst case; hence we fixed this value at 0.005 for each mode.

7.2.2.2.4. Hypothesis

A static unbalance equal to 1 g.cm (1.10-5 kg.m) has been taken into account. This unbalance causes a radial force:

$$F = Us * w^2$$

with Us = unbalance mass * radial distance of this mass.

The dynamic unbalance can range from 10 to 20 g.cm². However, it is impossible to use these values with µVision software: equivalent unbalances have to be estimated. Those equivalent unbalances are expressed in kg.m which permit to reach the same level of excitation than with dynamic unbalances. We used the curves given in § 6.3.2.5. – Data sheet #1) to determine those values. Only the 3 first harmonics were taken into account; the higher harmonics are negligible. Those curves were translated to obtain a stress equal to 1.4 N at 60 Hz, which corresponds to the effect of the static unbalance for the first harmonic. Thus, the equivalent unbalances are:

– 5.625 10-7 kg.m for the second harmonic

– 1.67 10-8 kg.m for the third harmonic.

This type of wheel has also one non-integer harmonic due to bearing-driven disturbances and especially to the balls: this harmonic has a frequency equal to 0.59 * f0. According to other studies, the equivalent unbalance has been estimated to 2.487 10-6 kg.m.

NOTE: The second and third harmonics are also negligible in comparison with the fundamental level: 99 % of the maximal displacement is explained by the first harmonic. Other harmonics explain few smaller maxima (cf. § 6.3.2.5. – Data sheet #2).

A linear sum has been done with all these harmonics in order to consider maximal values of displacement and acceleration.

Only the radial forces are modelled, because axial forces are negligible.

Calculations were carried out successively with excitation along X, Y and Z axes. A rotating effort in the planes XY, XZ and YZ corresponds to a combination of these efforts, and thus the response to this rotating disturbance is between the responses of excitations along the two axes of the plane considered separately (cf. § 6.3.2.5. – Data sheet #3).

7.2.2.3. Results

According to this hypothesis, this analysis shows that:

– the maximal acceleration of the optical equipment reaches 7.7 mg along the Z axis, at a frequency equal to 60 Hz, when disturbance is along the radial axis Z

– the global accelerations level is around 5 mg at many different frequencies from 29 Hz to 60 Hz (cf. § 6.3.2.5. – Data sheet #4)

– the maximal acceleration of the CVV, less damped than the focal plane, reaches 42 mg.

These results have a linear dependence towards damping assumptions and towards the amplitude of the excitation. It should be interesting to know more exactly which damping assumptions we could attribute to each mode (we decided to put 0.005 on each mode; an other hypothesis estimates that 0.02 is also realistic. This would allow to divide the level of acceleration by 4).

As a conclusion, those accelerations are very different from the desired level of 10 µg. However, a simple computation shows that this kind of wheel turning at 36.3 Hz (one of the mode of the structure), generates an associated effort of 0.521 N; if the structure is considered as a rigid body, this force creates an acceleration equal to:

$$\gamma = 0.521 / (3023 * g) = 17.5 \ \mu g$$
(3023 kg is the mass of Herschel satellite).

Thus, the acceleration without structure amplification already exceeds the specification. Consequently, it is not surprising that a structural mode generates acceleration 500 times higher than the specification.

This analysis shows that it seems difficult to be compliant with the desired level of 10 µg. It should be necessary to try to re-evaluate this specification and in a same time, to improve the model and our knowledge of the reaction wheel.

To reach the desired level of 10 μg (if this level is really justified), it could be possible to support the optical equipment with passive damping devices (an active control of the damping is excluded because this solution is not certified yet). An other solution could be either to change the wheels or to mount the wheel on a flexible support. This last solution has several system impacts:

- design of a support which is compatible with attitude control

- use of a launch lock system with in-orbit release

- thermal control of the wheel will be disturbed by the isolation support.

Due to the complexity of such device, it is not considered to be part of the baseline.

7.2.2.4. Preliminary conclusion

The results, as presented above, predict microvibration levels in the range of 1 to 10 mg on the FPU, and about 50 mg on the CVV. These rather high levels appear at the various resonances peaks of HERSCHEL PLM, when the wheel rotation speed sweeps up the same frequency range.

This analysis is considered as a reference for assessment of microvibration levels on Optical Bench of th HERSCHEL spacecraft. As a recall, it is to be mentioned that similar Reaction wheels were used on ISO without negative effects on detectors or mechanisms.

7.2.2.5. Technical data

Data sheet #1

Typical Reaction wheel Microvibration perturbations

Chart showing Induced Force (mN peak) versus Frequency of rotation (Hz) on logarithmic axes. Harmonic index legend: 1, 2, 3, 4, 5, 6, 7, 8, 9, 10, 20.
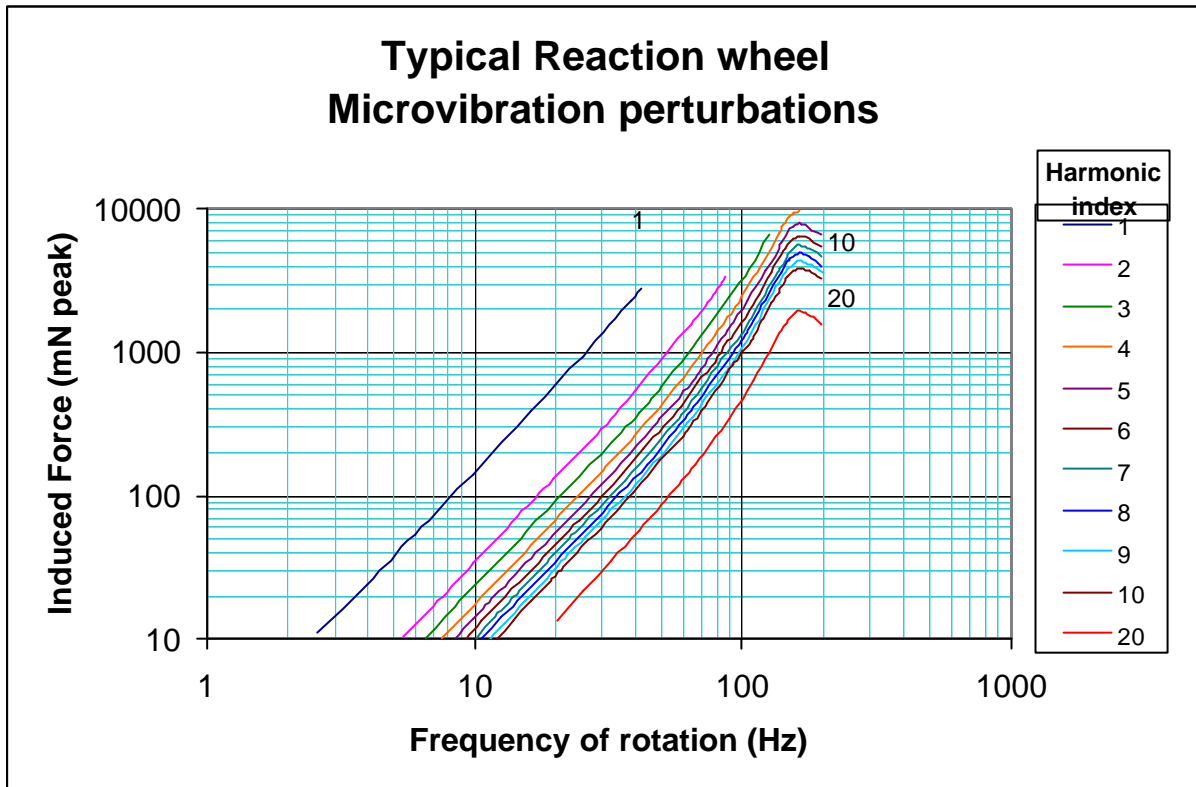
Data sheet #2

Explanation

Date	Dossier FSD
10-07-2001	c:\µVISION\Herschel2.fsd\Herschel2.fsd

Commentaire

Participation des harmoniques dans la réponse :
Courbe 1 en rouge : réponse avec toutes les harmoniques (l'harmonique 2 entraîne les pics autour de 17 Hz)
Courbe 2 en bleu : participation de l'harmonique 1
Courbe 3 en noir : participation du mode de cage

1 ——— Her-440H123c-xx : Critère Somme Linéaire -H4 Critère Translation opt Radian -Ry
2 ——— Hers-440-H1-xx : Critère Somme Linéaire -H1 Critère Translation opt Radian -Ry
3 ——— Hers-440-cage : Critère Somme Linéaire -H1 Critère Translation opt Radian -Ry

The response to the three harmonics (red curve) is mainly due to the disturbance corresponding to the fundamental level (Harmonic 1): the blue curve, associated to the Harmonic 1, is similar to the red one and justifies more than 99 % of the maximum value. The peaks located around 17 Hz are the consequence of the second harmonic: they are the image of the major peak (2.5 10-7 m) at a frequency divided by 2. The response due to the third harmonic is not visible. And the black curve which represents the effects of the bearing-driven disturbances, focuses on the fact that this non-integer harmonic generate minor peaks at a frequency divided by 0.59 in comparison with the main peaks.

Data sheet #3

Date	Dossier FSD
10-07-2001	c:\µVISION\Herschel2.fsd\Herschel2.fsd

Commentaire

Décomposition d'un effort tournant en deux efforts sur 2 axes :
Courbe 1 en bleu : excitation suivant l'axe X seul (réponse suivant Y)
Courbe 2 en vert : excitation suivant l'axe Y seul (réponse suivant Y)
Courbe 3 en rouge : excitation tournant dans le plan XY (réponse en Y) ; la courbe est contenue entre les 2 courbes sur X & Y

1 ——— Her-440H123c-xx : Critère Somme Linéaire -H4 Critère Translation opt Radian -Ry
2 ——— Her-440H123c-yy : Critère Somme Linéaire -H4 Critère Translation opt Radian -Ry
3 ——— Her-440H123c-xy : Critère Somme Linéaire -H4 Critère Translation opt Radian -Ry

Explanation

The red curve shows the excitation due to a revolving effort in the plane XY. This response is a combination of a sinusoidal disturbance along the axis X only (blue curve) and of a sinusoidal disturbance along the axis Y only. The two excitations along X and Y envelop the revovling excitation and thus, they correspond to the worst case.

Data sheet #4

Nœud de sortie	Instrument optique 1 (Nœud 48044)								
Axe d'excitation	X			Y			Z		
Axe des déplacements	x	y	z	x	y	z	x	y	z
Déplacement maximum (m)	1.48E-07	2.36E-07	4.50E-07	8.26E-08	5.00E-07	1.78E-07	5.45E-07	3.48E-07	9.33E-07
Fréquence du déplacement max (Hz)	59.4	32.9	29.3	42	44.8	42.5	59.4	36.2	36.3
Accélération associée au déplacement max (g)	0.00210148	0.001028	0.00155467	0.00058637	0.00403847	0.00129386	0.00773856	0.00183522	0.0049475
Accélératin maximale si différente (g)	0	0	0.00267126	0.00072764	0	0.00136846	0	0.00218885	0.00727272
Déplacement associé (m)			1.85E-07	5.87E-08		1.10E-07		2.71E-07	5.02E-07
Fréquence associée (Hz)			59.9	55.5		55.6		44.8	60
Accélération maximale (g)	0.00210148	0.001028	0.00267126	0.00072764	0.00403847	0.00136846	0.00773856	0.00218885	0.00727272
Nœud de sortie	Instrument optique 2 (nœud 48054)								
Axe d'excitation	X			Y			Z		
Axe des déplacements	x	y	z	x	y	z	x	y	z
Déplacement maximum (m)	1.09E-07	6.41E-07	4.31E-07	8.54E-08	5.11E-07	1.63E-07	4.95E-07	6.42E-07	8.22E-07
Fréquence du déplacement max (Hz)	60	35.3	29.3	42.4	44.8	29.4	53.5	43.3	36.3
Accélération associée au déplacement max (g)	0.00157914	0.00321439	0.00148903	0.00061785	0.00412732	0.00056699	0.00570169	0.00484397	0.00435889
Accélératin maximale si différente (g)	0	0.00344802	0	0.00472658	0	0.00093186	0	0	0
Déplacement associé (m)		2.38E-07		3.34E-07		1.27E-07			
Fréquence associée (Hz)		60		59.3		42.7			
Accélération maximale (g)	0.00157914	0.00344802	0.00148903	0.00472658	0.00412732	0.00093186	0.00570169	0.00484397	0.00435889
Nœud de sortie	Instrument optique 3 (nœud 48064)								
Axe d'excitation	X			Y			Z		
Axe des déplacements	x	y	z	x	y	z	x	y	z
Déplacement maximum (m)	1.31E-07	2.95E-07	4.41E-07	1.58E-07	5.45E-07	2.72E-07	4.06E-07	3.08E-07	8.96E-07
Fréquence du déplacement max (Hz)	59.5	35.4	29.3	44.8	44.9	35.4	59.4	36.2	36.3
Accélération associée au déplacement max (g)	0.00186636	0.00148771	0.00152358	0.00127616	0.0044216	0.00137172	0.00576487	0.00162427	0.00475129
Accélératin maximale si différente (g)	0	0.0016226	0.00340456	0	0	0.00157914	0	0.00247154	0.00496921
Déplacement associé (m)		1.12E-07	2.35E-07			1.09E-07		3.06E-07	3.43E-07
Fréquence associée (Hz)		60	60			60		44.8	60
Accélération maximale (g)	0.00186636	0.0016226	0.00340456	0.00127616	0.0044216	0.00157914	0.00576487	0.00247154	0.00496921
Nœud de sortie	Point du CVV (Nœud 50710)								
Axe d'excitation	X			Y			Z		
Axe des déplacements	x	y	z	x	y	z	x	y	z
Déplacement maximum (m)	8.24E-08	1.07E-07		4.67E-08	1.01E-07		2.99E-06	2.48E-07	
Fréquence du déplacement max (Hz)	59.8	43.3		55.8	43.3		59.4	43.4	
Accélération associée au déplacement max (g)	0.00118582	0.00080733	0	0.00058516	0.00076206	0	0.04245558	0.00187984	0
Accélératin maximale si différente (g)	0	0.00092989	0	0	0.00079247	0	0	0	0
Déplacement associé (m)		6.44E-08			5.47E-08				
Fréquence associée (Hz)		59.9			60				
Accélération maximale (g)	0.00118582	0.00092989	0.00318675	0.00058516	0.00079247	0.00127829	0.04245558	0.00187984	0.00138084
Accélération maximale des instruments optiques (g)	0.00773856								
Accélération maximale du point sur le CVV (g)	0.04245558								

Valeur issue de Nastran : accélération de 0.22ms² pour un echelon d'ampliude unité à 60.0Hz (or à cette fréquence l'excitation a une amplitude de 1.421)

Valeur issue de Nastran : accélération de 0.26ms² pour un echelon d'ampliude unité à 43.9Hz (or à cette fréquence l'excitation a une amplitude de 0.760)

Valeur issue de Nastran : accélération de 0.26ms² pour un echelon d'ampliude unité à 36.3Hz (or à cette fréquence l'excitation a une amplitude de 0.521)

7.2.3. Thermal Analyses

The system thermal analyses presented hereafter deal with the impact of the L2 injection scenario.

The present baseline for the spacecraft transfer to L2 is a direct injection by the launcher at the end of the coast arc. As discussed in Section 4, an alternative scenario is being studied: the envisaged strategy is that the ARIANE 5 upper stage inject both spacecraft in a highly eccentric orbit (called parking orbit) after the coast arc. After parking perigee passage, the final injection to the L2 transfer orbit will be achieved thanks to the spacecraft own propulsion system. An overview of the this strategy is outlined in Figure 7.2.3-1.

REMARK: Sketch not to scale.
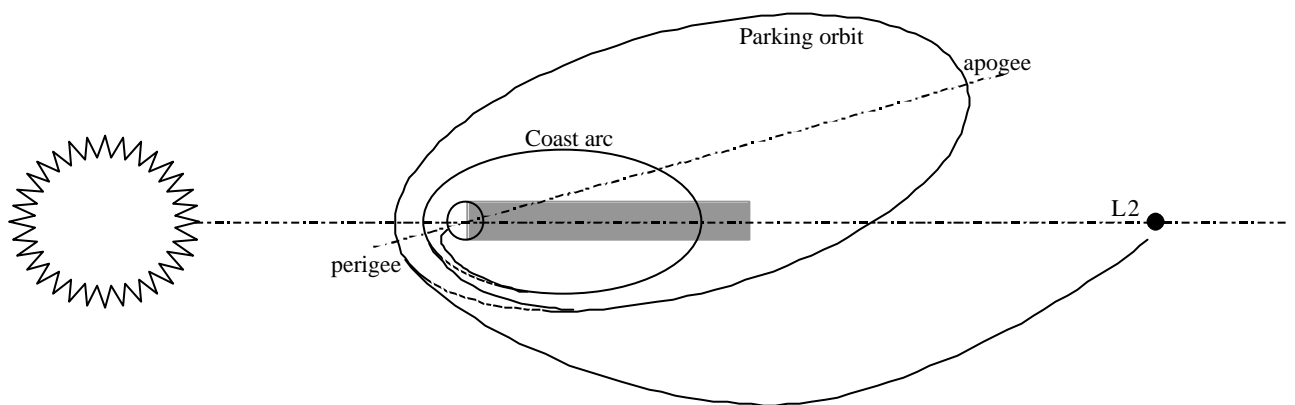
FIGURE 7.2.3-1 L2 ALTERNATIVE INJECTION SCENARIO

From a thermal performances point of view, the impact of such a scenario is clearly related to the CVV lifetime. Indeed, after cool down of the CVV when travelling to the parking orbit Apogee, the spacecraft is submitted again to Earth flux and Albedo when approaching the Earth to complete the parking orbit. The second impact on the CVV lifetime is obviously the time lost to complete this orbit (see assessment in Section 4).

The orbital parameters of the parking orbit are not yet frozen. However, the range of these parameters are known:

- Apogee: between 470 000 km and 700 000 km

- Perigee: between 230 km and 4 200 km

- eclipse will be avoided by selecting the right launch window

- period: between 14 days for a 470 000 km Apogee up to 21 days for a 700 000 km Apogee (Perigee altitude has no impact on the orbit duration).

In order to compute the external CVV temperature profile, we have compared first the results obtained with the simplified modelling of the HERSCHEL PLM (TMM used for the technical proposal) to the one given by the TMM including the detailed modelling of the CVV (provided by ASTRIUM)). The aim is to confirm validity of the simplified model in order to use it for system analyses which requires a large number of simulations. For the two analyses, the input parameters for computation are the following:

- CVV external envelop temperature at the beginning of the parking orbit: T = 300 K (this hypothesis shall be assessed in future works)

- Earth temperature for IR flux computation: 255 K

- albedo coefficient: 0.3

- solar constant: 1428 W/m^2 (Winter Solstice at Earth level).

- Spacecraft attitude: 3 axis stabilized.

  - +Z axis Sun-pointed during the whole parking orbit (the hypothesis will have to be refined for HERSCHEL as the current baseline plans to have a constant rotation of the spacecraft).

  - +X axis perpendicular to the ecliptic plane.

- Sunshield and sunshade temperature set respectively at 270 K and 370 K. Theses values are representative of the actual ones along the parking orbit. The exact numbers are not required since the rear side of these two elements facing the CVV are covered with MLI blankets, then damping the temperature variation effects on the CVV temperature.

- Telescope temperature set at 313 K to simulate the decontamination phase

The following figure shows the external CVV envelop cool down profile obtained respectively with the simplified and detailed CVV TMM.
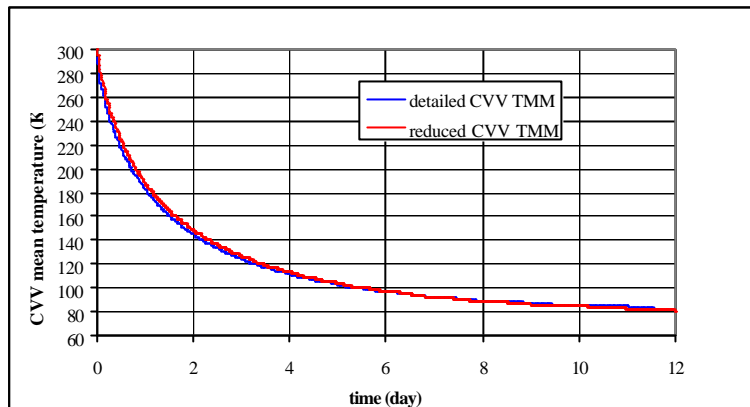
FIGURE 7.2.3-2 CVV COOL DOWN PROFILE CALCULATED WITH RESP. A SIMPLIFIED AND DETAILED CVV TMM

The previous curve demonstrate that the use of a simplified CVV TMM is representative enough to compute in a reasonable time transient system analyses. The results presented hereafter are consequently obtained with the reduced CVV TMM.

The next figure shows the CVV temperature increase when submitted to albedo and Earth flux for three perigee altitude, i.e. 200 km, 1100 km and 4200 km. The telescope decontamination duration has been set at three weeks.
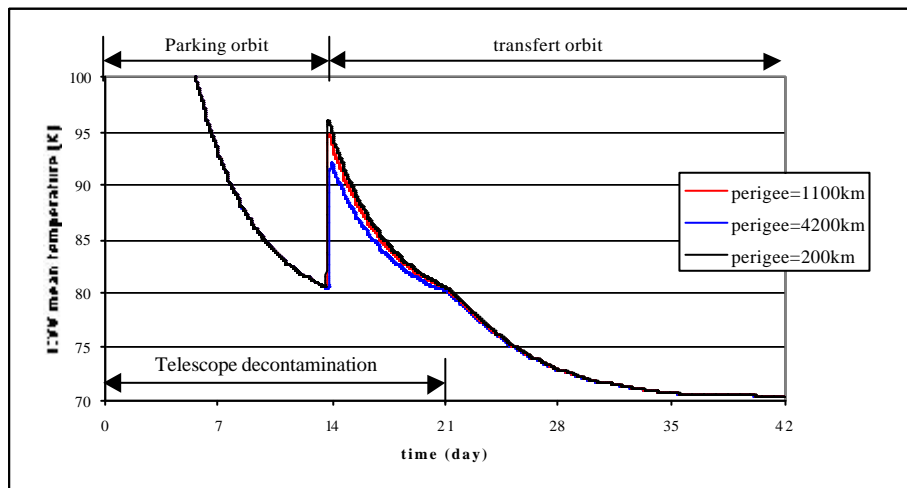
FIGURE 7.2.3-3 PERIGEE ALTITUDE INFLUENCE ON CVV EXTERNAL TEMPERATURE INCREASE

It has to be noted that aerothermal fluxes are not taken into account, which is a realistic hypothesis for high altitudes. For lower altitude, the aerothermal flux is important on surface perpendicular to the speed vector. The CVV external radiator should not be submitted to a high level of aerothermal flux. This point will be however assessed as soon as information expected from ARIANESPACE will be available.

The perigee passage induces a sharp increase in CVV temperature. At the end of the parking orbit, the CVV has reached a temperature of 80 K and the Perigee passage increases this temperature by 10 to 15 K. As expected, the lower Perigee altitude has more impact, but the difference between 200 km and 4200 km Perigee altitude is only 5 K on the cryostat temperature. The temperature recovery to 80 K takes one week in all cases.

The impact on the CVV Helium consumption and thus lifetime are undergoing. If the impact are considered significant, sensitivity studies shall be performed to find out the better spacecraft attitude to limit the extra Helium consumption, while meeting all the mission requirements.

7.2.4. Radiation analyses

7.2.4.1. General

The radiation environment is discussed in AD07.2, Environment Specification, § 3.4.4.2.

General radiation related damage mechanisms to which the satellites will be subjected include:

- total dose ionization damage of electronics and Solar Arrays due to Electrons and Protons

- single event phenomena (upsets, latchups, burnouts, Transient, Hard Error, Functional Interrupt, ...) of electronics due to the cosmic ray, solar flare environments and trapped Protons

- displacement damage induced mainly by Protons affecting Solar Arrays, CCDs, and optocouplers and bipolar electronics.

As a general statement, equipment are designed to survive the space radiation environment during the Radiation Design Lifetime.

The radiation and Single event effects hardness assurance is a general product assurance activity involving:

– dose depth curves and Let spectra calculations

– tasks related to Parts/materials selection, characterization and Radiation Lot Acceptance Testing

– deposited doses and upset rates calculations

– equipment Worst Case Analysis (WCA) and outage analysis.

The process of radiation hardening is illustrated in Figure 7.2.4-1 hereafter.
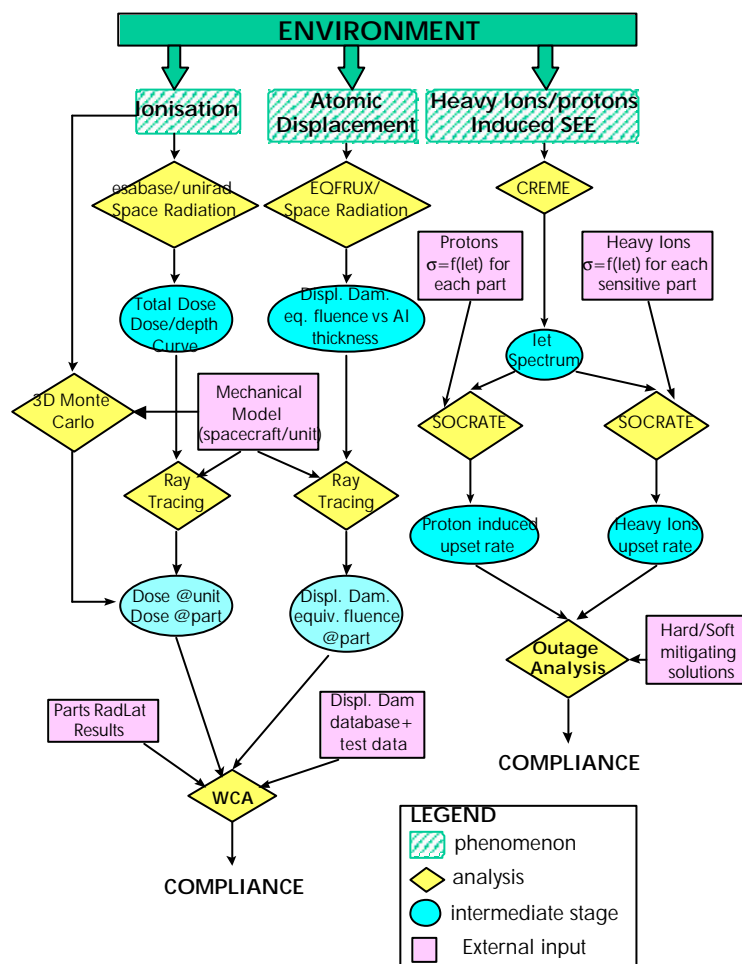
FIGURE 7.2.4-1   RADIATION ANALYSES PROCESS

Basically, it consists in, starting from the environment, to derive via analyses and tests, for each effect, the compliance of the design. It is demonstrated, in the end, via two types of analyses:

– the Worst Case Analysis (WCA) establishes, at unit level, the compatibility of the design with the worst case operating conditions, including end of life effects due to total dose and displacement damage effects of the radiative environment

– the outage analysis establishes, at unit or subsystem level, the compliance of the design with outage requirements, derived from system availability requirements, taking into account the non destructive Single Event Effects.

Several intermediate steps have to be achieved. Each of them is attained by dedicated analysis and/or tests:

– Environment analysis to deduce applicable specifications:

• further analysis to place the radiative environment in the spacecraft context, i.e. to introduce the spacecraft mechanical modelling; this is achieved nominally by ray tracing analysis using DOSRAD software (from ESABASE suite of software) or Novice software. The outputs of the task are sectorial analyses of the shielding brought by the satellite and the units in term of total dose and displacement damage; they providing environment figure at unit level

• analysis to place the Single Events environment in the spacecraft context. The Protons induced and Heavy Ions SEU rates computations are directly performed starting from sensitive parts test data and reporting them in the Single Event Upset Optimized Calculation RATE (SOCRATE) software, developed by ALCATEL.

7.2.4.2. HERSCHEL Analyses

The previous chapter has described the general approach. The specific conditions for HERSCHEL satellite are now described.

Total dose

It is expressed as a deposited dose vs Aluminium thickness curve. It is specified in AD07.2, and recalled hereafter in Figure 7.2.4-2.

A Radiation Design Margin of 2 shall be applied on top of the sectorial **analysis worst case results between HERSCHEL and PLANCK**, based on HERSCHEL & PLANCK CAD models. Later the unit WCA shall account for the parts degradation corresponding to the marged cumulated dose requirement.

However, AD07.2 asks for a minimum susceptibility level for the active parts, of 10 krad, which implies, considering the RDM of 2, that the spacecraft and units should bring a minimum shielding effect of an equivalent of 2 mm of Aluminium to any active component. This is believed a priori very easy to achieve, and it will be demonstrated by the sectorial analysis.
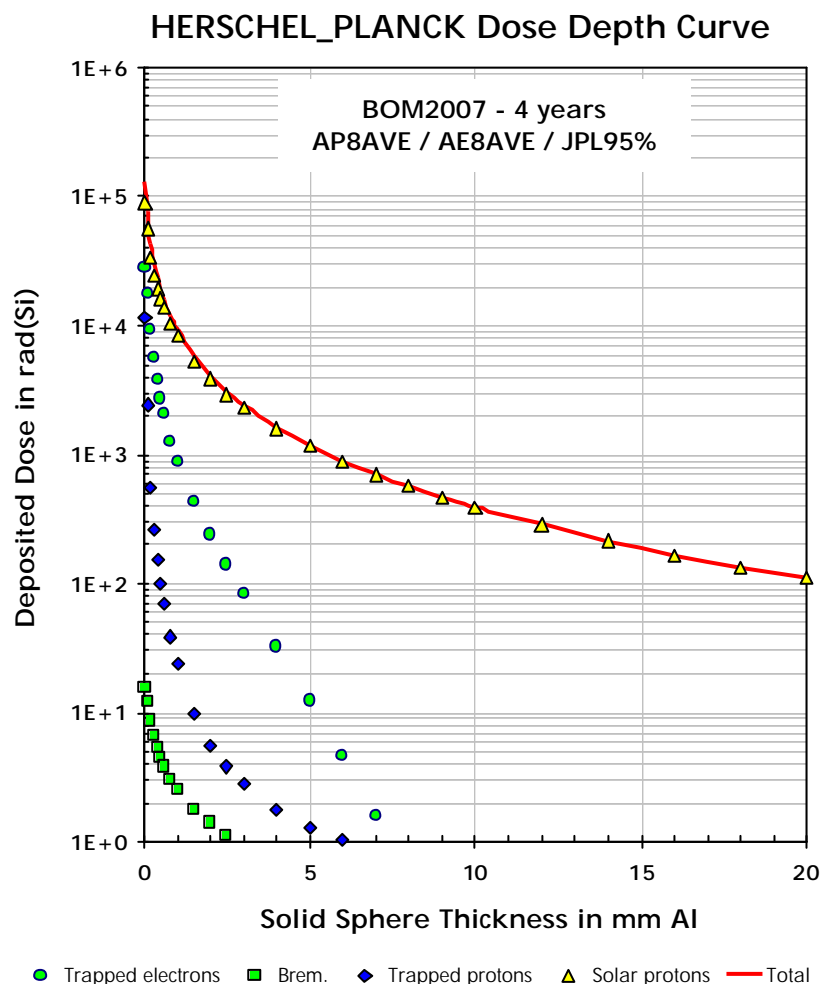
FIGURE 7.2.4-2 TOTAL DOSE CURVE

Displacement damage

The L2 environment is similar to GEO environment for particles involved in displacement damage (mainly high energy Protons).

Depending on the target, optoelectronic devices or semi conductor devices, the displacement damage requirement is expressed in different ways:

– **Opto electronic devices: solar cells**

It has here to be turned into 1 MeV e- equivalent fluence, for solar cells degradation assessment, and is specified in AD07.2. The effect of the mission Protons fluence on the Pmax of the selected GaAs cells type is recalled in Figure 7.2.4-3.

On the one hand, the thickness of the coverglass retained in the baseline is 100 μm for both spacecraft, leading to a 1MeV e- fluence of ~1^E14 e-/cm² for Pmax.

On the other hand, Figure 7.2.4-4 provides, for the dual junctions GaAs solar cells selected in the baseline, the specified degradation of their parameters as a function of the irradiation. This shows that Pmax should not degrade by more than 3.5 % over the HERSCHEL mission lifetime.

– **Semi conductor**

Here the part of energy deposited involved in displacement damage effects is called NonIonizing Energy Loss (NIEL). The particles fluxes spectra are converted into a fluence of monoenergetic particles producing the same amount of defects (10 MeV Protons).

This Displacement Damage Equivalent Fluence (in 10 MeV Protons) is specified in AD07.2 as a function of the Aluminum equivalent shielding surrounding the device, and is recalled in Figure 7.2.4-5.

However, AD07.2 asks for a minimum susceptibility level for the active parts, of 6.10^9 p+/cm² (in Si), which implies, considering the RDM of 2, that the spacecraft and units should bring a minimum shielding effect of an equivalent of 4 mm of Aluminium to any active component susceptible to displacement damage effect. This is believed feasible, and it will be demonstrated by the sectorial analysis.

This effect shall be considered within the units Worst Case Analyses.

Equivalent Fluences in GaAs - PMAX
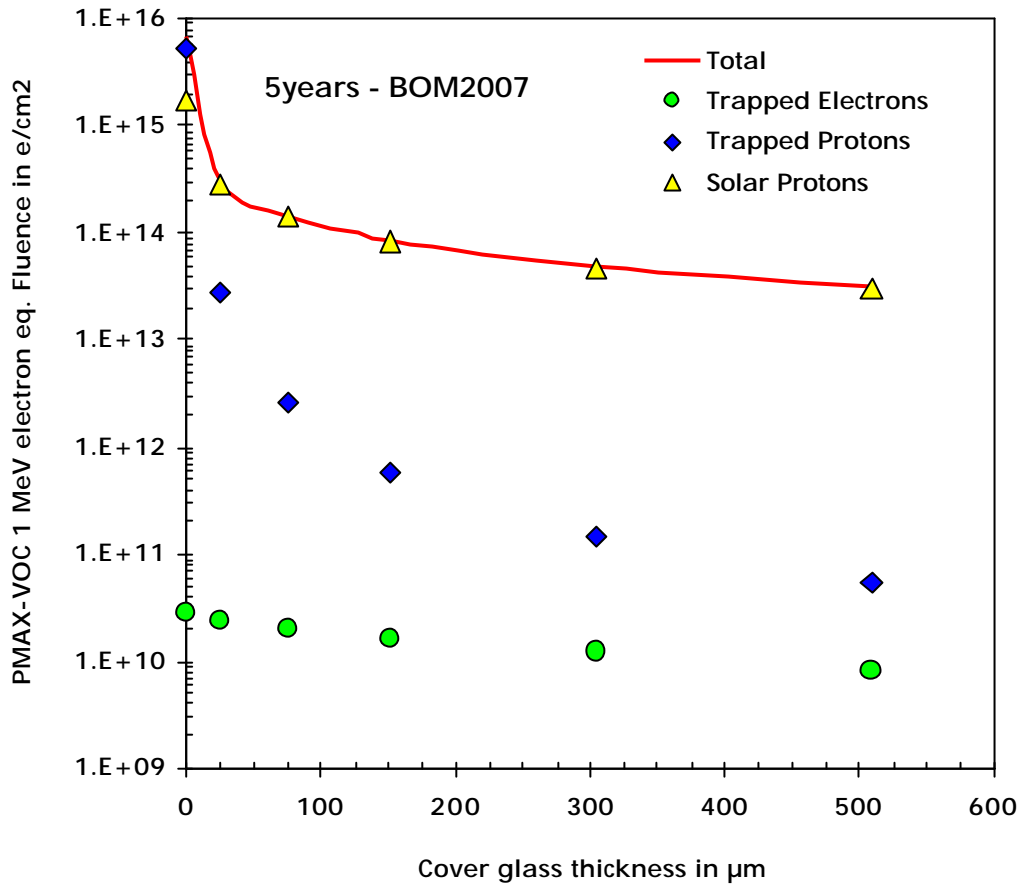
FIGURE 7.2.4-3 1 MEV ELECTRON FLUENCE
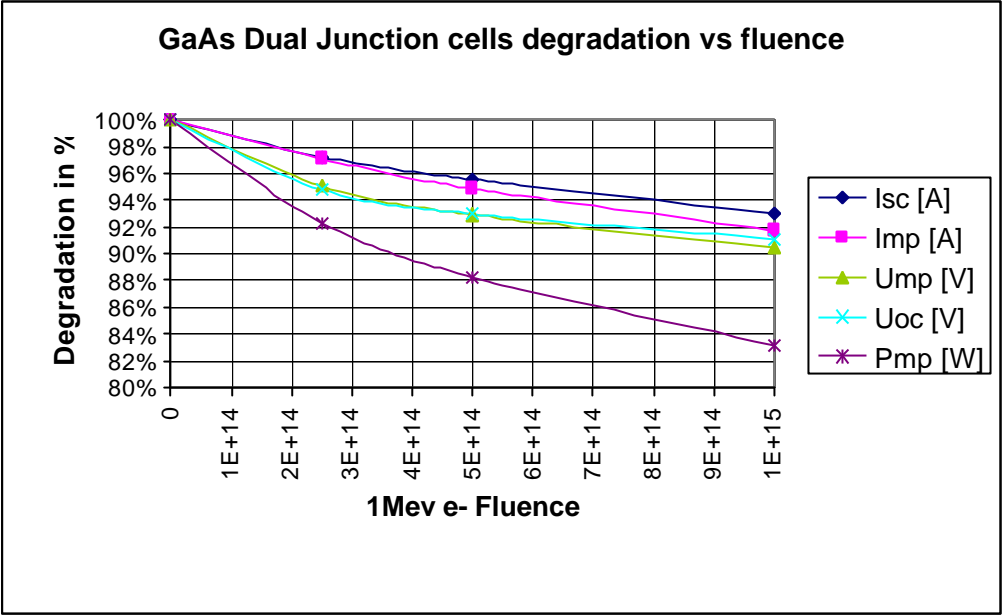
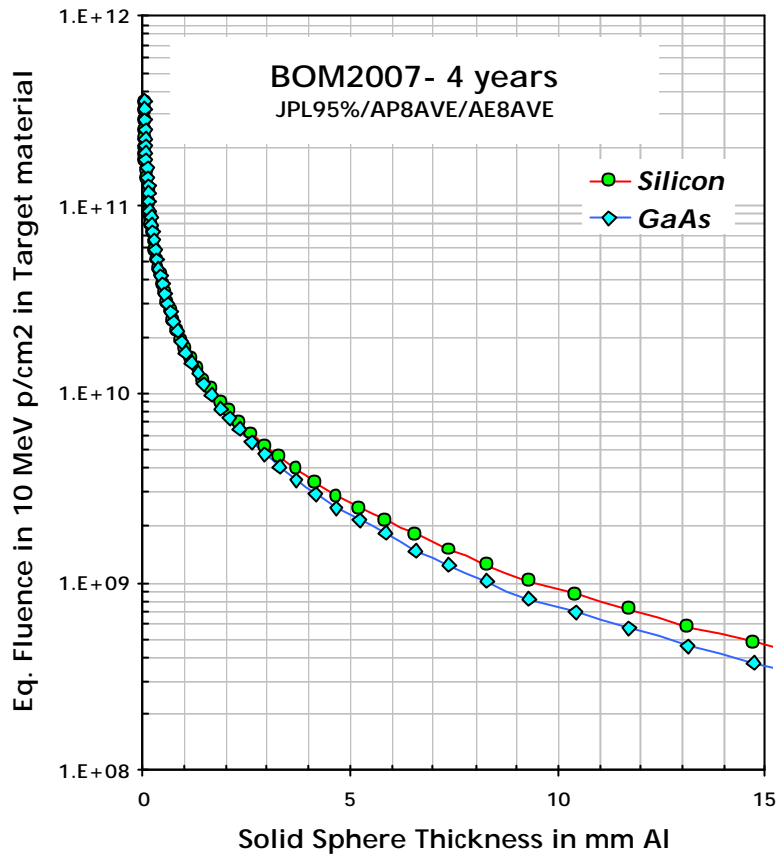**FIGURE 7.2.4-4 GAAS CELLS DEGRADATION VS IRRADIATION**

FIGURE 7.2.4-5 DISPLACEMENT DAMAGE FLUENCE CURVE

Single Event Effects

The environment applicable to L2 for heavy Ions is shown in AD07.2 Figure 3-29, expressed in LET spectrum; it is basically comparable to the GEO case. This environment is used to derive, in Figure 7.4.2-7, a Heavy ions induced SEU rate as a function of the LET threshold of the part.

It shall be used, together with the critical parts [cross section as a function of LET] characteristic, to compute a "single upset rate" in upset/bit (or/part)/s related to heavy ions.

The high energy Protons environment considered for SEU assessment is the October 89 solar flare peak 5 mn flux, shown in AD07.2 Figure 3-27. This environment is used to derive, in Figure 7.4.2-6, the Protons induced rate as a function of the Proton energy threshold A of the part.

It shall be used, together with the critical parts [cross section as a function of A] characteristic, to compute a "single upset rate" in upset/bit (or/part)/s related to Protons.

Note that, because of the Mass Memory, which high density parts are known to be susceptible to SEE, double error rates will also be derived.

The upset rates will be introduced as part as an overall units/subsystem availability analysis. This analysis will account for corrective actions implemented to mitigate the effect of SEE: EDAC for single errors correction, memory scrubbing to decrease the double error probability, mass memory organization. The memory scrubbing mechanism(s) overall period will be set based on the double error rate.
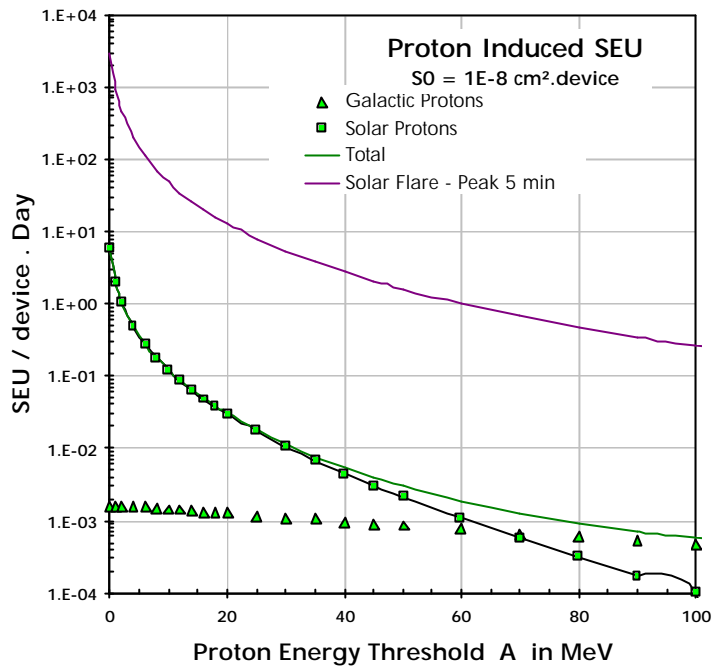
FIGURE 7.2.4-6   PROTONS INDUCED SEU RATE
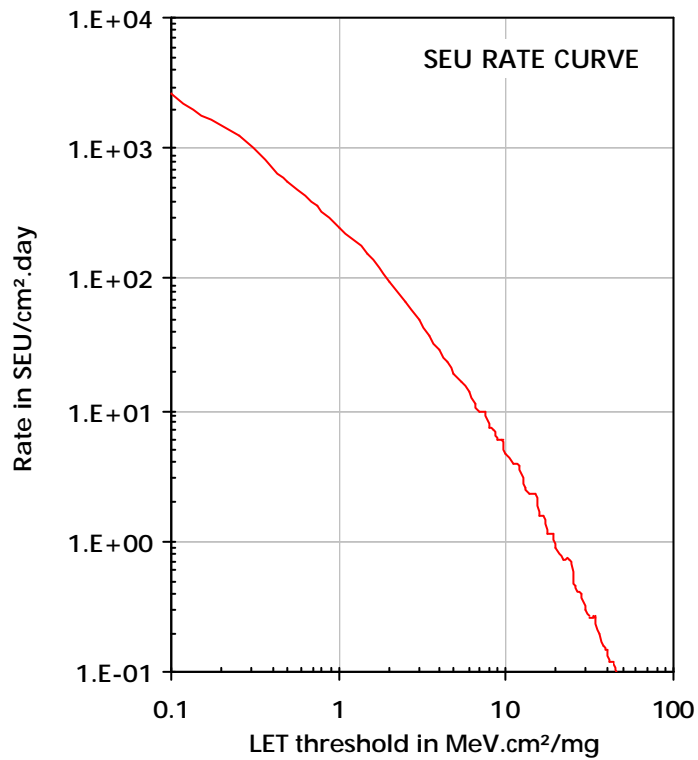
FIGURE 7.2.4-7   HEAVY IONS INDUCED SEU RATE

7.2.5. HERSCHEL EMC/ESD analyses

HIFI Radiated Susceptibility in IF band

HIFI units acceptable interference levels in IF band [3.5 – 9 GHz] is identified in a draft note from SRON "HIFI sensitivity to EMI". The conclusion is that the maximum allowable EMI level at the spectrometers (HRS and WBS) is – 115 dBm.

There are 3 types of limitations to the Shielding Efficiency (SE) of an RF unit:

- RF leakage due to D connector(s)

- RF leakage due to SMA connector(s)

- RF leakage due to space between RF body and cover.

These limitations are linked to the RF gaskets performances set between SMA connectors and unit structure, and between RF body and RF cover. The decoupling between the "TM/TC" part of the unit where D connectors are set and the purely RF part is achieved by feed-through connectors.

Concerning the venting holes, they should have no impact on the units overall shielding efficiency as long as the following relation between Length (l) and Diameter (D) is verified:

$$D < 4*l.$$

The venting holes then behave as waveguides below cut-off frequency and the shielding efficiency is approximately given by:

- SE ~ 30*l/D, i.e. SE > 120 dB, if the a.m. condition if fulfilled.

Measurements of the shielding efficiency of Channel Amplifiers Linearisers built by Alcatel Space Toulouse and operating in either C, X or Ku-Bands gave approximately SE = 100 dB.

Those measurements where performed in the frame of RS tests.

In the above measurement result, the SE is defined as SE (dB) = -G$_R$(dB), with:

$$P_R = \frac{E^2}{120\boldsymbol{p}} \times G_R \times \frac{\boldsymbol{l}^2}{4\boldsymbol{p}} \, .$$

- – E: illuminating E field.

- – P$_R$: spurious power received at unit input, i.e. spurious power at unit output/ active gain.

- – λ: wavelength.

HIFI IF units being more complex (bigger, more connectors, etc.) than the a.m. equipment, their shielding efficiency may not be as good. Anyway we take the hypothesis that a shielding efficiency of 90 dB is possible to reach.

The RS specification from IID-A is 2 V/m. With SE = 90 dB, the corresponding EMI level would be –113 dBm at 4 GHz. With SE = 100 dB, it would be –123 dBm at 4 GHz.

For that reason, ALCATEL is of the opinion that HIFI RF unit have good chances to pass successfully the RS test, and so that it is too early to envisage a specification relaxation.

HIFI compatibility with X-Band telemetry

The new RE specification is 64 dBµV/m at 4 GHz and 69 dBµV/m at 8 GHz.

RE tests performed on a 115W X-Band TWTA on a telecom program gave 89.4 dBµV/m at 1 m at 7.5 GHz at saturation.

Considering 30W for HERSCHEL TWTA, 84 dBµV/m can be expected, meaning that the RE specification (69 dBµV/m) is challenging for the tube.

If the distance between TWTA and HIFI RF units is roughly 1 m, assuming for a first approach that the field level from the TWTA at HIFI RF units location is the same as measured in the RE test, the picked-up EMI level will be the following, for the worst case hypotheses:

- – SE = 90 dB

- – E = 84 dBµV/m

- $P_R(dBm) = E(dB\mu V/m) - SE(dB) + 10 \cdot \log \dfrac{\lambda^2}{4\pi} - 115.76$

- Picked-up power level: -161 dBm (at 8 GHz).

Such a level would be acceptable for HIFI and would even leave a few tens of dB of system margin.

But the free space propagation assumption taken above is not valid.

At 8 GHz, the SVM behaviour should be modelled as a multimode - or oversized - cavity, intermediate between those of a free space and of a resonant cavity.

According to this theory, the ambient fields in the cavity are roughly homogenous and isotropic. The distance between units is not a relevant parameter, and the orientation and polarisation of a given leaking point does not matter.

A given amount of RF power injected into the cavity is uniformly attenuated; the power picked up by a receive Probe is independent of the probe location and orientation.

This fixed attenuation is called cavity insertion loss X_c. It is a function of the area of the apertures, wall conductivity and magnetic permeability, and of the frequency.

The cavity insertion loss X_c is a combination of a radiative component X_ρ (corresponding to the power radiated through the apertures and slots) and a conductive component X_σ (corresponding to the ohmic losses in the walls).

$$\frac{1}{X_c} = \frac{1}{X_\rho} + \frac{1}{X_\sigma} \text{ with } \frac{1}{X_\rho} = \frac{8\pi S_0}{\lambda^2} \text{ and } \frac{1}{X_\sigma} = \frac{8\pi(S - S_0)}{\lambda^2}\sqrt{\frac{\pi}{\lambda C \sigma \mu}}.$$

Where S is the overall area and S_0 the total surface of apertures and slots.

The spurious power radiated by the TWTA at the X-Band TM frequency is equal to:

- $P_r = \dfrac{E_r^2}{30}$ with E_r the RE field measured in free-space in the standard conditions of test at 1 m.

In the SVM oversized cavity, the spurious radiated power P_r suffers an attenuation equal to the cavity insertion loss X_c, that becoming $P_r' = X_c.P_r$

And the corresponding spurious field at any point of the satellite cavity is:

$$E_r^{'} = \frac{4\pi}{\lambda} \sqrt{30. P_r^{'}} \; .$$

Considering a typical value for X_c of − 30 dB, we obtain the following:

- For E_r = 84 dBµV/m:

  - P_r = -20 dBm, P_r' = -50 dBm (10 nW) and E_r' = 180 mV/m (105 dBµV/m).

With SE = 90 dB, the corresponding EMI level would be −140 dBm at 8 GHz.

Such an EMI pick-up level would be acceptable for HIFI.

The X_c = -30 dB will have to be consolidated at a later stage, but so far, the compatibility of the TWTA spurious radiated emission at X-Band TM frequency with HIFI spectrometers seems quite possible to achieve with realistic assumptions for the spectrometers shielding efficiency and for the TWTA RE.

For that reason, ALCATEL is of the opinion that the need to switch off the TWTA during HIFI observations is not demonstrated.

Cryostat shielding efficiency

In order to be able to assess the EMC between the radiated emission from the SVM and the low level detection signals in the cryostat, one must be able to estimate the cryostat shielding efficiency.

On ISO program, various approaches were investigated by AS, MBB and ESA. In the end, the following curve was commonly agreed:
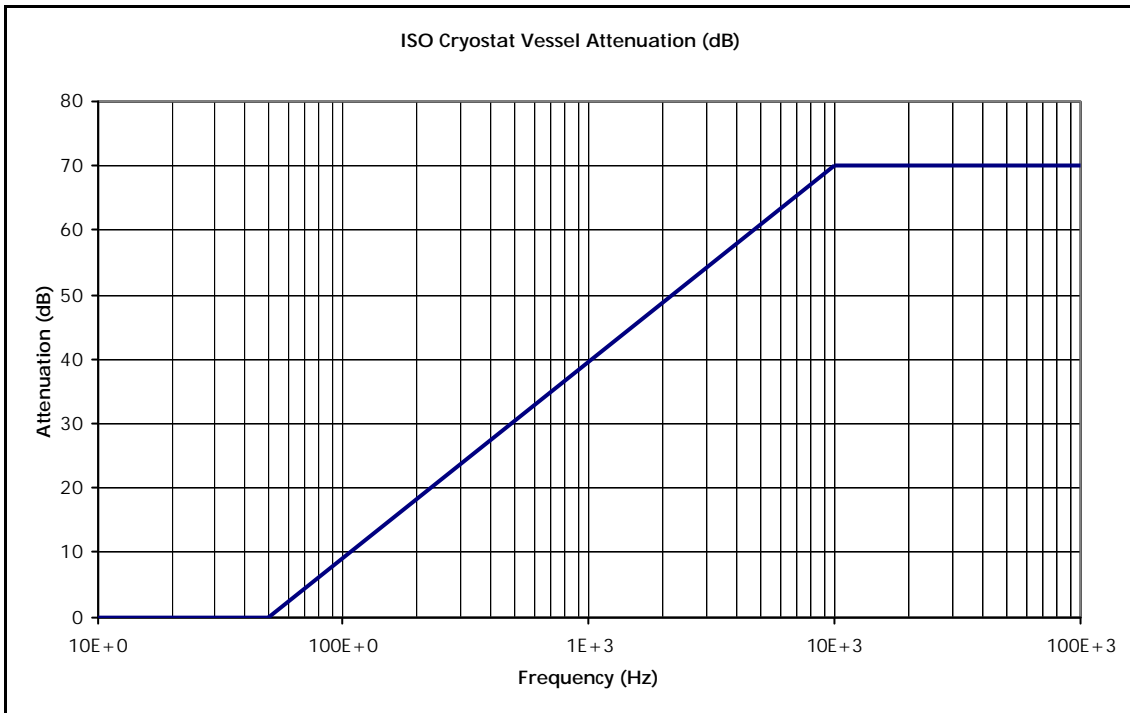
The shielding efficiency of a metallic barrier follows roughly the following behaviour:

– at low frequencies, the SE is the worst for a near H field source, and is driven by the metal properties; it increases according to frequency

– at high frequencies, the SE is limited by the openings and decreases according to frequency, until it reaches 0 dB.

The following formulas can be found in literature (Mardiguian).

The attenuation due to the metal properties can be decomposed in Reflection (R) and absorption (A) losses.

For a near magnetic field source (i.e. current loop), we have the following:

$$R(dB) = 74.6 + 20LogD(m) + 10LogF(MHz) - 10Log\frac{\mu_r}{\sigma_r}$$

with:

- D: Distance between source and shield

- μ$_r$: relative permeability

- σ: conductivity relative to copper.

$$A(dB) = 131 \cdot e(mm)\sqrt{F(MHz)\sigma_r\mu_r}$$

with:

- e : metal thickness.

This term is independent on the field conditions (near, far, E, H).

The attenuation due to the metal properties then expresses as:

$$SE_{material} (dB) = R(dB) + A (dB) - C(dB).$$

C is a correcting factor relative to reflections internal to metal thickness, when it is lower than skin depth.

C is a function of A:

A(dB)	1	2	3	5	7	10	> 10
C(dB)	14	9	6	4	2	1	→ 0

The computation of the attenuation due to openings (holes, slots, etc.) given here after assumes a far field source. The opening behaves as a dipole and radiates inside the shielding a part of the power received outside. Attenuation falls to 0 when the opening is as long as λ/2.

The attenuation due to the openings then expresses as:

$$SE_{openings} (dB) = 100 - 20LogI - 20LogF + 20Log(1 + 2.3LogI/h) + 30e/I$$

with:

- e =: metal thickness (mm)

- I =: opening length (mm)

- h =: opening height (mm)

- F =: frequency (MHz).

For near H field, this value should be corrected of $-20 \cdot \mathrm{Log} \dfrac{48}{D(m) \times F(MHz)}$ (Mardiguian).

To give an idea of orders of magnitude, figure 7.2.5-1 compares the shielding efficiency of a 4 mm Aluminium wall with a 1cm x 1mm slot (arbitrary) with the SE hypothesis taken in the frame of ISO program. The source distance taken into account is 1 m (order of magnitude of the distance between the Solar Array and the cryostat).
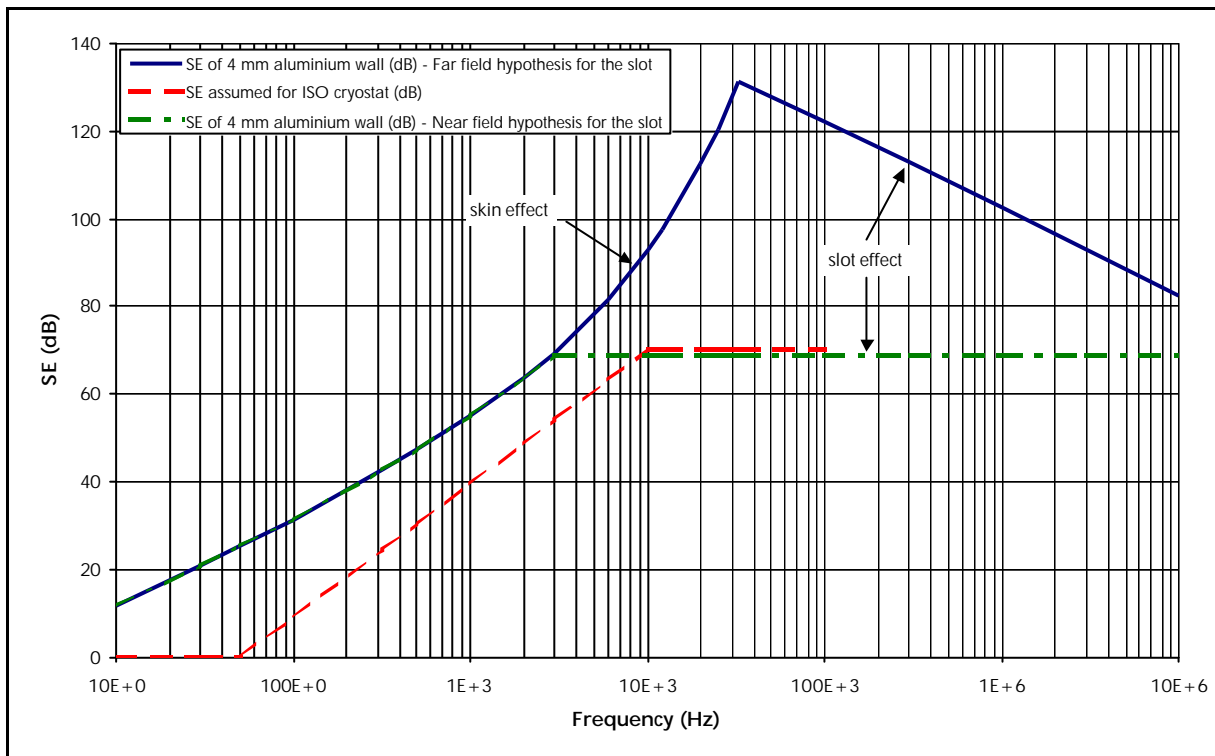

FIGURE 7.2.5-1 EXAMPLE OF SHIELDING EFFICIENCY COMPUTATION

It would seem that what is really critical for the SE value above ~ 1 or 10 kHz is the length of the biggest opening.

However, this last near field correction formula seems very pessimistic and doubtful, as it doesn't take the distance from the holes into account. Actually behind a hole, both E and H fields should decrease like $1/d^3$.

The following classic formulas give the attenuation of a circular or elliptical hole in a metallic wall illuminated by a far field source; if much smaller than the wavelength, these apertures radiate as electric/magnetic dipoles:

For a circular aperture of Diameter D:

$$S_E = \frac{D^3}{6} \cdot \frac{1}{4\pi d^3}$$

$$S_H = \frac{D^3}{3} \cdot \frac{1}{4\pi d^3} \cdot$$

For an elliptical aperture:

$$S_E = \frac{\pi}{12} \cdot a \cdot b^2 \cdot \frac{1}{4\pi d^3}$$

$$S_H = \frac{\pi}{12} \cdot a \cdot b^2 \cdot \frac{1}{4\pi d^3} \text{ for } H_0 \,/\!/\, b$$

$$S_H = \frac{\pi}{12} \cdot a^3 \cdot \frac{1}{Ln\left(\frac{4a}{b}\right) - 1} \cdot \frac{1}{4\pi d^3} \text{ for } H_0 \,/\!/a$$
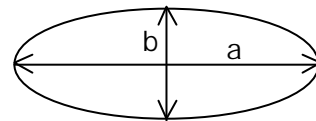
On ISO, the only identified apertures were the ones dedicated to cylindrical connectors of 30 mm diameter. Assuming that the connector itself does not provide any shielding effect, the attenuation of H field at 30 cm from the aperture is then – 91 dB (and – 63 dB for a distance of 10 cm).

For low frequency, an alternative approach also exists, considering the cryostat as a closed cylindrical body excited by an external uniform magnetic field H_0:
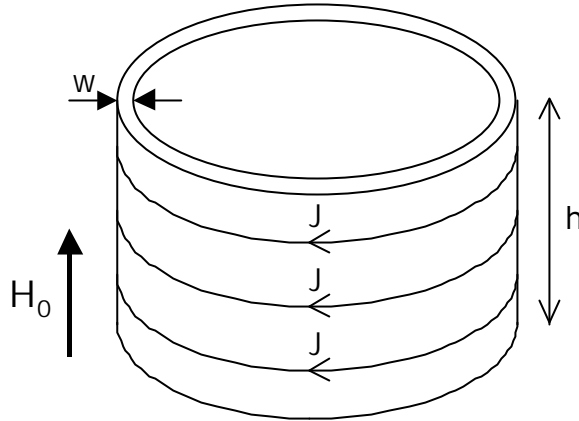
Induced currents appear in the structure that tend to create a field of opposite direction : inside the cavity the field is the sum of H_0 and of the field created by induced currents J, so is lower that H_0.

The induced currents are limited by the resistance and inductance of the wall.

It can be shown that between two sections orthogonal to H_0 and distant of h, the resistance and inductance crossed by induced currents are:

$$R_h = \frac{1}{\sigma} \frac{L}{w \cdot h}$$

$$L_h = \mu_0 \frac{S}{h}.$$

S and L being the surface and perimeter of a cross section.

There is then a cut-off frequency f_0 above which the magnetic field starts being attenuated, the cavity wall behaving as a R, L circuit limiting the current induced by the external magnetic field.

The filtering of the magnetic field will only appear above:

$$f_0 = \frac{1}{2\pi} \cdot \frac{R_h}{L_h} = \frac{1}{2\pi} \cdot \frac{1}{\mu_0 \sigma w \dfrac{S}{L}}.$$

Assuming 2 m diameter and 4 mm of Aluminium thickness, f_0 would be 3 Hz.

However it must be noted that any distributed contact resistance orthogonal to current lines (parallel to H_0) would increase this frequency that would become:

$$f'_0 = \frac{1}{2\pi} \cdot \frac{R_h + R}{L_h} \, .$$

Above f_0, the shielding effect increases of 20 dB/decade until it reaches $f_1 = \frac{1}{\pi \sigma \mu_0 w^2}$ were the skin effect appears.

With our assumptions we would have $f_1 \sim 800$ Hz.

We can conclude that the shielding efficiency assumed on ISO at low frequencies (before opening effect appears) seems reasonable and should be used for HERSCHEL, after consolidation by ASTRIUM.
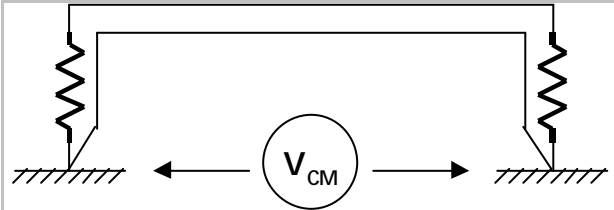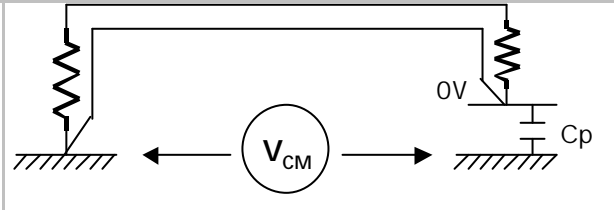
The effect of apertures is less easy to handle and should be discussed with ASTRIUM, ESA and the participants to the EMC Working Group in the near future.

Common mode rejection of SVM to PLM links

Some sensitive lines between SVM and PLM are single ended and carry low frequency (or even DC) signals.

In order to get the best possible common mode rejection at low frequency, the return wire is connected to chassis at one end only.

Indeed, we have the following:

No rejection for F < 10 kHz Slight rejection for F > 10 kHz	Very good CM rejection at low frequency Degenerating like F↗ or like F^2↗ because of the unavoidable parasitic capacitance

In the second case, we have actually a high pass filter, either first order if the wires resistance is predominant or second order if the wires inductance is predominant.

So the receiving side should be properly filtered in HF (above ~ 1 MHz], where the CMRR of the link becomes very bad.

If the link is shielded, it must be noted that the connection of the shield on both ends improves a lot the CMRR above ~ 1 MHz but degrades it at low frequency. This is an exception to the overall rule to connect shieldings at both ends: if we have a low level low frequency analogue signal (such as detectors signals), the shield should be connected to chassis at one end only, where the return is already connected:
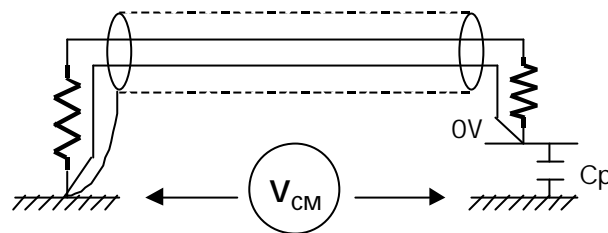
7.2.6. Disturbance torques

This section summarizes the disturbing torques applied on HERSCHEL.

External and internal torques are analysed.

External torque

At L2, HERSCHEL will benefit particularly quiet dynamic conditions. Gravity gradient, local geo-magnetic field and air density are vanishing and the torque they induce are insignificant compared to major sources detailed hereafter:

- **Solar pressure transverse to Sun Vector**

  The solar pressure torque is expected to be nominally large ($2.3 \ 10^{-4}$ N.m), due to the large surface exposed to Sun illumination (23 m²) and to the large lever arm (1.4 m) along the X-axis between the satellite centre of mass and the centre of pressure.

  In routine observations, it is expected that the satellite may stay in a constant attitude w.r.t. inertial space for a full observation period (22 hours). Meanwhile the direction of the Sun in the satellite reference frame will be almost constant (the Sun angular rate will be ~ 1 deg/day). Consequently, the satellite will undergo a constant solar pressure torque (in inertial reference frame). As wheel unloading phases are not scheduled during observation phases, this is a driver to the sizing of the RWA angular momentum storage capability.

The worst case solar pressure torque has been estimated under the assumption that all illuminated surfaces where 100 % reflective.

The following figure displays the solar pressure torque (in N.m.s per day) vs. the satellite SAA.
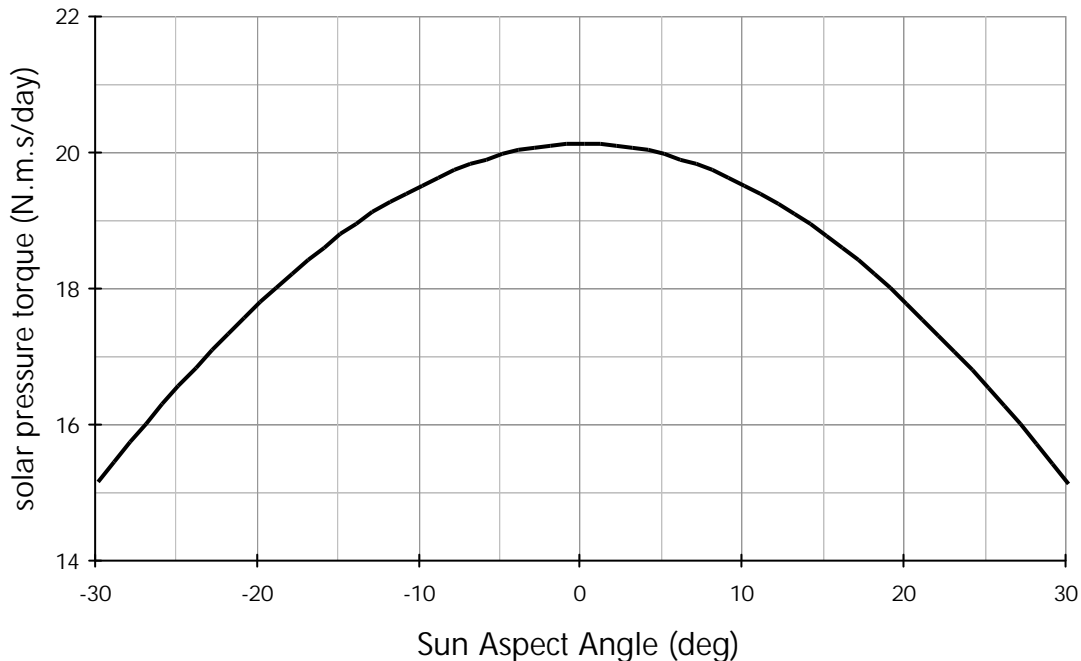
SOLAR PRESSURE TORQUE VS. SAA

– **Solar pressure windmill torque (along Sun Vector)**

An estimation of the worst case solar pressure windmill torque has been derived under the assumption that all surface where fully reflective and that alignments errors led to a 1 deg (1σ per axis) uncertainty in their orientation.

The resulting torque is 0.2 N.m.s / day. 3σ.

– **Thruster misalignments**

Thruster mispositioning and misalignments and deviations in the position of the satellite Centre of Mass (CoM) will result in perturbing torque during the orbit control mode and wheel unloading phases.

As all contributions to the thruster torque are biases, the 3σ worst case torque has been derived by co-adding linearly the different independent contributions.

The following assumptions have been used for the analysis:

Thrust level	10N (per thruster)
Thrust fluctuations	5 %
CoM migration along X	75 mm
CoM migration along Y	5 mm
CoM migration along Z	5 mm
Thrust misalignment	1 deg (half cone)

ALL 3s ERRORS

The resulting worst case perturbing torques are displayed in the following table:

(NM)	CONTROL THR	DV THR
X	0.8	0.4
Y	1.2	0.9
Z	1.1	0.6

WORST CASE THRUSTER PERTURBING TORQUE

These values are to be compared to the available torque produced by the control thrusters, displayed in the following table:

AXIS	X	Y	Z
CONTROL TORQUE (Nm)	23.9	24.4	23.9

AVAILABLE THRUSTER CONTROL TORQUE

Providing a fair commandability (ratio of torque capacity to worst case perturbing torque > 20).

Worst case perturbing torques have been considered for the derivation of the fuel budget.

– **Helium thruster obturation**

The failure of an Helium evacuation thruster has to be considered, it should lead to a $0.1 . 10^{-5}$ Nm disturbance torque thus resutling in a momentum accumulation of:

0.09 Nms/day.

which is very small compared with the solar disturbance torque.

Internal torque

– **RWS Friction**

The magnitude of the RWS friction torque is dependent on the wheel speed. During inertial pointing phases, when the pointing performance requirements must be met, the wheel speeds are almost constant (there are actually slowly drifting, due to the storage of the accumulated external solar pressure torque).

The magnitude of the RWS friction torque is maximum at maximum wheel speed and is evaluated to 0.02 Nm.

– **RWS resolution**

The RWS command is coded on 8 bits, corresponding to an LSB of $1.6 . 10^{-3}$ Nm.

Rounding errors will therefore produce a uniform error in the range $\pm 8 . 10^{-4}$ Nm with a standard deviation $5 . 10^{-4}$ Nm. The frequency of this noise is that of the control law sampling, i.e. 4 Hz (TBC).

– **Microvibration**

The Reaction wheel due to static and dynamic unbalances generate disturbance torque and force at harmonic frequencies of their rotation rate. These high frequency vibrations can be amplified by structure resonances and impact on the Relative Pointing Error. The following table summarises the RW microvibration main characteristics.

Static unbalance	1.1 g.cm
Dynamic unbalance	20 g.cm2

These unbalances lead to a maximum 0.005″ relative pointing error (at 1σ, corresponding to no structural amplification); thus proving margins wrt. the pointing budget.

– **Propellant and Helium sloshing**

The sloshes are low frequency disturbances, with reduced disturbance torques and have, as based on ISO and other spacecraft experience a reduced impact on the pointing performances in scientific modes.

In Sun Acquisition Mode the rotational energy dissipation in the propellant has to be considered, this lead to a reduced disturbance torque (typically < 0.02 Nm), which is handled by a 3-axis attitude control.

7.3. PLANCK SYSTEM ANALYSES

7.3.1. Mechanical analyses

7.3.1.1. Introduction

Several mathematical models (FEM) and mechanical analyses have been prepared and carried out in order :

– to assess the ability of the structural concept of PLANCK satellite (Launcher requirements)

– to define and update subsystem (P-PLM and SVM) structural requirements

– to update and complete the mechanical environment specification for PLANCK equipment

PLANCK mathematical model has been prepared from SVM FE model delivery coming from ALENIA and P-PLM FE model coming from ALCALEL proposal.

7.3.1.2. Analysis of PLANCK satellite dynamic behaviour

7.3.1.2.1. Subsystem mechanical performances

7.3.1.2.1.1. PLANCK Service Module

General

The Service Module (SVM) finite element model has been received from ALENIA.

This mathematical model has sufficient detail for the stiffness simulation in the dynamic analyses.

SVM FE model description

SVM cone:

Honeycomb : height H/C=15 mm

Three plies composite face sheet : T300 resin epoxy CFC 0°/60°/-60°
thickness for each sheet : t= 0.375 mm

SVM upper/lower closure plateform :

Honeycomb : total height H=20 mm

Three plies composite face sheet : thickness for each sheet 0°/60°/-60°: t= 0.375 mm

SVM / SCC lateral panels :

Honeycomb : height H/C=35 mm

Aluminium face sheet :   thickness for each sheet : t= 0.3 mm

SVM shear webs :

Honeycomb : height H/C=15 mm

Six plies composite face sheet : thickness for each sheet 0/60°/-60°/-60°/60°/0 : t= 0.75 mm

P-PLM sub-platform

The mechanical characteristics of the P-PLM sub-platform are:

Twelve plies composite face sheet thickness t=0.75mm

Honeycomb : height H/C = 60mm

NOTE: For **commonality** reasons, HERSCHEL SVM cone is used and implemented in the PLANCK Service module.

The main struts of the PLANCK Service Module are presented in the next table

Struts	Material	Young Modulus (E+6 N/m²)	Area (E-4 m²)	Inertia (E-8 m⁴)	Max Struts length (m)
SVM 1 (tank support)	CFRP	140 000	1.89	3.55	0.53

SVM FE model characteristics

The maim characteristics of the model are:

Number of Nodes :   9071
Number of Element :   9515

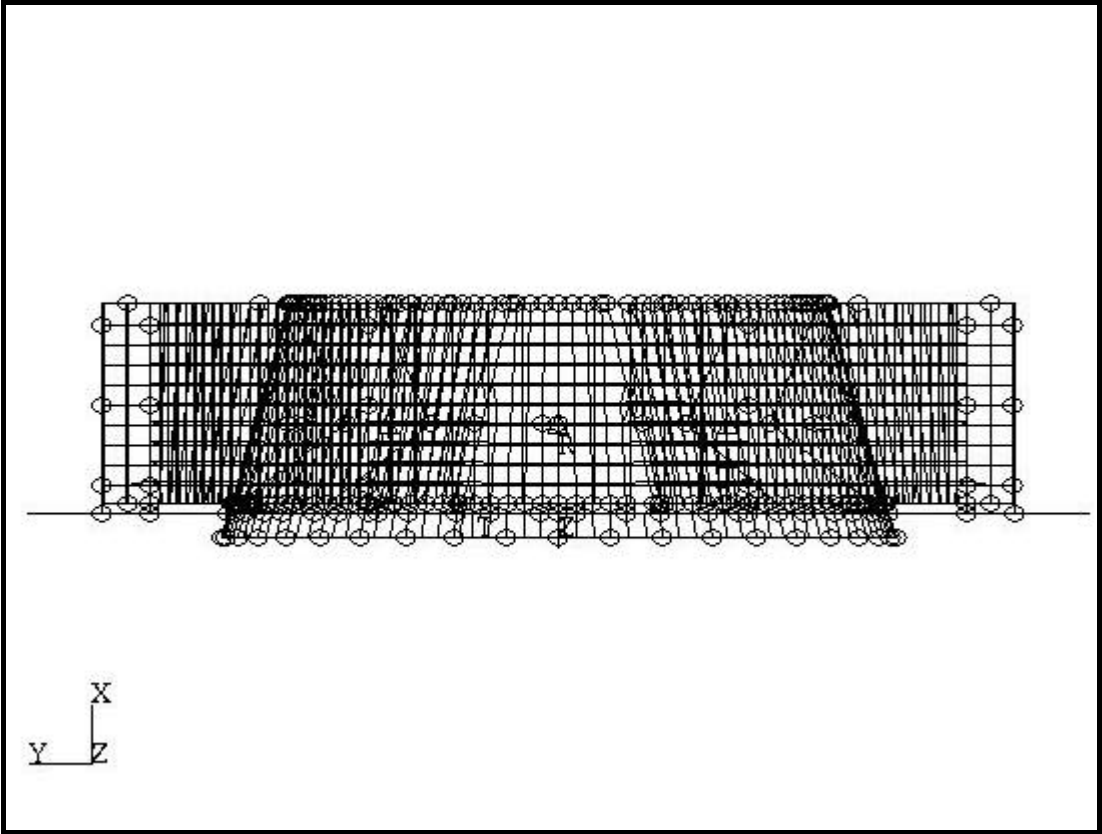SVM FEM has :   54426 d.o.f
SVM FEM mass is :   1110 Kg.

FIGURE 7.3.1-1 SVM FE MATHEMATICAL MODEL

Dynamic performances

PLANCK SVM dynamic global (global box modes, global lateral and longitudinal ones) and local stiffness (panels ..) are obtained from a modal analysis . These results are summarised in the following table.

Mode Frequency	Effective Masses (Kg)			Mode description
(Hz)	Mx	My	Mz	Mode description
30.3	25			Inner SA (X Axis)
48.5		53	170	First SVM lateral Z mode (bending mode)
51.6	68	10	6	Planck sub plat-form (bending mode X Axis)
52		189	134	First SVM lateral Y mode (bending mode)
53.4		92		SVM lateral Y mode + outer SA along X Axis
57.4			23	SVM lateral Z+ outer SA + lateral panel Z+
59.1		25	3	Lateral panel Z+ and Z+Y-
59.9		6		SVM lateral Z+ outer SA + lateral panel Z+
61.6	80			Outer SA along X Axis
69.4	117			SVM longitudinal X mode
70.3	155			SVM longitudinal X mode + lateral panel Y+
72.5			163	SVM lateral Z mode
74.2		94		SVM lateral Y mode

TABLE PLANCK SVM MODAL RESULTS

Comments:

PLANCK SVM main modes are close to 48 Hz in lateral and 70 Hz in longitudinal direction. PLANCK SVM is very stiff in the longitudinal direction with low effective mass .
The first out of plane panel modes are identified between 50 and 70Hz and occurred mainly in the Z direction around 60Hz and in the Y direction around 70Hz

PLANCK Payload Module

General

The PLANCK PLM finite element model implemented in the satellite system FEM model has been built by ALCATEL SPACE.

This mathematical model has sufficient detail for the stiffness simulation in the dynamic analyses.

FE model characteristics

PLANCK PLM FEM has   2515 elements
                            15666 degrees of freedom

PLANCK PLM FEM mass is   307 Kg

The FE model has been set up to the maximal mass. Planck payload structure is defined from the two following structural parts. PLANCK PLM FE model is presented in next figure.
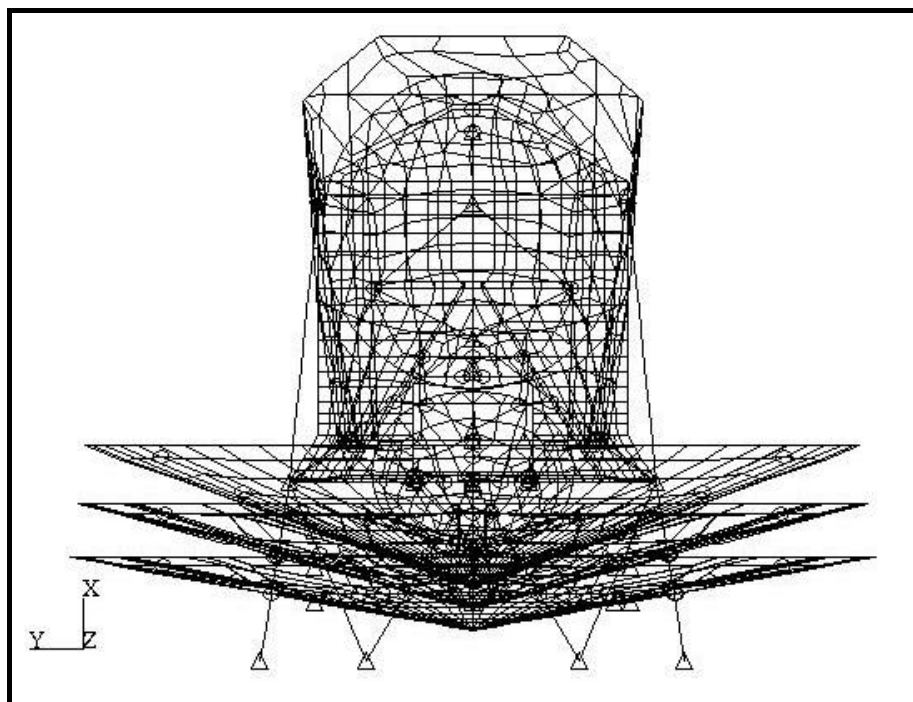
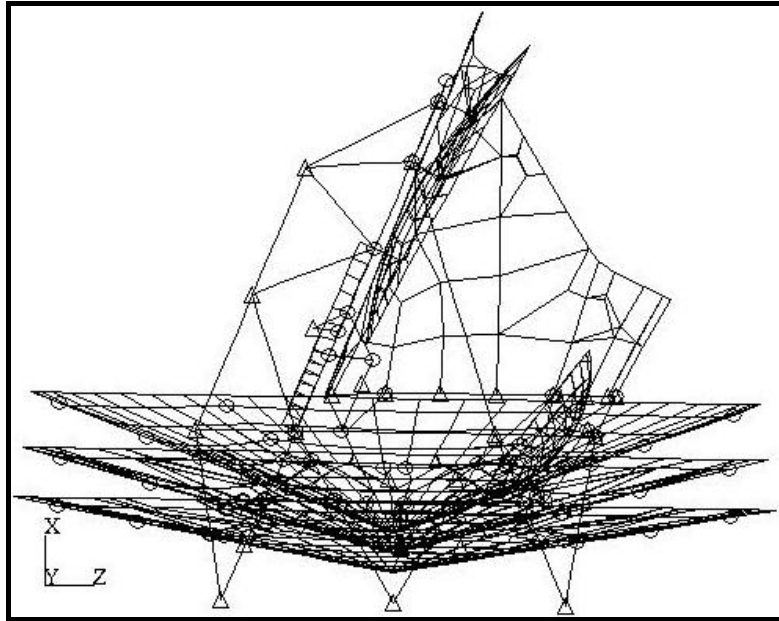

FIGURE 7.3.1-2 PLANCK PLM (Z VIEW)

FIGURE 7.3.1-3 PLANCK PLM (Y VIEW)

PLANCK telescope

PLANCK telescope structure is presented in the following figure.
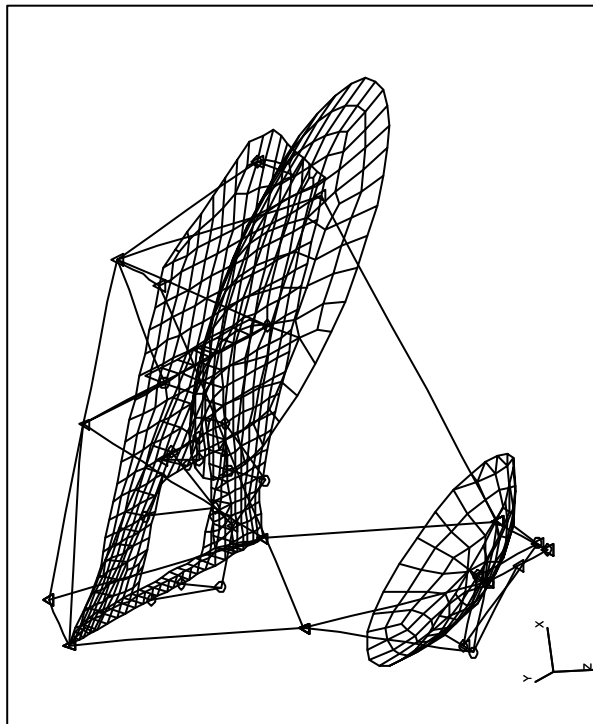

FIGURE 7.3.1-4 PLANCK TELESCOPE

The mechanical properties of PLANCK telescope structure are :

– -CFRP interface ring : Rectangular section 145mm X 85 mm X 4 mm

– -PR support : Plate with CFRP face sheet (thickness =1 mm) and NIDA 3-20 (thickness =50 mm)

– -Frame truss : CFRP circular section 40mm diameter with a thickness =2 mm

The concentrated mass associated to FPU instrument is connected to a support structure with 3 couples of bars. The description of the FPU support has been defined by LFI LABEN during PLANCK ARCHITEC study.

The main struts of the Telescope are presented in the next table

Struts	Material	Young Modulus (E+6 N/m²)	Area (E-4 m²)	Inertia (E-8 m⁴)	Max Struts length (m)
TELE 1	CFRP	130 450	1.76	1.73	0.28
TELE 2 (Interface ring)	CFRP	190 590	17.7	509	/
TELE 3	CFRP	190 590	2.38	3.3	1.19
TELE 4	CFRP	190 590	1.7	1.9	1.02
TELE 5	CFRP	190 590	2.04	3.7	1.52

TABLE 7.3.1-2 MAIN STRUTS CHARACTERISTICS

PLANCK Cryo substructure

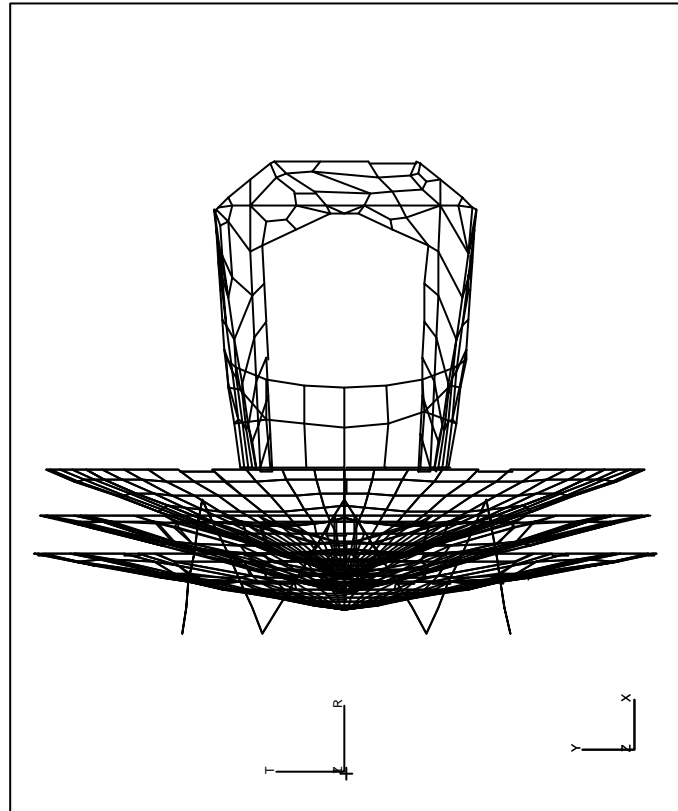PLANCK Cryo structure is presented in the following figure.

FIGURE 7.3.1-5 PLANCK CRYO-STRUCTURE

The main mechanical characteristics of the PLANCK cryo substructure are

- Grooves : Plate with Aluminium face sheet (thickness =0.3 mm) and NIDA 4-20 (thickness =20 mm)

- Baffle : NIDA Alu 9-20 (thickness 20mm) with Aluminium face sheet (thickness=0.3)

The main struts of the Cryo substructure are presented in the next table

Struts	Material	Young Modulus (E+6 N/m²)	Area (E-4 m²)	Inertia (E-8 m⁴)	Max Struts length (m)
PLM 1	GFRP	52 000	5.59	10.2	1.05

Dynamic performances

Telescope modal behaviour

The PLANCK Telescope structure has been determined in order to verify the stiffness requirements. The telescope structure is considered with simply supported boundary conditions introduced at each interface point with GFRP struts support. PLANCK Telescope main modes are presented hereafter.

Frequency [Hz]	Mass Mx [Kg]	Mass My [Kg]	Mass Mz [Kg]	Mode shape description
53	4	/	84.9	First lateral Z mode (FPU+PR)
84	/	60.7	/	First lateral Y mode (FPU)
85.3	25.4	/	11.2	Second Lateral Z/X mode (PR)
113.6	57.3	/	13.7	First longitudinal mode (FPU)

Table Planck Telescope modal analysis results

Comments:

For PLANCK baseline configuration, the lateral and longitudinal frequencies of PLANCK telescope main modes are correctly located and are sufficient to ensure a good dynamic behaviour of the PLANCK PLM.

Planck PLM modal behaviour

The PLANCK PLM structure has been determined in order to evaluate the stiffness of the complete PLM without SVM structure. The PLM structure is considered with simply supported boundary conditions introduced at each interface point with service module. PLANCK PLM main modes with effective mass > 5% of the total mass are listed in the next table.

Frequency [Hz]	Mass Mx [Kg]	Mass My [Kg]	Mass Mz [Kg]	Mode shape description
34.1	/	166	/	First lateral Z mode of PLANCK PLM
34.7	/	/	115	First lateral Y mode of PLANCK PLM
84	95	/	/	First longitudinal PPLM X mode

TABLE 7.3.1-3 PLANCK-PLM MAIN MODES

Comments:

PLANCK PLM main modes are identified around 34 Hz in lateral directions and above 84 Hz in longitudinal direction. These lateral main modes have high frequencies which ensure satisfactory global dynamic behaviour for PLANCK PLM.

PLANCK PLM modes with effective mass less than 5% are grooves and baffle modes which are identified :

- Grooves main mode : between 18 Hz and 27 Hz

- Baffle main mode : between 40 Hz and 45 Hz.

No particular modal coupling between subsystem is shown on the proposed PLANCK PLM design.

7.3.1.2.1.2. PLANCK satellite FE model

General

The mathematical model of the whole PLANCK satellite is assembled using the models of the various subsystems defined in the next chapter: payload module and service module.

The dynamic system analysis is carried out in two different steps:

- An overall dynamic modal analysis is performed with NASTRAN software in order to identify the primary and secondary main modes of PLANCK satellite and their modal weight (effective mass) and to check if there is no coupling between subsystems.

- A dynamic response analysis is performed to predict the accelerations responses of equipment during AR V launch. From the computed accelerations, quasi static loads are evaluated and design loads have been extrapolated for subsystems sizing and the equipment qualifications levels.

PLANCK FE model characteristics

Number of physical nodes: 12171
Number of elements: 11992
Total number of degrees of freedom: 73026.

Mass budget :

The following table presents the mass budget of PLANCK satellite

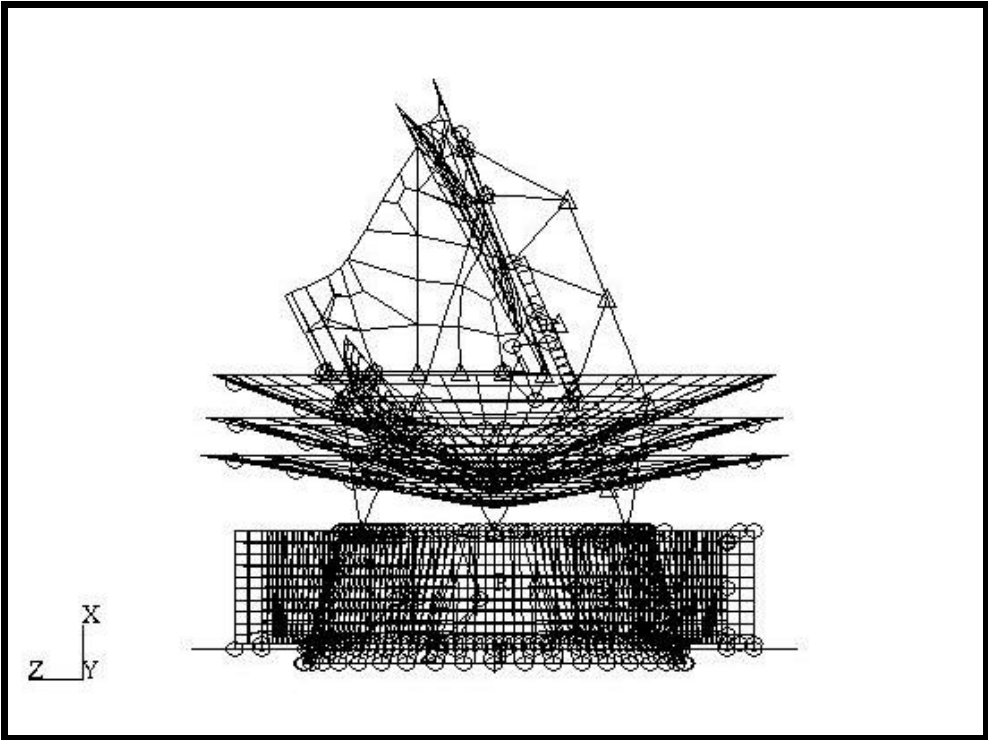| Subsystem	Mass in the model]Kg]
Telescope	103.7
Cryo structure	121.0
FPU	52.2
Equipment PPLM	29.5
SVM	1110
Total mass	**1417**

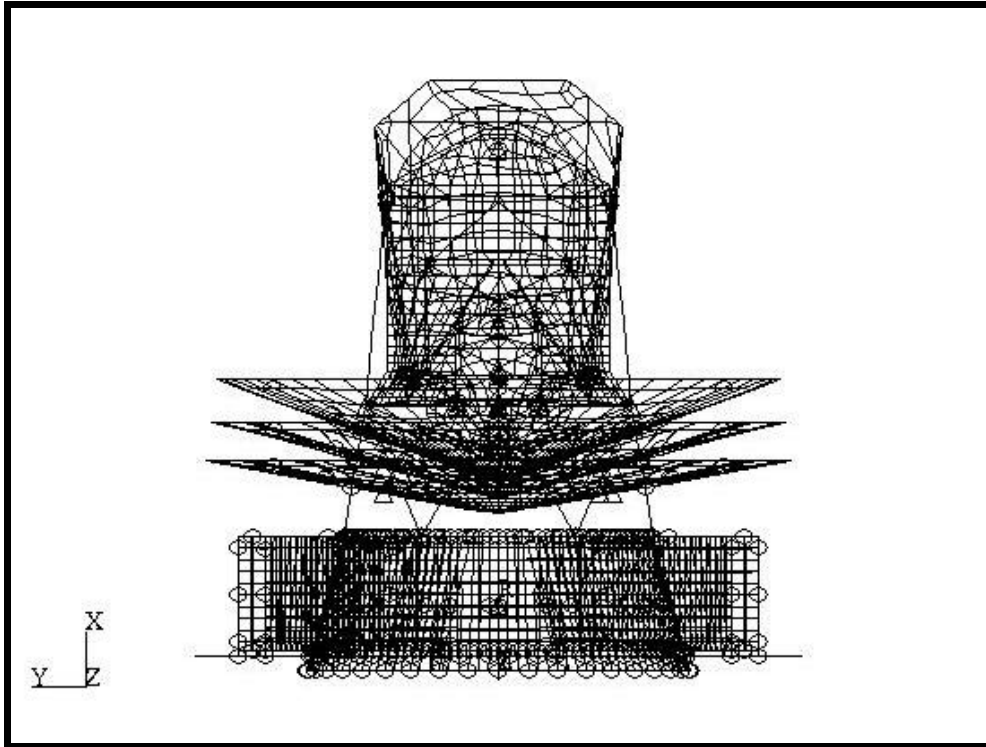**FIGURE 7.3.1-6 Y VIEW OF PLANCK SATELLITE**

FIGURE 7.3.1-7 Z VIEW OF PLANCK SATELLITE

7.3.1.2.2.   Overall system mechanical analyses

7.3.1.2.2.1. General

The dynamic system analysis is carried out in two different steps:

> An overall dynamic modal analysis is performed with NASTRAN software in
> order to identify
> the primary and secondary main modes of PLANCK satellite and their effective
> mass and to check if there is no coupling between subsystems.

> A dynamic response analysis is performed to predict the accelerations
> responses of equipment during AR V launch. From the computed accelerations,
> quasi static loads are evaluated and design loads are defined for subsystems
> sizing and the equipment qualifications levels.

7.3.1.2.2.2. PLANCK Satellite overall dynamic analyses
The dynamic analysis is performed up to 100Hz which corresponds to the frequency
bandwidth of the sine vibration tests.

Modal analysis

PLANCK satellite main modes with effective mass higher than 5 % of the total mass are
listed in next table.

Mode Frequency	Effective Masses [Kg]			Mode description
(Hz)	Mx	My	Mz	Mode description
30.1		239		First lateral PPLM Y mode
31.3			233	First lateral PPLM Z mode
48.6		42	125	Second lateral PPLM +SVM Y mode
52.4		155	106	Second lateral PPLM +SVM Z mode
69-70	309			Longitudinal main modes (PPLM+SVM)

Table PLANCK Satellite modal analysis results

Comments :

PLANCK satellite main modes

PLANCK satellite main modes are located at the following frequencies :

- First longitudinal mode = 70 Hz   > 31Hz (margin >> 20 %)

- First lateral mode = 30.1 Hz   > 9 Hz (margin >> 20 %)

First lateral PLANCK satellite main modes located around 30 Hz are mainly defined from the lateral stiffness of PLANCK PLM. The frequencies of PLANCK lateral main modes are more than 20 % higher than the minimal required frequency and fulfil the launcher frequency requirements.

Second lateral main modes (P-PLM+SVM) are located around 48Hz-52Hz.   This lateral dynamic behaviour is due to the high stiffness of the SVM cone (similar to HERSCHEL central cone) which generates two physical stages (PPLM and SVM) with significant stiffness discrepancies.

Longitudinal main mode of PLANCK satellite is identified at high frequency (above 69 Hz). This high frequency is mainly due to the high longitudinal stiffness of central tube. With high frequency margin, the frequency of the PLANCK longitudinal main mode is compliant with the Launcher stiffness Specification.

PLANCK secondary main modes

Other PLANCK modes with effective mass less than 5% of the total mass are located within the frequency bandwidth 0-60 Hz :

- 18.6 Hz-26.6 Hz Grooves bending modes

- 40Hz - 50 Hz Baffle bending modes.

- 80Hz –90Hz telescope modes

No significant modal coupling is identified between PLANCK substructures.

Dynamic Sine Response analyses

Methodology

The dynamic response analysis is performed using ARIANE 5 input flight levels. These levels are applied at the base of the spacecraft during sine vibration tests. These levels are :

- **Longitudinal axis :** ± 1g from 5Hz to 100Hz,

- **Lateral axis :** ± 0.8g from 5Hz to 25 Hz,

  ± 0.6g from 25Hz to 100Hz.

No notching is considered at this step of the analysis. The reduced damping factor considered in this analysis is 2 % for each mode which is usually consistent with most of the experimental tests.

Notching on the main modes

The following table presents the qualification maximal loads at the launcher interface due to the dynamic response (with qualification factor of 1.25), the maximum qualification quasi static loads at the interface and the foreseen notching values.

Item	ARIANE V QSL [g]	Quasi static Launcher Interface Loads	Dynamic Launcher Interface Loads	Frequency [Hz]	Flight Notching Level	Qualif Notching Level
Fx [N]	6	85000	83750	69.5	0.985g	1.23g
Fy [N]	2	28340	38750	30	0.439g	0.548g
Fz [N]	2	28340	39300	31.1	0.432g	0.540g
My [N.m]	2	23290	85750	31.1	0.163g	0.203g
Mz [N.m]	2	23290	87850	30	0.159g	0.198g

TABLE 7.3.1-4 PLANCK NOTCHING LEVELS

For the primary main modes, the predicted qualification notching levels are

- longitudinal direction   1.23g

- lateral Y direction   0.198g

- lateral Z direction   0.203g

The low effective mass (less than 30 %) on the longitudinal main mode at 69.5 Hz leads to high notching levels.

7.3.1.3.   Inputs to support subsystem spec

Dynamic loads and mechanical environments of structures and instruments have to be evaluated and specified through EVTR and GDIR specifications. The following chapter give a descriptions of these loads, environment and the mechanical requirements applicable to subsystems.

. Quasi static loads

The main flight limit loads extracted from the dynamic response analysis are presented in next tables. Notching on primary main modes are taken into account in these loads.

PLANCK TELESCOPE REFLECTORS

Flight Limit loads

	Flight limit loads			
Instrument	$\perp$ mounting plane (g)	// mounting plane (g)	Frequency (Hz)	Load Direction
Primary mirror	15	15	81	X
Secondary mirror	3.5 8	8 5	81 94	X Y/Z

TABLE 7.3.1-5 FLIGHT LIMIT LOADS FOR TELESCOPE REFLECTORS

<u>Comments:</u>

Compared to flight limit loads defined in ALCATEL proposal, these loads have increased. Nevertheless, these loads remain low and acceptable. The modification of the limit loads is probably due to the stiffness increase of central tube which modify and shifts a P-PLM longitudinal mode above 80Hz and induces modal coupling with lateral and longitudinal main modes of Telescope.

Flight limit loads

For instruments, the flight limit loads are presented in the next table.

Instrument	Flight limit loads			
	Axial [g]	Lateral [g]	Frequency (Hz)	Load Direction
BEU	28	0.6	51.6	X
	2.7	3.5	52.2	Y
FPU	24	6	81	X
	1.	9	31	Y/Z
JFET	20	8	81	X
	1.6	9.5	31	Z/Y

TABLE 7.3.1-6 PLANCK TELESCOPE INSTRUMENT FLIGHT LIMIT LOADS

Comments:

Flight limit loads of FPU and JFET have increased mainly in the axial direction at the frequency of 81Hz. The modification of the limit loads is due to the stiffness increase of central tube which shifts the P-PLM longitudinal mode above 80Hz. A modal coupling between P-PLM longitudinal mode (located around 81Hz) and lateral and longitudinal main modes of Telescope (located around 85.3 Hz) occurs. These limit loads could be reduced by :

- increasing the longitudinal main modes of PLANCK Telescope above 100Hz

- decreasing the stiffness of central tube

Instrument	Flight limit loads			
	⊥ [g]	// [g]	Frequency (Hz)	Load Direction
SCC panel	25	20	69.6	X

TABLE 7.3.1-10 SCC PANEL FLIGHT LIMIT LOADS

Comments:

The maximal out of plane loads have been computed at the frequency of the longitudinal main mode of PLANCK satellite. It will be possible to reduce these loads taking into account extra notching which could be possible at high frequencies.

SVM EQUIPMENT

Flight limit loads

For SVM equipment, flight limit loads have been computed and presented hereafter in the next tables.

	Flight limit Loads			
Equipment	⊥ (g)	// (g)	Frequency (Hz)	Load Direction
SVM lateral Panels	25	20	55.2	X
SVM Panel +Y /-Y	40(*)	20(*)	70	Y
Fuel tank	11.5	8	75	Z

TABLE 7.3.1-11 FLIGHT QUASI STATIC LOADS (TANKS AND LATERAL PANELS)

Comments:

Compared to the preliminary flight limit loads, flight limit loads of fuel tank have lightly increased . The analysis of quasi static loads modifications (modal analyses of global and local modes) will be done during B phase to optimised these values. Moreover, the high frequencies of the SVM and lateral panel modes where the limit loads are computed will allow to expect a significant reduction of these loads (using auxiliary notchings coming from preliminary LCDA results) down to the loads used for qualification testing.

For SVM lateral panels, compared to the preliminary flight limit loads, the updated flight limit loads have increased . The increase is probably due to a light modal coupling between SVM global box modes and out of plane lateral panel modes. The analysis of quasi static loads modifications (modal analyses of global and local modes) will be done during B phase to reduce these flight limit loads down to lower values. Moreover, the high frequencies of the SVM and lateral panel modes where the limit loads are computed will allow to expect a significant reduction of these loads with auxiliary notchings coming from preliminary LCDA results.

(*) these loads are not specified because these levels should be reduced by secondary notching.

Sine environments

The sine environment are defined for qualification test from the quasi static loads in order to be consistent with quasi static loads and to be sure that the loads levels will be applied during these tests.

The sine vibration levels are defined between 5Hz and 100Hz. The acceleration levels applied in this range are the acceptance levels defined in consitency with quasi static loads. Notching will be allowed not to exceed quasi static loads.

Equipment	Load Direction	Frequency Hz	Acc Level (g)
FPU	Long (X)	5 – 100 Hz	24
	Lat (Y/Z)		9
JFET	Long	5 – 100 Hz	20
	Lat		10
SCC	Long	5 – 100 Hz	25
	Lat		20
BEU	Long	5 – 100 Hz	28
	Lat		4
SVM	⊥	5 – 100Hz	25
	//		20

TABLE : SINE ACCEPTANCE LEVELS

Global SVM interface loads

Global SVM Quasi static load cases are presented in the next table.

Load Case	X Axis	Y Axis	Z axis
1	23g	/	1g
2	/	15g	/
3	/	/	11g

These loads have to be applied to the whole Telescope structure only (the resultant force is applied to centre of gravity). These global Quasi static loads coming from telescope behaviour only (V-groove masses being de-coupled at high frequencies), generate equivalent sizing forces is the struts at the interface points with SVM.

7.3.1.3.1. PLANCK Random vibration analyse

Methodology

The methodology for computing random acceleration levels on P-PLM equipment are based on two technical approach which give estimated levels from the weight of the equipment (HERSCHEL approach with ESA formulae) and from experimental results (second approach with XMM experimental random curve) provided by ESA. The final random results are defined from equipment location consideration on the panels.

For PDR, detailed Acoustic Analyses will be done with acoustic FE model taking into account CVV acoustic attenuation for improving and increasing the accuracy of random vibration specification levels.

P-PLM random vibration specification

The following levels presented in the next table are the random vibration levels specified for P-PLM equipment (FPU, JFET, BEU, PR, SR). These levels define a random spectrum with an horizontal maximal level

- 20-100Hz   : +3dB/Oct

- 100Hz-300Hz   : PSDmax [g²/Hz]

- 300Hz-2000Hz   : -5dB/Oct

Maximal PSD values (PSD max) of qualification random spectrum are defined in the following tables.

P-PLM Equipment	Mass [Kg]	In Plane Acc [g²/Hz]	Out of Plane Acc [g²/Hz]
FPU	52	0.1	0.1
JFET	2.3	0.1	0.2
BEU	30	0.5	1

TABLE 7.3.1-12 PLANCK PLM EQUIPMENT RANDOM VIBRATION SPECIFICATION (QUALIFICATION LEVELS)

NOTE : BEU random vibration levels have been estimated at high values. These high vibration acceleration levels are due to the surface of BEU support which is more than 3m² .The mass distribution of the BEU panel support is low which induces these high vibration levels. A reduction of the surface of the panel by adding auxiliary horizontal support beams and cutting out the panel could reduce significantly these levels down to 0.2g²/Hz for out of plane PSD levels.

PLANCK SVM equipment random vibration specification

The random qualification levels for PLANCK equipment located inside SVM are presented in the next table. These following Random vibration levels are the specified random vibration levels for SVM instruments.

Item	Mass [Kg]	Mounted Panel	Panel mass/surf [Kg/m²]	Out of Plane Level [g²/Hz]	In plane Level [g²/Hz]
SCC	37.2	[-Z;+Y]	36	0.3	0.15
4K CAU	8	[+Y]	34	0.3	0.15
4K CEU	7			0.3	0.15
4K CCU	16			0.3	0.15
Battery	6.8	[+Z;-Y]	55	0.2	0.1
PCDU	18.2			0.2	0.1
AOCS IF/Unit	8.69			0.2	0.1
CDMU-A	13.33			0.2	0.1
DCCU	25	[+Y;+Z]	30	0.3	0.15
FV Panel	5			0.4	0.2
SCC	37.2	[-Y;-Z]	38	0.2	0.1
QRS	1.43	[-Y]	16	1.2	0.6
X/B transponders	3.46			1.2	0.6
TWTA	0.75			1.2	0.6
EPC	1.4			1.2	0.6
Diplexer	0.3			1.2	0.6
REU	25	[+Z]	43	0.2	0.1
DPU	13			0.2	0.1
STR Mapper Elec	1			0.2	0.1
SCEB	10.5	[-Z]	23	1	0.5
REBA	6.8	Platf [+X]	18	1	0.5
PND	3	Web [–Z,+Y]	10	1.5	0.75

TABLE 7.3.1-13

7.3.1.3.2. PLANCK Shock analyses

General

A shock analysis is performed in order to evaluate the shock environment of PLANCK equipment inside P-PLM and SVM. PLANCK spacecraft position is the lower SC position on the Launcher.

Shock excitation assumptions

At the spacecraft interface, the shock response spectrum of shock excitation is supposed to be similar to the shock response spectrum presented in next table and used for ALCATEL proposal.

The interface shock response spectrum is defined by the following shock acceleration levels.

Frequency [Hz]	Shock Acceleration [g]
100	20
600	1000
10000	3600

TABLE 7.3.1-15 LAUNCHER SHOCK INTERFACE RESPONSE SPECTRUM (SB 1)

PLANCK-PLM Shock evaluation

A shock attenuation inside sandwich panels due to the distance from the excitation source has been clearly identified from experimental tests. Considering this shock attenuation, shock levels at the interface with P-PLM strut support located at 970 mm from the launcher interface plane are estimated reduced by about 15dB at high frequencies.

The estimated PLANCK-PLM Shock interface levels are presented in the following table.

Frequency [Hz]	Shock Acceleration [g]
500	200
1300	600
10000	600

TABLE 7.3.1-16 P-PLM INTERFACE SHOCK RESPONSE SPECTRUM (SRS P-PLM)

In PLANCK-PLM structures (not made with sandwich elements) , shock level is not considered to be significantly reduced except at interface points. The shock attenuation at each of interface point is supposed to be around 5dB (a conservative approach considered 4dB of shock reduction at each interface point). The shock levels applied to the P-PLM equipment and instruments is SRS 1

The severity shock response spectrum SRS is defined hereafter.

Frequency [Hz]	Shock Acceleration [g]
100	20
1300	200
10000	200

TABLE 7.3.1-17 SHOCK SEVERITY SRS 1

PLANCK PLM Shock specification

Taking into account the results obtained previously, shock levels specified for Planck PLM equipment (FPU, JFET, BEU, PR, SR) are summarised in the next table.

P-PLM Equipment	shock Specification
PR	**SRS 1**
SR	**SRS 1**
FPU	**SRS 1**
JFET	**SRS 1**
BEU	**SRS P-PLM**

TABLE 7.3.1-18 PLANCK PLM EQUIPMENT SHOCK SPECIFICATION

For telescope, V-groove and Planck PLM structures , the interface shock specification is presented hereafter.

P-PLM Structure	shock Specification
Telescope	**SRS P-PLM**
V-groove	**SRS P-PLM**
P –PLM	**SRS P-PLM**

TABLE 7.3.1-19 PLANCK PLM INTERFACE SHOCK SPECIFICATION

PLANCK SVM Shock specification

Waiting for results of ARIANESPACE new shock damping test and new Launcher interface shock data, for PLANCK SVM shock levels, the proposal main results presented hereafter are considered unchanged. Out of plane and In plane shock levels are supposed to be identical.

For main SVM equipments and instruments located on lateral panels , the shock specification to be considered is defined in the following table

Frequency (Hz)	Acceleration (g)
100	20
600	600
2800	2200
10000	2200

Shock response spectrum Sb 2 (qualification levels)

SVM equipment Shock Level STATUS

PLANCK SVM Equipment	shock level
RCS components	Sb 1
Lateral Panels -SCC -EPC -CDMU -TWTA -PCDU -DIPLEXER -AOCS I/F Unit -QRS -BAT -TRANSP -DCCU -HKCEU -FU Panel -STARM Elec -REU -DPU -SCE	Sb 2

7.3.1.4. Inputs to PLANCK SVM structural requirements specification

The mechanical design of PLANCK SVM has to be defined from mechanical environment and stiffness requirement to fulfil the Launcher frequency specification. These mechanical has been defined with the latest PLANCK SVM mass configuration and mechanical design .

PLANCK SVM Dynamic requirement specification

In order to avoid modal coupling between substructure, SVM dynamic requirements have been defined and concerns the frequency location of :

- Global SVM modes with rigid Payload:

  In relation with the global stiffness of central tube, the global SVM modes with rigid Payload have to be defined to reach and fulfil the Launcher frequency requirements with PLANCK Payload.

  - Frequency of the PLANCK longitudinal main mode   > 60 Hz

  - Frequency of the PLANCK lateral main mode   > 35 Hz

- SVM global Box modes :

  SVM global Box modes have to be de-coupled to PLANCK main modes (HERSCHEL longitudinal and secondary lateral). These technical considerations and the mechanical design lead to the following frequency requirements:

  - Frequency of the PLANCK SVM longitudinal global box mode   > 60 Hz

  - Frequency of the PLANCK SVM lateral global box mode   > 50 Hz

- Tank support modes:

  To avoid modal coupling between SVM modes located around 50 Hz and fuel tank main modes, the frequency requirements

  - Frequency of PLANCK fuel tank longitudinal X main mode   > 145 Hz

  - Frequency of PLANCK fuel tank lateral main mode   > 80 Hz

–   SVM Lateral panels:

The lateral panel frequency requirements have been defined from the lateral behaviour of PLANCK satellite for de-coupling out of plane modes of panels to second lateral Satellite main modes (around Fp = 50Hz). The main lateral panel frequency requirement is :

- Frequency of out of plane lateral panel > 1.4 * Fp

PLANCK SVM Stiffness requirement specification

–   Global lateral stiffness (central tube)

The global lateral and longitudinal stiffness is not specified because the central tube is identical to Herschel central tube. The lateral and longitudinal stiffness requirements specified for central tube are not needed for PLANCK which has a low weight Payload.

–   Local interface stiffness (interface SVM/P-PLM)

Local stiffness at SVM interface points with GFRP strut support are given by the central tube. For communality reasons, local stiffness are similar to HERSCHEL SVM but these local interface stiffness are not needed.

–   Local interface stiffness (interface SVM/fuel tank)

To avoid a significant frequency decrease coming from local SVM stiffness, local interface points between fuel tank and SVM have been estimated and derived as a local stiffness requirement.

PLANCK SVM interface specification

The global dynamic behaviour of PLANCK satellite generate forces (during sine test) at SVM/ GFRP struts interface points. These dynamic local loads depend on the frequency location of subsystem modes (P-PLM and SVM). These loads are specified for local and global SVM interface sizing

7.3.1.5. Inputs to P-PLM structural requirements specification

The objectives of the P-PLM structural requirements are to ensure a satisfactory global satellite dynamic behaviour and to define the main global P-PLM dynamic loads for PLANCK Payload Module sizing.

P-PLM frequency requirements

–   Global P-PLM Lateral and longitudinal stiffness

  •   Frequency of the P-PLM longitudinal (X)mode   > 85 Hz

  •   Frequency of the P-PLM lateral (Y/Z) mode   > 32 Hz

–   PLANCK Telescope stiffness specification

  •   Frequency of PLANCK Telescope longitudinal (X)mode   > 100 Hz

  •   Frequency of PLANCK Telescope lateral (Y/Z) mode   > 80 Hz.

P-PLM Flight limit loads

PLANCK PLM Quasi static loads cases are presented in the next table. These loads are not similar to SVM interface loads presented in chapter

Load Case	X Axis	Y Axis	Z axis
1	13g	/	2g
2	/	5g	/
3	/	/	7g

TABLE 7.3.1-20 P-PLM QUASI STATIC LOADS (FLIGHT LEVELS)

TELESCOPE Quasi static loads

Telescope quasi static loads have been defined and specified defined for interface and global sizing of the struts. These loads are presented in the following table. These loads are flight limit loads and have been evaluated from the computed interface forces.

Load Case	X Axis	Y Axis	Z Axis
1	21g	/	3g
2	/	6g	/
3	/	/	9g

TABLE 7.3.1-21 TELESCOPE QUASI STATIC LOADS (FLIGHT LEVELS)

Baffle Quasi static loads

Baffle quasi static loads have been defined and specified defined for Telescope interface and link sizing These loads are presented in the following table. These loads are flight limit loads and have been evaluated from the computed interface forces.

Load Case	X Axis	Y Axis	Z Axis
1	35g	/	10g
2	/	10g	/
3	/	/	10g

TABLE 7.3.1-21 BAFFLE QUASI STATIC LOADS (FLIGHT LEVELS)

7.3.2.   PLANCK Micro Vibration analysis

Objective of the study

The aim of PLANCK Micro vibration analysis was to determine :

– the acceleration levels on HFI due to 4K compressor perturbations

– the transfer function of PLANCK spacecraft.

Main assumptions

The main technical assumptions used in this study for analysing micro vibration transmission were :

– HFI susceptibility level is in the range of 0.1mg - 1 mg.

– Residual forces and moment generated by 4K cooler compressor are between 20 mN and 80 mN for the forces and between 2 mN and 8 mN for moment.

– The frequencies of excitation are 40 Hz for the fundamental force and 3 harmonic frequencies have been considered (80Hz, 120Hz, 160Hz)

– Damping ratio used is 0.005.

A finite FE model of PLANCK satellite and MVIB software developed by ALCATEL for micro vibration analysis was used.

Main Results

With the minimum pertubation loads (force=20mN), the estimated HFI micro vibration levels (0.4mg) are within the specification.

With the maximum pertubation loads (force=80mN), the estimated HFI micro vibration levels (1.7mg) are slightly above of the specification.

Conclusions

The HFI accelerations have been estimated close to the micro vibration specification. To decrease the HFI acceleration levels several technical solution could be considered :

- – Source optimisation

- – Use of dynamic damper

- – Optimisation of FPU support resonance

- – Adjustment of HFI support

Nevertheless, even if the HFI acceleration has been estimated at slightly higher values than expected, this technical approach is considered as pessimistic and shows that a satisfactory HFI micro vibration situation could be obtained.

7.3.3. Thermal analyses

7.3.3.1. L2 injection scenario impact

The potential impact on PLANCK of an injection scenario after a parking orbit is clearly related to the timeline of the PLANCK mission. One of the raised question deals with the possibility to switch ON the coolers during the parking orbit.

To perform the analyses with reduced CPU consumption, a simplified TMM of the PLANCK PLM has been elaborated. The orbital parameters for computation are identical to those used for HERSCHEL analyses. Furthermore, the specific input data for PLANCK are the following:

- SVM overall temperature is set at 300 K

- initial temperature of the whole PLM is set at 300 K at the beginning of the parking orbit (this hypothesis shall be assessed in future works)

    all the coolers are OFF, then no dissipation is applied on each of the "V-groove" shields

- -X axis of the spacecraft is Sun pointed (PLM always in the shadow of the Solar Array)

- no aero-thermal flux is taken into account.

The next figure represents the temperature profile of the Sorption Cooler Pipes interface with the third "V-groove" shield, i.e. the coldest one in operation.
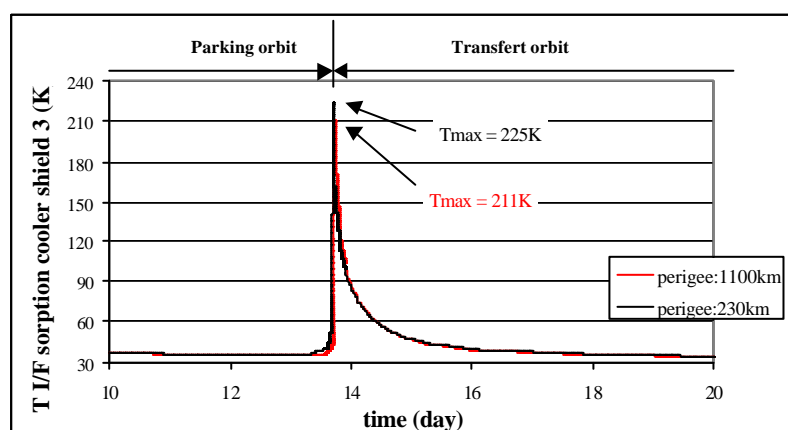
FIGURE 7.3.3-1 HEAT UP OF THE SORPTION COOLER COLDEST INTERFACE AROUND PARKING ORBIT PERIGEE

The temperature level of the Sorption Cooler interface on the third shield dictates the possibility to switch on the first level of the cooling system, i.e. the Sorption Cooler. The value given today by the instruments (JPL) is a maximum temperature of 140 K. The analyses show consequently that it is not worthwhile to switch on the cooling system during the parking orbit, because the third shield temperature level will exceed the maximum Sorption Cooler switch on temperature, then requiring to switch OFF this unit.

No solution is foreseen optimizing the spacecraft attitude. Indeed, the spacecraft configuration does not allow to avoid Sun and Earth fluxes at the same time.

7.3.3.2. Sorption Cooler Compressor TMM analyses

This part presents the analysis of the simplified Thermal and Mathematical Model of the Sorption Compressor, provided by JPL. This model has been delivered to ALCATEL in response to action AI1 took during the Sorption Cooler Interface Meeting, held in Cannes the 11/05/01 (Doc. n° HP.ASPI.MN.54).

The data provided by JPL are recalled hereafter. The important feature is that they are related to a End Of Life situation **with instrument margin**. The Sorption Compressor is basically modelled with 12 thermal nodes. 6 nodes are associated to the 6 inner beds, the part of the compressor which are periodically heated up to ~450 K for Hydrogen desorption. Each of the 6 inner beds is periodically thermally connected to its associated outer shell (6 outer shells total). The thermal conductance between one inner bed and one outer shell fluctuates during the Sorption Compressor cycle (6*667 s. = 4002 s.). The values depends on the status of the heat switches between the two components. Basically, the switch is open during the inner bed heating and desorbing phases, and closed during the inner bed cool down and absorbing phase. Finally, the 6 outer shells are thermally linked to the Sorption Cooler Radiator, in pratice to the crossing heat pipes.

The inputs provided by JPL are presented in the next figures.
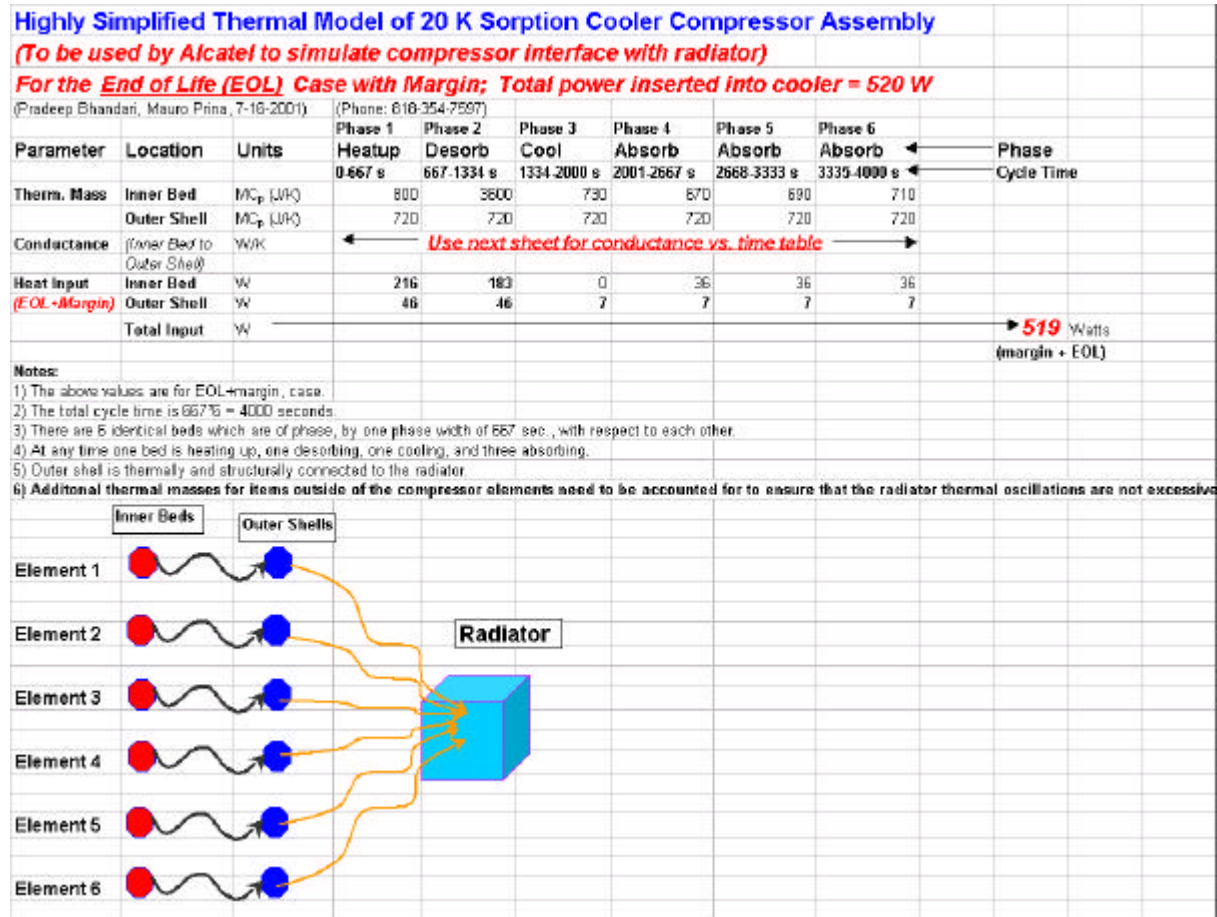

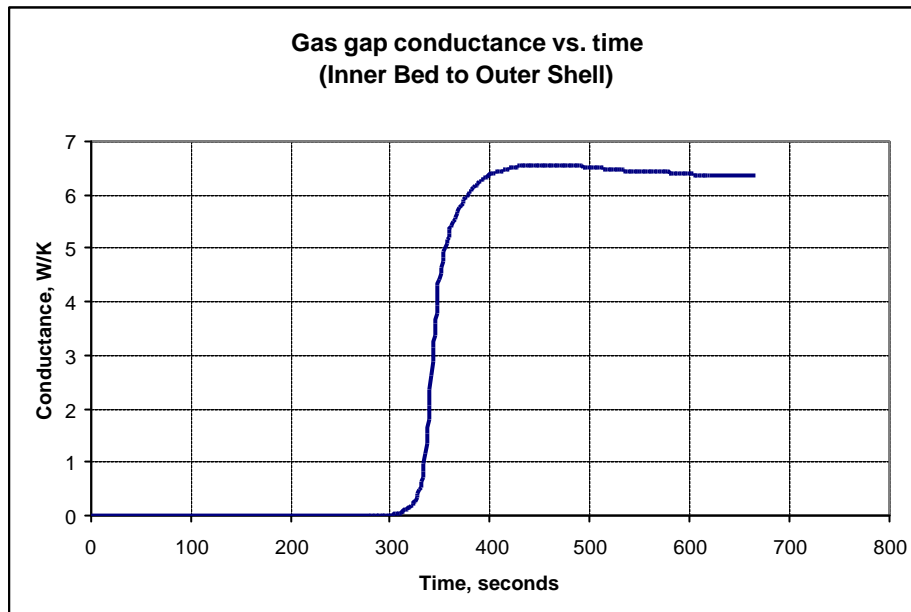FIGURE 7.3.3-2 JPL INPUT DATA FOR SCC MODELLING (1)

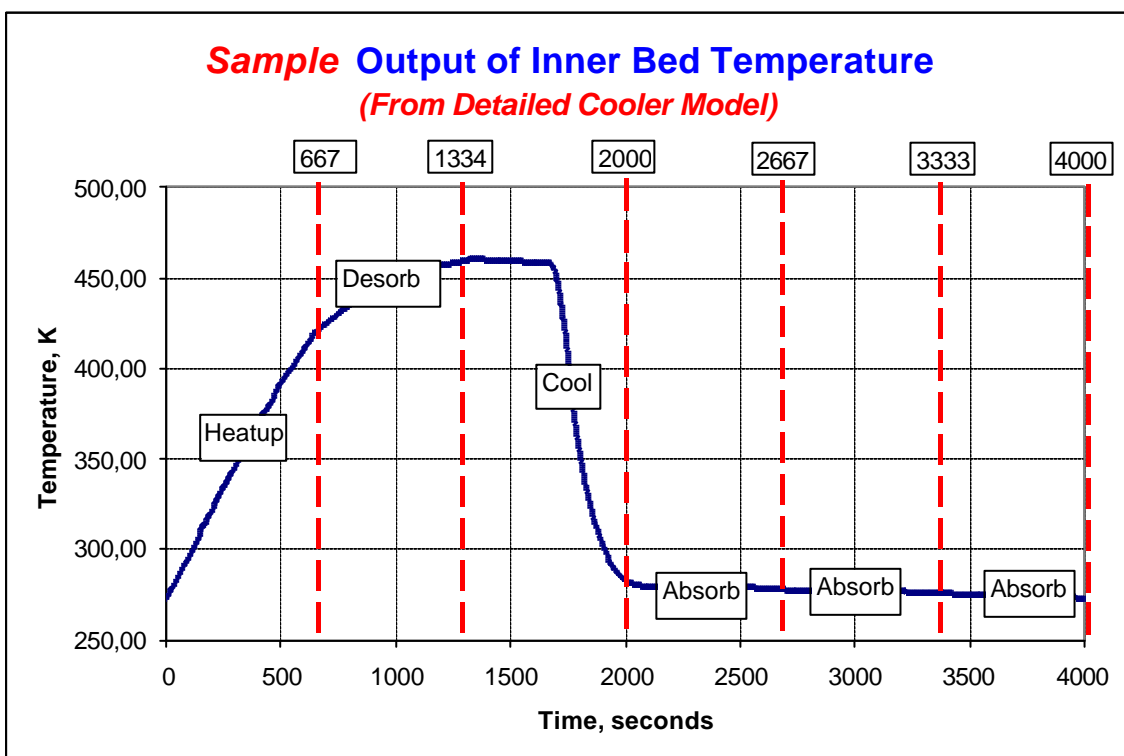FIGURE 7.3.3-3 JPL INPUT DATA FOR SCC MODELLING (2)

FIGURE 7.3.3-4 INNER BED TEMPERATURE PROFILE (FROM JPL)

An ESATAN TMM of the Sorption Compressor based on the previous data has been built in order to be included in the overall TMM of the Service Module.

Before this merging, the simplified TMM has been run alone to get a better understanding of the system as well as for verification. The aim was especially to compare the results with the information given by JPL, such as the inner beds temperature profile (see previous curve) as well as the thermal dissipation at the radiator interface, value which should be in accordance with the one given in the Interface Control Document.

For all the presented computations, the I/F temperature of the radiator is set at 260 K (boundary node).

The inner beds temperature profile calculated with the ESATAN model is similar the curve provided by JPL (see Figure 7.3.3-5).
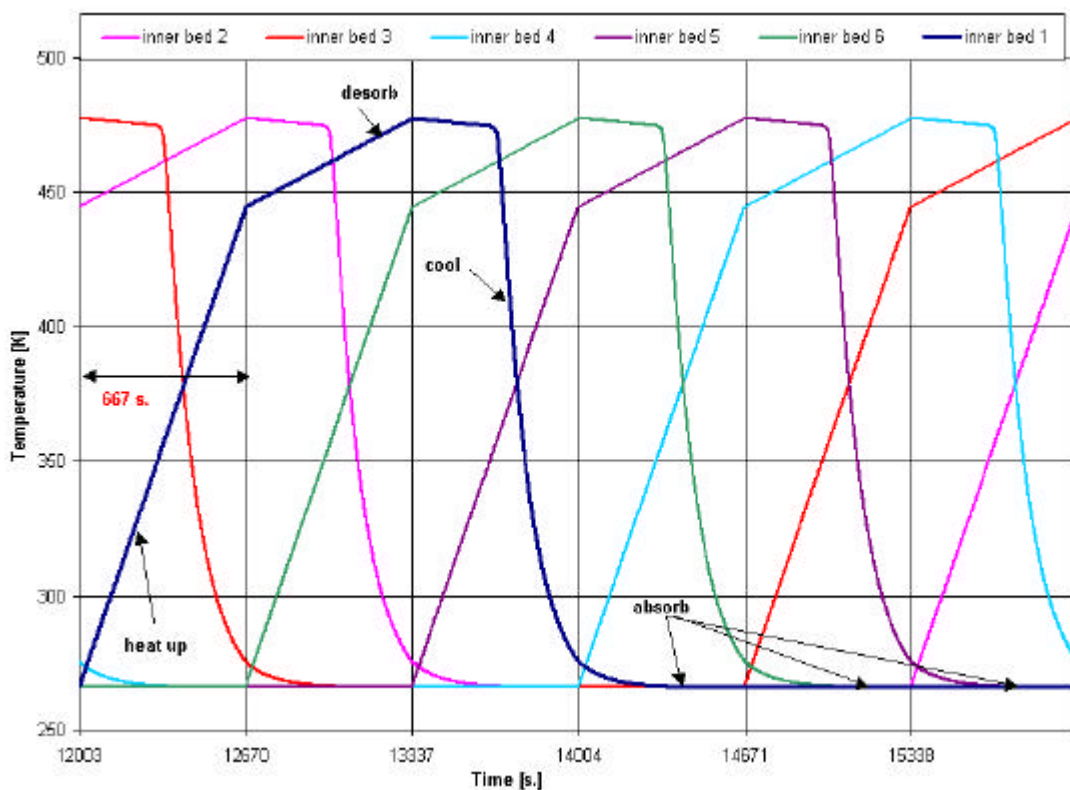
FIGURE 7.3.3-5 TEMPERATURE PROFILE OF THE INNER BEDS OVER ONE SCC CYCLE (6 *667 s)

The corresponding temperature profiles of the associated outer shells are the following:
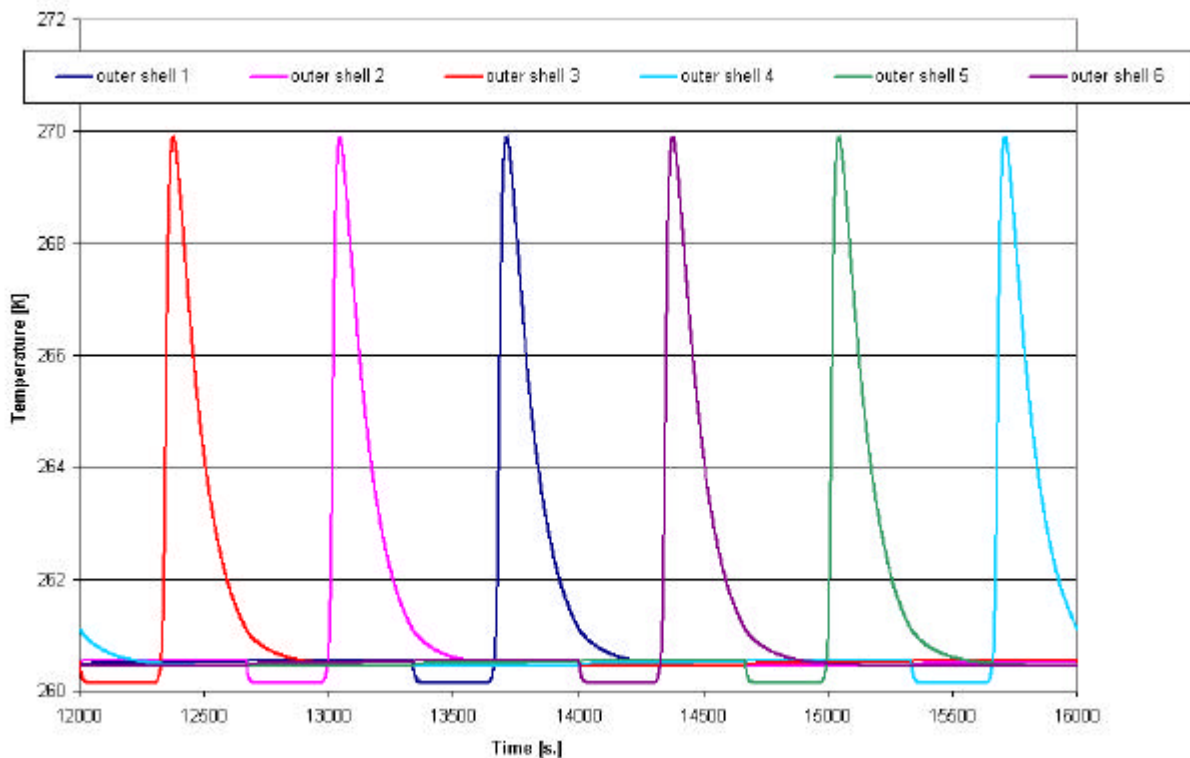

FIGURE 7.3.3-6 TEMPERATURE PROFILE OF THE OUTER SHELLS OVER ONE SCC CYCLE (6 *667 s)

The outer shell temperature fluctuate between 260 K and 270 K (radiator set at 260 K) which is a reduced range (10° C) compared to the proposal results (22° C). The temperature execursion had been pointed out at this because the SCC beds temperature as transiently higher than the specification (280 K maximum).

In any case, it has been clarified with JPL that the temperature requirements are not applicable during the "cool down phase' of a SCC element (this requirement change shall be reported in the issued IID-B). The remaining potential impact of this temperature excursion deals with thermo-elastic aspects, especially timelessness of the thermal contact between the outer shells and the radiator. The feeling of ALCATEL is that this point is not a major concern since the materials in contact are identical (Aluminium).

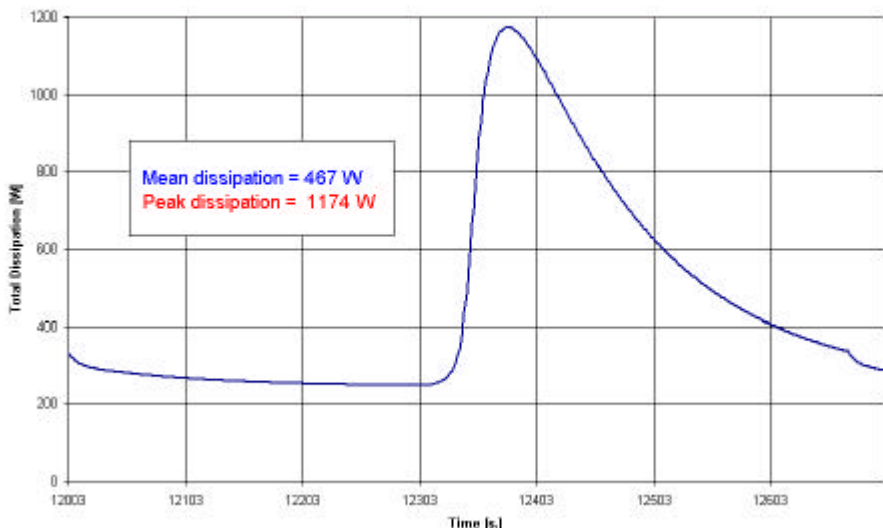The total heat flux received by the radiator interface is depicted is next figure:

FIGURE 7.3.3-7 TOTAL HEAT FLUX ON THE RADIATOR I/F

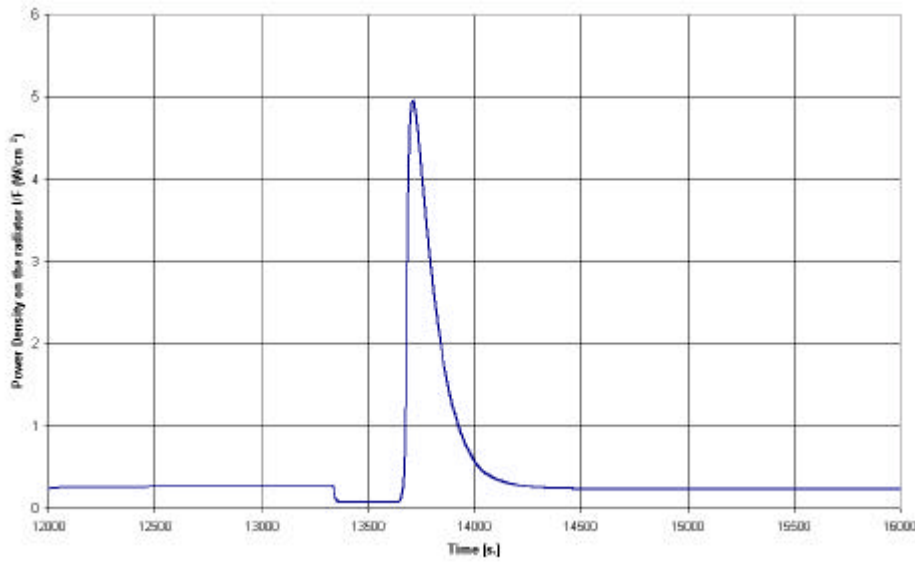The corresponding heat power density supported by a crossing heat pipe is presented hereafter.

**FIGURE 7.3.3-8 HEAT POWER DENSITY AT THE INTERFACE OUTER SHELL/
RADIATOR (CROSSING HEAT PIPE)**

Comments

– The mean flux is 467 W, consequently lower that the 520 W mean input dissipation on the inner beds (520 W is the mean power reflected in the Sorption Cooler ICD proposed update).

- This discrepancy between the two values has been clarified by JPL: it is due to simplifications of the complex Sorption Cooler thermal modelling. Reduction of the difference is possible using a more sophisticated Sorption Compressor TMM. The question to include or not a more complex model in the whole SVM is open.

– The peak dissipation is 1174 W, again slightly lower than what is reported in the proposed ICD update (1250 W).

- The peak dissipation depends on the time profile of the conductance between an inner and its associated outer shell. It is understood after some discussions with JPL that the heat switch activation process is not extremely predictable. JPL suggest to design the heat pipes layout with a total 1200 W peak dissipation.

– The calculated maximum power density at the interface between an outer shell and the radiator is 5 W/cm^2 (total corresponding dissipation: 1174 W).

- Taking into account 10 % system margin, and reduction of the surface contact between beds and heat pipes due to manufacturing accuracy and screws cross-section, will end up with a maximum power density lower than 6 W/cm^2. This level remains under the drying limit for "standard" heat pipes. The accurate maximum power density will be refined in the next future taking into account the SCC fixation layout onto the heat pipes. The maximum value a heat pipe can withstand without drying the evaporating zone will be confirmed after consultations of the potential heat pipes Suppliers. Indeed, this data depends on the heat pipe geometry and is not a "universal" requirement. However, it has been checked that heat pipes supplied by ALCATEL can withstand at least 6 W/cm^2. Higher values should be possible but elementary tests would be required to check this point.

– From the inputs provided by JPL, it is understood that the data are related to a EOL situation, with a margin of 88 W. An additional simplified TMM of the SCC have been provided, this one corresponding to a EOL situation WITHOUT MARGIN. For this configuration, the mean dissipation on the I/F radiator is 317 W.

- The difference between BOL without margin and EOL with margin mean dissipation is therefore 200 W, which represents a huge increase: + 64 %.

The results given by the JPL simplified TMM are more or less in accordance with the data suggested in the proposed ICD update. The slight discrepancies found out have been justified by JPL. There are related to the simplification of the modelling of the physical process of the cooler. This thermal model is being integrated in the overall SVM TMM. The aspect to check is related to the temperature stability under the cooling beds. This verification is motivated by the fact that stringent requirements are out coming from the proposed ICD update. They are listed in next table.

	PROPOSED ICD UPDATE
Temperature Stability at SCC I/F	± 3 K under absorbing bed adjacent to the cooling one
	± 0.5 K under the next adjacent
	± 0.1 K under the remaining absorbing bed

Results obtained for the technical proposal (based on IIDB Rev. 1.0) are not compliant with these new requirements. At this time, no specific heat was associated to the SCC. Computations shall be performed again using the simplified SCC TMM, which takes into account the actual thermal inertia of the system. It is however important to point out that the design of the radiator is totally constrained by the low operating temperature associated to a large dissipation of the unit. This feature dictates the implementation of the heat pipes network. Its function is basically to collect and distribute the dissipation all over the dedicated radiators. The three SCC panels will consequently operate roughly at the same temperature. Furthermore, the radiators and outer shells which are thermally coupled as much as possible, will consequently react in the same way to a fluctuating dissipation.

The direct consequence is that it is not feasible to actively control the outer shells interface temperature (on which are put the requirements). Indeed, it would require amount of heating power in the same order of magnitude than the source of fluctuations, i.e. up to ~1200 W. This is obviously impossible.

An alternative suggestion proposed by JPL is the use of phase change material in order to increase the thermal inertia of the system. Apart from development and qualification problems, the main drawback of this proposition is that the thermal conductance between the SCC and the radiators will be drastically reduced compared to the present situation. Given the critical problems encountered to reject the heat dissipated by the SCC, this proposition is considered as unacceptable.

We propose finally to first compute again the temperatures fluctuations with the simplified SCC TMM included in the SVM TMM. We will get therefore an actual status on the level of temperature instability obtained. This will give a basis for discussions with the instruments on the overall philosophy of maximum temperature fluctuations allocation on the different sources.

7.3.4.   Radiation analyses

The section 7.2.4 is fully applicable, with the following comments :

The Herschel/Planck radiative environment is mainly impacted by the transfer phase conditions, with the crossing of the radiation belts, as far as total ionising dose is concerned. Consequently, the difference in lifetime between Herschel and Planck, (respectively 4 years and 2.5 years) has a minor effect.

This difference in lifetime may be more significant for the solar flares contribution, which mainly affects the solar array degradation. However, among these 1.5 years difference, only 6 months should happen in Solar Maximum period. In addition, the effects of the protons fluence on the solar cells characteristics, as expressed in Figure 7.2.4-4, shows that the degradation on the Cells Pmax should not exceed 3.5% over 4 years. In conclusion, the benefit of considering a specific solar protons environment for Planck is believed marginal, and is not considered.

The same policy is applied for the heavy ions contribution.

7.3.5.   PLANCK EMC/ESD analyses

X-Band TM compatibility with LFI

One major point concerning PLANCK satellite self compatibility is the coupling between the TTC antenna and the PLANCK detectors: during scientific observation, data telemetry is nominally performed using the Medium Gain Antenna (MGA). It can also be envisaged to perform low rate data transmission using the Low Gain Antenna (LGA). For both antenna, a preliminary analysis has been carried out to estimate the observation signal to interference ratio, that is summarized hereafter.

Both LGA and MGA are implemented on the Solar Array oriented toward the Earth.

The aim is to compute the power level of the TTC reaching the detectors in the focal plane. The worst case analysis consists in performing the analysis for the detector working at the lowest frequency (LFI 27 at 30 GHz). This power has to be compared to the observation signal power.

The computation of the observation signal power is performed by computing the integrated black body luminance Φ [T].

$$\varphi [\nu,T] = (2.h/c^2) \ \nu^3 / (\exp[h. \ \nu/k.T]-1)$$

$$\Phi [T] = \int_{BW} \varphi [\nu,T] \ d\nu \approx 1/4 \ (\ \varphi [\nu_{min},T] + 2 \ \varphi [\nu_c,T] + \varphi [\nu_{max},T] \ ) \ * \ (\nu_{max}-\nu_{min}).$$

The black body luminance is multiplied by the primary mirror surface and by the telescope solid angle. This solid angle is obtained knowing the telescope on axis-directivity at 30 GHz using: $\Omega = 4^*\pi$ / Directivity.

Hence the power of the observed signal is:

$$DC_{power} = \Phi \ [T=2.7K] \ * \ \Omega \ * \ Mirror\_surface$$
$$DC_{power} = -91.22 \ dBm.$$

The required sensitivity is 2E-6 leading to temperature deviation of 5 µK.

Hence the power variation of the observed signal is:

$$AC_{power} = (\Phi[T_{max}]-\Phi[T_{min}]) \ * \ \Omega \ * \ Mirror\_surface$$
$$AC_{power} = -147.10 \ dBm.$$

Then the parasitic signal coming from the TTC antenna has to be compared to the AC_{power} level. The Table 7.3.5-1 provides the numerical details for this power computation.

Integrated luminance over 27 GHz – 33 GHz	Φ (W/sr/m²)	3.40E-09
Luminance deviation	$\Delta\Phi$ (W/sr/m²)	8.78812E-15
Primary surface	(m²)	1.77
Solid angle	(sr)	0.000125664
AC power	(W)	1.9547E-18
AC power	(dBW)	-177.1
AC power	(dBm)	-147.1
DC power	(W)	7.55873E-13
DC power	(dBW)	-121.2
DC power	(dBm)	-91.2

TABLE 7.3.5-1 INPUT POWER OF THE OBSERVATION SIGNAL COMPUTATION

The second phase of the analysis is to perform the link budget between the TTC antenna and the detector LFI 27. This is done using the standard formula:

$$P_r = P_e * G_e * L_{FS} * G_r$$

- P_e: TTC output power in X band attenuated by 30 dB for the harmonic at 30 GHz.

- G_e: TTC antenna gain

- L_{FS} : Free space losses $L_{FS} = (4^{*}\pi^{*}R / \lambda)^2$

- G_r: Gain of LFI 27 detector or, more precisely, coupling factor toward the TTC antenna.

The coupling factor between the horn LFI 27 and the TTC antenna was computed using GRASP 8 multi GTD. The ray combination is: diffraction on baffle edge then diffraction on the 3 cascaded grooves to finally diffract at the edge of the Solar Array.

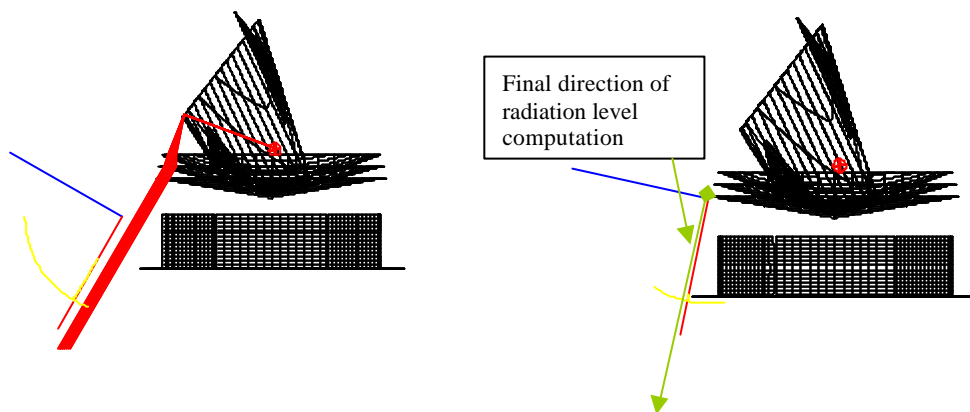This ray combination is displayed in Figure 7.3.5-1. A gain of –145 dBi is found.

Final direction of radiation level computation

FIGURE 7.3.5-1 RAYS COMBINATION BETWEEN DETECTOR AND TTC ANTENNA

A worst case link budget is displayed in Table 7.3.5-2. The 3 dB antenna gain is a worst case which envelopes both LGA and MGA gains at 90 deg from their axis. The TTC spurious signal reaching the LFI27 detector is 57 dB below the observed signal.

X-Band TTC antenna output power (W)	30
X-Band TTC antenna output power (dBW)	14.77
Out of band level attenuation (dB)	30 (typical conservative value)
TTC antenna output power at 30 GHz (dBW)	-15.23
LFI 27 horn reception gain (dBi)	-145
Frequency (GHz)	30
Wavelength (m)	0.01
Distance between LFI 27 horn and TTC antenna (m)	6.10
Free space losses (dB)	-77.69
TTC antenna transmit gain (dBi)	3.0
Received power (dBW)	-234.92
Received power (dBm)	-204.92
CMB AC level (dBm)	-147.1
Observation signal to interference ratio (dB)	57.8

TABLE 7.3.5-2 LINK BUDGET AND SIGNAL TO INTERFERENCE RATIO

The result of this preliminary analysis is that TTC antennas do not interfere with the mission with large margins.

The tests foreseen on the RFDM (Radio Frequency Development Model) and RFQM (Radio Frequency Qualification Model) will allow to check the validity of the computation methods used to determine the radiation pattern over 4π steradian (GRASP 8 validation).

Common mode rejection of SVM to PLM links

Cf. § 7.2.5.

7.3.6. Disturbance torques

This section summarizes the disturbing torques applied on PLANCK.

External and internal torques are distinguished.

External torque

At L2, PLANCK will benefit particularly quiet dynamic conditions. Gravity gradient, local geo-magnetic field and air density are vanishing and the torque they induce are insignificant compared to major sources detailed hereafter:

- **Solar pressure transverse to Sun Vector**

 The Solar Pressure torque is rather reduced due to the Sun Pointing attitude and the well centred attitude.

Sun exposed Surface	13.85 m^2
Force = P × S × (Ca+2.Cs+4/3.Cd)	75 μN
Lever Arm	< 3 cm
Maximal Transverse torque	< 2.3 μNm

  As the satellite is spinning the major part of the disturbance torque will be averaged out on 1 rotation. The temporary accumulation of momentum is maximised by: torque/spin rate = 22 μNms, which is negligible compared to the angular momentum due to the spin rate (200 Nms).

- **Solar pressure windmill torque (along Sun Vector)**

  There may also be a constant windmill torque induced by asymmetrical optical properties of the SVM -X surface. For example, the Solar Array may be described as a patchwork of facets which are not perfectly aligned.

On large spatial scales, some systematic deviation from uniformity may occur. Consider, for example, a division of the SVM surface into eight equal angular sectors, as displayed hereafter:
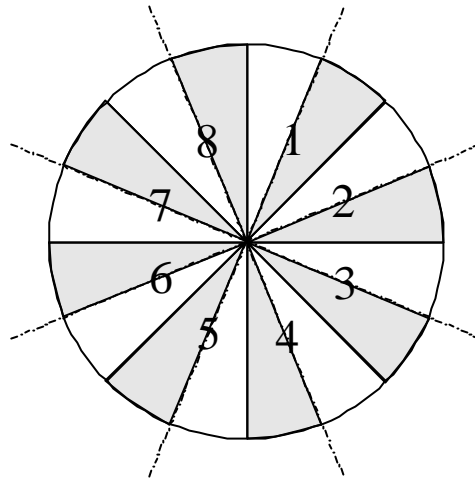
If all sectors are tilted by the same angle about their symmetry axis, the reflected part of the solar flux will induce a non zero windmill torque. However, the tilt angle required to cause spin rate variation above specification (10 - 4 rpm per hour) is 15 degrees, corresponding to deviations from a planar surface as large as 40 cm, while the shaping accuracy is below 1 mm. This means that the windmill torque will lead to spin rate disturbances well below the specified variation.

‒ **Thruster misalignments and repeatability**

The following contributors are accounted:

Thrust level	10N (per thruster)
Thrust fluctuations	5 %
CoM migration along X	45 mm
CoM migration along Y	2 mm
CoM migration along Z	2 mm
Thrust misalignment	1 deg (half cone)

ALL 3s ERRORS

This leads a maximum torque of 2.0 N.m, which is far below the control capacity (from 14 to 21 N.m according to thruster pair).

Internal torque

– **Propellant sloshing**

As the spacecraft is Spun around its maximum inertia axis, the fluids dynamics has a stabilization effect on the spacecraft when no maneuvers are performed.